

# Evolutionary morphology of body elongation in teleosts: aspects of convergent evolution

I - Text

Thesis submitted to obtain the degree of  
Doctor in Sciences (Biology)

Proefschrift voorgedragen tot het bekomen  
van de graad van Doctor in de Wetenschappen (Biologie)

Rector: Prof. Dr. Paul Van Cauwenberge

Decaan: Prof. Dr. Herwig Dejonghe

Promotor: Prof. Dr. Dominique Adriaens

De Schepper Natalie



Universiteit Gent  
Faculteit Wetenschappen  
Vakgroep Biologie

Academiejaar 2006-2007

Evolutionary  
Morphology of  
Vertebrates







# Examination Committee



**Evolutionary morphology of body elongation in teleosts:  
aspects of convergent evolution**

Members of the Examination Committee

Prof. Dr. Wim Vyverman, Chairman (Ugent, BE)

Prof. Dr. Dominique Adriaens, Promotor (Ugent, BE)

Prof. em. Dr. François Meunier (MNHN, FR)

Dr. Eric Parmentier (Ulg, BE)

Dr. Emmanuel Vreven (KMMA, BE)

Prof. Dr. Walter Verraes (Ugent, BE)

Prof. Dr. Ann Huysseune (Ugent, BE)

Prof. Dr. Luc Lens (Ugent, BE)





# Contents





## Table of Contents

### Chapter I - Introduction

I.1 General context .....	1
I.2 Description of the components .....	2
I.3 Decoupling of the components.....	6
I.4 Choice of species groups.....	8
I.5 Phylogenetic overview .....	14

### Chapter II - Aims and Structure of the thesis

II.1 Aims .....	27
II.2 Structure of the thesis.....	28

### Chapter III - Material and Methods

III.1. Material examined.....	31
III.2. Methods .....	38
III.2.1 Preparation of specimens.....	38
Anaesthesia, sacrifice and fixation.....	38
III.2.2 Morphology .....	38
<i>In toto</i> clearing and staining .....	38
Dissections.....	39
Serial sections .....	39
III.2.3 Morphometry .....	40
a) Landmarks <i>Anguilla anguilla</i> (IV.4.1) .....	40
b) Landmarks <i>Channallabes apus</i> (V.1) .....	41
c) Thin Plate Spline .....	43
III.2.4 Biometry.....	44
a) Cranial measurements <i>Anguilla anguilla</i> (IV.4.1) .....	44
b) Vertebral Biometry in <i>Channallabes apus</i> (V.1).....	45
III.2.5 Visualization .....	48
Camera lucida .....	48
CT-scanning .....	48
Radiographs .....	48
3D- reconstructions .....	48
III.2.6 Statistical analyses .....	49
Analysis of Variance.....	49
The Principal Component Analysis.....	49
The Discriminant Function Analysis .....	50
The Regression Analysis .....	50
The Bimodality Test .....	50
III.2.7 Bite force modelling.....	51
Biometrics of the lower jaw lever system.....	51
Model of mouth closing movements.....	52
Calculation of bite force .....	54
III.3. Terminology .....	55

## **Chapter IV - Anguilliformity in basal teleosts - Elopomorpha**

IV.1 Head-first burrowing species: <i>Moringua edwardsi</i>	
<b><i>Moringua edwardsi</i> (Moringuidae: Anguilliformes): Cranial specializations for Head-First Burrowing?</b>	61
Abstract	61
Introduction	62
Material and Methods	62
Results	63
Discussion	71
Acknowledgments	77
IV.2 Tail-first burrowing species: Heterocongrinae	
<b>Morphological Specializations in Heterocongrinae (Anguilliformes: Congridae) Related to Burrowing and Feeding?</b>	81
Abstract	81
Introduction	82
Material and Methods	83
Results	83
Discussion	91
Acknowledgments	95
IV.3 Head- and Tail-first burrowing species: <i>Pisodonophis boro</i>	
<b><i>Pisodonophis boro</i> (Ophichthidae: Anguilliformes): Specialization for Head-First and Tail-First Burrowing?</b>	99
Abstract	99
Introduction	100
Materials and Methods	101
Results	102
Discussion	107
Conclusions	115
Acknowledgments	116
IV.4 Non-burrowing species: <i>Anguilla anguilla</i> and <i>Conger conger</i>	
IV.4.1 Morphological variation in <i>Anguilla anguilla</i>	
<b>Variation in cranial morphology of the European eel: broad- and narrow-headedness</b>	119
Abstract	119
Introduction	119
Material and methods	121
Results	123
Discussion	124
Acknowledgements	126
IV.4.2 Cranial myology in <i>Anguilla anguilla</i>	
<b>Cranial musculature of <i>Anguilla anguilla</i> (Anguilliformes): functional implications related to narrow-headedness and broad-headedness</b>	129
Abstract	129
Introduction	129
Material and methods	131
Results	132

Discussion .....	136
Acknowledgements .....	140
IV.4.3 Cranial morphology in <i>Conger conger</i>	
<b>Cranial osteology and myology of <i>Conger conger</i> (Anguilliformes): comparison with burrowing species</b> .....	143
Abstract .....	143
Introduction .....	143
Material and methods .....	145
Results .....	145
Discussion .....	152
Acknowledgements .....	158
IV.4.4 Caudal morphology in <i>Anguilla anguilla</i> and <i>Conger conger</i>	
<b>The morphology of the caudal fin of <i>Anguilla anguilla</i> and <i>Conger conger</i>: comparison with the caudal fin of specialized Anguilliformes</b> .....	161
Abstract .....	161
Introduction .....	161
Material and methods .....	162
Results .....	163
Discussion .....	164
Acknowledgements .....	169
<b><u>Chapter V - Anguilliformity in basal teleosts - Ostariophysi</u></b>	
V.1 Vertebral morphology of <i>Channallabes apus</i>	
<b>Shape variation in the vertebrae of elongate Clariidae (Ostariophysi: Siluriformes): useful tool for taxonomy?</b> .....	173
Abstract .....	173
Introduction .....	174
Material and Methods .....	175
Results .....	176
Discussion .....	183
Acknowledgments.....	186
V.2 Caudal osteology of <i>Channallabes apus</i>	
<b>Intraspecific variation in the postcranial skeleton morphology in African clariids: a case study of extreme phenotypic plasticity</b> .....	189
Abstract .....	189
Introduction .....	190
Material and Methods .....	177
Results .....	178
Discussion .....	181
Acknowledgments.....	185
V.3 Caudal myology of <i>Channallabes apus</i>	
<b>Interspecific variation in the morphology of the caudal fin muscles in African clariids: a case in a fusiform and an elongate representative</b> .....	201
Abstract .....	201
Introduction .....	201
Material and Methods .....	202
Results .....	203
Discussion .....	204
Acknowledgments.....	206

## **Chapter VI - Anguilliformity in basal teleosts - Acanthopterygii**

VI.1.1 Cranial morphology: Mastacembelidae	
<b>A case study of extreme hypertrophy of the adductor mandibulae complex in Mastacembelidae: are cranial specializations related to powerful biting? ....</b>	<b>209</b>
Abstract .....	209
Introduction .....	209
Material and methods .....	210
Results .....	210
Discussion .....	214
Acknowledgments.....	217
VI.1.2 Caudal morphology: Mastacembelidae	
<b>A case study of the osteology and myology of the caudal fin in Mastacembelidae: are confluent median fins related to myological reductions in the caudal fin?.....</b>	<b>221</b>
Abstract .....	221
Introduction .....	221
Material and methods .....	222
Results .....	222
Discussion .....	224
Acknowledgments.....	226
VI.2 Cranial morphology: Trichiuridae	
<b>Morphology of the jaw system in trichiurids: trade-offs between mouth closing and biting performance.....</b>	<b>229</b>
Abstract .....	229
Introduction .....	229
Materials and methods.....	231
Results .....	232
Discussion .....	240
Acknowledgment.....	245

## **Chapter VII - General Discussion**

VII.1 Considerations and results of the functional-morphological component analysis.....	247
VII.2 Implications for <i>Channallabes apus</i> .....	259
VII.3 Convergent evolutionary traits .....	263
VII.4 Considerations regarding the use of vertebral morphology as a diagnostic trait.....	268
VII.5 Considerations regarding the use of morphological studies .....	271

## **Chapter VIII - Summary & Samenvatting**

VIII Summary .....	273
VIII Samenvatting.....	279

## **Chapter IX - Literature Cited**

Literature Cited .....	285
------------------------	-----

## **Chapter X - Publication List**

Publication list .....	305
------------------------	-----



Dankwoord



## DANKWOORD

Het blijkt traditie te zijn dat het dankwoord pas als laatste aan bod komt tijdens het schrijven, na het figuurlijke 'bloed, zweet en tranen'. Maar eigenlijk vormt dit naar mijn mening een van de belangrijkste paragrafen in een verhandeling, want zonder de hulp van al deze mensen zou dit werk nooit het licht hebben gezien.

Prof. Dr. W. Verraes verdient een heel bijzondere plaats in dit dankwoord. Eerst en vooral dank ik hem omdat hij me 6 jaar geleden de kans heeft gegeven mijn licentiaatsverhandeling te beginnen (en te voltooien) op zijn labo en mij aldus kennis te laten maken met de wondere wereld van de vertebrate morfologie. Dit was immers het beginpunt van een steeds groter wordende interesse in 'variatie in morfologie' wat uiteindelijk heeft geleid tot mijn wens deze topic dieper te benaderen.

Een uitermate groot woord van dank gaat uit naar mijn begeleider en promotor Prof. Dr. D. Adriaens. Hij leerde me de knepen van het vak en bracht zijn enthousiasme over zodat ik die 'palingen' zelfs MOOI begon te vinden (stel je voor). Hij heeft vaak geduld moeten oefenen bij het verbeteren van de teksten, maar hij kon door zijn ervaring en expertize alle werk tot een hoger niveau brengen. Door zijn onuitputtelijke enthousiasme kon hij me steeds weer motiveren het onderste uit de kan te halen. Zijn inbreng is dan ook van onschatbare waarde, waarvoor ik hem nogmaals wil, en niet genoeg kan, bedanken.

Hier wil ik iedereen van het 'derde verdiep' bedanken voor de goede sfeer. Uiteraard wil ik met name mijn collega's bedanken: Barbara, Stijn, Frank, Tom, Paul, Joachim, Mimi, Marleen, Soheil, Heleen en Celine. Zij waren de voorbije jaren niet alleen collega's waarmee kon gediscussieerd worden, zij waren ook mijn vrienden die van de 'ledeganck' een leuke plaats maakten om elke dag heen te gaan. Barbara, Marleen en Joachim wil ik nog eens uitdrukkelijk bedanken voor alle praktische hulp.

De thesistudenten (Kevin, Sara en Hon Fai) en maandwerkstudenten (Eveline, Brecht, Bart, Sara en Celine) wil ik eveneens vermelden daar zij door hun 'verkennd onderzoek' op hun manier een bijdragen hebben geleverd aan dit werk.

Verder verdient Dr. A. Herrel een uitgesproken woord van dank. Niet alleen gaf hij een diepere en meer toegepaste betekenis aan het begrip 'functionele morfologie', zijn

enthousiasme, geduld, vindingrijkheid en vakkundige hulp tijdens experimenten en statistische analyses hebben een enorme impact gehad op dit werk.

Ook Dr. S. Van Wassenbergh was een belangrijke steun. Zijn kennis en talent in de biomechanica en het wiskundig modeleren gaven mij de kans morfologie vanuit een andere invalshoek te benaderen. Verder wil ik hem bedanken voor het opstellen van het biomechanisch mondsluitingsmodel wat aanvullende en zeer relevante informatie opleverde in dit werk.

Prof. Dr. P. Aerts van de universiteit Antwerpen wil ik niet alleen bedanken om zijn labo ter beschikking te stellen voor de experimenten maar ook voor de waardevolle, opbouwende discussies.

Prof. Dr. A. Huyseunne wil ik bedanken om haar vakkundige kennis over histologie aan mij door te geven. Bovendien kon ik ook op haar rekenen bij het uitvoeren van histologische kleuringen daar zij mij zowel de nodige kennis als het nodige materiaal bezorgde.

I want to thank the following international scientists: Brad Moon, Jim O'Reilly, Andy Ward, Rita Mehta, Dean Adams, Jacqueline Webb (and many more) which are all working on the interesting group of burrowing and/or elongate fish and reptiles. We discussed related topics for hours. So, thanks for the inspiration and useful comments.

Dr. E. Vreven and wijlen Prof. Dr. G. Teugels mogen zeker niet in dit lijstje ontbreken. Zij gaven mij de kans om Mastacembelidae te bestuderen en een groot deel van de beschikbare literatuur over deze soorten te bemachtigen.

Onder de noemer 'het *Anguilla anguilla* team' wil ik een groot aantal personen bedanken. Eerst en vooral Claude Belpaire, Geert Goemans en Kathleen Peirsman wil ik bedanken voor hun onvangst en medewerking tijdens mijn bezoeken aan het IBW in Groenendaal. Ook Chris Liefveringe wil ik hartelijk bedanken voor de hulp tijdens de staalnames in het Lippenbroek evenals het technische team van IBW.

Prof. Dr. N. De Clerck en Dr. A. Postnov dank ik voor de bijdrage bij het maken van de CT-scans.

Barbara De Kegel en Hilde Vanwynsberghe dank ik voor alle hulp bij de administratieve rompslomp dat 'werken' met zich mee brengt.



Alle musea en commerciële handelaars die mijn vissen ter beschikking stelden verdienen uiteraard ook een plaatsje in dit dankwoord: Museum voor Dierkunde, Gent; Smithsonian National Museum of Natural History, Washington; Museum of comparative Zoology, Harvard; Koninklijk Museum voor Midden African, Tervuren; Poisson d'Or, Moeskroen, De Koraalduivel, Gent; Bassleer, Bergen op Zoom.

En natuurlijk mijn ouders en mijn zus ... Hen kan ik niet genoeg bedanken voor alles wat zij voor mij hebben gedaan. Voor hen mag deze paragraaf dan ook iets groter geschreven worden! Door hen heb ik de kans gekregen mijn studies aan de universiteit aan te vatten. Zij hebben mij vrij gelaten in de keuzes die ik maakte en hebben mij vervolgens ten volle gesteund in de goede maar ook in de kwade dagen. Zij stonden achter mij bij elke beslissing die ik nam en bleven mij motiveren. Dus nogmaals mama, papa en grote zus.. BEDANKT!

En dan als laatste, maar niet de minst belangrijke, een grote dank en een dikke kus aan mijn dodel, Stefan. Zonder jou zou deze zware periode waarschijnlijk honderd keer meer op mijn schouders hebben gewogen (met dan weer een trapeziumspierontsteking als gevolg!). Je stond altijd voor mij klaar op de momenten dat ik je nodig had en bleef me steunen ook op momenten waarop mijn humeur vermoedelijk op een heel laag pitje stond. Bedankt voor alles en nog veel meer.

Natalie De Schepper





# Introduction



## I.1 GENERAL CONTEXT

Catfish or Siluriformes (Fig. I.1- 1), are a highly diverse group of mainly freshwater species. They represent about one third of all freshwater fishes and have 34 families, about 437 genera and more than 2700 species (DE PINNA, 1996; TEUGELS, 1996; SABAJ ET AL., 2004). One of these families, the Clariidae, is a group of specialized, air-breathing catfish (TEUGELS AND ADRIAENS, 2003).

In the Clariidae a range of body plan forms from fusiform towards anguilliformity has been noted (PELLEGRIN, 1927) (Fig. I- 2A). Although body elongation is an evolutionary process that has occurred in other fish, primitive tetrapods (reptiles and amphibians) and some mammals as well (LANDE, 1978), it is never as extreme as within the Clariidae. Body elongation in the clariids is coupled to a whole set of morphological changes, such as reduction and loss of the adipose fin, continuous unpaired fins, reduction of paired fins, reduction of skull bones, increase of skull rigidity, increase in number of vertebrae, reduction of the eyes and hypertrophied jaw muscles (DEVAERE ET AL., 2001).

The present study will attempt to find out how these structural modifications in the clariid morphology are related to different components such as (1) miniaturized head, (2) a special fossorial lifestyle, (3) the presence of hypertrophied jaw muscles and (4) anguilliformity.

As most clariid representatives possess these components to some degree, it is impossible to trace the relation of each of these components on the rest of the Bauplan. Therefore, the design of this study involves an attempt to decouple the four components mentioned above, relying on a targeted selection of species from different evolutionary lineages. These lineages 1) are not related to the Clariidae in order to exclude phylogenetically defined modifications within the clariids, but 2) place the comparison of the relation of each component within the same phylogenetic context, in order to minimize phylogenetically defined differences between the applied species within one group. When two species, differing in one component only (as the components are assumed to be decoupled), are compared we may reveal to what degree structural modifications are related to that particular component. In order to recognize recurring morphological patterns that may be related to the above mentioned components, convergent structural modifications are studied and will subsequently be projected onto *C. apus*, chosen as the reference species for the clariids.

## I.2 DESCRIPTION OF THE COMPONENTS

The characteristic structural modifications of the elongate clariids are defined by a network of components, of which each component has a different morphological impact on the spatial architecture of the Bauplan. Based on current knowledge of morphology, ecology and lifestyle of these elongate clariids, the following prominent and probably the most crucial, components are recognized:

- 1) miniaturization of the skull,
- 2) burrowing lifestyle,
- 3) body elongation,
- 4) hypertrophy of the jaw muscles,

### 1) MINIATURIZATION AND REDUCTION OF THE CRANIAL SKELETON

Miniaturization can be defined as "the evolution of extremely small adult body size within a lineage" (HANKEN AND WAKE, 1993; RIEPPEL, 1996). Consequently, within the concept of miniaturization is the assumption that the species evolved from a larger ancestor (MILLER, 1979). Reduction in body size is considered a specialization that allowed the organisms to occupy a new niche (MILLER, 1979). This downsizing is observed in a variety of taxa such as mammals (JÜRGENS ET AL., 1996) and birds (CALDER, 1976), but it is more pronounced in reptiles, amphibians and fish (HANKEN AND WAKE, 1993). Moreover, the most extremely miniaturized vertebrate organisms are teleost representatives, e.g. the world's smallest vertebrate is a cyprinid fish of 7.9 mm, *Paedocypris progenetica* (KOTTELAT ET AL., 2006). Miniaturization is more common than generally thought, for example, among South American freshwater fish alone there are over 85 species regarded as miniature, spanning five orders, 11 families and 40 genera (HANKEN AND WAKE, 1993). Furthermore, miniaturization may occur more than once within one family, e.g. it occurred at least two times in the history of the ostariophysian family Alestidae (HUBERT ET AL., 2005).

Within the clariids, a range from fusiform to elongate body forms represented by the different genera has been noted (PELLEGRIN, 1927), as illustrated by figure I- 2A and with this tendency an increasing reduction of the cranial skeleton can be observed. Furthermore, with increasing anguilliformity, the head length with respect to total body length decreases (CABUY ET AL., 1999; DEVAERE ET AL., 2001). Consequently, the influence of

miniaturization onto the spatial composition of the clariid cranium can not be neglected and may even be substantial.

The genus *Heterobranchus*, is one of the fusiform clariid representatives and has the most strongly ossified head (DAVID, 1935). The cranial skeleton of this representative forms a firm and closed roof (Fig. I- 2C). The lateral sides of the cranium are formed by plate-like bones, thereby covering and protecting the jaw muscles. In most cases, increasing anguilliformity is coupled to a hypertrophy of the jaw muscles (CABUY ET AL., 1999; DEVAERE ET AL., 2001). The occurrence of cranial skeletal reductions may create space for the immense enlargement of the adductor mandibulae complex (Fig. I- 2B) (CABUY ET AL., 1999; DEVAERE ET AL., 2001). Some species (e.g. *Dinotopterus*, *Clarias*) dorsally show a fontanel-like space between the successive cranial bones (DAVID, 1935) (Fig. I- 2B, C). In *Channallabes apus*, which shows a high degree of anguilliformity (Fig. I- 2Ag), the lateral cranial bones (infraorbital and suprapraeopercular series) are even that highly reduced that both series are not connected anymore and widely dispersed (Fig. I- 2B). In general it can be stated that the neurocranium of eel-like representatives has become enormously narrow compared to the compact and broad skull of non-elongate species.

In clariids, the component ‘miniaturization’ is mainly present at the level of the head. Furthermore, the head length with respect to total body length is substantially smaller compared to that in other species where body length is similar but without elongation. Therefore, the term ‘miniaturization’, used throughout the dissertation and discussed in VII.1 and VII.2, refers to the downsizing of the head with respect to total body length.

## 2) BURROWING LIFESTYLE

---

A burrowing lifestyle has many advantageous as burrows create a space for habitation or temporary refuge or to retreat when environmental conditions are unfavorable (winter, dry season). Furthermore, it provides shelter to avoid predation. Burrowing into the sediment is commonly known among mammals, especially in insectivores and rodents, but is also found in invertebrates (TRUEMAN AND ANSELL, 1969), fish (ATKINSON AND PULLIN, 1996), amphibians (GANS, 1973; MEASEY AND HERREL, 2006) and reptiles (LEE, 1998) as well. Even though, anguilliform species are primitively adapted for wedging through small openings (GOSLINE, 1971; SMITH, 1989B), several anguilliform eels have evolved morphological adaptations for a burrowing lifestyle from head-first (*Moringua*) to tail-first (Heterocongrinae, Ophichtidae) (IV.1- 3). Burrowing vertebrates are often characterized by an elongate body and reduced or lost limbs (PARA-OLEA AND WAKE, 2001). The following

morphological characteristics are found to co-occur invariably in head-first burrowing vertebrates (GANS, 1975; WITHER, 1981; LEE, 1998): miniaturization, cranial consolidation, body elongation, limb reduction and eye reduction.

The Clariidae naturally inhabit freshwater rivers and lakes in Africa, Asia Minor, the Indian subcontinent and South-east Asia (GREENWOOD, 1961; BURGESS, 1989; TEUGELS, 1996), although they have been observed to enter brackish water as well (BURGESS, 1989). The more fusiform species (e.g. *Clarias gariepinus*) show a large distribution, whereas the elongate species occupy a more specialized, burrowing niche (Fig. I- 3A) (ALEXANDER, 1965; ADRIAENS ET AL., 2001). These species only occur in Equatorial Central and West Africa (DEVAERE ET AL., 2005; TEUGELS, 1996). The most remarkable adaptation to a benthic lifestyle, next to body elongation (GANS, 1975), is found in the dorso-ventral flattening of the skull, which improves stability on the sediment (ALEXANDER, 1965; ARRATIA, 2003A). Related to the nocturnal lifestyle, the eyes are reduced (POLL, 1973) (Fig. I- 3B). The reduction in visual input is compensated by input through the Weberian apparatus, long oral barbels, ampullary organs and the synapomorphic suprabranchial organ (GREENWOOD, 1961; ALEXANDER, 1965).

### 3) JAW MUSCLE HYPERTROPHY

Within the family of air-breathing clariid catfish, a remarkable evolution in the jaw adductor muscles has occurred as several species have developed hypertrophied jaw muscles, such as *Gymnallabes typus*, *Channallabes apus* en *Dolichallabes microphthalmus* (POLL, 1977) (Fig. I- 3B, 4). Such hypertrophy has evolved at least four times independently, originating from a fusiform *Clarias*-like ancestor (JANSEN ET AL., 2006). It has been assumed that reductions and modifications of several cranial structures are related to this extreme growth of the jaw muscles (CABUY ET AL., 1999) (Fig. I.4). A brief overview of the most striking and relevant differences in the morphology of the clariid skull, possibly related to the jaw adductor hypertrophy is given: 1) The external part of the jaw muscles ( $A_2A_3'$ ) is extremely large in the elongate *C. apus*, covering the entire postero-dorsal part of the skull and originating from the infraorbital, frontal, sphenotic and pteriotic; 2) *C. apus* is characterized by the narrow, reduced but fortified (sutures) skull roof and absence of a bony protection covering the jaw muscles, whereas the cranial bones of the fusiform *C. gariepinus* form a closed broad roof; 3) The eyes are substantially reduced and they have been shifted anteriorly in *C. apus*. Support by the infraorbitals is consequently not necessary. In *C. apus* the infraorbital series are reduced as they are tube-like. In the



fusiform *C. garipepinus* the eyes and the infraorbital series are larger, and the eyes are supported by the second infraorbital; 4) In *C. apus* the bony processes between the hyomandibula and the sphenotic are strongly interdigitated, whereas such interdigitation is absent in *C. garipepinus*; 5) The lower jaw tooth rows are posteriorly extended and the coronoid processes are larger in *C. apus* and *G. typus*. A more detailed description of the morphology of the cranial system is given in ADRIAENS AND VERRAES (1997), CABUY ET AL. (1999) and DEVAERE ET AL. (2001).

As the bite force that can be generated increased extremely in the elongate species with hypertrophied jaw muscles (HERREL ET AL., 2002), it is possible that these hypertrophied jaw muscles have evolved as an adaptation for dietary specialization (e.g. durophagy). The proportion of hard prey items included in the diet of *C. apus* seems to support this hypothesis idea (HUYSENTRUYT ET AL., 2004). Though several other factors have been suggested as possible explanations for the increase of the jaw muscles, such as the use of jaws for burrowing, aggressive interactions and even display (CABUY ET AL., 1999; HERREL ET AL., 2002).

#### 4) ANGUILLIFORMITY

Elongation of the body has occurred in all major groups of vertebrates but has less frequently evolved in endotherms probably as a result of heat-conserving constraints because surface area are proportionally greater (SHINE, 1986). Body elongation is observed in caecilians, many salamanders, amphisbaenians, snakes and in several lineages of lizards including skinks, anilids, cordylids, gerrhosaurids, anguids and microteiids. This phenomenon is frequently studied in a morphological, evolutionary and phylogenetic context (GANS, 1975; WITHERS, 1981; LEE, 1998; COATES AND RUTA, 2000; PARRA-OLEA AND WAKE, 2001; WIENS AND SLINGLUFF, 2001; CALDWELL, 2003; HIBBITS AND FRITZGERALD, 2005). Within the teleostei, elongate body forms have evolved multiple times from more deep-bodied forms such as in Osteoglossomorpha, Elopomorpha, Ostariophysi, Paracanthopterygii, Beloniformes, Synbranchiformes and Perciformes (NELSON, 2006; BELOUZE, 2003; WARD AND BRAINERD, 2007) (Fig. I- 1). In most amphibian and reptile lineages characterized by body elongation, limb reduction and even limblessness has occurred as well (WITHERS, 1981; LEE, 1998). GANS (1975) suggested some possible advantages for the evolution of body elongation and associated limblessness: 1) more efficient locomotion, 2) ability to use crevices for obtaining food, for thermoregulation or for shelter, 3) the ability to burrow in soil or sand.

The trend towards body elongation in clariids is accompanied by a whole set of morphological changes and structural reductions (BOULENGER, 1908; PELLEGRIN, 1927): reduction and loss of the adipose fin, elongate dorsal and anal fins, confluent median fins, reduction of paired fins (Fig. I- 3C) and increase in number of caudal vertebrae (DEVAERE ET AL., 2001). The presence or absence of the paired fins even appeared to differ on individual level, indicating the existence of a high level of phenotypic plasticity of traits that were generally considered as stable on a micro-evolutionary level, and even up to some degree on a macro-evolutionary level (ADRIAENS ET AL., 2002).

As already noted, other morphological features are considered to co-occur with body-elongation: reductions in cranial bones and hypertrophy of the adductor mandibulae complex. However, in clariids, the degree of cranial reductions and jaw muscle hypertrophy does not always seem to be coupled to anguilliformity. This is illustrated by *Tanganikallabes mortiauxi*. This clariid species is not elongate but it does have a markedly reduced neurocranium with large adductor muscles (POLL, 1943). On the other hand, *Channallabes*, which is more elongate compared to *Gymnallabes*, has less pronounced cranial bone reductions (DEVAERE ET AL., 2001). It is most likely that cranial modifications and jaw muscle hypertrophy are related to other components (e.g. miniaturization, burrowing or feeding) than to anguilliformity.

### I.3 DECOUPLING OF THE COMPONENTS

The study of interactions between these four various components (referred to as 'functional-morphological component analysis' throughout the study) can only reveal relevant information concerning the relation of each of these components on the rest of the Bauplan, when they do not co-occur (decoupling). Consequently, mutual influence may be eliminated. The decoupling of these assumed components may be possible by intentionally choosing comparison models (formed by two species) that, based on current knowledge, differ in only one of the above mentioned components. Of course differences related to other aspects will occur as well but these are not considered in the current functional-morphological component analysis.

The comparison models should preferably not be related to the clariids in order to eliminate phylogenetic predispositions. Within each of these models, however, the two species chosen should be phylogenetically closely related and should differ strikingly in only one of the considered components. When the species within such a model are closely related, the phylogenetic predispositions are assumed to be similar, and consequently observed morphological differences related to these components may not be masked (at

least by that). Obviously, special attention will be paid to possible phylogenetic differences.

One of the considered components for this functional-morphological component analysis is 'body elongation' and forms the main link through this dissertation as body elongation was one of the main selection criteria to choose the particular species. This doctoral thesis has focussed on 17 species, convergent in body elongation (the fusiform *Clarias gariepinus* not included) and representing three unrelated higher-level taxa: the subdivision Elopomorpha and superorders Ostariophysii and Acanthopterygii (NELSON, 2006; Fig. I- 1).

- Chapter IV (Fig. I- 5)
 

<u>Elopomorpha</u>	Anguilliformes	<i>Anguilla anguilla</i>
		<i>Conger conger</i>
		<i>Heteroconger hassi</i>
		<i>Heteroconger longissimus</i>
		<i>Moringua edwardsi</i>
		<i>Pisodonophis boro</i>
  
- Chapter V (Fig. I- 6)
 

<u>Ostariophysii</u>	Siluriformes	<i>Clarias gariepinus (fusiform)</i>
		<i>Platyallabes tihoni</i>
		<i>Platyclarias machadoi</i>
		<i>Gymnallabes typus</i>
		<i>Channallabes apus</i>
		<i>Dolichallabes microphthalmus</i>
  
- Chapter VI (Fig. I- 7, 8)
 

<u>Acanthopterygii</u>	Perciformes	<i>Aphanopus carbo</i>
		<i>Trichiurus lepturus</i>
	<u>Synbranchiformes</u>	<i>Mastacembelus mastacembelus</i>
		<i>Mastacembelus marcheii</i>
		<i>Mastacembelus brichardi</i>

Based on the results of the functional-morphological component analysis, we can verify whether an observed pattern (particularly the co-occurrence of a localized morphological change and one of the components) is correlated with phylogenetic differences rather than with structural trade-offs. For each of the above mentioned components a comparison models is chosen.

## I.4 CHOICE OF SPECIES GROUPS

### **CHANNALLABES APUS AS A REFERENCE SPECIES FOR ELONGATE CLARIIDS**

Several species within the Clariidae can be considered as potential reference organism for the present study because they show all the above mentioned characteristics that co-occur with anguilliformity. Though, *Channallabes apus* is the most appropriate species as all characteristic are more prominently present and as it is the most extensively elongated species (except for *Dolichallabes microphthalmus*):

- The hypertrophy of the adductor mandibulae-complex is most extensive (HERREL ET AL., 2002).
- The cryptic lifestyle and occurrence in murky swamps is known for many of the elongate representatives of this family (MATTHES, 1964). However, the cryptic behaviour is more extreme, as they live burrowed in the mud, in between roots of trees and best documented in *C. apus*. This species is found in Central-West Africa, and lives in swampy area, that become almost devoid of flowing surface water during the dry season (pers comm, Adriaens D; Fig. I- 3A).
- *C. apus* is the only clariid species on which a feeding-ecological study has been performed (HUYSENTRUYT ET AL., 2004). Consequently, additional data related to the feeding apparatus are available.
- An additional argument for the use of this species is the fact that many specimens were available in the lab as during preceding expeditions a lot of material, dead and alive, has been collected.

## **1) MINIATURIZATION AND REDUCTION OF THE CRANIAL SKELETON**

### THE ANGUILLA ANGUILLA - CONGER CONGER GROUP

- Shared component condition:
  - Phylogeny: Anguilliformes
  - Body shape: elongate
  - Lifestyle: non-burrowing
  - Jaw muscle size: hypertrophied
- Assumed different component condition:

- Head size: miniaturized versus large head

Even though *C. conger* and *A. anguilla* are not related at family-level, both are representatives of the same order Anguilliformes. Thus morphological differences due to phylogenetic predispositions may be more or less reduced. Both species have hypertrophied jaw muscles and an elongated body. As the condition of these components is similar, the influence of the components ‘body elongation’ and ‘jaw muscle hypertrophy’ are assumed to be negligible. Both species are assumed to be similar in their degree of ‘burrowing lifestyle’ as well. *C. conger* is a nocturnal non-burrowing species, found on rocky and sandy bottoms, where it retreats in holes, caves or wedges (LYTHGOE AND LYTHGOE, 1991). *A. anguilla* also displays nocturnal behaviour and exhibits cryptic habits during daytime (GRAHAM, 1997; TESCH, 2003), though there is little information available about the specific natural microhabitats where yellow eels actually settle and hide during daytime (SCHULZE ET AL., 2004). However, a recent study on *A. japonica* assumes that they are able to construct burrows in soft mud (AOYAMA ET AL., 2005). Furthermore, they would only adopt this behaviour when there is no other structural habitat available to hide in and when this kind of soft substrate is present (AOYAMA ET AL., 2005). It is not known whether *A. anguilla* is able to construct its own burrows in the sediment as well. Though, as burrowing is no obligate behaviour for *A. anguilla*, no extensive modifications for this behaviour were assumed. As both species appear to differ only in body and head size (other aspects are left out of consideration), this species group may be considered suitable to examine morphological influences of the component ‘miniaturization’.

## 2) BURROWING LIFESTYLE

---

### THE ANGUILLA ANGUILLA - HETEROCONGER GROUP

- Shared component condition:
  - Phylogeny: Anguilliformes
  - Body shape: elongate
  - Head size: miniaturized
  - Jaw muscle size: hypertrophied
- Assumed different component condition:
  - Lifestyle: non-burrowing versus tail-first burrowing

*Anguilla anguilla*, *Heteroconger hassi* and *H. longissimus* are related as they all belong to the order Anguilliformes (NELSON, 2006). The chosen species are clearly elongate. The head with respect to total body length of *A. anguilla* and the heterocongrids is considered miniaturized. The jaw muscles are superficially enlarged to the same extent. Consequently the influence of these three components ‘anguilliformity’, ‘miniaturization’ and ‘jaw muscle hypertrophy’ on the rest of the Bauplan may be considered equal and thus negligible. In contrast to *A. anguilla*, which exhibits cryptic habits during daytime (GRAHAM, 1997; TESCH, 2003), the heterocongrids are tail-first burrowers. Garden eels are known for their large colonies, where each individual lives permanently in separate, strengthened burrows (CASIMIR AND FRICKE, 1971; SMITH, 1989B). The front portion of the body is projected from the burrow to feed on zooplankton (CASIMIR AND FRICKE, 1971; SMITH, 1989B). They are able to withdraw entirely into their burrows but mostly they emerge three-fourths or more of their length from the burrow opening, while the tail remains inserted (BATH, 1960; SMITH, 1989B; VIGLIOLA ET AL., 1996; CASTLE AND RANDALL, 1999). During the course of the study more aspects in which these species differ became clear (e.g. jaw adductor size), though we attempted to focus on those morphological differences that are related with burrowing.

#### THE ANGUILLA ANGUILLA - MORINGUA EDWARDSI GROUP

- Shared component condition:
  - Phylogeny: Anguilloidei
  - Body shape: elongate
  - Head size: miniaturized
  - Jaw muscle size: hypertrophied
- Assumed different component condition:
  - Lifestyle: non-burrowing versus head-first burrowing

*Moringua edwardsi* (Moringuidae) and *Anguilla anguilla* (Anguillidae) are representatives of the same suborder, the Anguilloidei (ROBINS, 1989; NELSON, 2006).

These species are highly comparable when focussing on the components ‘anguilliformity’, ‘jaw muscle hypertrophy’ and ‘miniaturization’ are as both have elongate bodies, miniaturized heads and jaw muscles that are hypertrophied. Consequently, this species group is assumed to be highly suitable to examine possible structural modifications related to burrowing. *M. edwardsi* prefers sandy substrate which is penetrated head-first (CASTLE, 1968; SMITH AND CASTLE, 1972), whereas *A. anguilla* is a cryptic species (GRAHAM, 1997; TESCH, 2003). The relations between the observed

morphological differences and the difference in lifestyle (head-first burrowing versus non-burrowing) will be examined.

### PISODONOPHIS BORO

During the course of this study, we decided to add this ophichthid species to our list (for arguments see VII.1.2). It is an interesting study object as this species is able to burrow head-first as well as tail-first. Therefore, it may allow us to examine whether similar environmental demands (burrowing) has led to the evolution of similar morphological modifications in the head and in the caudal fin. Furthermore, observed structural modifications related to burrowing can be compared to those found in *Moringua edwardsi*, *Heteroconger hassi* and *H. longissimus*.

## 3) JAW MUSCLE HYPERTROPHY

### THE TRICHIURUS LEPTURUS - APHANOPUS CARBO GROUP

- Shared component condition:
  - Phylogeny: Trichiuridae
  - Body shape: elongate
  - Lifestyle: non-burrowing, benthopelagic
  - Head size: not miniaturized
- Assumed different component condition:
  - Jaw muscle size: not hypertrophied versus enlarged

*Trichiurus lepturus* and *Aphanopus carbo* are very closely related trichiurid species (GAGO, 1998). Both species have an elongated body, a benthopelagic lifestyle, they can grow to enormous proportions (> 1 m) and their head size is similar with respect to total body length (HELFMAN ET AL., 1997; GAGO, 1998). Thus, the components 'anguilliformity', 'burrowing lifestyle' and 'miniaturization' are comparable and negligible. Based on the external morphology, it can be noted that the jaw muscles of *T. lepturus* and *A. carbo* are not hypertrophied to the extent as observed in the elongate catfish and eels, dealt with in the present study. But as *T. lepturus* possesses an apparent elevated frontal crest (GAGO, 1998), we may hypothesize that this may enhance and enlarge the insertion site for the jaw muscles (amongst other, e.g. epaxials). Consequently, the degree of difference

between the jaw muscles of both species will be examined. If notable differences are present, than this species group is important as the component ‘jaw muscle hypertrophy’ is completely decoupled from the other components. If the results reveal no differences in the adductor mandibulae complex between both species, than this species group is still interesting to examine whether kinematic properties of the bite apparatus are similar, based on modelling techniques.

### THE *MASTACEMBELUS BRICHARDI* - *MASTACEMBELUS MARCHEI* GROUP

- Shared component condition:
  - Phylogeny: African Mastacembelidae
  - Body shape: elongate
  - Lifestyle: non-burrowing, benthic, cryptic
  - Head size: miniaturized
- Assumed different component condition:
  - Jaw muscle size: hypertrophied versus not-hypertrophied

*Mastacembelus brichardi* and *Mastacembelus marcheii* are closely related as both are representatives of the family Mastacembelidae (TRAVERS, 1984A, B; NELSON, 2006). Both species are considered to be similar in three components ‘anguilliformity’, ‘miniaturization’ and ‘burrowing lifestyle’. They are elongated and their head size is small with respect to total body length. Both species are cryptic. The African *M. marcheii* is a cryptic species, found in rocky habitats, and it prefers habitats of very swift velocity and more open spaces between rocks (VREVEN, 2001). The African mastacembelid *M. brichardi* is considered highly adapted to his cavernicolous life-style (POLL, 1973), especially in relation to its eye size (reduced) and coloration (depigmentation). *M. brichardi* is found out of the severe current of the surrounding rapids in hiding places situated under sandstone paving stones (VREVEN, 2001). It is a cryptophthalmic species, with small eyes deeply embedded in the head and covered by external integument and hypertrophied jaw muscles (POLL, 1973). As becomes evident from looking at the external head shape alone, *M. brichardi* has enormously bulging hypertrophied jaw muscles (TRAVERS, 1984A), whereas these are externally not clearly visible in *M. marcheii*. So, among the considered components, there is only one component in which they differ: ‘jaw muscle hypertrophy’. The components may be regarded as decoupled, which may enhance the identification of modifications related to the difference in hypertrophy of the jaw muscles. The adductor



mandibulae complex was examined into detail, in order to have a clear insight into related cranial modifications that may have occurred.

## 4) ANGUILLIFORMITY

---

### THE *MASTACEMBELUS MARCHEI* - *MASTACEMBELUS MASTACEMBELUS* GROUP

- Shared component condition:
  - Phylogeny: Mastacembelidae
  - Body shape: elongate
  - Lifestyle: non-burrowing
  - Jaw muscle size: not hypertrophied
  - Head size: miniaturized
- Assumed different component condition:
  - Body shape: confluence in median fins versus distinct fins

*M. marchei* and *M. mastacembelus* are representatives of the same family and consequently closely related (TRAVERS, 1984B; NELSON, 2006). Both species are non-burrowing species, thus the component ‘burrowing lifestyle’ can be neglected. The African *M. marchei* occurs in rocky habitats, and it prefers habitats of very swift velocity and more open spaces between rocks (VREVEN, 2001). The Asian *M. mastacembelus* (Mesopotamian spiny eel) is a demersal species, found only in the Tigris-Euphrates river systems (SAHINOZ ET AL., 2006). *M. mastacembelus* generally lives on sediments having considerable vegetation, mud and sand. At night they leave their hiding places (embedded in the mud) to feed (SAHINOZ ET AL., 2006). Both components ‘miniaturization’ and ‘jaw muscle hypertrophy’ are considered similar as both species have similar body and head size and no hypertrophied jaw muscle (TRAVERS, 1984A). Even though both species are elongate, differences in the unpaired fins are noted (TRAVERS, 1984A). *M. marchei* has confluent median fins, whereas in *M. mastacembelus* the dorsal, anal and caudal fins are distinct and clearly discernable. As the confluence of median fins is typical for species with elongated bodies, it might be interesting to examine whether more morphological differences occur, related to the differences in unpaired fin confluences and thus indirectly to the degree of anguilliformity. In this regard this species group can be used to examine specialization related to the component ‘anguilliformity’, without the influence of the other components.

## 1.5 PHYLOGENETIC OVERVIEW

As an introduction and background to the taxa discussed in this dissertation, a brief overview is given on the phylogenetic situation. It is not the aim of this chapter to list all the synapomorphic characters for all the examined species at all levels (familial, ordinal, or higher), though only the most conspicuous or relevant characters are given.

### ELOPOMORPHA

The Elopomorpha is one of the primitive subdivisions within the Teleostei (Fig. I- 1). *Moringua edwardsi* (Moringuidae), *Heteroconger hassi*, *Heteroconger longissimus* (Congridae), *Pisodonophis boro* (Ophichthidae), *Anguilla anguilla* (Anguillidae) and *Conger conger* (Congridae) are representatives of the Anguilliformes, one of the orders within this basal teleostean taxon.

➤ Chapter IV		Fig. I- 5
Elopomorpha	Anguilliformes	<i>Anguilla anguilla</i>
		<i>Conger conger</i>
		<i>Heteroconger hassi</i>
		<i>Heteroconger longissimus</i>
		<i>Moringua edwardsi</i>
		<i>Pisodonophis boro</i>

### ELOPOMORPHA

The subdivision Elopomorpha is the most diversified group of basal teleosts and comprises 856 species placed in three orders (Elopiformes, Albuliformes, Anguilliformes-Saccopharyngiformes), 24 families, and 156 genera (NELSON, 2006; INOUE ET AL., 2004). Elopomorpha vary widely in their morphology, behavior, and life history (BÖHLKE, 1989).

Since GREENWOOD ET AL. (1966) established the Elopomorpha on the basis of eight putative synapomorphies, many authors have discussed the validity of their monophyly through comparative observations of osteology, ontogeny, microstructure of spermatozoa, and physiology (for reviews, see FOREY ET AL., 1996; INOUE AND MIYA, 2001). It should be noted that some researchers did not support the monophyly of Elopomorpha and suggested that the leptocephalus larva simply represents a plesiomorphic trait of teleostean fishes (e.g., GOSLINE, 1971; HULET AND ROBINS, 1989). It appears that the adult morphological

heterogeneity (from very primitive elopiforms to highly derived anguilliforms) and ancient origin that presumably goes back more than a 100 million years ago, make it difficult to assess their phylogenies (INOUE AND MIYA, 2001). The interrelationships among anguilliforms and saccopharyngiforms have long been a problematic issue in systematic ichthyology (for details, see ROBINS, 1989). Although ROBINS (1989) regarded the saccopharyngiforms as the distantly related group to the other three orders, saccopharyngiforms have generally been considered as close relatives of the anguilliforms. Several molecular phylogenetic studies (FILLEUL AND LAVOUÉ, 2001; FOREY ET AL., 1996; WANG ET AL., 2003) have been conducted for resolving elopomorph phylogeny in relation to basal teleosts. Nevertheless, the monophyly and intrarelationships of Elopomorpha have remained ambiguous. The most recent classification of Elopomorpha is given by INOUE ET AL (2004). The order Elopiformes occupied the most basal position, with the Albuliformes and a clade comprising the Anguilliformes and the Saccopharyngiformes forming a sister group (WANG ET AL., 2003; INOUE ET AL., 2004).

### ANGUILLIFORMES

The Anguilliformes represent at present the most speciose group among the Elopomorpha (BELOUZE, 2001) and comprise 15 families, 141 genera and 791 species (NELSON, 2006). Eels are world-widely distributed and found in all large tropic and temperate oceans (NELSON, 2006; BELOUZE, 2001). Some species have even adapted to freshwater environments, though in order to complete the reproduction cycle, they are still dependant of marine circumstances (TESCH, 2003).

ROBINS (1989) has given an overview of 42 characters shared by all Anguilliformes, though most are no synapomorphies for the Anguilliformes as they are variously shared with other primitive fishes. A brief overview of striking or relevant features is given. The pelvic fins and girdle are absent. The dorsal and anal fins are confluent with the caudal fin. Scales are usually absent. The body is very elongate. The gill openings are usually extremely narrow and the gill region is elongate due to the posterior displacement of the gills. The hyomandibula is united with the quadrate. Even though the knowledge on the details of eel morphology is still fragmentary, ROBINS (1989) considered three suborders (Congroidei, Mureanoidei and Anguilloidei) within the Anguilliformes. Based on fused frontals, REGAN (1912) and ROBINS (1989), treated the Congroidei as a monophyletic taxon within the Anguilliformes. However, the molecular phylogenetic study of WANG ET AL. (2003) and morphological phylogenetic study of BELOUZE (2001) reject the monophyly of this suborder. The infraordinal relationships of the Anguilliformes as proposed by ROBINS (1989), are thus questionable. It has always been difficult to define and classify representatives of

the Anguilliformes, largely due to the uniformity in external appearance, with few marked characters available in most members. Even at present family-level relationships within the Anguilliformes are questionable as well and presently under investigation (PhD Eagderi S). A preliminary phylogeny proposed by BELOUZE (2001) is shown in Fig. I- 5.

### A) ANGUILLIDAE

The family Anguillidae or freshwater eels comprises 15 species within one genus *Anguilla* (SMITH, 1989A; NELSON, 2006). Representatives are found in tropical and temperal seas, except in the eastern Pacific and southern Atlantic (NELSON, 2006). This family forms a small group of species, with relatively unspecialized morphology (SMITH, 1989A). Anguillids are considered morphologically to be the most generalized eels of all Anguilliformes (SMITH, 1989A).

Based on the following characters, freshwater eels can be distinguished (SMITH, 1989A; NELSON, 2006): their elongate body is not excessively long nor short and stubby. The anus is situated slightly before the midlength of the body. The median fins are well developed. The pectoral fins are well developed and broadly rounded. The eyes are relatively large and the mouth is moderate. Anguillids possess scales, though small and inconspicuous. The anguillids are unique among eels because they are catadromous, spending most of their adult lives in freshwater, returning to the sea to spawn.

The phylogenetic analysis of EGE (1939) based on morphological characteristics, revealed four groups: (I) variegated species with broad, undivided maxillary and mandibular bands of teeth; (II) variegated species with a toothless, longitudinal groove in the maxillary and mandibular bands of teeth; (III) species without variegated markings and with a long dorsal fin, and (IV) species without variegated markings and with a short dorsal fin. This phylogeny has now been accepted, and early molecular studies seemed to agree with Ege's phylogenetic synopsis (AOYAMA ET AL. 1996; TSUKAMOTO AND AOYAMA 1998; BASTROP ET AL., 2000). However, this has been called into question by a recent, combined molecular and morphological, phylogenetic analysis (LIN ET AL., 2005).

CHAPTERS IV.4.1, IV.4.2 and IV.4.4: The anguillid representative (Fig. I- 5F) examined in this dissertation is *Anguilla anguilla*.

## B) MORINGUIDAE

The family Moringuidae or spaghetti eels comprise two genera, *Neoconger* and *Moringua*, with roughly six species (NELSON, 2006). *Neoconger* is considered the more primitive moringuid genus (CASTLE, 1968; SMITH AND CASTLE, 1972; SMITH, 1989D). Moringuids are a group of burrowing eels, which are, according to ROBINS (1989) related to the Anguillidae (SMITH, 1989A), and Heterenchelidae (SMITH, 1989C). Moringuids show pronounced morphological adaptations to their fossorial life (SMITH, 1989D): reduced eyes, lack of colour, low vertical fins, and reduced head pores. Moringuids are found in all tropical seas and even in freshwater, except in the eastern Atlantic (SMITH, 1989D; NELSON, 2006).

The following characters are used to define moringuid representatives (SMITH AND CASTLE, 1972; SMITH, 1989D; NELSON, 2006): they are extremely elongate and cylindrical, except near the caudal fin. The anus is situated near or behind the midlength of the body. Scales are absent. The dorsal and anal fins are reduced to low folds. The pectoral fins are small. The eyes are reduced, except in mature *Moringua*-specimens.

CHAPTER IV.1: The moringuid (Fig. I- 5C) representative examined in this dissertation was *Moringua edwardsi*.

## C) CONGRIDAE

The Congridae are one of the largest and most divers anguilliform family, the number of genera and species probably only exceeded by the Ophichthidae (SMITH, 1989B; BELOUZE, 2001). Congridae are found worldwide in tropical and subtropical latitudes and occurs in the Atlantic, Pacific and Indian Oceans (NELSON, 2006). A total of 32 genera and roughly 160 species are counted within the congrid family (NELSON, 2006). Former attempts to define and classify the congrid species have resulted in much confusion due to the lack of marked characters and the uniformity in their habitus. An overview of previous congrid classifications is given by SMITH (1989B). The foundation of modern congrid classification was proposed by ASANO (1962) and mainly based on numerous significant characters of osteological and other internal structures. Presently three subfamilies are recognized: Heterocongrinae, Bathymyrinae and Congrinae.

The Congrinae comprise 25 genera (NELSON, 2006) and is the largest and most divers subfamily (SMITH, 1989B). They are considered to represent the main stem of the congrid evolution (SMITH, 1989B).

The Heterocongrinae is a highly specialized group, comprising 25 species in two genera *Gorgasia* and *Heteroconger*, of which *Heteroconger* is the most derived genus (NELSON, 2006). They show some resemblances with the Bathymyrinae though they are more divergent and highly specialized (SMITH, 1989B). Their caudal fin is reduced and the tips are stiffened for burrowing, a trend that began in the Bathymyrinae (SMITH, 1989B). Their body is very elongate and slender. Their mouth is short and the lower jaw projects beyond the upper jaw (TYLER AND SMITH, 1992; CASTLE AND RANDALL, 1999). Garden eels live in large colonies, where each individual lives permanent in separate, strengthened burrows (CASIMIR AND FRICKE, 1971; SMITH, 1989B), the front portion of the body projected from the burrow to feed on zooplankton (CASIMIR AND FRICKE, 1971; SMITH, 1989B).

CHAPTERS IV.2, IV.4.3 and IV.4.4: Three congrid representatives were examined in this dissertation. *Conger conger* (Fig. I- 5D) belongs to the subfamily Congrinae, whereas *Heteroconger hassi* and *Heteroconger longissimus* belong the subfamily Heterocongrinae (Fig. I- 5E, G).

#### D) OPHICHTHIDAE

The Ophichthidae or snake eels are the most speciose and diverse family of the Anguilliformes, including 52 genera and more than 290 species (MCCOSKER ET AL., 1989). Two subfamilies are recognized, the Myrophinae (worm eels) and Ophichthinae (snake eels) (MCCOSKER ET AL., 1989; NELSON, 2006). Representatives of this large family have a worldwide distribution, inhabiting a wide range of different substrates, from coral reefs, to sand and mud in rivers and estuaries but mainly live burrowed in soft sediments (MCCOSKER ET AL., 1989). The following characters can be used to define the Ophichthidae (MCCOSKER ET AL., 1989; NELSON, 2006): the branchiostegal rays are numerous and broadly overlapping along the ventral midline. The supraorbital canals are united by the transverse frontal commissure. The supratemporal commissure is present. The frontals are fused. The pterygoids are well separated from the vomer and hyomandibulo-quadratum.

One of the most conspicuous characters defining the Ophichthinae (snake eels) is the presence a hard and fleshy tail tip, without caudal fin rays that are externally visible (MCCOSKER ET AL., 1989; NELSON, 2006). Within this subfamily, 41 genera are recognized with about 210 species.

CHAPTERS IV.3: One genus of the Ophichthidae (Fig. I- 5B) was examined in this dissertation. *Pisodonophis boro* belongs to the subfamily Ophichthinae.

## OSTARIOPHYSI

The Ostariophysi are considered, together with the Protoacanthopterygii, as the most primitive superorders within the Euteleostei (NELSON, 2006) (Fig. I- 1). The genera *Clarias*, *Platyclarias*, *Platyallabes*, *Gymnallabes*, *Channallabes* and *Dolichallabes* are representatives of the Clariidae, one of the 33 families within the Siluriformes, belonging to the superorder Ostariophysi (TEUGELS, 1996; NELSON, 2006).

➤ Chapter V		Fig. I- 6
<u>Ostariophysi</u>	<u>Siluriformes</u>	<i>Clarias gariepinus (fusiform)</i>
		<i>Platyallabes tihoni</i>
		<i>Platyclarias machadoi</i>
		<i>Gymnallabes typus</i>
		<i>Channallabes apus</i>
		<i>Dolichallabes microphthalmus</i>

## OSTARIOPHYSI

Recent molecular and morphological studies have demonstrated a sister-group relationship between the clupeomorphs and ostariophysans (anotophysans and otophysans) (e.g. LÊ ET AL., 1993; LECOINTRE AND NELSON, 1996; INOUE AND MIYA, 2001).

The Ostariophysi represent 27% of all known teleosts and 64% of all freshwater fishes (NELSON, 2006). The enormous ecological and evolutionary diversity and freshwater occurrence of the majority of the Ostariophysi have led to a large number of elaborate studies concerning evolution, biogeography and phylogenetic characteristics (synapomorphies) (REGAN, 1911; ROBERTS, 1973; GREENWOOD ET AL., 1979; FINK AND FINK, 1981). The presence of the Weberian apparatus and consequent, specialization for enhanced perception of vibrations is believed to be of the major adaptive characters at the base of their success and extensive diversity (REGAN, 1911; ALEXANDER, 1965). Another 'typical' Ostariophysian characteristic is the production of an alarm substance, inducing a wide range of fright reactions (GOSLINE, 1971; NELSON, 2006). Even though ostariophysians are characterized by a number of features that distinguish them from other teleost taxa (REGAN, 1911; ROBERTS, 1973; GREENWOOD ET AL., 1979; FINK AND FINK, 1981), listing these is beyond the scope of this chapter.

The Ostariophysi include five orders (NELSON, 2006; FINK AND FINK, 1996; TEUGELS, 1996): Gonorhynchiformes, Characiformes, Cypriniforme, Gymnotiformes and Siluriformes.

## SILURIFORMES

The order Siluriformes or catfish comprises 34 families, about 437 genera and more than 2700 species (DE PINNA, 1996; TEUGELS, 1996; SABAJ ET AL., 2006). This order represents about one third of all freshwater fishes, and is found in Africa, Eurasia, South-east Asia, Japan, Australia, North, Central and South America. Fossil taxa have also been found on Antarctica (GRANDE AND EASTMAN, 1986). A brief overview of the most striking morphological specializations in some siluriforms is given below.

In general the siluriform skull is broad, dorso-ventrally flattened and has small eyes (DAGET, 1964). The reduction in visual input and the fact that catfishes often live in murky waters or are nocturnal, is compensated by olfaction, taste and touch sensory organs (ALEXANDER, 1965). Catfish are characterized by the presence of highly sensorial oral barbels surrounding the snout region. A specialized palatine-maxillary mechanism has enabled a controlled movement of the maxillary oral barbels (Gosline, 1975). Another important sense organ is the Weberian apparatus. In catfish it is more specialized than in other ostariophysans, as the reduced swimbladder has become almost completely enclosed by the extended parapophyses of the fourth and fifth vertebrae (CHARDON ET AL., 2003). The swimbladder remains uncovered laterally, where it comes to lie close to the surface of the body, in an area with little body musculature, allowing external sound vibrations to enter the swimbladder. It allows an efficient transport of sound vibrations from the swimbladder to the inner ear (ALEXANDER, 1965; CHARDON ET AL., 2003). Besides sound perception, several catfishes are capable of producing sounds and this is assumed to be an effective defensive mechanism or used for intraspecific communication (ALEXANDER, 1965). At least two different sound producing mechanisms involve the swimbladder: contractions of the muscles on the swimbladder produce pulsations (e.g. Pimelodidae) and an elastic spring mechanism where the broad tip of the flexible, anterior part of the fourth parapophysis is responsible for sound production (e.g. Mochokidae)(ALEXANDER, 1965). A third mechanism for sound production is found in some catfish families and involves pectoral spine stridulation of the spine base in the pectoral socket (KAATZ AND STEWART, 1997). Furthermore, catfish display diverse defense mechanisms. Pectoral spines as well as dorsal spines can be erected and locked (based on a friction lock mechanism), making it difficult for predators to handle or swallow these species (ALEXANDER, 1965).



## CLARIIDAE

The clariid family comprises 15 genera with 93 species (TEUGELS, 1996; NG, 2003; SABAJ, 2006). They are found in Africa, Asia minor, the Indian subcontinent and South-east Asia (GREENWOOD, 1961; BURGESS, 1989; TEUGELS, 1996) and inhabit freshwater rivers and lakes, and even brackish water (BURGESS, 1989). The highly specialized elongate clariids are restricted to Central West Africa (BOULENGER, 1911; TEUGELS, 1986; ADRIAENS ET AL., 2001).

More generalized clariid species are defined by the heavy, dorso-ventrally flattened head with four pairs of oral barbels and small eyes (POLL, 1973). The presence of a suprabranchial organ enables them to perform aerial respiration and migrate through deoxygenated swamps and pools. This specialized arborescent, air-breathing organ is situated in the posterodorsal part of the branchial cavity (GRAHAM, 1997). Their ability for terrestrial migrations is facilitated by the specialized locomotor pattern, in which pectoral spines and undulatory body movements are used (TEUGELS, 1986).

In the Clariidae the existence of a range between fusiform and elongate genera has been noted (PELLEGRIN, 1922). Together with the elongate body, a set of morphological modifications are observed, such as the reduction and loss of the adipose fin, continuous unpaired fins, reduction of paired fins, reduction of the skull bones, reduction of the eyes and hypertrophied jaw muscles (CABUY ET AL., 1999; DEVAERE ET AL., 2001).

Originally, the Clariidae were thought to have undergone an anagenetic evolution, which involved transformations towards increasing anguilliformity, coupled to a hypertrophy of the jaw muscles (BOULENGER, 1908; PELLEGRIN, 1922). This idea was first doubted by (POLL, 1977). For a review on this see TEUGELS AND ADRIAENS (2003). Recent phylogenetic studies, however, provide evidence that supports the hypothesis that anguilliformity evolved several times (AGNÈSE AND TEUGELS, 2005; JANSEN ET AL., 2006; DEVAERE ET AL., 2007A; 2007B).

CHAPTER V: Six clariid species were examined in this dissertation: the fusiform *Clarias gariepinus*, and the elongate *Platyallabes tihoni*, *Platyclarias machadoi*, *Gymnallabes typus*, *Channallabes apus* and *Dolichallabes microphthalmus*.

## **ACANTHOPTERYGII**

The superorder Acanthopterygii is one of the nine superorders recognized by Nelson (2006) (Fig. I- 1). Three series are recognized within the Acanthopterygii, Mugilomorpha, Atherinomorpha and Percomorpha. All acanthopterygian species that were examined in this dissertation are representatives of the latter series (Percomorpha).

- Chapter VI Fig. I- 7, 8
- |                        |                         |                                    |
|------------------------|-------------------------|------------------------------------|
| <u>Acanthopterygii</u> | <u>Perciformes</u>      | <i>Aphanopus carbo</i>             |
|                        |                         | <i>Trichiurus lepturus</i>         |
|                        | <u>Synbranchiformes</u> | <i>Mastacembelus mastacembelus</i> |
|                        |                         | <i>Mastacembelus marcheii</i>      |
|                        |                         | <i>Mastacembelus brichardi</i>     |

## PERCOMORPHA

The Percomorpha are the most derived euteleostean clade and comprise 9 orders with 245 families, 2212 genera and 13173 species (NELSON, 2006). As intrarelationships of Percomorpha have remained ambiguous and major differences in recognized classifications occur (for details, see JOHNSON AND PATTERSON, 1993 and NELSON, 2006), the higher-level phylogeny within the Acanthopterygii remains a subject of debate (STIASSNY, 1986; JOHNSON AND PATTERSON, 1993; PARENTI, 1993; NELSON, 2006).

### A) PERCIFORMES

The order Perciformes is the most diversified of all fish orders as perciforms dominate in vertebrate ocean life and are the dominant fish group in many tropical and subtropical freshwaters (NELSON, 2006). The Perciformes contain 20 suborders, 160 families, about 1539 genera and over 10033 species (NELSON, 2006). The phylogenetic relationships within this extremely large group of perciform fish are still unsettled. NELSON (2006) supports a classification in which the order Perciformes is not monophyletic. A detailed examination of percomorph phylogeny performed by JOHNSON AND PATTERSON (1993) presents evidence that the perciforms may be part of a monophyletic group, though only when scorpaeniform, pleuronectiform and tetraodontiform representatives are included.

### SCOMBROIDEI

The superorder Scombroidei comprises six families with 46 genera and about 147 species (NELSON, 2006). This group includes species that may be the fastest swimming fish (e.g. sailfish, swordfish and bluefin tuna with speeds from 60 up to 100 km/h). Endothermy has evolved three times within the Scombroidei but not in the Trichiuridae.

The superorder Scombroidei was first considered by REGAN (1909) and included the Gempylidae, Istiophoridae, Luvaridae, Scombridae, Trichiuridae and Xiphiidae. Since then

several classifications are proposed. At present, the Istiophoridae and Luvaridae are excluded and the Sphyraenidae is additionally included in the Scombroidei (NELSON, 2006). In the classification proposed by JOHNSON (1986), the Sphyraenidae are recognized as the primitive sister group to the remaining taxa.

### TRICHIURIDAE

The Trichiuridae is considered a monophyletic group and comprises nine genera with at least 39 species (GAGO, 1998; NAKAMURA AND PARIN, 2001, NELSON, 2006). The cutlassfishes are marine species that are distributed in the Atlantic, Indian and Pacific Oceans (NELSON, 2006).

Trichiurid representatives can be described as follows (NELSON, 2006; GAGO, 1998): the body is very elongate and laterally compressed; the lower jaw is protruding and bears fanglike teeth; the opercle is splintered; the dorsal fin is extremely long; the anal fin has two spines and many soft ray; the caudal fin is reduced or absent; the pelvic fins are reduced or absent. Three subfamilies are recognized, i.e. the Aphanopodinae, the Lepidopodinae and the Trichiurinae (NELSON, 2006). The Aphanopodinae are characterized by a small and forked caudal fin and the presence of pelvic fins. The Trichiurinae are defined by the absence of a caudal fin (and hypurals) and by the absence of pelvic fins.

Several phylogenetic studies have been conducted for resolving the phylogeny of the cutlassfishes (TUCKER, 1956; JOHNSON, 1986; GAGO, 1998). Nevertheless, a formal classification for the cutlassfishes is presently unwarranted. Still, the phylogenetic study of GAGO (1998) revealed (amongst others) the monophyly of the trichiurids and the basal position of *Aphanopus* (Fig. I- 7A).

CHAPTERS IV.2: Two trichiurid representatives (Fig. I- 7B, C) were examined in the present dissertation. *Aphanopus carbo*, belongs to the subfamily Aphanopodinae and is considered the most basal trichiurid, whereas *Trichiurus lepturus* is more derived and belongs to the Trichiurinae (Fig. I- 7A).

### B) SYNBRANCHIFORMES

The Synbranchiformes is one of the orders belonging to the Percomorpha. This order comprises two suborders, three families, 15 genera and about 99 species (NELSON, 2006). The suborder Synbranchioidei comprises one family, the Synbranchidae or swamp-eels, whereas the second suborder, the Mastacembeloidei, comprises the Mastacembelidae and

Chaudhuriidae (JOHNSON AND PATTERSON, 1993; BRITZ AND KOTTELAT, 2003; NELSON, 2006). According to TRAVERS (1984A, B) the Mastacembelidae are a monophyletic group within the Mastacembeloidei, with the Chaudhuriidae being the sister family of the Mastacembelidae.

The Mastacembeloidei were originally placed within the Perciformes (GREENWOOD ET AL., 1966) but were removed to the Synbranchiformes by GOSLINE (1983), TRAVERS (1984A, B) and JOHNSON AND PATTERSON (1993). A detailed osteological and myological study of TRAVERS (1984A, B) led to the following diagnosis for the Synbranchiformes:

“DIAGNOSIS. Eel-shaped acanthomorph fishes of small to moderate size (attaining max. length of approx. 1 m). Burrowing and cavernicolous habit commonly displayed. Lack pelvic fins or girdle, with caudal fin reduced or absent. Gill membrane attached to lateral wall of body by expansion of the hyohyoidei adductores muscle; restricted opercular opening and insertion of levator operculi on lateral face of operculum. Prominent adductor mandibulae musculature, with part  $A_1$  lying ventral to  $A_2$ , the latter tending to encroach across dorsal surface of neurocranium and into orbital cavity. Eyes small and well forward in skull. Anterior and posterior nostrils. Cycloid scales, small and oval, sometimes absent. Neurocranium attenuated, particularly precommissural region involving frontals, pterospeneid, vomer and parasphenoid; dorsal surface lacks crests or any form of sculpturing. Frontals turned down with prominent descending lamina. Infraorbital bones reduced apart from 1st. Palatines joined firmly to vomer in midline; generally tooth bearing. Vomer a long thin strut. Ectopterygoid articulates with lateral ethmoid, vomer or both. Non-protrusile upper jaw. Maxilla and premaxilla long and strut-like, with symphyseal and articulatory processes reduced or absent. Dentary with posterior extension along ventral edge of anguloarticular. Pectoral girdle remote from basicranium, posttemporal bone reduced (accompanied by loss of connection to pectoral girdle) or lost. Flexible craniovertebral joint. Dorsal gill arch skeleton positioned posteriorly; lacks first pharyngobranchial bone, with second pharyngobranchial reduced to absent. Numerous vertebrae. Pantropical and subtropical fishes from freshwaters at high and low elevations; some individuals reported from brackish waters; tendency for facultative air-breathing and sex reversal. 83 extant species currently recognised (no fossil record) two suborders.”

### MASTACEMBELIDAE

The family Mastacembelidae or spiny eel have a wide distribution in tropical and subtropical regions of Africa, South East Asia and Middle Asia, and north to China (TRAVERS, 1984A; VREVEN, 2005). The following features are characteristic for this family (TRAVERS, 1984A, B; NELSON, 2006; VREVEN, 2005): the body is elongate and covered with a huge

number of small cycloid scales. A rostral appendage is present that bears two anterior nostrils on each side of the central rostral tentacle. The gill opening is reduced. A long series of well-developed dorsal spines and a short series of anal spines are present. Pelvic fins and girdles are absent. African species have confluent median fins. Even though TRAVERS (1984A, B) recognized two subfamilies (Mastacembelinae and Afromastacembelinae), which is followed by NELSON (2006), the use of subfamilies has recently been rejected by a thorough work of VREVEN (2005), as a sister relationship could not be confirmed. The genera *Aethiomastacembelus* and *Afromastacembelus* are subsequently placed in synonymy by VREVEN (2005) as the proposed monophyly could not be supported. Additional research on the phylogeny of the Mastacembelidae and even the Mastacembeloidei is necessary as the one proposed by TRAVERS (1984A, B) (Fig. I- 8) is confusing and unresolved (BRITZ AND KOTTELAT, 2003; VREVEN, 2005).

CHAPTERS IV.1.; VI.1.2: Three mastacembelid representatives (Fig. I- 8B, C, D) were examined in the present dissertation. *Mastacembelus mastacembelus* is an Asian species, whereas *Mastacembelus brichardi* and *Mastacembelus marcheii* are African representatives.





# Aims - Structure





## II.1 Aims

The principal conceptual strategy of this thesis is about a functional-morphological component analysis. This analysis is applied using species showing a convergent evolution in body elongation, in order to explore structural specializations that may be related (directly or indirectly) to one of more of these components. This dissertation tries to give some answers to the following general questions.

- 1) Are the proposed species complexes suitable for the study of one of the considered components ?
- 2) Is this kind of analysis useful to define and explain modifications related to a specific component ?
- 3) As the components considered for the analysis are assumed to form a tight network, defining the cranial morphology of the elongate clariids, can this network be decoupled in *Channallabes apus* ? And is it possible to explain the structural modifications observed in the specialized anguilliform clariids, and thus define these as adaptations based on the results of the functional-morphological component analysis as used in this study ?
- 4) Is a common evolutionary pattern present in distantly related species that are convergent in body elongation ?
- 5) To what degree have these species evolved to a similar overall Bauplan ?
- 6) What is the evolutionary advantage of an elongate body given the fact that body elongation has been developed many times independently ?

## II.2 Structure of the thesis

### CHAPTER I: INTRODUCTION

The first chapter '**Introduction**' formulates the working hypothesis of this study based on the proposed functional-morphological component analysis. An introduction is given on the family of clariids, showing a special and unique morphology in some elongate taxa, which has led to the present study. As an introduction to and background of the taxa discussed in this dissertation an overview of their systematic position is given.

### CHAPTER II: AIMS AND STRUCTURE

The current chapter resumes the main ideas and hypotheses that are tested and clarifies the structure of the thesis.

### CHAPTER III: MATERIAL AND METHODS

In the third chapter '**Material and methods**' an overview is given of the species and specimens that are used in this study. In order to avoid repetitions in the subsequent chapters, the methods used to obtain data and examine species are explained into detail with reference to the specific chapters where this technique is applied. The third part of this chapter deals with some terminologies used in this dissertation in order to avoid misunderstandings.

### CHAPTERS IV-V-VI: RESULTS

The fourth (Elopomorpha), fifth (Ostariophysi) and sixth (Acanthopterygii) chapters present the actual results of the dissertation. The order of the chapters is chosen based on the phylogenetic relationships between these taxa. The fourth chapter deals with the more basal teleost group, the Elopomorpha (Nelson, 2006). The Ostariophysi are presented in the subsequent chapter (V), as this group is considered a more basal suborder within the Euteleostei than the Acanthopterygii (chapter VI) (Nelson, 1994) (Fig. I.1- 1).

#### CHAPTER IV: ELOPOMORPHA

The morphological studies performed on elopomorph representatives are presented in this chapter. Four main parts are present, focussing on burrowing lifestyle, beginning with head-first burrowing (*Moringua edwardsi*, IV.1), and followed by respectively tail-first burrowing (*Heteroconger hassi* and *H. longissimus*, IV.2), the combination of head- and tail-first burrowing (*Pisodonophis boro*, IV.3), and ending with non-burrowing species (*Anguilla anguilla* and *Conger conger*, IV.4). The latter part subsequently presents results on cranial variation in trophic phenotypes of *A. anguilla* (IV.4.1), cranial myological variation related to trophic phenotypes of *A. anguilla* (IV.4.2), cranial morphology of *C. conger* (IV.4.3), morphology of the caudal fin in *A. anguilla* and *C. conger* (IV.4.4).

- 1) What kind of specializations define the head of the head-first burrowing anguilliform *Moringua edwardsi*? And can these be related to burrowing ?
- 2) Can morphological specializations present in *Heteroconger hassi* and *H. longissimus* be related to their tail-first burrowing habit ?
- 3) As *Pisodonophis boro* is able to burrow head-first as well as tail-first, can similar specializations be found at the level of the head and caudal fin or does it show trade-offs ? Are morphological specializations in *P. boro* similar to those found in the species that are restricted to head-first (*M. edwardsi*) and/or tail-first burrowing (*H. hassi* and *longissimus*) ?
- 4) What kind of morphological differences are found between two non-burrowing species *Anguilla anguilla* and *Conger conger* and between these species and the burrowing species? Are these differences related to differences in burrowing or to other aspects ?

### CHAPTER V : OSTARIOPHYSI

The ostariophysan species are considered in chapter V. Due to the lack of a reliable understanding of generic and specific characteristics in clariid catfish, the eel-like species were at that time difficult to discern. Part V.1 is focusing on the informative nature of vertebral shape variation for taxonomy and phylogeny, taking anguilliform clariids as a case study. Part V.2 focuses on the caudal skeleton of the elongate clariids. The caudal skeleton is often considered to be an important diagnostic trait but the degree of phenotypic plasticity has not been adequately assessed. Therefore, shape and variability of the caudal skeleton in *Channallabes apus* as a case study is examined. Part V.3 deals with the myological features of the Clariidae.

- 1) Can vertebral shape be used as an additional set of traits for taxonomy in the elongate clariids ?
- 2) Is the caudal skeleton of the clariid species inter- and intraspecifically variable ?
- 3) Can myological differences be related to body shape (fusiform versus anguilliform) ?

### CHAPTER VI : ACANTHOPTERYGII

In the sixth chapter, two representatives of acanthopterygan families are considered, Mastacembelidae and Trichiuridae. Part VI.1 deals with the head morphology of two mastacembelid species, *Mastacembelus marcheii* and *M. brichardi*, as they differ in the degree of development of the jaw muscles. Part VI.2 focuses on the morphology of the caudal fin of two mastacembelid species that differ in the degree of median fin confluence. The third part (VI.3) focuses on the cranial morphology and mouth closing kinematics (using the dynamic mouth closing model of Van Wassenbergh) of the two trichiurid species that differ in the height of the supraoccipital crest.

- 1) What kind of morphological specializations can be related to jaw muscle size ?

- 2) Are morphological specializations present at the level of the caudal fin in mastacembelid species, which may be related to the differences in median fin morphology (distinct versus confluent) ?
- 3) Are myological differences observed at the level of the head musculature of *A. carbo* and *T. lepturus*, which may be related to the difference the height of the supraoccipital crest ? Does the use of a biomechanical model of the mouth closing system reveal a compromise between biting and fast jaw closing in these trichiurids ?

## CHAPTER VII : GENERAL DISCUSSION

This chapter contains a general discussion on the use of the proposed species clusters and the functional-morphological component analysis in general. The results obtained in this thesis are reflected onto the morphology of the Clariidae and discussed. Some hypotheses with respect to convergent evolution in elongate species are discussed. Finally, the use of vertebral morphology, as well as morphological studies in general, is discussed.

## CHAPTER VIII: SUMMARY AND SAMENVATTING

A summary in English and Dutch is provided.



Material - Methods



### III.1. MATERIAL EXAMINED

A total of 958 specimens, representing 17 species, have been studied in this dissertation. Museum material was examined as well as commercially obtained specimens and specimens that were personally collected during samplings. In order to give a comprehensible overview of the species and specimens that were used, this section is subdivided according to the higher taxonomic level the species belongs to.

#### ELOPOMORPHA

For the morphological study of the elopomorph Anguilliformes, six species were used. The individual data of the specimens used to define the morphology of *Moringua edwardsi* (IV.1), *Heteroconger hassi* and *H longissimus* (IV.2), and *Pisodonophis boro* (IV.3) are listed in Table III.1- 1A.

The specimens of *M. edwardsi* and *H. longissimus* were obtained from the Museum of Comparative Zoology (Cambridge) and the Smithsonian National Museum of Natural History (Washington) respectively.

The specimens of *H. hassi*, deposited in the Zoological Museum of the Ghent University, and those of *P. boro* were commercially obtained (Poisson d'Or - Moeskroen).

Three specimens of *Conger conger* were commercially obtained, and two additional specimens, housed in the Zoological Museum of the Ghent University, were examined.

Additional information, such as total length, method (and staining) used to study the specimens and the chapter reference where the results are presented, is listed in Table III.1- 1A.

## Elopomorpha

species	Source	collection nr	TL	Method	staining	chapter
<i>Moringua edwardsi</i>	MCZ	MCZ 44686	219	CT-scanning	—	IV.1
<i>Moringua edwardsi</i>	MCZ	MCZ 44686	200	Clearing	AB+AR	IV.1
<i>Moringua edwardsi</i>	MCZ	MCZ 44686	172	Serial sections (2µm)	T	IV.1
<i>Heteroconger longissimus</i>	USMN	USNM 316037	225	Clearing	AB+AR	IV.2
<i>Heteroconger longissimus</i>	USMN	USNM 316037	226	Serial sections (2µm)	T	IV.2
<i>Heteroconger longissimus</i>	USMN	USNM 316037	240	Serial sections (2µm)	T	IV.2
<i>Heteroconger longissimus</i>	USMN	USNM 316037	268	CT-scanning	—	IV.2
<i>Heteroconger longissimus</i>	USMN	USNM 316037	268	Dissection	F	IV.2
<i>Heteroconger hassi</i>	UGMD	UGMD 175374	278	Clearing	AB+AR	IV.2
<i>Heteroconger hassi</i>	UGMD	UGMD 175374	237	Serial sections (2µm)	T	IV.2
<i>Heteroconger hassi</i>	UGMD	UGMD 175374	218	Clearing	AB+AR	IV.2
<i>Heteroconger hassi</i>	UGMD	UGMD 175374	226	Clearing	AB+AR	IV.2
<i>Heteroconger hassi</i>	UGMD	UGMD 175374	286	Serial sections (2µm)	T	IV.2
<i>Heteroconger hassi</i>	commercial trade		NA	observation	—	IV.2
<i>Heteroconger hassi</i>	commercial trade		NA	observation	—	IV.2
<i>Heteroconger hassi</i>	commercial trade		NA	observation	—	IV.2
<i>Heteroconger hassi</i>	commercial trade		NA	observation	—	IV.2
<i>Heteroconger hassi</i>	commercial trade		NA	observation	—	IV.2
<i>Pisodonophis boro</i>	commercial trade		209	Dissection + clearing	F+AR	IV.3
<i>Pisodonophis boro</i>	commercial trade		107	Serial sections (2µm)	T	IV.3
<i>Pisodonophis boro</i>	commercial trade		85	Serial sections (2µm)	T	IV.3
<i>Pisodonophis boro</i>	commercial trade		126	Dissection + clearing	F+AR	IV.3
<i>Pisodonophis boro</i>	commercial trade		187	Biometry	—	IV.3
<i>Pisodonophis boro</i>	commercial trade		309	Biometry	—	IV.3
<i>Pisodonophis boro</i>	commercial trade		198	Biometry	—	IV.3
<i>Pisodonophis boro</i>	commercial trade		259	Biometry	—	IV.3
<i>Conger conger</i>	commercial trade		1330	Dissection + clearing	F+AR	IV.4.3 + IV.4.4
<i>Conger conger</i>	commercial trade		1644	Dissection + clearing	F+AR	IV.4.3 + IV.4.4
<i>Conger conger</i>	commercial trade		1332	Dissection + clearing	F+AR	IV.4.3 + IV.4.4
<i>Conger conger</i>	UGMD	UGMD 53065	-	dry skeleton	—	IV.4.3 + IV.4.4
<i>Conger conger</i>	UGMD	UGMD 53089	523	Biometry	—	IV.4.3 + IV.4.4

**Table III.1- 1A:** Specimens used in IV.1, IV.2, IV.3, IV.4.3 and IV.4.4 as elopomorph representatives. AB, Alcian Blue; AR, Alizarine Red; F, iodine fibre staining; NA, not applicable as these specimens are still living; T, Toluidine Blue; TL, total length in mm.

For the biometric study of *Anguilla anguilla* (IV.4.1), two large sets of samples were used.

### 1) Sample Scheldt-Lippensbroek

***Anguilla anguilla*** collected in Scheldt-Lippensbroek used for the biometric study in IV.4.1

date of sampling	fyke code	n
25 04 2006	LB1	3
	LB2	7
	LB3	4
	S1	14
23 05 2006	LB1	1
	LB2	10
	LB3	13
	LB4	8
	S1	3
22 08 2006	S2	3
	LB2	8
	LB4	2
18 10 2006	S1	20
	LB2	5
	LB3	1
	S1	13
	S2	4

**Table III.1- 1B:** List of specimens of *Anguilla anguilla*, collected in the Scheldt-Lippensbroek. These specimens are used for biometry in IV.4.1. Four fyke nets were placed in the Lippensbroek (LB1-LB4) and tow in the scheldt (S1-S2). The amount of eels captured in each fyke is indicated

(LB1-LB4) and the Scheldt (S1-S2). Four samples of yellow eels were collected in the

The Lippensbroek is a controlled inundation area with reduced tidal movements, connected to the Scheldt (Fig. III.1- 1). The sampling is part of the “Harmonised River Basin Strategies for the North Sea” (HARBASINS) project (2005-2008) and partially within subproject 5 (fish communities) of the MODELKEY project, models for assessing and forecasting the impact of environmental key pollutants on marine and freshwater ecosystems and biodiversity.

*Anguilla anguilla* specimens were captured by several fyke nets from the Lippensbroek



months April, May, August and October 2006 (Table III.1- 1B). Each sample consisted of approximately 30 specimens. The specimens ( $n=121$ ) were collected alive, labelled and their total length (TL) was immediately measured with a ruler to the nearest 0.1 cm and they were weighed ( $W_e$ ) to the nearest 0.1g. All eels were killed by an overdose of anaesthetic (MS 222, Sigma Chemical Co), fixed in 10% formalin and preserved in 70% ethanol.

## 2) Sample INBO

This study (IV.4.1) also includes a biometric study of the head of 725 eels obtained from the INBO-eel pollutant monitoring network (see GOEMANS AND BELPAIRE, 2004). These specimens were collected from 65 different sample sites across Belgian waters between 2001 and 2005. Table III.1- 1C gives an overview of the total amount of eels collected in different waters across Belgium.

<i>Anguilla anguilla</i>					
INBO sample used for the biometric study in chapter IV.4.1					
Source	collection number	n	Source	collection number	n
Palingwekerij	010420 HEL	5	Schelde	020606 SCH4A	10
Zevenbronnen	010511 ZBR	3	Kanaal van Leuven naar de Dijle	020613 KLD2A	7
Ieperkanaal	010514 IK2	5	Dokken	020614 BEV	2
Weerderlaak	010516 WLL	4	Kanaal van Leuven naar de Dijle	020617 KLD	19
Zwart water	010517 ZWL	5	Oude Maas	020902 OMS	10
Witbeek	010606 WIK	2	Ieperkanaal	020909 IK	30
Itterbeek	010607 IB1	5	Oude Maas	020916 OMD	9
Congovaart + lagune	010810 COM	21	klein Zuunbekken	020924 KZ	10
Kanaal Nieuwpoort-Plassendale	010919 NP1A	5	Kanaal Bocholt-Herentals	021007 KBH1	19
Kanaal Nieuwpoort-Plassendale	010920 NP2	5	Kanaal Bocholt-Herentals	021008 KBH1C	10
Rotselaar meer	010928 RM1	4	Kanaal Bocholt-Herentals	021009 KBH	12
Waterwinningsput Kluisen	011001 SK	2	Kanaal Bocholt-Herentals	021010 KBH3	4
Oude Schelde Zomeput	011018 OSZ	5	Willebroekse vaart	021014 WBV6	5
Kanaal van Leuven naar de Dijle	011023 KLD1A	5	Willebroekse vaart	021017 WBV8	10
Kanaal van Leuven naar de Dijle	011023 KLD2	5	Oude Schelde	021023 OSK	9
Bergeleput	011105 BPG	10	Handzamevaart	021104 HV2	10
Kanaal van Leuven naar de Dijle	020207 KLD4	1	Handzamevaart	021104 HVX	7
Jeker	020311 JEK	2	Motte	030304 MOT	2
Zanderbeek	020314 ZB	1	Grote Neet	030318 GN4	6
Langelede	020318 LLS	6	Grote Nete	030319 GN	17
Zuidlede	020321 ZLO	1	Kleine Nete	030320 KN2	10
Dender	020327 DE3	22	Netekanaal	030320 NKE	10
Asdonkbeek	020402 ASA	1	Boerekreek	030325 BRK	8
Balengracht	020402 BGX	2	Hollandersgatkreek	030325 HGK	5
Mol Neet	020403 MNB	6	Oostpolderkreek	030325 OPK	5
Voorste Neet	020403 VNX	2	Roesselarekreek	030327 RLK	4
Kleine (Witte) Nete	020404 KN1	9	Demer	030409 DEM 3A	3
Wamp	020404 WMX	7	Dijle	030506 DIJ1	7
Aabeek	020424 AA	1	Leerzevaart	030514 LEV	5
Poperingevaart	020506 PV1	3	Slijkvaart	030515 PDV	8
Kemmelbeek	020507 KBR	3		0306 KAL	7
Martjevaart	020508 MVX	2	Blankenbergse Vaart	030604 BBV	10
Zaadgracht	020508 ZGL	2	Noord-Ede	030604 NEK	10
Grensmaas	020513 MA3	27	Darse	030607 DA	4
Grensmaas	020514 MA	23	Grote Beverdijk	030616 GB1	1
Grensmaas	020515 MA	29	Leie	030623 L	10
Groot Schijn	020523 GS	10	Leie	030623 LE1	5
Kleinbeek	020523 KLB	5	Leie	030623 LE6	8
Kanaal van Leuven naar de Dijle	020523 KLD4	10	Demer	030902 DEM2	3
Driesbeek	020528 DBU	1	Demer	030902 DEM6	2
Ede	020528 ED	5	Demer	030904 DEM	2
Ede	020528 ED2	4	Kanaal van Dessel naar Schoten	030915 KDS	51
Hertsbergebeek	020529 HBN	1	Kanaal van Dessel naar Schoten	030917 KDS6	30
Schelde	020604 SCH	18	Kleine Neet	030925 KN2C	10
Geuzenbeek	020605 GBO	4			

**Table III.1- 1C:** List of specimens of *Anguilla anguilla*, collected from the INBO- eel pollutant monitoring network. These specimens are used for biometry in IV.4.1.

For the geometric morphometric study of *Anguilla anguilla* (IV.4.1) a total of 64 specimens were used. These specimens were obtained from the INBO-eel pollutant monitoring network (see GOEMANS AND BELPAIRE, 2004). Table III.1- 1D lists where and how many specimens were caught, the sample code, and eel identification number.

<b><i>Anguilla anguilla</i></b>		<b>morphometric study in chapter VI.4.1</b>	
<b>Source</b>	<b>collection number</b>	<b>n</b>	<b>specimen</b>
Congovaart + lagune	010810 COM	2	P1-P12
Rotselaar meer	010928 RM1	1	P1
Waterwinningsput Kluizen	011001 SK	1	P2
Oude Schelde Zonneput	011018 OSZ	3	P1-P4-P7
Kanaal van Leuven naar de Dijle	011023 KLD1A	1	P1
Langelede	020318 LLS	3	P2-P4-P6
Dender	020327 DE3A	1	P1
Dender	020328 DE3C	2	P5-P10
Mol Neet	020403 MNB	1	P2
Kleine (Witte) Nete	020404 KN1	1	P9
Grensmaas	020513 MA3E	1	P9
Grensmaas	020514 MA3A	1	P10
Grensmaas	020515 MA2	1	P8
Ede	020528 ED2	1	P4
Hertsbergebeek	020529 HBN	1	P1
Schelde	020604 SCH3A	2	P2-P5
Schelde	020606 SCH4A	1	P1
Dokken	020614 BEV1	1	P2
Kanaal van Leuven naar de Dijle	020617 KLD1A	3	P1-P3-P4
Oude Maas	020902 OMS	2	P1-P10
Kanaal Bocholt-Herentals	021007 KBH1	3	P1-P2-P3
Kanaal Bocholt-Herentals	021008 KBH1C	1	P5
Kanaal Bocholt-Herentals	021009 KBH2	2	P1-P2
Kanaal Bocholt-Herentals	021010 KBH3	1	P1
Grote Neet	030318 GN4	3	P4-P5-P6
Grote Nete	030319 GN2A	1	P9
	0306 KAL	7	P1-P2-P3-P4-P5-P6-P7
Leie	030623 L	4	P1-P4-P7-P10
Leie	030623 LE1	2	P2-P5
Leie	030623 LE6	2	P6-P8
Demer	030902 DEM2	1	P1
Demer	030902 DEM6	1	P1
Kanaal van Dessel naar Schoten	030915 KDS2	1	P2
Kanaal van Dessel naar Schoten	030915 KDS4	1	P1
Kanaal van Dessel naar Schoten	030915 KDS5	1	P3
Kanaal van Dessel naar Schoten	030915 KDS7A	1	P4
Kleine Neet	030925 KN2C	2	P3-P8

**Table III.1- 1D:** List of specimens of *Anguilla anguilla*, collected from the INBO- eel pollutant monitoring network. These specimens are used for morphometry in IV.4.1.

To study the morphology of *Anguilla anguilla*, 39 specimens are used of which 27 were commercially obtained and 12 were collected in the Scheldt-Lippensbroek. Additional information (collection number, total length, method (and staining) and chapter reference) is listed in Table III.1- 1E.

<i>Anguilla anguilla</i>						
specimens used for the morphological study in chapter VI.4.2						
Source	collection nr	TL	Method	staining	chapter	
commercial trade - wild catch	03 AA BH 1	541	Dissection + clearing	F+AR	IV.4.2	
commercial trade - wild catch	03 AA BH 2	522	Dissection + clearing	F+AR	IV.4.2	
commercial trade - wild catch	03 AA BH 3	561	Dissection + clearing	F+AR	IV.4.2	
commercial trade - wild catch	03 AA BH 4	556	Dissection + clearing	F+AR	IV.4.2	
commercial trade - wild catch	03 AA BH 5	—	Dissection + clearing	F+AR	IV.4.2	
commercial trade - nursery	06 AA NH 1	438	Dissection + clearing	F+AR	IV.4.2	
commercial trade - nursery	06 AA NH 2	429	Dissection + clearing	F+AR	IV.4.2	
commercial trade - nursery	06 AA NH 3	358	Dissection + clearing	F+AR	IV.4.2	
commercial trade - nursery	06 AA NH 4	365	Dissection + clearing	F+AR	IV.4.2	
commercial trade - nursery	06 AA NH 5	454	Dissection + clearing	F+AR	IV.4.2	
commercial trade - nursery	06 AA NH 6	352	Dissection + clearing	F+AR	IV.4.2	
commercial trade - nursery	06 AA NH 7	439	Dissection + clearing	F+AR	IV.4.2	
commercial trade - nursery	06 AA NH 8	390	Dissection + clearing	F+AR	IV.4.2	
commercial trade - nursery	06 AA NH 9	414	Dissection + clearing	F+AR	IV.4.2	
commercial trade - nursery	06 AA NH 10	497	Dissection + clearing	F+AR	IV.4.2	
commercial trade - nursery	06 AA NH 11	438	Dissection + clearing	F+AR	IV.4.2	
commercial trade - nursery	06 AA NH 12	400	Dissection + clearing	F+AR	IV.4.2 + IV.4.4	
commercial trade - nursery	06 AA NH 13	410	Dissection + clearing	F+AR	IV.4.2 + IV.4.4	
commercial trade - nursery	06 AA NH 14	432	Dissection + clearing	F+AR	IV.4.2 + IV.4.4	
commercial trade - nursery	06 AA NH 15	490	Dissection + clearing	F+AR	IV.4.2 + IV.4.4	
commercial trade - wild catch	06 AA BH 1	498	Dissection + clearing	F+AR	IV.4.2 + IV.4.4	
commercial trade - wild catch	06 AA BH 3	555	Dissection + clearing	F+AR	IV.4.2 + IV.4.4	
commercial trade - wild catch	06 AA BH 4	514	Dissection + clearing	F+AR	IV.4.2	
commercial trade - wild catch	06 AA BH 5	495	Dissection + clearing	F+AR	IV.4.2	
commercial trade - wild catch	06 AA BH 6	541	Dissection + clearing	F+AR	IV.4.2	
commercial trade - wild catch	06 AA BH 9	503	Dissection + clearing	F+AR	IV.4.2	
commercial trade - wild catch	06 AA BH 10	517	Dissection + clearing	F+AR	IV.4.2	
Lippensbroek - Scheldt	230506 LB2 P10	315	Biometry + Dissection + weight	F	IV.4.2	
Lippensbroek - Scheldt	220806 LB2 P2	341	Biometry + Dissection + weight	F	IV.4.2	
Lippensbroek - Scheldt	220806 LB2 P4	410	Biometry + Dissection + weight	F	IV.4.2	
Lippensbroek - Scheldt	220806 LB2 P6	415	Biometry + Dissection + weight	F	IV.4.2	
Lippensbroek - Scheldt	220806 LB2 P8	405	Biometry + Dissection + weight	F	IV.4.2	
Lippensbroek - Scheldt	220806 LB4 P1	560	Biometry + Dissection + weight	F	IV.4.2	
Lippensbroek - Scheldt	220806 S1 P10	347	Biometry + Dissection + weight	F	IV.4.2	
Lippensbroek - Scheldt	220806 S1 P14	406	Biometry + Dissection + weight	F	IV.4.2	
Lippensbroek - Scheldt	220806 S1 P15	447	Biometry + Dissection + weight	F	IV.4.2	
Lippensbroek - Scheldt	220806 S1 P18	414	Biometry + Dissection + weight	F	IV.4.2	
Lippensbroek - Scheldt	220806 S1 P3	671	Biometry + Dissection + weight	F	IV.4.2	
Lippensbroek - Scheldt	220806 S1 P6	574	Biometry + Dissection + weight	F	IV.4.2	

**Table III.1- 1E:** List of specimens of *Anguilla anguilla*, used for the morphological study in IV.4.2 and IV.4.4. TL, total length in mm; AR, Alizarine Red; F, iodine fibre staining

## OSTARIOPHYSI

For the study of ostariophysan morphology (V), 33 specimens belonging to six species, *Clarias gariepinus*, *Platyallabes tihoni*, *Platyclarias machadoi*, *Gymnallabes typus*, *Channallabes apus* and *Dolichallabes microphthalmus* were examined. All of these, except for *Clarias gariepinus*, were housed in the ‘Musée Royal de l’Afrique Centrale / Koninklijk Museum voor Midden Afrika’ (Tervuren). Additional information (collection number, total length, method (+ staining) and chapter reference) is listed (Table III.1- 2).

Three specimens of *Clarias gariepinus* were examined, two of which were cultivated at the ‘Laboratory of Aquatic Ecology’ (KU Leuven) and one at the research group ‘Evolutionary Morphology of Vertebrates’ (Ghent University).

A sample of 25 specimens of *Channallabes apus* was examined (Table III.1-2). These specimens were collected in Gabon, at three different sample sites during an expedition by Adriaens D, Devaere S and Herrel A in 1999 and 2000 (Fig. III.1- 2). This collection was housed in Musée Royal de l’Afrique Centrale / Koninklijk Museum voor Midden Afrika (Tervuren). Nine specimens were collected in northern Gabon (Oyem), six in eastern Gabon (Makokou) and ten in southern Gabon (Congo-Brazzaville and Franceville).

<b>Ostariophysys</b>						
<b>species</b>	<b>Source</b>	<b>collection number</b>	<b>TL</b>	<b>Method</b>	<b>staining</b>	<b>chapter</b>
<b>Northern Gabon</b>						
<i>Channallabes apus</i>	MRAC/KMMA	MRAC A4-31-P-19 (C-01)	335	Clearing	AB+AR	V.1 - V.2
<i>Channallabes apus</i>	MRAC/KMMA	MRAC A4-31-P-20 (D-01)	312	Clearing	AB+AR	V.1 - V.2
<i>Channallabes apus</i>	MRAC/KMMA	MRAC A4-31-P-22-23 (F-01)	323	Clearing	AB+AR	V.1 - V.2
<i>Channallabes apus</i>	MRAC/KMMA	MRAC A4-31-P-22-23 (F-02)	445	Clearing	AB+AR	V.1 - V.2
<i>Channallabes apus</i>	MRAC/KMMA	MRAC A4-31-P-24 (G-01)	370	Clearing	AB+AR	V.1 - V.2
<i>Channallabes apus</i>	MRAC/KMMA	MRAC A4-31-P-26 (I-01)	324	Clearing	AB+AR	V.1 - V.2
<i>Channallabes apus</i>	MRAC/KMMA	MRAC A4-31-P-33-35 (J-02)	349	Clearing	AB+AR	V.1 - V.2
<i>Channallabes apus</i>	MRAC/KMMA	MRAC A4-31-P-33-35 (J-03)	411	Clearing	AB+AR	V.1 - V.2
<i>Channallabes apus</i>	MRAC/KMMA	MRAC A4-31-P-27-28 (K-02)	312	Clearing	AB+AR	V.1 - V.2
<b>Eastern Gabon</b>						
<i>Channallabes apus</i>	MRAC/KMMA	MRAC A4-31-P-106-131 (w-01)	283	Clearing	AB+AR	V.1 - V.2
<i>Channallabes apus</i>	MRAC/KMMA	MRAC A4-31-P-106-131 (w-05)	290	Clearing	AB+AR	V.1 - V.2
<i>Channallabes apus</i>	MRAC/KMMA	MRAC A4-31-P-106-131 (w-09)	213	Clearing	AB+AR	V.1 - V.2
<i>Channallabes apus</i>	MRAC/KMMA	MRAC A4-31-P-106-131 (w-14)	170	Clearing	AB+AR	V.1 - V.2
<i>Channallabes apus</i>	MRAC/KMMA	MRAC A4-31-P-106-131 (w-17)	185	Clearing	AB+AR	V.1 - V.2
<i>Channallabes apus</i>	MRAC/KMMA	MRAC A4-31-P-106-131 (w-21)	206	Clearing	AB+AR	V.1 - V.2
<b>Southern Gabon</b>						
<i>Channallabes apus</i>	MRAC/KMMA	MRAC A4-31-P-171-183 (AB1)		Clearing	AB+AR	V.1 - V.2
<i>Channallabes apus</i>	MRAC/KMMA	MRAC A4-31-P-171-183 (AB5)	133	Clearing	AB+AR	V.1 - V.2
<i>Channallabes apus</i>	MRAC/KMMA	MRAC A4-31-P-171-183 (AB8)	220	Clearing	AB+AR	V.1 - V.2
<i>Channallabes apus</i>	MRAC/KMMA	MRAC A4-31-P-171-183 (AB11)	180	Clearing	AB+AR	V.1 - V.2
<i>Channallabes apus</i>	MRAC/KMMA	MRAC A4-31-P-171-183 (AB12)	148	Clearing	AB+AR	V.1 - V.2
<i>Channallabes apus</i>	MRAC/KMMA	MRAC A4-31-P-165-169 (Z1)	145	Clearing	AB+AR	V.1 - V.2
<i>Channallabes apus</i>	MRAC/KMMA	MRAC A4-31-P-165-169 (Z4)	120	Clearing	AB+AR	V.1 - V.2
<i>Channallabes apus</i>	MRAC/KMMA	MRAC A4-31-P-184-185 (Ca 7)	186	Dissection	F	V.3
<i>Channallabes apus</i>	MRAC/KMMA	MRAC A4-31-P-184-185 (Ca 8)	138	Dissection	F	V.3
<i>Channallabes apus</i>	MRAC/KMMA	MRAC A4-31-P-184-185 (Ca 11)	204	Dissection	F	V.3
<i>Clarias gariepinus</i>	cultivated at KUL AE	KULCg 1	165	Dissection	F	V.3
<i>Clarias gariepinus</i>	cultivated at KUL AE	KULCg 2	250	Dissection	F	V.3
<i>Clarias gariepinus</i>	cultivated at Ugent	041098n4	37	Clearing	AB+AR	V.1 - V.2
<i>Platyallabes tihoni</i>	MRAC/KMMA	MRAC 73-23-P-5912	165	Clearing	AB+AR	V.1 - V.2
<i>Platyclarias machadoi</i>	MRAC/KMMA	MRAC 78-6-P-1348-364	132	Clearing	AB+AR	V.1 - V.2
<i>Gymnallabes typus</i>	MRAC/KMMA	MRAC 75-84-P-683-693	229	Clearing	AB+AR	V.1 - V.2
<i>Channallabes apus</i>	MRAC/KMMA	MRAC 88-25-P-2192-227	299	Clearing	AB+AR	V.1 - V.2
<i>Dolichallabes microphthalmus</i>	MRAC/KMMA	MRAC 78808-810	113	Clearing	AB+AR	V.1 - V.2

**Table III.1- 2:** List of ostariophysian specimens (Clariidae) used in V.1, V.2 and V.3. AB, Alcian Blue; AR, Alizarine Red; F, iodine fibre staining; T, Toluidine Blue; TL, total length in mm.

## ACANTHOPTERYGII

The mastacembelid morphology (VI.1) was examined based on three species and ten specimens (Table III.1- 3). *Mastacembelus brichardi* and *M. marcheii* were obtained from the ‘Musée Royal de l’Afrique Centrale / Koninklijk Museum voor Midden Afrika’ (Tervuren), whereas *M. mastacembelus* was obtained from the Natural History Museum of Iran.

The trichiurid morphology (VI.2) was studied using eleven specimens representing two species (Table III.1- 3). *Trichiurus lepturus* was obtained from the ‘Smithsonian National Museum of Natural History’ (Washington), whereas the *Aphanopus carbo*

specimens were commercially obtained. Table III.1- 3 lists additional information such as collection number, total length, method (+ staining) and chapter reference.

#### Acanthopterygii

species	Source	collection number	TL	Method	staining	chapter
<i>Mastacembelus brichardi</i>	MRAC/KMMA	RG 96-35-P1-29	158	Dissection	F	VI.1
<i>Mastacembelus brichardi</i>	MRAC/KMMA	RG 96-35-P1-29	114	Dissection + clearing	F+AR	VI.1
<i>Mastacembelus brichardi</i>	MRAC/KMMA	RG 96-35-P1-29	121	Dissection + clearing	F+AR	VI.1
<i>Mastacembelus marcheii</i>	MRAC/KMMA	RG-98-29-P-6-9	210	Dissection + clearing	F+AR	VI.1
<i>Mastacembelus marcheii</i>	MRAC/KMMA	RG-98-29-P-6-9	280	Dissection + clearing	F+AR	VI.1
<i>Mastacembelus marcheii</i>	MRAC/KMMA	RG-98-29-P-6-9	323	Dissection + clearing	F+AR	VI.1
<i>Mastacembelus mastacembelus</i>	INHM	IR-068	404	Dissection + clearing	F+AR	VI.1
<i>Mastacembelus mastacembelus</i>	INHM	IR-012	292	Dissection + clearing	F+AR	VI.1
<i>Mastacembelus mastacembelus</i>	INHM	IR-110	448	Dissection + clearing	F+AR	VI.1
<i>Mastacembelus mastacembelus</i>	INHM	IR-003	224	Dissection + clearing	F+AR	VI.1
<i>Aphanopus carbo</i>	commercial trade		111	Dissection + clearing	F+AR	VI.2
<i>Aphanopus carbo</i>	commercial trade		117	Dissection + clearing	F+AR	VI.2
<i>Aphanopus carbo</i>	commercial trade		121	Dissection + clearing	F+AR	VI.2
<i>Aphanopus carbo</i>	commercial trade		118	Dissection + clearing	F+AR	VI.2
<i>Aphanopus carbo</i>	commercial trade		125	Dissection + clearing	F+AR	VI.2
<i>Trichiurus lepturus</i>	MCZ	MCZ 58488	83	Dissection	F	VI.2
<i>Trichiurus lepturus</i>	MCZ	MCZ 58488	95	Dissection	F	VI.2
<i>Trichiurus lepturus</i>	MCZ	MCZ 58488	101	Dissection	F	VI.2
<i>Trichiurus lepturus</i>	USMN	USMN 369981-168	99	Clearing	AB+AR	VI.2
<i>Trichiurus lepturus</i>	USMN	USMN 369981-168	32	Clearing	AB+AR	VI.2
<i>Trichiurus lepturus</i>	USMN	USMN 369981-168	35	Clearing	AB+AR	VI.2

**Table III.1- 3:** List of actinopterygian specimens (Mastacembelidae and Trichiuridae) used in VI.1 and VI.2. AB, Alcian Blue; AR, Alizarine Red; F, iodine fibre staining; T, Toluidine Blue; TL, total length in mm.

As the examined species are housed in several institutions all over the world, a list of the museum and institution abbreviations (LEVINTON ET AL, 1985), used in this work is given below.

- INHM:** Natural History Museum of Iran, 9 Qaem Maqam Farahani Ave, Teheran, Iran.
- KULeuven (AE):** Katholieke Universiteit Leuven - Laboratory of Aquatic Ecology, Charles Deberiotstraat 32, B-3000 Leuven, Belgium
- MCZ:** Harvard University, Museum of Comparative Zoology, Cambridge, Massachusetts 02138, USA
- MRAC/KMMA:** Musée Royal de l'Afrique Centrale / Koninklijk Museum voor Midden Afrika, Afdeling vertebraten, Laboratorium Ichthyologie, Leuvensesteenweg 13, B-3080 Tervuren, Belgium
- UGent (EMV):** Ghent University - Laboratory of Evolutionary Morphology of Vertebrates, K.L. Ledeganckstraat 35, B-9000 Ghent, Belgium.
- UGMD:** Zoological Museum of the Ghent University, K.L. Ledeganckstraat 35, B-9000 Ghent, Belgium.
- USMN:** Smithsonian National Museum of Natural History, 10th Street & Constitution Ave. NW, in Washington, D.C. 20560, USA

## III.2. METHODS

### III.2.1 PREPARATION OF SPECIMENS

#### ANAESTHESIA, SACRIFICE AND FIXATION

Specimens were anaesthetized in a 0.001% water solution MS 222 (ethyl 3-aminobenzoic acid methanesulfonate salt - Sigma Chemical Co) and subsequently sacrificed by an overdose MS 222. Procedure occurred in accordance with the Belgian law in the protection of laboratory animals (KB d.d. November 14<sup>th</sup>, 1993). Euthanized specimens were fixed using a 4% buffered formalin solution (at neutral pH). This widely used fixative was additionally injected in larger specimens to improve and allow steady fixation of deeper tissue as well. Using this fixative allowed us to apply the fixed specimens for serial sections and for clearing and staining.

### III.2.2 MORPHOLOGY

In order to study the detailed morphology of soft and hard tissue, different procedures were applied. The osteology was examined, using *in toto* cleared and stained material. Myological as well as osteological features were studied based on dissections. Additional information and detail of hard as well as soft tissue were gathered using serial sections. Furthermore these proved to be very useful for checking internal structures, ossifications, attachment of ligaments, distinction of muscle bundles, connection or fusion of bones etc.

#### IN TOTO CLEARING AND STAINING

The specimens were cleared and stained according to the protocol of HANKEN AND WASSERZUG (1981). Though, this protocol was slightly modified as the slowly active trypsin was replaced by the more aggressive potassium hydroxide (KOH), leading to equally good results (Table III.2- 1). In general, concentrations ranging between 1% and 3% were used though in large specimens concentrations up to 10% were applied. Alizarine red S (Sigma) and alcian blue 8GX (Sigma) allowed differential staining of bones and cartilage respectively. As the alcian blue 8GX had to be dissolved in ethanol and glacial acetic acid, decalcification of the bone was induced. Ossifications may be masked by this decalcification process as alizarine red S actually binds onto the calcified matrix of bone. For that reason some specimens were stained with alizarine red S alone.

Step	Solution/Action	Duration
Fixation	4% buffered formalin	Days to weeks
Washing	tap water	24h
Cartilage staining	Alcian Blue (8GX, Sigma): 10mg in 70ml alcohol (96%) + 30 ml acetic acid	6-8h
Dehydration	96-100% (two times alcohol renewal)	24h
Maceration	75% alcohol	2h
	50% alcohol	2h
	25% alcohol	2h
	Aqua dest (two times water renewal)	4h
Bleaching	3-10% H <sub>2</sub> O <sub>2</sub> in 0.5% KOH	1-2h
Washing	tap water	24h
Clearing	Trypsine solution: 1-4% KOH/trypsin (0.6g in 400ml 30% NaBO <sub>3</sub> )	24h-...
	OR KOH solution: 0.5%-4%	24h-...
Bone staining	Alizarine red (Sigma): 0.5% KOH in (0.1% alizarine red S in aqua dest)	12h
preservation	25% glycerine + 75% 0.5% KOH	24h
	50% glycerine + 50% 0.5% KOH	24h
	75% glycerine + 25% 0.5% KOH	24h
	100% glycerine	24h

**Table III.2- 1:** modified protocol of Hanken and Wasserzug (1981) for bone and cartilage staining in whole specimens.

## DISSECTIONS

For the study of both hard and soft tissue structures, dissections were performed. Visualization of muscle fibre arrangement, insertion sites and origin was enhanced by the use of a iodine solution (BOCK AND SHEAR, 1972). The examination of specimens was performed by means of an Olympus SZX 9- stereomicroscope, equipped with a camera lucida and a digital camera (Colorview 8). Valuable additional information or confirmation concerning muscular insertion and origin sites was obtained by subsequent treatment of the *in toto* clearing and staining protocol.

## SERIAL SECTIONS

Specimens were embedded in the plastic Technovit 7100 (Table III.2- 2). Sections with a thickness of 2 µm were cut using a Reichert-Jung Polycut microtome and subsequently mounted onto microscopic glass slides, stained with toluidine blue and covered. This procedure may induce some imperfections as the result of shrinking of external tissue (skin) during preparation or embedding or minor distortion can occur in the whole section by imperfect stretching. The examination of sections was performed by means of a Reichert-Jung Polyvar light microscope, equipped with a camera lucida and a digital camera (Colorview 8).

Step	Solution/Action	Duration
Vacuum fixation	4% buffered formalin	Days to weeks
Washing	tap water	8h
Decalcification	Decalc (Histolab)	36h
Washing	tap water	8h
Dehydratation	30% alcohol	12h
	50% alcohol	12h
	70% alcohol	12h
	96% alcohol (two times alcohol renewal)	12h
Embedding	Technovit 7100 solution A (Hereaus Kulzer)	min. 24h
	Technovit 7100 solution A renewal	min. 48h
	add Technovit 7100 solution Harder II	12h
	Place in deepfreeze	12h
Polymerization	Place at room temperature (check progress)	2h
	Place in oven (approx 40° C)	1h

Table III.2- 2: Technovit 7100 embedding protocol for serial sections.

### III.2.3 MORPHOMETRY

For the geometric morphometric analyses, shape variation (neurocrania - IV.4.1, precaudal and caudal vertebrae - V.1) was studied based on landmark configurations, representing the shapes from the respective structures (BOOKSTEIN, 1991). Digital images of neurocrania and vertebrae were used to define landmarks. These digital images were captured using a digital camera (Colorview 8, Soft Imaging System), mounted on a stereomicroscope (Olympus SZX 9) and taken with Analysis Docu (Soft Imaging System GmbH, version 3.0).

#### A) LANDMARKS USED TO DEFINE NEUROCRANIAL SHAPE VARIATION WITHIN *ANGUILLA ANGUILLA* (IV.4.1)

Ten landmarks were defined to describe the shape of the neurocranium in a lateral view (Fig. III.2- 1A).

- LL1: posterior margin of the tooth row on the ventral surface of the premaxillo-ethmovomerine complex;
- LL2: anterior tip of the premaxillo-ethmovomerine complex;
- LL3: anterior tip of the pterotic;
- LL4: rostral tip of sphenotic process;
- LL5: dorso-caudal process of epiotic;
- LL6: dorso-caudal process of pterotic;
- LL7: ventro-caudal tip of basioccipital;
- LL8: posterior tip of orbit;



- LL9: dorso-caudal tip of orbit;
- LL10: anterior tip of orbit.

Twenty-four landmarks were defined to describe the shape of the neurocranium in a dorsal view (Fig. III.2- 1B):

- LD1: rostral tip of the premaxillo-ethmovomerine complex;
- LD2-24: lateral tips of rhombus-like anterior extension of the premaxillo-ethmovomerine complex;
- LD3-23: caudal points of the rhombus-like extension;
- LD4-22: rostral tips of the frontal arches;
- LD5-21: rostral tips of the pterotics;
- LD6-20 sutures between pterotic and sphenotic in front of sphenotic processes;
- LD7-19: inclination points of the concave side of the sphenotic processes;
- LD8-18: rostral tips of sphenotic processes;
- LD9-17: lateral points of the convex side of the sphenotic processes;
- LD10-16: sutures between pterotic and sphenotic behind sphenotic processes;
- LD11-15: caudal tips of pterotic processes;
- LD12-14: caudal tips of epiotic processes;
- LD13: caudal tip of supraoccipital.

#### B) LANDMARKS USED TO DEFINE VERTEBRAL SHAPE VARIATION WITHIN *CHANNALLABES APUS*

##### (V.1)

Nine landmarks (LPL) were defined to describe the shape of the precaudal vertebrae in a lateral view (Fig. III.2- 2A).

- LPL 1: tip of the neural spine;
- LPL 2: posterior base of the neural arch;
- LPL 3: tip of the processus postneuralis;
- LPL 4: posterodorsal margin of the vertebral centrum;
- LPL 5: posteroventral margin of the vertebral centrum;
- LPL 6: tip of the parapophyses;
- LPL 7: anterodorsal margin of the vertebral centrum;
- LPL 8: anteroventral margin of the vertebral centrum;
- LPL 9: tip of the processus praeneuralis.

Ten landmarks (LPC) were defined to describe the shape of the precaudal vertebrae in a caudal view (Fig. III.2- 2B).

- LPC 1: tip of the left parapophysis;
- LPC 2: left margin of the vertebral centrum;
- LPC 3: tip of the left processus postneuralis;
- LPC 4: tip of the neural spine;
- LPC 5: tip of the right processus postneuralis;
- LPC 6: dorsal margin of the vertebral centrum;
- LPC 7: right margin of the vertebral centrum;
- LPC 8: tip of the right parapophysis;
- LPC 9: ventral margin of the vertebral centrum;
- LPC 10: central point of the vertebral centrum;

Fourteen landmarks (LCL) were defined to describe the shape of the caudal vertebrae in lateral view (Fig. III.2- 2C).

- LCL 1: tip of the haemal spine;
- LCL 2: posterior base of the haemal arch;
- LCL 3: tip of the processus posthaemalis;
- LCL 4: postero-ventral margin of the vertebral centrum;
- LCL 5: postero-dorsal margin of the vertebral centrum;
- LCL 6: tip of the processus postneuralis;
- LCL 7: anterior base of the processus postneuralis;
- LCL 8: posterior base of the neural arch;
- LCL 9: tip of the neural spine;
- LCL 10: posterior base of the processus praeneuralis;
- LCL 11: tip of the processus praeneuralis;
- LCL 12: antero-dorsal margin of the vertebral centrum;
- LCL 13: antero-ventral margin of the vertebral centrum;
- LCL 14: tip of the processus praehaemalis.

For the caudal vertebrae in caudal view eleven landmarks (LCC) were defined (Fig. III.2- 2V).

- LCC 1: tip of the haemal spine;
- LCC 2: tip of the right processus praehaemalis;
- LCC 3: right margin of the vertebral centrum;

- LCC 4: tip of the right processus praeneuralis;
- LCC 5: tip of the neural spine;
- LCC 6: tip of the left processus praeneuralis;
- LCC 7: dorsal margin of the vertebral centrum;
- LCC 8: left margin of the vertebral centrum;
- LCC 9: tip of the left processus praehaemalis;
- LCC 10: ventral margin of the vertebral centrum;
- LCC 11: centrum of the vertebral centrum.

In some specimens it was hard to define the correct location of the landmarks because of the presence of soft tissue. These vertebrae are consequently not included in the analysis in order to decrease inaccuracies. This explains the variable number of vertebrae in the geometric morphometric analyses (e.g. V.1, Fig. V.1- 7, 8, the eastern population counted 8 specimens in the analysis of the lateral view of the caudal vertebrae, whereas the eastern populations counted 5 specimens in the analysis of the caudal view of the caudal vertebrae).

#### C) THIN PLATE SPLINE (IV.4.1 AND V.1)

X and Y-coordinates for each landmark were digitized using TPS-DIG (ROHLF, 2001A). In order to evaluate the approximation of the distribution of the specimens in the Kendall shape space by that in the tangent space, the Procrustes distances between the specimens were compared to the corresponding Euclidean distance using TPS-SMALL (ROHLF, 1996; 1998). The relationship between shape variation and an independent variable (e.g. V.1, degree of anguilliformity) was examined using TPS-REGR (ROHLF, 2000).

The shape of both the precaudal and caudal vertebrae in caudal view is symmetrical. To avoid duplication of information and to avoid asymmetry noise, the landmark coordinates of both sides were averaged.

To explore patterns in shape variation, a relative warp analysis was conducted. Landmark configurations were aligned, translated, rotated and scaled to unit centroid size by applying Generalized Least-Squares (GLS) superimposition, using TPS-RELW (ROHLF AND SLICE, 1990). Partial and relative warp scores, calculated by TPS-RELW were used as descriptors for the variation in shape at different scales of shape variation. Relative warp scores actually represent principle component scores of the partial warp scores, with the relative warps being analogous to principle components (BOOKSTEIN, 1991; ROHLF, 1993; 2001B).

To investigate whether the different populations showed different patterns in shape variation, a backward stepwise Discriminant Function Analysis (DFA) (Statistica 5.5, Statosoft, Inc.) was performed using the weight matrix of partial warp scores (IV.4.1).

Visualization of the landmark plots and deformations grids were generated using TPS-RELW (BOOKSTEIN, 1991; ROHLF, 1993; 2001B). A multivariate test, included in the TPS-REGR program, examines how well variation in shape can be predicted using one or more independent variables (ROHLF, 2000).

## III.2.4 BIOMETRY

### A) CRANIAL MEASUREMENTS IN *ANGUILLA ANGUILLA* (IV.4.1)

#### SAMPLE SCHELDT-LIPPENSBROEK

A total of 19 head measurements were taken point to point using a digital calliper (Mausser) to the nearest 0.01 mm (Fig. III- 3). The absolute values for each length is given in Addendum III.2 - 1.

- 1 L Sn-E L: length from the snout tip to the rostral border of eye in lateral view;
- 2 L Sn-E D: length from the snout tip to the rostral border of eye in dorsal view;
- 3 L Sn-E c: length from the snout to the caudal border of the eye;
- 4 L E-nos r: length from rostral nostril to the rostral border of the eye;
- 5 L Sn-Pe: length from the tip of the snout to the pectoral girdle;
- 6 H H [E r]: height of the head at the level of the rostral border of the eye;
- 7 H H [E c]: height of the head at the level of the caudal border of the eye;
- 8 H H [nos r]: height of the head at the level of the rostral nostril;
- 9 H Pe; height of the body at the level of the pectoral girdle;
- 10 W H [E r]: width of the head at the level of the rostral border of the eye;
- 11 W H [E c]: width of the head at the level of the caudal border of the eye;
- 12 W H [nos r]: width of the head at the level of the rostral nostril;
- 13 W Pe: width of the body at the level of the pectoral girdle;
- 14 D: length of the lower jaw from the tip of the lower jaw to the mouth angle;
- 15 H E: height of the eye;
- 16 L E: length of the eye;
- 17 IOD r: interorbital distance at the level of the rostral border of the eye;
- 18 IOD c: interorbital distance at the level of the caudal border of the eye;
- 19 IOD m: interorbital distance at the centre of the eye.

## SAMPLE INBO

Measurements taken on 725 specimens from the INBO- eel pollutant monitoring network were restricted to We; SL; L Sn-Pe; IOD m; H H [E c]; W Pe. The absolute values for each length is given in Addendum III.2 -2.

### B) VERTEBRAL BIOMETRY IN *CHANNALLABES APUS* (V.1)

For the precaudal as well as the caudal vertebrae, different lengths have been defined (Fig. III.2- 4, 5). Digital images and point to point measurements of these images were taken with Analysis Docu (Soft Imaging System GmbH, version 3.0).

All biometric data were expressed in relation to standard length to be able to compare lengths between different specimens. Each length was plotted to standard length to analyze which length could be used to distinguish between different populations. Additionally these data were analyzed by a Principle Component Analysis (PCA). The absolute values of all measurements are given in Addendum III.2- 3 for the northern population (Oyem), in Addendum III.2- 4 for the southern population (Congo-Brazzaville and Franceville) and in Addendum III.2- 5 for the eastern population (Makokou). A Discriminant Function Analysis is subsequently performed.

### CHOICE OF VERTEBRAE

	<b>F</b>	<b>p</b>
L1	234.73	0.0000
L2	148.57	0.0000
L3	289.49	0.0000
L4	49.71	0.0004
L5	60.14	0.0002
L6	341.94	0.0000
L7	634.91	0.0000
L8	278.98	0.0000
L9	73.97	0.0001
L10	247.45	0.0000
L11	140.67	0.0000

**Table III.2- 3:** An Anova was performed on the biometric data of the successive caudal vertebrae in two *Channallabes apus* specimens. All measurements were significantly different.

In order to compare aspects of shape in the vertebral column of all specimens of *Channallabes apus* (V.1), two vertebrae were isolated: the fifth precaudal and the fortieth caudal vertebrae. The counting of the vertebrae began with the first vertebra not included in the weberian apparatus, which thus corresponds to the 6<sup>th</sup> vertebra. In order to allow a proper comparison of vertebral shapes, it is necessary that homologous vertebrae are used. As the total number of vertebrae varies among specimens, it is difficult to identify which vertebrae are homologous for all

specimens and the homology of these two vertebrae among different specimens can be questioned. Therefore, four successive vertebrae (39-42) of two specimens (w17, w21), were isolated and compared. Eleven measurements, L1 - L11 (Fig. III.2- 4B; Add III.2- 6) were taken on the lateral sides of the caudal vertebrae. An analysis of variance (Anova) was performed on the biometric data of these successive vertebrae. It could be concluded that no significant differences between the four successive vertebrae of the two specimens

are present (Table III.2- 4). Consequently, these vertebrae may be considered homologous, or at least as shape homologues.

### PRECAUDAL VERTEBRAE

A total of nine and ten lengths were defined on the lateral and caudal view of the precaudal vertebrae respectively (Fig. III- 4A, B).

### PRECAUDAL VERTEBRAE IN LATERAL VIEW

- PL1: distance between the tip of the neural spine and processus postneuralis;
- PL2: distance between the tip of the neural spine and processus praeneuralis;
- PL3: distance between the tip of the processus praeneuralis and processus postneuralis;
- PL4: distance between the tip of the processus praeneuralis and processus praehaemalis;
- PL5: distance between the tip of the processus postneuralis and processus posthaemalis;
- PL6: distance between the tip of the processus praehaemalis and processus posthaemalis;
- PL7: distance between the two extensions of the processus postneuralis;
- PL8: height of the posterior side of the vertebral centrum;
- PL9: height of the anterior side of the vertebral centrum.

### PRECAUDAL VERTEBRAE IN CAUDAL VIEW

- PC1: distance between the parapophyses;
- PC2: height of the vertebral centrum;
- PC3: width of the vertebral centrum;
- PC4: distance (left side) between the tip of the parapophysis and processus postneuralis;
- PC5: distance (right side) between the tip of the parapophysis and processus postneuralis;
- PC6: distance between the tips of both processus postneuralis;
- PC7: height of the neural canal;
- PC8: distance between the dorsal surface of the vertebral centrum and the tip of the neural spine;
- PC9: length of the right processus postneuralis;
- PC10: length of the left processus postneuralis.

### CAUDAL VERTEBRAE

The caudal vertebrae in lateral view were defined by 14 lengths (Fig. III- 5A).

- L1: distance between the tips of the neural and haemal spines;
- L2: distance between the tip of the neural spine and processus postneuralis;
- L3: distance between the tip of the neural spine and processus praeneuralis;
- L4: distance between the tip of the haemal spine and processus posthaemalis;
- L5: distance between the tip of the haemal spine and processus praehaemalis;
- L6: distance between the tip of the processus praeneuralis and processus postneuralis;
- L7: distance between the tip of the processus praehaemalis and processus posthaemalis;
- L8: distance between the tip of the processus postneuralis and processus posthaemalis;
- L9: distance between the tip of the processus praeneuralis and processus praehaemalis;
- L10: narrowest height of the vertebral centrum, in front of the spine bases;
- L11: narrowest height of the vertebral centrum, behind the spine bases;
- L12: height of the posterior side of the vertebral centrum;
- L13: height of the anterior side of the vertebral centrum;
- L14: width of the vertebral centrum.

### PECTORAL SPINE LENGTHS

A total of 6 measurements were defined on the lateral view of the pectoral spines (Fig. III- 5B).

- PS1: total length of the pectoral spine;
- PS2: height of the pectoral ridge;
- PS3: distance between the ridge and caudal process;
- PS4: distance between articular condyle and ridge;
- PS5: width of the pectoral spine behind the articular condyle;
- PS6: width of the pectoral spine in front of the pectoral teeth.

### MERISTIC DATA

In order to investigate whether the total number of vertebrae is a discriminative characteristic (V.1), the total number of vertebrae was counted for most of the examined specimens of *Channallabes apus*. Vertebral counts were made on specimens using

radiographs. The average of the total number of vertebrae was calculated for each population.

## III.2.5 VISUALIZATION

---

### CAMERA LUCIDA

Drawings of the osteology, based on cleared and stained specimens, and myology, based on dissected specimens, were made during stereoscopic observations on the Olympus SZX9.

### CT-SCANNING

To visualize the osteological structures of the head and tail of *Heteroconger longissimus* and *Moringua edwardsi* a CT-scanning was performed, using a high-resolution desktop X-ray microtomography instrument (Skyscan-1072, Belgium) (IV.1, IV.2). This was performed with the help of Dr. A Postnov and Prof. Dr. N De Clerck in the Department of Biomedical Sciences, University of Antwerp (RUCA).

### RADIOGRAPHS

In order to obtain meristic counts of the total number of vertebrae in clariid species (V.1), radiographs were made. These were made with a MPG 65 generator and a RSN 620X-ray tube (General Electric). The following settings allowed the most optimized images as possible: a focus distance of 1m, an exposure time of 10 ms, a power of 42 kV and a number of 320 mA. Radiographs were taken at the research group 'Interne geneeskunde en klinische biologie van de grote huisdieren, Ghent University'.

### 3D- RECONSTRUCTIONS

Computer-generated 3D-reconstructions were generated to visualize musculo-skeletal structures of small sized species (e.g. *Heteroconger hassi*, *H. longissimus*, *Moringua edwardsi*, *Pisodonophis boro*) (IV.1, IV.2, IV.3).

Serial sections were first examined using a Reichert-Jung Polyvar light microscope equipped with a digital camera (Colorview 8). Digital images of serial sections were captured using the AnalySIS 5.0 software (Olympus), as digital images of serial sections form the source material for the computer-based reconstruction-method. In order to obtain high quality images (with higher magnification) of sections with a larger cross-section, several images, with an overlapping area had to be taken to compose the section completely. These partial images were assembled using the Multi-Image-Arrangement (MIA)



function of AnalySIS. The interval between successive sections was 30  $\mu\text{m}$ , as every 15<sup>th</sup> section was used.

The selected digital images were imported in the software package Amira 3.1.1 (TGS). One of the most crucial steps included the alignment, which was done manually to decrease errors. This program also allowed to trace manually the target structures (bones, muscles, tendons,..). This step was also of high importance as here imperfections (see III.2.2 Serial sections) have to be detected and corrected. Each target structure was reconstructed separately and rendered. The resultant objects were subsequently smoothed to decrease the roughness of the generated surfaces, resulting in a smooth surface.

At last, all reconstructed elements were imported in Rhinoceros 3.0 (McNeel). This program allows to generate composite images. According to the user preferences, all or some reconstructed elements can be viewed, rotated in all directions and photographed.

## III.2.6 STATISTICAL ANALYSES

---

### ANALYSIS OF VARIANCE

In general, an analysis of variance (ANOVA) is performed to test for significant differences between means. The statistical method was applied to identify whether successive vertebrae are shape homologous (III.2.4b) and whether the biometric data, taken on the precaudal and caudal vertebrae in lateral and caudal view, are significantly different among different Gabonese population of *Channallabes apus* (V.1).

### THE PRINCIPAL COMPONENT ANALYSIS

The principal component analysis (PCA) is a method for simplifying a dataset in order to identify patterns in data, and expressing the data in such a way as to highlight their similarities and differences. The data are transformed to a new coordinate system such that the greatest variance by any projection of the data comes to lie on the first coordinate (PC1), the second greatest variance on the second coordinate (PC2), and so on. The lower order components (e.g. PC1, PC2) reflect those characteristics that contribute most to its variance and thus contain the most important aspects of the data (SOKAL AND ROHLF, 1995).

The principal component analysis was used as the multivariate analysis in V.1. The data, obtained from precaudal and caudal vertebrae, were logarithmically transformed and submitted to a PCA, using Statistica 6.0 (StatSoft Inc).

### THE DISCRIMINANT FUNCTION ANALYSIS

The discriminant function analysis was applied to determine which variables discriminate between two or more naturally occurring groups in IV.4.1 (SOKAL AND ROHLF, 1995). A Discriminant Function Analysis to examine vertebral shape differences in different geographic populations of *Channallabes apus* (V.1). This analysis was performed using Statistica 6.0 (StatSoft Inc).

### THE REGRESSION ANALYSIS

A regression analysis is a statistical tool for the investigation of relationships between variables. In the linear regression model, the dependent variable is assumed to be a linear function of the independent variable plus an error introduced to account for all other factors (SOKAL AND ROHLF, 1995). The regression analyses were performed in Statistica 6.0 (StatSoft Inc). In IV.4.1 the regression analyses were performed for all cranial measurements on total length ( $p < 0.05$  for all variables). In IV.4.2 regression lines were calculated in order to detect whether the weight of different cranial muscles increases equally in both phenotypes. In V.1 a regression analysis was performed, using TPS-REGR to explore the relationship between shape variation and two independent variables (degree of anguilliformity, size).

### THE BIMODALITY TEST

The chapter IV.4.1 provides a quantitative analysis of head size and shape in the *Anguilla anguilla* population (in Belgium) and tests for the presence of bimodality in cranial size and shape 1) within a single population in the Scheldt-Lippensbroek in Belgium and 2) across a broad range of waters in Belgium. The following statistical test was performed by Herrel A.

Three complementary methods were used to infer bimodality (BREWER, 2003).

(1) Frequency histograms of each  $\log_{10}$ -transformed measurement were examined.

(2) For each measurement the observed cumulative values were plotted against cumulative values expected under normality. The plot for a single normal distribution takes the form of a straight line, whereas bimodal distributions have a characteristically curved shape.

(3) It was statistically tested (BREWER, 2003; HENDRY ET AL., 2006) whether each sample was better represented by a single normal distribution or by a mixture of two normal distributions. Based on Akaike's Information Criterion (AIC), the fit of a single normal distribution was compared to that of a mixture of two normal distributions. The  $\Delta AIC$  was calculated as AIC (for the single normal distribution) minus AIC (for the fitted

mixture of two normal distributions). For interpretation, the following guidelines were used (BREWER, 2003; HENDRY *ET AL.*, 2006). If  $\Delta AIC < -8$ , a single normal distribution is strongly supported; If  $-8 \leq \Delta AIC < -5$ , a single normal distribution is moderately supported; If  $-5 \leq \Delta AIC < 5$ , a single normal distribution or a mixture of two normal distribution are roughly equivalently supported; If  $\Delta AIC > 8$ , a mixture of two normal distributions is strongly supported.

## III.2.7 BITE FORCE MODELLING

The mechanism of the jaw closing system of *Anguilla anguilla* (IV.4.1) and both representatives of the Trichiuridae, *Aphanopus carbo* and *Trichiurus lepturus* (VI.2) was predicted using the bite force model of VAN WASSENBERGH *ET AL.* (2005). The model of mouth closing movements was made and the analysis was performed by Van Wassenbergh S.

### BIOMETRICS OF THE LOWER JAW LEVER SYSTEM

In order to model the jaw-closing system of the examined species, a number of morphological variables were measured from preserved specimens (Fig. III.2- 6). These measurements are given for both the narrow-headed and broad-headed eels of the species *Anguilla anguilla* (Table III.2- 4) and for both trichiurids *Trichiurus lepturus* and *Aphanopus carbo* (Table III.2- 5). First, the XY-coordinates in the lateral view plane were determined for the lower jaw rotation point, the rostral tip of the lower jaw, and the insertion points on the lower jaw and the approximate origins on the neurocranium of each of the subdivisions of the adductor mandibulae complex ( $A_0$ ,  $A_1$ - $A_2$  and  $A_3$ ). Secondly, the average pennation angle ( $\theta$ ) was estimated for each of these muscle bundles by measuring the angle between the central tendon of the muscle and muscle fibres at different locations across the muscle. Thirdly, the jaw adductors of both sides were removed and weighed. Next, the muscle bundles were immersed in an  $HNO_3$  30% solution for 24 hours to dissolve the connective tissue. Fibres were gently teased apart and transferred to and stored in a 50% glycerol solution. Twenty muscle fibres per bundle were selected randomly and drawn using an Olympus SZX9 microscope with a camera lucida, from which the average fibre length per bundle was determined. The physiological cross-sectional area (PCSA) of each bundle could then be calculated by:

$$PCSA = \frac{muscle\ mass(g) * \cos(\theta)}{\rho(g/cm^3) * fibre\ length(cm)}$$

, where  $\theta$  is the average fibre pennation angle, and  $1.0597\ g/cm^3$  (MENDEZ & KEYS, 1960) was used as an approximation for the density of the muscle tissue ( $\rho$ ). Note that  $\theta$  is a function

of the instantaneous muscle length (NARICI, 1999), and thus depends on gape angle. It is therefore assumed that the measured lengths from isolated muscle fibres (Table III.2- 4, 5) correspond to the closed-mouth configuration of the jaw adductor muscles.

Species	lower jaw length (mm)	lower jaw width (mm)	Muscle	$L_{in}$ (mm)	$\beta$ (°)	Muscle length (mm)	$\sigma$ (°)	PCSA (cm <sup>2</sup> )	$\theta$ (°)	avg. fibre length (mm)
<i>Narrow-headed</i>	18.11	5.14	A <sub>1</sub> -A <sub>2</sub>	5.39	11	21.97	77	0.52	6	7.7
<i>CL=32.69 mm</i>			A <sub>3</sub>	4.29	17	14.28	60	0.06	32	7.1
<i>Broad-headed</i>	23.65	6.02	A <sub>1</sub> -A <sub>2</sub>	5.51	8	24.18	68	0.35	12	9.2
<i>CL=32.69 mm</i>			A <sub>3</sub>	3.73	16	13.95	60	0.07	30	8.1

**Table III.2- 4:** The morphological variables, measured in narrow-headed, and broad-headed eels, *Anguilla anguilla* In order to model the jaw-closing system of both species.

Species	lower jaw length (mm)	lower jaw width (mm)	Muscle	$L_{in}$ (mm)	$\beta$ (°)	Muscle length (mm)	$\sigma$ (°)	PCSA (cm <sup>2</sup> )	$\theta$ (°)	avg. fibre length (mm)
<i>T.lepturus</i>	76.9	8.5	A <sub>00</sub>	34.4	10	54.5	20	2.51	6	6.6
<i>CL=100.3 mm</i>			A <sub>1</sub> -A <sub>2</sub>	24.0	26	45.9	52	0.99	32	17.5
			A <sub>3</sub>	10.1	22	32.3	45	0.27	25	14.0
<i>A. carbo</i>										
<i>CL=160.6 mm</i>	136.9 (85.5)	16.4 (10.2)	A <sub>00</sub>	53.6 (33.5)	10	106.2 (66.3)	20	16.84 (6.57)	12	13.4 (8.37)
			A <sub>1</sub> -A <sub>2</sub>	27.3 (17.0)	38	72.0 (45.0)	68	7.79 (3.04)	30	27.3 (17.0)
			A <sub>3</sub>	23.8 (14.9)	36	44.0 (27.5)	75	1.50 (0.59)	28	20.2 (12.6)

**Table III.2- 5:** The morphological variables, measured in *Trichiurus lepturus* and *Aphanopus carbo* In order to model the jaw-closing system of both species.

### MODEL OF MOUTH CLOSING MOVEMENTS

Mouth closing movements are simulated using the model of VAN WASSENBERGH ET AL. (2005). This model calculates angular motion of the lower jaw based on the dynamic equilibrium of the external moments of force acting on the system. It has shown to predict jaw-closing velocity of several morphologically different species of air-breathing catfishes (Clariidae) with reasonable accuracy. More specifically, there was generally less than 15 % difference between experimentally observed data and the model's output for the time it takes to close the mouth (VAN WASSENBERGH ET AL., 2005). The model is therefore suitable to evaluate the effects of specific morphological changes to the jaw system of fishes, and to investigate in what aspects the jaw system is (or is not) optimised for fast mouth closing.

In this model, the lower jaw is modelled as a half-elliptic plate of which the length and width correspond to the measured dimensions of the lower jaw measure for the trichiurid species (Table III.2- 5). Upon rotation of this plate, a certain amount of water surrounding it will be put in motion as well. Therefore, the inertia of the rotating lower

jaw is increased by including a virtual, or added mass component that has the volume of the half-ellipsoid comprising the half-ellipse (VAN WASSENBERGH ET AL., 2005).

Upward rotation of the lower jaw is caused by the contraction of the jaw adductor muscles. The model calculates the instantaneous angular acceleration ( $\ddot{\alpha}$ ) of the lower jaw by using the following equation of motion:

$$I \ddot{\alpha} = M_m + M_d + M_{pr}$$

, where  $I$  is the moment of inertia of the lower jaw and added mass with respect to the quadratomandibular axis of rotation,  $M_m$ ,  $M_d$  and  $M_{pr}$  are the moments of force from respectively the jaw muscle activity, hydrodynamic drag, and a factor of resistance to jaw closing that combines the effects of the gradually increasing super-ambient pressure observed in the mouth cavity of suction feeding fishes near the end of the jaw closing phase (VAN LEEUWEN AND MULLER, 1983) and the damping by elongation of the mouth-opening muscles and other tissues during mouth closing. For further information about estimates of the magnitude of each of these included factors during jaw closure, we refer to the original publication of the model (VAN WASSENBERGH ET AL., 2005).

The instantaneous moment of force generated by the jaw muscles ( $M_m$ ) is calculated by:

$$M_m = \sum F_m \sin(\sigma) L_{in}$$

, where  $F_m$  is the instantaneous force along the line of action of one of the jaw muscle's subdivisions,  $\sigma$  the instantaneous (gape dependent) inclination of the jaw muscle with respect to the inlever with length  $L_{in}$  (Fig. III.2- 6). The contractile properties determining the instantaneous force produced by the jaw muscle ( $F_m$ ) are modelled as described in VAN WASSENBERGH ET AL. (2005). In this way, we accounted for the force-velocity dependence (Hill-curve), force-length dependence (optimal sarcomere overlap for a relevant range of gape angles), parallel elastic forces (elasticity in the muscle builds when it is stretched in a wide mouth opening) and included a sinusoidally rising activation profile (reaching full activation after 20 ms). In order to account for the force-length relationship, it was assumed that both species have optimal sarcomere-overlap in each of their jaw muscles at a gape angle of  $37^\circ$ . In this way, there is favourable sarcomere-overlap for a wide range of biomechanically relevant gape angles and the muscles do not reach the unstable, descending limb of the force-length curve when the mouth is opened to the maximal anatomical gape, which was estimated to be around  $55^\circ$  (manipulation of preserved specimens).

### CALCULATION OF BITE FORCE

Maximal bite force is calculated from the static equilibrium of forces at the tip of the lower jaw. In our calculations, maximal bite forces ( $F_{bite}$ ) and the resultant prey reaction forces on the lower jaw tip are always perpendicular to the longitudinal axis of the lower jaw running from the centre of the quadratomandibular articulation to the tip of the lower jaw and are determined for different gape angles by:

$$F_{bite} = M_m / \text{lower jaw length}$$

, where  $M_m$  is the moment of force from the different jaw muscles in isometric, fully activated state.

### III.3. TERMINOLOGY

#### TERMINOLOGY OF ANATOMICAL STRUCTURES

In order to avoid misinterpretations, the terminology applied throughout this dissertation as well as the principal equivalents found in literature are defined below.

##### ELOPOMORPHA (IV)

Terminology of cranial bones mostly follows that of ASANO (1962) and BÖHLKE (1989B). Terms used to define sutures and articulations follow HILDEBRAND (1995). The caudal skeleton follows the terminology proposed by MONOD (1968). Myology terminology follows WINTERBOTTOM (1974).

- Premaxillo-ethmovomerine complex: the rostral neurocranial complex where the mesethmoid, vomer and premaxillaries are indistinctly fused.
- Pars ethmoidalis: part of the premaxillo-ethmovomerine complex that is situated dorsal to the orbits.
- Pars vomeralis: part of the premaxillo-ethmovomerine complex that is situated ventral to the orbits.
- Pars premaxillaris: most rostral part of the premaxillo-ethmovomerine complex.
- Angular complex: the result of the fusion of the articular with the retro-articulo-angular complex (ROBINS, 1989; TAVERNE, 1999). In adult eels neither a separate angular nor a retroarticular is discernable. They generally fuse to form a uniform bone element. The angular with the retroarticular fuse first and later in ontogeny this fuses with the articular (TESCH, 2003).
- Dentary: the largest part of the lower jaw that surrounds the coronomeckelian.
- Coronomeckelian = a small bone on the postero-lateral part of Meckel's cartilage of the lower jaw. Often a point of insertion of the adductor mandibulae muscle. Also called sesamoid angular, supraangular, sesamoid articular, articular sesamoid, splenial, or os meckeli (ROJO, 1991; COAD AND MCALLISTER, 2007).
- Meckel's cartilage = the embryonic lower jaw of gnathostomous vertebrates which ossifies at least in part as the mentomeckelian, mediomeckelian, coronomeckelian, articular and retroarticular. It remains in some adult fishes as a pointed rod embedded in the dentary and angular. Also called mandibular cartilage, ceratomandibular cartilage or primary mandible (ROJO, 1991; COAD AND MCALLISTER, 2007).

- Cephalic lateral line system: following terminology of ADRIAENS ET AL., (1997) and BELOUZE (2001):
  - supraorbital canal,
  - infraorbital canal,
  - preoperculo-mandibular canal,
  - ethmoid canal: remnant of larval rostral commissure (TESCH, 2003), ventral branch of the supraorbital canals (BÖHLKE, 1989B),
  - adnasal canal, unique for elopomorphs, dorsal branch of the infraorbital canals (BÖHLKE, 1989B),
  - otic canal, canal between the supra- / infraorbital anastomosis and postotic / preoperculo-mandibular anastomosis, = temporal canal of BÖHLKE, 1989B),
  - postotic canal: canal behind preoperculo-mandibular branch and in front of supratemporal commissure,
  - temporal canal (canal behind supratemporal commissure),
  - frontal commissure (connects the left and right supraorbital canal),
  - supratemporal commissures (connecting left and right otic canals).
- Circumorbital bones of the cephalic lateral line system follows BÖHLKE (1989B):
  - nasal,
  - adnasal: ossification in front of the preorbital, protecting the adnasal canal,
    - = adnasal of MCDOWELL (1973) for elopomorphs;
    - = supraorbital of ASANO (1962),
    - = antorbital of TAVERNE (1986);
  - preorbital: first element of the infraorbital series, this term is preferred above the antorbital, proposed by BELOUZE (2001), as this may be confused with the antorbital of TAVERNE (1986), which corresponds to the adnasal;
    - = 1e infraorbital;
    - = lacrimale, ADRIAENS ET AL., (1997),
  - infra- and postorbitals, elements respectively ventral and caudal to orbits.
- Anterior ceratohyal: = ceratohyal of BÖHLKE (1989B),
- Posterior ceratohyal: = the epihyal of BÖHLKE (1989B) incorrectly insinuates homology with the epihyal of mammals, as well as an epihyal structure represents the dorsal element of the hyoid arch, the term posterior ceratohyal should be used,
- Hyomandibula: considered as composed by the fusion of the hyomandibula ss and metapterygoid (BELOUZE, 2001), strongly connected or even fused with quadrate. As homology of suspensorial elements in Anguilliformes is still ambiguous, terms of BELOUZE (2001) are followed.



- Pterygoid: = palatopterygoid bone (BELOUZE, 2001), this element may represent the ectopterygoid of teleosts (TESCH, 2003),
- Suspensorial inclination: the suspensorium can be considered ‘anteriorly or forwardly inclined’ when the quadrato-mandibular articulation is situated in front of the hyomandibular articulation condyle. Difference in suspensorial inclination is considered diagnostic trait at family level (BELOUZE, 2001),
- Caudal fin rays: rays supported by the hypurals and parhypural.

### OSTARIOPHYSI (V)

Terminology of the cranial skeleton follows CABUY ET AL. (1999) and DEVAERE ET AL. (2001), The caudal skeleton follows the terminology of ARRATIA (2003), MONOD (1968), ROJO (1991) and GOSLINE (1997). Cranial and caudal myology corresponds to that of WINTERBOTTOM (1974).

- Precaudal vertebrae: vertebrae characterized by the presence of parapophyses, supporting ribs (if present), and the absence of haemal spines (LAKSHMI AND SRINIVASA, 1989).
- Caudal vertebrae: vertebrae characterized by the presence of haemal arches, which enclose the large ventral blood vessels and which are elongated by a haemal spine (ROCKWELL, 1938; RAMZU AND MEUNIER, 1999).
- Processus prae- and posthaemalis: generally referred to as dorsal pre- and postzygapophyses. But, these terms are used to describe the articulation processes of vertebral arches in tetrapodes (HILDEBRAND, 1995). However, the extensions that are present in fish are considered non-homologous (GRASSÉ, 1958; GOSLINE, 1971; HILDEBRAND, 1995).
- Processus prae- and postneuralis: ventral pre- and postzygapophyses (HILDEBRAND, 1995).

### ACANTHOPTERYGII (VI)

Terminology of cranial bones and muscles of the mastacembelid species follows that of TRAVERS (1984A,B). For the trichiurids the terminology of cranial bones follows that of GAGO (1998), whereas the cranial myology follows WINTERBOTTOM (1974).



# IV

Anguilliformity in basal teleosts

Elopomorpha



**IV.1 HEAD-FIRST BURROWING SPECIES: *MORINGUA EDWARDSI***



---

## **MORINGUA EDWARDSI (MORINGUIDAE: ANGUILLIFORMES): CRANIAL SPECIALIZATIONS FOR HEAD-FIRST BURROWING?**

---

Modified from the paper published as:

De Schepper N, Adriaens D, De Kegel B. 2005.

*Moringua edwardsi* (Moringuidae: Anguilliformes): Cranial specializations for Head-First  
Burrowing?

Journal of Morphology 266 (3): 356-368.

### **ABSTRACT**

---

The order Anguilliformes forms a natural group of eel-like species. *Moringua edwardsi* (Moringuidae) is of special interest because of its peculiar fossorial lifestyle: this species burrows head-first. Consequently, we might hypothesize that morphological constraints are predominantly present at the level of the skull, whereas the caudal fin morphology is rather not specialized. Externally pronounced morphological specializations for a fossorial lifestyle include: reduced eyes, lack of color, low or absent paired vertical fins, elongate, cylindrical body, reduced head pores of the lateral line system, etc. Many fossorial amphibians, reptiles and even mammals have evolved similar external specialisations related to burrowing. The present study focuses on osteological and myological features of *M. edwardsi*, in order to evaluate the structural modifications that may have evolved as adaptations to burrowing. Convergent evolutionary structures and possible relations with head-first burrowing, miniaturization, feeding habits, etc, are investigated. Body elongation, reduction of the eyes, modified cranial lateral line system, and modified skull shape (pointed though firm) can be considered as specialization for head-first burrowing. Hyperossification can probably be regarded more as a specialization to both head-first burrowing and feeding, even though an impact of miniaturization cannot be excluded. Hypertrophied adductor mandibulae muscles and the enlarged coronoid process can be associated with both feeding requirements (it enhances bite forces necessary for their predatory behavior) and with a burrowing lifestyle, as well as miniaturization. The caudal fin is similar to non-burrowing eels and thus can be considered as not specialized.

---

## INTRODUCTION

---

*Moringua edwardsi*, belongs to the family Moringuidae (Anguilliformes; REGAN, 1912; NELSON, 1994) and is commonly known as spaghetti eels. Despite the common features shared with other Anguilliformes, this species caused considerable confusion in the past because of its striking ontogenetic polymorphism. Many different ontogenetic stages were even described as distinct genera (SMITH AND CASTLE, 1972). Moringuidae (SMITH, 1989D) appear to be phylogenetically related to Anguillidae (SMITH, 1989A) and Heterenchelidae (SMITH, 1989C). According to SMITH (1989D), Moringuidae share pronounced morphological specializations for a fossorial lifestyle with Heterenchelidae and Ophichthidae: reduced eyes, lack of color, low vertical fins, elongate, cylindrical body and reduced head pores. Though, in contrast to tail-first burrowing ophichthid species, both Heterenchelidae and Moringuidae burrow head-first (CASTLE, 1968; SMITH AND CASTLE, 1972; SMITH, 1989D). It is striking that only immature specimens of *M. edwardsi* spend all their time burrowed in the sand (GORDON, 1954; GOSLINE, 1956). Adults seem to limit their burrowing behavior, as they leave their burrows during the night (SMITH, 1989D). SMITH (1989D) mentions rapid movements of the body, just beneath the surface for subterranean hunting and feeding. The solid conical snout, combined with a protruding lower jaw, facilitate burrowing, where power is provided by the cylindrical body (CASTLE, 1968; SMITH, 1989D).

As immature specimens spend most of their time buried in the sand, they form the most obvious study object to examine the degree of structural specializations for head-first burrowing. First, a detailed description of the cranial osteological and cranial myological features of such immature moringuids (*M. edwardsi*) was performed. The detailed morphology of the head was examined with the goal to apportion the anatomical specializations among head-first burrowing, miniaturization and predatory feeding. Second, as *M. edwardsi* is a head-first burrowing species, we might hypothesize that morphological constraints are predominantly present at the level of the skull, whereas the caudal fin morphology is rather not specialized.

## MATERIAL AND METHODS

---

For this study three alcohol-preserved immature specimens of *Moringua edwardsi* (MCZ 44686) were used, obtained from the Museum of Comparative Zoology, Harvard University: ME1: Total length (TL) = 219 mm; ME2: TL = 200 mm and ME3: TL = 172 mm. Obtained osteological data were compared with previous papers published by TREWAVAS



(1932) and SMITH (1989D). See chapter III.1 for details on specimens (Table III.1- 1A). In this study, specimens were anaesthetized, sacrificed and fixed (see III.2.1). specimens were cleared and stained, serial sections were made and a CT-scanning and 3D-reconstructions was performed (see III.2.2 and III.2.5).

## RESULTS

---

### HEAD: CRANIAL LATERAL LINE SYSTEM

The cranial lateral line system comprises the supra- and infraorbital canals, the otic canal, the mandibular canal, the preopercular canal, the ethmoid canal, the adnasal canal, the frontal commissure and the supratemporal commissure (Fig. IV.1- 1A). The supra- and infraorbital canals are mainly supported by the following circumorbital bones: a large nasal, small adnasal, long preorbital and three postorbitals (Fig. IV.1- 1B). The nasal bone comprises three parts. The first and anterior part of the nasal is tube-like and lies in front of the olfactory organ. The second part of the nasal bone, covering the dorsal roof of the olfactory organ, has a horizontal position. The medial side of this part contains the supraorbital canal, while thin wings expand laterally. Behind the nasal sac, the third part of the nasal is again tube-like, lacking the horizontal plates. The supraorbital canal has an ethmoid canal, running ventrally and enclosed by the premaxillo-ethmovomerine complex. Behind the nasals, the supraorbital canal is enclosed by the frontal. More caudally it is partially enclosed by incomplete extensions or arches of the frontal. The frontal commissure connects the left and right supraorbital canal (Fig. IV.1- 2A). The rostral part of the infraorbital canal is enclosed in the preorbital. The dorsal adnasal canal is enclosed by the adnasal. Behind the eyes, the infraorbital canal is surrounded by three postorbitals and meets the supraorbital canal (Fig. IV.1- 2Ba). Both fuse in the anterior process of the pterotic, continuing as the otic canal. This otic canal is enclosed by the pterotic and runs up to the caudal part of the skull. The mandibular canal is enclosed by the dentary (Fig. IV.1- 2C). Posterior to the mandibular articulation the preopercular canal is enclosed by the preopercle. The otic canals are connected through a supratemporal commissure. The bases of this commissure are situated in front of the fusion of the preopercular canal and the otic canal (no longer surrounded anymore by the pterotic; Fig. IV.1- 2D).

No external head pores are present, implying that the cranial lateral line system is not connected to the environment, at least in the head region. Though, the circumorbital bones (nasal, adnasal, preorbital and postorbitals), as well as the dentary are pierced by many internal pores (Fig. IV.1- 1A). These pores lead to interconnected, dermal cavities,

situated lateral to and along the total length of the supra- and infraorbital canals (Fig. IV.1- 1C, 2A,Ba). It is remarkable that these cavities are not connected with any external pores or with the environment. Neuromasts are observed in all canals and are well developed.

The eyes of the immature specimens are very small, dark spots and are covered with semi-opaque skin (Fig. IV.1- 2Ba). The orbits, which enclose the eyes, are small as well (Fig. IV.1- 3A).

## HEAD: OSTEOLOGY

The neurocranium is heavily ossified, forming one solid unit, with the exception of a movable maxillary (Fig. IV.1- 3A,B). The shape of the neurocranium is elongate, tapering from its widest part, the otic region, toward the tip of the snout. The orbits are small. Large recurved teeth are present and supported by the premaxillo-ethmovomerine complex, maxillary and lower jaw. Tooth size decreases caudally. Neighbouring bones are interconnected by dense connective tissue and form scarf joints (Fig. IV.1- 2Ba,b). The bones forming the skull roof (frontals, parietals, supraoccipital, epiotics and exoccipitals) show a high amount of overlap, formed by the extension of the scarf joint (Fig. IV.1- 4B) (terminology of joints follows HILDEBRAND, 1995). Both frontals show less extended scarf joints between each other, though the scarf joints between the frontals and parietals are extremely extended.

The ethmoid region comprises the premaxillo-ethmovomerine complex and the nasals. The latter are described with respect to the lateral line system (Fig. IV.1- 1). A robust and compact premaxillo-ethmovomerine complex is present, forming the rostral tip of the neurocranium. Two small, cartilaginous nasal bars are situated ventral to the nasal organ and lateral to the premaxillo-ethmovomerine complex. These cartilaginous nasal bars contact the premaxillo-ethmovomerine complex posteriorly. These bars may aid in support of the nasal organ (Britz R, pers comm). Lateral to the complex, robust but elongate maxillaries are present. The anterior part of the maxillary bears small ventral and dorsal processes, which rest in the anterior and posterior maxillo-premaxillo-ethmovomerine articular facets on the premaxillo-ethmovomerine complex respectively. The posterior end of the maxillary is surrounded by the primordial ligament, which attaches to the dorso-lateral face of the lower jaw (Fig. IV.1- 2C).

The orbital region comprises the pterospheoids, frontals, adnasals, preorbitals and postorbitals. Orbitospheoid and basisphenoid are absent. The paired frontals meet in the midline and are strongly interconnected by a scarf joint (Fig. IV.1- 2Bb). Dense connective

tissue is present between both bones. Anteriorly, the frontals border the posterior edge of the premaxillo-ethmovomerine complex. The pterotics cover the frontals caudo-laterally. The caudo-ventral part contacts the parasphenoid ventrally and the pterosphenoid caudally, all as a result of scarf joints (Fig. IV.1- 2Bc). The caudo-dorsal parts of the frontals overlie the parietals caudally, as a result of extreme extension of the scarf joint. Part of the supraorbital canal runs in incompletely expanded canals formed by frontal extensions, referred to as frontal arches (Fig. IV.1- 2Ba). More caudally this canal is completely enclosed in the frontal. The pterosphenoid contacts the pterotic dorsally and the parasphenoid ventrally. Again scarf joints connect these bones. Preorbital, postorbitals and adnasal are described with respect to the lateral line system (Fig. IV.1- 1).

The otic region comprises the sphenotics, pterotics, prootics, epiotics and parietals, in which all neighboring bones are connected by scarf joints. The ventral surface of the sphenotic contacts the dorso-lateral side of the prootic, forming the anterior articular groove, or dilatator fossa for the connection between the hyomandibula. The lateral sphenotic process is supported by a bony strut, which is partially formed by the antero-dorsal surface of the prootic and partially by the sphenotic. This process contributes to the anterior suspensorial articular facet. The pterotic forms the lateral wall of the skull and contains the otic canal. The dorsal edge connects to the frontal, parietal, epiotic and exoccipital. Ventrally it contacts the frontal, the pterosphenoid, the sphenotic, the prootic and exoccipital. Caudally the posterior suspensorial articular facet contributes to the articulation between the suspensorial hyomandibula and the neurocranium. The prootic forms the anterior part of the otic bullae. The dorsal edge of the prootic abuts the pterosphenoid, the sphenotic and pterotic. Ventrally it connects the parasphenoid and the basioccipital. The pterotic and the prootic form an articulating groove for the dorsal edge of the hyomandibulo-quadrate. The epiotics are connected to the supraoccipital and exoccipital, and their anterior parts contact the pterotic and parietals. The first third of the parietals is overlain by the frontals, thus forming an extended scarf joint. A scarf joint connects both parietals. The parietals overlie the supraoccipital caudally (Fig. IV.1- 2D) and the epiotics.

The occipital region comprises the exoccipitals, basioccipital, supraoccipital and parasphenoid, which are connected by scarf joints. The anterior part of the exoccipitals contacts the pterotic dorsally and the prootics ventrally. The medial part joins the supraoccipital dorsally and the basioccipital ventrally, whereas both exoccipitals interconnect postero-medially. The foramen magnum is surrounded by the exoccipitals laterally and dorsally. The occipital region is, in ventral view, dominated by the basioccipital (Fig. IV.1- 3B). The basioccipital and prootic are expanded forming the

posterior part of a large otic bulla. The foramen magnum is bordered ventrally by the basioccipital. The anterior half of the supraoccipital is overlain by the parietals. Posteriorly it abuts the epiotics and exoccipitals. Postero-dorsally the bone bears a small ridge on which attaches the aponeurosis of the two halves of the adductor mandibulae muscle A2 (see below) (Fig. IV.1- 2D). The parasphenoid spans from the orbital region to the occipital region. It is a rhomboid-like bone and covers the dorsal surface of the ventro-posterior tip of the premaxillo-ethmovomerine complex. It attains its maximum width near its junction with the pterosphenoid and the prootics. The parasphenoid extends caudally as two slender parasphenoidal processes from about the middle of the prootics (Fig. IV.1- 2D, 3B).

The suspensorium is slightly longer than deep, resembling an inverted triangle, and consists of three robust bones (Fig. IV.1- 5). The hyomandibula and quadrate are fused, forming a single, massive complex: the hyomandibulo-quadrate. The hyomandibula of the complex bears three articular condyles: the anterior suspensorial condyle articulates with the sphenotic and prootic; the posterior suspensorial condyle articulates with the pterotic; and the rostro-dorsal opercular articular condyle articulates with the opercle (Fig. IV.1- 3A, 5). In between the two condyles, the cartilaginous dorsal edge of the hyomandibula additionally is connected to the articular groove. The angular complex of the lower jaw articulates at the level of the mandibular articular facet with the quadrate by the quadrato-mandibular articular condyle (Fig. IV.1- 5). The pterygoid is reduced to a small slender bone, which lies anterior to the hyomandibulo-quadrate (Fig. IV.1- 5).

The opercular bones consist of a series of four bones: opercle, preopercle, interopercle and subopercle (Fig. IV.1- 3A, 5). The opercle is triangular. The dorsal process of the opercle bears the opercular articular facet for the opercular condyle of the hyomandibula. The preopercle encloses the sensorial preopercular canal (Fig. IV.1- 1). The dorsal process of the preopercle is connected to the lateral side of the hyomandibula through dense connective tissue. Ventrocaudally the medial side of the preopercle is covered by and strongly attached to the interopercle by dense connective tissue. The interopercle is triangular. The subopercle is triangular and situated ventro-medially to the opercle.

The anterior and largest part of the lower jaw is formed by the dentary (Fig. IV.1- 6A). Dorsally it bears a large coronoid process (Fig. IV.1- 6A). The dentary is penetrated by the mandibular canal of the cranial lateral line system (Fig. IV.1- 1, 2C). The Meckel's cartilage appears as a slender rod enclosed by the dentary (Fig. IV.1- 2C). The posterior end of the lower jaw consists of three fused bones (the angular, the articular and the retroarticular; Taverne, 1999), which are fused to form the angular complex (Fig. IV.1-

6A). The angular complex is pointed anteriorly and wedges into the dentary. Posteriorly at three quarters of the length of the lower jaw, the angular complex becomes exposed dorsally and medially. Caudally the complex bears the mandibular articular facet for the quadrate (Fig. IV.1- 6A). Both complexes are L-shaped in cross-section, with the horizontal ridge pointing medially.

The hyoid apparatus consists of a median basihyal; a median urohyal, with a short posterior extension; and paired anterior and posterior ceratohyals (Fig. IV.1- 6B). Hypohyals and interhyals are absent.

### HEAD: LIGAMENTS

The primordial ligament surrounds the caudal surface of the maxillary and extends caudally to insert on the dorso-lateral face of the lower jaw (Fig. IV.1- 2C). This ligament shows an extensive dorsal outgrowth, covering the anterior part of the adductor mandibulae complex (A1 and A2) and its tendons (Fig. IV.1- 7). The posterior tip of the posterior ceratohyals is connected to the medial surface of the interopercle by means of the interoperculo-ceratohyal ligament and to the hyomandibula by means of the hyomandibulo-ceratohyal ligament (Fig. IV.1- 5, 6C). A strong pterygoid ligament stretches from the dorsal edge of the pterygoid to the parasphenoid; it more caudally connects the pterygoid to the anterior projection of the hyomandibulo-quadrate (Fig. IV.1- 5). The dorsal edge of the interopercle is connected through a dorsoventrally directed operculo-interopercular ligament to the ventrolateral face of the opercular dorsal process (Fig. IV.1- 5). Anteriorly a rostro-caudally directed angulo-interopercular ligament connects the anterodorsal side of the interopercle to the ventro-caudal side of the angular complex (Fig. IV.1- 5, 6A). The preoperculo-opercular ligament connects the opercular process to the caudal edge of the preopercle (Fig. IV.1- 5). The basihyo-ceratohyal ligament connects the caudo-lateral surface of the basihyal with the ventral surface of the anterior ceratohyals (Fig. IV.1- 2C). The urohyo-ceratohyal ligament connects the antero-ventral surface of the urohyal to the dorso-lateral surface of the anterior ceratohyal (Fig. IV.1- 2C). The angulo-preopercular ligament connects the ventro-caudal surface of the angular complex to the anterior edge of the preopercle (Fig. IV.1- 5, 6A).

### HEAD: MYOLOGY

The adductor mandibulae complex comprises four parts: A1, A2, A3 and A $\omega$  (Fig. IV.1- 7). The complex is hypertrophied so that the counterparts of A2 meet dorsally, thus

covering the skull. Caudally, an aponeurotic connection is present between the jaw muscles and the epaxials. The fibres of adductor mandibulae A1 appear as a separate, thin and short bundle, lateral to A2 and are ventro-rostrally directed. The medial fibres of A1 are connected to the tendon of the medial A2m, whereas the ventral and lateral fibres of A1 are connected to the expanded outgrowth of the primordial ligament (Fig. IV.1- 7A). The adductor mandibulae A2, comprising three bundles, is the largest part of the complex and extends dorsally and caudally. Dorsal to the neurocranium, both left and right halves of the A2 interconnect by an aponeurosis, originating from the dorsal bones of the skull (frontal, parietal, supraoccipital ridge) (Fig. IV.1- 2D). The muscular origin includes the lateral and dorsal elements of the neurocranium: frontal, pterotic, parietal, epiotic and supraoccipital. The anterodorsal part A2d is situated laterally to A3 and is covered by the tendinous plate-like extension of the primordial ligament (Fig. IV.1- 7B). The fibres of A2d are ventrocaudally directed (Fig. IV.1- 8) and merge into the well-developed tendon of A2m. This tendon covers the medial A2m and inserts on the posterior edge of the coronoid process of the lower jaw and on the inner side of the dentary, medial to the primordial ligament. The fibres of A2m and A2v are ventro-rostrally directed (Fig. IV.1- 8). The ventral part of the A2m tendon also receives fibres of the  $A\omega$ , thus separating the A2m and  $A\omega$ . At the level of the end of the pterotic, the caudoventral A2v is separated from A2m by an aponeurosis. The fibres of the ventral bundle A2v attach tendinously to the dorsolateral side of the hyomandibula (Fig. IV.1- 2D). The adductor mandibulae A3, with ventro-caudally directed fibres, originates muscularly from the ventro-lateral surface of the frontal and the pterosphenoid. The ventral fibres of the A3 attach to a tendon T A3 that inserts on the ventromedial ridge of the angular complex, ventromedial to the fibres of  $A\omega$ . The adductor mandibulae  $A\omega$  inserts on the Meckelian fossa on the medial face of the dentary and the angular complex. Fibres of  $A\omega$  arise from the anteroventral part of the A2m tendon, separating  $A\omega$  from A2m. More caudally the posterior fibres of  $A\omega$  and the ventral fibres of A2m interconnect. The merged fibres of A2m and  $A\omega$  attach medioventrally by a tendon to the pterygoid, quadrate and hyomandibula.

The levator arcus palatini runs between the suspensorium and the neurocranium (Fig. IV.1- 7C). This muscle is covered laterally by the adductor mandibulae A2- $A\omega$  complex. The fibres are directed dorso-ventrally and are slightly inclined caudally. The fibres merge into a tendon that originates on the lateral ridge of the sphenotic. Fibres insert on the lateral face of the hyomandibula and the quadrate.

The adductor arcus palatini runs in the roof of the buccal cavity and connects the neurocranium to the inner face of the suspensorium (Fig. IV.1- 7D). The fibres are directed dorsocaudally but inclined ventrolaterally. It has muscular attachments, running from the

parasphenoid to the medial side of the pterygoid, hyomandibula and the quadrate. A second bundle of the adductor arcus palatini appears at the level of the articulation between the lower jaw and the quadrate. It shows a different fibre direction and inserts on the dorsolateral face of the parasphenoid near its suture with the prootic.

The adductor hyomandibulae is situated posteriorly to the adductor arcus palatini (Fig. IV.1- 7D). Its fibres attach to the dorsolateral face of the prootic, and dorsolateral surface of the exoccipital (Fig. IV.1- 2D). The muscular insertion sites include the dorsomedial surface of the quadrate and hyomandibula. Its anterior fibres are dorsoventrally directed, forming a right angle with the posterior fibres of the adductor arcus palatini, whereas a ventrolateral direction is present caudally. Posteriorly the fibres merge with the anterior fibres of the adductor operculi.

The dilatator operculi is conically shaped with the apex lying ventrally (Fig. IV.1- 7C). It is overlain laterally by the adductor mandibulae A2-A $\omega$  complex. The dorsoventrally directed fibres of the dilatator operculi originate from the posterior part of the pterotic. Its tendon borders the ventral edge of the muscle and inserts on the dorsal opercular process.

The adductor operculi covers the caudal part of the adductor hyomandibulae ventrally and can be distinguished from the latter by a different fibre direction: those of the adductor operculi are dorsoventrally directed, whereas the posterior fibres of the adductor hyomandibulae are directed more rostrocaudally (Fig. IV.1- 2D). The fibres originate on the exoccipital and insert on the dorsomedial surface of the dorsal opercular process and to the dorsomedial surface of the opercle, posterior to its articulation with the quadrate (Fig. IV.1- 7D).

The levator operculi originates tendinously from the ventral face of the posterior process of the hyomandibula, near its articulation with the neurocranium (Fig. IV.1- 7C). The dorsoventrally directed and caudally inclined fibres insert on the dorsal opercular process and dorsal edge of the opercle, and extend ventrally to cover its external and medial side. Some fibres even extend ventrally to insert on the lateral face of the interopercle (Fig. IV.1- 2D).

The intermandibularis is absent.

The protractor hyoidei, characterized by its X-shape, connects the hyoid arch to the lower jaw. Near the dental symphysis, well-developed anterior tendons attach the right and left bundle to the medial surface of the dentary (Fig. IV.1- 6C). These tendons cover the lateral surface of both bundles anteriorly. More caudally each muscle half is divided aponeurotically into a dorsal  $\beta$  and ventral  $\alpha$  part (Fig. IV.1- 2C, 6C). The ventral part meets its counterpart on a median aponeurosis, forming a single unit. Both left and right parts diverge at the level of the rostral tip of the basihyal, (Fig. IV.1- 2C). The posterior

fibres of both dorsal and ventral parts each attach to a posterior tendon. These tendons fuse to a single tendon, which attaches to the dorsolateral surface of the anterior ceratohyal.

The sternohyoideus consists of three myomeres, separated by two myocommata. The fibres insert by means of a strong, well-developed tendon on the posterodorsal region of the urohyal (Fig. IV.1- 6C). Fibres have a bipennate insertion on the tendon. The sites of origin include the medial side of the cleithrum, whereas the posterior fibres insert on a myocomma, separating them from the hypaxial muscles.

The hyohyoidei adductores form a sheet of fibres which interconnects the successive branchiostegal rays (Fig. IV.1- 2D). Both muscle halves continue ventrally to meet their opposite halves in a ventromedial hyohyoideal aponeurosis. Dorsally fibres attach to the ventromedial side of the dorsal opercular process (Fig. IV.1- 2D). Posterior to the process this muscle attaches to the medial surface of the opercle. Both muscle halves remain separate at the end of the orobranchial cavity, bordering the ventrolateral sides of each gill opening. Posterior to the opercle, the fibres attach dorsally to the horizontal septum, between the epaxials and hypaxials. According to the nomenclature of WINTERBOTTOM (1974) the hyohyoideus inferioris is present and arises from an aponeurosis in the ventral midline. The medial fibres run to the ventro-lateral surface of the ceratohyal, whereas the ventro-medial fibres radiate, attaching to ventro-medial surface of branchiostegal rays. It is not clear whether the hyohyoidei abductores are absent or not differentiated. Ontogenetic series are necessary to resolve this.

The supracarinalis anterior originates from the supraoccipital and inserts on the first neural spine.

The epaxials insert aponeurotically on the epiotic, the pterotic and the supraoccipital (Fig. IV.1- 2D, 7D). The myocommata between successive myomeres are visible in cross-sections.

The hypaxials insert onto the ventrocaudal border of the exoccipitals, the basioccipital, the horizontal myoseptum and the myocomma of the sternohyoideus (Fig. IV.1- 2D).

### CAUDAL FIN: OSTEOLOGY

The number of caudal fin rays, supported by the caudal skeleton varies between 7 and 8 (Fig. IV.1- 9; 10). The caudal fin is confluent with the dorsal and anal fins, though this is externally less clear in immature specimens (Fig. IV.1- 10). The caudal fin rays are long and pliable. Hypural fusions are noted. The dorsal hypural plate is formed by the



fusion of the third and fourth hypurals. Only the proximal parts the first and second hypurals are fused. A distinct hypural fenestra cannot be discerned. The urostyle, formed by the fusion of the first and second ural centrum, bears one pair of uroneurals, which are dorso-medially fused. An epural element is absent. Distinct hypurapophyses on the lateral surface of the ventral hypural plate are present. The parhypural, modified haemal spine of the first preural centrum is absent. The neural and haemal arches of the first preural vertebra are medially fused. The neural spines of the preural vertebrae are absent.

### CAUDAL FIN: MYOLOGY

The supracarinalis posterior and infracarinalis posterior are absent. Interradials are present and interconnect dorsal caudal fin rays (Fig. IV.1- 9B). The flexor dorsalis originates from the lateral surface of the uroneural and dorso-lateral surface of the dorsal hypural plate (Fig. IV.1- 9D). This muscles inserts onto 4 or 5 dorsal caudal fin rays. The flexor ventralis originates from the lateral surface of the first hypural and inserts on three ventral caudal fin rays (Fig. IV.1- 9D). The hypochordal longitudinalis runs from the dorso-lateral surface of the first hypural to the ventro-lateral surface of the dorsal hypural plate (Fig. IV.1- 9B). Origin and insertion are tendinous. The proximalis originates from the caudal surface of the hypurapophysis and inserts onto the lateral surface of the second hypural and dorsal hypural plate (Fig. IV.1- 9C). The epaxial and hypaxial musculature inserts by means of broad tendinous sheets onto dorsal and ventral caudal fin rays respectively.

## **DISCUSSION**

---

### MORPHOLOGY RELATED TO HEAD-FIRST BURROWING?

Eye reduction - Elongation of the body is rather common in fishes, amphibians, reptiles and mammals (LANDE, 1978; HANKEN, 1993; RIEPPEL, 1996; MECKLENBURG, 2003A, B) and is frequently linked to a whole set of morphological transformations. The most recurrent changes are eye reduction, increasing rigidity of the skull, increase in number of vertebrae and limblessness (GANS, 1973; 1975; WITHERS, 1981). Most of these changes have been linked to a burrowing lifestyle. Body elongation combined with limblessness allows unhindered movements below the substrate surface (GANS, 1975; POUGH ET AL., 1998). Eye reduction is also believed to be related to burrowing, as well as a benthic or cryptic lifestyle (GANS, 1973; 1975; WITHERS, 1981; LEE, 1998). For example, eye reduction is known

in elongate clariid catfish (*Channallabes apus*) living in submerged swamp mud (POLL, 1973; ADRIAENS ET AL., 2002); the blind spiny eel (*Caecomastacembelus brichardi*) known to inhabit rock crevices (POLL, 1973); and the blind cave salamander (*Proteus vulgaris*) (POLL, 1973). For *Moringua edwardsi*, not only does this species show similar features, but they can also be related to an ontogenetic shift in burrowing behavior. The burrowing immature specimens have reduced eyes, whereas the pelagic adults do not (SMITH, 1989D). Adults are also known to be visual predators, whereas immature specimens are believed to detect benthic and burrowing prey through olfaction and touch (GORDON, 1954; SMITH, 1989D). In those immature specimens, the eyes are covered with thick semi-opaque skin (Fig. IV.1-2Ba), which presumably has a protective role during burrowing. In *Ophichthus rufus* the eye is similarly protected externally from injury by a dermal cornea and a thick corneal epithelium covered by protective mucus (BOZZANO, 2003). Protective structures for the eyes have been observed in other burrowing vertebrates as well (e.g., caecilians), but are not always related to eye reduction (e.g., some snakes and lizards; GANS, 1975).

Lateral line system - In those vertebrates in which the eyes have become completely lost, other sensory systems become more important (e.g., in fishes the lateral line system becomes the most important sensory organ for scanning the surroundings; MONTGOMERY, 1989). In blind cave characins (*Anoptichthys jordani*), for example, the eyes are absent but the cranial lateral line system is well developed, comprising canals enclosed in bones and containing neuromasts that are in contact with the exterior through canal openings (HASSAN, 1989). In *Moringua edwardsi*, however, the cranial lateral line system is markedly different: external pores are absent and canals are widened into dermal cavities. Even though the connection with the exterior seems to be lost, the neuromasts are still well developed. We hypothesize that the lack of pores is a specialization for burrowing, as this avoids the entering of sediment into the canals during head-first burrowing. The dermal cavities may function as a kind of sensory pads that are stimulated mechanically during burrowing or when in contact with prey, subsequently pushing fluid into the canals and thus stimulating the neuromasts in the canals (J. Webb, pers comm).

Jaw adductor hypertrophy - The reduction of the eye, especially in a macrophthalmic ancestral state, can be expected to have a substantial impact on the spatial design of the head. In elongate clariids, hypertrophy of the jaw muscles has been linked to reduction of the eyes (DEVAERE ET AL., 2001). We may assume that in *Moringua edwardsi* the reduced eyes similarly create space allowing the expansion of the adductor mandibular muscles (+ unusual orientation of fibres; see below). Hypertrophy of jaw

adductor muscles has been linked before to either head-first burrowing (ATKINSON AND TAYLOR, 1991; NELSON, 1994) or a predatory lifestyle (HELPMAN ET AL., 1997).

Hypertrophied mouth-closing muscles suggest the ability for powerful biting, with a consequent increase of mechanical loads on skeletal elements (HERREL ET AL., 2002; VAN WASSENBERGH ET AL., 2004). The link with predation has been made for muraenids, which also show structural adaptations for muscular attachment in the dental coronoid process and suspensorium (BÖHLKE ET AL., 1989). It is possible that the presence of hypertrophied jaw muscles is the plesiomorph state in the order Anguilliformes since a predatory lifestyle represents the primitive condition of the Anguilliformes (GOSLINE, 1971; SMITH, 1989B), since hypertrophied jaw muscles and a strong bite are advantageous for predation, and since hypertrophied jaw muscles are frequent in Anguilliformes (e.g. in Anguillidae, Muraenidae, Congridae, Ophichthidae, etc). Of course such assumptions have to be taken carefully and a cladistic analysis has to be performed to test this. *Monopterus* and *Synbranchus*, which are also eel-shaped burrowers, show striking convergence in the hypertrophy and fibre direction of the adductor mandibulae complex, shape and size (reduced) of the opercular apparatus and shape and orientation of the levator operculi. These features have been linked before to their specialized predacious feeding mode (LIEM, 1980). Several additional features in *Moringua edwardsi* can be linked to a predatory lifestyle, apart from jaw muscle hypertrophy. Some examples are the large recurved teeth on the upper and lower jaws (including vomeralis), robust upper and lower jaws for holding prey, and a large gape. The robustness of the upper jaw results from the fusion of the premaxillary, mesethmoid and vomer to form the premaxillo-ethmovomerine complex. Even though this fusion is synapomorphic for Anguilliformes, it is assumed to be a specialization for predatory feeding (EATON, 1935; GOSLINE, 1980; SMITH, 1989D). In those teleosts, handling of prey occurs through rotational feeding, inducing large torque forces onto the skull. Structural changes for resisting these forces can thus be expected, both at the skeletal and myological level (see below).

In *Moringua edwardsi*, the hypertrophied jaw muscles are likely to be advantageous in head-first burrowing as well. Head-first burrowing can occur through mouth excavation (e.g., *Cepola rubescens*) or through shovelling movements of the snout, in which both forward forces are generated through body undulations (CASTLE, 1968; SMITH, 1989D, c; ATKINSON AND TAYLOR, 1991). *Moringua edwardsi* is known to penetrate the substrate with its conical snout and protruding lower jaw, without actual oral excavation. Consequently, powerful biting during excavation cannot explain the presence of the hypertrophied jaw muscles in *Moringua edwardsi*, even though a large coronoid process and rigid suspensorium (to which the jaw muscles attach) are present. Still, as these muscles

substantially enclose the posterior part of the skull, they may reinforce the lower jaw during shovelling, thereby protecting it from disarticulation (see below). Also, as a gap between the jaw adductors and epaxials is absent, because of them interconnecting, the transition from head to body is smooth (thus improving substrate penetration).

Hyperossification - Apart from structural reinforcements to deal with increasing loads during jaw adductor contraction, elevated levels of ossification have been associated directly to head-first burrowing as well (RIEPEL, 1996; LEE, 1998). Amphisbaenids, uropeltid and scolecophid snakes, caecilia (GANS, 1975; HANKEN, 1993; DUELLMAN AND TRUEB, 1986) and even some frogs (e.g., *Hemisus*; POUGH ET AL., 1998), which are true head-first burrowers, show extreme skull modifications that can be linked to resisting compressive forces during burrowing. Not only the bones themselves but also connections between bones contribute to skull strength. The distribution of different types of joints (e.g., scarf or butt joints) or fusions between bones may reflect the presence of high mechanical loadings (DUELLMAN AND TRUEB, 1986; HILDEBRAND, 1995) (Fig. IV.1-4). In *Moringua edwardsi*, fusions occur in the upper jaw (forming the solid premaxillo-ethmovomerine complex), and scarf joints, with large overlaps between bones, are present between most bones in the skull roof (Fig. IV.1- 2Bb,c). The large interorbital distance, as a result of the reduced eyes and consequently reduced orbits, also improves skull fortification.

### MORPHOLOGY RELATED TO MINIATURIZATION?

Morphological transformations related to miniaturization, rather than to head-first burrowing, cannot be excluded, as miniaturization frequently occurs in burrowing vertebrates (HANKEN, 1993; RIEPEL, 1996). Elongation of the body, reduction of limbs, and dental and cranial transformation (reduction in skull size, hypertrophy of the adductor mandibulae complex, hyperossification) are also characteristic features of many miniaturized taxa, including caecilia (e.g., *Idiocranium russelli*) and lizards (e.g., *Dibamus novaeguineae*; HANKEN, 1993). Hyperossification is frequently interpreted as compensation for mechanical weakening (due to decrease in body size and reduction of bones). Large coronoid processes have also been explained in the context of miniaturization. Isometric reduction of skull size would imply shortening of jaw muscle fibres, thus compromising their functionality (HANKEN, 1993). The formation of a higher coronoid process, combined with a posterior expansion of jaw muscle insertion, increases biting force within a smaller spatial design. RIEPEL (1996) concludes however that such cranial transformations in miniaturized lizards are consequences of a burrowing lifestyle and not due to miniaturization. However, for *Moringua edwardsi* it is not clear whether the observed

features are related to one of both, or both. The fact that paedomorphosis, which frequently co-occurs with miniaturization (RIEPEL, 1996), seems to be absent in *Moringua edwardsi*, might suggest a closer relation with the burrowing (and feeding) lifestyle.

### MORPHOLOGY RELATED TO FEEDING HABITS AND PREY CAPTURE?

Rotational feeding - As mentioned above, limblessness and body elongation in vertebrates frequently co-occurs with rotational feeding and has been observed both in teleosts (e.g., *Anguilla anguilla*) and tetrapods (e.g., caecilians) (DUELLMAN AND TRUEB, 1986; HELFMAN AND CLARK, 1986). Here, spinning movements of the elongated body are coupled to a powerful grasping of the prey. The physical coupling of epaxials and jaw muscles could thus be considered an advantage for transferring forces from the body onto the head. The insertion of the lateral fibres of the epaxials onto an aponeurosis, separating it from the jaw muscles, has been observed in caecilians, *Anguilla anguilla* and *Monopterus* (LIEM, 1980). The same is the case for *Moringua edwardsi*. Additionally, in this species the spatial constraints for the insertion of the epaxials, due to the jaw muscle hypertrophy, are circumvented by the expansion of the latter aponeurosis (Fig. IV.1- 2D).

Rotational feeding also requires a solid grip onto the prey, which is enhanced in caecilians, *Anguilla anguilla*, and in *Moringua edwardsi* due to the presence of setiform or recurved teeth on both upper and lower jaws. However, a solid grip during rotations requires an increased structural rigidity of the jaws to resist torque forces, especially at the level of their attachment onto the neurocranium. The fusion of the upper jaw bones (see above), as well as the neurocranium, solid lower jaw and suspensorium can assist in resisting these forces. The absence of a direct, rigid connection between the anterior part of the suspensorium and the neurocranium (as the pterygoid has become decoupled from the hyomandibulo-quadrates) may seem to contradict this. However, modelling of forces has shown that in catfishes, which also lack this connection, the suspensorium and lower jaw articulation can resist elevated forces simply by the way they are positioned and shaped (HERREL ET AL., 2002). The occurrence of the extensive lap joints in the skull roof of *Moringua edwardsi* undoubtedly attribute to the neurocranial rigidity.

The lower jaw may also be prevented from being dislodged thanks to the hypertrophied jaw muscle complex, in combination with the large coronoid process. Not only the jaw muscle size, but also the orientation of the different bundles composing this complex may attribute (Fig. IV.1- 7B). A surprising feature of the jaw muscle morphology is the anteriorly directed A2d and A3, combined with the posteriorly directed A2m and A2v (Fig. IV.1- 7B). Consequently, their corresponding forces, i.e., F3 and F2, respectively,

generate an adduction component (F2v and F3v) and a component working onto the lower jaw articulation (F2h and F3h) (Fig. IV.1- 8). The latter two thus point in opposite directions and partially neutralize each other. This prevents dislocation of the joint, even though large forces are exerted that can assist in resisting torque forces during rotational feeding (P Aerts, pers comm). Rotational feeding is known for *Monopterus* and *Synbranchus* as well (LIEM, 1980). The morphological convergence with *Moringua edwardsi* is striking: the adductor mandibulae complex is hypertrophied and the anterior fibres of the A2 are anteriorly directed as well. The statement of LIEM (1980) considering rotational feeding in *Monopterus* “Once prey is captured, the highly hypertrophied adductor mandibulae complex plays a key role in conjunction with the corkscrew-like twisting motion of the body in breaking up the prey into pieces” confirms our assumptions.

Body elongation, reduction of the eyes, modified cranial lateral line system, and modified skull shape (pointed though firm) can be considered as specializations with respect to head-first burrowing. Hyperossification can probably be regarded more of a specialization for head-first burrowing and feeding, even though an impact of miniaturization cannot be excluded. Hypertrophied adductor mandibulae muscles and the enlarged coronoid process can be associated with both feeding requirements (enables bite forces necessary for their predatory behavior) and with a burrowing lifestyle, as well as miniaturization.

#### MORPHOLOGY OF THE CAUDAL FIN RELATED TO BURROWING?

As *M. edwardsi* burrows head-first, no extreme morphological specializations in the caudal fin are expected. *A. anguilla* and *C. conger* are non-burrowing species and basal anguilliforms (BELOUZE, 2001). The morphology of the caudal fin of *M. edwardsi* is generally similar to that of *A. anguilla* and *C. conger* (IV.4.4): interradials are present, caudal fin rays are long and movable, the caudal skeleton is not extremely fortified or fused. This, in contrast to tail-first burrowing species (IV.2- 3).

However, an interesting difference can be observed at the level of the confluent median fins. The immature specimens of *M. edwardsi* live permanently burrowed (GORDON, 1954; GOSLINE, 1956). As the anal and dorsal fins are low, the confluence of the median fins is less apparent in immature specimens (Fig. IV.1- 10). When specimens switch from a burrowing lifestyle (as juveniles) to a pelagic lifestyle (as adults), the height of the anal and dorsal fins increase (SMITH AND CASTLE, 1972). These morphological modifications may indicate the importance of confluent and high unpaired fins in a pelagic lifestyle to be able to generate propulsion during swimming or to maneuver.

## ACKNOWLEDGMENTS

---

Thanks to P Aerts (Antwerp University, Belgium) and J Webb (Villanova University, USA) for discussing the paper and offering valuable suggestions. We thank KE Hartel of the Museum of Comparative Zoology (Harvard University) for offering museum specimens. Research was partially funded by the FWO (G. 0388.00).





## **IV.2 TAIL-FIRST BURROWING SPECIES: HETEROCONGRINAE**



# MORPHOLOGICAL SPECIALIZATIONS IN HETEROCONGRINAE (ANGUILLIFORMES: CONGRIDAE) RELATED TO BURROWING AND FEEDING?

---

Modified from the paper published as:

De Schepper N, De Kegel B, Adriaens. *accepted*.

Morphological Specializations in Heterocongrinae (Anguilliformes: Congridae) Related  
to Burrowing and Feeding?  
*Journal of Morphology accepted*

## ABSTRACT

---

The remarkable lifestyle of heterocongrines has drawn the attention of many authors in the past, though no or little attention has been paid to the morphology of the caudal fin and the head of these species. In order to examine the true nature of possible morphological specializations of the head and caudal fin and their relation to their tail-first burrowing habit and/or feeding mode, a detailed myological and osteological study of *Heteroconger hassi* and *Heteroconger longissimus* was performed. The osteological similarities of the cranial skeleton between *H. hassi* and *H. longissimus* are striking. Most of the cranial muscles show no variation in presence, insertion or origin among these two species except for the adductor mandibulae complex, the adductor hyomandibulae and the intermandibularis. The adductor mandibulae complex is small, compared to other anguilliform species, and is probably related to their suction-dominated feeding mode and a diet, comprising mainly small, soft prey items. Heterocongrinae have undergone several morphological specializations in the caudal fin for their tail-first burrowing lifestyle. The skeleton and musculature of the caudal fin of *H. hassi* and *H. longissimus* are similar. In both species the caudal skeleton is highly reduced and fortified, forming a firm, pointed burrowing tool. Intrinsic caudal musculature is reduced and some muscles (interradials, supracarinalis) are even absent.

## INTRODUCTION

---

Congridae are found worldwide in tropical and subtropical latitudes and are one of the largest and most diverse families of the Anguilliformes (SMITH, 1989B, BELOUZE, 2001). Except for the heterocongrine subfamily, Congridae are bottom dwellers that feed on a variety of fishes and invertebrates (SMITH, 1989B).

Heterocongrinae are a subfamily of the Congridae (SMITH, 1989B) and are the most distinct of the congrids, and among the few that show conspicuous morphological specializations related to their tail-first burrowing lifestyle. The taxonomy of Heterocongrinae has been ambiguous in the past, although recently two genera were recognized: *Heteroconger* and *Gorgasia* (CASTLE, 1999; CASTLE AND RANDALL, 1999). *Gorgasia* is regarded as the most primitive genus of the Heterocongrinae (TYLER AND SMITH, 1992; CASTLE AND RANDALL, 1999). Garden eels live in large colonies. Each individual lives permanent in separate, strengthened burrows, in sandy or silty-sand substrate (CASIMIR AND FRICKE, 1971; SMITH, 1989B). They project the front portion of the body from the burrow to feed on zooplankton (CASIMIR AND FRICKE, 1971; SMITH, 1989B). They are able to withdraw entirely into their burrows but mostly they emerge three-fourths or more of their length from the burrow opening, while the caudal fin remains inserted, their heads turned to the plankton-loaded currents to snap and pick small zooplanktonic particles (BATH, 1960; SMITH, 1989B; VIGLIOLA ET AL., 1996; CASTLE AND RANDALL, 1999). Heterocongrinae feed mainly on copepods (66.3 % of total stomach content volume). Tunicates form 18.6 % of the stomach contents and the remaining part consists of pteropods, ostracods, shrimp larvae, unidentified eggs and copepod larvae (SMITH, 1989B).

This study is part of an ongoing project that deals with evolutionary trade-offs related to head- and tail-first burrowing. In this case-study the cranial and caudal morphology of true head-first burrowers are examined. So, morphological constraints are predominantly expected in the caudal fin morphology as no fortification constraints on the skull are required. We hypothesize that 1) marked specializations in the musculo-skeletal system of the caudal fin are present to cope with and generate large mechanical forces, and 2) the cranial musculo-skeletal system is not specialized, as suction-feeding is applied by these species.

The remarkable lifestyle of heterocongrines has drawn the attention of many authors in the past, although no attention has been paid to the musculature of the caudal fin and the head. In order to examine the true nature of morphological specializations of the head and caudal fin a detailed myological and osteological study of *Heteroconger hassi* and *H. longissimus* was performed. First, the cranial morphology is described for

*Heteroconger hassi* into detail and subsequently a brief survey of the observed cranial morphological differences in *Heteroconger longissimus* is given. Second, the detailed morphological description of the caudal fin of *Heteroconger hassi* is given and subsequently compared with that of *Heteroconger longissimus*. The relation between cranial morphology and feeding mode on the one hand and between morphology of the caudal fin and tail-first burrowing on the other hand are discussed in order to understand possible structural specializations of the systems involved.

## MATERIAL AND METHODS

---

For this study four specimens of *Heteroconger longissimus* (total length varies between 225 mm and 268 mm) and five *Heteroconger hassi* (218 mm and 286 mm) were used. All specimens were preserved in ethanol (70%). *Heteroconger longissimus* specimens were obtained from the Smithsonian National Museum of Natural History - Washington (USNM 316037). Specimens of *H. hassi* were commercially obtained (Moeskroen, Belgium) and deposited in the Zoological Museum at Ghent University (UGMD 175374). A detailed description of the osteological features of the head morphology of *H. longissimus* is provided by BÖHLKE (1957) and SMITH (1989B). See chapter III.1 for details on specimens (Table III.1- 1A). In this study, specimens were anaesthetized, sacrificed and fixed (see III.2.1). Some specimens were cleared and stained, dissected, serial sections were made and a CT-scanning and 3D-reconstructions was performed (see III.2.2 and III.2.5).

## RESULTS

---

### HEAD OSTEOLOGY: *HETEROCONGER HASSI*

The *ethmoid region and upper jaw* is composed of the massive premaxillo-ethmovomerine complex, formed by ankylosed premaxillaries, mesethmoid and vomer (Fig. IV.2- 1). Ethmoid processes are absent. The lateral process of the pars vomeralis is well developed and elevated, bearing the vomero-ptyergoidal articular facet, to which the pterygoid is connected (Fig. IV.2- 1C). The anterior part of the maxillary bears small ventral and dorsal processes, which rest in the anterior and posterior maxillo-premaxillo-ethmovomerine articular facets on the premaxillo-ethmovomerine complex respectively (Fig. IV.2- 1A, B). The posterior teeth of the maxilla are markedly enlarged and pointed forward.

The *orbital region* comprises the basisphenoid, frontals and pterosphenoids (Fig. IV.2- 1). Orbitosphenoid is absent. An irregularly shaped cartilage is present in front of the orbit. A relatively small, unpaired basisphenoid borders the ventro-posterior edge of the orbits. A small medial basisphenoidal process, directed towards the orbits, serves for the attachment of some of the eye muscles (Fig. IV.2- 1A). The frontals occupy the largest part of the skull roof and have fused. The tips of the frontals taper rostrally and are dorsally covered by the dorso-caudal projection of the pars ethmoidalis. The dorso-caudal border of the orbits is formed by the rostral part of the frontals. Above the caudal margin of the orbit, the frontals bear a groove for the entrance of the supraorbital canal (Fig. IV.2- 1B). The pterosphenoids borders the ventro-caudal margin of the orbits. The parasphenoid spans from the orbital region to the occipital region forming the longest cranial element in ventral aspect. Two symmetrical, latero-dorsal projections stretch towards the sphenotics, where it reaches its highest width. The anterior part of the parasphenoid borders the orbits ventrally and is in this region extremely narrow. Caudally, the parasphenoid splits into two long, narrow arms, i.e. the parasphenoidal processes.

The *otic region* comprises the sphenotics, pterotics, prootics, epiotics and parietals (Fig. IV.2- 1). The sphenotics are situated latero-dorsally and bear an extensive sphenotic process or sphenotic wing (Fig. IV.2- 1B). The posterior part of this sphenotic process contributes to the anterior suspensorial articulation facet (Fig. IV.2- 1C). The paired pterotics, bearing a large anterior process, form a large part of the lateral skull wall and house the otic canals (Fig. IV.2- 10A). The posterior suspensorial articulatory facet is formed by the pterotics (Fig. IV.2- 1C). The prootics, the pterotics and sphenotics contribute to the suspensorial articulatory groove. The prootics are situated latero-ventrally. The prootics, basioccipital and exoccipitals are expanded to form otic bullae. The epiotics are situated at the postero-dorsally. Both epiotics border the foramen magnum dorsally. The two parietals have a rectangular shape, rostro-caudally extended, and cover a large part of the skull roof. Both parietals contact in the midline.

The *occipital region* comprises the exoccipitals, basioccipital and supraoccipital. The ventral border of the foramen magnum is formed by the unpaired basioccipital. The exoccipitals surround the foramen magnum dorso-laterally and form the ventro-lateral part of the cranium in caudal view. Two exoccipital processes are present caudo-laterally. The unpaired medial supraoccipital is situated dorso-caudally, in front of the caudal border of the skull, and lacks a ridge and spiny projections.

The *suspensorium* comprises three bones, the hyomandibula, quadrate and pterygoid (Fig. IV.2- 2C). The preopercle is described with respect to the opercular apparatus. The hyomandibula and quadrate are strongly connected, forming a massive,

strong trapezoidal entity, which is elongate and forwardly inclined. The lateral surfaces show slightly elevated ridges for the insertion of the adductor mandibulae complex. The anterior and posterior dorsal articulatory condyles fit into the anterior and posterior suspensorial articulatory facets of the neurocranium, respectively (Fig. IV.2- 1A). The hyomandibula bears the opercular articular condyl dorso-caudally for the articulation with the operculare. The posterior part of the hyomandibula is connected to the posterior ceratohyal by a strong ligament. The quadrate bears the mandibular articulation condyle. The pterygoid is a slender, elongate bone. The rostral tip of the bone is ligamentously connected to the vomero-ptyerygoidal articulatory facet on the pars vomeralis.

The *opercular apparatus* comprises four bones (opercle, preopercle, interopercle and subopercle, Fig. IV.2- 2D). The preopercle is situated rostrally. Its anterior edge is tightly connected to the hyomandibula through dense connective tissue (Fig. IV.2- 10A). The interopercle has an approximately triangular shape and is elongated in the rostro-caudal axis. Rostrally, this element is concealed by the caudal part of the preopercle. The curved subopercle follows the caudal edge of the opercle, to which it is firmly attached by dense connective tissue, both elements the level of the fourth vertebra. The fan-shaped opercle articulates by means of the rostro-dorsal opercular articulation facet with the dorsal opercular condyle of the hyomandibula. This facet is situated at the distal end of the rostro-dorsal process of the opercle (Fig. IV.2- 2D).

The *lower jaw* is longer than the upper jaw (Figs. IV.2- 1, 2B). The anterior and largest part of the lower jaw is formed by the dentary. The caudo-dorsal edge of this part bears the small coronoid process. The dentary encloses the Meckel's cartilage anteriorly and covers its posterior part laterally. The posterior part of the lower jaw consists of the fusion of retroarticular, articular and angular bones (TAVERNE, 1999), referred to as the angular complex. The angular complex is pointed anteriorly and partially enclosed by the dentary. The retroarticular process is short and directed caudally. The mandibular articulation facet, ventral to the angular process, involves the articulation between the angular complex and the quadrate.

The *hyoid apparatus* comprises an unpaired median basihyal and urohyal and paired anterior ceratohyals and posterior ceratohyals (Figs. IV.2- 2A, 5). Hypohyals are absent, an observation that was confirmed using the serial histological sections. The basihyal is a long, cylindrical element. It articulates on both sides with the anterior ceratohyals and ventrally with the rostral tip of the urohyal. Caudally, the urohyal tapers and ends in a trifold process (in lateral view), which mediates the insertion of the sternohyoid tendon. A total of 16 to 22 branchiostegal rays are supported by the anterior ceratohyal and posterior ceratohyal (Fig. IV.2- 5A, C). The branchiostegal rays are dorsally curved and reach up to

the caudal border of the opercle. The anterior ceratohyal occupies the largest part of the hyoid arch and anteriorly bears the articulation facet for the basihyal, urohyal and contralateral hyoid arch.

The cephalic lateral line system has the usual major components as in all congrid (SMITH, 1989B): the supra- and infraorbital canals, ethmoid canals, otic canals, mandibular canals, preopercular canals, and supratemporal commissure (Fig. IV.2- 2E). The supratemporal commissure has no pore. The otic canals run rostrally through the pterotics and anteriorly branch in the supraorbital and infraorbital canals. The infraorbitals course forward to the tip of the snout, partially over the lateral surface of the frontals and along the edge of the ethmo-vomerine complex. These canals are supported by three postorbitals caudal to the eyes, two suborbitals below the eyes and one preorbital in front of the eyes. All these ossifications are small, reduced, irregular and tube-like but open above. The supraorbital canal has no frontal commissure and no median dorsal frontal pore. This canal runs shortly through the frontal bone and is anteriorly supported by the nasal (Fig. IV.2- 1B). The ethmoid canal ends in one pore. The mandibular and preopercular canals run through the lower jaw and preopercular respectively.

#### HEAD MYOLOGY: *HETEROCONGER HASSI*

Adductor mandibulae complex - This complex comprises three parts, their fibres only partially separated (Figs. IV.2- 3, 4). It is difficult to distinguish the different components of the complex but based on the terminology of WINTERBOTTOM (1974) the following subdivisions can be recognized: A2, A3 and A $\omega$ . The absence of a muscular or tendinous connection with the maxilla or primordial ligament suggests that the A1 is absent. The left and right halves are not connected in the midline (Fig. IV.2- 10A). The A $\omega$  is present though very small. It inserts through a tendon on the medial surface of the dentary (Fig. IV.2- 5A). This tendon fuses posteriorly with the A2. The A2 is situated laterally and comprises the largest part of the complex. The A2 inserts tendinously on the dorsal edge and the lateral side of the coronoid process. It originates muscularly from the lateral surface of the quadrate, frontal, pterosphenoid, sphenotic, pterotic, parietal and epiotic (Fig. IV.2- 3A). Ventrally the fibres even reach the preopercle. The fibres of A3 merge caudally with those of the A2. The A3 is the most medial part of the complex, inserting tendinously onto the medial surface of the dentary and originating from the lateral surface of the pterosphenoid and antero-lateral surface of the sphenotic (Fig. IV.2- 5A).



Levator arcus palatini - The apex of this muscle points dorsally and the fibres diverge ventrally (Fig. IV.2- 3B). The tendinous origin includes the lateral and ventral surface of the sphenotic process. This tendon is situated internally in the (bipennate) muscle. The fibres insert muscularly on the lateral surface of the pterygoid, hyomandibula and quadrate (Fig. IV.2- 5A).

Adductor arcus palatini - This muscle forms the floor of the orbits (Fig. IV.2- 3). The fibres originate muscularly from the ventral surface of prootic and ventral surface of the parasphenoid, lateral to its median ridge, which separates the left and right parts of the muscle. The muscle inserts muscularly on the caudo-medial surface of the pterygoid and the medial surface of the hyomandibula (Fig. IV.2- 5A). The fibres are directed rostro-laterally. The anterior margin is situated at one fourth of the length of the orbit.

Adductor hyomandibulae - This muscle is situated caudally to the adductor arcus palatini (Fig. IV.2- 5A). The muscle tapers caudally, with its origin on the prootic. It inserts on the medial surface of the hyomandibula. Its anterior margin is situated at the level of the anterior suspensorial articulatory facet.

Levator operculi - The fibres of the levator operculi are directed caudo-ventrally (Fig. IV.2- 3A). Its tendon originates from the pterotic, just behind the caudal margin of the adductor mandibulae complex. The fibres insert muscularly on the lateral surface, up to its ventro-lateral border, and the dorsal edge of the opercle.

*Dilatator operculi* This muscle has a conical shape, with the apex pointing caudo-ventrally (Fig. IV.2- 3C). The site of origin comprises the caudo-lateral surface of the sphenotic and the ventro-lateral surface of the pterotic. Internally a tendon is present which inserts on the lateral surface of the rostro-dorsal process of the opercle.

Adductor operculi - This muscle originates muscularly from the ventro-lateral surface of the prootic and exoccipitals (Fig. IV.2- 3C). No tendons are present. The fibres insert on the medial surface of the opercle (Fig. IV.2- 5A). The insertion site varies from the surface just beneath the dorsal edge of the opercle or may extend to the middle of the opercle.

Intermandibularis - The intermandibularis is present (Fig. IV.2- 3B; 5). This small muscle runs transversely between the medial surfaces of the left and right dentary.

Protractor hyoidei - This muscle connects the lower jaw to the hyoid arch (Fig. IV.2- 3; 5). The fibres are directed rostro-caudally. The fibres insert tendinously on the latero-ventral surface of the posterior ceratohyal, and the rostro-ventral edge of the interopercle. The protractor hyoidei originates tendinously from the ventro-medial surface of the dentary, just behind the dental symphysis (Fig. IV.2- 5). The left and right bundles are separated over their whole length.

*Sternohyoideus* This muscle consists of three myomeres, divided by two myocommata. The left and right, strong, well-developed tendons insert on the lateral surfaces of the caudal trifold end of the urohyal (Fig. IV.2- 5A, B). The posterior fibres of the sternohyoideus are muscularly attached to the lateral surface of the ventro-rostral projection of the cleithrum. The sternohyoideus merges ventro-caudally with the hypaxial muscles by means of a myocomma.

Hyohyoideus - The hyohyoideus inferioris is present (following the nomenclature of WINTERBOTTOM, 1974) and arises from an aponeurosis in the ventral midline (Fig. IV.2- 5C, 7D). The medial fibres run to the ventro-lateral surface of the anterior ceratohyal, whereas the ventral fibres radiate, attaching to dorso-medial surface of branchiostegal rays. The hyohyoidei adductores surround the gill chamber ventrally, forming a 'sac-like' muscle sheet, situated just beneath the opercular system and above the branchiostegal rays (Figs. IV.2- 3, 5B, C). This sheet attaches to the medial surface of the opercle, and more caudally, attaches to the horizontal septum (ventral to the epaxial muscles). At the level of the opercle, the sheet is interrupted by the insertion of the adductor operculi. The sheet continues ventrally, dorsal to the rays, the opposite halves meeting in the midline. As it is difficult to differentiate the hyohyoideus abductor from the hyohyoidei adductores, the hyohyoidei abductores may be absent or not differentiated. Ontogenetic series are necessary to resolve this.

Epaxials - These muscles attach to the exoccipitals and supraoccipital (Fig. IV.2-3A, C). No aponeurotic connection between the adductor mandibulae complex and the epaxials is present.

Hypaxials - The fibres of the hypaxials attach to the basioccipital, the horizontal septum and the myocomma of the sternohyoideus.

#### INTERSPECIFIC VARIATION IN CRANIAL MORPHOLOGY (*HETEROCONGER HASSI* COMPARED WITH *H. LONGISSIMUS*)

The osteological similarities of the cranial skeleton between *Heteroconger hassi* and *H. longissimus* are striking (Fig. IV.2- 6). Minor differences are found at the level of the suspensorium. The pterygoid of *H. longissimus* is broader, compared to its slender shape in *H. hassi*. The elevated ridge on the lateral surface of the hyomandibula is present in *H. longissimus*, though it is larger in *H. hassi*.

Most of the cranial muscles show no variation in presence, insertion or origin among these two species except for the adductor mandibulae complex, the adductor hyomandibulae and the intermandibularis (Fig. IV.2- 7). The adductor mandibulae complex in both species is considerably smaller compared to several other anguilliform species

(e.g., *Moringua edwardsi*, DE SCHEPPER ET AL., 2005, (IV.1), Fig. IV.2- 10C). Comparisons among both heterocongrid species reveals that the origin of the adductor mandibulae complex includes the same structures (quadrate, frontal, pterosphenoid, sphenotic, pterotic, parietal and preopercle), though species vary in size and volume of the jaw muscles. In *H. longissimus* the origin of the jaw muscles is smaller anteriorly as well as caudally compared to that of *H. hassi*: the antero-dorsal margin is restricted to a very small part of the ventro-caudal margin of the frontal; the dorsal fibres originate lower on the latero-ventral surface of the parietals; caudally no fibres reach the epiotics and a larger part of the caudal surface of the pterotic is not part of the insertion site (Fig. IV.2- 3A, 7A). In cross section the jaw muscles appear as a thin sheet of fibres, so it becomes clear that the volume of the jaw muscles in *H. longissimus* is smaller as well (Fig. IV.2- 10B). The adductor hyomandibulae shows interspecific variation as well (Fig. IV.2- 10B). Its anterior margin is situated in front of the anterior suspensorial articulation condyle of the hyomandibula, whereas in *H. hassi* this is situated behind this articulation. The intermandibularis, which is present in *H. hassi*, is absent in *H. longissimus*. The hyohyoideus of *H. hassi* forms a large, thick muscle mass and occupies the ventro-lateral surface of the branchial region. It comprises two parts, defined as hyohyoideus inferioris and hyohyoidei adductores. It is not clear whether the hyohyoideus abductor is fused with the hyohyoidei adductores or whether it is not yet completely differentiated, taking into account the basal phylogenetical position of the Anguilliformes. In *H. longissimus* the hyohyoideus inferioris and adductores are similar in origin and insertion sites, though the hyohyoideus inferioris is smaller in *H. longissimus* (Fig. IV.2-7D). Furthermore, the anterior margin of the hyohyoideus inferioris is anteriorly displaced in *H. longissimus*.

#### CAUDAL FIN OSTEOLOGY: *HETEROCONGER HASSI*

The caudal fin is reduced (Fig. IV.2- 8A). Six caudal fin rays are present, though not visible from the outside. They are covered by thick layer of soft tissue. The anal and dorsal fins are confluent with the caudal fin rays. Caudal fin rays are supported by hypurals whereas dorsal and anal fin rays are supported by pterygiophores. The caudal skeleton comprises a dorsal hypural plate (fused hypurals 3 and 4) and a ventral hypural plate (fused hypurals 1 and 2). A hypural fenestra is present in the latter. The first preural vertebra is situated in front of the caudal skeleton. The boundary between preural and ural vertebrae is marked by the bifurcation point of the dorsal aorta, as could be observed in the serial sections. The parhypural, modified hemal spine of the first preural centrum, is the last hemal spine crossed by the dorsal aorta. The urostyle, formed by the fusion of the

first and second ural vertebrae, bears one pair of uroneurals, as is found in all Anguilliformes (GOSLINE, 1971). The ventral hypural plate bears strongly developed hypurapophyses on both sides. The epural is absent. The neural canal of the first preural centrum is bordered laterally by the left and right bases of the neural arch. The neural arch is not fused in the midline. The base of the arch is as wide as the centrum. The neural spine is lacking. Neural and haemal spines are absent in the preceding caudal vertebrae. In some cases, one vertebra may bear two neural arches and two hemal arches. This may indicate the fusion of two vertebrae during development.

#### CAUDAL FIN MYOLOGY: *HETEROCONGER HASSI*

Interradials are absent (Fig. IV.2- 8). The flexor dorsalis originates from the lateral surface of the uroneural and inserts onto the four uppermost caudal fin rays through a tendinous sheet (Fig. IV.2- 8C). The hypochordal longitudinalis originates from the lateral surface of the ventral hypural plate and passes to the lateral surface of the dorsal hypural plate (Fig. IV.2- 8D). Both origin and insertion are tendinous. The flexor ventralis originates from the lateral surface of the parhypurapophysis and lateral surface of the ventral hypural plate and inserts through a tendon on the three ventral caudal fin rays (Fig. IV.2- 8C). The proximalis is situated medial to the hypochordal longitudinalis (Fig. IV.2- 8E). This muscle runs from the hypurapophysis to the lateral surface of the ventral and dorsal hypural plate. The body musculature, epaxials en hypaxials, is attached to the base of the caudal fin rays by broad tendinous sheets (Fig. IV.2- 8B).

#### INTERSPECIFIC VARIATION IN CAUDAL FIN MORPHOLOGY (*HETEROCONGER HASSI* COMPARED WITH *H. LONGISSIMUS*)

The skeleton and musculature of the caudal fin of *Heteroconger hassi* and *H. longissimus* are similar. In both species the caudal skeleton is highly reduced and fortified, forming a firm pointed burrow tool. Some small differences are found in the flexor dorsalis (Fig. IV.2- 9C). The anterior margin of the flexor dorsalis of *H. longissimus* is situated more anteriorly, where it reaches the anterior margin of the uroneural. The insertion site of the flexor dorsalis is restricted to the dorsal caudal fin rays in *H. longissimus* whereas in *H. hassi* its tendon additionally inserts onto the first ventral caudal fin ray below the midline.

## DISCUSSION

---

### MORPHOLOGY RELATED TO FEEDING

*Heteroconger hassi* and *H. longissimus* are plankton feeders. This feeding style is reflected in the morphology of Heterocongrinae as stated by ROSENBLATT (1967), SMITH (1989B) and CASTLE AND RANDALL (1999): one of the principal characteristics is the shortening of the snout, which brings the extremely large eyes closer to the tip, allowing close-up binocular vision. Their vision is assumed to be additionally improved by the presence of anteriorly elongated pupils (SMITH, 1989B). The mouth, which is small and oblique as in planktonic feeding serranids (e.g., *Paranthias*) and embiotocids (e.g., *Brachyistius*). This is regarded as a specialization for snapping planktonic prey (ROSENBLATT, 1967). The skin of the throat covering the pharyngeal cavity shows grooves and folds. SMITH (1989B) stated that these folds indicate the possibility of a considerable expansion of the former, improving buccal expansions during suction feeding, necessary to catch prey from the passing current. Personal observations of feeding *H. hassi* confirm that prey capture occurs predominantly by suction as the predator's head moves slowly towards the prey item while the prey is drawn rapidly towards the mouth as the result of rapid depression of the mouth floor, thus expanding the mouth and creating suction (LIEM, 1980). Prey items are ingested intact. As heterocongrines have a suction-dominated feeding mode, mainly on small, soft prey items, (SMITH, 1989B), no powerful bite is required (BAREL, 1983; VAN WASSENBERGH ET AL., 2005). Consequently no hypertrophied jaw muscles are needed and no special structural reinforcements at the level of oral skeletal elements (e.g., dentary, suspensorium and neurocranium) to resist increased mechanical loads, are required (BAREL, 1983; VAN WASSENBERGH ET AL., 2005).

*Adductor mandibulae complex* - The feeding mode in *Heteroconger hassi* and *H. longissimus* is reflected in the configuration of the adductor mandibulae complex. This mouth closing muscle complex is small and the comprising subdivisions form one unit. The two halves do not meet dorsally. So, in contrast to other anguilliform species which have hypertrophied jaw muscles and which all are predators (e.g., in Anguillidae, Muraenidae, Congridae, Ophichthidae, Moringuidae, etc...), *H. hassi* and *H. longissimus* have no hypertrophied mouth-closing muscles (BÖHLKE ET AL., 1989; MCCOSKER ET AL., 1989; SMITH, 1989A, B; DE SCHEPPER ET AL., 2005) (IV.1). Hypertrophied adductor mandibulae muscles provide a powerful bite, thus implying an increased mechanical load on skeletal elements such as dentary, suspensorium and neurocranium (HERREL ET AL., 2002; VAN WASSENBERGH ET

AL., 2004). As mentioned above, a strong bite is not needed in *H. hassi* and *H. longissimus*. Thus, small mouth closing muscles, without special structural reinforcements (e.g. dentary, suspensorium and neurocranium), presumably serve their needs (Fig. IV.2- 10A, B). Because 1) a predatory lifestyle represents the primitive condition of the Anguilliformes (GOSLINE, 1971; SMITH, 1989B), 2) hypertrophied jaw muscles and thus a strong bite are advantageous for predation (VAN WASSENBERGH ET AL., 2005), and 3) hypertrophied jaw muscles are frequent in Anguilliformes (BÖHLKE, 1989), the question should be raised whether the presence of hypertrophied jaw muscles is the plesiomorphic condition in the Anguilliformes. This implies that the configuration of the jaw muscles of *H. hassi* and *H. longissimus* represents a derived condition. Of course such assumptions have to be tested.

*Spatial impact of large eyes - Heteroconger hassi* and *H. longissimus* are visual predators of small planktonic prey (CASTLE AND RANDALL, 1999). This requires the presence of well-developed, large eyes. As they burrow tail-first and retreat in burrows with a wider diameter than their body (TYLER AND SMITH, 1992), the eyes of *H. hassi* and *H. longissimus* need no special protection for mechanical injuries during substrate contact. This is in contrast to most head-first burrowers, which have reduced eyes (BOZZANO, 2003; DE SCHEPPER ET AL., 2005) (IV.1). The size of the eyes may have a substantial impact on the spatial design of the skull (BAREL, 1984). We may assume that the large eyes in *H. hassi* and *H. longissimus* are related to the smaller interorbital space of the neurocranium. Consequently, narrowing of the skull involves reduction in strength. Focussing on the sessile lifestyle of this species, a strong skull to resist external forces (e.g. during burrowing) or to resist large mechanical loads from muscle insertions (e.g. hypertrophied jaw muscles) are not required. Furthermore the large eyes limit the space for the adductor mandibulae complex and adductor arcus palatini. Ventral to the eyes the adductor mandibulae appears as a compact mass which is dorsally restricted by the large eyes. Underneath the eyes the adductor arcus palatini appears as a thin muscle plate. Behind the eyes, a dorsal expansion of this muscle can be observed.

#### MORPHOLOGY RELATED TO TAIL-FIRST BURROWING

Anguilliform species are primitively adapted for wedging through small openings (GOSLINE, 1971; SMITH, 1989B). However, several anguilliform eels have evolved adaptations to a range of different lifestyles. Some are pelagic, others are adapted to burrowing lifestyles, from head-first (*Moringua*, *Neoconger*) to tail-first (Heterocongrinae, Ophichtidae). The true head-first burrowing anguilliform species (e.g. *Moringua edwardsi*)

have a conical, strengthened skull (DE SCHEPPER ET AL., 2005) (IV.1). Conversely, extremely fortified skulls to resist large compressive forces during burrowing (GANS, 1975; HANKEN, 1983; DUELLMAN AND TRUEB, 1986; POUGH ET AL., 1998) are unnecessary in non-burrowing or tail-first burrowing species. Since *H. hassi* and *H. longissimus* burrow tail-first, the observed reduced skull fortification (thin, non-overlapping bones) may be sufficient considering its sessile lifestyle.

Heterocongrinae have undergone several morphological specializations for their tail-first burrowing lifestyle: the caudal fin is reduced to a stiff fleshy point (CASTLE AND RANDALL, 1999); the caudal skeleton is firm and strengthened, lacking an externally visible caudal fin; the caudal fin rays (reduced in size and number), externally invisible, are covered with muscles, connective tissue and thick skin, resulting in a pointed, burrowing tool. All this appears to provide an advantage to tail-first burrowing. Similar external caudal fin morphology, modified to enable the excavation of burrows tail-first, is observed in ophichthid eels (TILAK AND KANJI, 1969; SUBRAMANIAN, 1984; ATKINSON AND TAYLOR, 1991; DE SCHEPPER ET AL., 2007) (IV.3). Considering the reduction of the caudal skeleton of *Heteroconger hassi* and *H. longissimus*, highly reduced caudal fin musculature could be expected. Furthermore, subtle movements of individual fin rays to generate propulsion or to maneuver are not needed because 1) a strong, stiff caudal fin is needed to penetrate the substrate tail-first and 2) they rarely leave their burrows and consequently they seldom swim (ROSENBLATT, 1967; CASTLE AND RANDALL, 1999). More over, flexible and movable fin rays might even be disadvantageous during tail-first burrowing as reduction of strength of the tail tip or damage during burrowing might occur. Thus, complex caudal fin musculature as observed in generalized teleosts (LAUDER AND DRUCKER, 2004) is no longer required.

In teleosts the caudal fin musculature generally allows a precise control of caudal fin movements through caudal fin conformation (LAUDER AND DRUCKER, 2004). The interradials generally interconnect and adduct caudal fin rays, reducing the caudal fin area in teleosts (WINTERBOTTOM, 1974). In *Heteroconger hassi* and *H. longissimus* these muscles are completely absent. Consequently, the covered caudal fin rays are immovable, increasing strength of the tail tip. In teleosts, the flexor dorsalis usually connects the last few neural spines and centra and the upper hypurals to the dorsal caudal fin rays. The flexor ventralis usually runs from the lateral surfaces of the hemal spines and arches of the last few vertebrae, parhypural and lower hypurals to the lateral bases of the ventral caudal fin rays (WINTERBOTTOM, 1974). The flexor dorsalis and flexor ventralis are known in teleosts to move the dorsal and ventral caudal fin rays separately (LAUDER AND DRUCKER, 2004). In *H. hassi* and *H. longissimus* the flexor dorsalis and ventralis are reduced in size

and the origin does not include the last few vertebrae, as the origin is restricted to the uroneurals and parhypurapophysis and ventral hypural plate, respectively. In teleosts, the hypochordal longitudinalis passes from the lower hypurals to three or four of the more dorsal fin rays in the dorsal half of the caudal fin (WINTERBOTTOM, 1974). It allows the dorsal fin margin to move separately from the ventral fin margin, turning them into the leading edge during swimming (LAUDER AND DRUCKER, 2004). It is surprising that in *H. hassi* and *H. longissimus* this muscle connects two immobile elements (ventral and dorsal hypural plates). Due to the absence of insertions onto caudal fin rays, contraction will not lead to the movement of rays, though it may offer strength, avoiding the tail-tip to bend during burrowing. Reduction and even absence of this muscle has been observed in several species with highly reduced caudal skeletons and where fine movements of separate caudal fin rays are also less important (e.g., tuna: LAUDER AND DRUCKER, 2004). The origin and insertion of the proximalis is highly variable in teleosts though it generally connects the centra of the last few vertebrae (WINTERBOTTOM, 1974). In *H. hassi* and *H. longissimus* the proximalis muscle connects the hypurapophyse to the ventral and dorsal hypural plates. The proximalis muscle and the broad tendinous insertions of the body musculature (epaxials and hypaxials) onto the caudal fin rays may strengthen the caudal fin to withstand bending forces during tail-first burrowing. Reduction or even loss of the proximalis and reduction of the insertion sites of the epaxials and hypaxials has already been observed in species where sophisticated movements of individual fin rays are no longer required (WINTERBOTTOM, 1974; LAUDER AND DRUCKER, 2004). In teleosts, the supracarinalis posterior generally connects the last basal pterygiophore of the dorsal fin to the neural spine, epurals, uroneurals or dorsal caudal fin rays, whereas the infracarinalis posterior runs from the last basal pterygiophore of the anal fin to the hemal spine of the last complete vertebrae, parhypural or ventral caudal fin rays. These muscles are not discerned in *H. hassi* and *H. longissimus* which is likely related to the fact that the dorsal, anal and caudal fins are confluent.

#### MORPHOLOGY RELATED TO MINIATURIZATION

These species are fearily small animals, though extremely elongate (with respect to other Anguilliform representatives such as *Anguilla anguilla* and *Conger conger*, IV.4.1; IV.4.3) and their head size is extremely small as well as it accounts for only 6% of the total body length (CASTLE AND RANDALL, 1999). Consequently, the some of the reductional features as discussed previously might be related to the phenomenon of miniaturization as well.



## **ACKNOWLEDGMENTS**

---

We thank the FWO (Project G.0388.00) for financing this research and the National Museum of Natural History - Smithsonian Institution (Washington) for the loan of specimens.



**IV.3 HEAD- AND TAIL-FIRST BURROWING SPECIES: *PISODONOPHIS BORO***



---

## ***PISODONOPHIS BORO* (OPHICHTHIDAE: ANGUILLIFORMES):**

### **SPECIALIZATION FOR HEAD-FIRST AND TAIL-FIRST BURROWING?**

---

Modified from the paper published as:

De Schepper N, De Kegel B, Adriaens. 2007.

*Pisodonophis boro* (Ophichthidae: Anguilliformes): Specialization for Head-First and Tail-First Burrowing?

Journal of Morphology 268(2): 112-126.

#### **ABSTRACT**

---

The rice paddy eel, *Pisodonophis boro*, is of special interest because of its peculiar burrowing habits. *Pisodonophis boro* penetrates the substrate tail-first, a technique common for ophichthids, but it is able to burrow head-first as well. *Pisodonophis boro* exhibits three feeding modes: inertial feeding, grasping and spinning. Rotational feeding is a highly specialized feeding mode, adopted by several elongate, aquatic vertebrates and it is likely that some morphological modifications are related to this feeding mode. The detailed morphology of the head and caudal fin of *Pisodonophis boro* is examined with the goal to apportion the anatomical specializations among head-first burrowing, tail-first burrowing and rotational feeding. The reduced eyes, covered with thick corneas may be beneficial for protection during head-first burrowing, but at the same time decreased visual acuity may have an impact on other sensory systems (e.g. cephalic lateral line system). The elongated and pointed shape of the skull is beneficial for substrate penetration. The cranial bones and their joints, which are fortified, are advantageous for resisting high mechanical loads during head-first burrowing. The aponeurotic connection between epaxial and jaw muscles is considered beneficial for transferring these forces from the body to the head during rotational feeding. Hypertrophied jaw muscles facilitate a powerful bite, which is required to hold prey during spinning movements and variability in the fibre angles of subdivisions of jaw muscles may be beneficial for preventing the lower jaw from being dislodged or opened. Furthermore, firm upper (premaxillo-ethmovomerine complex) and lower jaws (with robust coronoid processes) and high neurocranial rigidity are advantageous for a solid grip to hold prey during rotational feeding. The pointed shape of the tail and the consolidated caudal skeleton are beneficial for their tail-first burrowing habits. It is likely that the reduction of the caudal

musculature is related to the tail-first burrowing behavior because the subtle movements of the caudal fin rays are no longer required.

## INTRODUCTION

---

Anguilliformes is a large group of elongated, cosmopolitan teleosts (NELSON, 1994). Eels are considered to be well adapted for wedging through small openings, which is their basic mode of life (GOSLINE, 1971; SMITH, 1989B). In this regard several morphological specializations may benefit the entering of such crevices (elongated body and skull), moving back and forth (scales not overlapping or absent) or preventing sediments from entering into the gill cavities (gill openings small) (GOSLINE, 1971; SMITH, 1989B). However, several clades of Anguilliformes adopted different fossorial lifestyles: Heterocongrinae and Ophichthidae penetrate the substrate tail-first, whereas Heterenchelyidae and Moringuidae burrow head-first (CASTLE, 1968; SMITH AND CASTLE, 1972; SMITH, 1989B, C, D).

*Pisodonophis boro*, the species dealt with in this study, belongs to the family Ophichthidae (TILAK AND KANJI, 1969). Ophichthids, or snake eels, have a worldwide distribution and inhabit a wide range of different substrates, from coral reefs, to sand and mud in rivers and estuaries (MCCOSKER ET AL., 1989). This diverse group of species (> 250) live mainly burrowed in soft sediments (MCCOSKER ET AL., 1989). *P. boro* penetrates the substrate tail-first, a technique common for ophichthids, but it is able to burrow head-first as well (TILAK AND KANJI, 1969; SUBRAMANIAN, 1984; ATKINSON AND TAYLOR, 1991). *P. boro* burrows for shelter and feeding and it exhibits three feeding modes: inertial feeding, grasping and spinning (SUBRAMANIAN, 1984).

Understanding possible structural specializations of the systems involved in burrowing in *Pisodonophis boro*, i.e. the head and the caudal fin, requires a comparison at two levels. First, outgroups must be phylogenetically closely related in order to eliminate possible evolutionary shared traits (thus independent of burrowing) as much as possible. Second, outgroups must use the systems involved especially for burrowing (so adaptations for it can be expected) or not at all for burrowing (so adaptations for it can be expected to be absent). This may allow extracting indications about (1) the presence of specializations that could be adaptations for a specific way of burrowing, and (2) the possible trade-offs in the allocation of structural adaptations in the head and caudal fin. For that reason, outgroups in this study are *Moringua edwardsi* and *Heteroconger longissimus*, both Anguilliformes. *M. edwardsi* is a strict head-first burrower with a well developed caudal fin (CASTLE, 1968; SMITH AND CASTLE, 1972; SMITH, 1989D; DE SCHEPPER ET AL., 2005) (IV.1),

whereas *H. longissimus* is a strict tail-first burrower (ROSENBLATT, 1967; CASTLE AND RANDALL, 1999).

*Moringua edwardsi* belongs to the Moringuidae, which appear to be phylogenetically related to Anguillidae and Heterenchelidae (SMITH, 1989A,C, D; NELSON, 1994). According to (SMITH, 1989D), Moringuidae share pronounced morphological specializations for a fossorial lifestyle with Heterenchelidae and Ophichthidae: reduced eyes, lack of color, low vertical fins, elongated, cylindrical body and reduced head pores. Being a head-first burrower, *M. edwardsi* has shown to possess some extreme adaptive skull modifications (DE SCHEPPER ET AL., 2005). SMITH (1989D) also mentions rapid movements of the body, just beneath the surface for subterranean hunting and feeding, thus also relying on the head for substrate penetration.

*Heteroconger longissimus* is an obligate tail-first burrower belonging to the Heterocongrinae, that shows extreme modifications in its caudal fin morphology (SMITH, 1989B). According to SMITH (1989B) and NELSON (1994) Heterocongrinae belong, as the Ophichthidae, to the suborder Congroidei. Though the monophyly of the Congroidei is recently questioned (BELOUZE, 2001; WANG ET AL., 2003). Garden eels, as they are called, live in a colony, where each individual lives in separate, strengthened burrows in sandy or silty-sand substrate, which are used for long periods (CASIMIR AND FRICKE, 1971; SMITH, 1989B). They project the front portion of the body from the burrow, their heads turned to the plankton loaded currents to snap and pick small zooplanktonic particles (BATH, 1960; FRICKE, 1969; SMITH, 1989B; VIGLIOLA ET AL., 1996; CASTLE AND RANDALL, 1999).

## MATERIALS AND METHODS

---

Eight specimens of *Pisodonophis boro* (Hamilton, 1822) were used, measuring between 85 mm and 309 mm. These specimens were obtained commercially (Poisson d'Or - Moeskroen, Belgium) and preserved on ethanol (70%). Four ethanol preserved specimens of *Heteroconger longissimus* were used from the United States National Museum of Natural History (USNM 316037). Their total length ranged from 225 mm to 268 mm. Standard lengths were measured with a ruler to the nearest 0.1 cm. Standard length was used instead of total length due to potential damage to the fin rays of caudal fins during collection and preservation or due to potential reductions of the caudal fin. For osteological descriptions of *P. boro* we refer to TILAK AND KANJI (1969). See chapter III for details on procedures and list of specimens (Table III.1- 1A). In this study, specimens were anaesthetized, sacrificed and fixed (see III.2.1). Some specimens were cleared and

stained, dissected, serial sections were made and a CT-scanning and 3D-reconstructions was performed (see III.2.2 and III.2.5).

## RESULTS

---

### CRANIAL OSTEOLOGY

The osteology of *Pisodonophis boro* has already been described in detail by TILAK AND KANJI (1969). Figure IV.3- 1 shows a 3D reconstruction of the cranial skeleton and its constituent elements. The skull is elongate, tapering from the otic region to the tip of the snout. The cranial bones are heavily ossified and strongly connected to each other, with the exception of the mobile maxillae. The frontals are fused and form one massive element. A robust and compact premaxillo-ethmovomerine complex is present. The orbits are small and separated dorsally by a wide interorbital distance. Neighboring bones form joints with oblique edges (scarf joints, according to the terminology of Hildebrand, 1995) and are interconnected by dense connective tissue (Fig. IV.3- 2A, C). The bones forming the skull roof (premaxillo-ethmovomerine complex, frontals, parietals, supraoccipital, epiotics and exoccipitals) show a high amount of overlap, formed by the extension of the oblique edges of the scarf joints (Fig. IV.3- 2B). The suspensorium comprises the quadrate, hyomandibula and pterygoid (separated bones not shown in Fig. IV.3- 1), which are strongly interconnected by ligaments. The pterygoid is reduced, and is loosely connected to the parasphenoid. The hyomandibula bears an anterior suspensorial articulation condyle for the articulation with the sphenotic and a posterior one for the articulation with the pterotic. Dorsocaudally the hyomandibula bears the opercular articular condyle for the articulation with the articular facet of the opercle.

Cranial lateral line system - The cephalic lateral line system comprises the supra- and infraorbital canals, ethmoidal canals, otic canals, mandibular canals, preopercular canals, and frontal and supratemporal commissures (Fig. IV.3- 3). The ethmoidal canals are ventral branches of the supraorbital canals, surrounded by the premaxillo-ethmovomerine complex. Anteriorly, each ethmoidal canal opens in an anteroventral, external pore. The supraorbital canal includes four external pores (exclusive of the ethmoid and frontal commissural pores) and is enclosed anteriorly by the main part of the winglike nasal bone (Fig. IV.3- 4A). A branch exiting the nasal runs ventrally and has no pore. The posterior part of the supraorbital canal runs in the frontal. The frontal commissure, situated above the eyes, connects the left and right parts of the supraorbital canal dorsally, and opens in a single dorsal, external pore. The infraorbital canal opens through four external pores and



is surrounded anteriorly by the preorbital, whereas the posterior part is enclosed by two infraorbitals and 3 postorbitals. Behind the eyes, the supra- and infraorbital canals anastomose, forming the otic canal. The otic canal is enclosed completely by the pterotic and the left and right halves of the canal are interconnected through the supratemporal commissure. This commissure is connected to the external environment by one external pore (Figs. IV.4.3- 4, 6A). The mandibular canal is enclosed in the dentary and angular complexes. Behind the articulation between the lower jaw and the suspensorium, the preopercular bone surrounds the preopercular canal. This canal bears a non-enclosed ventrocaudal branch, ending in an external pore. The mandibulo-preopercular canal bears six external pores. The preopercular canal and otic canal fuse, extending caudally in the lateral line system of the body, which is supported by ossicles. No dermal cavities, connected with the canals of the cranial lateral line system are observed (cfr. DE SCHEPPER ET AL., 2005) (IV.1).

The nasals are flat triangular bones, lying apposed to the dorsolateral edges of the premaxillo-ethmovomerine complex and covering the olfactory chamber. The small orbits are surrounded by a ring of 6 small, thin and weak bones: the preorbital forms the anterior edge and is connected to the nasal, the 2 infraorbitals form the ventral edge and the 3 postorbitals form the posterior edge (Fig. IV.3- 3).

Some aspects of the eyes - The eye diameter of *P. boro* measures between 1.05-2.24 mm (53% of skull height). The cornea in *P. boro* is thick, presumably to protect the eyes during head-first burrowing. The eyes of *M. edwardsi* are smaller compared to those of *P. boro*. The corneal epithelium and especially the corneal dermis are extremely thick (Fig. IV.3- 9B). In *Heteroconger longissimus* the eyes are extremely large and the cornea is markedly thinner (Fig. IV.3- 9D), compared to that of *M. edwardsi* and *P. boro*.

## CRANIAL MYOLOGY

The adductor mandibulae complex, comprising four parts (A1, A2, A3 and A $\omega$ ), is hypertrophied and expanded dorsocaudally (Fig. IV.3- 4). The counterparts of the A2 contact each other medially, covering the dorsal skull roof up to the level of the supratemporal commissural pore. The jaw muscles are connected caudally to the epaxial musculature by an aponeurosis (Fig. IV.3- 6A). The A1, lying superficial to the A2, forms a thin sheet of muscle fibres. Its medial fibres are connected to the frontals and more posteriorly to the lateral tendon of the A2 (Fig. IV.3- 4A). The A1 inserts by a tendinous sheet (T A1: Fig. IV.3- 4A) on the dorsal edge of the dentary, medial to the primordial

ligament (Fig. IV.3- 6B). This ligament runs from the maxilla to the dorsolateral edge of the dentary (Fig. IV.3- 4A); the fibres are directed ventrocaudally.

The A2 has no subdivisions and forms the largest part of the adductor mandibulae complex, extending dorsally and caudally (Figs. IV.3- 4A, B). The counterparts of the A2 are interconnected dorsally by an aponeurosis, originating from the frontal, parietal, epiotic and supraoccipital surfaces. The muscular origin includes the frontal, pterotic, parietal, epiotic and supraoccipital. The A2 has a tendinous insertion (T A2: Fig. IV.3- 4B) on the dorsal edge of the coronoid process of the lower jaw (Fig. IV.3- 6B). This tendon partially covers the lateral surface of the A2. The A2 inserts indirectly on the inner surface of dentary by the fusion of the ventral fibres of the A2 with the posterior fibres of the  $A\omega$  (Fig. IV.3- 6B). The anterior fibres are ventrocaudally directed, whereas the remaining fibres are directed ventrally to rostroventrally.

The muscular origin of the A3 includes the ventrolateral surface of the posterior part of the frontal, the ventrolateral surface of the anterior part of the pterotic, and the dorsolateral surface of the pterosphenoid, the hyomandibula and pterygoid (Figs. IV.3- 4C, 6B). The A3 inserts tendinously (T A3) on the ventromedial ridge of the angular complex, ventromedial to the fibres of  $A\omega$  (Fig. IV.3- 5B). The fibres are directed ventrocaudally.

The fibres of the  $A\omega$  arise from the anteroventral part of the tendon T A2. More caudally fibres of the  $A\omega$  fuse with ventral fibres of the A2 and this complex is connected to the pterygoid. The  $A\omega$  inserts into the Meckelian fossa on the mediodorsal surface of the angular complex and the medial surface of the dentary (Fig. IV.3- 6B).

The levator arcus palatini inserts muscularly on the lateral surface of the hyomandibula and dorsal edge of the pterygoid (Fig. IV.3- 4C). Its fibres, directed ventrocaudally, merge onto a tendon, which originates from the lateral ridge of the sphenotic and pterosphenoid.

The adductor arcus palatini has muscular origin and insertion sites (Fig. IV.3- 6A). Its fibres, inclined ventrolaterally, originate from the parasphenoid and insert on the medial surfaces of the pterygoid and ventromedial surface of the hyomandibula.

The adductor hyomandibulae originates muscularly from the prootic and inserts muscularly on the dorsomedial surface of the hyomandibula (Fig. IV.3- 5B). The fibres are directed ventrolaterally.

The dilatator operculi lies with its apex pointing caudoventrally (Fig. IV.3- 4C). The fibres are directed ventrocaudally. The muscle originates muscularly from the lateral surface of the pterotics and the posterior process-like extension of the dorsal edge of the hyomandibula (Fig. IV.3- 6A). It inserts by its tendon on the dorsal process of the opercle.

The adductor operculi has both a muscular origin and insertion (Figs. IV.3- 4C, 5B, 6A). The fibres originate from the ventrolateral surface of the pterotics and exoccipitals and insert on the dorsomedial surface of the dorsal process of the opercle and on the anterior part of the dorsal edge of the opercle. The fibres are directed dorsoventrally and inclined caudally.

The levator operculi runs from the neurocranium to the opercle. Its tendon originates from the caudoventral surface of the exoccipitals and the posterodorsal edge of the hyomandibula (Fig. IV.3- 6A). This muscle inserts muscularly on the dorsal opercular process and the dorsal edge and lateral surface of the opercle. The fibres of this large muscle are directed dorsoventrally and inclined caudally.

The intermandibularis is absent.

The protractor hyoidei comprises a separated left and right bundle, which are attached tendinously to the medial surfaces of the left and right dentary, respectively (Figs. IV.3- 4A, 5B). Anteriorly these tendons cover the dorsal surface of the anterior part of the muscle bundles. Posteriorly, both bundles diverge and arise separately by a posterior tendon from the laterodorsal surface of the anterior ceratohyal.

The left and right bundles of the sternohyoideus insert by means of a common, well developed tendon (Figs. IV.3- 5B, 6A) on the posterodorsal region of the urohyal. This muscle comprises three myomeres separated by two myocommata, and the left and right bundles connect aponeurotically in the midline. The sites of origin include the medial side of the cleithrum dorsally, whereas the ventral fibres insert on a myocomma, separating them from the hypaxial muscles.

The successive branchiostegal rays are interconnected by the hyohyoideus, forming a sheet of fibres (Fig. IV.3- 6A). The muscle halves extend ventrally and connect to an aponeurosis in the ventral midline. Dorsally the fibres attach muscularly on the ventromedial surface of the dorsal opercular process and the medial surface of the opercle (Fig. IV.3- 6A). Posteriorly, the fibres attach to the horizontal septum, that interconnects the hypaxial and epaxial muscles. Whether the hyohyoidei inferior, abductor and adductores are absent or not differentiated remains uncertain, and ontogenetic series are necessary to resolve this.

The epaxial muscles insert on the epiotics and the dorsal ridge of the supraoccipital by an aponeurosis (Fig. IV.3- 6A). The hypaxial muscles inserts aponeurotically on the ventrocaudal border of the basioccipital and exoccipitals (Fig. IV.3- 6A).

## CAUDAL FIN: OSTEOLOGY

*Pisodonophis boro* has a reduced caudal fin (Fig. IV.3- 8A). The caudal skeleton comprises a dorsal and ventral hypural plate, the result of the fusion of hypurals 3 and 4 and hypurals 1 and 2, respectively. The bifurcation point of the dorsal aorta marks the boundary between preural and ural vertebrae. The first and second ural vertebrae are fused, forming the urostyle. This integrates the uroneurals. Rostrolaterally on each side of the ventral hypural plate, a hypurapophysis can be discerned. An epural element is absent. The first preural vertebra is situated in front of the caudal skeleton. The parhypural is the modified hemal spine of the first preural centrum and is the last hemal spine crossed by the dorsal aorta. The neural arches of the preural centra are large and robust. Their bases are as wide as the centra and they are fused dorsally in the midline, covering the neural canal. A neural spine is lacking. The left and right halves of the haemal arch of the preural centra are not fused in the midline. The posterior base of the haemal arch supports a large processus posthaemalis. Neural and haemal spines are absent in the proceeding caudal vertebrae. In some cases two neural arches and two hemal arches are discerned (Fig. IV.3- 8A). This may indicate the fusion of two vertebrae during development. Ontogenetic studies are needed to confirm this hypothesis.

## CAUDAL FIN: MYOLOGY

Interradials are absent (Fig. IV.3- 8B-D). The flexor dorsalis passes from the lateral surface of the uroneural to the three uppermost caudal fin rays, inserting via a tendinous sheet. The hypochordal longitudinalis originates from the ventrolateral surface of the ventral hypural plate and passes to the ventrolateral surface of the uroneural. The flexor ventralis originates from the lateral surface of the parhypural and inserts through a tendon on the ventral caudal fin ray. Medial to the hypochordal longitudinalis, the proximalis is present. This muscle connects the parhypural and first preural centrum to the lateral surface of the ventral and dorsal hypural plate. The trunk musculature, including both epaxial and hypaxial muscles, attaches to the bases of the caudal fin rays by broad tendinous sheets.

## DISCUSSION

---

### MORPHOLOGY RELATED TO HEAD-FIRST BURROWING?

Eye protection and eye reduction - The eyes of *Pisodonophis boro* (TILAK AND KANJI, 1969), measuring 53% of the skull height, and those of other Ophichthids (BOZZANO, 2003) are reduced (Fig. IV.3- 9A). Eye reduction is a feature observed in several groups of vertebrates adapted to the benthic, cryptic or fossorial environments (RIEPEL, 1996). In some mammals (e.g., Spalacidae [mole rats], Chrysochloridae [golden moles] and Notoryctidae [marsupial moles]) the eyes are almost completely reduced and this is associated with the use of the head as a wedge while digging (BORCHI ET AL., 2002). Reduced eyes have been documented for reptiles (amphisbeanians, some lizards and many primitive snakes (LEE, 1998; WIENS AND SLINGLUFF, 2001), as well as for several elongate fishes (e.g. Clariidae [DEVAERE ET AL., 2001, 2004], Mastacembelidae [POLL, 1973], Anguilliformes [BOZZANO, 2003; DE SCHEPPER ET AL., 2005; 2007; IV.1; IV.3; AOYAMA ET AL., 2005]) in which the eye reduction is generally considered to be adaptive for a cryptic or burrowing lifestyle. Due to the reduction of vision, other sensory systems (olfaction, touch, lateral line system, etc.) may become more important to provide environmental information (GORDON, 1954; POLL, 1973; MONTGOMERY, 1989). The importance of olfaction, touch and taste in eels in general is well known (BANTSEEV ET AL., 2004) and has been documented in detail for Muraenidae (SANTOS AND CASTRO, 2003), Anguillidae (PANKHURST AND LYTHGOE, 1983) and Ophichthidae (BOZZANO, 2003). Observations on foraging behavior of *P. boro* confirm the importance of olfaction and touch, as the fish move actively along the bottom, regularly probing into the sediment with their snout (personal observation).

The cornea comprises the corneal epithelium, dermis and endothelium (BOZZANO, 2003) (Fig. IV.3- 6A). The thick cornea in *P. boro* presumably has a protective role during head-first burrowing. In *Moringua edwardsi*, which has smaller eyes compared to *P. boro*, the corneal epithelium and especially the corneal dermis are extremely thickened (Fig. IV.3- 9B), in contrast to the tail-first burrowing species *Heteroconger longissimus*, in which the cornea is markedly thinner (Fig. IV.3- 9D). The eyes of burrowing fish need to be protected from mechanical injuries during substrate contact. In *Ophichthus rufus*, another anguilliform head-first burrowing species, protection of the eye is offered by the presence of a corneal dermis and thick corneal epithelium covered by protective mucus (BOZZANO, 2003). This supports our hypothesis of the protective role of the thick cornea in *P. boro*.

A substantial impact on the spatial design of the head due to the reduction of the eyes can be expected, especially given the macrophthalmic ancestral state in Anguilliformes (BÖHLKE, 1989). In other eel-like teleosts, like the elongate clariid catfish, hypertrophy of the jaw muscles has been linked to eye reduction (DEVAERE ET AL., 2001). In *Pisodonophis boro* and *Moringua edwardsi* (DE SCHEPPER ET AL., 2005) (IV.1) the reduced eyes also create space for housing enlarged adductor mandibulae muscles and for allowing an unusual orientation of some fibres (see below). Next to the relation between hypertrophy of the jaw muscles and eye reduction in clariids (DEVAERE ET AL., 2001), eye reduction is linked to the reduction of circumorbital bones (reduced to small tubular bones) (DEVAERE ET AL., 2004). In *P. boro* these bones are small and tubular as well. Interestingly and in accordance with the situation in clariids (DEVAERE ET AL., 2004), the reduction in size of the circumorbital bones and the reduction in eye size co-occur in Ophichthids (TILAK AND KANJI, 1969; MCCOSKER ET AL., 1989; BOZZANO, 2003).

Lateral line system - The cephalic lateral line system of *Pisodonophis boro* is well-developed and follows the general pattern characteristic for other Anguilliformes as described by BÖHLKE (1989). This pattern contrasts with that of *Moringua edwardsi*, in which the cephalic lateral line system is aberrant (DE SCHEPPER ET AL., 2005) (IV.1); dermal cavities are present, presumably functioning as a kind of sensory pads, which are stimulated mechanically during burrowing or when in contact with prey. External pores are absent in *M. edwardsi*, impeding the connection with the environment, but avoiding the entrance of sediment. Focusing on the head-first burrowing behavior, the question may arise why the cephalic lateral line system in *P. boro* isn't modified as in *M. edwardsi*, to protect the canals from obstruction with sediment. The answer may be found in differences in the burrowing behavior between *P. boro* and *M. edwardsi*, especially related to the level of mechanical loading exerted onto the skull while burrowing. Immature specimens of *M. edwardsi* (dealt with in DE SCHEPPER ET AL., 2005) (IV.1) spend all their time burrowed in the sand (GORDON, 1954; GOSLINE, 1956), hunting and feeding subterraneously (SMITH, 1989D). Behavioral observations in our lab on *P. boro*, and on a closely related ophichthid, *Ophichthus rufus* (BOZZANO, 2003), indicate that, after burrowing, this species remains stationary for a long period of time with its head protruding from the burrow entrance. Living in burrows with the head protruding is useful for protection and hiding against predators and for ambushing prey. Of course, locating predators or prey in time is crucial and may be mediated by the cephalic lateral line system. Because the eyes are reduced in *P. boro*, the cephalic lateral line system may be one of the dominant sensory systems. This has likewise been reported for blind fish (e.g. *Anoptichthys jordani*), in which the lateral line system becomes the most important sensory organ for scanning the

surroundings (HASSAN, 1989; MONTGOMERY, 1989). So, the absence of external pores in *M. edwardsi* may be related to being permanently subterranean (but the system remains functional due to its modifications), whereas in *P. boro* the presence of external pores is likely to be related to the habit of scanning the surroundings.

Hyperossification - LEE (1998) demonstrated that in amphisbaenians, dibamid lizards and snakes convergent evolutionary traits (miniaturization, cranial consolidation, body elongation, limb reduction), are clearly related to head-first burrowing. These characters frequently co-occur in other tetrapods (e.g. caecilians, frogs) with similar habits, showing that extreme skull modifications can be linked to resisting compressive and torque forces during burrowing (GANS, 1975; HANKEN, 1983; DUELLMAN AND TRUEB, 1986; POUGH ET AL., 1998). Interestingly, *Pisodonophis boro* shows similar traits that are considered to be advantageous for head-first burrowing.

The skull of *Pisodonophis boro* is elongated and tapers towards the tip of the snout, facilitating penetration into the substrate. Fortification of the skull is improved by the broad, strong bones, by the fusions in the upper jaw and between the frontals, by the wide interorbital skull roof (as a result of the reduction of the eyes and orbits), by the large nasals (protecting the olfactory organ), by scarf joints and by large overlaps between successive bones of the skull roof (Figs. IV.3- 1, 9C). DUELLMAN AND TRUEB (1986) reported that the distribution of different types of joints or fusions between bones may reflect the presence of high mechanical loads. RAFFERTY ET AL. (2003) and SUN ET AL. (2004) similarly found in pigs that fusions and enhanced bone growth appeared to be associated with increased suture strain. Some of these skull modifications in *M. edwardsi* are even more extreme compared to *P. boro*: paired dorsal skull bones are broader in cross section and show a larger surfaces of overlap at the midline (DE SCHEPPER ET AL., 2005) (IV.1).

Jaw adductor hypertrophy - The jaw muscles of *Pisodonophis boro* are hypertrophied and expanded dorsocaudally, covering the complete postorbital skull roof (Figs. IV.3- 2, 5). The adductor mandibulae complex comprises four parts (A1, A2, A3 and A $\omega$ ). The A2 has no subdivisions. The anterior fibres of the A2 are directed slightly ventrocaudally, whereas the remaining fibres are directed ventrally to rostroventrally. In *Moringua edwardsi* the anterior part of the A2, in which the fibres are more oblique and directed ventrocaudally, is separated from the medial part of the A2 by the tendon T A2. An additional difference in jaw muscles of both species is found at the level of the A1. In *P. boro*, fibres of the A1 are directed ventrocaudally to ventrally and the tendon of this part is separate from the primordial ligament. In *M. edwardsi*, these fibres are directed ventrorostrally, with the A1 tendon merging with the primordial ligament.

In *Pisodonophis boro* head-first burrowing occurs via head probing and body undulations (personal observations), not through mouth excavation (e.g. *Cepola rubescens* (Cepolidae, Perciformes; ATKINSON AND TAYLOR, 1991). Consequently, powerful biting during excavation cannot explain the presence of the hypertrophied jaw muscles in *P. boro*. As the jaw muscles are hypertrophied in *P. boro*, it is reasonable to assume that these have a negative impact on head-first burrowing performance because of the increase in the head diameter. Logically the force required to penetrate the substrate increases exponentially with head diameter, so head-first burrowing puts severe constraints on maximal head diameter (MEASEY AND HERREL, 2006). However, hypertrophied jaw muscles may hold some benefit for head-first burrowing. As some parts of the jaw muscles show the aberrant fibre direction and as these muscles substantially enclose the posterior part of the skull, they may reinforce the lower jaw during head probing, thereby protecting it from being disarticulated (see below). The above-mentioned benefits of hypertrophied jaw muscles in head-first burrowing can count for *Moringua edwardsi* as well (DE SCHEPPER ET AL., 2005). As mentioned above, in *M. edwardsi* more fibres (A2d, A3) show the aberrant (ventrocaudal) fibre direction than is the case in *P. boro* (anterior fibres of A2 and A3 only). This may reflect the stronger need for reinforcement of the lower jaw during head-first burrowing in *M. edwardsi* because this species is an obligate head-first burrower, whereas *P. boro* burrows tail-first as well.

### MORPHOLOGY RELATED TO FEEDING HABITS AND PREY CAPTURE?

Rotational feeding - Three feeding modes (suction, shaking and rotational feeding) to capture and handle food are observed in *Pisodonophis boro*, depending on the size and consistency of the offered food items (personal observation). HELFMAN AND WINKELMAN (1991) already discerned the feeding modes in anguillids: (1) inertial suction, which draws small items into the mouth; (2) shaking, which entails grasping of large items and shaking or twisting the head and body, tearing small pieces from the prey; 3) rotational feeding, which entails grasping large prey items and spinning around the body axis, thereby tearing small pieces from the prey. As the choice of feeding mode depends on prey size and food consistency, rotational feeding is performed when the prey item is firm and exceeds 85% of the eel's jaw width (HELFMAN AND CLARK, 1986; HELFMAN AND WINKELMAN, 1991). The importance of rotational feeding in *P. boro* can be deduced from the dietary data reported by SUBRAMANIAN (1984). Field observations showed selective feeding of *P. boro* on the crab *Uca annulipes*. The large size and high consistency of the carapace of these prey types require a spinning feeding mode to tear off consumable pieces.



Several morphological modifications in *Pisodonophis boro* may be related to this specialized feeding mode. Rotational feeding starts at the anterior one-third of the body (HELFMAN AND CLARK, 1986). The common aponeurosis separating the epaxial muscles and adductor mandibulae complex in *P. boro* may be considered beneficial for transferring these rotational forces from the body to the head (Figs. IV.3- 2D, 6A). During rotational feeding a powerful bite is required to be able to hold prey during spinning movements and to help prevent the lower jaw from being dislodged. Hypertrophied jaw muscles may exert large forces that can help resist torque forces during rotational feeding. The presence of a hypertrophied adductor mandibulae complex, which leads to the assumption that powerful biting may occur (DEVAERE ET AL., 2001; HERREL ET AL., 2002; VAN WASSENBERGH ET AL., 2004), could be considered in this context. Consequently, an increase in mechanical loads at the level of the insertion of the muscle complex onto the neurocranium and the upper and lower jaw may be expected, as well as in their articulations. Neurocranial rigidity in *P. boro* is improved by the extensive overlap between successive cranial bones, which are additionally very broad in cross section (Fig. IV.3- 2D). The lower jaw of *P. boro* is robust and bears a coronoid process. This process, however, is substantially shorter than in *Moringua edwardsi*. Similar structural adaptations in the lower jaw and the coronoid process have been linked previously to predation and powerful biting (BÖHLKE ET AL., 1989; CABUY ET AL., 1999; DEVAERE ET AL., 2001).

Rotational feeding also requires a solid grip on the prey, which is enhanced by the presence of numerous, pointed and recurved teeth, as observed in *Pisodonophis boro*. The absence of cutting dentition excludes the possibility to remove pieces of prey by nibbling, as reported by HELFMAN AND CLARK (1986) for anguillid eels. A solid grip during rotational feeding also requires a high structural rigidity of the upper and lower jaws to resist torque forces. In Anguilliformes, the robustness of the upper jaw results from the fusion of the premaxilla, mesethmoid and vomer to form the premaxillo-ethmovomerine complex. This fusion is synapomorphic for Anguilliformes and is assumed to be a specialization for predatory feeding (EATON, 1935; GOSLINE, 1980; BÖHLKE, 1989B). Independently in Synbranchidae the upper jaw has become a strong, non-protrusible element as a specialization for this particular feeding method (LIEM, 1980).

Not only the jaw muscle size, but also the orientation of the different bundles composing this complex and the robust coronoid process, may contribute preventing the lower jaw from being dislodged during rotational feeding (Figs. IV.3- 4A). The anterior fibres of the A1 and A2, and the fibres of the A3 are directed ventrocaudally. This is in contrast to the posterior fibres of the A1 and A2, which are directed rostroventrally. The resulting forces generate both a vertical adduction component and a horizontal component

acting on the lower jaw articulation (Fig. IV.1- 8 in DE SCHEPPER ET AL., 2005) (IV.1). Both horizontal components pointing in opposite directions and partially neutralize each other, and thus both vertical components prevent dislocation of the jaw joint (P. Aerts, pers comm).

Rotational feeding has been reported for eels (Anguilliformes, HELFMAN AND CLARK, 1986), eel-like fish (Clariidae, CABUY ET AL., 1999; Synbranchidae, LIEM, 1980) and vertebrates with elongate bodies and small or lost appendages (sirens, caecilians, crocodylians, HELFMAN AND CLARK, 1986). The convergence in some aspects of the morphology and behavior of these species with *Pisodonophis boro* and *Moringua edwardsi* (DE SCHEPPER ET AL., 2005) (IV.1) is noteworthy. The following characteristics are observed in these spinning species and are assumed to be related to rotational feeding: the aponeurotic connection between epaxials and jaw muscles, hypertrophied jaw muscles (except in caecilians), increased neurocranial rigidity, robust lower jaws, non-cutting dentition and rigid upper jaw. These features have been linked to their specialized rotational feeding mode (LIEM, 1980). The statement of LIEM (1980) considering rotational feeding in *Monopterus*, "Once prey is captured, the highly hypertrophied adductor mandibulae complex plays a key role in conjunction with the corkscrew-like twisting motion of the body in breaking up the prey into pieces," further supports our assumptions.

### MORPHOLOGY RELATED TO TAIL-FIRST BURROWING?

Osteology and caudal fin rays - The caudal skeleton is highly consolidated, lacking an externally visible caudal fin. The caudal fin rays are present but they are covered with muscles, a thick layer of connective tissue and a thick dermis and epidermis. This results in a hard, pointed tail, which appears to provide an added advantage to tail-first burrowing. The presence of long and pliable caudal fin rays would not benefit penetration of the substrate tail first. Garden eels (Heterocongrinae: *Heteroconger* and *Gorgasia*) also excavate their burrows tail-first and show a similarly modified caudal fin morphology (shortened caudal fin rays, with stout and reduced caudal skeleton) to ensure an effective penetration into the sediment (ATKINSON AND TAYLOR, 1991; CASTLE AND RANDALL, 1999).

Caudal fin myology - The intrinsic caudal musculature of the caudal fin of *Pisodonophis boro* is highly reduced and presumably related to the modifications of the caudal fin skeleton and its function. In teleosts the caudal fin musculature generally allows a precise control of caudal fin movements through caudal fin conformation (LAUDER AND DRUCKER, 2004). With respect to the caudal fin myology in teleosts (WINTERBOTTOM, 1974),

that of *P. boro* is reduced. The interradians are absent completely in *P. boro*. In *P. boro* the flexor dorsalis and flexor ventralis are reduced in size and their origins do not include the last few vertebrae. It is surprising that in *P. boro* the hypochordal longitudinalis connects two immobile elements (ventral hypural plate to uroneural), this in contrast to teleosts.

The actions of the intrinsic caudal fin musculature in *P. boro* are presumably no longer required with the loss of the need for subtle movements of individual fin rays. This may explain the absence of the interradians, the size reduction of the flexors and the absence of the insertion of the hypochordal longitudinalis onto the dorsal caudal fin rays in *P. boro*. Reduction and even absence of this muscle has been observed in several species with highly reduced caudal skeletons, especially those known for high-speed locomotion (e.g., tuna; LAUDER AND DRUCKER, 2004). In these cruisers fine movements of separate caudal fin rays are also less important. The proximalis generally connects the centra of the last few vertebrae, though its occurrence and position is highly variable in teleosts (WINTERBOTTOM, 1974). In *P. boro* the proximalis muscle connects the parhypural and first preural centrum to the ventral and dorsal hypural plates. The presence of the proximalis muscle and the presence of broad tendinous insertions of the epaxial and hypaxial muscles onto the caudal fin rays may strengthen the caudal fin to withstand bending forces during tail-first burrowing. Reduction or loss of these intrinsic muscles has been observed previously in species in which sophisticated movements of individual fin rays are no longer required (WINTERBOTTOM, 1974; LAUDER AND DRUCKER, 2004). The supracarinalis posterior generally runs from the last basal pterygiophore of the dorsal fin to the neural spine, epurals, uroneurals or dorsal caudal fin rays. The infracarinalis posterior runs from the last basal pterygiophore of the anal fin to the hemal spine of the last complete vertebrae, parhypural or ventral caudal fin rays. These muscles are not discerned in *P. boro*, which is likely related to the fact that the dorsal, anal and caudal fins are confluent.

## FUNCTIONAL TRADE-OFFS

### COMPARISON OF MORPHOLOGICAL ALTERATIONS IN HEAD AND CAUDAL FIN OF *PISODONOPHIS BORO*

As in *P. boro* both terminal parts of the body need to be able to penetrate the substrate, one would expect similar kinds of external and internal modifications in the head and caudal fin. However, as the head is not only used for burrowing but also has to accommodate the apparatus for feeding, constraints on the functional morphology of the head, associated with feeding and respiration are expected and are likely to prevent certain kinds of transformations or reductions.

Theoretically, a pointed end that has a small cross section and that is supported by a strong, consolidated skeleton would be the optimal design for burrowing. Indeed, such modifications (stout and reduced caudal skeleton) are found in the caudal fin of *P. boro* (Fig. IV.3- 8). The head on the other hand is also pointed and slender, but due to the hypertrophy of the jaw muscles, the cross section of the head is decreased to a lesser degree. Further more, several skull bones are fused and thick, thus providing extra strength. Though some degree of kinesis (jaws, suspensorium) is still needed in the skull for feeding, consequently consolidation in the skull is limited at this level.

As protruding structures would have a negative effect or would be damaged during burrowing or substrate contact, it is expected that external structures would be reduced. This is again found in the caudal fin with caudal fin rays being reduced. Again, similar modifications are found to a lesser degree in the head morphology. The eyes are reduced though still present and functional even though they may be damaged during substrate contact. The lateral line system is well developed, even though the canals are not specifically protected from being obstructed with sediment (which is the case in for example *Moringua edwardsi* [DE SCHEPPER ET AL., 2005; IV.1]).

At the level of the musculature, reductions are expected, except when they consolidate the structural components of the burrowing apparatus. The muscles in the caudal fin are reduced when compared to the situation in generalized teleosts that need complex movements of individual fin rays. The muscles, which are present in the caudal fin in *P. boro* are likely to strengthen the tail during burrowing. In agreement with our hypothesis, the skull shows no myological reductions, but incorporates hypertrophied jaw muscles (see below).

It is obvious the head is specialized for burrowing to some degree, though shows less far going transformations than the caudal fin. Clearly the mechanical design of the head allows animals to perform in different functions (locomotion and feeding) and shows trade-offs.

Trade-offs - A number of crucial biological functions must be fulfilled by the cranial musculo-skeletal system: capturing, processing and transporting prey, breathing water or air, providing protection for the major sense organs and brain, and serving as a streamlined bow in locomotion (LIEM, 1980). Whenever two relevant functions require opposing biomechanical or physiological adaptations, the evolution towards optimal performance is assumed to be prevented (STEARNS, 1992; VAN WASSENBERGH ET AL., 2004). An important goal in functional morphology is to identify how the mechanical design allows animals to perform in different functions that are essential, but require a trade-off with

each other. As this study is based on morphological data, only indirect assumptions can be made of their biological function.

Feeding and head-first burrowing in *Pisodonophis boro* can be two important functions that call for different requirements in the morphology of the jaw muscles. In the previous sections the hypertrophied jaw muscles of *Pisodonophis boro* are associated with a strong bite needed to crush hard and large prey (cancrivory) and with their possible advantage during rotational feeding. Additionally they may be advantageous during head-first burrowing as they may reinforce the lower jaw during head probing, thereby protecting it from being disarticulated. However, the comment may arise that large jaw muscles would decrease head-first burrowing performance as the force required to penetrate the substrate increases exponentially with head diameter (reflecting the amount of pressure drag experienced during substrate penetration). The jaw muscles are likely to be involved in feeding and locomotion, and as *P. boro* performs head-first burrowing despite the presence of a wider head diameter, we consequently may assume trade-offs occur in these jaw muscles.

## CONCLUSIONS

---

*Pisodonophis boro* is able to burrow head-first but can penetrate the substrate tail-first as well. Focusing on the morphology of *P. boro*, several features may be related to either one or both burrowing habits. The reduced eyes, covered with thick protecting cornea, may be beneficial for protection during head-first, but at the same time decreased vision acuity may have an impact on other sensory systems (increase of olfaction, touch, lateral line system). Eye reduction may be related to the hypertrophy of the jaw muscles. The presence of a well-developed cephalic lateral line system is advantageous when the head is positioned at the entrance of a burrow. Hypertrophied jaw muscles may be advantageous for protecting the lower jaw from disarticulation during head-first burrowing. However, they probably are more important during feeding. The shape of the skull is beneficial for substrate penetration. The cranial bones and their joints, which are fortified, are advantageous to resist high mechanical loads during head-first burrowing. It is likely the hypertrophied mouth closing muscles yield a benefit for a predatory lifestyle. A specialized feeding mode is observed in *P. boro*: rotational feeding. The aponeurotic connection between epaxial and jaw muscles is considered beneficial for transferring forces from the body to the head during spinning. Hypertrophied jaw muscles enhance a powerful bite, which is required to hold prey during spinning movements. Different orientations of lower jaw muscle bundles may be beneficial to prevent the lower jaw from

being dislodged. Furthermore, firm upper jaws (premaxillo-ethmovomerine complex) and lower jaws (with robust coronoid process), high neurocranial rigidity and non-cutting dentition are advantageous for a solid grip to hold prey during rotational feeding. The pointed shape of the tail and the consolidated caudal skeleton are beneficial for tail-first burrowing. It is likely that the reduction of the caudal musculature is related to the tail-first burrowing, because subtle movements of the caudal fin rays are no longer required. Furthermore, additional strength may be offered by the presence of broad tendinous connection of the epaxial and hypaxial muscles as well as by the presence of the proximalis.

## **ACKNOWLEDGMENTS**

---

Thanks to P. Aerts (Antwerp University, Belgium) for discussing the paper and offering valuable suggestions. Research was partially funded by the FWO (G. 0388.00).

**IV.4 NON-BURROWING SPECIES: *ANGUILLA ANGUILLA* AND *CONGER***  
***CONGER***

**IV.4.1 MORPHOLOGICAL VARIATION IN *ANGUILLA ANGUILLA***





# VARIATION IN CRANIAL MORPHOLOGY OF THE EUROPEAN EEL: BROAD- AND NARROW-HEADEDNESS

---

Modified from the paper published as:

De Schepper N, Lateur S, Christiaens J, Van Liefferinge C, Herrel A, Goemans G, Meire P, Belpaire C, Adriaens D

Variation in cranial morphology of the European eel: broad- and narrow-headedness  
Biological journal of the Linnean Society. *SUBMITTED A*

## ABSTRACT

---

The presence of two varieties, broad- and narrow-headed, of eels (*Anguilla anguilla*) is common knowledge among fishermen and eel biologists in Europe. Yet, no qualitative or statistical analyses testing for a dimorphism in head size or shape of Belgian eel populations have been performed to date. A total of 121 specimens from a single location (Scheldt-Lippensbroek - Belgium) as well as a larger data set of 725 eels from water systems across Belgium are examined in the present study. Biometric data are explored by means of histograms, normality plots, and tested for the presence of a dimorphism using Brewer's bimodality test. Morphometric data of the skull are examined using Thin Plate Spline analyses. All methods used in this study point towards the presence of a dimorphism in head size and shape, and the variation in head size and shape of European eels is significantly better described having a bimodal rather than a unimodal distribution. As the head dimorphism is the result of a phenotypically plastic response to food availability and as cultured eels are exclusively narrow-headed, our data point towards the importance of conservation measures aimed specifically at preserving the existing dimorphism in the population of European eels, which may be crucial to maintain the stability of freshwater ecosystems.

## INTRODUCTION

---

The European eel, *Anguilla anguilla*, is one of nature's most durable, mysterious and remarkable animals. Their mysterious life cycle has fascinated scientists ever since it was first commented upon by Aristotle around 350 BC, in his Natural History (see SCHWEID, 2004). Yet, many aspects of their biology, life cycle, migration routes and ecology remain

a mystery to date (DANNEWITZ ET AL., 2005). Though, as the smallest larvae are found in the Sargasso Sea, eels are generally believed to spawn and die in this region (RINGUET ET AL., 2002; TESCH, 2003).

European eels are not only of scientific interest, but also have a long culinary history as they have been part of the human diet, especially in Europe and Asia, for hundreds and even thousands of years (RINGUET ET AL., 2002; SCHWEID, 2004). Consequently, *Anguilla anguilla* has always been an important (economical, aquacultural and recreational) fish for fisherman. Today, it is considered of great economical significance in world trade, as in 1995 the global eel harvest from fishing and aquaculture amounted up to 205000 tons (TESCH, 2003) and approximately 25000 people across Europe gain an income by fishing for eels.

However, the population of European eels has mysteriously declined (around 90-98%) and has reached a critically low level (recruitment of less than 1%) since the 1970's (WIRTH AND BERNATCHEZ, 2003; DANNEWITZ ET AL., 2005; WG EEL, 2006). Up to present, there is no sign of recovery and explanations for this decline (natural or anthropogenic) are unknown (DANNEWITZ ET AL., 2005; VAN GINNEKEN, 2006A). Although, recently VAN GINNEKEN (2006B) mentioned that PCB's and eel viruses seem to have important effects on swimming performances and mass mortality after a migration distance of 1000 km, in contrast to the normal 5000 km (distance to the Sargasso Sea) of non infected eels. Similarly, the closely-related American eel, *Anguilla rostrata*, (BEAK INT INC, 2001; AFMSC, 2004; TRAUTNER, 2006) and Japanese eel, *Anguilla japonica* (TSENG ET AL., 2003) are also threatened with extinction (WG EEL, 2006). At present there is a general agreement from the International Council for the Exploration of the Seas (ICES) and the European Inland Fisheries Advisory Commission (EIFAC) that addresses the need for management actions as the current eel fishery is not sustainable and is outside safe biological limits (STARKIE, 2003; WG EEL, 2006).

At present the reduced recruitment and catches of eels (and thus conservation of the species) are the principle motives for international conservation management. However, conservation of morphological variability within the species has never been the motivation for management initiatives as the knowledge of this phenomenon is limited.

For example, it is common knowledge among fishermen that two varieties (broad- and narrow-headed) of European eels appear to occur and is described for populations in Germany (TÖRLITZ, 1922; THUROW, 1958), the Netherlands (LAMMENS AND VISSER, 1989) and Ireland (PROMAN AND REYNOLDS, 2000). Former studies suggest that this so-called dimorphism is tied to differences in diet as broad-headed specimens tend to be piscivorous, whereas the narrow-headed specimens predominantly feed on benthic invertebrates (TÖRLITZ, 1922; THUROW, 1958; LAMMENS AND VISSER, 1989; PROMAN AND REYNOLDS, 2000; TESCH, 2003).

Interestingly, the study of PROMAN AND REYNOLDS (2000), based on wild and cultured Irish eel populations, revealed that cultured eels were exclusively narrow headed, supporting the general consideration that the apparent flexibility of mouth width (and thus head shape) is related to environmental conditions (e.g. availability of trophic resources) (LAMMENS AND VISSER, 1989).

Phenotypically induced head dimorphism, with a close relation to the trophic ecology of European eels, calls for a detailed screening of causalities and consequences when conservation efforts are envisioned. The present study provides a quantitative analysis of head size and shape in the *Anguilla anguilla* population (in Belgium) and tests for the presence of bimodality in cranial size and shape 1) within a single population in the Scheldt-Lippensbroek in Belgium and 2) across a broad range of waters in Belgium.

## MATERIAL AND METHODS

---

### SAMPLING

The sampling is part of the “Harmonised River Basin Strategies for the North Sea” (HARBASINS) project (2005-2008) and partially within subproject 5 (fish communities) of the MODELKEY project, models for assessing and forecasting the impact of environmental key pollutants on marine and freshwater ecosystems and biodiversity (see III.1). Specimens were captured by fyke nets from the Lippensbroek (which is a controlled inundation area with reduced tidal movements) and the Scheldt (Fig. III.1- 1). We collected four samples of yellow eels in the months April, May, August and October 2006. Each sample consisted of approximately 30 specimens. The specimens ( $n=121$ ) were collected alive, labelled and their total length (TL) was immediately measured with a ruler to the nearest 0.1 cm and weighed (We) to the nearest 0.1g. All eels were killed by an overdose of anaesthetic, fixed in 10% formalin and preserved in 70% ethanol. This study also includes a biometric study of the head of 725 eels obtained from the INBO-eel pollutant monitoring network (see GOEMANS AND BELPAIRE, 2004). These specimens were collected from 65 different sample sites across Belgian waters between 2001 and 2005. The total length of the eels of the Scheldt-Lippensbroek sample ranged from 25.6 to 76.0 cm (mean, 45.3 cm). The total length from the eels from the INBO-pollutant network ranged from 22.9 to 102.3 cm (mean, 42.9 cm).

## BIOMETRY

1) Sample Scheldt-Lippensbroek: A total of 19 head measurements were taken point to point using a digital calliper (Mauser) to the nearest 0.01 mm. Measurements are described and illustrated in III.2.4A. Specimens, collected in the Scheldt-Lippensbroek, used for the biometric study are listed in Table III.1- 1B.

2) Sample INBO: Measurements taken on 725 specimens from the INBO- eel pollutant monitoring network were restricted to We; SL; L Sn-Pe; IOD m; H H [E c]; W Pe. Measurements are described and illustrated in III.2.4A. Specimens from the INBO sample, used for the biometric study are listed in Table III.1- 1C.

## ANALYSES

Prior to the statistical analyses, measurements were logarithmically transformed. To examine whether the four subsamples, taken at different months differed from one another, a Discriminant Function Analysis ( $F_{63,290}=1.0006$ ;  $p<0.482$ ) was performed. As the data of all subsamples were not different from one another, samples were combined for further analyses. Next, regression analyses were performed for all cranial measurements on total length ( $p<0.05$  for all variables). Three complementary methods were used to infer bimodality (BREWER, 2003). See III.2.6 for more details.

## MORPHOMETRY

The skull of a total of 64 specimens was morphometrically examined based on digital images. These specimens were initially defined as being narrow- or broad-headed. In some specimens the correct location of the landmarks was hard to define because of the presence of soft tissue. These vertebrae are consequently not included in the analysis in order to decrease inaccuracies. Specimens used for the morphometric study are listed in Table III.1- 1D. For a detailed description of the landmarks, I refer to III.2.3A.

## RESULTS

### BIOMETRY - SAMPLE FROM THE SCHELDT-LIPPENSBROEK

Frequency histograms of the cranial measurements for the Scheldt-Lippensbroek sample show discontinuities, which suggest a bimodal pattern (e.g. Fig. IV.4.1- 1a, c). The observed cumulative values plotted against the cumulative values expected under normality reveal strong deviation from normality, again suggesting a bimodal pattern in the biometric data (see Fig. IV.4.1- 1b, d). The mixture model approach (BREWER, 2003) gives strong support for bimodality in all cranial measurements ( $\Delta AIC > 8$ ) (Table IV.4.1- 1). However, for some measurements (e.g. IOD c; H E; L E), bimodality can to a lesser extent be deduced visually from histograms and normality plots (Fig. IV.4.1- 1e) as overlap between the tails of two distributions can fill the gap between them or as the data may have a normal distribution, which is however rejected by Brewer's bimodality test (Table IV.4.1- 1).

Broad- and narrow-headedness are independent of total length (Fig. IV.4.1-1f). When both extremes are arbitrarily separated (broad-headed  $HW/SL > 0.034$ ) and measurements (e.g. IOD c) are plotted to total length (Fig. IV.4.1- 1f), it becomes clear that broad-headedness is not restricted to the largest specimens only.

### BIOMETRY - SAMPLE COLLECTED FROM WATER SYSTEMS ACROSS BELGIUM (INBO)

The frequency histograms, probability plots and bimodality test of the logarithmically transformed cranial measurements in this dataset even more strongly support a bimodal pattern as substantially better fits ( $\Delta AIC$ ) for mixtures of two normal distributions are found (Table IV.4.1- 1). The  $\Delta AIC$  values are larger, compared to those from the Scheldt-Lippensbroek sample, and indicate that the bimodal pattern is even stronger supported, as a result of the larger sample size (pers comm, Brewer).

### MORPHOMETRY - SAMPLE COLLECTED FROM THE SCHELDT-LIPPENSBROEK

For the analyses of the landmark configurations of the neurocrania in dorsal and lateral view, the distributions in tangent space are a sufficient approximation for that in the Kendall shape space, as indicated by a correlation coefficient between Procrustes distance (in Kendall shape space) and tangent distance (in tangent shape space) of 1.000.

The relative warp analysis based on the lateral view data set, yielded 16 relative warps. The first two relative warps (RW1 and RW2) account for 28.43% and 17.78% of the total shape variation, respectively (Fig. IV.4.1- 2b). The pattern of shape change explained by the first two relative warps (Fig. IV.4.1- 2b) reveals the existence of two partially overlapping groups (due to intermediates), separated along the 'Shape1-Shape2' axis (S1-S2), with S1 being extremely broad-headed and S2 being extremely narrow-headed. The landmark configuration of extreme broad-headed specimens (S1) is visualized in figure IV.4.1- 2. The vectors indicate the difference in landmark configuration between S1 and S2 and represent the main shape differences between the broad- (S1) and narrow-headed (S2) specimens (Fig. IV.4.1- 2). The visualized landmark displacements for extreme narrow-headed specimens involve an increase in snout length, increase in skull height at the level of the occipital region, decrease in postorbital length of the skull, decrease in inclination of the sphenotic process, increase in length of the pterotic process and decrease in length of the epiotic process. The third and fourth relative warps respectively explain 13.33% and 11.39% of the shape variation (Fig. IV.4.1- 2c). No dimorphism is revealed in this scatter plot as the shape changes completely overlap, however, it does indicate that the shape variation within the group of broad-headed specimens is larger compared to that of the narrow-headed specimens.

The relative warp analysis based on the dorsal view data set, yielded 44 relative warps. The first two explain 29.66% and 14.93% of the total shape variation, respectively. Despite a larger amount of overlap in skull shape among the narrow-headed group and broad-headed group, a trend of shape differences is apparent along the S3-S4 axis (Fig. IV.4.1- 2e). The landmark configuration of the extreme broad-headed specimens (S3) is visualized in figure IV.4.1- 2. The vectors again represent the main shape differences between the broad- (S3) and narrow-headed (S4) specimens (Fig. IV.4.1- 2). These observed landmark displacements correspond to a longer snout, narrower post-orbital region, smaller and more slender sphenotic processes and longer epiotic processes in narrow-headed specimens. The third and fourth relative warps respectively explain 10.03% and 6.51% of the shape variation, however, not describing a dimorphic shape pattern (Fig. IV.4.1- 2f). Again, shape variation in the skull in broad-headed specimens seems to be larger than in the group of narrow-headed specimens.

## DISCUSSION

---

The presence of two trophic phenotypes in the European eel is widely accepted among fisherman and eel biologists and is considered the result of diet induced phenotypic

plasticity (LAMMENS AND VISSER, 1989). The influence of feeding conditions or random factors on head form has been subsequently examined, providing support for the hypothesis that these trophic phenotypes are an adaptive response to available trophic resources (TÖRLITZ, 1922; THUROW, 1958; LAMMENS AND VISSER, 1989; STEARNS, 1989; PROMAN AND REYNOLDS, 2000; TESCH, 2003; AUBRET ET AL., 2004). However, in most studied populations only one phenotype was dominant and measurements of mouth widths did not show clear bimodal distributions (LAMMENS AND VISSER, 1989).

Yet, both our biometric and morphometric data indicate a striking head shape dimorphism in Belgian eel populations. Thus, both broad- and narrow-headed eels co-occur syntopically in the Scheldt-Lippensbroek as well as across waters in Belgium. Eel population density and prey diversity / abundance may give an explanation for this syntopical occurrence of the phenotypes as shown in this study. According to the competition theory, high eel population densities would suggest that differentiation in feeding specialization (and consequently the phenotype) is more likely, which was supported by data of LAMMENS AND VISSER (1989). Of course, the biomass of small and soft (invertebrates) as well as larger and harder (fish, crustaceans) prey has to be sufficiently high to maintain this high level of predation. The fact that clear bimodal distributions in previous studies could not be detected may be the result of overlap of two closely resembling normal distributions. As indicated by our results, bimodality can not always be deduced from histograms, (Fig. IV.4.1- 1e) but requires a statistical bimodality test as applied in this study.

Our results reveal that the two phenotypes do, however, not form two discrete phenotypes but rather are reflected by two normal distributions with overlapping tails. Thus the shape of the skull/heads of specimens can be intermediate, which complicates discrete characterization of the two phenotypes. The most important and conspicuous differences between phenotypes are jaw length, head width and head height, similar results as found by TÖRLITZ (1922) and THUROW (1958).

Even though the subsamples of the Scheldt-Lippensbroek taken at different months (April, May, August, October) are too small to statistically test for bimodality, histograms suggest the presence of a bimodal pattern. Additionally, as the distribution of biometric data among the four subsamples is equal (DFA,  $F_{63,290}=1.0006$ ;  $p<0.482$ ), it can be assumed that both phenotypes are present throughout the year (no seasonality), which is supported by the data of LAMMENS AND VISSER (1989). As eel monitoring of the Scheldt-Lippensbroek is planned for the following four years, this will be examined more extensively. Interestingly, the biometric sample taken from eels dispersed across many different Belgian waters, also reveals bimodality, thus suggesting that the two phenotypes are distributed throughout

Belgium. As this dimorphism had been suggested previously for eels in Germany (TÖRLITZ, 1922; TESCH, 2003), the Netherlands (LAMMENS AND VISSER, 1989) and Ireland (PROMAN AND REYNOLDS, 2000), it is likely that this phenomenon is widespread throughout Europe.

Bimodality in head shape is also known in the Japanese eels (THUROW, 1958). Interestingly, such a head dimorphism has not yet been suggested for the American eel despite their strong morphological resemblances, close phylogenetic relationship, similar lifestyle and similar life cycle and spawning grounds (TESCH, 2003; TRAUTNER, 2006). However, as the bimodality may be hard to detect in small samples or when the distributions are overlapping strongly, it would be worth testing using a large biometric sample of American eels.

As both phenotypes have different prey preferences, as suggested before (PROMAN AND REYNOLDS, 2000; LAMMENS AND VISSER, 1989), any shift in the ratio of both phenotypes in natural populations may have an important impact on freshwater ecosystems.

The observation by PROMAN AND REYNOLDS (2000) that eels raised in captivity are exclusively narrow-headed indicates the need for well planned management actions when restocking. Re-introducing only one phenotype may induce changes in the food chain, with a consequent increase in the trophic competition of the eels introduced.

On the other hand, changes in the trophic ecosystem, whether natural or anthropogenic, will affect the presence or proportion of one or both phenotypes. In this case, any effort towards conservation requires the assessment of the degree plasticity to switch between the two phenotypes, as well as the rate of the phenotypic response involved. This will be the focus of further studies.

## ACKNOWLEDGEMENTS

---

We wish to thank the FWO (Project G.0388.00) for partially financing this research. Herrel A is a postdoctoral researcher of the Fund for Scientific Research Flanders, Belgium (FWO-VI). We further acknowledge J. Breine and the INBO technicians involved in the field sampling.



## IV.4.2 CRANIAL MYOLOGY IN *ANGUILLA ANGUILLA*



---

# CRANIAL MUSCULATURE OF *ANGUILLA ANGUILLA* (ANGUILLIFORMES): FUNCTIONAL IMPLICATIONS RELATED TO NARROW-HEADEDNESS AND BROAD-HEADEDNESS

---

De Schepper N, Van Liefferinge C, Herrel A, Goemans G, Belpaire C, Adriaens D

## ABSTRACT

---

The presence of two trophic phenotypes in the European eel is widely accepted among fisherman and eel biologists and is considered the result of diet induced phenotypic plasticity. As the broad-headed eels have larger jaw muscles and have a predominantly piscivorous diet compared to the narrow-headed specimens, we hypothesize that the broad-headed eels are able to exert larger bite forces. Jaw muscle bite forces are predicted for both phenotypes by the use of a dynamic model of mouth closing movements. In this study a detailed description of the cranial myology in *Anguilla anguilla* specimens sampled in the Lippensbroek is given as well as morphological and quantitative differences in cranial musculature between narrow-headed and broad-headed eels. Functional properties of the jaw muscles of both varieties (narrow-headed and broad-headed) are theoretically examined using the biomechanical model for mouth closing. Furthermore, hypothesis concerning ecological implications are provided

## INTRODUCTION

---

In Europe and Asia, eels (*Anguilla anguilla*) have a long culinary history as they have been part of the human diet for hundreds and even thousands of years (RINGUET ET AL., 2002; SCHWEID, 2004). Consequently, *Anguilla anguilla* has always been a popular (economical, aquacultural and recreational) fish for fisherman. It is common knowledge among fishermen and eel biologists that two phenotypes (broad- and narrow-headed) of European eels are present. This phenomenon, biometrically supported for populations in Germany (TÖRLITZ, 1922), the Netherlands (LAMMENS AND VISSER, 1989) and Ireland (PROMAN AND REYNOLDS, 2000) is considered the result of diet induced phenotypic plasticity (THUROW, 1958; TESCH, 2003; AUBRET ET AL., 2004). Broad-headed specimens tend to be piscivorous,

whereas the narrow-headed specimens predominantly feed on benthic invertebrates (BERTIN, 1942; TÖRLITZ, 1922; PROMAN AND REYNOLDS, 2000; TESCH, 2003).

A recent study on eels caught in Belgian waters (DE SCHEPPER ET AL., SUBMITTED A) (IV.4.1), provides a multidisciplinary approach of the cranial variation in the phenotype and a statistical bimodality test for cranial size and shape. The phenotypic variation is reflected in external head shape (mainly head width, head height and jaw length) as well as in the shape of the skull (snout length, skull height, width and length of the post-orbital region, length and inclination of the sphenotic processes, length of the pterotic and epiotic processes).

Consequently changes are expected in the head musculature as well and especially in the jaw muscles. Such like myological variation with respect to the head shape of phenotypes is demonstrated by TÖRLITZ (1922) for a German eel population. The question raises whether the phenotypes, collected in the Belgian Lippensbroek (for details see IV.4.1) also display variation in the morphology of cranial muscles and whether this can be related to narrow- or broad-headedness. Furthermore, if myological variation between the phenotypes in the Lippensbroek occurs, is the variation more or less extensive compared to the variation observed in the German population (TÖRLITZ, 1922). LAMMENS AND VISSER (1989) note that in most eel populations only one phenotype occurs. As in the Lippensbroek (DE SCHEPPER ET AL., SUBMITTED A) (IV.4.1) and in the TÖRLITZ' population both phenotypes co-occur, they are an ideal case-study to examine and compare myological data of the head of European eels.

Due to the larger jaw muscles and the piscivorous diet of the broad-headed eels compared to the narrow-headed specimens, we hypothesis that the broad-headed eels are able to exert larger bite forces. Bite forces, generated by the jaw muscles are predicted for both phenotypes by the use of a dynamic model of mouth closing movements (VAN WASSENBERGH ET AL., 2005).

The present study provides 1) a detailed description of the cranial myology in *Anguilla anguilla* specimens sampled in the Lippensbroek and 2) morphological and quantitative differences in cranial musculature between narrow-headed and broad-headed eels of the Lippensbroek. 3) Quantitative variation in cranial musculature is compared with data of the German eel population studied by TÖRLITZ (1922). 4) Functional properties of the jaw muscles of both varieties (narrow-headed and broad-headed) are theoretically examined using the biomechanical model for mouth closing of VAN WASSENBERGH ET AL. (2005) as bite forces for both phenotypes are predicted and subsequently compared. Furthermore, hypothesis concerning ecological implications are provided.

---

## MATERIAL AND METHODS

---

### SPECIMENS

To study the morphology of the cranial musculature in narrow-headed and broad-headed eels, a total of 27 commercially obtained specimens were used (see Table III.1-1E). Twelve broad-headed and fifteen narrow-headed eels were selected by vision, consequently only the extremes are retained and intermediately shaped eels were rejected. Additionally, twelve specimens, collected in the Lippensbroek-Scheldt, were biometrically examined, dissected and used to define the weight of some of the cranial muscles. In this study, specimens were anaesthetized, sacrificed and fixed (see III.2.1). Specimens were cleared and stained and dissected. For details of used protocols, see III.2.2.

### WEIGHT OF THE CRANIAL MUSCLES

Six narrow-headed eels and six broad-headed eels were selected to determine the weight of the adductor mandibulae complex, levator arcus palatini, levator operculi, dilatator operculi and protractor hyoidei. Other cranial muscles were considered but it appeared impossible to dissect these muscles out of the skull, without damaging or pulling them apart (Table IV.4.2- 1). Of three additional broad-headed and three narrow-headed specimens, the weight was measured of only the adductor mandibulae complex (Table IV.4.2- 1). To diminish inaccuracies in measurements due to manipulation of the tissue during dissections, the adductor mandibulae complex was weighed as one entity. Weight of the muscles was defined using a digital balance (OHAUS Adventurer) to the nearest 0.001 g. Weight of the body was defined to the nearest 0.1 g. Total length of the specimens was measured with a ruler to the nearest 0.1 cm. These specimens are listed in Table III.1- 1E)

### BIOMECHANICAL MODELLING

Two specimens of the Lippensbroek-Scheldt were dissected and biometrical data were used to predict biomechanical dynamics during mouth closure based on the model of (VAN WASSENBERGH ET AL., 2005). For details of the mouth closing model of Van Wassenbergh see III.2.7.

## RESULTS

### TERMINOLOGY OF THE CRANIAL MYOLOGY

The terminology used to describe the cranial musculature of the European eel in the present manuscript follows that of WINTERBOTTOM (1974). Four of the cranial muscles in *Anguilla anguilla* (i.e. adductor mandibulae, levator operculi, dilatator operculi and levator arcus palatini) were previously studied and described by TÖRLITZ (1922) for narrow-headed and broad-headed European eels. But, as not all cranial muscles are considered (e.g. adductor arcus palatine, adductor hyomandibulae, adductor operculi, protractor hyoidei, sternohyoideus, hyohyoidei,..), a detailed description is presented in this study. No distinguishable differences in configuration of these four cranial muscles between TÖRLITZ' eels and the Lippensbroek eel population could be detected. Even though TÖRLITZ' work forms a solid (but limited) base for detailed anatomical descriptions of Anguilliformes, one can and should argue the applied terminology. Even though TÖRLITZ (1922) shortly mentions the more accurate 'musculus adductor mandibulae' as proposed by VETTER (1878), he denominates the mouth closing muscles throughout the manuscript erroneously as 'musculus temporalis'. As this term does infer incorrectly to the cheek muscles of mammals, we prefer the 'adductor mandibulae complex' according to the nomenclature of VETTER (1878) and WINTERBOTTOM (1974). The 'Portion I, II and III' of the 'musculus temporalis' of TÖRLITZ (1922) correspond to the subdivisions A1, A2 and A3 respectively, as applied in the current manuscript, based on the criteria of WINTERBOTTOM (1974). Similarly, the 'levator palatini' used by TÖRLITZ (1922), is synonymized with 'levator arcus palatini' by WINTERBOTTOM (1974) and applied in this manuscript.

### MYOLOGY OF THE HEAD OF NARROW-HEADED EELS

The adductor mandibulae complex is hypertrophied in such a way that the lateral as well as the dorsal surface of the head is covered by this large muscle mass (Fig. IV.4.2- 1, 2). Furthermore, both halves on each side of the head contact dorsally in the midline. This complex stretches dorso-caudally to contact the epaxials by means of an aponeurosis. Three subdivisions A1, A2 and A3 are recognized. Fibers of the different subdivisions do not intermingle. The A1 is the largest and dominant subdivision of the complex. Two lengthwise running tendons divide the A1 into 3 parts which are hardly separable. The fibres of the two dorsal most A1-parts are more antero-ventrally directed, whereas the

fibres of the ventral A1-part are more rostro-caudally directed. These two tendons unite anteriorly in the common tendon, T A1. This tendon (T A1) inserts onto the primordial ligament, which stretches to the antero-dorsal surface of the maxillary, and onto the caudal margin of the coronoid process. The origin of the A1 is extended over the dorsal and lateral surfaces of the frontals, parietals, epiotics and pterotics. The fibres are attached to the skull by the presence of a dorso-medial ridge and a lateral ridge on the frontals and by a deep groove in the epiotics and pterotics. The protruding sphenotic wing covered by the adductor mandibulae complex, hence forms no part of its origin. The A1 originates ventro-caudally from the preopercle and hyomandibula. The A2 is situated medial to the A1 and also inserts onto caudal edge of the coronoid process as well as the medial surface of the dentary. This deeper subdivision originates from the ventro-lateral surface of the frontals, lateral surface of the basisphenoid and pterosphenoid, and the anterior surface of the protruding sphenotic. The A3 originates from the lateral surface of the hyomandibula and quadrate. The fibres radiate from a strong anterior tendon, which inserts onto the medial surface of the dentary.

The dilatator operculi originates from the caudal surface of the sphenotic and the latero-caudal surface of the pterotic (Fig. IV.4.2- 1B). The fibres converge caudo-ventrally in a tendon, which inserts onto the lateral surface of the opercular dorsal process.

The levator operculi originates tendinously and musculously from the ventro-caudal surface of the pterotic (Fig. IV.4.2- 1A, 2). The fibres insert onto the dorsal edge of the opercle and onto the lateral surface of the opercle. Except for a thin ventral margin, the opercle is completely covered by fibres of the levator operculi.

The adductor operculi originates from the lateral surface of the exoccipital and the dorso-lateral surface of the basioccipital (Fig. IV.4.2- 1B). The fibres insert onto the medial surface of the opercle and reach half of the length of the opercle.

The levator arcus palatini is a triangular muscle, covered by the three subdivisions of the adductor mandibulae complex and the dilatator operculi (Fig. IV.4.2- 1B). The fibres originate from the outer surface of the protruding sphenotic wing as well as from the ventral surface of the sphenotic. The anterior fibres are more anteriorly directed and insert onto the pterygoid while the rest of the fibres insert onto the quadrate and hyomandibula.

The adductor arcus palatini originates mainly from the parasphenoid but caudally some fibres attach to the prootic (Fig. IV.4.2- 1B). The median ridge of the parasphenoid is free of fibres, thus separating the left and right part of the muscle. The muscle inserts partially onto the dorsal edge and medial surface of the caudal part of the pterygoid and

mainly onto quadrate and hyomandibula. The caudal margin of this muscle is situated at the level of the caudal border of the sphenotic.

The adductor hyomandibulae is absent.

The protractor hyoidei originates tendinously from the medial surface of the dentary, just behind the symphysis between the left and right lower jaw (Fig. IV.4.2- 1, 2). The fibres insert musculously and tendinously onto the lateral surface of the posterior ceratohyal. The thin caudal tendinous sheet stretches out to about half the length of the posterior ceratohyal. The left and right halves of the muscles are not fused in the midline.

The hyohyoidei adductores surround the gill chamber ventrally, forming a 'sac-like' structure (Fig. IV.4.2- 2). This sheet attaches dorsally to the medial surface of the opercle and more caudally to the horizontal septum (ventral to the epaxial muscles). The sheet continues ventrally, interconnecting the branchiostegal rays and meets its antimeres in the midline by means of an aponeurosis. It is not clear whether the hyohyoideus abductor is fused with the hyohyoidei adductores or whether it is not yet completely differentiated, given the basal phylogenetical position of the Anguilliformes.

The sternohyoideus is partially covered by the hyohyoidei adductores (Fig. IV.4.2- 2). This muscle comprises a left and right part, which attach rostrally on a medial aponeurosis. Both parts are connected in the midline. Each part originates from the left and right cleithrum, respectively. Though, the caudo-ventral fibres merge with the anterior fibres of the hypaxials. The sternohyoideus inserts rostrally onto the urohyal by means of a well developed tendon. This long tendon diverges more caudally covering the lateral surface of the muscle.

#### DIFFERENCES IN MUSCULATURE BETWEEN NARROW-HEADED AND BROAD-HEADED EELS

No marked differences between the narrow-headed and broad-headed eels are found with respect to origin or insertion of the cranial muscles. Though, the weight of the cranial muscles differs between the two phenotypes as shown in figure IV.4.2- 3A-E. The weight of the adductor mandibulae complex, levator arcus palatini, dilatator operculi, levator operculi and protractor hyoidei in the narrow-headed phenotypes is lower compared to that of broad-headed specimens with similar total lengths (Fig. IV.4.2- 3A-E). In narrow-headed eels, the mean weight of the adductor mandibulae complex is 1.97 ‰ of the total body weight, whereas in the broad-headed specimens this is 5.45 ‰ (Table IV.4.2- 1). Comparing the absolute values of the weight of the jaw muscles, those of the broad-headed eels are about three times higher compared to that of the narrow-headed eels of the same length. In narrow-headed eels, the mean weight of the levator arcus



palatini is 0.18 ‰ of the total body weight, whereas in the broad-headed specimens this is 0.41 ‰ (Table IV.4.2- 1). The mean weight of the dilatator and levator operculi of the narrow-headed eels is respectively 0.06 ‰ and 0.30 ‰ of the total body weight, whereas in broad-headed specimens the weight is respectively 0.08 ‰ and 0.39 ‰ (Table IV.4.2- 1). In narrow-headed eels, the mean weight of the protractor hyoidei is 0.25 ‰ of the total body weight, whereas in the broad-headed specimens this is 0.40 ‰ (Table IV.4.2- 1).

## BIOMECHANICAL MODELLING OF JAW ADDUCTOR FORCES BETWEEN NARROW-HEADED AND BROAD-HEADED EELS

The dynamic model of jaw closing is developed by VAN WASSENBERGH ET AL. (2005) to evaluate the importance of jaw adductor muscles on the speed of mouth closure. The model allows the prediction of bite forces generated during the closing of the mouth and includes inertia, pressure, tissue resistance and hydrodynamic drag forces on the lower jaw. Both phenotypes are scaled to equal head size in order to allow a quantitative comparison.

### DYNAMICS OF MOUTH CLOSING

The simulations with the mouth-closing model show the following general pattern. The duration of jaw closure (0.05 s) is identical in both phenotypes, and the general pattern of total muscular forces generated by the jaw muscles (gradually increasing) during jaw closing is quite similar in both extreme phenotypes. The magnitude of force, in contrast, in the extreme broad-headed eel is, at each moment, about twice of that predicted for the extreme narrow-headed eel (Fig. IV.4.2- 4C, D).

Figure IV.4.2- 4 gives an overview of the model output of the forces that are involved during a specific jaw closure in the two varieties of *Anguilla anguilla*. The simulations show the following general pattern. The model predicts that the time needed to close the lower jaw, from  $-50^\circ$  to  $-10^\circ$ , is about 45 milliseconds in the narrow- and broad-headed specimens (Fig. IV.4.2- 4A, B). Initially, muscular forces are mainly required to accelerate the lower jaw, and thus overcoming its inertia (Fig. IV.4.2- 4C, D). In the narrow-headed eels this takes about 5 milliseconds, whereas in broad-headed eels about 7 milliseconds are needed. After this phase, the model predicts that forces from the lower jaw muscle activity are largely used to overcome the increasing positive pressure in the buccal cavity and the resistance from soft tissues. In both phenotypes, the importance of drag forces on the rotation of the lower jaw is negligible. During the final 30 milliseconds

of the mouth-closing phase, the force generated by the jaw adductors is predominantly countering resistance caused by stretching of the jaw-opener muscles and the forces exerted on the lower jaw resulting from super-ambient pressure inside the mouth that typically appears near the end of mouth-closing (pers comm., Van Wassenbergh) (Fig. IV.4.2- 4).

## DISCUSSION

---

First, it has to be addressed that the results of this paper do not provide evidence that allows directional interpretations of causalities or consequences. Subsequently, assumptions made in the following discussion should rather be considered as reflections on possible and rather logical spatial interactions.

Second, even though the above mentioned results and following discussion are based on extreme broad-headed and extreme narrow-headed eels, it has to be addressed that an eel population does not solely include these two phenotypes. Most of the specimens are intermediate morphs, showing mixed values (TÖRLITZ, 1922; THUROW, 1958; DE SCHEPPER ET AL., SUBMITTED A) (IV.4.1). Consequently mixtures in diet and feeding behaviour (TESCH, 2003) should be kept in mind.

### VARIABILITY IN WEIGHT OF CRANIAL MUSCLES RELATED TO NARROW- AND BROAD-HEADEDNESS?

The absolute weight (g) of the mouth closing muscles of the broad-headed eels of the Lippensbroek is about 2.5 to 3 times higher compared to that of the narrow-headed eels of the same total length (Fig. IV 4.2- 3A). Relative to the total body weight, the weight of the jaw muscles of the broad-headed eels is on average about 3 times that of narrow-headed eels (Table IV.4.2- 1). This was also found by TÖRLITZ (1922). In this study, the subdivisions of the adductor mandibulae complex are not measured separately in order to avoid additional inaccuracies in the measurements due to manipulation. TÖRLITZ (1922) did separate subdivision A3 from A1 and A2, with A3 showing much less difference between the two phenotypes (0.07‰ and 0.11‰) than for A1 + A2 (1.5‰ and 4.9‰). Space constraints on the deeper A3 could explain why this subdivision shows a similar weight ratio (HERREL ET AL., 2002). The total length of TÖRLITZ' eels ranged from 58.5cm to 74.5cm, with an average jaw muscle weight for the narrow-headed and broad-headed eels of respectively 1.6‰ and 5.0‰, whereas the eels of the present study are smaller with larger

average jaw muscle weight (Table IV.4.2- 1). TÖRLITZ (1922) already noted that eels with larger body size had relatively smaller (lighter) jaw muscles compared to those of smaller eels of the same phenotype and our data seem to confirm this trend.

Based on both studies we can conclude that extreme narrow-headed eels in general have smaller jaw muscles (about three times), than extreme broad-headed ones. It is expected that the weight of the mouth closing muscles of intermediates, expressed as permille, is situated somewhere in between both ranges of the phenotypes or even within the range of a phenotype.

The average weight of the levator arcus palatini, expressed as permille of the total body weight, is respectively 0.165‰ and 0.45‰ for the narrow- and broad-headed eels of the German eel population (TÖRLITZ, 1922). Our results show similar values (0.18‰ and 0.41‰; Table IV.4.2- 1). As can be deduced from the difference in average weight of the levator arcus palatini, as well as from the slopes of the regression lines (Fig. IV.4.2- 3B), this muscle is larger in the broad-headed eels.

The average weight values for the dilatator operculi differ between the two populations, being larger for both phenotypes in TÖRLITZ' eel population (0.085‰ and 0.105‰) (Lippensbroek population, 0.06‰ and 0.08‰, Table IV.4.2- 1). This is assumed to be related to the fact that the examined specimens in TÖRLITZ' study are larger, compared to those examined here (Lippensbroek population, Table IV.4.2- 1). This hypothesis is supported by the data of TÖRLITZ (1922). The smallest narrow-headed eel (53.5 cm) has a permille for the dilatator operculi of 0.06‰, whereas this accounts for 0.08‰ in the smallest broad-headed eel (58.5 cm). These values indeed correspond to our values (Table IV.4.2- 1). The average weight of the dilatator operculi, with respect to the total body weight, tends to be larger in the broad-headed eels in both populations, though the differences are not that extensive as also can be deduced from the more similar slopes of the regression lines (Fig. IV.4.2- 3C).

The values of the average weight for the levator operculi are less discriminative between the two phenotypes (0.30‰ and 0.39‰, Table IV.4.2- 1) as could also be deduced from the more similar slopes of the regression lines of both phenotypes (Fig. IV.4.2- 3D). As this muscle is not measured in the study of TÖRLITZ (1922), no comparison is possible.

The difference in the average weight permille of the protractor hyoidei (0.25‰ and 0.40‰, Table IV.4.2- 1) for the narrow- and broad-headed eels of the Lippensbroek eel population and the slopes of the regression lines between the two phenotypes are more prominent (Fig. IV.4.2- 3D, E), compared to that in the dilatator and levator operculi. This muscle has not been examined by TÖRLITZ (1922) so no comparison is possible.

The muscular differences are most prominent in the mouth closing muscles, but also to the lesser extent in the levator arcus palatini and in the protractor hyoidei (Table IV.4.2- 1). The adductor mandibulae complex is situated laterally and dorsally on the skull, and consequently the mass differences between the phenotypes contribute highly to the observed cranial shape differences as discussed in DE SCHEPPER ET AL. (SUBMITTED A; IV.4.1).

#### PREDICTED BITE FORCES GENERATED BY ENLARGED JAW MUSCLES

From an evolutionary point of view, it is assumed that jaw muscle hypertrophy and consequent large bite forces are evolved as an adaptation for durophagy (HERREL ET AL., 2002; WESTNEAT, 2003; VAN WASSENBERGH ET AL., 2005). This idea is applicable to *Anguilla anguilla* in general, leaving the dimorphism out of consideration, as all specimens have dorso-caudally expanded, large jaw muscles, enabling them to generate large bite forces. In narrow-headed as well as broad-headed eels this is applied for cracking shells of crustaceans, snails and muscles, even though worms form the largest part of the diet of narrow-headed eels, whereas broad-headed eels tend to eat more fish (TÖRLITZ, 1922; THUROW, 1958; LAMMENS AND VISSER, 1989; PROMAN AND REYNOLDS, 2000; TESCH, 2003). So, former studies on dimorphism of eels revealed that the head-dimorphism is tied to differences in diet.

According to the mouth-closing model of VAN WASSENBERGH ET AL. (2005) based on morphological data of extreme narrow- and broad-headed specimens the magnitude of force in the extreme broad-headed eel is about twice the size of that predicted for the extreme narrow-headed eel (Fig. IV.4.2- 4). Even though these are only preliminary data, and future studies will add model-predicted data as well as experimental data, the model supports our hypothesis that the expanded jaw muscles of the broad-headed eels are able to generate enlarged bite forces. As supported by dietary data (TÖRLITZ, 1922; THUROW, 1958; LAMMENS AND VISSER, 1989; PROMAN AND REYNOLDS, 2000; TESCH, 2003) these enlarged bite forces may be beneficial for increased piscivorous feeding habits in broad-headed eels. Again it needs to be mentioned that fish as prey items are not limited to broad-headed eels, though are occasionally found in narrow-headed specimens and intermediates as well.

#### ENLARGED JAW MUSCLES IN BROAD-HEADED EELS RELATED TO SPATIAL CHANGES?

The expansion of the adductor mandibulae complex can be expected to be related to spatial changes in the feeding apparatus. As the enlarged jaw muscles lead to a

powerful bite (model output), increased mechanical loads and thus increased cranial rigidity are expected at the level of the jaw muscles insertion sites. Indeed, the observed variation in skull morphology of narrow- and broad-headed eels reveals structural differences belonging to the feeding apparatus (TÖRLITZ, 1922; THUROW, 1958; DE SCHEPPER ET AL., SUBMITTED A; IV.4.1). The lower jaw and maxillaries, involved in the insertion of the A1 and A2, are lengthened, more robust and form a wider arch in the broad-headed eels (TÖRLITZ, 1922; THUROW, 1958). Furthermore, THUROW (1958) noted the larger size of the coronoid process in broad-headed eels, to which the A1 and A2 insert. This indicates a stronger bite as a higher coronoid process implicates a longer force input arm (CABUY ET AL., 1999; HERREL ET AL., 2002). Even though the hyomandibula and quadrate are shortened in the broad-headed eels (TÖRLITZ, 1922; THUROW, 1958) no additional fortification is observed. Interestingly, these elements form the insertion site for the A3, which is not remarkably different between the two phenotypes (TÖRLITZ, 1922).

Osteological variation associated with extreme broad- and narrow-headedness is not only detected at the level of the insertion sites, also the attachment site of the jaw muscles appear modified: Broad-headed eels have larger and more robust protruding sphenotic processes, one of the origins of the A2 (DE SCHEPPER ET AL., SUBMITTED A; IV.4.1); The available area for muscle (A1 and A2) attachment is expanded in broad-headed eels as the skull of broad-headed eels is larger compared to that of a narrow-headed eel of similar length (TÖRLITZ, 1922; THUROW, 1958; DE SCHEPPER ET AL., SUBMITTED A; IV.4.1).

### MORPHOLOGICAL VARIATION RELATED TO FEEDING MODE?

Three feeding modes, depending on prey size and food consistency, are discerned in anguillids: inertial suction, shaking and rotational feeding (HELPMAN AND CLARK, 1986; HELPMAN AND WINKELMAN, 1991). Rotational feeding is usually performed when the prey item is firm and exceeds 85% of the eel's jaw width (HELPMAN AND CLARK, 1986; HELPMAN AND WINKELMAN, 1991). As dietary studies revealed piscivorous diet preferences of broad-headed eels (BERTIN, 1942; TÖRLITZ, 1922; PROMAN AND REYNOLDS, 2000; TESCH, 2003), rotational feeding may be assumed the dominant (though not exclusive) feeding mode of this phenotype, whereas the narrow-headed eels are likely to spin feed less frequent. In this regard, the more robust, broader and shorter premaxillo-ethmovomerine complex, and the strengthened upper and lower jaws, distinguishing the broad-headed eels from the narrow-headed eels (TÖRLITZ, 1922; THUROW, 1958; DE SCHEPPER ET AL., SUBMITTED A; IV.4.1), may be considered structural changes to enhance a solid grip onto the prey during spinning movements. However it needs to be addressed that narrow-headed eels occasionally eat

fish as well and that preferential differences in the application of the types of feeding modes still needs to be studied.

## **ACKNOWLEDGEMENTS**

---

We wish to thank the FWO (Project G.0388.00) for partially financing this research. Thanks to Van Wassenbergh S and Herrel A for meaningful discussions concerning the mouth closing model. Herrel A is a postdoctoral researcher of the Fund for Scientific Research Flanders, Belgium (FWO-VI). We further acknowledge J. Breine and the INBO technicians involved in the field sampling.

### IV.4.3 CRANIAL MORPHOLOGY IN *CONGER CONGER*





---

# CRANIAL OSTEOLOGY AND MYOLOGY OF *CONGER CONGER* (ANGUILLIFORMES): COMPARISON WITH BURROWING SPECIES

---

De Schepper N, Lambeets K, De Kegel B, Adriaens D

## ABSTRACT

---

Anguilliformes are primitively adapted for wedging through small openings, which is assumed to be the basic mode of life but many eels are adapted to a range of different lifestyles (pelagic, head-first burrowing and tail-first). In order to examine the true nature of cranial specializations related to burrowing, the detailed morphology of many species, displaying different kinds of (non-)burrowing needs to be studied. As the predatory feeding behaviour and non-burrowing lifestyle, as also observed in *Conger conger*, is considered the primitive condition, this species forms an ideal subject to study the non-specialized anguilliform morphology. This study provides a detailed description of the cranial myology and osteology of *C. conger*. These prophylogical data are subsequently compared to those of anguilliform species displaying a burrowing lifestyle.

## INTRODUCTION

---

The order Anguilliformes forms a large group of cosmopolitan elongate teleosts (NELSON, 1994). Eels are predominantly adapted to a predatory way of feeding (SMITH, 1989B). Furthermore, as stated by GOSLINE (1971) Anguilliformes are primitively adapted for wedging through small openings, which is assumed to be the basic mode of life. In this regard several morphological specializations are considered to benefit the penetration capacities of such wedges (elongated body and solid skull), moving back and forth (scales not overlapping or absent, thus preventing damaging) or preventing the entering of sediment in the gill cavity (gill openings small) (GOSLINE, 1971; SMITH, 1989B). As a consequence of the latter, eels will rather engulf water to obtain water streaming over the gills than create suction to force water over the gills by contraction and expansion of the opercular apparatus (GOSLINE, 1971).

This study focuses on *Conger conger* (Linnaeus, 1758), a representative of the family Congridae and subfamily Congrinae (Order Anguilliformes) (NELSON, 1994; SMITH, 1989B). The Congridae are seen as 'relative generalized eels, most without unusual

modifications' (SMITH, 1989B), with the exception of the highly modified Heterocongrinae (DE SCHEPPER ET AL., IN PRESS A) (IV.2). *Conger conger* represents the above mentioned primitive condition: non-burrowing lifestyle and predatory feeding behaviour. *C. conger* displays nocturnal activity, and is specialized in preying upon fishes, crustaceans and squid. Several studies based on stomach analysis of *C. conger* (CAU AND MANCONI, 1984; OLASO AND RODRIGUEZ-MARIN, 1995; MORATO ET AL., 1999; O'SULLIVAN ET AL., 2004) reported the dominance of fish in their diet. Although *C. conger* is a benthopelagic species, usually found on hard and sandy bottoms, it consumes fish species living in benthopelagic, benthic and even pelagic and mesopelagic environments, indicating their active predatory feeding behaviour. During the day, *C. conger* is found on rocky and sandy bottoms, where it retreats in holes, caves or wedges (LYTHGOE AND LYTHGOE, 1991).

Previous studies have described the cranial osteology of some anguilliform representatives in detail (BÖHLKE, 1989) but almost no attention has been paid to the morphology of the cranial musculature (except in DE SCHEPPER ET AL., 2005; 2007; IN PRESS A) (IV.1; IV.2; IV.3; IV.4.2). As anguilliform eels are adapted to a range of different lifestyles (pelagic Serrivomeridae, head-first burrowing Moringuidae or tail-first burrowing Ophichthidae and Heterocongrinae), considerable morphological diversity within such a large group related to a particular lifestyle is encountered (NELSON, 1994). Consequently, considering morphology in relation to lifestyle can yield a better insight in the evolutionary morphology of Anguilliformes. In order to examine the true nature of cranial specializations, the detailed morphology of many species, displaying different kinds of (non-)burrowing and feeding behaviour, needs to be studied (DE SCHEPPER ET AL., 2005; 2007; IN PRESS A) (IV.1; IV.2; IV.3). As the predatory feeding behaviour and non-burrowing lifestyle, as also observed in *C. conger*, is considered the primitive condition (GOSLINE, 1971), this species forms an ideal subject to study the non-specialized anguilliform morphology.

This paper provides a detailed description of the cranial myology and osteology of *C. conger*. Even though some data are already published on morphology, behaviour, diet and biology (CAU AND MANCONI, 1984; OLASO AND RODRIGUEZ-MARIN, 1995; MORATO ET AL., 1999; BELOUZE, 2001), a detailed description of its cranial myology is currently lacking. Any inferences with respect to functional implications of their particular predatory feeding behaviour or benthic lifestyle on morphology (or vice-versa) are lacking and will be discussed here where possible.

## MATERIAL AND METHODS

---

For this study five specimens of *Conger conger* (total length varying between 0.52 m and 1.64 m) were used. Three *C. conger* specimens were commercially obtained, caught at the North Sea shore (Nieuwpoort, Belgium), and preserved in alcohol. One dried specimen (UGMD 53065) and one alcohol preserved specimen (UGMD 53089) were obtained from the Zoology Museum, Ghent University - Belgium. See chapter III.1 for details on specimens (Table III.1- 1A). For more information about dissections, clearing and staining protocols and visualization, I refer to see III.2.2 and III.2.5).

## RESULTS

---

### OSTEOLOGY

The firm and solid *neurocranium* is dorso-ventrally flattened and slender (Fig. IV.4.3- 1, 2). The upper jaw is slightly longer than the lower jaw. The upper (pars vomeralis included) and lower jaws show an outer row of big incisiform teeth as well as recurved teeth, forming a cutting edge and an inner row of smaller conical, sharp teeth (Fig. IV.4.3- 1, 4). The bones of the cranium connect by butt joints, which means that the sutures are approximately straight, except for the bones of the dorsal and lateral skull wall, where the interdigitation is elaborate or where the bones have even fused (Fig. IV.4.3- 2B).

The *ethmoid region* comprises the premaxillo-ethmovomerine complex, consisting of an ankylosed premaxillary, mesethmoid and vomer. Ethmoid processes are absent. The anterior part of the orbit is dorsally and ventrally bordered by respectively the pars ethmoidalis and pars vomeralis. Caudally the pars ethmoidalis covers the dorsal surface of the fused frontals. The lateral processes of the pars vomeralis bear the vomero-ptyergoidal articular facet (Fig. IV.4.3- 2A, B; 3A). In between this facet and the pterygoid a strip of connective tissue is found, resulting in a strong though slightly movable connection. The articulation between the premaxillo-ethmovomerine complex and the maxillary comprises two articular facets (Fig. IV.4.3- 2A). The anterior and posterior processes of the maxillary (Fig. IV.4.3- 5A) rest on the maxillo-premaxillo-ethmovomerine articular facet, which is situated antero-laterally on the ethmovomerine part of the complex.

The *orbital region* comprises the basisphenoid, frontals, pterosphenoids and parasphenoid (Fig. IV.4.3- 2). Orbitosphenoid is absent. A relatively small unpaired

basisphenoid borders the ventro-caudal edge of the orbits. The basisphenoidal process (Fig. IV.4.3- 2A), directed towards the orbits, serves for the attachment of some of the eye muscles. The frontals occupy the largest part of the skull roof. They are fused, forming a single dorsal element. The tip of the fused frontals tapers rostrally and is dorsally covered by the dorso-caudal projection of the pars ethmoidalis. The dorsal border of the orbit is formed by the rostral part of the frontals. At the level of the caudal margin of the orbit, frontal processes are present at both sides of the skull, which encloses the entrance of the supraorbital canal (Fig. IV.4.3- 2A). The largest part of the lateral skull wall, in front of the sphenotics, is formed by the pterosphenoids. The anterior pterosphenoidal margin is situated at the same level as the anterior margin of the prootic. The parasphenoid spans from the anterior orbital region to the occipital region forming the longest cranial element. Two symmetrical, latero-dorsal projections contact the sphenotics, where the parasphenoid reaches its highest width. Anteriorly a bifid, thin extension tapers and covers the pars vomeralis dorsally. Caudally, the parasphenoid splits into two long, narrow arms, *i.e.* the parasphenoidal processes, enclosing the basioccipital (Fig. IV.4.3- 2D).

The *otic region* comprises the sphenotics, pterotics, prootics, epiotics and parietals. The sphenotic is latero-dorsally situated in the skull and bears an extensive sphenotic process or sphenotic wing (Fig. IV.4.3- 2B, D). The posterior part of the base of the sphenotic process contributes to the anterior suspensorial articulation facet (Fig. IV.4.3- 2A). The pterotic is a paired bone forming a large part of the lateral skull wall, from the frontal processes to the caudal skull border. The rostral part is elongate, forming a slender bar, enclosing the temporal canal. Posteriorly this bone becomes wider, contributing to the dorso-lateral skull wall. The dilatator fossa, for the attachment of several cranial muscles, is situated at the ventro-lateral side of the pterotic and is ventrally bordered by the dorsal edge of the hyomandibula (Fig. IV.4.3- 2A). The dorsal part of the fossa dilatator is bordered by the pterotic. The fossa lies between the suspensorial articulatory facets for the hyomandibula. The pterotic contributes to the caudal part of the anterior suspensorial articulatory facet. The posterior suspensorial articulatory facet is formed completely by the pterotic (Fig. IV.4.3- 2B). The caudal part of the pterotics forms together with the exoccipital and prootic the fossa subtemporalis, which serves as an attachment site of the adductor hyomandibula (Fig. IV.4.3- 2A). A large part of the lateral and ventral skull wall is formed by the prootics. Otic bullae are hardly developed. The epiotics are paired and are situated at the postero-dorsal surface of the neurocranium (Fig. IV.4.3- 2C). The epiotics form two symmetrical projections towards the supraoccipital giving the skull a dorso-caudally sloping appearance. Numerous grooves are found on the epiotics, pterotics and exoccipitals. The two parietals have a rectangular

shape, rostro-caudally extended, and form a large part of the skull roof. Both parietals contact in the midline.

The *occipital region* comprises the exoccipitals, basioccipital and supraoccipital. The exoccipitals surround the foramen magnum dorso-laterally, forming the ventro-lateral part of the cranium in caudal view (Fig. IV.4.3- 2C). Two caudo-lateral exoccipital processes are present (Fig. IV.4.3- 2C). The medial supraoccipital is unpaired and is dorso-caudally situated, reaching behind the posterior border of the skull. It shows medio-caudally an extensive transvers ridge and bears two caudal spiny projections. This small bone contributes, together with the epiotics to the dorso-caudal slope of the neurocranium. The caudal edge serves as attachment for the aponeurosis between the adductor mandibulae complex and the epaxials, which is laterally expanded to the epiotics and pterotics.

The *suspensorium* comprises three bones, the hyomandibula, quadrate and pterygoid (Fig. IV.4.3- 3A). The hyomandibula, quadrate and pterygoid are strongly connected by interdigitating sutures, forming a massive, strong trapezoidal entity, with an oblique long-axis. The lateral surface shows highly elevated ridges for the insertion of the adductor mandibulae complex (Fig. IV.4.3- 3A). The anterior and posterior dorsal suspensorial articular condyles fit respectively into the anterior and posterior suspensorial articular facets of the neurocranium. The hyomandibula articulates with the opercle through a opercular articular condyl. The quadrate bears the mandibular articular condyl which articulates with the mandibular articular facet of the angular complex. The pterygoid is a slender, elongated bone. The rostral tip of the bone is ligamentously and strongly connected the vomero-ptyergoidal articular facet on the pars vomeralis.

The *opercular apparatus* comprises four bones: opercle, preopercle, interopercle and subopercle (Fig. IV.4.3- 3B-E). The preopercle is with its anterior edge tightly connected to the hyomandibula through dense connective tissue. The interopercle is rather triangularly shaped and elongated in the rostro-caudal axis. The dorsal edge of this element is concealed by the caudal part of the preopercle. The subopercle follows the ventro-caudal edge of the opercle, to which it is firmly attached by dense connective tissue. The caudal borders of the subopercle and opercle reach the level of the second vertebra. The opercle articulates by means of the rostro-dorsal opercular articular facet with the opercular condyl of the hyomandibula. This facet is situated at the distal end of the rostro-dorsal process of the opercle.

The *lower jaw* is shorter than the upper jaw and is composed of the dentary, the Meckel's cartilage and the angular complex (Fig. IV.4.3- 4). It encloses the mandibular

canal of the cephalic lateral line system. The left and right halves form one firm entity by means of a large bony symphysis. The anterior and largest part of the lower jaw is formed by the dentary. The dorso-lateral edge of this part bears the coronoid process. The dentary encloses the Meckel's cartilage anteriorly and covers its posterior part laterally. The angular complex is the result of the fusion of the articular with the retro-articulo-angular complex (autapomorphic for Anguilliformes (ROBINS, 1989; TAVERNE, 1999)). The angular complex is anteriorly pointed and partially enclosed by the dentary complex. The retroarticular process is long and is caudally directed. The mandibular articulation facet, ventral to the angular process mediates the articulation between the angular complex and the quadrate.

The *hyoid apparatus* comprises an unpaired median basihyal and urohyal and paired anterior and posterior ceratohyals. Hypohyals are fused with the anterior ceratohyals. Interhyals are absent. In the past (BÖHLKE, 1989B) the term epihyal was used to indicate the posterior ceratohyal. Though, as this term incorrectly insinuates homology with the epihyal of mammals, as well as an epihyal structure represents the dorsal element of the hyoid arch, the term posterior ceratohyal should be used. The basihyal is a long, cylindrical element (Fig. IV.4.3- 5C). It articulates with the anterior ceratohyals and ventrally with the rostral tip of the urohyal. The articulation facet of the urohyal for the basihyal is situated rostrally and those for the anterior ceratohyals are situated dorso-laterally (Fig. IV.4.3- 5D). Caudally, the urohyal tapers and ends in a trifid process (in lateral view). A total of 18 to 22 branchiostegal rays are present. The branchiostegal rays are dorsally curved and reach no further than the caudal border of the opercle. The anterior ceratohyal occupies the largest part of the hyoid bar and anteriorly bears the articulation facet for the basihyal, urohyal and contra-lateral hyoid arch.

The lateral line system - The frontal commissure and adnasal canals are absent. The supraorbital canal is supported by the nasal. The ethmoid canal is a ventral branch of the supraorbital canal, running in the premaxillo-ethmovomerine complex. The infraorbital canal is supported by the preorbital, two infraorbitals and three postorbitals. The otic canal is supported by the pterotic. The preoperculo-mandibular canal is supported by the lower jaw and preopercle. The supratemporal canal connects the left and right otic canals caudally.

## MYOLOGY

The adductor mandibulae complex is well developed and caudally and dorsally expanded (Fig. IV.4.3- 6). The muscle complex covers the neurocranium from the orbital

region to the supraoccipital. The contra-lateral parts of the A1 and A2 meet in the dorsal midline (Fig. IV.4.3- 6B). The caudal fibres of the whole complex are aponeurotically connected to the epaxials. This aponeurosis is also attached to the caudal border of the neurocranium. This complex comprises three parts: an antero-lateral A1, a postero-lateral A2 and a medial A3. The  $A_{\omega}$  is absent. The A1 is attached to the frontals, parietals, epiotics and rostro-dorsally to the supraoccipital. The A1, shares an anterior tendon with the  $A2_{\alpha}$  and the A3, which mediates their insertion onto the medial surface of the dentary and the primordial ligament. This anterior, dorsal A1- $A2_{\alpha}$ -A3 tendon, is situated on the lateral surface of the A3 and on the medial side of the A1 and  $A2_{\alpha}$ , and bears a longitudinal, laterally directed extension in between the latter parts. The adductor mandibulae A2 occupies the ventro-lateral region of the cheek and two parts can be recognized based on attachment sites of the bundles: the proportionally large, ventro-lateral  $A2_{\alpha}$  and the relatively small, but deeper  $A2_{\beta}$  (Fig. IV.4.3- 7B). The  $A2_{\alpha}$  originates tendinously (T  $A2_{\alpha}$ ) from the ventral surface of the quadrate, the caudo-lateral surface of the hyomandibula (posterior to the lateral ridge) the dorso-lateral surface of the preopercle, the caudo-dorsal part of the pterotic, frontal, parietal, epiotic, supraoccipital and the epaxial aponeurosis. This broad tendon sheet is found on the medial surface of the  $A2_{\alpha}$ . The  $A2_{\beta}$  is covered by the ventral part of the  $A2_{\alpha}$ . The  $A2_{\beta}$  part originates musculously from the rostro-lateral surface of the hyomandibula, in front of the longitudinal lateral ridge (Fig. IV.4.3- 7B; 3A). Both share an anterior tendon (T A2), which mediates their insertion onto the medial surface of the dentary. Medial to this A2-complex lies the dorso-medial A3-complex, comprising two parts: the dorsal  $A3_{\alpha}$  and the smaller, ventrally situated  $A3_{\beta}$ . Both A3 parts are covered by the A1 and  $A2_{\alpha}$ . The muscular origin of  $A3_{\alpha}$  is situated latero-dorsally on the skull roof and comprises the lateral surfaces of the frontals, parietals, epiotics and additionally the dorso-lateral part of the pterotics. The  $A3_{\beta}$  originates by means of a tendon (T  $A3_{\beta}$ ) from the rostral extension of the sphenotic process and musculously from the pterotic, in front of the sphenotic process. Both parts insert on the medial surface of the coronoid process by means of the anterior (T A1- $A2_{\alpha}$ -A3) tendon. The A3 covers the anterior part of the levator arcus palatini.

The levator arcus palatini has a conical shape with the apex pointing dorsally. The tendinous origin includes the lateral and ventral surface of the sphenotic process and the pterosphenoid. The fibres insert musculously on the lateral surface of the pterygoid, hyomandibula and quadrate.

The adductor arcus palatini caudally forms the floor of the orbits (Fig. IV.4.3- 8A). The fibres originate musculously from the parasphenoid, lateral to its median ridge, separating the left and right parts of the muscle, and partially from the prootics. The

muscle inserts musculously on the suspensorium, at the level of the caudo-medial surface of the pterygoid and the medial surface of the hyomandibula.

The adductor hyomandibulae is situated medially to the adductor arcus palatine (Figs. IV.4.3- 8B; 9A). The muscle tapers caudally. It is difficult to distinguish it from the adductor arcus palatini since both have the same fibre direction. The origin is situated in the fossa subtemporalis, formed by the prootics and exoccipitals. It inserts on the medial surface of the hyomandibula.

The fibres of the levator operculi are caudo-ventrally directed (Figs. IV.4.3- 7A; 8A). Two tendons originate from the pterotic, just behind the attachment of the adductor mandibulae complex, and run ventro-caudally covering the lateral surface of the muscle. The fibres insert musculously on the dorso-lateral surface of the opercle.

The dilatator operculi has a conical shape, with the apex pointing caudo-ventrally (Figs. IV.4.3- 7; 8A). The site of origin comprises the caudo-lateral and partially the caudo-dorsal surface of the sphenotic process and the ventro-lateral surface of the pterotic. Internally, a tendon is present that inserts on the lateral surface of the dorsal process of the opercle.

The adductor operculi is situated caudal to and partially covered by the dilatator operculi (Fig. IV.4.3- 9A). The muscle originates tendinously from the caudal part of the pterotic and the exoccipital. Some fibres are musculously attached to the hyomandibula at the level of its neurocranial articulation. The fibres insert on the medial surface of the opercle. The insertion site varies from the surface just beneath the dorsal edge of the opercle to half the height of the opercle.

The intermandibularis is absent.

The protractor hyoidei connects the lower jaw to the hyoid arch (Fig. IV.4.3- 9B). The fibres are rostro-caudally directed, originating musculously from the anterior ceratohyal and the ventro-rostral edge of the interopercle. The protractor hyoidei inserts tendinously on the ventro-medial surface of the dentary complex, just behind the dental symphysis.

The sternohyoideus consists of three myomeres, divided by two myocommata (Fig. IV.4.3- 9). The left and right, strong, well developed tendons insert independently on the postero-lateral surfaces of the caudal trifold end of the urohyal. Posterior to the insertion site, both tendons border the lateral surfaces of the sternohyoideus. The posterior fibres of the sternohyoideus are musculously attached to the lateral surface of the ventro-rostral projection of the cleithrum. Ventro-caudal fibres of the sternohyoideus merge with the hypaxial muscles.



The hyohyoidei adductores surround the gill chamber ventrally, forming a ‘sac-like’ structure, situated just beneath the opercular system and above the branchiostegal rays (Fig. IV.4.3- 9B). This sheet attaches dorsally to the medial surface of the opercle and more caudally to the horizontal septum (ventral to the epaxial muscles). The sheet continues ventrally, interconnecting the branchiostegal rays and meets its antimere in the midline by means of an aponeurosis. It is not clear whether hyohyoideus abductor is fused with the hyohyoidei adductores or whether it is not yet completely differentiated, given the basal phylogenetical position of the Anguilliformes in teleosts.

The anterior epaxial muscles originate from several neurocranial bones: the exoccipitals, epiotics, pterotics and supraoccipital (Fig. IV.4.3- 6). The supraoccipital has two caudal spiny projections for the insertion site of the epaxials. An aponeurosis is present between the epaxial muscles and the adductor mandibulae complex. The hypaxials originate from the basioccipital, the horizontal septum and the myocomma of the sternohyoideus.

## LIGAMENTS

The rostro-lateral surface of the pterygoid is connected to the dorsal surface of the maxillary by the pterygo-maxillary ligament (Fig. IV.4.3- 7B). The primordial ligament connects the caudo-dorsal surface of the maxillary to the dorsal edge the dental coronoid process (Fig. IV.4.3- 6A). A second ligament between the coronoid process and maxillary, the maxillo-dental ligament, is observed. It is attached to the maxillary, ventrally to the primordial ligament, and inserts more rostro-dorsally on the coronoid process. In one specimen these two ligaments (primordial ligament and the maxillo-dental ligament) are found to be fused. The angulo-preopercular ligament runs from the caudal surface of the dentary to the rostro-medial surface of the preopercle (Fig. IV.4.3- 6A, 7). The angulo-interopercular ligament is attached ventro-laterally on the interopercle and runs to the retro-articular process of the angular complex (Fig. IV.4.3- 7B). The hyomandibulo-ceratohyal ligament runs between the dorso-medial surface of the hyomandibula and the posterior tip of the posterior ceratohyal (Fig. IV.4.3- 8B). The preoperculo-ceratohyal ligament forms a dorso-ventral ligamentous connection between the dorso-medial surface of the preopercle and the caudo-lateral surface of the posterior ceratohyal (Fig. IV.4.3- 8B). The operculo-ceratohyal ligament connects the lateral surface of the rostro-dorsal articulation facet of the opercle to the latero-caudal surface of the ceratohyal, though this ligament has not been found in all specimens (Fig. IV.4.3- 8A). The angulo-ceratohyal ligament connects the retro-articular process to the posterior ceratohyal (Fig. IV.4.3- 8B).

The interoperculo-ceratohyal ligament connects the interopercular process to the caudo-lateral surface of the posterior ceratohyal (Figs. IV.4.3- 7B, 9A). The preoperculo-opercular ligament attaches dorso-caudally to the lateral surface of the preopercle and runs to the ventral surface of the dorsal opercular process (Fig. IV.4.3- 7A). The hyomandibula is dorso-medially connected to the ventral surface of the sphenotic process by means of the sphenotico-hyomandibular ligament (Fig. IV.4.3- 8B).

## DISCUSSION

---

In accordance with the elongated body, eels have a rather narrow head. The head as well as the gill region is elongated and the gill chamber is displaced backwards to almost behind the skull (NELSON, 1994; ROBINS, 1989). GOSLINE (1971) assumed that all their peculiarities reduce the head and body diameter and seem attributable to the one basic habit of wedging themselves through small holes in the coral or rocks. As *C. conger* and *A. anguilla* are considered to be generalized, morphologically unspecialized eels (SMITH, 1989A, B), their morphology is expected to differ from eels that are adapted to specialized lifestyles such as head-first or tail-first burrowing. In what follows the morphology of such specialized eels, *M. edwardsi* (DE SCHEPPER ET AL., 2005; IV.1), *P. boro* (DE SCHEPPER ET AL., 2007; IV.3), *H. hassi* and *H. longissimus* (DE SCHEPPER ET AL., IN PRESS A) (IV.2), is discussed with that of the more generalized eels, *A. anguilla* (TESCH, 2003; BELOUZE, 2001; IV.4.2) and the presently studied *C. conger*.

### PREMAXILLO-ETHMOVOMERINE COMPLEX

The upper jaw is an immobile bone formed by the fusion of the premaxillary, vomer and mesethmoid and is synapomorphic for Anguilliformes (ROBINS, 1989; TESCH, 2003). It is assumed to be a specialization for predatory feeding (EATON, 1935; GOSLINE, 1980; SMITH, 1989B) as this premaxillo-ethmovomerine complex limits the mobility of the bordering elements of the upper jaw and seems to assist an excellent grasping and holding ability.

As *C. conger* displays active predatory feeding behaviour and is specialized in preying upon fishes, crustaceans and squid (CAU AND MANCONI, 1984; OLASO AND RODRIGUEZ-MARIN, 1995; MORATO ET AL., 1999), a solid grip and increased structural rigidity of the jaws is required and provided by the fused upper jaw elements. Moreover, all the in this dissertation studied eels, except for *H. hassi* and *H. longissimus*, (DE SCHEPPER ET AL., IN PRESS A) (IV.2), are predators capable of biting hard (DE SCHEPPER ET AL., 2005; 2007) (IV.1;

IV.3). In other predacious teleost forms, requirements of a strong bite have often led to the secondary loss of inherited upper jaw movements (GOSLINE, 1980).

As the heterocongrines have a suction-dominated feeding mode, which is assumed to be a derived condition (SMITH, 1989B; DE SCHEPPER ET AL., IN PRESS A) (IV.2), no powerful bite (BAREL, 1983; VAN WASSENBERGH ET AL., 2005) or no special structural reinforcements are required. The reduction of the jaw muscles can be explained in this regard. Nevertheless, the premaxillo-ethmovomerine complex has not been modified as the elements are fused. Though the length of the complex is reduced (Fig. IV.4.3- 10). This is assumed to be an adaptation to their feeding style as the shortening of the snout, which brings the extremely large eyes closer to the tip, may allow close-up binocular vision (ROSENBLATT, 1967; SMITH, 1989B; CASTLE AND RANDALL, 1999).

In the burrowing eels (*M. edwardsi* and *P. boro*) an added advantage of this fused immobile upper jaw is ascribed to their head-first way of burrowing, in order to resist compressive forces during substrate penetration (DE SCHEPPER ET AL., 2005; 2007) (IV.1; IV.3), as similar structural conformations in amphisbaenians, dibamid lizards and snakes are demonstrated to be convergent evolutionary traits, clearly related to head-first burrowing (LEE, 1998). Even though this strengthening is advantageous, it cannot be considered an added adaptation to their head-first burrowing lifestyle considering the synpleisiomorphic condition for Anguilliformes.

#### SHAPE OF THE NEUROCRANIUM AND SIZE OF THE ORBITS

In *C. conger* the neurocranium is dorso-ventrally flattened. The orbits are large. The skull roof is straight, though from the anterior margin of the epiotics the skull is caudally sloping upwards. In ventral and dorsal view the neurocranium of *C. conger* is narrow in the ethmoid and orbital regions, and widens markedly at the level of the protruding sphenotic processes (Fig. IV.4.3- 10). Even though the proportions of neurocranial parts in *A. anguilla* differ between two ecological varieties of broad-headed and narrow-headed eels (DE SCHEPPER ET AL., SUBMITTED A) (IV.4.1), the shape of the neurocranium of *A. anguilla* is strongly comparable to that of *C. conger*. The skull has large orbits, the roof is straight and at the level of the protruding sphenotic processes the skull becomes markedly wider (Fig. IV.4.3- 10). These traits are generally applicable to the anguillids and congrid as becomes evident from Smiths' drawings of 18 congrid species (SMITH, 1989B), though large interspecific variability in size and shape of individual cranial bones can be discerned. Even though cranial morphology is variable among Anguilliformes

(ROBINS, 1989), some cranial features, which are likely to be linked to a specific specialized lifestyle, are recognised in the present study.

The skull of the tail-first burrowing heterocongrines (DE SCHEPPER ET AL., IN PRESS A) (IV.2) differs markedly from that of *A. anguilla* and *C. conger* in the ethmoid, orbital and postorbital regions. The snout is markedly shortened (Fig. IV.4.3- 11A). The orbits are markedly larger (Fig. IV.4.3- 11B) and the interorbital distances (pars ethmoidalis) is narrower (Fig. IV.4.3- 10E). The skull is caudally higher, due to the dorso-ventral expansion of the pterotic, the increased size of the prootics and basioccipital and the less protruding sphenotic processes.

The overall shape of the skull of the head-first burrowers, *M. edwardsi* and *P. boro* differs markedly from that of the non- and tail-first burrowers (Fig. IV.4.3- 10). The orbital region is shorter but more robust. The orbits are reduced (Fig. IV.4.3- 11B) and consequently the interorbital distance is increased in *M. edwardsi* and *P. boro*, and this is most pronounced in *M. edwardsi* (Fig. IV.4.3- 10C). The skull widens gradually from the anterior margin of the orbits, mainly due to the widening of the frontals and parasphenoid. Furthermore, serial cross sections reveal that the cranial bones are thicker and show a higher amount of overlap in *M. edwardsi* and *P. boro*, compared to those in the heterocongrines. As no data on bone thickness of *A. anguilla* and *C. conger* are available, no comparison is possible and the former notes should consequently not be generalized. All the above mentioned neurocranial features contribute to an increase in skull strength, are advantageous in head-first burrowing and may be seen as adaptations to head-first burrowing. This is supported by preliminary results of a finite-element-analysis of the neurocrania of *H. hassi* and *P. boro* (Fig. IV.4.3- 12). At equal values for respectively frontal and lateral loadings onto the neurocrania, stress is up to 10 times lower in *P. boro* compared to that in *H. hassi*. Furthermore stress is evenly distributed over the surface of the skull in *P. boro*, whereas it is concentrated at the end of the orbits, due to the abrupt transition from a narrow element to a broad structure (CHOI, 2006). So, the shape of the skull and thickness of the cranial bones appear to be advantageous in the distribution of stress, generated during head-first burrowing.

## LOWER JAW

Comparing the lower jaw morphology of *C. conger* to that of the other anguilliform species discussed in this dissertation, the most remarkable differences are found in the total length of the lower jaw with respect to the upper jaw, orientation and inclination of

the lower jaw when the mouth is closed and the inclination or location of the mandibular articulatory facet.

In the heterocongrines (DE SCHEPPER ET AL., IN PRESS A) (IV.2), the lower jaw is remarkably shortened and obliquely orientated. This modified lower jaw is regarded as a specialization for snapping planktonic prey (ROSENBLATT, 1967), though no arguments specifying to which degree this is actually the case are given.

In *M. edwardsi*, *A. anguilla* and the heterocongrines the lower jaw extends beyond the upper jaw, whereas it is shorter in *P. boro* and *C. conger*. The mandibular articulatory facet is dorso-caudally directed in *A. anguilla*, *C. conger* and *P. boro*, whereas caudally directed in the heterocongrines and *M. edwardsi*.

The occurrence of morphological differences appears random in the, in this study examined, species, as was also noted for the congrid (SMITH, 1989B; BELOUZE, 2001). The examination of the lower jaws of 18 congrid species (SMITH, 1989B) revealed that the relative proportion of the dentary to the angular complex, and the inclination or location of the mandibular articulatory facet are highly variable within this family.

However, all species share some morphological traits, which can be related to the fact that all these species have a predacious lifestyle.

In all studied species, except the heterocongrines, the lower jaws are robust and firm. This is advantageous for predators to grasp and hold prey, especially when feeding occurs using spinning of the body of when prey items are hard (LIEM, 1980; HELFMAN ET AL., 1997). Furthermore the lower jaws of all species examined, except for the heterocongrines, are rostrally strongly connected by a large bony symphysis. As the exertion of an asymmetrical loading onto the contra-lateral mandibular bars during forceful biting with spinning movements may occur and may be substantial, the large and firm symphysis may prevent anterior dislocation of the jaws.

## SUSPENSORIUM

The suspensorium is elongate and the ventral elements are forwardly inclined in *C. conger*, *A. anguilla* and the heterocongrines. The pterygoid is long, slightly curved and attaches to the vomero-ptyergoidal articulatory facet on the pars vomeralis. Caudally it is strongly connected to the hyomandibula-quadratum complex.

In *M. edwardsi* and *P. boro* however, the suspensorium is more robust, the length-axis has a dorso-ventral orientation and a reduced pterygoid that has become decoupled from the hyomandibulo-quadrata and is connected to the parasphenoid.

Even though the morphology of the suspensorium unites the head-first burrowers in this study, it should not be related to their burrowing habit as the degree of suspensorial inclination and the presence or absence of the anterior attachment of the suspensorium varies considerably among the anguilliform families (BELOUZE, 2001; ROBINS, 1989).

### HYPERTROPHY OF THE ADDUCTOR MANDIBULAE COMPLEX

The most notable myological feature in *C. conger* involves the extremely enlarged mouth closing muscles, i.e. the adductor mandibulae complex, which are dorso-caudally expanded, covering the skull roof. As the adductor mandibulae complex of *C. conger* is hypertrophied, not only an extensive insertion site is noted but also the complexity appears to be high (apart from the A1, A2, A3 parts) as becomes evident from the subdivided A2 (A2 $\alpha$ , A2 $\beta$ ) and A3 (A3 $\alpha$ , A3 $\beta$ ) (Fig. IV.4.3- 6, 7). In *A. anguilla* three subdivisions are recognized in the A1 (IV.4.1) and in *M. edwardsi* three subdivisions are present in the A2 (DE SCHEPPER ET AL., 2005) (IV.1). Though, the increase of complexity of the adductor mandibulae complex with increasing muscle hypertrophy does not always co-occur as is demonstrated in *P. boro* (DE SCHEPPER ET AL., 2007) (IV.3) and within the clariid family (DEVAERE ET AL., 2001).

*C. conger* is a predator that is feeding on fish, crustaceans and cephalopods (SMITH, 1989B). As such prey items imply a strong bite, the hypertrophied jaw muscles of *C. conger* may be advantageous to seize and hold prey and also to crack shells of crustaceans. Similarly, hypertrophied jaw muscles associated with predatory feeding habits are found in *M. edwardsi* (DE SCHEPPER ET AL., 2005) (IV.1), *A. anguilla* (IV.4.2), *P. boro* (DE SCHEPPER ET AL., 2007) (IV.3), catfish (VAN WASSENBERGH ET AL., 2005) and synbranchiforms (LIEM, 1980; TRAVERS, 1984A; BRITZ AND KOTTELAT, 2003). An additional confirmatory argument is found in the jaw muscle size variation and its relation to dietary preferences in the two morphotypes of *A. anguilla* (IV.4.1; IV.4.2). In accordance with this statement, the jaw muscles of the suction-feeding heterocongrines are small as no large bite forces are required (DE SCHEPPER ET AL., IN PRESS A) (IV.2).

Hypertrophied jaw muscles have been related to eye reduction in other eel-like fish such as clariids (DEVAERE ET AL., 2001) and synbranchids (LIEM, 1980). This relation appears present in the examined anguilliforms as well. In both head-first burrowers the reduced eyes create space for housing enlarged adductor mandibulae muscles thereby also allowing an unusual orientation of the anterior fibres, i.e. being ventrocaudally directed (DE SCHEPPER ET AL., 2005; 2007) (IV.1; IV.3). This is assumed to be related to rotational feeding and head-first burrowing as this may assist in preventing the mandibular joint from being

dislocated. Furthermore such an aberrant fibre direction is also noted in *Monopterus* and *Synbranchus*, which also have reduced eyes and are known to burrow and feed using rotations (LIEM, 1980). In *C. conger* the eyes are moderate large and no fibres of the jaw muscles are ventro-caudally directed. In the heterocongrines with extremely enlarged eyes, the jaw muscles are even reduced.

### REINFORCEMENTS

As could be deduced from the presence of hypertrophied jaw muscles, coupled to the predatory feeding behaviour with powerful biting, associated reinforcements and specializations involving the spatial design in *C. conger* can be expected. So a substantial increase in mechanical loads on several skeletal elements composing the biting apparatus (especially neurocranium, lower jaw and suspensorium as they involve the origin and insertion sites of the jaw muscles) (VAN WASSENBERGH ET AL., 2005) are assumed to exist. In *C. conger* the degree of interdigitations between the successive bones (frontals, parietals, epiotics, pterotics, sphenotics and supraoccipital forming the attachment site of the jaw muscles) in the skull roof is substantial, thus increasing the strength of the neurocranium. The sphenoid processes are robust and firm. The sutures between the pterygoid, hyomandibula and quadrate are tight and strong, forming a firm entity. The lateral surface of the suspensoria show highly elevated ridges for the insertion of the adductor mandibulae complex. The degree of interdigitation between the ventral and latero-ventral bones is less pronounced. Structural adaptations in the dentary, its coronoid process and suspensorium for muscular attachment of enlarged jaw muscles are observed in other eels as well, such as muraenids (BÖHLKE ET AL., 1989).

In the heterocongrines no hypertrophied jaw muscles are needed and no special structural reinforcements at the level of oral skeletal elements (e.g., dentary, suspensorium and neurocranium) to resist increased mechanical loads, are required (BAREL, 1983; VAN WASSENBERGH ET AL., 2005).

### ROTATIONAL FEEDING

Rotational feeding is a highly specialized feeding mode, adopted by several elongate, aquatic vertebrates (LIEM, 1980; HELFMAN AND CLARK, 1986; MEASEY AND HERREL, 2006). Some convergent morphological modifications, enhancing a solid grip and probably assisting in resisting torque forces during rotations, are: the aponeurotic connection between epaxials and jaw muscles, hypertrophied jaw muscles, increased neurocranial

rigidity, robust lower jaws and coronoid process, rigid upper jaw, and differing orientations of the adductor mandibulae complex bundles (IV.1; IV.3; IV.4.2). Even though only few data dealing with feeding behaviour in *C. conger* are published and its feeding behaviour has never been reported before for *C. conger*, the above mentioned morphological data address the possibility for this kind of feeding. Additionally, these morphological features are shared with that of *Pisodonophis boro* (DE SCHEPPER ET AL., 2007) (IV.3) and *Anguilla anguilla* (IV.4.2), which are known to actually perform this kind of feeding.

So, the presence of hypertrophied jaw muscles may be advantageous for this feeding mode as these muscle transfer rotational forces from the body to the head and provide a powerful bite to hold prey during spinning movements and to prevent the lower jaw from being dislodged during spinning.

## **ACKNOWLEDGEMENTS**

---

We wish to thank the FWO (Project G.0388.00) for financing this research.



#### **IV.4.4 CAUDAL MORPHOLOGY IN *ANGUILLA ANGUILLA* AND *CONGER***

##### ***CONGER***



---

# THE MORPHOLOGY OF THE CAUDAL FIN OF *ANGUILLA ANGUILLA* AND *CONGER CONGER*: COMPARISON WITH THE CAUDAL FIN OF SPECIALIZED ANGUILLIFORMES

---

De Schepper N, De Kegel B, Adriaens D

## ABSTRACT

---

Anguilliformes are primitively adapted for wedging through small openings, which is assumed to be the basic mode of life but several anguilliforms show a range of different lifestyles, with morphological specializations that may be associated with it. As *Conger conger* and *Anguilla anguilla* represent non-burrowing species exhibiting the primitive way of life (wedging through small openings), they may be useful to reveal possible adaptations to a specific, specialized lifestyle (e.g. burrowing). Therefore, the caudal fins of these non-burrowing species are examined and subsequently compared to those of burrowing species. Differences in caudal skeleton consolidation and caudal fin rays are noted. Muscular differences are observed as well. The morphological differences at the level of the caudal fin are likely to be related to differences in lifestyle.

## INTRODUCTION

---

The extant Anguilliformes are characterized by a caudal fin which is confluent with the dorsal and anal fins (ROBINS, 1989; BELOUZE ET AL., 2003). From anguilliform fossil records it could be deduced that in the extant Anguilliformes the caudal skeleton is reduced (from 5 distinct hypurals to 2 hypural plates) and the number of caudal fin rays is decreased (below 16) (BELOUZE, 2001; BELOUZE ET AL., 2003). Within the Anguilliformes the osteological elements of the caudal fin appear to vary in the degree of reductions and fusions as well (DE SCHEPPER ET AL., 2005; 2007; IN PRESS A) (IV.1; IV.2; IV.3) and this is believed to be related to their lifestyle (BÖHLKE, 1989; BELOUZE, 2001).

The caudal skeleton of Anguilliformes always consists of two more or less fused hypural plates, which are also fused to the ural vertebrae, the uroneurals and to the epurals (if present). Some degree of variation was detected in whether the parhypural supports caudal fin rays (as in Anguillidae, Moringuidae and some representatives of the

Congridae) or not; in the degree of development of the hypural fenestra and in the degree of fusions in caudal elements (BELOUZE, 2001; BELOUZE ET AL., 2003; DE SCHEPPER ET AL., 2005; 2007; IN PRESS A) (IV.1; IV.2; IV.3).

Reduction of the caudal fin (towards sharply tapering, filament-like structures [Nettastomatidae, Nemichthyidae, and in some Congridae e.g. *Uroconger*] or a hard, pointed tip without a fin [Heterocongrinae and Ophichtidae]) has been observed in several species and is related to the use of restricted spaces or tail-first burrowing respectively (BELOUZE, 2001; BELOUZE ET AL., 2003; DE SCHEPPER ET AL., 2005; 2007; IN PRESS A) (IV.1; IV.2; IV.3).

Anguilliform species are adapted for wedging through small openings (GOSLINE, 1971; SMITH, 1989B). However several anguilliforms show a range of different lifestyles, with morphological specializations that may be associated with it. Some are pelagic, others are adapted to burrowing lifestyles, from head-first (*Moringua*, *Neoconger*) to tail-first (Heterocongrinae, Ophichtidae). As the caudal fin generally is of great importance during locomotion (LAUDER, 2000), differences in lifestyle (e.g. pelagic, burrowing, sessile) are expected to be reflected in the osteological morphology but also in the musculature involved (DE SCHEPPER ET AL., 2005; 2007; IN PRESS A) (IV.1; IV.2; IV.3).

The main goal of this study is to recognize morphological specializations that may be related to tail-first burrowing. As *Conger conger* and *Anguilla anguilla* represent non-burrowing species exhibiting the primitive way of life (wedging through small openings), they may be useful to reveal possible adaptations to a specific, specialized lifestyle (e.g. burrowing). The caudal fin morphology was previously examined in *H. hassi* and *H. longissimus*, (DE SCHEPPER ET AL., IN PRESS A) (IV.2), *M. edwardsi* (DE SCHEPPER ET AL., 2005) (IV.1) and *P. boro* (DE SCHEPPER ET AL., 2007) (IV.3). Furthermore, they are more specialized (BELOUZE, 2001) and show differing burrowing lifestyles (tail-first, head-first and a mixture of both respectively).

Therefore, these burrowing anguilliform species are applied in this study to compare their morphological of the caudal fin with that of the more primitive and non-burrowing species *A. anguilla* and *C. conger*, aiming to reveal morphological specializations that may be related to tail-first burrowing.

## MATERIAL AND METHODS

---

For this study five specimens of *Conger conger* (total length varying between 523 mm and 1644 mm) were used. Three *C. conger* specimens were commercially obtained, caught at the North Sea shore (Nieuwpoort, Belgium), and preserved in alcohol. One dried

specimen (UGMD 53065) and one alcohol preserved specimen (UGMD 53089) were obtained from the Zoology Museum, Ghent University - Belgium. See chapter III.1 for details on specimens (Table III.1- 1A).

To examine the caudal fin morphology of *Anguilla anguilla*, six specimens ranging between 400 mm and 555 mm are used. These specimens were commercially obtained and preserved in alcohol. Specimens used in this study are listed in Table III.1- 1E.

For more information about dissections, clearing and staining protocols and visualization, I refer to III.2.2 and III.2.5.

## RESULTS

---

### EXTERNAL MORPHOLOGY OF THE CAUDAL FIN

The caudal fin of *A. anguilla* and *C. conger* is confluent with the anal and dorsal fins (Fig. IV.4.4- 1A, B). The caudal fins are similar as both have a broadly rounded caudal fin, with long and flexible caudal fin rays.

### MYOLOGY OF THE CAUDAL FIN

The flexor dorsalis of *Anguilla anguilla* and *Conger conger* originates from the lateral surface of the uroneural and rostro-dorsal surface of the dorsal hypural plate (Fig. IV.4.4- 2A, B). It inserts onto the three or four uppermost caudal fin rays through a tendinous sheet.

The hypochordal longitudinalis originates from the ventro-lateral surface of the ventral hypural plate and passes to the ventro-lateral surface of the dorsal hypural plate (Fig. IV.4.4- 2A, B). Both origin and insertion are tendinous.

The flexor ventralis originates from the lateral surface of the parhypural and antero-ventral surface of the base of the ventral hypural plate in *A. anguilla* and *C. conger* (Fig. IV.4.4- 2A, B). This muscle inserts tendinously onto three of four ventral caudal fin rays.

The proximalis is situated medial to the hypochordal longitudinalis, and originates musculously from the posterior surface of the hypurapophysis (Fig. IV.4.4- 2A, B). In *A. anguilla* and *C. conger* the proximalis inserts onto to the lateral surface of the ventral and

dorsal hypural plate and caudo-lateral fibres extend posteriorly, inserting onto three to four caudal fin rays.

Interradials are present in *A. anguilla* and *C. conger*, and formed by several bundles of muscle fibres (Fig. IV.4.4- 2A, B). These bundles radiate dorsally and ventrally. The bundles above the midline run upwards and backwards, inserting on the ventro-lateral side of dorsal caudal fin rays, while the ventral bundles run downwards and backwards, inserting on the dorso-lateral side of the ventral caudal fin rays.

The body musculature, including both epaxial and hypaxial muscles, attaches to the bases of the caudal fin rays by broad tendinous sheets.

## DISCUSSION

---

### OSTEOLOGY OF THE CAUDAL FIN IN ANGUILLIFORMES

A trend of unpaired fin confluence that is associated with reduction in the caudal skeleton (hypurals, epurals) and number of caudal fin rays in Anguilliformes becomes apparent (BELOUZE ET AL., 2003), when primitive taxa are considered. One of the apomorph characters, grouping the more specialized taxa (the fossil *Urenchelys avus* and *Hayenchelys germanus* and the living *A. anguilla* and *C. conger*) is the confluence of the unpaired fins; *A. anguilla* and *C. conger* share the following synapomorphies: upper hypurals fused into a single dorsal plate, caudal rays number less than 8 in both lobes. Interestingly, such a relation appears to be present in the unrelated synbranchiform Mastacembelidae as well (TRAVERS, 1984A, B).

Even though, the confluence of the median fins, reduction of the caudal skeleton and reduction in number of the caudal fin rays are synapomorphic for all extant Anguilliformes (BELOUZE ET AL., 2003), morphological differences in the caudal fin can be detected in the examined species as discussed below. The features of the caudal skeleton of *A. anguilla* and *C. conger* have been studied in detail by BELOUZE (2001). For detailed description of the caudal skeleton of *M. edwardsi*, *H. hassi*, *H. longissimus* and *P. boro*, I refer to IV.1; IV.2; IV.3.

The urostyle bears one pair of uroneurals. An epural element is found only in *A. anguilla*. All examined species possess distinct hypurapophyses on the lateral surface of the ventral hypural plate, however these are relatively small in *A. anguilla*. The parhypural supports caudal fin rays in *A. anguilla* and *C. conger*, which is not the case in *H. hassi*, *H. longissimus*, *P. boro* and *M. edwardsi*. Though, the parhypural of the Moringuidae may be intraspecifically variable as, according to BELOUZE (2001), it is caudally extended,

supporting caudal fin rays, whereas in this study, it is absent. The neural arches of the first preural vertebra are medially fused in all examined species, except for the heterocongrines. Neural spines of the first and second preural vertebrae are absent in all examined species, except for *A. anguilla*. The caudal skeleton of all examined species comprises two hypural plates. The sutures between the fused hypurals are still apparent in *A. anguilla* and *C. conger* (Fig. IV.4.4- 3A, B). In *M. edwardsi* only the proximal parts of the first and second hypurals are fused (Fig. IV.4.4- 3D). In *A. anguilla*, *C. conger*, *H. hassi* and *H. longissimus*, the distal parts of the hypurals 1 and 2 are fused as well, resulting in ventral hypural plate pierced by a hypural fenestra. *P. boro* lacks the hypural fenestra (Fig. IV.4.4- 3C). The first hypural in *P. boro* bears a rostrally directed projection, which is not observed in the other species. In *P. boro* the dorsal hypural plate is longer than the ventral one and the distal ends of both plates are laterally broadened (Fig. IV.4.4- 3C), giving the tail tip a robust and firm appearance. Similarly, a robust, firm and strengthened caudal skeleton is found in *H. hassi* and *H. longissimus* due to the high degree of fusions and the stout, broad hypural plates (oval in cross section; Fig. IV.4.4- 2E, F).

The number of caudal fin rays differs among the examined species: 10-12 in *A. anguilla*, 9-10 in *C. conger*, 8-9 in *M. edwardsi*, 6-7 in *H. hassi* and *H. longissimus* and 4-5 in *P. boro*. Even though the difference in amount of caudal fin rays among the examined species is small, a reductive trend seems present: the non- ( *A. anguilla* and *C. conger* ) and head-first burrowing species ( *M. edwardsi* ) without consolidated caudal skeletons tend to have more caudal fin rays. Furthermore the caudal fin rays also differ in length and movability among the examined anguilliform species. In *A. anguilla*, *C. conger* and *M. edwardsi* the caudal fin rays are long and pliable and they are able to move in the horizontal as well as in the ventral plane. As the caudal fin rays are short and fixed by thick tissue in *H. hassi*, *H. longissimus* and *P. boro*, dorso-ventral movements are less obvious (see below).

#### EXTERNAL MORPHOLOGY AND OSTEOLOGY OF THE CAUDAL FIN RELATED TO LIFESTYLES

The tail-first burrowing species *H. hassi*, *H. longissimus* and *P. boro* have a firm, pointed tail. The caudal skeleton is fortified and consolidated by fusions. Fewer caudal fin rays are present and they are externally not visible as they are covered by a thick layer of connective tissue and thick dermal and epidermal layers. As discussed in IV.2 and IV.3, these modifications are an advantage for tail-first burrowing as they ensure an efficient penetration of the sediment and are thus considered an adaptation for tail-first burrowing (TILAK AND KANJI, 1969; SUBRAMANIAN, 1984; ATKINSON AND TAYLOR, 1991; CASTLE AND RANDALL,

1999). *Gymnothorax ocellatus* (Muraenidae), known for entering their burrows tail-first, but using burrows excavated by other animals, do not have modified caudal fins (SANTOS AND CASTRO, 2003). The adaptive nature of the caudal fin morphology for tail-first burrowing as found in *H. hassi*, *H. longissimus* and *P. boro* (hardened tip) is supported by the morphology of the primitive ophichtids (MCCOSKER ET AL., 1989) and primitive congrid (SMITH, 1989B) as they do not show the modified, pointed tail tip. The modified caudal fin for burrowing as found in *H. hassi*, *H. longissimus* and *P. boro* may consequently be regarded as a convergent evolutionary trait related with tail-first burrowing.

The caudal fin of the head-first burrower, *M. edwardsi*, resembles that of *A. anguilla* and *C. conger* as the elements of the caudal skeleton are fused to a lesser degree and the caudal fin rays are externally visible (Fig. IV.4.4- 1D). Though, in immature specimens of *M. edwardsi*, which live burrowed in the substrate, the confluence of the median fins is less apparent as the anal and dorsal fins are low, whereas in adult specimens, which are pelagic, the confluence is apparent as the height of anal and dorsal fins has increased (SMITH AND CASTLE, 1972; IV.1). Based on the morphological modifications that occur when specimens switch from a burrowing to a pelagic lifestyle, the importance of a well developed, continuous fringe of median fins can be assumed.

In the non-burrowing *A. anguilla* and *C. conger* the confluence results in a broad, apparent fringe around the tail (Fig. IV.4.4- 1A, B). The importance of the confluent median fins in eels during swimming is suggested by GILLIS (1997) and LIAO (2002) as the continuous median fins increase the lateral surface area, providing a greater transfer of momentum from the body to the water. It can be assumed that swimming performance is important in *A. anguilla* as it has to migrate more than 5000 km (VAN GINNEKEN ET AL., 2005), and in the predacious *C. conger* as it hunts in open water (LYTHGOE AND LYTHGOE, 1991). Consequently, it may be suggested that a modified caudal fin, as found in the tail-first burrowers, would be disadvantageous. The caudal skeleton of the non-burrowers (*A. anguilla* and *C. conger*) and head-first-burrower (*M. edwardsi*) are less fortified and consolidated and may indicate that the tail is not applied as a burrowing tool.

## REDUCTION IN THE CAUDAL FIN MORPHOLOGY IN ANGUILLIFORMES WITH RESPECT TO

### ELOPS

Together with the overall reduction of the caudal skeleton in Anguilliformes (BELOUZE ET AL., 2003), reductions in caudal fin musculature appear to have occurred as well, with respect to that of *Elops saurus*, a basal elopomorph (WINTERBOTTOM, 1974), a representative of the sister-group of the Anguilliformes (BELOUZE, 2001; BELOUZE ET AL.,



2003). For a detailed description of the caudal fin musculature of the Anguilliformes, I refer to DE SCHEPPER ET AL. (2005; 2007; IN PRESS A) and (IV.1, IV.2, IV.3).

In *Elops saurus*, the supracarinalis posterior connects the last basal pterygiophore of the dorsal fin to the dorsal caudal fin rays, while the infracarinalis posterior runs from the last basal pterygiophore of the anal fin to the hemal spines of the last complete vertebrae (WINTERBOTTOM, 1974). The supracarinalis posterior and infracarinalis posterior are not discerned in any of the examined anguilliform species, which is likely to be related to the confluence of the dorsal, anal and caudal fins.

The interradians are present in *Elops saurus* and interconnect and adduct caudal fin rays, consequently reducing the caudal fin area (WINTERBOTTOM, 1974; LAUDER AND DRUCKER, 2004). The presence of interradians seems to be variable in Anguilliformes. The interradians are present in *A. anguilla*, *C. conger* and *M. edwardsi*, where the caudal fin rays are free to move. Logically, muscles causing dorso-lateral movements of caudal fin rays are redundant in species where caudal fin rays movements are restricted due to covering tissue, which is indeed observed in the tail-first burrowers (*H. hassi*, *H. longissimus* and *P. boro*), lacking the interradians.

The flexor dorsalis of teleosts runs from the last few neural spines and the upper hypurals to the dorsal caudal fin rays (WINTERBOTTOM, 1974). The flexor ventralis connects the lateral surfaces of the hemal spines, arches and centra of the last few vertebrae, the parhypural and the lower hypurals to the lateral bases of the ventral caudal fin rays (WINTERBOTTOM, 1974). The flexor dorsalis and flexor ventralis are known to move the dorsal and ventral caudal fin rays separately (LAUDER AND DRUCKER, 2004). The flexors dorsalis and ventralis are reduced in all examined species, with respect to *Elops*, as their origin is restricted to the caudal skeleton (*A. anguilla*, *C. conger*, *H. hassi*, *H. longissimus* and *M. edwardsi*) or to the first preural vertebra as in *P. boro*.

The hypochordal longitudinalis of teleosts passes from the lower hypurals to three or four of the more dorsal fin rays of the caudal fin and allows the dorsal fin margin to move separately from the ventral fin margin, turning them into the leading edge (WINTERBOTTOM, 1974; LAUDER AND DRUCKER, 2004). The hypochordal longitudinalis is highly reduced in all anguilliform species examined as it is no longer inserted onto the caudal fin rays but, surprisingly, connects two immobile elements (ventral hypural plate to dorsal plate/uroneural).

No data are available of the proximalis in *Elops*. In the anguilliform species the proximalis is present though differences in insertion site are observed. In *A. anguilla* and *C. conger*, this muscle inserts onto the hypural plates, and thus connects two immobile elements.

The caudal fin musculature of the Anguilliformes is reduced with respect to *Elops* and generalized teleosts. Even though the caudal fin musculature of the tail-first burrowers is reduced with respect *A. anguilla*, the reductions are limited: the interradians are absent and the proximalis is not connected to caudal fin rays. These differences can be related to the tail-first burrowing lifestyle but reductions are limited due to trade-offs (see below).

### MYOLOGY OF THE CAUDAL FIN RELATED TO LIFESTYLES

Even though the caudal fin musculature of *A. anguilla* (and Anguilliformes in general) is reduced, with respect to *Elops*, it does not seem to affect swimming performance or functionality: *A. anguilla* is capable to migrate over 6000 km to reach their spawning grounds, i.e the Sargasso sea (DANNEWITZ ET AL., 2005); and a recent study demonstrates that the swimming efficiency of *A. anguilla* is even 4 to 6 times higher compared to that of non-anguilliform fish (VAN GINNEKEN ET AL., 2005). This high swimming efficiency appears not to be restricted to *A. anguilla* or *A. rostrata*. A kinematic study revealed that the swimming efficiencies and forward swimming kinematics for *P. boro* and *H. hassi*, with reduced caudal fin musculature (compared to *A. anguilla*), are high and comparable to those found for *A. anguilla* (CHOI ET AL., SUBMITTED). This is certainly remarkable for these species given their burrowing lifestyles, modified caudal fins and reduced musculature, and especially for *H. hassi* as this species is semi-sedentary (TILAK AND KANJI, 1969). The function of the caudal fin may be more important for manoeuvrability (LAUDER, 2000) or backward swimming (D'AOÛT AND AERTS, 1999): video images of the tail during swimming in *Anguilla rostrata* (and probably also in *A. anguilla*) show that the caudal fin undergoes complex patterns of deformations, assuming precise and complex muscular control of subtle fin ray movements (LAUDER, 2000). During backward swimming the caudal fin cleaves the water, delivering propulsion and it is proposed by D'AOÛT AND AERTS (1999) that the caudal fin muscles operate as stiffness regulators, avoiding collapse of the caudal fin.

The interradians are assumed to be important muscles for dorso-ventral movements of the caudal fin rays and may partially cause the complex movements of the caudal fin of *A. rostrata* observed by LAUDER (2000). The absence of the interradians in the tail-first burrowing species is likely to be related to their burrowing lifestyle, as some actions of the caudal fin musculature are presumably no longer required for generating subtle movements of individual fin rays in a dorso-ventral direction. Furthermore, due to the thick layers of tissue, covering the caudal fin rays, movability is likely to be restricted.

Reduction or even loss of some of the caudal fin muscles has been observed before in teleost species in which sophisticated movements of individual fin rays are no longer required (WINTERBOTTOM, 1974; LAUDER AND DRUCKER, 2004).

Based on aquarium observations of *H. hassi* in the lab, the tip of the tail, even though modified, appears to be able to exert elaborate lateral movements. These movements may be important during the actual burrowing process and are likely to be obtained by unilateral contraction of the caudal fin muscles such as the flexors dorsalis and ventralis. From a functional point of view, it becomes clear that a trade-off between flexibility and strength of the caudal fin is required during burrowing. A strong, pointed, inflexible element to penetrate the substrate without bending is needed, however, at the same time, the ability to exert bilateral movements of the caudal end of the body/tail during the actual penetration is required. The caudal fin musculature is likely to offer flexibility and bilateral movability to some degree as well as strength. It might be assumed that the muscles inserting onto caudal fin rays may cause lateral movements (flexor dorsalis and ventralis), whereas the muscles, connecting two immobile elements may provide strength (proximalis, hypochordal longitudinalis). Interestingly, during backward swimming in *A. anguilla* the caudal fin musculature is proposed to exert the same function as stiffness regulator to avoid collapse of the caudal fin (D'AOÛT AND AERTS, 1999). This trade-off may explain the limited muscular reduction in the caudal fin of the tail-first burrowing species.

## ACKNOWLEDGEMENTS

---

We wish to thank the FWO (Project G.0388.00) for partially financing this research.



**V**

Anguilliformity in derived teleosts

Ostariophysii



**V.1 VERTEBRAL MORPHOLOGY OF *CHANNALLABES APUS***





## SHAPE VARIATION IN THE VERTEBRAE OF ELONGATE CLARIIDAE (OSTARIOPHYSI: SILURIFORMES): USEFUL TOOL FOR TAXONOMY?

---

Modified from the paper published as:

De Schepper N, Adriaens D, Teugels GG, Devaere S, Verraes W. 2007.

Shape variation in the vertebrae of Anguilliform Clariidae (Ostariophysi: Siluriformes):  
useful tool for taxonomy?

Journal of Afrotropical Zoology, *in press*.

### ABSTRACT

---

This study focuses on the postcranial skeleton of *Channallabes apus*. They are representatives of a specialized family of African catfish, the Clariidae. This family is of special interest because of a trend towards an increasing anguilliformity. But due to the lack of a reliable understanding of generic and specific characteristics, it is difficult to discern between the different eel-like species. Based on morphological characteristics, biometric data and vertebral counts, it has been difficult to distinguish the different species so far. Vertebral shape has not been studied before and may give an outcome to this problem. As a result, this study focused on the informative nature of vertebral shape variation for taxonomy and phylogeny, taking elongate clariids as a case study. Shape variation was quantified and qualified within one species. This has been done for specimens of three different populations of *C. apus*, collected in northern (Oyem), southern (Congo-Brazzaville and Franceville) and eastern Gabon (Makokou). To study the morphological variation of the vertebrae, geometric morphometrics based on thin plate spline (TPS) is applied. In order to compare aspects of shape in the vertebral column of all specimens, two vertebrae were isolated (the fifth precaudal and the fortieth caudal vertebrae). The results of the morphometrics reveal some geographic vertebral variation of the different populations of *C. apus*. Two hypotheses may explain the presence of these two groups within one species: (1) interspecific variation and (2) intraspecific variation. It can be concluded that vertebral shape variation is a good and useful tool in systematics and phylogenetics, however, at this moment and in case of *C. apus*, it is not clear at which taxonomic-level (species or subspecies) vertebral shape variation is explicatory.

## INTRODUCTION

---

The Clariidae (Teleostei: Ostariophysi: Siluriformes), distributed throughout northern and central Africa and extending to western Asia, is a specialized family of African catfishes, comprising 12 African genera with 74 species and 2 endemic Asian genera (TEUGELS, 1996). This family is of special interest because of a trend towards increasing anguilliformity, as reported by BOULENGER (1908) and PELLEGRIN (1927). Although this tendency is present in other families of teleosts, amphibians, reptiles, and some mammals, the distinct transformation from fusiformity to complete anguilliformity has almost never been as extensive as in Clariidae (LANDE, 1978). The most notable feature of this transformation is the elongation of the postcranial skeleton. However, a whole set of morphological transformations has been observed: disappearance of the adipose fin, continuous anal, dorsal and caudal fins, reduction of the pectoral and pelvic fins (limblessness), reduction of skull bones, reduction of the eyes, and hypertrophy of the adductor-mandibulae complex (PELLEGRIN, 1927; POLL, 1977; CABUY ET AL., 1999; DEVAERE ET AL., 2001). The species *Channallabes apus* Günther, 1873 shows all these traits. Currently, the taxonomic relationships of some species within the Clariidae, especially the elongate ones (as for example *C. apus*), are ambiguous (DEVAERE ET AL., 2001). In order to study the functional implications of these adaptations, a reliable understanding of generic and specific characteristics, which is presently lacking, is required. Based on the current determination key for the Clariidae (POLL, 1977), it is difficult to discern between the different eel-like species because the range of variation for different features has not been considered adequately, largely due to the limited numbers of specimens used to describe the species.

This paper focuses on the shape variation in vertebral elements in order to evaluate whether this proves to be useful as an additional set of traits for taxonomy. The vertebrae of most of the less primitive teleosts are composed by one centrum (monospondylous). In general, caudal vertebrae of teleosts are characterized by the presence of neural arches and spines and haemal arches and spines, whereas precaudal vertebrae have neural arches and spines and parapophyses, fused to their centra (GRASSÉ, 1958; JARVIK, 1980; ARRATIA, 2003B). Vertical rotational movements between adjacent vertebrae are limited by the presence of bony extensions (zygapophyses) on each neural and haemal arch (GOSLINE, 1971; HILDEBRAND, 1995). These extensions are by many authors referred to as dorsal and ventral pre- and postzygapophyses. But, these terms are used to describe the articulation processes of vertebral arches in Tetrapodes (HILDEBRAND, 1995). However, the extensions that are present in fish are considered non-homologous with those of Tetrapodes (GRASSÉ,

1958; GOSLINE, 1971; HILDEBRAND, 1995). Consequently, in order to avoid misinterpretations, the following terms are used in this paper: processus prae- and posthaemalis and processus prae- and postneuralis (Fig. V.1- 1).

The vertebral column can be divided in two regions: the precaudal and the caudal zone (ROCKWELL ET AL., 1938; RAMZU AND MEUNIER, 1999). The precaudal zone consists of vertebrae characterized by the presence of parapophyses, supporting ribs (if present), and the absence of haemal spines (LAKSHMI AND SRINIVASA, 1989). The vertebrae of the caudal zone have haemal arches, which enclose the large ventral blood vessels and which are elongated by a haemal spine (ROCKWELL, 1938; RAMZU AND MEUNIER, 1999). Both zones have neural arches and spines (ROCKWELL, 1938).

At present the systematics and phylogeny of the Clariidae is still a problem due to the lack of unambiguous, diagnostic traits to distinguish the different elongate clariid species. The study of the postcranial skeleton may provide an outcome to this problem. In order to examine the informative nature of vertebral shape variation for taxonomy and phylogenetic research, it is important to quantify and qualify this variation adequately. To study the shape variation of the vertebrae, geometric morphometrics based on thin plate spline, is used as it completely uncouples variation in shape from variation in size (ROHLF, 1990).

Up to now, to our knowledge, no geometric morphometric analyses based on landmark data have been used to describe intraspecific shape variation in the postcranial skeleton of teleosts.

## MATERIAL AND METHODS

---

The specimens used in this study are listed in Table III.1- 2. The sample of *C. apus* comprised 30 specimens, of which nine specimens were collected in northern Gabon (Oyem), six in eastern Gabon (Makokou) and ten in southern Gabon (Congo-Brazzaville and Franceville) by D. Adriaens, S. Devaere and A. Herrel in 1999 and 2000 (Fig. V.1- 2). The specimens collected in northern Gabon (Oyem (1)), were found in the Woleu-river, which is part of the Woleu-Ntem-system. The eastern population, collected in Makokou (2), was found in the Liboumba-river, lying within the Ivindo-basin. The specimens collected in southern Gabon (Congo-Brazzaville and Franceville) (3), were obtained from two different river systems. Two specimens were found in the Kahjaka kanjaka-river (Franceville 3a), which is part of the Ogooué-basin, whereas the other specimens are collected in the Djou-river (3b), part of the Congo-basin.

For the geometric morphometric analyses, shape variation in both the precaudal and caudal vertebrae was studied based on landmark configurations. Ten landmarks were defined to describe the shape of the precaudal vertebrae in a caudal view and nine for the lateral view (Fig. V.1- 1A). For the caudal and lateral view of the caudal vertebrae, eleven and fourteen landmarks were defined, respectively (Fig. V.1- 1B). For a detailed description see III.2.3B.

For the precaudal as well as the caudal vertebrae, different lengths have been defined and measured (Fig. V.1- 3, 4A). A total of 9 and 10 lengths were defined on the lateral and caudal view of the precaudal vertebrae respectively (Fig. V.1- 3A, B). On the lateral view of the caudal vertebrae, 14 lengths were measured (Fig. V.1- 4A). A total of 6 measurements were defined on the lateral view of the pectoral spines (Fig. V.1- 4B). For a detailed description I refer to III.2.4B. These data were submitted to a Principal Component Analysis, using Statistica (StatSoft Inc) (see III.2.6).

A detailed description of the clearing and staining protocol and visualization is given in III.2.2 and III.2.5 respectively.

## RESULTS

---

For the analyses of the landmark configurations of the precaudal vertebrae (in caudal and lateral view) and those of the caudal vertebrae (in caudal and lateral view), the distribution in tangent space is a sufficient approximation for that in the Kendall shape space, as indicated by a correlation coefficient between Procrustes distance (in Kendall shape space) and tangent distance (in tangent shape space) of 1.000.

### MORPHOMETRY - PRECAUDAL VERTEBRAE

The relative warp analysis based on the data set of the precaudal vertebrae in lateral view, yielded 14 relative warps, of which relative warp 1 (RW1) explains most of the variation in shape (68.61%). A plot of RW1 versus RW2 thus represents the pattern of the most important shape variation in the sample of landmark configurations. Despite of the overall similarity in morphology of the precaudal vertebrae this plot shows some marked shape variation: two geographical groups can be discerned (Fig. V.1- 5). Specimens collected in the northern region of Gabon (Oyem), form the first group whereas the second group originates from the southern part of Gabon (Congo-Brazzaville and Franceville) and the eastern part of Gabon (Makokou). RW1 explains most of the shape variation in the sample (44.35%). This shape vector reflects the variation in length and inclination of the

neural spines and the size of the postneural processes. With respect to the consensus, which is the calculated mean landmark configuration of the sample and which is situated at the origin of the biplot, positive RW1-values represent longer, ventrally displaced neural spines and smaller processus postneurales. The opposite is true for the negative values. Variation expressed by RW2 (23.81% of variation explained) involves the length of the neural spines and the vertebral centra (in rostro-caudal direction). Negative RW2-scores involve elongated neural spines and higher vertebral centra. The two geographic groups are separated along axis S. The landmark configurations of the extreme negative (S1) and positive values (S2) of this axis S is visualized in figure V.1- 5 and these represent the main shape differences between the two groups. A Discriminant Function Analysis reveals highly significant geographic variation and confirms the distinct shape differences in the two geographic groups (Table V.1- 1A).

Data based on the caudal view of the precaudal vertebrae are plotted in figure V.1- 6. The scatterplot of the scores of RW1 (explains 44.32% of variation) versus those of RW2 (22.18%) indicates a different ordination of three groups. The first group consists of the specimens collected in northern Gabon (Oyem). The second group consists of the specimens collected in eastern Gabon (Makokou), which somewhat cluster with the specimens collected in southern Gabon (Franceville). The third group consists of specimens collected in Congo-Brazzaville. Positive RW1-scores represent vertebrae with shorter neural spines and with parapophyses being more dorsally displaced. Along RW2, positive scores represent, with respect to the consensus, vertebrae with longer, ventrally displaced parapophyses and vertebral centra that have a smaller diameter, whereas negative scores involve dorsally displaced parapophyses and vertebral centra with broader diameter. The displacement of landmarks 1, 4 and 8 corresponds to the main shape variation observed on the lateral view of the precaudal vertebrae (Fig. V.1- 5). A Discriminant Function Analysis of the data indicates significant differences between all groups except for the specimens collected in eastern Gabon (Makokou) and the specimens collected in Congo-Brazzaville, these show no significant differences (Table V.1- 1B).

Based on the biometric results (see below) and the morphometric results of the lateral and caudal view of the precaudal vertebrae the conclusion can be made that the northern population has neural spines, which are ventrally inclined and shorter. The biometric as well as the morphometric analyses indicate that the parapophyses of the northern population are dorsally inclined. The biometric results also confirm that the vertebral centrum of the northern population is larger. These shape differences of the precaudal vertebrae in lateral view between the northern population and the other populations are visualized by axis S in figure V.1- 5.

## MORPHOMETRY - CAUDAL VERTEBRAE

Analyses of the morphometric data based on the caudal vertebrae in lateral view, follow the pattern where a distinction between the specimens of northern Gabon (Oyem), and those of eastern (Makokou) and southern Gabon (Congo-Brazzaville and Franceville) is present and the distinction is even more clearly (Fig. V.1- 7). Both groups are separated along RW1, which explains 62.22% of the shape variation. RW1-scores of the northern population all are positive, which involves (with respect to the consensus) shorter neural and haemal spines and larger vertebral centra. The second group, which has negative relative warp scores only, is formed by the eastern (Makokou) and southern populations (Congo-Brazzaville and Franceville), and has caudal vertebrae with elongated neural and haemal spines and smaller vertebral centra. The RW2 explains 16.35% of the variation. Positive scores of this axis include specimens, which have, elongated neural and haemal spines, smaller processus prae- and postneurales, and neural and haemal spines that are respectively inclined in rostro-dorsal and rostro-ventral direction. These results are confirmed by the results of the biometric analysis of the data of the precaudal vertebrae in lateral view (see below). A Discriminant Function Analysis indicates highly significant differences between the northern population and the eastern population and between the northern population and the southern population (Table V.1- 1C).

The scatter plot of RW1 versus RW2, based on the data of the caudal vertebrae (in caudal view) again shows a separation of two groups: the northern population (Oyem) on the one hand and the eastern (Makokou) and southern population (Congo-Brazzaville and Franceville) on the other hand (Fig. V.1- 8). The northern population has negative RW1-scores only, with RW1 explaining 63.86% of the variation. Combined with the information obtained from the lateral view of the caudal vertebrae (Fig. V.1- 7), it can be concluded that the vertebrae in the specimens of the northern population (Oyem) have shorter neural and haemal spines, vertebral centra with a larger diameter and shorter processus postneuralis in contrast to the vertebrae of the other populations (Makokou, Congo-Brazzaville and Franceville). Specimens of the group composed by the eastern and southern populations (Makokou, Congo-Brazzaville and Franceville), which all have positive RW1-scores, have caudal vertebrae with elongated neural and haemal spines, vertebral centra with smaller diameter and longer processus postneuralis. The second relative warp axis explains 22.49% of the shape variation. As could be suspected from the results of the relative warp analyses, the differences are highly significant (Table V.1- 1D).

## DEGREE OF ANGUILLIFORMITY

The degree of anguilliformity can be defined as the ratio of the abdominal body depth versus the standard length (Fig. V.1- 9). A Discriminant Function Analysis (Table V.1- 2) indicates that the differences, based on the degree of anguilliformity, between the northern population (Oyem) and the eastern and southern populations (Makokou, Congo-Brazzaville and Franceville) are significant. The specimens of northern Gabon (Oyem) show a higher degree of anguilliformity.

TPS-REGR was used to explore the relationship between shape variation and independent variables (degree of anguilliformity, size). Based on the morphometric data of the lateral view of the caudal vertebrae it is not possible to conclude whether a relationship exists between shape and degree of anguilliformity, because the sample size is too small and too many landmarks are defined. This implies that too less degrees of freedom are defined so a multivariate regression cannot be done.

Regressing the shape variation based on the data of the precaudal vertebrae in lateral and caudal view, the relation found between shape and the degree of anguilliformity is in both cases low. 1) Based on the data of the precaudal vertebrae in caudal view, only 21% of the variance is explained by the regression of shape to the degree of anguilliformity. The amount of variance is significant ( $F=5.986$ ,  $p<0.00001$ ). The program also performs a permutation of Goodall's F-tests, where all of the shape variables for each specimen are randomly assigned to any specimen and where the regression is performed 1000 times. With the permutation procedure, it calculates how many times it found a better regression than the one the program indicates. Performing the permutation test, no alternative regression was found, which yielded a better or equal result than the one observed. 2) The amount of variance explained by the regression based on the data of the precaudal vertebrae in lateral view is 29% and is also significant ( $F=8.7855$ ,  $p<0.00001$ ). Again, no better or equal alternative regression using the permutation test is found. 3) Forty-one % of the variance (significance:  $F=13.413$ ,  $p<0.00001$ ) is explained by the regression between the shape of caudal vertebrae in caudal view and the degree of anguilliformity. The Goodall F-tests found no better or equal alternative regression.

The relation between shape variation and standard length has also been examined. The variance explained by the regression based on the precaudal and caudal vertebrae in lateral and caudal view is respectively 22.01%, 31.89%, 49.95 and 45.27%. In all cases, no better or equal alternative regressions are found by the Goodall F-tests. Despite the fact that the northern specimens have higher standard lengths than the other populations, no relation is present between shape variation and standard length.

Thus, we may conclude that shape variation observed in these vertebrae is independent of size and the degree of anguilliformity, and presumably thus reflects geographic differences. This implies that the degree of anguilliformity could thus be considered a taxonomic trait.

## BIOMETRY

Exploring the relative values of the measurements, taken on the precaudal and caudal vertebrae, led to the conclusion that all relative biometric vertebral variables have lower values in specimens collected in northern Gabon (Oyem), whereas the values of the southern (Congo-Brazzaville and Franceville) and eastern (Makokou) populations are distributed within the same range. Based on an Anova (Table V.1- 3), the values of most vertebral measurements of specimens found in Oyem are shown to be significantly different from those of the other geographic populations (Makokou, Congo-Brazzaville and Franceville). Some measurements appear to separate the specimens from the northern population (Oyem) completely from the other populations and thus may hold some value as potential diagnostic traits. Therefore these are illustrated in figures V.1- 10, V.1- 11, V.1- 12 and V.1- 13.

### BIOMETRY - PRECAUDAL VERTEBRAE

Precaudal vertebrae in lateral view - The relative values (with respect to standard length) of two measurements, (PL4) the distance between the processus praehaemalis and the processus praeneuralis and (PL5) the distance between the processus posthaemalis and the processus postneuralis (Fig. V.1- 3A) are significantly lower in the northern population (Oyem) compared to those of the other populations (Makokou, Congo-Brazzaville and Franceville) (Fig. V.1- 10) and no overlap between these two groups is found. This trend (lower values in the northern population) is observed for each measurement taken on the precaudal vertebrae in lateral view. An Anova reveals that all variables are significantly different between the northern population (Oyem) on the one hand and the other populations (Makokou, Congo-Brazzaville and Franceville) on the other hand (Table V.1- 3A). These significantly lower relative values for PL4 and PL5 correspond with smaller processus prae- and postneurales because the relative values of the vertebral centra are similar in the different populations. These results are confirmed by the geometric morphometric analyses.



Precaudal vertebrae in caudal view - The relative values (with respect to standard length) of the distance between the parapophyses (PC1), the length of the neural canal (PC7), and the distance between the vertebral centrum and the tip of the neural spine (PC8) (Fig. V.1- 3B) are significantly lower for the northern population (Oyem) (Fig. V.1- 11) and show no overlap. The Anova reveals that all measurements, defined on the precaudal vertebrae in caudal view, of the northern population (Oyem) are significantly lower than those of the other populations (Makokou, Congo-Brazzaville and Franceville) as shown in Table V.1- 3B. The geometric morphometric analysis showed that the neural spines of the northern population (Oyem) are ventrally inclined and that their parapophyses are dorsally inclined, which respectively explains the relatively lower values of PC1, PC7 and PC8.

### BIOMETRY - CAUDAL VERTEBRAE

A total of 14 measurements were defined on the caudal vertebrae in lateral view (Fig. V.1- 4A). Based on the relative values of 5 measurements (L1- L5, with respect to the standard length), again the specimens collected in northern Gabon (Oyem) are completely separated from those collected in the other parts of Gabon (Makokou, Congo-Brazzaville and Franceville). The relative values of (L1) the distance between the tip of the neural spine and the tip of the haemal spine, (L2) distance between the tip of the neural spine and the processus postneuralis, (L3) distance between the tip of the neural spine and the processus praeneuralis, (L4) distance between the tip of the haemal spine and the processus posthaemalis and (L5) distance between the tip of the haemal spine and the processus praehaemalis are significantly (Anova) lower for the northern Gabon population (Oyem) (Fig. V.1- 12; Table V.1- 3C). L6, L8 and L9 are also significantly lower for the northern population, though the values show some degree of overlap. The lengths of the pterygiophores of specimens of the northern population (Oyem), supporting the fin rays of the anal and the dorsal fins, also have lower values compared to the other populations (Makokou, Congo-Brazzaville and Franceville). The above-mentioned measurements (L1-L5) explain the lower relative values of the abdominal body depth of the specimens of northern population (Oyem). Geometric morphometric analysis reveals the presence of shorter neural and haemal spines in the northern population (Oyem). This is confirmed by the biometric analysis, which shows that the corresponding measurements L2, L3, L4 and L5 have lower relative values as well. The neural and haemal spines are respectively dorsally and ventrally inclined, which corresponds with the biometric results (L1).

## BIOMETRY - PECTORAL SPINES

Based on pectoral spine measurements (Fig. V.1- 4B), with respect to skull length, the northern population (Oyem) can also be distinguished from the eastern and southern populations (Makokou, Congo-Brazzaville and Franceville) as all variables are significantly different between these two groups (Anova, Table V.1- 3D). The northern population (Oyem) has lower relative values (and without overlap) for the total length of the pectoral spine (PS1), width of the base of the ridge (PS5) and width of the spine (PS6).

## BIOMETRY - PRINCIPAL COMPONENT ANALYSIS

A Principal Component Analysis was performed, using the log-transformed data matrix of 26 measurements. The first principal component proved to be an overall size factor and was thus omitted (BOOKSTEIN ET AL., 1985). Plotting the second principal component scores versus the third scores, we obtain four completely separated groups, each group containing specimens of the same geographical location. One group, located mainly in the upper left quadrant, contains specimens collected in eastern Gabon (Makokou). A second group is situated in the upper right quadrant and comprises specimens of Congo-Brazzaville. The third group, mainly located in the lower right quadrant is formed by specimens collected in northern Gabon (Oyem). The fourth group comprises specimens from Congo-Brazzaville and is situated in the lower left quadrant of the plot (Fig. V.1- 14A). The factor loadings are listed in Table V.1- 4 and plotted in figure V.1- 14B. The dominant characters for the second principal component for the biometric data are PS1, PS2, PS5, PS6, L2 and L11. The dominant characters for the third principal component for the biometric data are L10, L4, L1, L12, PL9.

It is remarkable that based on the PCA, the specimens from Franceville form a separate group (not clustered with specimens from Congo-Brazzaville). Furthermore, the eastern Makokou specimens are also separated from both southern populations, Congo-Brazzaville and Franceville. The geometric morphometric studies based on the precaudal vertebrae in lateral view (Fig. V.1- 5) and the caudal vertebrae in lateral and caudal view (Fig. V.1- 7, 8), group the eastern and southern specimens. That specimens from eastern (Makokou) and southern Gabon (Congo-Brazzaville and Franceville) form one group was also noted by exploring the relative biometric data. Though the geometric morphometric analysis of the precaudal vertebrae in caudal view (Fig. V.1- 6) and the biometric PCA (Fig. V.1- 14A) split all geographic populations.

The dominant measurements, with highest factor loadings, correspond to neural and haemal spine lengths and height of the precaudal and caudal vertebral centra, all morphological features which have geometric morphometrically been proven to be of high value to separate groups (though only two). This analysis additionally shows the importance of pectoral spine lengths, especially to define (or separate) specimens from both southern populations, Congo-Brazzaville and Franceville.

### MERISTIC DATA

Based on the number of vertebrae, it is possible to distinguish the northern population, which has more vertebral elements (90-103), from the eastern (86-89) and the southern populations (86-88) (Fig. V.1- 15).

## DISCUSSION

---

Vertebral counts are often used in systematics and phylogenetical research. The aim of this study was to investigate whether the shape of vertebrae is also a useful tool for taxonomic purposes.

The results indicate that vertebral shape differences are present between the different populations of elongate clariids. The analysis of the data based on the lateral and caudal view of the precaudal as well as the caudal vertebrae, reveals a pattern of at least two geographical groups and probably four groups. The specimens originating from northern Gabon (Oyem) are always completely separated from those collected in eastern (Makokou) and southern Gabon (Congo-Brazzaville and Franceville). The specimens from eastern and southern Gabon form the second geographical group. However, based on the caudal view of the precaudal vertebrae and the PCA, three additional groups are detected as the specimens of Congo-Brazzaville can be separated from those collected in Franceville as well as from those found in Makokou.

The northern population (Oyem) is characterized by the following features: (1) the precaudal vertebrae have smaller processus postneurales, ventrally inclined neural spines, dorsally displaced parapophyses and larger vertebral centra; (2) the caudal vertebrae show shorter neural and haemal spines, respectively dorsally and ventrally inclined, vertebral centra with a larger diameter and shorter processus postneurales. These shape differences are observed based on the geometric morphometric analysis and are confirmed by biometric data.

Due to the lack of a reliable understanding of generic and specific characteristics, it is difficult to discern between the different eel-like species (DEVAERE ET AL., 2001). The current determination key of POLL (1977) did not consider the range of variation of the different features because few specimens were used to describe the species. For example, one specimen, found in Makokou, was cataloged in the collection of the M.R.A.C. as *Gymnallabes alvarezi* Roman, 1970, based on the currently available determination key of POLL (1977). According to POLL (1977) the presence of the pelvic fins is considered to be a diagnostic character for *G. alvarezi*. However, the presence or absence of these fins has been demonstrated to be a highly variable trait in some elongate clariids, including *G. alvarezi* (ADRIAENS ET AL., 2002). Specimens of the northern population (Oyem), which show the highest degree of anguilliformity, lack pelvic fins, whereas in specimens, collected in eastern Gabon (Makokou), pelvic fins are present. This leads to the conclusion that proposed diagnostic characters to distinguish different species are not unambiguous and thus cannot be used to distinguish species or subspecies (at least as they are described today).

A Discriminative Function Analysis on several biometric characters, performed by ADRIAENS ET AL. (2002) shows that differences between *G. alvarezi* and *C. apus* are significant. This analysis is based on only few specimens of *G. alvarezi* and thus could give a wrong representation of the group variation. A more recent PCA-analysis of metric and meristic characters of *C. apus* (collected in northern, southern and eastern Gabon), *C. apus* (present in M.R.A.C.) and *G. alvarezi* (present in M.R.A.C.), based on more specimens of each species, shows a substantial degree of overlap, and distinct groups can no longer be recognized (Fig. V.1- 16). However, since DFA reflects the maximal variation between groups, which is not the case for PCA, a DFA should be done on this data set as well. Currently an anova of this data is not possible because the different groups of species or subspecies are not clearly understood yet. Additionally, the type specimen of *G. alvarezi*, is located in the plot near specimens belonging to *C. apus*, as on-going research is showing (Devaere, per comm.).

This indicates the difficulty to designate a species name to the specimens, collected in the different regions of Gabon, and the need of good diagnostic tools to distinguish the different species from each other.

The morphometric analyses of both precaudal and caudal vertebrae thus reveal some kind of geographic variation in the postcranial skeleton of "*C. apus*". Two hypotheses may explain the presence of two groups within the currently examined specimens: (1) interspecific variation and (2) intraspecific, geographic variation.

(1) Morphometric analyses of the precaudal as well as the caudal vertebrae reveal shape differences between the northern population (Oyem) on the one hand and the eastern (Makokou) and southern population (Congo-Brazzaville and Franceville) on the other hand. Next to the vertebral differences between the different populations, other postcranial differences can be observed as well within the northern population. These differences are the absence of serrations on the anterior side of the pectoral spine, shorter and more slender pectoral spines, the absence of pelvic fins, a higher total number of vertebrae, a higher degree of anguilliformity, and shorter pterygiophores. Features as serrations of the pectoral spine, abdominal height, the presence of the pelvic fin and the number of vertebrae are characteristics which are often used to describe species (POLL, 1942; 1957; ROBERT AND STEWART, 1976). The differences in these characters may be additional arguments for the hypothesis that the observed morphological differences are due to interspecific variation, rather than intraspecific variation. But as mentioned before some of these features (e.g. pelvic fins) are highly variable within the Clariidae (ADRIAENS ET AL., 2002) and thus may not be useful in systematic research. In case the morphological vertebral differences and other postcranial differences between the northern population (Oyem) on the one hand and the eastern (Makokou) and southern population (Congo-Brazzaville and Franceville) on the other hand are due to interspecific variation, the differences may indicate that the former belongs to *C. apus* and the latter belongs to *G. alvarezi*. To confirm these statements, further studies are required and in progress (Devaere, pers comm.). If the on-going research reveals the presence of two or more species, the morphology and shape of precaudal and caudal vertebrae can be used to distinguish different species.

(2) The morphological vertebral differences may be due to intraspecific variation. In this case, all specimens should be considered as *C. apus*, where the observed vertebral shape differences occur at a subspecies-level. Intraspecific variation can be the result of different natural processes. Due to the isolation of a population, genetic drift may occur (JOCKUSH, 1997). Additionally, variation of environmental factors will select for different adaptations, which supports (sub)speciation (HOLCIK AND JEDLIKA, 1994). Within a geographic population, differences in the vertebral column have been observed which can be related to fluctuating abiotic factors, such as temperature (GABRIEL, 1944), climatologic or geographic circumstances (HOLCIK AND JEDLIKA, 1994). Each year, the number of vertebral elements of specimens of a population can vary, which depends on the temperature to which the embryo has been exposed during development (GABRIEL, 1944). Since the studied populations are collected in different regions of Gabon, different factors are controlling the development of the embryos and may be responsible for the observed

geographic variation. Focusing on the habitat of the different populations, the habitats of the northern (Oyem) and eastern populations (Makokou) are similar. These two populations live in the moist soil of the rain forest, whereas the southern populations (Congo-Brazzaville and Franceville) live in a dryer region, closer to the Gabonese savannah. But the results suggest that the morphology of the eastern and southern populations is more similar. This may indicate that in this case shape variation is no consequence of different developmental controlling factors.

As mentioned above, a recent PCA-analysis of metric and meristic characters of *C. apus*-specimens of different geographic regions and *G. alvarezi*, shows no distinct groups. The hypothesis of intraspecific variation is furthermore supported by the high degree of phenotypic plasticity in the fusion of hypurals in the caudal skeleton, the absence or presence of the pectoral and pelvic fins and the presence of shorter neural and haemal spines (ADRIAENS ET AL., 2002; DE SCHEPPER ET AL., 2004) (V.2).

The length of the pterygiophores of the specimens of the northern population (Oyem) is smaller compared to that of the other populations (Makokou, Congo-Brazzaville and Franceville). These observations are reflected in the higher degree of anguilliformity. However, the statistical analysis (TPS-REGR) reveals no relation between shape of precaudal and caudal vertebrae and the degree of anguilliformity. Furthermore, no relations between vertebral shape and the presence or absence of paired fins and hypural fusions of the caudal fin are observed. Thus, these characteristics may be examples of features, which are highly variable and thus can't be used as diagnostic traits.

The geometric morphometric analysis of vertebral shape variation in three different population of *C. apus*, collected in Gabon, leads us to the conclusion that vertebral shape is a useful diagnostic tool in taxonomy. But at this moment it is not clear at which species-level (species or subspecies) vertebral shape variation can be considered in the case of these elongate clariids.

## ACKNOWLEDGMENTS

---

The authors wish to thank M. Stiasny, C. Hopkins, J.-D. Mbega and the I.F.A.F. (Gabon) for assistance during sampling. This research was funded by the BOF (projects 01104299 and 01103401) and the FWO (project G 0388.00).

## V.2 CAUDAL OSTEOLOGY OF *CHANNALLABES APUS*





# INTRASPECIFIC VARIATION IN THE POSTCRANIAL SKELETON MORPHOLOGY IN AFRICAN CLARIIDS: A CASE STUDY OF EXTREME PHENOTYPIC PLASTICITY

---

Modified from the paper published as:

De Schepper N, Adriaens D, Teugels GG, Devaere S, Verraes W. 2004.  
Intraspecific variation in the postcranial skeleton morphology in African clariids: a case  
study of extreme phenotypic plasticity  
Zoological Journal of the Linnean Society. 140: 437-446.

## ABSTRACT

---

Taxonomic relationships within the Clariidae, especially within the elongate species, are currently ambiguous due to the lack of a reliable structure of valid generic and specific characteristics. Based on the information available, it is difficult to properly diagnose the different elongated genera and species. This is due in part to a high degree of variability of certain traits generally considered to be important taxonomically. For example, the caudal skeleton is often considered to be an important diagnostic trait. However, the degree of phenotypic plasticity has not hitherto been adequately assessed. This paper deals with interspecific variation of the caudal skeleton of *Clarias gariepinus*, *Platyallabes tihoni*, *Platyclarias machadoi*, *Gymnallabes typus*, *Channallabes apus* and *Dolichallabes microphthalmus*. The caudal skeleton of *C. apus* is studied, using specimens from three regions in Gabon. Hypural fusions and haemal and neural spines show most variation. The observed morphological variation appears to be geographically independent, in contrast to other morphological features such as vertebrae.

## INTRODUCTION

---

The Clariidae (Teleostei: Siluriformes) is a family of catfishes distributed throughout northern and central Africa and extending to south-east Asia. In Africa there are 12 genera (74 species) and in Asia three genera (18 species), two of which are endemic (TEUGELS, 1996). The family shows a trend toward increasing anguilliformity as reported by

BOULENGER (1908) and PELLEGRIN (1927). Although this tendency is present in other families of teleosts, amphibians, reptiles and mammals, the extensiveness of the transformation from fusiform to elongate in Clariidae is distinctive (LANDE, 1978; WITHERS, 1981). Its most notable characteristic is the elongation of the postcranial skeleton, although a whole set of other morphological transformations has been observed: disappearance of adipose fin; continuous dorsal, caudal and anal fins; reduction of pectoral and pelvic fins (limblessness); reduction of skull bones; reduction of eyes; and hypertrophy of the adductor mandibulae muscle complex (PELLEGRIN, 1927; POLL, 1977; CABUY ET AL., 1999; DEVAERE ET AL., 2001; ADRIAENS ET AL., 2002).

Currently, the taxonomy of some genera and species within the Clariidae, especially those which are elongate, is confusing. In order to study the functional implications of these adaptations, a reliable structure of generic and specific characteristics is required. Based on the identification key produced by POLL (1977), it is difficult to discern between the different elongated genera and species because the degree of phenotypic plasticity has not been considered adequately, largely due to the limited numbers of specimens used to describe the species. Features of the caudal skeleton are considered by many authors to be important diagnostic traits and are used for interpreting systematic and phylogenetic relationships within Teleostei (ARRATIA, 1983, 1997, 1999; SCHULTZE AND ARRATIA, 1988). However, intraspecific variation in different parts of the caudal skeleton has rarely been investigated, and conclusions are often based on a handful of specimens. Morphological variation in the postcranial and caudal skeletons within species of elongated clariids, however, appears to be frequent and substantial.

The objective of this paper is to focus on the caudal skeletal morphology of different representatives of the Clariidae in order to: (1) describe interspecific morphological variation and (2) describe intraspecific variation of the caudal skeleton in *Channallabes apus*, one of the most abundant elongate species.

## MATERIAL AND METHODS

---

For the study of interspecific variation, specimens preserved in alcohol were used, obtained from the Africa Museum (MRAC), Tervuren, Belgium. This study is focused on six clariid species (ranked in order of increasing anguilliformity): *Clarias gariepinus* (Burchell, 1822) (04-12-98n3, 1 specimen), *Platyclarias machadoi* Poll, 1977 (MRAC 78-6-P-1348-364, 1 specimen), *Platyallabes tihoni* (Poll, 1944) (MRAC 73-68-P-144, 1 specimen), *Channallabes apus* (Günther, 1873) (unregistered samples from Gabon, 37 specimens), *Gymnallabes typus* Günther, 1867 (KMMA-75-84-P-683-693, 1 specimen) and *Dolichallabes*

*microphthalmus* Poll, 1942 (MRAC 78808- 810, 1 specimen). Additional data on the caudal skeleton of *Platyclarias machadoi*, *Platyallabes tihoni* and *Gymnallabes typus* were obtained from POLL (1977). The specimens used in this study are listed in Table III.1- 2.

In order to study intraspecific variation, 30 specimens of *Channallabes apus* were used, which were collected in 1999 and 2000 in three different regions in Gabon (West-Central Africa). Nine specimens originated from the Woleu River system in northern Gabon (Oyem), whereas six were from eastern Gabon (Liboumba River Makokou, which is part of the Ivindo Basin, Ogowe System). A southern population was represented by ten specimens collected in two different river systems: the Djoué River (Congo Basin), and the Ogowe Basin.

A detailed description of the clearing and staining protocol and visualization is respectively given in III.2.2 and III.2.5.

## RESULTS

---

### INTERSPECIFIC VARIATION

The caudal skeleton of *Clarias gariepinus* shows no fusions between the different hypurals (Fig. V.2- 1). All hypurals, the parhypural and the urostyl are separate structures. However, these elements, except the upper hypurals, are fused at their bases both with each other and with the compound centrum. The two halves of the neural arch of the compound centrum do not fuse dorsally. The epural is supported by both these halves. The dorsal lobe, which supports 14 caudal fin-rays, is formed by hypurals 3, 4 and 5, the urostyl and the epural. The neural spine of the third preural centrum, which is elongated and plate-like, is, in contrast to the other species, added to the dorsal lobe of the caudal fin. The ventral lobe, supporting 12 caudal fin-rays, is not exclusively formed by the parhypural and hypurals 1 and 2 - the haemal spines of the second and third preural centrum are also involved. This contrasts with other clariid species (see below). The caudal fin is not confluent with the anal and dorsal fins.

The caudal skeleton of two specimens of *Platyclarias machadoi* shows some intraspecific variation. In the first specimen, hypurals 4 and 5 and 3 and 4 are fused, whereas the second specimen shows no hypural fusions (Fig. V.2- 2A, B). Other features are similar in the two specimens. Incomplete neural and haemal arches of the compound centrum are present. The epural is proximally supported by both halves of the neural arch. The plate-like neural and haemal spines of the second preural centrum are elongated. The caudal fin is not confluent with the anal and dorsal fins.

The caudal skeleton of *Platyallabes tihoni* consists of a caudal plate formed by fused hypurals and urostyl and of the parhypural and the plate-like haemal spine of the second preural centrum, which flank the caudal plate (Fig. V.2- 2C) (POLL, 1977). An incomplete neural arch of the compound centrum is present and supports the epural. The second preural centrum has an elongated haemal spine and a short neural spine. The caudal fin is confluent with the anal and dorsal fins.

The caudal skeleton of *Gymnallabes typus* is divided into ventral and dorsal lobes. In one specimen, the dorsal lobe is formed by a distinct urostyl and fused hypurals 3, 4 and 5 (Fig. V.2- 2D). The ventral lobe consists of a separate parhypural and fused hypurals 1 and 2. Anterior to the epural, a neural spine of the neural arch of the compound centrum is present. The second preural centrum has double haemal arches and spines, whereas the third preural centrum has double neural and haemal arches and spines. A second specimen has a ventral lobe that, in contrast to the other specimen, is formed by the fusion of the parhypural and hypurals 1 and 2 (Fig. V.2- 2E). Only the second preural centrum has double haemal arches and spines. The caudal fin is confluent with the anal and dorsal fins.

The caudal skeleton of *Dolichallabes microphthalmus* consists of an independent parhypural and a caudal plate, formed by fusion of all hypurals and the urostyl (Fig. V.2- 2F). The neural arch of the compound centrum is open distally. Both halves of the neural arch, which are relatively long, articulate with the epural. Ventral to the compound centrum, two haemal arches and spines can be observed. The parhypural supports caudal fin rays. The other haemal spine is shorter and does not support caudal fin rays. The second preural centrum has two neural and haemal arches and spines, which have partially fused. The caudal fin is confluent with the anal and dorsal fins.

### INTRASPECIFIC VARIATION

The caudal skeleton of *Channallabes apus* displays a high degree of intraspecific variation in the pattern of hypural fusions. The caudal fin is confluent with the anal and dorsal fins.

The unfused configuration (five separate hypurals and a separate parhypural) is found in 45% of the specimens of *C. apus* examined (Fig. V.2- 3A). However, 63% of these have at least two hypurals that are partially fused at their bases. In 25% and 19% of the individuals examined, only the bases of hypurals 1 and 2 or 3 and 4, respectively, are fused. In 19%, partial fusions of these hypurals can be observed (Fig. V.2- 3B). An overview of all the different patterns of hypural fusion observed is given in Table V.2- 1. Apparently, fusions between hypurals 3 and 4 (30%) and 1 and 2 (27%), with or without additional

fusions, occur most frequently (Fig. V.2- 3C, D). Fusions of hypurals 3, 4 and 5, forming a dorsal plate, are present in 8% of the specimens, whereas the presence of a dorsal (H3 + H4 + H5) and a ventral plate (PH + H1 + H2), was observed in 3% (Fig. V.2- 3E). A complete fusion, forming one plate (PH + H1-5), was observed in only 3% (Fig. V.2- 3F), as was fusion of the parhypural with the first hypural (Fig. V.2- 4A).

The frequency of the different patterns of hypural fusion of the different populations has been examined. Half of the southern (Congo-Brazzaville and Franceville) and northern populations (Oyem), and 29% of the eastern population (Makokou) have caudal skeletons lacking hypural fusions. Hypurals 1 and 2 are fused in, respectively, 17%, 21% and 57% of the southern (Congo-Brazzaville and Franceville), northern (Oyem) and eastern populations (Makokou); the equivalent percentages for fusion of hypurals 3 and 4 are 17%, 33% and 29%. Half of the northern population and 14% of the eastern population show fusions of hypurals 3, 4 and 5, forming a dorsal plate. Fourteen percent of the eastern population (Makokou) has two plates, a dorsal and a ventral one. Fusion of all hypurals and the parhypural is observed once (eastern population, Makokou). No specimens of the southern population (Congo-Brazzaville and Franceville) have dorsal or ventral caudal plates. A correlation between the pattern of hypural fusion and geographical distribution appears to be non existent. However, in the eastern population (Makokou), 75% of specimens show hypural fusions in the ventral lobe. This number is substantially lower in the two other populations (i.e. 20% in the southern (Congo-Brazzaville and Franceville), 0.4% in the northern population, Oyem).

Unfused neural arches of the compound centrum appears to be a shared feature of the Clariidae. In *C. apus* two halves of the neural arch can be distinguished. The epural is supported by either or both bases. The caudal skeleton of 6% of the examined specimens of *C. apus* lacks an epural (Fig. V.2- 3A). In this case, the neural spine of the second preural centrum functions as an epural. The epural is present in 95% of the specimens, of which 59% have an epural supported by both halves of the neural arch. On the other hand, in 38% the epural is supported by only one of the neural halves: 18% by the right half (Fig. V.2- 3B) and 21% by the left (Fig. V.2- 4A). Two specimens possess an atypically elongated and broad epural: in one it is fused to the neural spine of the second preural centrum (Fig. V.2- 3C), whereas in the other it consists of two parts (Fig. V.2- 4B). Probably, the morphology of the latter is the result of healing after a trauma.

The morphology of the parhypural shows little variation. In some cases a double haemal arch and spine appear to precede the parhypural (Fig. V.2- 4C). There are many specimens with aberrant neural or haemal spines on the first preural centrum. In *C. apus*, the neural spines of the second preural centrum have a characteristic spine-like

morphology and show little variation in shape. In 8% of the specimens such a neural spine is lacking (Fig. V.2- 4B), whereas in 6% the second preural centrum has two neural arches and spines (Fig. V.2- 4D). In 11% the neural spines of the second preural centrum are supported by the right half only of the neural arch (Fig. V.2- 4E). In 5% both left and right neural arches of the second preural centrum bear a separate neural spine (Fig. V.2- 3A). Only one specimen has a neural spine that is fused to the third preural centrum (Fig. V.2- 4E).

The haemal spines of the second preural centrum articulate with caudal fin-rays. These usually elongated and broad spines show some variation in their morphology. In 6% of the specimens, two spines are present (Fig. V.2- 4C), whereas in 11% the spines are branched (Fig. V.2- 4D). The spine of only one specimen is fused with the parhypural (Fig. V.2- 4F).

The neural and haemal spines of the third preural centrum show little variation. None of the examined third preural centra have double neural spines or spines that are elongated and support caudal fin-rays. In 8% of the specimens the neural spines are branched (Fig. V.2- 3D), whereas in one the spine is fused to that of the second preural centrum (Fig. V.2- 4E).

## DISCUSSION

Two types of diurnal caudal skeleton are observed in teleosts (DE PINNA, 1996). In most of the higher Teleostei it is of the stegural type, whereas in Ostarioclupeomorpha it is pleurostylar (GOSLINE, 1971). The stegural urocentrum is formed by the fusion of the first and second ural vertebrae as well as the first preural centrum and supports the parhypural and the first and second hypurals (ARRATIA, 1997). The stegural urostyl is formed by the fusion of the remaining ural vertebrae and supports the third up to the sixth hypurals. The pleurostylar urocentrum is formed by fusion of the first preural centrum and the first and second ural vertebrae, and supports the parhypural and the first and second hypurals. The pleurostylar urostyl, however, is formed by the fusion of the first and second uroneurals and supports the remaining hypurals (FINK AND FINK, 1981; ARRATIA, 1983).

The caudal skeleton of Siluriformes consists of a series of characters, explained below. The compound centrum is generally formed by the fusion of the first preural centrum and one or two ural centra (ARRATIA, 2003B; MONOD, 1968; GOSLINE, 1997). A second ural centrum, which in most cases is fused to the base of hypurals 3 and 4, is present (LUNDBERG AND BASKIN, 1969). The caudal skeleton of Siluriformes consists of a maximum of six hypurals, which is considered to be the most primitive pattern. The hypurals and parhypural are located ventral to the urostyl (ROJO, 1991). Two lobes can be distinguished:

a dorsal lobe, of a maximum of four, independent hypurals, and a ventral lobe, which consists of the first and second hypurals and the parhypural (EASTMAN, 1980). A small, incomplete and commonly dorsally positioned neural arch of the compound centrum is present. Usually one of the halves of the neural arch supports the epural (MONOD, 1968). In some specimens, both halves of the neural arch are fused to the epural, which has also been observed in different species by ARRATIA (1983) and SCHULTZE AND ARRATIA (1988). The epural can vary phenotypically and may be elongated, rounded, oval or absent (ARRATIA, 1983). The posterior part of the compound centrum is fused to the uroneural element, the urostyl. The haemal arch of the parhypural bears a small processus or hypurapophysis (NURSALL, 1963). A second hypurapophysis may be present on the first or the second hypural (LUNDBERG AND BASKIN, 1969; ARRATIA, 2003B).

Different fusion patterns of hypurals can be observed. Within the Siluriformes, as in other teleosts, a trend towards loss and fusion of hypurals has been noted (ARRATIA, 2003B; LUNDBERG AND BASKIN, 1969; POLL, 1977; TEUGELS AND ADRIAENS, 2003). Thus, the observed variation in *C. apus* may be an evolutionary transition towards fused hypurals.

The features described in the following section are generally applicable to the caudal skeletons of all Clariidae, although a great amount of variation between the different species can be observed. In Clariidae, five hypurals are present. The dorsal lobe consists of hypurals 3, 4 and 5. The ventral lobe consists of hypurals 1 and 2 and the parhypural. The second ural centrum (U2), which precedes the urostyl, is fused to the bases of hypurals 3 and 4. In some species neural and/or haemal spines of the second and/or third preural vertebrae are elongated to support caudal fin rays. The haemal arch of the parhypural lacks hypurapophyses, a feature in which the Clariidae differ from the closely related Heteropneustidae (LUNDBERG AND BASKIN, 1969) (Fig. V.2- 5). Secondary hypurapophyses are absent as well. An elongated, bony epural, articulating with the bases of one or two procurrent caudal lepidotrichia is present (LUNDBERG AND BASKIN, 1969; ARRATIA, 1983).

According to BOULENGER (1908) and PELLEGRIN (1927), the following clariid species form an orthogenetic series, starting with a more fusiform species and ending with an extremely elongated species: *Clarias gariepinus*, *Platyallabes tihoni*, *Platyclarias machadoi*, *Gymnallabes typus*, *Channallabes apus* and *Dolichallabes microphthalmus*. However, later studies revealed the polyphyletic nature of these genera (TEUGELS AND ADRIAENS, 2003). In Figure V.2- 6 the average degree of anguilliformity and the minimum and maximum value (ratio of the standard length and the abdominal depth) for each species used in this study is shown. Obviously, the series based on the degree of

anguilliformity does not correspond with the orthogenetic series of BOULENGER. This confirms the polyphyletic statement of TEUGELS AND ADRIAENS (2003).

As mentioned by LUNDBERG AND BASKIN (1969), caudal skeletons with a trend towards loss and fusion of hypurals are considered to be more advanced. Among the different species examined, different patterns of fusion occur. One could expect that with an increasing degree of anguilliformity, the degree of hypural fusion would increase as well, as this is frequently the case in other elongate species (see below) (Fig. V.2- 7) (SMITH AND CASTLE, 1972; GAGO, 1998). Nevertheless, no relation with degree of anguilliformity appears to exist in clariids. However, the degree of hypural fusions seems to be related to the confluence of the unpaired fins. Focussing the caudal skeleton of the Clariidae, different hypural fusion patterns can be observed: *Clarias gariepinus* is a fusiform representative of the Clariidae and the hypurals in the caudal skeleton of this species are distinct elements; *Platyclarias machadoi* has a dorso-ventrally flattened and elongate body and the dorsal, anal and caudal fins are not fused; The degree of fusion between the hypurals of the caudal skeleton of *Platyclarias machadoi* appears to be variable; The body of *Platyallabes tihoni* is elongate and the unpaired fins are fused; The caudal skeleton of *Platyallabes tihoni* comprises one hypural plate, formed by fused hypurals and urostyl; The elongate clariid *Gymnallabes typus* has confluent unpaired fins and the caudal skeleton show variations in degree of fusions between parhypural element and ventral hypural plate; *Dolichallabes microphthalmus* has an elongate body, with confluent unpaired fins (DEVAERE ET AL., 2004) and the caudal skeleton shows a high degree of hypural fusions. The observed high amount of variation in fusions in the caudal skeleton of *Channallabes apus* may be an evolutionary transition towards fused hypurals. There appears to be a relation between the confluence of unpaired fins and degree of hypural fusions.

The caudal skeleton of *C. apus* reveals a high degree of intraspecific variation in hypural fusions. Analysing the patterns of fusions within the three different geographical regions, a similar morphological variation is observed, which means that the observed variation is randomly distributed among the specimens and populations. Another aspect of this research (DE SCHEPPER ET AL., IN PRESS B) (V.2) deals with variation in the shape of vertebrae. Vertebral structures also show morphological variation between the different specimens. A geometric morphometric analysis of the vertebral morphology reveals distinct groups: the northern population (Oyem) can be distinguished from the eastern (Makokou) and southern ones (Congo-Brazzaville and Franceville).

Therefore, two hypotheses can be posited. First, if all specimens from the three populations from Gabon belong to *C. apus* and thus are one species, the observed variation is intraspecific. Second, if the eastern (Makokou) and southern populations (Congo-



Brazzaville and Franceville) belong to one or more other species, it could turn out to be interspecific. Current research on the taxonomical status of these populations is in progress. Based on the results reported in this paper, the variation appears to be intraspecific.

The morphological variation can be the result of different factors. The relationship between the gender of the specimens and the morphology of the caudal skeleton could not be studied because the majority of the specimens examined were males. However, the presence of considerable variation in the caudal skeleton of males may indicate that there is no relationship between variation and gender. According to ARRATIA (1983) intraspecific variation in Trichomycteridae occurs independently of age. Even though the current study does not deal with the ontogeny of the caudal skeleton, a relationship between standard length and hypural fusion appears to be absent in these clariids, which confirms the observations in trichomycterids.

According to GOSLINE (1997) fusion of hypurals occurs in both slow and fast swimmers. Therefore, it does not seem possible to generalize the functional significance of the caudal skeleton in clariids. All species studied have an elongated, rod-like epural, which articulates distally with caudal fin-rays and is supported at the base by the neural arch of the compound centrum. The unpaired fins of more eel-like clariids tend to be confluent. Therefore, the presence of an epural can be considered a functional advantage to support fin-rays at the transition from the dorsal to the caudal fin. Some representatives of the Siluriformes (Trichomycteridae) show intraspecific variation in the shape of the epural (ARRATIA, 1983). All studied clariids, as well as representatives of the Heteropneustidae (Fig. V.2- 5) appear to have a similar (elongated and rod-like) epural.

Shape and size of the neural arch of the compound centrum of the Clariidae is highly variable. One common feature can be observed: the neural arch of the compound centrum is dorsally open and supports the epural. Furthermore, both halves of the neural arch may be of equal size or one half can be reduced. This character thus has little systematic value.

The presence of two neural and/or haemal spines on the second preural centrum has been observed in several clariid species (*Dolichallabes microphthalmus*, *Gymnallabes typus*, *Channallabes apus*). CHANET AND WAGEMANS (1997) note that this feature has been found in Pleuronectinae, Gadidae, Samaridae, Soleidae, Bothidae, Rhombosoleinae, Cynoglossidae and Scopthalmidae. A developmental study of the turbot (*Scophthalmus maximus*) reveals that the multiple occurrences of these neural and haemal spines are the result of the fusion of the second and the third preural centrum. It is possible that in clariids the same developmental pattern occurs. However, this hypothesis has to be

confirmed by ontogenetic studies on the caudal skeleton of Clariidae. FUJITA (1992) described the ontogeny of the caudal skeleton of *Clarias batrachus*, although deformities and/or variation were not included.

According to LUNDBERG AND BASKIN (1969) all species with weak or undeveloped hypurapophyses tend toward an anguilliform type of locomotion. As mentioned above, Clariidae do not have hypurapophyses. Due to the fact that all species used in this study have a pronounced elongate body, strict anguilliform locomotion can be expected. Even though *Clarias gariepinus* does not have a strictly elongate body shape, the applied type of locomotion is presumably a combination of both anguilliform and subcarangiform types of locomotion. The results of this study thus confirm the statement proposed by LUNDBERG AND BASKIN (1969).

## ACKNOWLEDGMENTS

---

Special thanks to M Stiasny, C Hopkins, JD Mbega and the IRAF (Gabon) for assistance during sampling. Thanks to J. Okouyi (M'Passa, Makokou) for his assistance with taking pitfall traps. Research was financed by the BOF of the Ghent University (project 01104299 and 01103401) and the FWO (project G.0388.00).

### V.3 CAUDAL MYOLOGY OF *CHANNALLABES APUS*



# INTERSPECIFIC VARIATION IN THE MORPHOLOGY OF THE CAUDAL FIN MUSCULATURE IN AFRICAN CLARIIDS: A CASE IN A FUSIFORM AND AN ELONGATE REPRESENTATIVE

---

De Schepper N, Adriaens D

## ABSTRACT

---

Body elongation within the catfish family Clariidae appears to have arisen independently at least four times, and together with body elongation the median fins seem to have become confluent. The caudal skeleton each time seems to be reduced to some degree as well. Consequently, we hypothesize that to some degree reduction in the caudal fin musculature may occur in these elongate species. The caudal fin musculature of the fusiform *Clarias gariepinus* highly resembles that of generalized teleosts except for the proximalis, which is absent. The muscles of the caudal fin of *Channallabes apus* are reduced with respect to those found in *Clarias gariepinus* and other generalized teleosts. Reductions are found in the size of the interradians, absence of posterior carinalis muscles and the origin of the flexor dorsalis and flexor ventralis in particular.

## INTRODUCTION

---

Clariidae belong to the teleostean order Siluriformes (Ostariophysi) and comprises fifteen genera of which 12 are endemic to Africa and two endemic to Asia (SABAJ ET AL., 2006). A total of 93 species are presently recognized (SABAJ ET AL., 2006). The genera *Clarias* and *Heterobranchus*, being fusiform clariid representatives, occur widespread in Africa, whereas the elongate representatives, *Channallabes*, *Gymnallabes*, *Dolichallabes*, *Platyallabes*, and *Platyclarias* are found in the swamps of the Western and Central African rain forests (CABUY ET AL., 1999; DEVAERE ET AL., 2001).

The latter African clariid group is of special interest and unique among teleosts because of the evolutionary transformation from fusiform to elongate at the species level (PELLEGRIN, 1927). Initially, anguilliformity was considered to have evolved gradually in a series starting with *Heterobranchus* and ending with the extreme elongate *Dolichallabes* (BOULENGER, 1908; DAVID, 1935; PELLEGRIN, 1927). According to JANSEN ET AL., (2006),

anguilliformity appears to have arisen at least four times independently, each time having a sister group relation with a fusiform *Clarias*-like ancestor.

Together with this tendency towards anguilliformity, a whole set of morphological changes have been observed, such as reduction of the pectoral and pelvic fins, hypertrophied jaw muscles, narrow skull roof and reduction in skull bones, decrease and loss of the adipose fin, reduction of the eyes and continuous unpaired fins (CABUY ET AL., 1999; DEVAERE ET AL., 2001).

In DE SCHEPPER ET AL., (2004) (V.2) the caudal skeleton of fusiform and elongate representatives of the family Clariidae has been examined and revealed the presence of different hypural fusion patterns, even at an ontraspecific level. Furthermore, these hypural fusions appear to be related to the degree of anguilliformity as the fusiform clariid representatives (e.g. *Clarias gariepinus*) have caudal skeletons with distinct elements, whereas elongated clariid representatives (e.g. *Platyclarias*, *Platyallabes*, *Gymnallabes*, *Channallabes*, *Dolichallabes*, etc.) have to some degree fused elements in the caudal skeleton (DE SCHEPPER ET AL., 2004) (V.2). The observed high amount of variation in fusions in the caudal skeleton of *Channallabes* may be an intermediate step in the evolutionary transition towards completely fused hypurals (DE SCHEPPER ET AL., 2004) (V.2).

As together with anguilliformity the median fins seem to have become confluent and the caudal skeleton has become reduced to some degree (DE SCHEPPER ET AL., 2004) (V.2), we hypothesize that at least some aspects of the caudal fin musculature might be reduced.

For a comparison we used two morphotypes, with respect to the degree of body elongation. *Clarias gariepinus* was chosen as the fusiform morphotype with distinct median fins and *Channallabes apus* being the elongate morphotype with confluent median fins.

## MATERIAL AND METHODS

---

Three specimens of *Channallabes apus*, with a total length of 138, 186 and 204 mm, were examined as elongate representatives of the Clariidae. The caudal skeleton of this species has been extensively examined and described (DE SCHEPPER ET AL., 2004) (V.2). *Clarias gariepinus* (total length 165 mm and 250 mm), was chosen because of its fusiform body shape and its close phylogenetic relationship with the elongate *Channallabes apus* (DEVAERE ET AL., 2007A). These specimens were obtained from the laboratory of Aquatic Ecology (KU Leuven). The specimens used in this study are listed in Table III.1- 2. For a detailed description of the clearing and staining protocol and visualization see III.2.2 and III.2.5.

## RESULTS

---

### MYOLOGY OF CAUDAL FIN

The muscles of the caudal fin are covered by the epaxial and hypaxial muscles, which insert tendinously onto the caudal fin rays (Fig. V.3- 1A). No interspecific variation between *Clarias gariepinus* and *Channallabes apus* in the caudal epaxial and hypaxial muscles are observed.

The supra- and infracarinalis posterior are present in *C. gariepinus* (Fig. V.3- 1A). These muscles originate from the last few pterygiophores of the dorsal and anal fin respectively. The supra- and infracarinalis posterior insert onto dorsal (7-8) and ventral (4) caudal rays, respectively. The posterior carinalis muscles are absent in *C. apus*.

The interradiialis muscles are present in *C. gariepinus* and *C. apus* between the successive caudal fin rays (Fig. V.3- 1B, C). In *C. gariepinus* this muscle is more elaborate as it inserts onto more caudal fin rays. The muscle fibres between the fin rays of the upper lob are antero-ventrally directed, whereas those between the fin rays of the lower lob are antero-dorsally directed.

The hypochordal longitudinalis of *C. gariepinus* and *C. apus* originates from the antero-dorsal border of the second hypural and ventral hypural plate respectively (Fig. V.3- 1B, C). In *C. gariepinus* the posterior tendon inserts tendinously on two dorsal caudal fin rays. In *C. apus* the hypochordal longitudinalis is larger, compared to that in *C. gariepinus*. It inserts tendinously onto four dorsal caudal fin rays. The fibres are postero-dorsally directed.

The flexor dorsalis superior is present in *C. gariepinus* and *C. apus* and is situated dorsal to the flexor dorsalis (Fig. V.3- 1B, C). The fibres of the flexor dorsalis superior of *C. gariepinus* are muscoulously attached to the lateral surface of the neural spines of the second and third preural vertebrae, the epural and the dorso-lateral border of the urostyl. The muscle inserts tendinously onto four dorsal caudal fin rays. In *C. apus* the flexor dorsalis superior inserts onto the epural and the dorso-lateral border of the urostyl, and the second preural centrum. No fibres are attached to neural spine of the third preural vertebra as in *C. gariepinus*. In *C. apus* the insertion site is restricted to one, the dorsal most caudal fin ray.

The flexor dorsalis of *C. gariepinus* is caudally directed and is attached to the lateral surface of the second and third preural vertebra, the urostyl and the lateral surface of the fourth and fifth hypural (Fig. V.3- 1B, C). In *C. apus* the attachments site does not

include the second or third preural vertebra. Fibers originate from the urostyle and dorsal hypural plate. The muscle of both species inserts tendinously on the caudal fin rays.

The fibres of the flexor ventralis are caudally directed. In *C. gariiepinus* the muscle originates from the lateral surface of the second and third preural vertebrae, the parhypural and first and second hypurals (Fig. V.3- 1B, C). In *C. apus* the origin includes ventral hypurals (or plate) and parhypural. No fibres are attached to the second or third preural vertebrae as in *C. gariiepinus*. In both species it inserts tendinously on the caudal fin rays.

The flexor ventralis inferior of *C. gariiepinus* is attached to the lateral surface of the haemal spine of the second preural vertebra and the ventral border of the parhypural (Fig. V.3- 1B, C). This muscle inserts tendinously on one ventral caudal fin ray. In *C. apus* the muscle also originates from the haemal spine of the second preural vertebra and the ventral border of the parhypural. The caudally directed fibres insert tendinously on the most ventral caudal fin ray.

## DISCUSSION

---

NURSALL (1963) noted a gradual evolution towards a increasing complexity of the caudal fin musculature in a phylogenetic sequence based on *Polypterus*, *Amia*, *Carassius* and *Scomberomorus*. The caudal fin musculature of teleosts is complex and generally includes interradians, flexor dorsalis, flexor ventralis, hypochordal longitudinalis, proximalis and (not in all teleosts) flexor dorsalis superior, flexor ventralis inferior and flexor ventralis externus (NURSALL, 1963; WINTERBOTTOM, 1974), allowing a precise control of tail movements (LAUDER, 2000; LAUDER AND DRUCKER, 2004).

The interradians in teleosts span the middle caudal fin rays (WINTERBOTTOM, 1974), which is similar in *Clarias gariiepinus* and *Channallabes apus*. Though fewer caudal fin rays are inserted by fibers in *C. apus*, which is of course associated with the lower number of caudal fin rays present in this species (DE SCHEPPER ET AL., 2004) (V.2). The presence of interradians in both clariid species may indicate that these clariids can still move the caudal fin rays in a vertical plane.

In teleosts, the supra- and infracarinalis posterior usually connect the last basal pterygiophore of the dorsal or anal fin, respectively, to elements of the caudal fin (NURSALL, 1963; WINTERBOTTOM, 1974). This is found in *C. gariiepinus* as well. In *C. apus* on the other hand, the supra- and infracarinalis posterior muscles are absent. The confluence of the dorsal, anal and caudal fins may explain the absence of these muscle, as the supra- and infracarinalis posterior interconnect the usually distinct dorsal and respectively the



anal fins to the caudal fin. This hypothesis seems to be supported by the fact that in Anguilliformes (IV.4.4) and Mastacembelidae (VI.1) the absence of the supra- and infracarinalis posterior co-occurs with the confluence of unpaired fins.

In teleosts the flexor dorsalis usually runs from the last few neural spines and centra and the upper hypurals to the dorsal caudal fin rays in teleosts (WINTERBOTTOM, 1974), and the flexor ventralis usually connects the lateral surfaces of the haemal spines and arches of the last few vertebrae, parhypural and lower hypurals to the lateral bases of the ventral caudal fin rays (WINTERBOTTOM, 1974). As in teleosts, the last few vertebrae (up to the third preural) are included in the origin of the flexors in *C. gariepinus*, whereas in *C. apus* the origins of the flexors are reduced to the caudal skeleton.

No differences between teleosts and both clariids are observed in the morphology of the hypochordal longitudinalis, as this passes similarly from the lower hypurals to three or four of the more dorsal fin rays in the dorsal half of the caudal fin (WINTERBOTTOM, 1974).

The flexor dorsalis superior and flexor ventralis inferior are not commonly found in teleosts, but if they are present, they appear to be found always in association with each other (WINTERBOTTOM, 1974). As both muscles are present in both clariid species (and have a similar morphology), our data seems to confirm this.

With respect to generalized teleost caudal fin musculature, both clariid species lack the flexor ventralis externus (Fig. V.3- 1B, C).

To resume, the caudal fin musculature of the fusiform *C. gariepinus* resembles that of generalized teleosts (see NURSALL, 1963; WINTERBOTTOM, 1974; LAUDER, 2000) in many aspects, except for the proximalis, which is absent. With respect to *C. gariepinus* and other teleosts (see NURSALL, 1963; WINTERBOTTOM, 1974), the caudal fin musculature of *C. apus* has become reduced. Reductions are found in the size of the interradians, absence of the posterior carinalis muscles and the origin of the flexor dorsalis and flexor ventralis in particular. But the hypochordal longitudinalis appears to be enlarged.

Two hypotheses can be posited. 1) Reductions found in the caudal fin muscles of *C. apus*, may be related to body elongation and the confluence of median fins. 2) Reductions in caudal fin muscles may be related to the hypural fusions in the caudal skeleton (DE SCHEPPER ET AL., 2004). However, at present, none of these two hypotheses can be supported or rejected. Reductions of the caudal fin muscles observed in Anguilliformes may support both hypotheses as these species are elongate, have confluent unpaired fins and show hypural fusions (IV.4.4). The mastacembelids (VI.1.2), in contrast, may reject both hypotheses as in these species almost no myological reductions in the caudal fin are

observed (except for the proximalis and carinalis muscles). Therefore, the caudal musculature of all elongate clariid species should be examined as well. Furthermore, the examination of other elongate teleosts (Notograpidae, Gymnotidae, Plotoptidae, Synbranchidae etc.) may provide an outcome to this problem.

## ACKNOWLEDGMENTS

---

We would like to thank the laboratory of Aquatic Ecology of the Katholieke Universiteit Leuven (KU Leuven) for offering specimens of *Clarias gariepinus*. Special thanks to D. Adriaens, S. Devaere and A. Herrel for collecting the samples in Gabon (1999 and 2000). Research was partially funded by the FWO (G. 0388.00).

**VI**

Anguilliformity in derived teleosts

**Acanthopterygii**



### **VI.1.1 CRANIAL MORPHOLOGY: MASTACEMBELIDAE**



---

# A CASE STUDY OF EXTREME HYPERTROPHY OF THE ADDUCTOR MANDIBULAE COMPLEX IN MASTACEMBELIDAE: ARE CRANIAL SPECIALIZATIONS RELATED TO POWERFUL BITING?

---

De Schepper N, Adriaens D

## ABSTRACT

---

Within the Mastacembelidae, a remarkable evolution in one of the components of the cranial systems can be observed: extremely large jaw adductors have arisen in the more derived species (e.g. *Mastacembelus brichardi*). The question arises what the implications are of such hypertrophied jaw muscles on the morphology of the cranial system. Therefore, the morphology of the jaw apparatus in a closely related species *Mastacembelus marcheii* is examined and subsequently compared. Jaw muscle enlargement in *M. brichardi* mainly occurs in the A1 and A2 subdivisions and does not involve an increase in complexity. The size of the A3 may be constrained. Space for the expanded jaw muscle may be provided by the reduction of the eyes and the infraorbital bones. The neurocranium, suspensorium and infraorbital bones are reduced. Based on the jaw muscle size and high coronoid process, a stronger bit force can be expected.

## INTRODUCTION

---

Mastacembelidae are regarded as highly advanced synbranchiform fishes, with a slender, eel-like body, no pelvic fins, confluent unpaired fins, a peculiar rostral appendage and a series of separate spines in front of the soft dorsal fin (TRAVERS, 1984A, B; NELSON, 1994; VREVEN, 2005). Within this family, a remarkable evolution in one of the components of the cranial systems can be observed: extremely large jaw adductors have arisen in the more derived species (lineage O - S in figure VI.1.1- 1; TRAVERS, 1984B). One of these species is the African *Mastacembelus brichardi* (Poll, 1958) (lineage P in figure VI.1.1- 1), exhibiting some anatomical peculiarities. First, it is a cryptophthalmic species, with small eyes, deeply embedded in the head and covered by external integument and muscles (POLL, 1973). A second feature of special interest is the mouth closing muscles, which are hypertrophied in larger specimens (TRAVERS, 1984A, B). These muscles, described by TRAVERS

(1984A), are externally visible as bulging structures, causing the lateral profile of the head to have a sigmoid shape.

The question arises what the implications are of such hypertrophied jaw muscles on the morphology of the cranial system. Therefore, the morphology of the jaw apparatus in a closely related African mastacembelid species *Mastacembelus marcheii* (lineage L in figure VI.1.1- 1), lacking the hypertrophy is studied in order to screen for possible implications of such hypertrophied jaw muscles on the morphology of the cranial system. Secondly, the myological and osteological data are compared with those of a more basal, mastacembelid species *Mastacembelus mastacembelus*, as described by TRAVERS (1984A, B).

## MATERIAL AND METHODS

---

A total of 10 alcohol preserved (70%) specimens were examined. Three specimens of *Mastacembelus marcheii* Sauvage, 1879, (RG-98-29-P-6-9), and three specimens of *Mastacembelus brichardi* (Poll, 1958) (RG-96-35-P-1-29), were obtained and used from the Royal Museum for Central Africa. Four specimens of *Mastacembelus mastacembelus* (Banks and Solander, 1794), were examined and obtained from the Iranian Natural History Museum (IR-068; IR-012; IR-110; IR-003). A list of the specimens used in this study is given in Table III.1- 3. The specimens were dissected and cleared and stained. For details of the applied protocols I refer to III.2.2.

The mastacembelids species were chosen based on the different degree of jaw muscle hypertrophy, availability of morphological information and availability of museum specimens. *M. marcheii* is chosen because of its close phylogenetic relationship with *M. brichardi* (Fig. VI.1.1- 1). As the myology of this species (synonyms: *M. marchii* and *M. sclateri*) is not described by TRAVERS (1984A, B) a detailed myological description and illustration is provided here. *M. mastacembelus* and *M. brichardi* are described into detail by TRAVERS (1984A, B) and belongs to the most basal lineage.

For detailed osteological descriptions of the cranial structures, see TRAVERS (1984A).

## RESULTS

---

### MYOLOGY OF THE HEAD OF *MASTACEMBELUS MARCHEII*

The adductor mandibulae complex comprise four clearly separated subdivisions (A1, A2, A3, A $\omega$ ). The A1 subdivision is situated ventral to the A2 (Fig. VI.1.1- 3A). Its origin



includes the dorso-lateral preopercular surface and anterior edge of the preopercular horizontal arm, ventro-lateral surface of the hyomandibula, symplecticum, quadrate and metapterygoid and the caudo-lateral surface of the angulo-articular. It has both a tendinous and muscular insertion. A long and broad tendon (T A1) runs anteriorly from the lateral surface of the A1 and inserts onto the dorsal surface of the premaxilla and ventro-lateral margin of the maxilla. Some fibres of the antero-medial surface of the A1 merge with the antero-lateral surface of the anterior tendon of the A2. The fibres of the A1, dorsal to its tendon, are predominantly rostr-caudally directed, whereas the ventral ones are shorter and antero-dorsally directed.

The second superficial subdivision of the adductor mandibulae complex is situated dorsal to the A1 subdivision and lateral to the inner A3 subdivision (Fig. VI.1.1- 2A, B). Its antero-dorsal margin curves around the caudo-ventral margin of the orbit. This subdivision comprises a dorsal ( $A2\beta$ ) and ventral ( $A2\alpha$ ) part which only can be distinguished by their separate anterior tendons. The tendon of  $A2\beta$  is the largest and broadest one and inserts onto the postero-dorsal edge of the coronoid process, while the tendon of  $A2\alpha$  is narrow and merges antero-medially with the tendon of the  $A\omega$  subdivision. The medial fibers of the A2 originate ventrally from the lateral surface of the metapterygoid, symplecticum, hyomandibula and vertical arm of the preopercle (just above the origin of A1 and beneath the origin of A3 and LAP).

The third and deeper subdivision of the adductor mandibulae complex, the A3, is separated from the superficial subdivisions by the levator arcus palatini (Fig. VI.1.1- 2B). A thin sheet of connective tissue is situated between the A3 and the latter muscle. The fibers of the A3 converge into the anterior tendon resulting in a large, fanshaped muscle. This tendon T A3 is connected to the posterior end of the unusually large (compared to other teleosts) coronomeckelian, which is subsequently connected to the medial side of the meckelian fossa. The A3 originates dorsally from the lateral surface of the frontal descending lamina, the sphenotic, pterosphonoid and dorso-lateral surface of the prootic and originates ventrally from the dorso-lateral surface of the endopterygoid, metapterygoid and hyomandibula. No fibers originate from the quadrate.

The  $A\omega$  is the anterior and smallest subdivision of the adductor mandibulae complex (Fig. VI.1.1- 2B). The fibers insert on the ventro-medial surface of the dentary and the medial surface of the retro-articular and anguloarticular. The fibers converge into a medial tendon which originates from the antero-medial margin of the quadrate.

The levator arcus palatini is situated between the A2 and A3 of the adductor mandibulae complex (Fig. VI.1.1- 2B). The fibers are organized into a thin sheet and originate from a narrow area on the dorso-lateral surface of the frontal, pterotic and

sphenotic process. The fibers are caudo-ventrally directed and insert onto the dorso-lateral surface of the symplectic and ventro-lateral surface of the metapterygoid and hyomandibula. The posterior fibers merge dorsally with the anterior fibers of the dilatator operculi.

The adductor arcus palatini originates mainly from the lateral surface of the parasphenoid but also from the ventro-lateral surface of the prootic and basisphenoid (Fig. VI.1.1- 2B, C). This muscle inserts tendinously onto the caudo-medial surface endopterygoid, and musculously onto the medial surface of the metapterygoid, dorso-medial surface of the endo- and ectopterygoid and dorsal surface of the palatine. The muscle stretches far anteriorly and is flattened in the suborbital region.

The adductor hyomandibula originates from the latero-ventral surface of the parasphenoid and anterior part of the prootic, up to the level of the small otic bullae. The fibers are latero-ventrally directed and insert onto the ventro-medial surface of the hyomandibula (Fig. VI.1.1- 2C). The anterior fibers extend below the posterior part of the adductor arcus palatini, inserting onto the dorso-medial surface of the symplectic.

The dilatator operculi is partially covered by the vertical preopercular arm and by the postero-dorsal edge of the A2 subdivision (Fig. VI.1.1- 2B). Its origin includes the dorso-lateral surface of the pterotic and the ventro-caudal edge of the sphenotic. The fibers run caudo-ventrally and merge into a short tendon, which inserts onto the dorsal surface of the dorsal opercular process.

The adductor operculi is a small triangular muscle, with its apex lying antero-dorsally (Fig. VI.1.1- 2B). In lateral view, the adductor operculi is covered by the levator operculi and the opercle. It originates by means of a tendon from the dorso-lateral surface of the exoccipitals, just below the posterior suspensorial articulatory facet. The fibers diverge ventro-caudally and insert onto the medial surface of the opercle, reaching its ventral margin. The posterior fibers merge with the antero-dorsal fibers of the hyohyoidei adductores.

The levator operculi is a large, superficial, opercular muscle. It originates from the caudo-lateral surface of the pterotic, just above the posterior suspensorial articulatory facet (Fig. VI.1.1- 2A). The fibers radiate caudo-ventrally and insert onto the dorso-lateral surface of the opercle. The ventral fibers insert onto the narrow dorsal edge of the opercular ridge, which is situated along the lateral surface of the opercle and which separates the levator operculi from the intraoperculi.

The intraoperculi originates from the postero-lateral edge of the preopercle (Fig. VI.1.1- 2A, B). The fibers run caudo-ventrally and insert onto the antero-lateral surface of the opercle, ventral to the opercular ridge.

TRAVERS (1984A) correctly described the hyohyoidei adductores as large, expanded muscles with no interspecific variation among the mastacembelids. But no hyohyoidei abductores or inferior are reported or described. In all species examined, the hyohyoidei adductores and hyohyoidei abductores are found and morphologically similar, whereas no hyohyoidei inferior is found in any of the examined species. The hyohyoidei adductores form a sheet of fibers between the successive branchiostegal rays (Fig. VI.1.1- 2, 3). The lateral fibers extend dorsally, above the posterior branchiostegal ray to connect loosely to the medial surface of the opercle. The dorso-medial fibers of this extended sheet attach musculously to the epaxials, whereas the caudal fibers attach to the ventral surface of the post-temporal tubules, lateral surface of the supracleithrum and dorso-lateral surface of the cleithrum. The hyohyoidei abductores comprise a left and right bundle, arising tendinously from the anterior ceratohyal and inserting musculously onto the medial surface of the first branchiostegal rays of the opposite sides (Fig. VI.1.1- 2, 3). Both bundles cross each other in the midline, the right bundle overlaying the left one.

The protractor hyoidei halves insert by a strong anterior tendon onto the medial surface of the dentaries, near the symphysis (Fig. VI.1.1- 2, 3). The left and right bundles, arising respectively from the lateral surfaces of the left and right anterior ceratohyals, fuse in the midline anterior to the hyoid arch.

The intermandibularis stretches transversally between the two halves of the lower jaw, just in front of the insertion site of the protractor hyoidei (Fig. VI.1.1- 2B).

The sternohyoideus originates from the ventro-lateral surfaces of both cleithra. Both halves of the muscle are fused in the midline (Fig. VI.1.1- 3). This muscle comprises two myocommata, the second one, separating it from the hypaxials. The fibers pass anteriorly to insert tendinously onto the lateral sides of the urohyal.

#### COMPARISON OF THE CRANIAL MYOLOGY WITH *MASTACEMBELUS BRICHARDI* AND *MASTACEMBELUS MASTACEMBELUS*

The following section focuses on those muscles that differ among the three species examined. Interspecific variation in the morphology of the adductor mandibulae complex is particularly noticeable in the A1 and A2 subdivisions and to some degree in the levator and adductor arcus palatini.

1) The size of the adductor mandibulae complex of *M. marcheii* is smaller compared to that of *M. mastacembelus* and *M. brichardi* (Fig. VI.1.1- 5). The A1 and A2 in *M. brichardi* are extremely enlarged and externally visible as bulging structures (Fig. VI.1.1- 4A, 5C). The A2 in *M. brichardi* is dorsally and caudally expanded, originating from the postorbital dorsal surface of the frontals up to the midline and the entire dorsal surface of

the parietals (Fig. VI.1.1- 4A). The dorso-caudal fibers are aponeurotically connected to the epaxials. Even though the jaw muscles of *M. mastacembelus* are small compared to those of *M. brichardi*, they are enlarged with respect to the majority of Asian mastacembeloids (TRAVERS, 1984A). In contrast, in both *M. mastacembelus* and *M. brichardi*, the A3 subdivision is smaller compared to that in *M. marcheii*.

2) The origin of the levator arcus palatini is anteriorly enlarged in *M. brichardi*. The anterior fibers reach the small orbits, and cover the reduced eyes (Fig. VI.1.1- 4B).

3) The adductor arcus palatini extends more anteriorly, towards the anterior border of the orbit in *M. marcheii*.

## DISCUSSION

---

### HYPERTROPHY OF THE JAW MUSCLES

The adductor mandibulae complex has been hypertrophied in several species of the Mastacembelidae and has enlarged to extreme proportions in *M. brachyrhinus*, *M. brichardi*, *M. crassus* and *M. aviceps* (TRAVERS, 1984A). Such hypertrophy, however, has been noted in other teleosts lineages as well, such as Anguilliformes (IV.4.4), Chaudhuriidae (BRITZ AND KOTTELAT, 2003), Synbranchidae (LIEM, 1980) and Clariidae (CABUY ET AL., 1999; DEVAERE ET AL., 2001).

### HYPERTROPHY OF THE JAW MUSCLES AND ASSOCIATED CRANIAL MODIFICATIONS

*M. brichardi*, *M. crassus*, *M. latens* and *M. aviceps* are micro- or cryptophthalmic and have hypertrophied jaw muscles. Furthermore these species share the following morphological traits (for details see TRAVERS, 1984A, B): reduced neurocrania including the loss and reduction of many neurocranial bones, more or less ‘tubular’ shape of the postorbital region, reduced suspensorium (endopterygoid), reduced cranial lateral line sensory pores and reduced infraorbital elements (TRAVERS, 1984A). Even though the eyes of *M. aviceps* are small, they are larger compared to the other species with enlarged jaw muscles (VREVEN, 2001). *M. brichardi* is exceptional with respect to the other species in having hypertrophied sensory canal pores (edges of the pores are inflated forming a ring around the pore opening) on the head and pectoral region (VREVEN, 2001). The cranial lateral line system is hard or not discernable in *M. crassus*, *M. latens* and *M. aviceps*. These morphological may however also be the result of cranial miniaturization (TRAVERS, 1984A, B).

## IMPACT OF HYPERTROPHIED JAW MUSCLES

The following comparison focuses on the impact of jaw muscle hypertrophy in mastacembelids, with muscle *M. brichardi* and *M. marcheii* as representatives of the group with enlarged and non-enlarged jaw muscles, respectively. Links with other teleosts are made where relevant.

The hypertrophy of the mandibular adductor muscle of *M. brichardi* does not involve an increase in complexity, as it closely resembles that of *M. marcheii* and consistently comprises three subdivisions in all species. In some representatives of Synbranchidae (LIEM, 1980), Clariidae (DEVAERE ET AL., 2001) and Anguilliformes (DE SCHEPPER ET AL., 2007) (IV.3), the hypertrophy of the jaw muscles is also substantial and not combined with increasing complexity either.

The impact of jaw muscle enlargement is more notably at the level of the eye and infraorbital elements. The eyes and the infraorbital bones are reduced, the latter in amount, size and degree of ossification, thus providing space for the expanded muscle. The remaining infraorbital bones (2 in *M. brichardi*; 0 in *M. aviceps*) are small, tubular and weakly ossified. In elongated clariid catfish and some anguilliforms with hypertrophied jaw muscles, the enlargement of the adductor mandibulae complex is similarly related to the eye reduction and reduction and displacement of the infraorbitals and suprapraeopercular bones (CABUY ET AL., 1999; DEVAERE ET AL., 2001; IV.1; IV.3).

It has been noted that jaw muscle hypertrophy in mastacembelids is the result of the expansion of the A1 and A2. Space constraints on the deeper A3 could explain its restricted enlargement. In *Anguilla anguilla* the enlargement of the jaw muscles in the broad-headed phenotype also occurs in the A1 and A2, whereas the A3 is constrained (IV.4.2).

## STRONGER BITE POTENTIAL

Why different species of mastacembelids have developed such large jaw muscles in the course of evolution is unclear. The most obvious possibility is that jaw muscle hypertrophy has evolved as an adaptation for durophagy, enabling these mastacembelids to crush hard prey by producing large bite forces. Indeed, data of preferred prey items seems to confirm this statement. Analysis of stomach contents revealed that *M. brichardi* feeds on snails (VREVEN, 2001), whereas *M. marcheii* predominantly feeds on aquatic insects (VREVEN, 2001). Of course powerful biting implies a substantial increase in mechanical

loading on certain skeletal elements composing the bite apparatus: lower jaw and upper jaw.

Some features of the lower jaw of *M. mastacembelus* and *M. brichardi* indicate a relatively stronger bite potential compared with that of *M. marcheii*. *M. mastacembelus* and *M. brichardi* have a tall and narrow coronoid process. The coronoid process of *M. marcheii* shows the opposite condition: low and broad. The height of the coronoid process may indicate a stronger bite as a higher coronoid process implicates a longer input force lever (LIEM, 1980; HERREL ET AL., 2002). Consequently, both *M. mastacembelus* and *M. brichardi* may be able to generate a stronger bite. This has likewise been demonstrated for *C. apus* and *G. typus*, clariid species of which the coronoid processes are larger and the jaw muscles are hypertrophied. The clariid species *C. gariepinus*, with small jaw muscles has a small coronoid process (CABUY ET AL., 1999; HERREL ET AL., 2002).

Mastacembelidae have a non-protrusible upper jaw, which is exceptional among percomorphs as jaw protrusibility is characteristic for most neoteleosts (TRAVERS, 1984B). Likewise, the premaxillo-ethmovomerine complex found in Anguilliformes, limits the mobility of the bordering upper jaw elements and assist in an excellent grasping and holding ability in predators (TESCH, 2003). GOSLINE (1980) noted in teleosts that also in other predacious forms requirements of a strong bite have led to secondary loss of upper jaw movements.

## EYE REDUCTION

The impact of the jaw muscles on the development of the eye in *M. brichardi* is apparently substantial as the eyes are reduced and even covered by the jaw muscles (POLL, 1973). The other species have also a decreased eye size, though to the lesser extent as in *M. brichardi*. The question that consequently can be raised is at what cost the eye reduction has occurred, as this will surely influence the visual capacities.

Mastacembelidae in general have relatively small eyes (POLL, 1973). As a compensation, the olfactory sensory system is well developed and extended by a mobile (and tactile) rostral tentacle, which bears two tubulated anterior nostrils (POLL, 1973; BENJAMIN AND SANDHU, 1990; VREVEN, 2005). During evolution this highly specialized sensory system (POLL, 1973) may have allowed the eyes to become reduced even more as it may have overruled the importance of visual observation, especially considering their occurrence in dark spaces underneath and between the rocks in the rapids. Visual capacities are assumed to be reduced in the other mastacembelid species as well (*M. crassus*, *M. latens* and *M. aviceps*) as the eyes would mainly be used to detect light from

which they flee (POLL, 1973; VREVEN, 2001). Eye reduction is often regarded as an adaptation to fossorial or cavernicole habits (GANS, 1973, 1975; WITHERS, 1981; LEE, 1998), and appears to be true for most mastacembelids (Vreven, 2001) as well.

## **ACKNOWLEDGMENTS**

---

We would like to thank the Royal Museum of Central Africa in Tervuren (Belgium) and Natural History Museum (Iran) for offering museum specimens. Research was partially funded by the FWO (G. 0388.00).





## **VI.1.2 CAUDAL MORPHOLOGY: MASTACEMBELIDAE**



---

# A CASE STUDY OF THE OSTEOLOGY AND MYOLOGY OF THE CAUDAL FIN IN MASTACEMBELIDAE: ARE CONFLUENT MEDIAN FINS RELATED TO MYOLOGICAL REDUCTIONS IN THE CAUDAL FIN?

---

De Schepper N, Adriaens D

## ABSTRACT

---

This study has focused on the morphology of the caudal fin of *Mastacembelus mastacembelus*, with distinct median fins, and *M. marcheii* and *M. brichardi* which have confluent median fins. The confluent unpaired fins appear to be associated with the reduced number of hypurals and a lower number of caudal fin rays. We hypothesize that reductions or modifications at the level of the caudal fin musculature may co-occur with reductions in the caudal skeleton, confluence of the median fins and lower number of caudal fin rays. The results indicate, however that no such relation is present in the examined mastacembelids. The caudal myology of *M. mastacembelus* resembles in origin and insertion to that of generalized teleosts. Compared to *M. mastacembelus*, *M. marcheii* and *M. brichardi* solely lack the carinalis posterior muscles, which is likely to be related to the confluent unpaired fins.

## INTRODUCTION

---

Mastacembelidae are a group of freshwater teleost fish and regarded as highly advanced Synbranchiformes (TRAVERS, 1984A, B; NELSON, 1994). This group is characterized by an eel-like appearance, numerous vertebrae, the lack of pelvic fins, confluent unpaired fins, a narrow, tapered skull ending in a peculiar rostral appendage and a series of separate spines in front of the soft dorsal fin (TRAVERS, 1984A, B; NELSON, 1994; VREVEN, 2005).

This study focuses on the morphology of the caudal fin of *M. mastacembelus*, *M. marcheii* and *M. brichardi*. TRAVERS (1984B) recognized convergent evolutionary traits in some mastacembelid lineages, as hypural fusions forming one or two hypural plates appear to be combined with confluent median fins and a lower number of caudal fin rays. *M. marcheii* and *M. brichardi* have confluent median fins (Fig. VI.1.2- 1B, C), fused hypurals

and few caudal fin rays (TRAVERS, 1984A), whereas *M. mastacembelus* has a distinct caudal fin without hypural fusions and a higher number of caudal fin rays (TRAVERS, 1984A) (Fig. VI.1.2- 1A).

We hypothesize that reductions or modifications at the level of the caudal fin musculature may co-occur with reductions in the caudal skeleton, confluence of the median fins and lower number of caudal fin rays. Consequently, the caudal fin musculature of *M. mastacembelus* is compared with that of the African mastacembelids.

A recent taxonomical study and critical revision of features of the caudal fin, is provided by VREVEN (2001, 2005). As this study revealed some inconsistencies to what was previously described of the osteology of the caudal fin, a short comparison of the caudal fin components of these three species is made.

## MATERIAL AND METHODS

---

A total of 10 alcohol preserved (70%) specimens were examined. Three specimens of *Mastacembelus marcheii* Sauvage, 1879, (RG-98-29-P-6-9), and three specimens of *Mastacembelus brichardi* (Poll, 1958) (RG-96-35-P-1-29), were used and obtained from the Royal Museum for Central Africa (MRAC). Four specimens of *Mastacembelus mastacembelus* (Banks and Solander, 1794), were examined and obtained from the Iranian Natural History Museum (IR-068; IR-012; IR-110; IR-003). These specimens were dissected and cleared and stained. A list is provided in Table III.1- 3. A detailed description of the protocols used here is given in III.2.2.

## RESULTS

---

### MYOLOGY OF CAUDAL FIN OF *M. MASTACEMBELUS*, *M. MARCHEII*, *M. BRICHARDI*

The epaxial and hypaxial muscles, shown for *M. mastacembelus* Fig. VI.1.2- 2A) cover the caudal fin musculature. The caudal fibers of both muscles insert tendinously onto the lateral surfaces of caudal fin rays. The arrangement is the same as in both *M. marcheii* and *M. brichardi*.

The supracarinalis posterior in *M. mastacembelus* originates from the last few pterygiophores of the dorsal fin and runs caudally (Fig. VI.1.2- 2A). The posterior tendon of this muscle inserts onto two or three dorsal caudal fin rays. *M. marcheii* and *M. brichardi* lack this muscle.

The infracarinalis posterior in *M. mastacembelus* originates from the last few anal fin pterygiophores and inserts tendinously onto six or seven caudal fin rays (Fig. VI.1.2- 2A). This muscle is also absent in *M. marcheii* and *M. brichardi*.

The interradians of *M. mastacembelus* (Fig. VI.1.2- 2A), *M. marcheii* and *M. brichardi* (Fig. VI.1.2- 3) are formed by several bundles of muscle fibres which radiate dorsally and ventrally. The bundles above the midline run upwards and backwards to insert tendinously on the ventro-lateral side of dorsal caudal fin rays, while the ventral bundles run downwards and backwards, inserting on the dorso-lateral side of the ventral caudal fin rays. The dorsal bundles in *M. mastacembelus* are larger than the ventral bundles, whereas the ventral and dorsal bundles are of similar size in the African mastacembelids. The interradians insert onto 13 caudal fin rays in *M. mastacembelus*, 10 in *M. marcheii* and 7 in *M. brichardi*.

In *M. mastacembelus*, *M. marcheii* and *M. brichardi* the hypochordal longitudinalis originates partially from a narrow area on the ventro-lateral surface of the dorsal hypural plate and on the dorso-lateral surface of the ventral hypural plate (Fig. VI.1.2- 2B, 3). The muscle inserts tendinously on one dorsal caudal fin ray. The base of the muscle is broader in *M. marcheii*, compared to the other mastacembelids. In *M. mastacembelus* the inserting tendon is noticeably longer.

The flexor dorsalis superior of *M. mastacembelus* and *M. marcheii* is situated dorsal to the flexor dorsalis and originates from the lateral surface of the neural spine of the second preural centrum (Fig. VI.1.2- 2B, 3). It inserts tendinously onto the dorsalmost caudal fin ray. In *M. brichardi* the flexor dorsalis superior originates from the neural spine of the second and third preural centra.

The flexor dorsalis of *M. mastacembelus*, *M. marcheii* and *M. brichardi* originates from the lateral surface of the second and third preural centrum, the urostyle, the dorsal hypural plate and the epural (Fig. VI.1.2- 2B, 3). The fibres of the flexor dorsalis are caudally directed and insert tendinously on 8-10, 4-6 and 3-4 dorsal caudal fin rays in *M. mastacembelus*, *M. marcheii* and *M. brichardi* respectively.

In *M. mastacembelus*, *M. marcheii* and *M. brichardi* the flexor ventralis externus originates from the ventro-lateral surface of the third and second preural centra and the lateral surface of the parhypural (Fig. VI.1.2- 2B, 3). In *M. marcheii* some fibres additionally attach to the haemal arch of the third preural vertebra. The fibres are ventro-caudally directed and insert onto 4-5, 3 and 3 ventral caudal fin rays respectively.

The flexor ventralis in *M. mastacembelus*, *M. marcheii* and *M. brichardi* is similar, originating from the lateral surface of the urostyle, the parhypural and the ventral hypural plate (Fig. VI.1.2- 2B, 3). The fibres are caudo-ventrally directed and insert on 4 to 5

ventral caudal fin rays in *M. mastacembelus* and *M. marcheii* and onto 3 caudal fin rays in *M. brichardi*.

The flexor ventralis inferior in *M. mastacembelus* and *M. brichardi* originates from the haemal spine of the second preural centrum. In *M. marcheii* the flexor ventralis inferior is smaller and attaches to the lateral surface of the parhypural. It inserts tendinously on the ventralmost caudal fin ray.

## DISCUSSION

---

### OSTEOLOGY OF THE CAUDAL FIN

The caudal skeleton of the Mastacembelidae has been examined extensively by TRAVERS (1984A, B) and a detailed and critical revision of features of the caudal fin, based on an amazing high amount of specimens is provided by VREVEN (2005). For a detailed description of the caudal skeleton we consequently refer to the latter manuscripts. The present study compared the osteological features to those described by TRAVERS (1984A) and VREVEN (2005), as presented in Table (VI.1.2- 1). Our results confirm the presence of inconsistencies in Travers' work, as reported by VREVEN (2005), e.g. the amount of hypural fusions varies intraspecifically in *M. mastacembelus* as well.

Interspecific variation is not only found in the topology of the structural elements of the caudal skeleton (TRAVERS, 1984A; VREVEN, 2005), but also in the shape of the caudal fin. Even though both examined African species have confluent median fins, the caudal fin of *M. marcheii* is rather narrow and pointed, whereas broad and rounded in *M. brichardi* (Fig. VI.1.2- 2).

### CONVERGENT EVOLUTIONARY TRAITS RELATED TO ANGUILLIFORM LOCOMOTION?

TRAVERS (1984B) recognized convergent evolutionary traits in mastacembelid lineages (Oriental taxa: *Sinobdella*, *Pillaia*; African taxa) as the reduced number of hypurals (2-1) appears to be associated with confluent unpaired fins and a lower number of caudal fin rays (8-10). However, some African taxa have higher caudal fin ray counts.

Still, a similar relation between confluence of the unpaired fins, hypural fusions and reduction in number of caudal fin rays is found in the Anguilliformes studied (IV.4.4) and was observed in elongate clariid catfish (DE SCHEPPER ET AL., 2004).

GOSLINE (1997) considered the occurrence of hypural fusions to be a recurring theme in teleostean evolution. Fusions are present in species that do not exert rapid forward

movements (Anguilliformes), though also in strongly swimming fish (e.g. *Thunnus*). Therefore, no generalization concerning the functional significance of fusions seems possible (GOSLINE, 1997).

LUNDBERG AND BASKIN (1969) and GOSLINE (1997) stated that all species with weak or undeveloped hypurapophyses tend toward an anguilliform type of locomotion. None of the presently examined mastacembelid species or those mastacembelids studied by TRAVERS (1984A), which have a pronounced elongate body and indeed swim using anguilliform body undulations, have hypurapophyses, thus confirming their statement. Furthermore, an elongated body combined with the absence of a hypurapophysis is found in the elongate clariid catfish (DE SCHEPPER ET AL., 2004) (V.2) and the perciform, elongated Notograptidae (MOOI AND GILL, 2004). However, the absence of the hypurapophysis is not strictly related to species with elongate bodies (e.g. *Normanichthys crockeri*, Scorpaeniformes; YABE AND UYENO, 1996) as well as it can be present in elongate species (e.g. Anguilliformes, IV.4.4). Therefore, no generalization concerning the functional significance of hypurapophyses seems possible (GOSLINE, 1997).

#### MYOLOGY OF THE CAUDAL FIN

The caudal fin musculature of the mastacembelids (at least those examined in the present study) include interradians, flexor dorsalis, flexor ventralis, hypochordal longitudinalis, flexor dorsalis superior, flexor ventralis inferior and flexor ventralis externus. With respect to other teleosts (e.g. *Lepomis macrochirus*, WINTERBOTTOM, 1974; *Scomberomorus*, NURSALL, 1963; *Trachurus japonicus*, SUDA, 1996), the myology of the caudal fin of *M. mastacembelus* solely differs in the absence of the proximalis. But, as reported by WINTERBOTTOM (1974) this muscle has an erratic occurrence in teleosts and has presumably arisen more than once during evolution. The rest of the caudal fin musculature of *M. mastacembelus* resembles in origin and insertion to that of generalized teleosts (e.g. *Lepomis macrochirus*, WINTERBOTTOM, 1974).

#### DIFFERENCES IN MYOLOGY OF THE CAUDAL FIN RELATED TO MEDIAN FIN CONFLUENCE?

*M. mastacembelus* is characterized by a distinct caudal fin (TRAVERS, 1984A, NELSON, 1994; VREVEN, 2005), whereas the African mastacembeloids *M. marcheii* and *M. brichardi* have confluent median fins (TRAVERS, 1984A, NELSON, 1994; VREVEN, 2005). As the supra- and infracarinalis muscles are absent in the African mastacembelids, it is likely to be related to the confluence of the unpaired fins in *M. marcheii* and *M. brichardi* because these muscles

in teleosts generally originate from the last basal pterygiophore of the, usually separate, dorsal or anal fins (WINTERBOTTOM, 1974). The relation is further supported by the co-occurrence of confluent unpaired fins and reduced supra- and infracarinalis posterior muscles in Anguilliformes (IV.4.4) and elongate clariid catfish (V.3).

The origins of the other caudal fin muscles are highly similar in all examined mastacembelid species, except for the flexor ventralis inferior which originates from the parhypural in *M. marcheii*. Differences in insertion of the caudal fin muscles, more specific in the number of caudal fin rays involved, are noted, especially in *M. brichardi*. This is of course associated with the reduced number in caudal fin rays.

## ACKNOWLEDGMENTS

---

We would like to thank the Royal Museum of Central Africa in Tervuren (Belgium) and Natural History Museum (Iran) for offering museum specimens. Research was partially funded by the FWO (G. 0388.00).



## VI.2 CRANIAL MORPHOLOGY: TRICHIURIDAE



# MORPHOLOGY OF THE JAW SYSTEM IN TRICHIURIDS: TRADE-OFFS BETWEEN MOUTH CLOSING AND BITING PERFORMANCE

---

Modified from the paper published as:

De Schepper N, Van Wassenbergh S and Adriaens D submitted.

Morphology of the jaw system in trichiurids: trade-offs between mouth closing and biting performance.

Biological Journal of the Linnean Society submitted.

## ABSTRACT

---

In this study, we focus on two piscivore species of cutlassfishes (Trichiuridae) that show some degree of differences in morphology of the jaw system: *Aphanopus carbo* and *Trichiurus lepturus*. As studies dealing with myological features of *A. carbo* and *T. lepturus* are presently lacking, we first provide a detailed description of the head musculature of *A. carbo* and *T. lepturus*. Secondly, we will focus on the mechanics of the mouth closing system of these trichiurids by using biomechanical modeling. More specifically, models will allow us to: (1) describe the differences between how the lower jaw lever system works during mouth closure and during generating static bite force, (2) evaluate the effects of morphological change on the performance of both functions, (3) determine whether the configuration of each component of the lower jaw lever system is a compromise between both functions, or whether there is a partition of function (optimization for either hard biting or fast jaw closing) between the different parts of the jaw closing musculature, and (4) discuss the dynamical implications of having elongate jaws for capturing prey.

## INTRODUCTION

---

A central goal in understanding evolutionary processes associated with species radiation is the recognition of conflicts in the performance of functions with high ecological significance (BAREL, 1983). Two functions are conflicting when they require opposing biomechanical or physiological adaptations. In that case, both functions cannot be optimized in the course of evolution (STEARNS, 1992). Consequently, trade-offs are often observed in case certain components of the musculo-skeletal system have to participate in

different functions (e.g. LOSOS ET AL., 1993; BRAINERD AND SIMONS, 2000; IRSCHICK, 2002; PASI AND CARRIER, 2003; SCHONDUBE AND DEL RIO, 2003).

The head of fishes is one of the best examples of a complex and integrated system that has to accomplish several crucial biological functions (LIEM, 1980): capturing, processing and transporting prey, breathing water or air, participating in sensory perceptions, providing protection for the major sense organs and brains, and serving as a streamlined bow in locomotion. In order to survive, fish must have an architectonic configuration of the head that specifically meets the structural and dynamical needs of each of these functions.

The lower jaw lever system of predatory fishes has to cope with two important performance traits: (1) quickly closing the mouth at the moment the prey is entering the mouth aperture or when the prey can be caught somewhere between the oral teeth and (2) producing bite force in order to immobilize, crush, or tear pieces out prey. However, previous modelling studies have shown that fast mouth closing and forceful biting have different morphological demands (WESTNEAT, 1994; TURINGAN ET AL., 1995; WESTNEAT, 2004; COLLAR ET AL., 2005; KAMMERER ET AL., 2005; VAN WASSENBERGH ET AL., 2005). As a result, it has been observed that fish hunting for evasive prey generally have a lever system of the lower jaw that appears to favour rapid closure of the mouth, while the jaws of fish preying on hard items are generally built to generate high bite forces at the cost of the speed at which the jaws can be moved (WESTNEAT, 1994; TURINGAN ET AL., 1995; WESTNEAT, 2004; COLLAR ET AL., 2005; KAMMERER ET AL., 2005).

From a biomechanical point of view, an intriguing situation occurs when prey capture performance depends equally on the maximal speed at which a fish can snap its jaws and on the maximal force its oral teeth can be pressed against or into the prey. This situation occurs in long-jawed fishes that have large, sharp teeth on the mandible, like for example most Lepisosteidae, Bellonidae, Sphyrnaeidae or Trichiuridae. These fishes predominantly rely on piercing of the teeth into agile prey (SIBBING AND NAGELKERKE, 2001). How does the jaw system in these fishes deal with the trade-off between speed and force when it needs both to capture prey efficiently?

In this study, we focus on two piscivore species of cutlassfishes (Trichiuridae) that show some degree of differences in morphology of the jaw system: *Aphanopus carbo* and *Trichiurus lepturus*. As studies dealing with myological features of *A. carbo* and *T. lepturus* are presently lacking, we first provide a detailed description of the head musculature of *A. carbo* and *T. lepturus*. Secondly, we will focus on the mechanics of the mouth closing system of these trichiurids by using biomechanical modeling. More specifically, models will allow us to: (1) describe the differences between how the lower jaw lever system works

during mouth closure and when generating static bite force, (2) evaluate the effects of morphological change on the performance of both functions, (3) determine whether the configuration of each component of the lower jaw lever system is a compromise between both functions, or whether there is a partition of function (optimization for either hard biting or fast jaw closing) between the different parts of the jaw closing musculature (FRIEL AND WAINWRIGHT, 1999), and (4) discuss the dynamical implications of having elongate jaws for capturing prey.

## MATERIALS AND METHODS

---

### SPECIES

*Aphanopus carbo* Lowe 1839 is a remarkably elongate and laterally compressed species, found in the North Atlantic Ocean (ANON, 2000; NAKAMURA AND PARIN, 1993). This species is a benthopelagic predator but migrates to midwater during the night to feed. Their predatory life style, especially the fact that they span considerable depth differences when hunting, is even reflected in the modified and reinforced gas bladder (HOWE, 1979; BONE, 1971). The diet mainly comprises crustaceans and cephalopods and fishes (mostly macrourids, morids, alepocephalids, *Micromesistius*, *Argentina*) (SWAN ET AL., 2003). Larger specimens tend to feed on larger prey (fish and cephalopods) and less on crustaceans (COSTA ET AL., 2000).

*Trichiurus lepturus* Linnaeus 1758, a cosmopolitan coastal species, is distributed throughout tropical and temperate waters between 60°N and 45°S (MARTINS AND HAIMOVICI, 1997; KWOK AND NI, 2000; CHENG ET AL., 2001). These benthopelagic, elongated fish are found in shallow coastal waters over muddy-sand bottoms of the continental shelf. They are known to feed near the surface during daytime and migrate to the bottom during the night (CHENG ET AL., 2001). *T. lepturus* are predators, mainly feeding on large sized pelagic and benthic fish (90.9%), crustaceans (10.9%) and cephalopods (2.5%) (WOJCIECHOWSKI, 1972; MARTINS AND HAIMOVICI, 1997; CHIOU ET AL., 2006). Food composition differences changes with size: small specimens predominantly feed on crustaceans, while large specimens mainly feed on fish and cephalopods (WOJCIECHOWSKI, 1972).

The osteology and phylogeny of the cutlassfishes has been examined before by GAGO (1998). The most notable osteological difference between *A. carbo* and *T. lepturus* is found at the level of the supraoccipital. *T. lepturus* possesses an elevated supraoccipital crest, formed by the confluence of the frontal ridges, whereas in *A. carbo* the posterior confluence of the frontal ridges does not form a crest (TUCKER, 1956; GAGO, 1998).

Additional, though small, cranial differences are observed in the length of the epiotics, pterotics and vomer (GAGO, 1998). Although both species are popular subjects in studies focusing on phylogeny, diet, predation, distribution, abundances, movements, age and growth to determine stock dynamics (PEPIN ET AL., 1988; MARTINS AND HAIMOVICI, 1997; STUDHOLME ET AL., 1999; FIGUEIREDO ET AL., 2003), morphological data concerning cranial myology is currently lacking and is therefore provided in detail in this study.

## SPECIMENS

Five *Aphanopus carbo* specimens were commercially obtained from Madeira (Portugal). Three males and two females were examined, measuring between 111 cm and 125 cm standard length. Five specimens, three males and two females of *Trichiurus lepturus* were obtained from the Museum of Comparative Zoology-Harvard (MCZ 58488), measuring between 32 cm and 101 cm standard length. A list of the specimens used is given in Table III.1- 3. The specimens were dissected and cleared and stained. For details of the protocols used, I refer to III.2.2.

## BIOMECHANICAL MODELLING

Biometrical data (see Table III.2- 6) were used to predict biomechanical dynamics during mouth closure based on the model of (VAN WASSENBERGH ET AL., 2005). For details of the mouth closing model of Van Wassenbergh see III.2.7.

## **RESULTS**

---

A detailed description of the head muscles of *A. carbo* is given in the following paragraph. To avoid repetition, only the myological differences observed in *T. lepturus* are mentioned.

### APHANOPUS CARBO

*Adductor mandibulae complex* - The adductor mandibulae complex is a large muscle complex of the cheek region that covers the lateral surface of the suspensorium, below and behind the eye (Fig. VI.2- 2A). Three main parts can be recognized: the adductor mandibulae A<sub>1</sub>-A<sub>2</sub>, separated from the A<sub>3</sub> (Fig. VI.2- 3A) and the A<sub>ω</sub> (Fig. VI.2- 4A).

(1) The superficial part of the adductor mandibulae complex is referred to as  $A_1-A_2$  since no clear-cut subdivisions (into the  $A_1$  and  $A_2$ ) are observed (Fig. VI.2- 2A). Though based on the nomenclature of Winterbottom (1974) the presence of a tendinous connection (T Mx) with the maxilla, lachrymal and primordial ligament suggests the presence of the  $A_1$ . The bulk of the fibers of this complex may represent the  $A_2$  of the adductor mandibulae complex, according to the nomenclature of Winterbottom (1974) since they are latero-ventrally situated and insert indirectly onto the Meckelian fossa by means of the tendon T  $A_1-A_2$  (Fig. VI.2- 4A). This tendon additionally merges with the tendon of  $A\omega$ . Most of the fibres of the  $A_1-A_2$  complex are antero-ventrally directed. Some fibres bordering the posterior edge of the orbit are more dorso-ventrally oriented. These fibres originate musculously from the lateral surface of the frontal and the antero-lateral surface of the sphenotic, and cover the levator arcus palatini and the anterior part of the dilatator operculi. The remaining fibres originate musculously from the lateral ridge of the elongate ventral arm of the hyomandibula (Fig. VI.2- 3A), the anterior border of the preopercle, the antero-ventral part of the lateral surface of the quadrate and the antero-dorsal part of the metapterygoid.

(2) The second part of the adductor mandibulae complex, the  $A_3$ , is the most medial part (Fig. VI.2- 3A). The origin of the  $A_3$  includes the ventral two-thirds of the crescentic anterior edge of the preopercle, the ventro-posterior part of the lateral surface of the metapterygoid, the lateral surface of the symplectic and the ventro-posterior part of the lateral surface of the quadrate. The tendon of the  $A_3$  inserts between the medial surface of the dentary and the lateral surface of the  $A\omega$ , in the Meckelian fossa (Fig. VI.2- 4A).

(3) The third part and anterior expansion of the adductor mandibulae complex,  $A\omega$ , consists of many short fibres which are antero-dorsally to antero-ventrally directed (Fig. VI.2- 4A). The insertion site includes the medial surface of the dentary and is expanded by the presence of a longitudinal bony ridge. These fibers are connected to a broad and strong tendon T  $A\omega$ , which fuses with the tendon of  $A_1-A_2$  (Fig. VI.2- 4A). Additionally, the T  $A\omega$  splits postero-ventrally into two tendons: T  $A\omega-Q$  attaches to the medial surface of the quadrate, near its caudal border, while T  $A\omega-IOp$  attaches to the medio-lateral surface of the interopercle, near its rostral border.

*Levator arcus palatini* - The levator arcus palatini is a triangular muscle, with postero-ventrally orientated fibres (Fig. VI.2- 3A). This muscle stretches from its origin, being the frontal, pterosphenoid and sphenotic to a rather large insertion surface, *i.e.* the dorsal two-third of the dorso-lateral surface of the metapterygoid and the dorso-anterior edge of the hyomandibula. The insertion is accomplished by means of a superficial, flat

tendon. The posterior fibres are incompletely separated from the anterior fibres of the dilatator operculi.

*Adductor arcus palatini* - This muscle is situated in the roof of the buccal cavity and extends between the skull and the suspensorium, forming the posterior and postero-ventral margin of the orbit (Fig. VI.2- 3A). The postero-dorsal half of the adductor arcus palatini is covered by the levator arcus palatini. The rostral half of the muscle is relatively thin and becomes gradually thicker posteriorly. The fibres are latero-ventrally directed and originate from the parasphenoid and prootic. They insert musculously as a narrow strip on the medial surface of the metapterygoid and antero-medial edge of the hyomandibula.

*Levator operculi* - The levator operculi runs between the lateral skull wall and the opercle (Fig. VI.2- 3A). Its anterior fibres are confluent with the posterior fibres of the dilatator operculi. The levator operculi arises from the neurocranium at the level of the pterotic and epiotic by means of a tendon sheet along the dorsal edge of the levator operculi over its total length (Fig. VI.2- 3A). The latero-ventrally oriented fibres insert musculously on the dorso-medial surface of the opercle and on the medial surface of the opercle at the level of a medial ridge.

*Adductor operculi* - The adductor operculi is laterally covered by the anterior part of the levator operculi (Fig. VI.2- 3A). The fibres arise musculously from the ventro-lateral surface of the pterotic and partially from the prootic. They insert on the medial surface of the opercle. The fibres run postero-ventrally and are laterally inclined.

*Dilatator operculi* - The dilatator operculi is subdivided into two parts: a dorsal and a ventral part. The dorsal part is long and slender and situated in the dilatator fossa (Fig. VI.2- 3A). Its origin is extensive and includes the frontal, pterosphenoid, sphenotic, pterotic, hyomandibula and supratemporal. The anterior fibres form a bipennate muscle with a long tendon, which is clearly visible, inserting on the lateral plate-like process on the articular head of the opercle. Some posterior fibres of the dorsal part insert musculously on the lateral plate-like process of the articular head of the opercle as well. These fibres merge ventrally with the dorsal fibres of the second part. This second, ventral part of the dilatator operculi arises from the posterior edge of the hyomandibula and the medial surface of the preopercle. These fibres converge postero-dorsally to insert musculously on the latero-ventral side of the same lateral plate-like process on the articular head of the opercle.

*Intermandibularis* - The fibres of the intermandibularis stretches out transversally between the two halves of the dentary and lie caudal to the dental symphyse (Fig. VI.2- 4A, 5A).



*Protractor hyoidei* - The protractor hyoidei interconnects the hyoid with the dentary (Fig. VI.2- 5A). The protractor hyoidei comprises two parts, an inferior  $\alpha$ - and a smaller superior  $\beta$ -part. The two halves of the PH $\beta$  form two distinct bundles, separated by a deep, longitudinal groove containing the basihyal. The left and right halves of the PH $\alpha$  are ventro-medially fused. The PH $\beta$  is ventrally fused to the PH $\alpha$ . The anterior tendon of the PH $\beta$  is anteriorly fused with that of PH $\alpha$ , forming the anterior common tendon T PH A. This tendon inserts onto the dentary, just behind the intermandibularis. Posteriorly, the protractor hyoidei originates from the lateral surface of the anterior ceratohyal. The posterior tendons of the left and right PH $\beta$  run backwards to attach on the dorso-lateral surface of the anterior ceratohyal. The left and right halves of the PH $\alpha$  share a common posterior tendon. This common tendon splits posteriorly and each branch runs towards the ventro-lateral surface of respectively the left and right anterior ceratohyal. The posterior tendons of PH $\alpha$  and PH $\beta$  are connected by a tendinous sheet which covers the antero-lateral surface of the anterior ceratohyal.

*Hyohyoideus abductor* - The hyohyoideus abductor connects the dorsal hypohyal to the first branchiostegal ray of each side (Fig. VI.2- 6A). The anterior fibres of the hyohyoideus abductor originate through a broad flat tendon from the ventro-lateral surface of the ventral hypohyal. The two robust urohyal-hypohyal ligaments are partially covered by these tendons. The posterior fibres of the hyohyoideus abductor of each side insert through a flat tendon on the anterior surface of the first branchiostegal ray of the opposite side. Both tendons of the left and right side thus cross each other in the midline.

*Hyohyoidei adductores* - Hyohyoidei adductores lie between the successive branchiostegal rays (Fig. VI.2- 6A). Lateral fibres pass between the successive rays while the medial fibres form a continuous sheet on the medial side of the branchiostegal rays and continue behind the postero-dorsal most branchiostegal ray to attach to the medial surface of the opercle.

*Sternohyoideus* - Two myocommata divide the sternohyoideus into three myomeres (Fig. VI.2- 7A). The two halves of the sternohyoideus are separated in the midline by an aponeurosis. The postero-dorsal fibres of the sternohyoideus originate from the lateral, anterior and medial surface of the cleithrum. The origin onto the cleithrum is postero-dorsally extended, dorsal to the origin of the pharyngoclavicularis internus. The pharyngoclavicularis externus and internus cover the sternohyoideal fibres, both originating from the lateral surface of the cleithrum. The postero-ventral fibres of the sternohyoideus are continuous with fibres of the hypaxialis and are laterally covered by a fascia. The anterior fibres of the muscle insert musculously and tendinously through the sternohyoideal tendon on the lateral surface of the urohyal. The antero-dorsally directed

sternobranchial tendon is merged with the aponeurosis between the two halves of the sternohyoideus. Only the tip of this tendon lies superficially, and runs forward to attach to the ventral processus of the third hypobranchial element, after fusion with the tendon of the opposite side.

*Pharyngoclavicularis internus* - This muscle lies medial and posterior to the pharyngoclavicularis externus (Fig. VI.2- 7A). It is both tendinous at its origin and insertion. The posterior fibres attach tendinously to a small groove in the antero-lateral margin of the cleithrum. The fibres run in dorso-rostral direction. The anterior tendon inserts on the antero-ventral region of the fifth ceratobranchial.

*Pharyngoclavicularis externus* - This muscle originates from a groove on the antero-lateral surface of the cleithrum and inserts underneath a dorsal ridge on the dorso-mesial surface of the fifth ceratobranchial (Fig. VI.2- 7A). The fibres run dorsally and slightly rostrally.

*Epaxials* - The epaxials originate from the dorsal surface of the neurocranium, above the posterior edge of the eye (Fig. VI.2- 2A). The origin includes the frontals, parietals, exoccipitals, supraoccipital and epiotics. The origin is not additionally extended by a supraoccipital ridge.

*Supracarinalis anterior* - The anterior fibres of the supracarinalis anterior insert musculously on the postero-dorsal region of the skull forming a cord-like muscle bundle in the dorsal midline (Fig. VI.2- 2A). The posterior fibres originate by means of two postero-lateral tendons on the first pterygiophore of the dorsal fin. The fibres are antero-posterior directed.

#### Myological differences found in *Trichiurus lepturus*

The cranial muscles in *T. lepturus* are highly comparable to those in *A. carbo* (Fig. VI.2- 2B-7B). Origin, insertion and configuration are similar in the levator arcus palatini, adductor arcus palatini, adductor operculi, dilatator operculi, intermandibularis, hyohyoidei abductores, hyohyoidei adductores, pharyngoclavicularis internus and pharyngoclavicularis externus.

*Adductor mandibulae complex* - In *T. lepturus* the configuration of the adductor mandibulae complex is similar, though small differences are observed (Fig. VI.2- 2B; 3B). Some fibres arising from the dorsal half of the lateral surface of the preopercle seem to be somewhat separate from the body of the muscle mass, but are strongly connected by a superficial sheet of faint tendons, which is absent in *A. carbo*. The tendon T A<sub>1</sub>-A<sub>2</sub> splits, in contrast to that in *A. carbo*, into two smaller parts which separately insert onto the edge of the dentary (Fig. VI.2- 4B).

*Levator operculi* - The origin includes similar sites as in *A. carbo* though in *T. lepturus* the fibres arise musculously from the neurocranium (Fig. VI.2- 3A). The tendon is absent.

*Protractor hyoidei* - As in *A. carbo*, both halves of the PH $\alpha$  are ventro-medially fused (Fig. VI.2- 5B). Though in *T. lepturus* the fibres of the anterior tendons of the PH $\alpha$  halves are fused, forming one common ventral tendon which extends rostrally to insert on the dentary behind the intermandibularis. In contrast to *A. carbo*, the posterior tendons of the PH $\alpha$  remain separate in *T. lepturus*, while in *A. carbo* the posterior tendons of PH $\alpha$  are rostrally fused.

*Sternohyoideus* - The sternohyoideal tendon is shorter and situated in the anterior part of the muscle (Fig. VI.2- 7B). The origin of the sternohyoideus includes the medial, anterior and lateral surface of the cleithrum. The origin of the pharyngoclavicularis externus is similar though its lateral surface is covered by a thin sheet of fibres of the sternohyoideus, inserting onto the cleithrum as well. The postero-ventral fibres of the sternohyoideus, also continuous with the hypaxials, are not laterally covered by a fascia. The sternobranchial tendon has a more superficial position (visible on the lateral surface of the sternohyoideus) compared to that in *A. carbo*. At about two thirds of the length of the muscle this tendon becomes superficial.

*Epaxials* - Origin, insertion and configuration are similar, though the origin is expanded due to the presence of the supraoccipital ridge (Fig. VI.2- 2B).

*Supracarinalis anterior* - The supracarinalis muscle is present in *T. lepturus* but due to the anterior displacement of the dorsal fin, compared to *A. carbo*, this muscle is less antero-caudally extended (Fig. VI.2- 2B).

### DYNAMICS OF MOUTH CLOSING

The simulations with the mouth-closing model of *A. carbo* and *T. lepturus* show the following general pattern. Initially, during the first 15 milliseconds after the start of mouth closing, jaw muscle force is almost entirely used to accelerate the lower jaw (Fig. VI.2- 8). Shortly after this, when the lower jaw has nearly reached its maximal velocity (peak near 20 ms), drag becomes the most important factor of resistance to lower jaw rotation. During the final half of the mouth-closing phase (around 30 ms to 65 ms), the force generated by the jaw adductors is predominantly countering resistance caused by stretching of the jaw-opener muscles and the forces exerted on the lower jaw resulting from super-ambient pressure inside the mouth that typically appears near the end of

mouth-closing (Fig. VI.2- 8). According to the model, *A. carbo* is able to close its mouth from a gape angle of 50° to 10° in 64.8 ms, while *T. lepturus* needs 74.2 ms for this.

### FUNCTION OF THE DIFFERENT JAW MUSCLES DURING JAW CLOSING AND BITING

The *musculus adductor mandibulae* consists of three subdivisions ( $A_{\omega}$ ,  $A_1$ - $A_2$ ,  $A_3$ ). The jaw muscle part with the highest physiological cross-sectional area (PCSA), the  $A_{\omega}$ , is also the longest muscle (Table VI.2- 1). It attaches to the lower jaw at a relatively low and distant position from the quadrato-mandibular joint. It consists of a large number of relatively short fibres. The PCSA of the  $A_1$ - $A_2$  subdivision is only 46.3 % and 39.4 % of that of the  $A_{\omega}$  for, respectively, *A. carbo* and *T. lepturus* (Table VI.2- 1). It attaches higher on the lower jaw compared to the  $A_{\omega}$ , close to the coronoid process.

The insertion, inclination, and pennation of the slenderest muscle part, the  $A_3$ , resemble closely to that of the  $A_1$ - $A_2$ , but its PCSA, muscle length and fibre length is considerably lower (Table VI.2- 1).

According to the dynamic and static modelling, the individual adductor mandibulae subdivisions differ notably in function during mouth closing and biting (Fig. VI.2- 9). At the onset of jaw closing, each of the jaw muscle parts generate a considerable moment of force to accelerate the lower jaw rotation, with magnitudes roughly relative to their PCSA (Fig. VI.2- 9A, B). Shortly after this, the total moment of force produced by the  $A_1$ - $A_2$ , and also the  $A_3$  in *A. carbo*, drops entirely and the  $A_{\omega}$  becomes dominant in powering mouth closure, being able to generate its highest mouth-closing torques during this period (Fig. VI.2- 9A, B). Toward the end of mouth closure, the  $A_1$ - $A_2$  again becomes increasingly important; ultimately even doubling the amount of moment of force the  $A_{\omega}$  is able to produce at this instant, despite the larger PCSA of the latter muscle (Fig. VI.2- 9A, B). The contribution of the slender  $A_3$  in causing lower jaw adduction gradually increases as mouth closing goes on in *T. lepturus*, or similarly, recovers progressively in the second half of mouth closure in *A. carbo* (Fig. VI.2- 9A, B)

Maximal bite force is produced at a gape angle of 20.2° in *A. carbo* and 26.0° in *T. lepturus*. More than 90 % of this maximum bite force can be exerted on prey at gape angles between 13.2° - 30.2° and 19.1° - 35.5° for, respectively, *A. carbo* and *T. lepturus*. According to the model, the  $A_{\omega}$  in both species is unable to produce force optimally for a wide range of gape angles, because of the force-length relationship. Because of its geometrical configuration within the jaw system (Table VI.2- 1), the  $A_{\omega}$  is elongated considerably when the mouth is opened to a 50° gape angle. As a consequence, the muscle is predicted to lose substantial tension at short muscle lengths, when gape angles are

narrow (Fig. VI.2- 9C, D). The  $A_1$ - $A_2$  and  $A_3$  subdivisions are able to generate bite force at a much wider range of gape angles compared to the  $A_\omega$ .

### EFFECTS OF MORPHOLOGICAL CHANGE ON BITING AND JAW CLOSING PERFORMANCE

A trade-off between mouth-closing and biting performance is demonstrated by model simulations for three morphological variables: (1) the effects of changes in the length of the input lever arm for jaw closing (Fig. VI.2- 10A), (2) the effects of changes in the length and cross-sectional area of the muscle, making the condition that the total volume of the jaw muscle is kept constant (Fig. VI.2- 10B) and (3) the effects of an increased or decreased inclination of the jaw muscle (Fig. VI.2- 10C). The results show that the morphology of the jaw system of *A. carbo* and *T. lepturus* is neither optimal for generating high bite forces nor for minimizing the time to close the mouth. The functional trade-off appears from the result that, in general, morphological change has the opposite effect on both functions: if bite performance is enhanced, then mouth-closing performance is reduced and *vice versa* (Fig. VI.2- 10).

Some exceptions are observed for which the optimal configuration in a certain aspect of the jaw system is indicated for jaw-closing performance, but not for biting. Firstly, jaw-closing performance could not be improved in any way by changing the input lever length, the jaw muscle shape or the inclination of the jaw muscle of the  $A_3$  of *T. lepturus* (Fig. VI.2- 10A2, B2, C2), indicating that this design is close to optimal for this function. A second noteworthy example is that there is very little room to increase the  $A_\omega$ 's input-lever length or to decrease the inclination of this muscle in both species and still being able of closing the mouth from a gape angle of  $50^\circ$ . When implementing these morphological changes in the model, the  $A_\omega$ 's line of action soon crosses the rotational axis of the lower jaw, through which the muscle will open instead of close the mouth upon activation. As a consequence, the geometrical configuration of the  $A_\omega$  in the jaw system is close to its limits for allowing a mouth opening of  $50^\circ$ . Given that interference with the capacity of opening the mouth widely is probably not favourable for the animal's feeding performance, the muscle is performing very close to its optimum for fast mouth closing (Fig. VI.2- 10A, C).

## DISCUSSION

---

### MORPHOLOGY

The morphology, origin and insertion of the cranial muscles are highly comparable in *T. lepturus* and *A. carbo*. Differences are found in the insertion of the epaxials and supracarinalis muscles. These differences are presumably related to the difference in cranial shape at the level of the supraoccipital crest (Fig. VI.2- 2). In *T. lepturus* a higher supraoccipital crest is formed by the confluence of the frontal ridges, whereas in *A. carbo* the posterior confluence of the frontal ridges does not form a crest (TUCKER, 1956; GAGO, 1998). The supraoccipital is known to serve as insertion site for the epaxials. Expanded insertion sites and increased input lever for the epaxials (by the presence of a crest) may have effect on the functionality or efficiency of these dorsal body muscles (BONE ET AL., 1995; LIEM AND OSSE, 1975; CAROLL ET AL., 2004). The differences in supracarinalis anterior muscles between both species is likely to be related to the anterior position of the dorsal fin in *T. lepturus*. The shape and size of the dilatator operculi is aberrant compared to that of most teleosts. In *T. lepturus* and *A. carbo*, this muscle comprises two parts and its origin is extended to the posterior edge of the hyomandibula and the medial surface of the preopercle. Although this configuration is unusual, fibres originating from the preopercle is observed a few teleost (e.g. *Cyclepus*, *Helostoma*; WINTERBOTTOM, 1974).

### FUNCTIONAL MORPHOLOGY

An important goal in functional morphology is to identify how the mechanical design allows animals to perform in different functions that are essential, but require trade-off with each other. The mathematical modeling in the present study showed that the morphology of the jaw-closing system in *Aphanopus carbo* and *Trichiurus lepturus* indeed displays a compromise in the performance to produce a powerful bite force and the ability to swing the lower jaw towards the upper jaw as quickly as possible (Fig. VI.2- 10).

This result, however, is not surprising as trade-offs between maximization of force and velocity transfer in mouth closing systems have been suggested before and are found to be manifested in the natural diets of terrestrial vertebrates such as salamanders (ADAMS AND ROHLF, 2000) and of fish species (WESTNEAT, 1994; TURINGAN ET AL., 1995; WESTNEAT, 2004; COLLAR ET AL., 2005; KAMMERER ET AL., 2005; VAN WASSENBERGH ET AL., 2005). Piscivores generally require the rapid capture of evasive prey and therefore benefit by favouring fast

mouth closure. On the other hand, animals relying on static biting to eat hard prey will favour the capacity to transfer force to the jaws, by which they inevitably reduce their performance to close the mouth rapidly. However, this still leaves the question how the complex jaw system, with the different parts of the jaw-adducting musculature (Fig. VI.2-2), is built for performing both functions sufficiently well in the examined trichiurid species, which need a quickly moving as well as a forceful jaw to pierce their teeth into elusive prey such as fish.

### ELONGATE JAWS

An important aspect of a predator's prey capture success, especially when feeding on elusive prey, is rapid mouth closure. The chance of prey escape may be reduced significantly by closing the mouth rapidly. Trichiurids mainly feed on large fish, which are usually fast and agile prey, and additionally on harder or tougher prey e.g. cephalopods and crustaceans. Therefore rapid snapping of the jaws onto prey can be important to reduce the chance of prey escape as well as a powerful bite is needed as well (WOJCIECHOWSKI, 1972; MARTINS AND HAIMOVICI, 1997; FRIEL AND WAINWRIGHT, 1998; COSTA ET AL., 2000; SWAN ET AL., 2003). These requirements seem to be reflected in the morphology of the jaws. Both trichiurids have elongate jaws (relative lengths with respect to cranial length of 0.76 (*T. lepturus*) and 0.85 (*A. carbo*). The presence of long jaws is also observed in other aquatic vertebrates and appears to be particularly effective for capturing mobile and elusive prey and they rely on high velocity jaw closure for capturing prey (TURINGAN AND WAINWRIGHT, 1993; FERRY-GRAHAM ET AL., 2001A; FERRY-GRAHAM ET AL., 2001b; KAMMERER ET AL., 2005; NORTON AND BRAINERD, 1993; PORTER AND MOTTA, 2004). They are well suited for closing the tips of the jaws at high linear velocities but they have a mechanical disadvantage at their tips in terms of force production (PORTER AND MOTTA, 2004). Furthermore long jaws increase gape size, allowing to engulf or to seize relatively large prey between the jaws (NORTON AND BRAINERD, 1993; PORTER AND MOTTA, 2004).

In previous research, the mechanical advantage of the mouth closing system has often been calculated to compare the ability of species in mouth-closing velocity and biting capacity. Measured lengths of the in- and outlevers of the lower jaw enable calculating lever ratios that give some information about the force and velocity transmission or "gearing" of the lower jaw: a large outlever relative to the inlever gives a high displacement advantage, while a relatively large inlever gives a high mechanical advantage. This relatively simple approach to the biomechanics of the lower jaw has

proven to be valuable to predict differences in diet between species (CUTWA AND TURINGAN, 2000; WAINWRIGHT AND RICHARD, 1995; TURINGAN ET AL., 1995; WESTNEAT, 1994).

However, the more detailed modelling presented here shows some limitations to this approach, in particular for fish with elongate jaws. Firstly, our analysis shows that the forces resisting jaw closure (inertia, drag, pressure and tissue resistance) become more important in limiting the maximal speed of mouth closing in the long-jawed trichiurids compared to, for example, the relatively shorter jaws of clariid catfishes (VAN WASSENBERGH ET AL., 2005). This implies that, during mouth closure, force transmission (and thus mechanical advantage) can also be important for building and maintaining velocity and not only for the displacement advantage of the leverage system must be considered to evaluate jaw-closing performance. This is analogous to the situation in which we want to close an open door as quickly as possible: if the door is relatively long and heavy (a long, robust jaw), it is often advantageous to push the door at a point further away from the hinge (higher mechanical advantage) than it is to push near the hinge (high displacement or kinematical advantage). As a result, the power of the jaw muscles relative to the force-resistance to movement of the jaw is an important aspect in this process.

Yet, the results show that the trichiurid species still follow the traditional relationship between lever ratio and jaw closing performance when a jaw rotation is simulated from a gape angle of  $50^\circ$  to  $10^\circ$  (Fig. VI.2- 10A). The acceleration phase, in which force transmission is important for increasing the angular velocity of the jaw, is limited to the first quarter of the total duration of this mouth closure. However, if we triple the length of the lower jaw of *T. lepturus* and simulate a  $30^\circ$  to  $10^\circ$  jaw rotation (which roughly approximates, for example, an extremely long jaw of a gar), the total duration (originally 0.166 s) becomes longer (0.203 s) if the inlever length is decreased by a factor of 0.8. This shows that we must be careful with the interpretation of lever ratios in relation to feeding performance in fishes with extremely elongated jaws (e.g. KAMMERER ET AL., 2005).

The results of the present study also show that not only lever ratios, but also muscle inclination (Fig. VI.2- 10C) and the aspect ratio of the muscle (Fig. VI.2- 10B) are almost equally important factors in imposing the trade-off between biting and jaw closing performance. It can therefore be argued that further comparative research should, whenever possible, try to include these morphological variables as well (see also WESTNEAT, 2004).



## ADDUCTOR MANDIBULAE COMPLEX

The ability of predators to bite hard depends on the isometric force generated by the jaw-adductor muscles, while the speed of jaw closure depends on this muscle's shortening velocity and how it is transmitted through the lever system (BAREL, 1983; WESTNEAT, 1994; COLLAR ET AL., 2005). The teleost adductor mandibulae complex usually comprises different subdivisions. However, up to now, remarkably little information about potential independent actions of subdivisions on the lower jaw is available. Yet, increased morphological complexity in jaw muscles (e.g. Tetraodontiformes, Loricarioidea) has shown to be associated with increased functional complexity (SCHAEFER AND LAUDER, 1996; FRIEL AND WAINWRIGHT, 1998; 1999; KORFF AND WAINWRIGHT, 2004).

Apart from some differences in the timing and the amount of force generated (Fig. VI.2- 9), both trichiurid species show a similar pattern in the dynamic and static modelling results for the subdivisions of the mouth closing apparatus. However, comparing the model output between the different adductor mandibulae subdivisions, we see that the function of the individual subdivisions differs notably during mouth closing and biting (Fig. VI.2- 8B).

The  $A_{\omega}$  subdivision has the largest PCSA and is the longest subdivision as well (Table VI.2- 1). This subdivision generates considerable moment of force to accelerate the jaw rotation at the onset of jaw closing and remains the dominant subdivision to power mouth closure during the first half of mouth closure (Fig. VI.2- 9). Due to the force-length relationship and its elongation at wide gape angles, its position within the jaw system is probably less optimal to produce force at narrow gape angles. Still, the  $A_{\omega}$  clearly plays a dominant role in powering mouth closing, especially at the initial phase of mouth closing, where the  $A_1$ - $A_2$  and  $A_3$  become suppressed (Fig. VI.2- 9).

Because the  $A_{\omega}$  makes a relatively small angle with the inlever compared to the other subdivisions, the  $A_{\omega}$  limits the maximal gape of both trichiurids. Interestingly, its configuration within the jaw system appears to be almost optimised for generating fast mouth closing if we assume that the mouth is opened up to an angle of about  $50^{\circ}$  during prey capture (Fig. VI.2- 10). For producing high bite forces, the optimal inclination, for example, is much steeper (Fig. VI.2- 10C). This may indicate that this muscle has evolved specifically to increase the speed of mouth closing.

Despite its smaller size compared to the  $A_{\omega}$ , the  $A_1$ - $A_2$  becomes the most important muscle at the moment of prey impact (Fig. VI.2- 9). This muscle, and also the  $A_3$ , can operate rather constantly over a larger range of lower jaw angles compared to the  $A_{\omega}$ . The  $A_1$ - $A_2$ 's position in the jaw system is clearly a compromise between closing speed and static bite force. The design of the  $A_3$  subdivision, on the other hand, appears to be optimised for

fast mouth closing since its performance in this task could not improved by changing any of the morphological traits (Fig. VI.2- 10).

These results indicate that the different parts of the adductor mandibulae complex could have evolved because of the different selective pressures to improve bite force or to improve the speed of jaw closing. The  $A_{\omega}$  apparently seems adapted for the role of high-power jaw closing muscle, and is probably constrained in its configuration to preserve a sufficient gape size. The  $A_1$ - $A_2$  and  $A_3$ , on the other hand, are better adapted to produce bite force over a wider range of gape angles and rotate the lower jaw at the instant of impact on the prey (Fig. VI.2- 9). The following paragraphs give a reason why none of the adductor's subdivision can be optimised for producing a powerful bite force (Fig. VI.2- 10).

### STREAMLINED HEAD

Having a streamlined head shape facilitates aquatic animals to approach potential prey closely before striking. In addition, streamlined heads allows laminar flow of the surrounding water, even at higher swimming speeds (PORTER AND MOTTA, 2004). A consequent reduction of momentum generated on the water in front of the head (minimizing the bow wave) will reduce predator recognition by the prey. The trichiurid species typically approach their prey slowly (with a carangiform swimming pattern in *A. carbo* or an undulating dorsal fin in *T. lepturus*), the body held rigid (BONE, 1971). As prey fish are sensitive to size, shape and velocity of possible predators, the rigid body (reducing lateral undulatory movements) will reduce visual predator recognition by the prey (PORTER AND MOTTA, 2004). Also, a slow approach (e.g. *Lepisosteus platyrhinus*) can be used to eliminate predator recognition by the prey (PORTER AND MOTTA, 2004).

Consequently, a streamlined head is advantageous for locomotion as well as for prey capture in fish. However, a streamlined head cannot always be combined with a jaw system optimized for producing large bite forces: Fig. VI.2- 10 shows that if both trichiurid species would exhibit maximal bite force (especially for the  $A_{\omega}$ ), a conversion of the head configuration is required. In order to increase maximum bite force, an increase in input lever length and muscle inclination and a decrease in jaw muscle length are beneficial. An increase in maximal bite force may also be accomplished by jaw muscle hypertrophy as observed in the clariid family (VAN WASSENBERGH ET AL., 2005). As these morphological modifications make the head higher and broader, this may be disadvantageous for swimming (increase in drag), and optimizing streamlined head shape is therefore in a trade-off with maximizing biting performance (BAREL, 1983). This illustrates that not only within different aspect of feeding (biting and closing the mouth), but also between feeding

and locomotion, trade-offs have to be considered if we fully want to understand the functional morphology of the jaw system in fishes.

## **ACKNOWLEDGMENT**

---

We would like to thank K.E. Hartel of the Museum of Comparative Zoology (Harvard) for offering museum specimens. Research was partially funded by the FWO (G. 0388.00).



**VII**

**General Discussion**



## VII.1 CONSIDERATIONS AND RESULTS OF THE APPLIED FUNCTIONAL-MORPHOLOGICAL COMPONENT ANALYSIS

A short explanatory note concerning the functional-morphological component analysis, as described in the introduction (I.1), is recapitulated for clarity and to avoid misunderstandings. Four components that are considered to largely define the morphology of the elongate Clariidae are considered: (1) miniaturized head, (2) a special fossorial lifestyle, (3) the presence of hypertrophied jaw muscles and (4) anguilliformity. Even though, we are aware of the fact that morphological diversity is not only the result of the above mentioned components but is related to other driving factors as well, these four are considered to be highly important components for the clariid catfish and are therefore more elaborately examined. As most clariid representatives possess these components to some degree, it is impossible to trace the influence of each of these components on the rest of the Bauplan. Therefore, several species groups are selected in this study. These species groups 1) are not related to the Clariidae in order to exclude phylogenetically defined modifications within the clariids, but 2) allocate the comparison of the influence of each component within a similar phylogenetic context, in order to minimize phylogenetically defined differences between the studied species within one group. When two species differing in one component only (as the components are assumed to be decoupled), are compared we may reveal to what degree structural modifications are related to that component.

The following discussion thus focuses onto these four components, however it needs to be addressed that other components, not dealt with here, may be of equal importance and should be kept in mind.

### 1) MINIATURIZATION

---

#### THE *ANGUILLA ANGUILLA* - *CONGER CONGER* GROUP

Initially *A. anguilla* and *C. conger* were thought to be good subjects for comparing the relation of the component 'head miniaturization' to the rest of the Bauplan, as this was assumed to be the only component, in which they markedly differed. However, the more this topic was deepened, the more it became evident that our choice was not as suitable as initially thought.

The concept of miniaturization includes the assumption that the species evolved from a larger ancestor within a lineage (MILLER, 1979; HANKEN AND WAKE, 1993). Even though the phylogeny within the Anguilliformes is far away from resolved and stable, at present *A. anguilla* is considered a more basal representative of the Anguilliformes with respect to *C. conger* (ROBINS, 1989; BELOUZE, 2001). Whether the ancestor of *A. anguilla* had a larger body size is not known. In short, based on phylogenetic data it is dubious whether *A. anguilla* is really a miniaturized species. It is more likely that the opposite phenomenon of miniaturization is represented in *C. conger*. In agreement with Copes' Law (referring to a widespread tendency for evolution towards larger physical size, MILLER, 1979) *C. conger* can reach huge standard lengths (up to 3m) and is considered the largest anguilliform representative to date (SMITH, 1990).

Miniaturisation? - AS DE PINNA (1996) noted that an extreme modification towards decreased body size seems to occur in a continuum across lineages, and miniaturisation is an extreme endpoint of what may be a gradual trend, we proceeded from the idea that *A. anguilla* may represent an intermediate state, without extreme modifications. However, as discussed below, it appears that *A. anguilla* does not fit in any aspect of the definition of a miniature species based on the criteria of WEITZMAN AND VARI (1988). The following characters were found to be associated with miniaturization in fishes (WEITZMAN AND VARI, 1988; HANKEN AND WAKE, 1993; SOARES-PORTO ET AL., 1999; BRITZ AND KOTTELAT, 2003): reductions in number of fin rays and body scales, structural simplification, reduced ossification, reduction of the cranial and body lateral line sensory system, increased variability and morphological novelty.

Criterion: Body size - A standard length below 26 mm in adults and sexual maturity under 23.5 mm is suggested by WEITZMAN AND VARI (1988) as an arbitrary cutoff for separating miniaturized from non-miniaturized fish species (COSTA AND LE BAIL, 1999; BRITZ AND KOTTELAT, 2003). However, it was noted that in some elongate fishes, head length may be a more appropriate parameter as they may possess head sizes comparable to those of miniature fish below the 26 mm cutoff despite higher standard lengths (BRITZ AND KOTTELAT, 2003).

The body size of *A. anguilla* (max 133 cm, DEKKER ET AL., 1998) clearly exceeds the total body length cutoff value (26 mm) and its head size (Table VII- 1), is far from comparable to that of miniature fish, following the criterion for elongate fish of BRITZ AND KOTTELAT (2003). Even though the body size and head size of *A. anguilla* is dramatically



lower with respect to *C. conger* (max 300 cm, SMITH, 1990), it should not be regarded as miniaturized.

Criterion: Structural cranial simplifications - A relationship between structure of the body and body size is noted in miniaturized species (MILLER, 1979), and frequently this downsizing results in structural and functional changes within the animal. In downsized salamanders (HANKEN 1983; 1993; EHMCKE AND CLEMEN, 2003), caecilians (WAKE, 1986), and fish (MILLER, 1979; FRIEL AND LUNDBERG, 1996; SOARES-PORTO ET AL., 1999; BRITZ AND KOTTELAT, 2003) cranial miniaturization was achieved at the expense of ossification (HANKEN, 1983). Much of the ossified skeleton is lost or reduced, especially in the anterior elements, and a number of components of the skull remain cartilaginous. In contrast to this ossified downsizing, many of the sensory organs were not diminished in size. The reduction of bony skull elements in small vertebrates occurs in favor of the sensory organs and the central nervous system, which need to have an absolute minimum size even in small animals (HANKEN, 1983; WAKE, 1986).

With respect to the neurocranium of *C. conger* (VI.4.3), *A. anguilla* (TESCH, 2003) shows no cranial reduced ossifications or absent cranial elements nor novelties. The size of elements of the sensory units, such as the eyes and otic bullae, are not markedly different or enlarged either. Except for some osteological differences that are characteristic for the families they belong to (e.g. fusion of frontals in *C. conger*, SMITH, 1989B), few conspicuous differences occur.

Criterion: Reduction of the cranial lateral line sensory system - In miniaturized fish, the cranial and body lateral line sensory system is frequently reduced (FRIEL AND LUNDBERG, 1996; SOARES-PORTO ET AL., 1999; BRITZ AND KOTTELAT, 2003).

With respect to *C. conger* and other Anguilliformes, the sensory system of *A. anguilla* and its supporting bones are not reduced. In *A. anguilla* the circumorbital bones are represented merely by thin shell-shaped ossifications (TESCH, 2003) as in *C. conger* (IV.4.3) and most Anguilliformes (BELOUZE, 2001).

Consequently, *A. anguilla* should not be regarded as a miniaturized species. This comparison group is therefore considered not suitable to study morphological implications of head miniaturization in elongate fish.

#### MINIATURIZATION AND BURROWING

Some of the species (e.g. *Heteroconger hassi*, *H. longissimus*, *Moringua edwardsi* and *Pisodonophis boro*) (IV), examined in this dissertation, have small head sizes and may

be miniaturized. Whether these species meet the criteria for miniaturization is explored in the following section.

Criterion: Body size - Despite their relatively high body lengths, the head lengths (Table VII- 1), measured from the tip of the snout to the opercular opening, of the latter species are low and might be comparable to that of miniaturized fish, especially considering that head length includes the elongated and posteriorly displaced gill chamber.

#### A) TAIL-FIRST BURROWERS

The cranial morphology of *H. hassi* and *H. longissimus* appears to correspond to some degree to the definition of miniature species as some aspects of the criteria of WEITZMAN AND VARI (1988) are met. Though, not all reductions are as extensive.

Criterion: Structural cranial simplifications - The downsizing in *H. hassi* and *H. longissimus* may, to some extent, be reflected in some structural changes in the skull (IV.2). The skull of adult heterocongrines has no additional cartilaginous components that would not be present in other relatives (e.g. the related basal *C. conger*) or does not lack any cranial bones. Though, the following features might be related to miniaturization. The cranial bones in *H. hassi* and *H. longissimus* are thin and non-overlapping and the edges of successive cranial bones are straight (Fig. IV.2- 1, 6). In the heterocongrines the snout region and jaws are clearly shortened and the bones of the orbital region have become extremely narrow. To my opinion, the most convincing argument in favour of miniaturization in the heterocongrids can be found in the sensory units. As noted by WAKE (1986) and HANKEN (1983) some elements of the skull may be reduced further than the sensory units as the latter are defined by a minimal functional size (Wake, 1986). This appears to be the case in the heterocongrines as the eyes are extremely large, and the otic bullae are clearly distinguishable (Fig. IV.2- 1C).

Criterion: Reduction of the cranial lateral line sensory system - The cephalic lateral line system of the heterocongrines is not reduced as it corresponds to the overall morphology as found in all congrids (SMITH, 1989B). Still, its supporting bones (circumorbitals) are small, reduced, irregular and tube-like but open above (Fig. IV.2- 2E).

Even though the heterocongrids present cranial reductions that may be related to miniaturization, the downsizing has not co-occurred with numerous and extensive reduction as reported for other miniaturized fish (MILLER, 1979; FRIEL AND LUNDBERG, 1996; Soares-Porto et al., 1999; BRITZ AND KOTTELAT, 2003). This may be explained by the following hypotheses:

- This may indicate that heterocongrines do not represent the extreme end (with according extreme modifications) of the continuous gradual trend (as supposed by DE PINNA, 1996) that occurs across lineages towards miniaturization.

- Head-first burrowing clearly puts severe constraints on the skull morphology and size. In tail-first burrowing species, a smaller size is also advantageous for sediment penetration, though constraints due to burrowing are expected to be less prominent at the level of the skull, as skull fortifications to resist forces during burrowing are not required. This may explain why the reductions and modifications found in the skull of tail-first burrowers, which are probably related to miniaturization, are more extensive compared to 'possible' modifications related to miniaturization found in head-first burrowers (see below).

- On the other hand, constraints on the functional morphology of the head, associated with feeding (suction-feeding, SMITH, 1989B) and respiration may prevent certain kinds of transformations or reductions. After all, one has to keep in mind that both heterocongrines are specialized for its tail-first burrowing lifestyle and suction feeding (SMITH, 1989B).

- The myological study of the heterocongrines revealed that the mouth closing muscles are not hypertrophied (IV.2), in contrast to the other examined species. So the observed reductional cranial features may be related to the presence of small jaw muscles as well, because special structural reinforcements at the level of the cranium are probably not needed and consequently may be to the lesser extent the result of miniaturization.

## B) HEAD-FIRST BURROWING

The studies on head-first burrowing eels, *Moringua edwardsi* (DE SCHEPPER ET AL., 2005) (IV.1) and *Pisodonophis boro* (DE SCHEPPER ET AL., 2007) (IV.3), reveal that specializations that are associated with their burrowing behavior appear to be tightly related to modifications related to miniaturization.

Criterion: Structural cranial simplifications - Even though *P. boro* and *M. edwardsi* may be miniaturized eels, both show no reduced ossifications or absence of cranial elements, as observed in other miniaturized fish (SOARES-PORTO ET AL., 1999) (IV.1; IV.3). However, *M. edwardsi* lacks one cranial bone, the basisphenoid. Elements related to the sensory units such as the otic bullae are not extremely large. The eyes are even reduced in *P. boro*, and even more extremely in *M. edwardsi* (IV.1; IV.3) but this is likely to be related to fossoriality (WAKE, 1986; LEE, 1998).

In head-first burrowing species, the extensive ossification and fusion of several cranial bones are assumed to compensate for the reduction or loss of some other cranial

elements and are assumed to be correlated with the head-first burrowing mode (TRAVERS, 1984A; WAKE, 1986; LEE, 1998; BRITZ AND KOTTELAT, 2003; MEASEY AND HERREL, 2006). This may be true for *M. edwardsi* (DE SCHEPPER ET AL., 2005) and *P. boro* as well (DE SCHEPPER ET AL., 2007).

Criterion: Reduction of the cranial lateral line sensory system - In *P. boro* the cephalic lateral line system shows no modifications at all (IV.3), compared to the pattern generally found in Anguilliformes (BÖHLKE, 1989B), whereas that of *M. edwardsi* is highly modified as external pores are absent and canals are widened into dermal cavities (IV.1).

Not all morphological features in the skull of downsized animals are simply consequences of miniaturization, but some are correlated with demands of function and habitat (LEE, 1998). Morphological transformations related to burrowing rather than to miniaturization, cannot be excluded, as miniaturization frequently occurred in burrowing vertebrates (HANKEN, 1993; RIEPPEL, 1996). As burrowing puts severe constraints on the maximal head and body diameter (MEASEY AND HERREL, 2006), the most specialized burrowing species exhibit small diameters and increased elongation of the body. These two traits must reduce relative effort during digging (NAVAS ET AL., 2004). Consequently modifications such as extremely fortified skulls or tails to resist large compressive forces during burrowing (GANS, 1975; HANKEN, 1983; DUELLMAN AND TRUEB, 1986; POUGH ET AL., 1998) and modifications as a consequence of miniaturization are likely to co-occur (LEE, 1998). As discussed above, specializations for burrowing appear to be tightly related to modifications due to miniaturization. Of course this complicates the distinction of possible morphological specializations to one of both components. On the other hand it may indicate that, due to the close relation between the components, both should not be separated but treated as one entity.

## 2) BURROWING LIFESTYLE

---

### THE ANGUILLA ANGUILLA - HETEROCONGER GROUP

It was initially assumed that *A. anguilla* differs only from the heterocongrids in the burrowing component as *A. anguilla* is considered to be a non-burrowing species (SCHULZE ET AL., 2004), whereas the heterocongrids are known for their peculiar tail-first burrowing behaviour (SMITH, 1989B).

During the course of the study, it became apparent that mutual relations between the different components are more complex than originally presumed. The morphological

study of *A. anguilla* (IV.4.2) revealed that the head, though highly variable (IV.4.1), has no miniaturized features (see above). *Heteroconger hassi* and *H. longissimus* (IV.2) on the other hand indeed are miniaturized species, but their jaw muscles are not enlarged. Consequently, the assumptions that these species are similar in the components ‘jaw muscle hypertrophy’ and ‘miniaturization’ need to be rejected. Therefore, this comparison group is considered not suitable to study possible morphological modifications that may be related to a burrowing lifestyle.

#### THE ANGUILLA ANGUILLA - MORINGUA EDWARDSI GROUP

*Anguilla anguilla* and *M. edwardsi* were considered appropriate comparison subjects as their burrowing lifestyle was thought to be the only component in which they differed. Though as mentioned before, *A. anguilla* is no miniaturized species. As the assumptions for both components ‘burrowing lifestyle’ and ‘miniaturization’ are not fulfilled, revealed morphological differences may not be unambiguously related to either burrowing or miniaturization. Therefore, this comparison group, comprising these two species, is considered not suitable, at least as was originally conceived.

#### PISODONOPHIS BORO

At the start of this study, this species was not selected as a study subject. But during the course of the present study, some arguments have led to the decision to add *Pisodonophis boro* to the species list:

- *P. boro* is of special interest because it is able to burrow head-first as well as tail-first.
- As living specimens were available in the lab, biomechanical studies, finite-element analyses and observations provided additional proof or verifications of hypothesis based on morphological features (CHOI, 2006; CHOI ET AL., SUBMITTED).
- As this species belongs to the family Ophichthidae, it allows us to examine whether similar environmental demands has led to the evolution of similar morphological modifications in the head (compared to *Moringua edwardsi*) and in the caudal fin (compared to *Heteroconger hassi* and *H. longissimus*) (IV.3).

As this species is also assumed to be miniaturized, it could however not replace *M. edwardsi* nor the heterocongrines in the comparison groups.

The head of *P. boro* is assumed to be specialized for burrowing to some degree, though cranial modifications are less extensive due to trade-offs than modifications observed in its caudal fin (for details see discussion IV.3). Clearly the mechanical design of

the head allows head-first burrowing animals (*P. boro* as well as *M. edwardsi*) to perform in different functions (e.g. burrowing locomotion and feeding).

#### A) TAIL-FIRST BURROWING

In order to identify trends that may be related to tail-first burrowing, the osteological and myological features of the caudal fin were examined in *Anguilla anguilla* and *Conger conger* (IV.4.4), *Heteroconger hassi* and *H. longissimus* (IV.2), *Moringua edwardsi* (IV.1) and *Pisodonophis boro* (IV.3). Tail-first burrowing is expected to have a major impact on the caudal skeleton and its muscles. Subsequently the morphological features of all these species are compared and an attempt has been made to relate morphology to differences in lifestyle (IV.4.4). In order to avoid redundant repetitions, the major differences that are likely to be related to tail-first burrowing are mentioned here. An elaborate discussion can be found in IV.4.4.

Modifications related to tail-first burrowing: A robust, firm and strengthened caudal skeleton is found in the tail-first burrowers *P. boro*, *H. hassi* and *H. longissimus* due to the high degree of fusions and the stout, broad hypural plates. The tail is externally pointed. The total amount of caudal fin rays is lower in the tail-first burrowers and the fin rays are short and fixed by the thick skin and connective tissue, so dorso-ventral movements are less obvious. These modifications can be an advantage for tail-first burrowing, ensuring an effective penetration into the sediment, and may thus be considered adaptations for tail-first burrowing. The caudal fin muscles are not extremely reduced with respect to the non- and head-first burrowers and may be related to a possible trade-off between flexibility and strength of the tail. The absence of the interradials in the tail-first burrowing species is likely to be related to the tail-first burrowing lifestyle, as some actions of the caudal fin musculature are presumably no longer required and not even possible.

The modified caudal fin as found in *H. hassi*, *H. longissimus* and *P. boro* may be regarded as a convergent evolutionary trait, modified for and related to tail-first burrowing.

#### B) HEAD-FIRST BURROWING

The morphology of the head of *A. anguilla* (IV.4.2), *C. conger* (IV.4.3), *H. hassi* and *H. longissimus* (IV.2), *M. edwardsi* (IV.1) and *P. boro* (IV.3) has been studied into detail and are subsequently compared in order to identify possible trends that may be related to head-first burrowing. Though it needs to be addressed that, observed modifications may be related to either 'burrowing' or 'miniaturization' or both components. An elaborate

discussion, concerning cranial modifications among the examined Anguilliformes can be found in IV.4.3. Thus this section is limited to the major finding to avoid repetition.

Modifications related to head-first burrowing: The head-first burrowing species *M. edwardsi* and *P. boro* have a relatively shorter but compact ethmoid region. The orbital region is shorter but more robust as the orbits are reduced and the interorbital distance is increased. This is most pronounced in *M. edwardsi*. Due to the widening of the frontals and parasphenoid, the skull widens gradually from the anterior margin of the orbits. The shape of the skull, increased thickness of the cranial bones and high amount of overlap between successive bones appear to be advantageous in the distribution of stress, generated during head-first burrowing. The eyes are reduced, as visual capacities are assumed less important beneath the substrate, and this is considered advantageous during burrowing to avoid damage of these sense organs. The enlarged jaw muscles, probably related to predatory feeding behaviour and rotational feeding as well, are assumed to be related to head-first burrowing as this may prevent the dislocation of the mandibular joint as a result of torque forces experienced during substrate penetration.

### 3) JAW MUSCLES HYPERTROPHY

---

#### THE *TRICHIURUS LEPTURUS* - *APHANOPUS CARBO* GROUP

The component assumptions, made at the start of this study, are proven to be correct, though to some extent. Both trichiurid species indeed differ solely in the component ‘jaw muscle hypertrophy’ but initially it was thought that *T. lepturus* had enlarged jaw muscles. As *T. lepturus* possesses an apparent elevated supraoccipital crest, it was believed that this structure may enhance and enlarge the insertion site for the jaw muscles (amongst other, e.g. epaxials). However the jaw muscles of *T. lepturus* turned out to be smaller with respect to those of *A. carbo* and the supraoccipital crest, not involved in the insertion of the jaw muscles, serves solely for the attachment of the epaxials.

The morphology, origin and insertion of the cranial muscles, even the adductor mandibulae complex, are highly comparable in *T. lepturus* and *A. carbo* (VI.2). Even though the variables, defining the adductor mandibulae complex (Table VI.2- 1), are similar for both species, the scaled physiological cross section area (PCSA) is about 3 times larger for each subdivision of the jaw muscle complex in *A. carbo*. This difference results in larger forces generated and some small differences in timing during mouth closing in *A. carbo* (Fig. VI.2- 9). Though apart from these differences in the timing and the amount of

force generated (Fig. VI.2- 9), the overall pattern in the dynamic and static modelling results are similar in both species.

Even though the PCSA and consequent generated forces are larger in *A. carbo*, the insertion site is equally large in both species and no notable osteological differences related to increased mechanical loads are observed. However, increased bone thickness can not be excluded. As no histological cross section are available (and technically difficult to produce due to their large size) this can not be confirmed.

With respect to *M. edwardsi*, *P. boro*, *A. anguilla* and *C. conger*, the enlarged jaw muscles of *A. carbo* solely involved an increase in PCSA, whereas in the former species the insertion site of the jaw muscles are enormously expanded as well.

#### THE MASTACEMBELUS BRICHARDI - MASTACEMBELUS MARCHEI GROUP

It was initially thought that in *M. brichardi* and *M. marchei* the only differing component was ‘jaw muscle hypertrophy’. However, as became evident from dissections and from anatomical descriptions of other, more derived mastacembelids (TRAVERS, 1984A), *M. brichardi*, should be considered intermediate in the component ‘miniaturization’ or even miniaturized. Consequently, morphological modifications may be related to both ‘miniaturization’ and ‘jaw muscle hypertrophy’.

The enlargement of the adductor mandibulae complex in *M. brichardi* is largely due to the enlargement of the A1 and A2, and this may have occurred at the expense of the A3. The eyes are substantially reduced. The neurocranium is more cylindrical as the skull roof and skull floor are posteriorly much more narrow. The infraorbital bones are reduced in number, size and degree of ossification (TRAVERS, 1984A). The neurocranium is reduced as many neurocranial bones are lost or reduced (for details see TRAVERS, 1984A, B). These latter reductional features are more likely to be related to ‘miniaturization’.

As both species differ in both components ‘miniaturization’ and ‘jaw muscle hypertrophy’ the observed morphological differences can not with certainty be assigned to one of both.

#### ANGUILLA ANGUILLA

That *A. anguilla* occurs in two varieties (broad- and narrow-headed) as extremes of a continuous spectrum is elaborately discussed in IV.4.1. The influence of feeding conditions or random factors on head form has been subsequently examined, providing support for the hypothesis that these trophic phenotypes are an adaptive response to available trophic resources (TÖRLITZ, 1922; THUROW, 1958; LAMMENS AND VISSER, 1989; STEARNS, 1989; PROMAN AND REYNOLD, 2000; TESCH, 2003; AUBRET *ET AL.*, 2004). As, among the four



components considered, these phenotypes (within one species!) differ solely in the component 'jaw muscle hypertrophy', *A. anguilla* appears to be an ideal species to examine whether the enlargement of jaw muscles has effect on the architecture and morphology of the skull and if so, to define what kind of modifications occur. The broad-headed eels have enlarged jaw muscles compared to the narrow-headed phenotypes (IV.4.2). The absolute weight (g) of the mouth closing muscles of the broad-headed eels is about 2.5 to 3 times higher compared to that of the narrow-headed eels of the same total length. The magnitude of force in the extreme broad-headed eel is about twice the size predicted for the extreme narrow-headed eel.

The following morphological differences, related to the jaw muscle enlargements are noted. The skull of broad-headed eels is larger compared to that of a narrow-headed eel of similar length. The phenotypic variation is reflected in external head shape (mainly head width, head height and jaw length) as well as in the shape of the skull (shorter snout, higher skull, wider (width) and shorter (length) post-orbital region, smaller and dorsally inclined sphenotic processes, shorter pterotic processes and longer epiotic processes. The lower jaw and maxillaries, involved in the insertion of the A1 and A2, are lengthened, more robust and form a wider arch in the broad-headed eels (TÖRLITZ, 1922; THUROW, 1958). Furthermore, THUROW (1958) noted the larger size of the coronoid process, to which the A1 and A2 insert, in broad-headed eels. This indicates a stronger bite as a higher coronoid process implicates a longer power arm (CABUY ET AL., 1999; HERREL ET AL., 2002). Broad-headed eels have larger jaw muscles and are able to generate higher bite forces (based on the mouth closing model of VAN WASSENBERGH ET AL., 2005)

Based on the results of the morphological examination of the phenotypes of *A. anguilla*, we can conclude that the enlargement of the jaw muscles may result in cranial modifications. Furthermore, as this variation is diet-dependant, the relation between hypertrophied jaw muscles and feeding behavior is emphasized. The possibility that the jaw muscle hypertrophy has evolved as an adaptation for predatory feeding habits and rotational feeding was previously addressed for *A. anguilla* (IV.4.2), *C. conger* (IV.4.3), *M. edwardsi* (IV.1) and *P. boro* (IV.3) and was further supported by the small sized jaw muscles in the suction-feeding heterocongrines (IV.2).

## 4) BODY ELONGATION

### THE *MASTACEMBELUS MARCHEI* - *MASTACEMBELUS MASTACEMBELUS* GROUP

The component assumptions as considered at the start of the present dissertation can still be applied. These species indeed solely differ in the confluence of median fins, which is still regarded as a modification related to anguilliformity.

The cranial morphology of *M. marcheii* and *M. mastacembelus* is similar (VI.1.1). Although, some aspects of the skull and cranial myology show some differences as discussed in VI.1.1, which are likely to be related to subtle differences in feeding behaviour rather than to differences in ‘anguilliformity’. Some aspects of the osteological and myological features of the caudal fin are presumably related to the component ‘anguilliformity’.

A relation apparently exists between body elongation and the elongated dorsal and anal fins, the confluence of the unpaired fins, increased reductions and fusions in skeletal elements of the caudal fin and reduction in number of caudal fin rays (VI.1.2). This is further supported by the observations in the other examined species as they all are elongate and show elongate dorsal and anal fins, confluent unpaired fins, with reduced (and fused) caudal skeletal elements, and a low number of caudal fin rays (IV.4.4). The trichiurids also have an elongate body, though it is additionally laterally flattened (to increase swimming capacities; BONE, 1971). *T. lepturus* also shows the elongated dorsal and anal fins, reduced caudal fin skeleton (1 hypural present) and reduced caudal fin rays (absent) (GAGO, 1998). *A. carbo* forms an exception as it has a clearly distinct (and lunate) caudal fin, though its dorsal and anal fins are extremely long and caudally extended and the elements of the caudal skeleton are highly fused as well. In short, body elongation appears to be to some extent reflected in the median fin morphology.

The absence of the supracarinalis posterior and infracarinalis posterior muscles seems to be related to the confluence of the median fins as their absence is observed in all presently examined species with confluent fins (s IV.1; IV.2; IV.3; IV.4.4; V.3; VI.1.2).

The rest of the caudal fin musculature of the examined mastacembelids resembles the muscular conformation of generalized teleosts both in origin and insertion (VI.1.2) whereas the examined as well as Anguilliformes have reduced caudal fin muscles with respect to generalized teleosts (IV.4.4). Consequently phylogeny appears to be reflected in the myological features as Anguilliformes are basal teleosts, whereas Mastacembelidae are more derived percomorphs. It may be assumed that reductions in caudal fin myology are

not necessarily directed related to body elongation or reductions in the caudal skeleton. It is more likely that myological reductions reflect differences in lifestyle such as burrowing (IV.2; IV.3 and IV.4.4) or cruising specialists (LAUDER AND DRUCKER, 2004).

## VII.2 IMPLICATIONS FOR *CHANNALLABES APUS*

Morphological examination of some representatives of the Anguilliformes (IV), Mastacembelidae (VI.1) and Trichiuridae (VI.2), combined with a literature review of relevant papers on morphology and ecology of fish and even amphibians and reptiles, allows a discussion on those components that may be reflected in the cranial morphology of the elongate clariids. This was the primary goal for the onset of this study.

Until recently, the genus *Channallabes* was considered as monotypic, including *Channallabes apus* (PELLEGRIN, 1927). But, morphological studies revealed high variability in biometric and meristic features (ADRIAENS ET AL., 2002), caudal skeleton (DE SCHEPPER ET AL., 2004) (V.2), vertebrae (DE SCHEPPER ET AL., IN PRESS B) (V.1) as well as the pectoral and pelvic fins and girdles (ADRIAENS ET AL., 2002). Consequently, a survey of elongate African clariids was performed and indicated the existence of two new species and two reassigned species within the genus *Channallabes*, adding the total number of valid species of *Channallabes* occurring in the lower Guinea ichthyological province to four species (*C. alvaresi*, *C. ogoensis*, *C. teugelsi* and *C. longicaudatus*) (DEVAERE ET AL., 2007A). Another two species (*C. apus* and *C. sanghaensis*) are known from the Congo basin (DEVAERE ET AL., 2007B). Phylogenetic analyses indicated that these *Channallabes* taxa have arisen at least four times independently from different *Clarias*-like ancestors (DEVAERE ET AL., 2007C; JANSEN ET AL., 2006).

### BODY ELONGATION

The results of the phylogenetic analyses consequently imply that body elongation in these *Channallabes* species is the result of parallel evolution (DEVAERE ET AL., 2007C; JANSEN ET AL., 2006). The refuge theory Haffer (1982) may offer a plausible explanation for the idea that the evolution towards body elongation may have occurred more than once. It is suggested that forest contraction could have triggered a selective pressure towards anguilliformity, enabling these elongate species to colonize new niches, such as swamps (DEVAERE ET AL., 2007C).

It is furthermore observed that in each of these lineages, the same set of morphological changes co-occurred with body-elongation such as the increase in number of vertebrae (DE SCHEPPER ET AL., IN PRESS B) (V.1) and reduction of paired fins (ADRIAENS ET AL.,

2002). Limb reduction coupled to body elongation is similarly observed in the non-clariid species examined here (IV, V, VI) and has occurred independently in many higher level taxa (GANS, 1975; WITHER, 1981; LEE, 1998). This is not so surprisingly as it is known that an expansion of the Hox gene expression domains along the body axis, both accounts for elongation of the body as well as the generally co-occurring loss of limbs (COHN AND TICKLE, 1999).

Based on the results of the examination of Anguilliformes (IV.4.4), Clariidae (V.3) and Mastacembelidae (VI.1.2), a relation apparently exists between body elongation and the elongated dorsal and anal fins, the confluence of the unpaired fins, increased reductions and fusions in skeletal elements of the caudal fin and reduction in number of caudal fin rays. Furthermore a possible relation between the absence of the supracarinalis posterior and infracarinalis posterior muscle and the confluence of the median fins has been suggested (IV.4.4). Even though this may be true to some extent for fossorial and burrowing species, pelagic species may differ from this pattern (see Trichiuridae; GAGO, 1998), especially in median fin morphology and confluence.

The skulls of all elongate clariids are convergent as these are reduced and in the jaw muscles as they are hypertrophied (DEVAERE ET AL., 2007A, B). Though this should not be associated with the component ‘body elongation’ as illustrated by 1) *Tanganikallabes mortiauxi*, which is not elongate but has a markedly reduced neurocranium with large adductor muscles (POLL, 1943), and by 2) *Channallabes*, which is more elongate compared to *Gymnallabes*, but has less pronounced reduced cranial bones (DEVAERE ET AL., 2001). *Heteroconger hassi* and *H. longissimus* (IV.2), *Trichiurus lepturus*, *Aphanopus carbo* (VI.2) and *Mastacembelus marcheii* (VI.1.1) support this as these species are elongated but have no enlarged jaw muscles.

#### REDUCTION IN CRANIAL BONES

The reduction of the eyes (DEVAERE ET AL., 2001), reduction in cranial bones and increasing rigidity of the skull (CABUY ET AL., 1999; DEVAERE ET AL., 2001) are convergent characters of the *Channallabes* species (DEVAERE ET AL., 2007A) as well as in the other elongate clariids. All these species are found in swampy areas, occupying a similar burrowing niche (ADRIAENS ET AL., 2002; DEVAERE ET AL., 2007A), and have downsized skulls (DEVAERE ET AL., 2001; 2007A). Consequently, the close connection between these convergent morphological specializations and both components ‘miniaturization’ and ‘burrowing lifestyle’, as assumed for the burrowing species examined in this dissertation, is addressed. ‘Why’ these convergent traits have occurred remains unclear and can not unambiguously be assigned to either one or both of these components.

Based on the results of the morphological studies on the burrowing species examined in this dissertation (De SCHEPPER ET AL., 2005; 2007) (IV.1; IV.3), and from literature (RIEPEL, 1996; LEE, 1998; DANIELS ET AL., 2005; MEASEY AND HERREL, 2006) it could be deduced that burrowing puts severe constraints on the maximal head and body diameter and that a burrowing lifestyle mostly co-occurs with body elongation and those convergent morphological changes in cranial bone reduction and rigidity. This additionally emphasizes the close connection between ‘burrowing lifestyle’ and ‘miniaturization’, consequently interfering with the examination of these components individually in burrowing species. Therefore, in this context, these components may be considered rather as one entity, that may be related to modifications in the cranial morphology.

In this regard, the narrowing of the skull, the reduction of the lateral neurocranial bones (infraorbital and suprapraeopercular series) and eye reduction in the elongate clariids may be explained as being associated with both the ‘burrowing lifestyle’ and ‘miniaturization’ components. The increased neurocranial rigidity, due to the outgrowth of several interdigitation zones (DEVAERE ET AL., 2001) in *Channallabes* can also be associated with both components. The additional fortification may provide sufficient strength to the miniaturized clariid skull to resist forces that are involved with burrowing. Fortifications at the level of the hyomandibular-neurocranial joint may be related to the enlargement of the mouth closing muscles as well (CABUY ET AL., 1999; HERREL ET AL., 2002; VAN WASSENBERGH ET AL., 2004).

#### HYPERTROPHIED JAW MUSCLES

In course of the evolution, different lineages of clariid catfish have developed extremely large mouth closing muscles (DEVAERE ET AL., 2007A). The question remains why such large mouth closing muscles have developed in these elongate clariids. Dietary studies on *Channallabes apus* revealed that hard prey (especially beetles) form the main part of their diet (HUYSENTRUYT ET AL., 2004). Biomechanical studies on several clariid species, including *Channallabes apus*, demonstrated the relationship between the size of the jaw muscles and the maximal amount of bite force that can be generated (Herrel et al., 2002; VAN WASSENBERGH ET AL., 2005). The relation between hypertrophied jaw muscles, bite force and feeding behavior is emphasized by the trophic variation observed in *A. anguilla* (IV.4.2) and further supported by the studies of *C. conger* (IV.4.3), *M. edwardsi* (IV.1), *P. boro* (IV.3), the trichiurids (VI.2) and the mastacembelids (VI.1.1). Additional support is provided by the fact that the jaw muscles are small in the suction-feeding heterocongrines (IV.2).

As the jaw muscles are drastically enlarged in the elongate clariid species, consequences of these changes may be expected on the surrounding structures. In this regard, the hyomandibular-neurocranial joints are strengthened, connecting the suspensoria firmly to the neurocranium and the suspensoria are tightly covered by these enlarged jaw muscles (CABUY ET AL., 1999). Consequently, diminished lateral expansions during suction are expected, and confirmed (VAN WASSENBERGH ET AL., 2004).

A relation between the enlargement of the jaw muscles and the reduction of eyes in the elongate clariids has been proposed as a result of additional space being provided by the reduction and forward displacement of the eyes in the elongate catfish, allowing the expansion of the jaw muscles (CABUY ET AL., 1999; DEVAERE ET AL., 2001). This appears to be true for *M. edwardsi* (DE SCHEPPER ET AL., 2005) (IV.1), *P. boro* (DE SCHEPPER ET AL., 2007) and *M. brichardi* (VI.1.1) as well. Though, our results assume that both features are not necessarily connected, especially as the eyes of *A. anguilla* (IV.4.2) and *C. conger* (IV.4.3) are not as extremely reduced, whereas the jaw muscles are extremely enlarged. Those species with reduced eyes do share a burrowing or cryptic lifestyle. As much, to my opinion, eye reduction is more likely to be related to the fact that these species occupy burrowing niche.

Again, the component ‘miniaturization’ can not be disregarded as it may partially account for the enlargement of the jaw muscles of the elongate clariids as well. Isometric reduction of skull size would imply shortening of jaw muscle fibres, thus compromising their functionality (HANKEN, 1993). The posterior expansion of jaw muscle insertion may increase biting force within a smaller spatial design (HANKEN, 1993). Furthermore, it is assumed that the enlarged jaw muscles are advantageous for head-first burrowing as they may prevent the dislocation of the mandibular joint (DE SCHEPPER ET AL., 2005; 2007) (IV.1; IV.3). However, as enlarged jaw muscles are found in the closely related, non-miniaturized and non-burrowing eels, *A. anguilla* (IV.4.2) and *C. conger* (IV.4.3) as well, this should be interpreted with caution.

Conclusion: The cranial musculo-skeletal system of fishes in general has to accomplish a large number of crucial biological functions, coping with capturing, processing and transporting prey, breathing water or air, participating in sensory perceptions, providing protection for the major sense organs and brains, and serving as a streamlined bow in locomotion (LIEM, 1980). Consequently, changing the features of one of the structural elements in such a complex integrated system can alter several, structurally coupled functions of the system. In similar manner, several factors to which cranial elements might be adapted, form a tight complex network as well, which might be

unfeasible to decouple. As many features of the cranial system of the elongate catfish are in favor of an increased biting force (hypertrophied jaw muscles, stronger bony connections between skeletal elements), the cranial musculo-skeletal apparatus of the elongate clariids can be considered as highly specialized (VAN WASSENBERGH ET AL., 2005). These enlarged jaw muscles may have contributed to some extent to the change of structural elements in the cranial system but so may have other components such as 'miniaturization', 'body elongation' and 'burrowing'. As becomes clear from the results in the present dissertation, the considered components form a closely related network within the cranial system as whole. It is therefore unfeasible to define changes in structural elements unambiguously to only one of the considered components.

The present dissertation has led to a deeper insight in relations between morphological modifications and components that may lead or alter such modifications. The main conclusion is the realization that potential modification components, regardless which ones are chosen or how many are considered, are mutually linked to each other and may have an indirect effect on several other structural elements. They form a close network, hindering the demarcation of the effect of the individual components.

### VII.3 CONVERGENT EVOLUTIONARY TRAITS

Morphological similarities among species may be the result of a common ancestry or it may have evolved independently in several lineages as a result of convergent evolution (WIENS ET AL., 2003; HIBBITS AND FRITZGERALD, 2005). Groups of species that are convergent in body elongation form the main focus of this dissertation (1.2). Body elongation is an evolutionary process that has evolved numerous times in many independent lineages and on a broad scale within vertebrates (WARD AND BRAINARD, 2007). Three different types of morphological changes are recognized that may contribute to the evolution of elongate body forms in vertebrates: (1) an increase in the number of vertebrae; (2) an increase in the length of the vertebral centra and (3) a decrease in depth of the body (WARD AND BRAINARD, 2007). Body elongation observed in those species examined in this dissertation, is the result of an increase in number of caudal vertebrae. (DE SCHEPPER ET AL., IN PRESS B; WARD AND BRAINARD, 2007).

Intriguing evolutionary questions emerge when curious similarities are noted in distantly related species. Can we find a common evolutionary pattern in elongate fish? To what degree have these species evolved to a similar overall Bauplan? What is the

evolutionary advantage of an elongate body given the fact that it has evolved many times independently?

### CONVERGENT TRAITS: DEVELOPMENTAL MECHANISMS ?

Convergent traits shared by all species examined in this dissertation, are:

- The pelvic fins are absent.
- The dorsal and anal fins are elongated.
- The caudal skeleton is characterized by hypural fusions.

As reported before, body elongation often co-occurs with limb reduction and even limblessness (WITHERS, 1981; LEE, 1998). Based on the data of this dissertation, the convergence in body elongation is for each species paralleled by convergence in fin morphology but is not restricted to the limb homologues (i.e. paired fins): 1) reduction of pelvic fins, 2) dorsal and anal fin elongation, and 3) hypural fusions in the caudal skeleton. However, elongate species with short anal and dorsal fins have been described as well, such as those belonging to the Beloniformes (LIAO, 2002), or the Sphyraenidae (NELSON, 2006). Genetic studies of snake development have shown that the expansion of the *Hox* gene expression domains along the body axis both accounts for elongation of the body as well as the generally co-occurring loss of limbs (COHN AND TICKLE, 1999). As in snakes (COHN AND TICKLE, 1999), the combined occurrence of body elongation and fin reduction in fish may suggest that these changes may be linked to a common developmental mechanism. A recent study however, proposed prolongation of somitogenesis in the tail as a common developmental mechanism that may be associated with increases in caudal vertebral number. *Hox* genes are not thought to play a patterning role in the caudal region (WARD AND BRAINARD, 2007). Future studies should test these hypotheses of evolutionary changes in underlying processes that may determine phenotypic outcomes, resulting in body elongation.

### LATERALLY FLATTENED VERSUS ROUND BODY CROSS SECTION IN ELONGATED FISH: THE SAME KIND OF NATURAL SELECTION PRESSURES ?

One of the consistent conclusions revealed by evolutionary morphological studies is that any given feature of an organism is enclosed in a complex functional musculo-skeletal system (VANHOYDONCK AND VAN DAMME, 2001; PASI AND CARRIER, 2003). As selection acts on this integrated system, the total effect of selection on a component of the Bauplan and its functionality is therefore probably the result of direct and indirect effects of selection on surrounding structures as well. The outcome of selection can thus be influenced by



different types of selection on the same trait, e.g. predation and sexual selection on color patterns in fish (ENDLER, 1982) and stream velocity, foraging mode, and predation on the evolution of swimming (WEBB, 1984; SKULASON AND SMITH, 1995; WALKER, 1997). As many aspects of the morphology of the trichiurids are highly different compared to those of the other elongated species examined here, it may be more compelling to view the trichiurid body shape as a reflection of different types of environmental pressures (as all examined species are derived from ancestors with a laterally flattened body at some point). In these trichiurids, selection has favoured the evolution of a (bentho-)pelagic and predacious lifestyle with an elongate and laterally flattened body shape, whereas in the examined Anguilliformes, Mastacembelidae and Clariidae other influences have favoured the evolution of a lifestyle in close contact with or in the substrate with an elongate and round body. In order to recognize possible common evolutionary patterns it consequently might be more relevant to consider those elongate species that are similar in lifestyle, especially as convergence is thought to be primarily the result of species experiencing the same kinds of natural selection pressures (WIENS ET AL., 2003; HIBBITS AND FRITZGERALD, 2005). Therefore, the species examined here are separated into two groups: the pelagic species (trichiuridae) and those that are cavernicole, burrowing or benthic (anguilliforms, clariids and mastacembelids).

CONVERGENT TRAITS SHARED BY THE CAVERNICOLE, BURROWING OR BENTHIC SPECIES  
EXAMINED IN THIS DISSERTATION: SELECTIVE ADVANTAGE ?

Many of these convergences are also found in other elongate teleosts such as swamp inhabiting Notograptidae (MOOI AND GILL, 2004) and burrowing Synbranchidae (LIEM, 1980) and Chaudhuriidae (BRITZ AND KOTTELAT, 2003). The convergent traits shared by the anguilliforms, clariids and mastacembelids which are cavernicole, burrowing or benthic species are:

- Capacities to perform air-breathing.
- The median fins are confluent or nearly confluent (Asian mastacembelids). Species with confluent median fins all lack supra- and infracarinalis posterior muscles.
- The number of caudal fin rays is reduced.
- The body (except tail region) is approximately rounded in cross section.
- The circumorbital bones are to some degree reduced in size and/or number.

That air-breathing may yield a large selective advantage for the species examined here and for burrowing species or species living in swamps in general (e.g. Synbranchidae, ROSEN AND GREENWOOD, 1976; Galaxiidae, WATERS AND MCDOWALL, 2005), may be deduced from

the fact that air-breathing capabilities are reported for the Anguillidae, Clariidae and Mastacembelidae as well (GRAHAM, 1997). Many fishes, however, have evolved methods for extracting oxygen from air. Such adaptations permit these fishes to live in waters subjected to drying, or in oxygen-poor waters (e.g. swamps and burrows). Furthermore, this may enable a species to exploit environments, unavailable to other fishes. Air-breathing presents a clear advantage to species that live in hypoxic conditions (BICUDO AND JOHANSEN, 1979; KRAMER AND MCCLURE, 1982; CHAPMAN ET AL., 2002), but is not restricted to elongated ones (e.g. air-breathing in labyrinth fishes or suckermouth catfishes) (GRAHAM, 1997).

Species with elongate bodies perform undulatory locomotion, which is suited to high manoeuvrability as the whole body participates in large amplitude undulations (LAUDER, 2000). Many anguilliform swimmers are capable of backward as well as forward swimming by altering the propagation direction of the propulsive wave (GILLIS, 1996; 1997; CHOI ET AL, SUBMITTED). This ability is advantageous in burrowing and cavernicole species. The reduction in fins and round body may be seen as additional advantages when entering the burrows or narrow openings. Furthermore, an elongated body and the ability to perform extensive lateral undulatory movements, combined with the possibility to breath air, is advantageous for terrestrial locomotion as it uses the presence of sites of lateral resistance against which the animal can push and propel itself forwards (GILLIS, 1998). The anguillids and *Channallabes apus* are reported to make terrestrial excursions (GILLIS, 1998; VAN WASSENBERGH ET AL., 2006). *C. apus* is even known to feed on land (VAN WASSENBERGH ET AL., 2006). Being elongate may hold another evolutionary advantage as well: the ability to perform rotational feeding. Rotational feeding is a highly specialized feeding mode, adopted by several elongate, aquatic vertebrates (HELFMAN AND WINKELMAN, 1991; MEASEY AND HERREL, 2006) and it is likely that some morphological modifications are related to this feeding mode (e.g. hypertrophied jaw muscles, aponeurotic connection between epaxials and jaw muscles, etc., see IV.1; IV.3; IV.4.2).

Another mechanism that may influence or alter evolutionary outcomes, especially those related to specializations, involves trade-offs. For example, ant-eating mammals are well adapted for foraging and feeding on their specific prey type as they have a long, sticky, wormlike tongue, specialized salivary glands (sticky secretion), claws for digging and no teeth (REISS, 2001). Consequently, other food sources, that for example require teeth, cannot be exploited. The reduced eyes may present an example of such a trade-off as in those species with reduced eyes, other sensory systems probably compensate the reduced visual capacities (*Moringua edwardsi*, modified lateral line system, IV.1). Or the presence of well developed sensory systems may have allowed the eyes to become reduced

(e.g. Clariidae, Weberian apparatus and barbels, I.5: Mastacembelidae, elongate olfactory system, VI.1.1).

### CONVERGENT TRAITS SHARED BY THE MASTACEMBEDIDS AND ELONGATE CLARIIDS: CONSTRAINTS ?

Three architectural parallelisms are found in the Anguilliformes and Mastacembelidae examined here, but not in the elongate clariids. In these species, the hyohyoidei adductores has dorso-ventrally and caudally expanded, forming a sac-like structure surrounding the gill chamber; the levator operculi is ventrally expanded, covering a large area of the lateral surface of the opercle and the gill opening has become extremely small. A similar pattern has been noted in the burrowing synbranchiform species (Liem, 1980). The restricted opercular opening may be seen as an adaptation to avoid sediment from entering and subsequently obstructing the gill chamber. Why the hyohyoidei adductores and levator operculi are expanded is unclear. In general, contraction of the hyohyoidei adductores results in the constriction of the branchiostegal membrane (Winterbottom, 1974). As the opercular opening is restricted, it might be possible that pushing the water out of the gill cavity is needed, explaining its expansion. Another possibility is that this muscular organisation allows the opercular opening to close, which may be advantageous during terrestrial excursions or during burrowing. The levator operculi inserts onto the lateral surface of the opercle, whereas the hyohyoidei adductores on the medial surface of the opercle. The expansion of the levator operculi may have occurred in response to the expansion of the hyohyoidei adductores or vice versa (as both act as antagonists).

Constraints can be defined as restrictions that limit the evolutionary response of a character to external selection (ARNOLD, 1992; SCHWENK AND WAGNER, 2003). In this context, the importance of the air-breathing capacity and thus presence and functionality of the suprabranchial organ in elongate clariids may have constrained the hyohyoidei adductores, levator operculi and opercular opening to evolve in the same pattern as observed in the examined anguilliform and mastacembelid species. These elongate clariids thus may be less optimally adapted with regard to gill protection but a restricted opercular opening with enlarged hyohyoidei muscles may prevent optimal use of the in the posterodorsal part of the branchial cavity situated suprabranchial organ. Miniaturization is another example of constraints, as burrowing puts constraints on the diameter of the head and the body as well (see miniaturization VII.1.1).

## GENERAL CONCLUSION

The results of the morphological studies indicate that convergence in body elongation is not unambiguously related to a particular lifestyle, feeding mode, diet or other aspects. As body elongation has evolved many times and in different environmental and ecological circumstances (WARD AND BRAINARD, 2007) it might be considered a body shape that is advantageous for a large range of lifestyles. To my opinion it is not body elongation but rather other morphological modifications (e.g. at the level of the cranium, fins, tail, sensory systems, etc.) that allow species to adapt accordingly to their particular environmental and ecological requirements. However, it should be addressed that an elongate body might be considered a highly advantageous body form for wedging through small openings or for burrowing.

## **VII.4 CONSIDERATIONS REGARDING THE USE OF VERTEBRAL MORPHOLOGY AS A DIAGNOSTIC TRAIT**

Chapter V.1 (DE SCHEPPER ET AL., IN PRESS B) of this dissertation focused on the informative nature of vertebral shape variation. The aim of the study was to examine whether the shape of vertebrae is also a useful tool for taxonomic purposes. The elongate clariids were chosen as a case study as at that time, the systematics and phylogeny of the Clariidae was still a problem due to the lack of unambiguous, diagnostic traits to distinguish the different elongate clariid species. We hypothesized that the study of the postcranial skeleton could provide an outcome to this problem.

The geometric morphometric analysis of vertebral shape variation in three geographic populations of *C. apus*, collected in Gabon, led us to the conclusion that vertebral shape indeed is a useful diagnostic tool in taxonomy as it is able to detect subtle morphological differences and can group geographically separated specimens (V.1). In short, the geometric morphometric and biometric support for the separation of the northern population (Oyem) is high as this population always forms a distinct group (Figs V.1- 5-9). Based on the geometric morphometric analysis of the precaudal vertebrae in caudal view (Fig. V.1- 6) and the biometric analysis (Fig. V.1- 9), three additional groups are discernable (Makokou, Congo-Brazzaville and Franceville). To confirm whether the specimens represent two or four groups, additional morphological diagnostic traits needed to be defined.

The observed vertebral variation and clustering of specimens was cautiously explained through two possible hypotheses, being inter- and intraspecific variation. But the

moment the research took place, it was not clear at which species-level (species or subspecies) vertebral shape variation could be considered in the case of these elongate clariids because the taxonomic and phylogenetic research at the alpha-level of catfish from the Congo drainage was still in progress. As the phylogenetic study proceeded (DEVAERE, 2005) and data concerning the current systematic and taxonomic state of the clariid catfish family are recently published (DEVAERE ET AL., 2007A, B), we can reform and deepen the former hypothesis of V.1.

All specimens used in V.1 were initially considered representatives of the species '*Channallabes apus*'. Recent studies, however, have shown that these specimens actually belong to four species within the genus *Channallabes* (DEVAERE ET AL., 2007A, B). The northern population collected in Gabon represents *Channallabes alvarezi* (Devaere, 2007). The eastern population found in Makokou belongs to *Channallabes longicaudatus* (Devaere, 2007). Within the southern population, the specimens collected in Congo-Brazzaville represent the new species *Channallabes sanghaensis* Devaere, 2007, whereas those found in Franceville belong to the new species *Channallabes ogoensis* Devaere, 2007.

So, as discussed earlier, two hypotheses were proposed to explain the vertebral variation between the examined populations (V.1). As the four geographic populations represent four different species (DEVAERE ET AL., 2007A, B), the observed vertebral variation is to be considered interspecific now. Consequently the second hypothesis, where variation was thought to be intraspecific, is to be rejected. Furthermore, the data obtained by the geometric morphometric analysis of the precaudal vertebrae in caudal view and the biometric analysis, appear to be the best approaches in case of these African elongate catfish.

Analysing the patterns of hypural fusions (caudal skeleton) within and between the three different geographical regions, a similar morphological variation is observed, which means that the observed variation in hypural fusions is randomly distributed among the specimens and populations (DE SCHEPPER ET AL., 2004). Consequently, the morphology of the caudal skeleton of elongate Gabonese clariids turns out to be highly variable and can not be used as a diagnostic tool to distinguish the four geographically distributed species described by DEVAERE ET AL. (2007A, B).

Thus, vertebral shape indeed appears to be a useful diagnostic tool in taxonomy, applicable to recognize species.

Nevertheless, to my opinion some crucial considerations concerning the usefulness need to be addressed. A number of arguments that can counter its use are listed.

- 1) This research is highly invasive and destruction of the specimens is inevitable. This means that for some specimens (e.g. holotypes, paratypes), where studies are limited to non-invasive research alone, the study of vertebral shape is out of the question. The study of vertebral morphology is also excluded for species known from only one or few specimens (e.g. *Gymnallabes nops*, DEVAERE ET AL., 2005A).
- 2) The procedure is elaborate and time-consuming as all specimens need to be cleared and stained (HANKEN AND WASSERZUG, 1984). Furthermore, after the extensive procedure, the ability to use some of the individual vertebrae is not assured. Even the smallest remnants of incompletely cleared tissue, at crucial locations can obscure the exact position of landmarks. Fragile structures (e.g. small processes) may be damaged, erode or break off due to the aggressive chemicals or manipulation, again preventing to define the landmark position accurately.
- 3) Indispensable for field sampling is obviously externally visible morphological characters and an accurate though relatively simple identification key. It is obvious that the currently discussed diagnostic tool (vertebral shape) can not be taken into consideration in this regard as well. Furthermore, this technique is not usable for living specimens, so their sacrifice is needed.

To avoid some of the above mentioned disadvantageous qualities of the use of vertebral shape as a diagnostic trait, radiographs or CT-scanning may offer a solution as this technique is non-invasive, less complicated and certainly less time-consuming. Whether radiographs will display similarly high morphological details is not likely. Moreover if the resolution of the images and consequent morphological details will be sufficient to allow accurate placement of landmarks is questionable though may be worth while examining. Up to now, radiographs are frequently applied in systematic research for vertebral, hypural, pterygoid counts etc. (COLETTE AND CHAO, 1975; TRAVERS, 1984A; BÖHLKE, 1989, CASTLE, 1999). CT-scanning has proven to generate high quality images (DEVAERE ET AL., 2005A) and is likely to provide a high-quality non-invasive alternative.

## VII.5 CONSIDERATIONS REGARDING THE USE OF MORPHOLOGICAL STUDIES

One of the topics that is attended to in this dissertation is morphological variation. Fishes are known to display an enormous high amount of variation in form and function (Nelson, 1994) but this is even further addressed here. Even within a group of species, selected for their convergent morphological features, the observed variation in morphology, ecology, behaviour, etc. is striking, not to mention the variation that occurs within one species (e.g. *Anguilla anguilla*).

Variation is a central topic in evolutionary biology, both conceptually and historically (HALLGRIMSSON AND HALL, 2005). Understanding the nature of variation and comparing the anatomical features of organisms has been a central element of biology for centuries. Yet, methodological approaches to define variation remains a major problem within the evolution theory since Darwins' introduction of the term (BOWLER, 2005), despite the diverse approaches, from a descriptive field to a quantitative science, and attempts to analyse, define and explain variation (ADAMS ET AL., 2004; RICHTSMIEIER ET AL., 2005; VAN VALEN, 2005). One basic and central topic, regardless the methodical approach of variation, still returns: the description of anatomical features of the organisms. Basically, the detailed knowledge of the anatomical basis of biological systems is crucial for the study of any biological aspect. Nevertheless, it is surprising how many species, even though well known, lack solid anatomical descriptions. This is illustrated by the species studied in the present dissertation, which are, however, well known to the general public.

The current need for detailed, solid, morphological descriptions is expressed in the fact that those, presented in this dissertation, are already applied in further research.

- The myological and osteological descriptions of the representatives of the Anguilliformes (IV) are currently applied for phylogenetic purposes, in order to unravel evolutionary relationships within the order Anguilliformes (PhD Eagderi S)
- The detailed descriptions of myology, osteology as well as those dealing with the trophic phenotypic variation within *Anguilla anguilla* have subsequently led to the recently started study with the phenotypic plasticity of *Anguilla anguilla*, and its relation to feeding ecology and pollution as the central aspect. The theoretical results concerning bite forces will be used and compared with experimentally collected data (PhD Ide C).
- The morphological data of the head- and tail-first burrowing *Pisodonophis boro* and the tail-first burrowing species (*Heteroconger hassi* and *H. longissimus*) have

led to and have allowed a biomechanical study focussing onto forward and backward swimming as well as burrowing movements of these species (Choi HF).

- Current biomechanical studies performed at the University of California (Mehta R and Wainwright PC), focussing on prey capture functional morphology in eels, are interested in a collaboration project, where our morphological data will be combined with their biomechanical studies.



**VIII**

Summary - Samenvatting



## VIII SUMMARY

This dissertation has focussed on a targeted selection of species that are convergent in having an elongate body. The central aim of this study was to identify how a whole set of structural modifications in the morphology of elongate clariid catfishes are related to different components such as (1) miniaturized head, (2) a special fossorial lifestyle, (3) the presence of hypertrophied jaw muscles and (4) anguilliformity. Therefore, a functional-morphological component analysis, attempting to decouple these four components, has been performed, with *Channallabes apus*, chosen as the reference species for the elongate clariids.

I In the introduction, an overview is given of the general frame of this study, explaining why a functional-morphological component analysis was proposed. First, the four components are described. Subsequently, the hypothesis of decoupling these components, based on a targeted selection of phylogenetically related species differing in one component only, is explained. Argumentation is given for the choice of the clariid reference species and an explanation is given about the choice of the comparison models (species groups) that are used to examine a particular component. The different higher level taxa are introduced with a brief introduction and background of the phylogenetic position of the species used in this dissertation.

III 'Material and methods' lists the specimens of all species that were used in this thesis. A total of 958 specimens belonging to 17 species and representing three unrelated higher level taxa, are examined using a multidisciplinary approach. These include morphological, morphometrical, biometrical and modelling approaches. A detailed description of the methods that were applied in the course of this study is given. The morphological approach comprises preparation of specimens, clearing and staining protocols, dissections, and serial histological and CT sections. Visualization occurred through light and stereomicroscope equipped with a camera lucida, where CT- and histological sections were used for generating graphical 3D-reconstructions. The morphometric approach describes the shape of crania and vertebrae based on landmarks. For the biometric approach, cranial, vertebral and pectoral spine measurements, as well as some meristic data were collected. The data were processed applying several statistical analyses. To avoid misinterpretations some terminologies, applied throughout this study are explained.

This summary lists the most important results and conclusions of this study, reflecting the aims stated in chapter II.

IV. This chapter presents the morphological descriptions and discussion on several aspects of the cranial and postcranial Bauplan in elongated representatives of a basal teleostean lineage: Elopomorpha.

IV.1 *Moringua edwardsi* - The osteological and myological morphology of the head and caudal fin are described in this head-first burrowing species. Externally, pronounced morphological specializations for a fossorial lifestyle are observed and these include reduced eyes; lack of color; absent paired, low dorsal and anal fins; elongate, cylindrical body; and reduced head pores of the lateral line system. We hypothesize that the lack of these pores is a specialization for burrowing, avoiding the entering of sediment into the canals but at the same time allowing mechanical stimulation of the neuromasts due to the presence of internal dermal cavities. The reduced eyes, advantageous during head-first burrowing from a protective point of view, possibly create space allowing the expansion of the adductor mandibulae muscles. Jaw adductor muscle size and fibre direction can be linked to either head-first burrowing (preventing the lower jaw from being dislodged) or a predatory lifestyle (increased bite forces). Skull fortification, advantageous for head-first burrowing is improved by scarf joints, with large overlaps between bones, and by the large interorbital distance. Cranial modifications related to miniaturization can not be excluded. The caudal fin is similar to that in non-burrowing eels and thus can be considered as not specialized.

IV.2 *Heteroconger hassi* and *H. longissimus* - The osteology and myology of the head and caudal fin are described in these tail-first burrowing species. The small jaw muscles and large eyes (with consequent narrow interorbital distance) are probably related to their suction-dominated feeding mode. Since *H. hassi* and *H. longissimus* burrow tail-first, the observed reduced skull fortification (thin, non-overlapping bones) may be sufficient considering its sessile lifestyle, but may be related to miniaturization as well. The heterocongrines have undergone several morphological caudal fin specializations for their tail-first burrowing lifestyle, resulting in a strong, pointed, burrowing tool. Muscular modifications are observed and considered to restrict caudal fin (and rays) movements, thus offering strength avoiding the tail-tip to bend during burrowing.

IV.3 *Pisodonophis boro* - This species is of special interest as it is able to burrow head-first as well as tail-first. The morphology of the head and the caudal fin are described. Many aspects of the morphology of the head of both head-first burrowing species (*P. boro* and *M. edwardsi*) are highly similar and likely related to their burrowing

lifestyle, except for the lateral line system, not modified in *P. boro*. The absence of external pores in *M. edwardsi* may be related to being mostly subterranean (but the system remains functional due to its modifications), whereas in *P. boro* the presence of external pores is likely to be related to the habit of scanning the surroundings. The caudal fins of *P. boro* and the heterocongrines are similarly modified for tail-first burrowing. Even though both terminal parts of the body penetrate the substrate in *P. boro*, external and internal modifications are less extensive at the level of the head. As the head is not only used for burrowing but also has to accommodate for feeding and respiration, constraints and trade-offs on the mechanical cranial design are recognized.

**IV.4.3** *Anguilla anguilla* - The cranial variation resulting in two extreme phenotypes, i.e. broad- and narrow-headed eels, are examined using a multidisciplinary approach. This study shows that these phenotypes co-occur syntopically in the Scheldt-Lippensbroek as well as across waters in Belgium. All methods used in this study point towards the presence of a dimorphism in head size (biometry) and shape (morphometry), and the cranial variation is significantly better described having a bimodal rather than a unimodal distribution. The phenotypic variation is reflected in external head shape (mainly head width, head height and jaw length) as well as in the shape of the skull (snout length, skull height, width and length of the post-orbital region, length and inclination of the sphenotic processes, length of the pterotic and epiotic processes).

**IV.4.2** *Anguilla anguilla* - In this study a detailed description of the cranial myology of the narrow-headed and broad-headed phenotypes of *A. anguilla* is provided. Morphological and quantitative differences in cranial musculature between these phenotypes are examined as well as bite forces and functional properties are predicted using a biomechanical model for mouth closing. The mass of the mouth closing muscles of the broad-headed eels was about three times higher compared to that of the narrow-headed eels of the same total length. The A3-part shows much less difference between the two phenotypes, which could be explained by space constraints on this deep subdivision. The mass of the levator arcus palatini and dilatator operculi muscles is larger in the broad-headed eels. That of the levator operculi and protractor hyoidei is less discriminative between the two phenotypes. The predicted magnitude of force generated in the extreme broad-headed eels is about twice the size of that predicted for the extreme narrow-headed eel and is reflected in structural differences belonging to the feeding apparatus. These differences may be beneficial for the increased piscivorous feeding habits, and thus rotational feeding in broad-headed eels.

**IV.4.3** *Conger conger* - The cranial osteology and myology is described in this non-burrowing species and subsequently compared to that of other burrowing species. Few

differences in skull morphology are observed between the two non-burrowing species (*A. anguilla* and *C. conger*). The shape of the neurocranium is markedly different among the non-, head-first and tail-first burrowers. The morphology of the lower jaw, jaw muscles and associated structural modifications is different in the heterocongrines but similar in the other species and presumably related to differences in feeding but may be associated to burrowing as well.

**IV.4.1** *Conger conger* and *Anguilla anguilla* - The osteology and myology of the caudal fin is described for two non-burrowing species, *A. anguilla* and *C. conger*. The non- and head-first burrowing species (*M. edwardsi*), without consolidated caudal skeletons tend to have more, longer and movable caudal fin rays. As the caudal fin rays are short and fixed by thick tissue in *H. hassi*, *H. longissimus* and *P. boro*, dorso-ventral movements are less obvious. These modifications are advantageous as they ensure an efficient penetration of the sediment. Even though the caudal fin muscles of Anguilliformes in general are reduced, reductions in the tail-first burrowers are more extreme. A trade-off between flexibility and strength of the caudal fin in tail-first burrowers is probably present. The caudal fin musculature is likely to offer flexibility and bilateral mobility to some degree as well as strength.

**IV.** This chapter presents the morphological descriptions and discussion on several aspects of the cranial and postcranial Bauplan in elongated representatives of a basal euteleostean lineage: Ostariophysi.

**V.1** *Channallabes apus* - This study focuses on the informative nature of vertebral shape variation for taxonomy, taking elongate clariids as a case study. Two hypotheses are proposed to explain the observed vertebra variation: (1) interspecific variation and (2) intraspecific variation. It can be concluded that vertebral shape variation is a good and useful tool in systematics, however, at this moment (see VII.4) and in case of *C. apus*, it is not clear at which taxonomic-level (species or subspecies) vertebral shape variation is explicatory.

**V.2** *Channallabes apus* - The inter- and intraspecific variability in the caudal skeleton of elongate clariids is examined and described. Hypural fusions and haemal and neural spines show most variation. The observed morphological variation appears to be geographically independent, in contrast to other morphological features such as vertebrae.

**V.3** *Channallabes apus* and *Clarias gariepinus* - The caudal fin muscles of a fusiform and an elongated clariid representative are described. The muscles of the caudal fin of *Channallabes apus* are reduced with respect to those found in *Clarias gariepinus* and other generalized teleosts. Reductions are found in the size of the interradians, absence of

posterior carinalis muscles and the origin of the flexor dorsalis and flexor ventralis in particular.

IV. This chapter presents the morphological descriptions and discussion on several aspects of the cranial and postcranial Bauplan in elongated representatives of a derived teleostean lineage: Acanthomorpha.

VI.1.1 Mastacembelidae - This study focuses on the cranial myological features of mastacembelids, with *M. marcheii*, *M. brichardi* and *M. mastacembelus* as case studies. Jaw muscle enlargement in *M. brichardi* mainly occurs in the A1 and A2 subdivisions. The size of the A3 may be constrained. A stronger bite is suggested based on the jaw muscle size and high coronoid process, and is also reflected in dietary differences. Space for the expanded jaw muscle may be provided by the reduction of the eyes and the infraorbital bones. Some aspects of the neurocranium, suspensorium and infraorbital bones are reduced, which may be related to jaw muscle expansion but miniaturization can not be excluded.

VI.1.2 Mastacembelidae - The morphology of the caudal fins of *Mastacembelus mastacembelus*, with distinct median fins, and *M. marcheii* and *M. brichardi* which have confluent median fins, are described. The results indicate that no relation between skeletal reductions and myological reductions is present in the examined mastacembelids. Compared to *M. mastacembelus*, *M. marcheii* and *M. brichardi* solely lack the carinalis posterior muscles, which is likely to be related to the confluence of the unpaired fins.

VI.2 Trichiuridae - This study provides a detailed description of the head muscles of *Aphanopus carbo* and *Trichiurus lepturus*. Differences are found in the insertion of the epaxials and supracarinalis muscles. These differences are presumably related to the difference in cranial shape at the level of the supraoccipital crest. Secondly, the mechanics of the mouth closing system of these trichiurids has been examined using biomechanical modeling. This study illustrates that not only within different aspects of feeding (biting and closing the mouth), but also between feeding and locomotion, trade-offs have to be considered if we fully want to understand the functional morphology of the jaw system in fishes.

VII The 'General Discussion' combines all data collected in this study. The proposed functional-morphological component analysis is critically examined. First all comparison models (species groups), decoupled for a particular component are considered and accepted or rejected as suitable models. As becomes clear in this comparative section, the considered components form a closely related network within the cranial system as a

whole, hindering the demarcation of the effect of or interaction between individual components. Second, the obtained information is projected onto the elongated clariid reference species, *C. apus*. It can be concluded that potential components, regardless which ones are chosen or how many are considered, are mutually linked to each other and may have an indirect effect on several other structural elements. Third, some evolutionary hypotheses with respect to convergent evolution in elongate species and some examples are supplemented. More morphological traits are convergent in species experiencing more similar kinds of natural selection pressures. But evolutionary outcomes are highly influenced by constraints and trade-offs as well. Finally some considerations regarding the use of vertebral morphology as a diagnostic trait and morphological studies in general are made.



## VIII SAMENVATTING

Deze doctoraatsverhandeling behandelt doelgericht geselecteerde soorten die allen convergent zijn in lichaamsverlenging. De centrale doelstelling van deze studie bestond erin te bepalen hoe een hele set aan structurele morfologische veranderingen bij verlengde clariïde katvissen gerelateerd zijn aan verschillende componenten zoals 1) geminiaturizeerde kop, 2) een speciale gravende levenswijze, 3) de aanwezigheid van hypertrofe kaakspieren en 4) lichaamsverlenging. Vandaar dat in deze studie een functionele-morfologische componentenanalyse werd uitgevoerd, teneinde deze vier componenten te kunnen ontkoppelen. Hierbij werd *Channallabes apus* gekozen als referentie soort voor de verlengde clariïde katvissen.

I In de inleiding wordt een overzicht gegeven van het algemeen kader van deze studie. Ook de redenen voor het aanwenden van een dergelijke functionele-morfologische componentenanalyse, de keuze van *C. apus* als referentie soort voor de verlengde clariïde katvissen en de keuzes van de vergelijkings modellen (groepen nauw verwante soorten) om een bepaalde component te bestuderen, worden toegelicht. Tenslotte wordt in dit hoofdstuk een korte inleiding en achtergrond gegeven van de phylogenetische plaats van de hier bestudeerde soorten.

III Het hoofdstuk 'Materiaal en Methode' bevat een lijst van alle specimens van de verschillende soorten die in deze studie gebruikt werden. In totaal werden 958 vissen, behorende tot 17 soorten en 3 hogere taxa met een multidisciplinaire benadering (morfologisch, morfometrisch, biometrisch en modelmatig) bestudeerd. De methodes die in de loop van deze studie werden aangewend worden gedetailleerd besproken. De morfologische studies gebeuren aan de hand van specimens, die eerst verdoofd, gedood en gefixeerd werden (voorbereiding), ophelderingen, dissecties en seriële coupe reeksen. Visualizatie gebeurde aan de hand een licht- en stereomicroscoop waarop een camera lucida is gemonteerd, CT-scannings, radiografiën en 3D-reconstructies. De morfometrische studie beschrijft de vorm van schedels en wervels aan de hand van landmarks. In de biometrische studies werden metingen (en tellingen) op de kop, wervels en pectorale stekels uitgevoerd. De verkregen data werden geanalyseerd met behulp van verschillende statistische analyses. Tenslotte wordt een verklarende lijst gegeven van gebruikte termen teneinde misinterpretaties te voorkomen.

In deze samenvatting worden de meest belangrijke resultaten en conclusies van deze study opgesomd en biedt zodoende een antwoord op de doelstellingen geformuleerd in chapter II.

IV. Dit hoofdstuk toont de morfologische beschrijvingen en discussie van verschillende aspecten van het craniale en postcraniale Bauplan in verlengde vertegenwoordigers van de Elopomorpha.

IV.1 *Moringua edwardsi* - De osteologische en myologische kenmerken van de kop en de staartvin worden beschreven. Uwendig kunnen uitgesproken morfologische specialisaties voor een gravende levenswijze geobserveerd worden en deze omvatten, gereduceerde ogen, depigmentatie, afwezige parige vinnen, verlengde anale en dorsale vinnen, verlengd en cilindrisch lichaam en gereduceerde openingen van het kop lateraal zijlijnsysteem. We vermoeden dat de afwezigheid van deze openingen een specialisatie is voor een gravende levenswijze aangezien dit het binnenkomen van sediment in de sensorische kanalen verhindert maar tegelijkertijd de mechanische stimulatie van de neuromasten toelaat door de aanwezigheid van interne dermale holtes. De gereduceerde ogen creëren mogelijk plaats voor een verbreding van de kaakspieren. De grootte van de kaakspier even als de vezelrichting kunnen enerzijds gerelateerd worden aan het graven met de kop eerst (vermijdt het ontwrichten van de onderkaak) en anderzijds aan een predatorische levenswijze (toename van de bijtkracht). De brede interorbital ruimte en 'scarf joints' die bovendien een hoge mate van overlap vertonen, bieden een hogere stevigheid aan de schedel. Craniale modificaties kunnen echter ook gerelateerd zijn aan miniaturisatie. De staartvin is gelijkaardig aan deze van de niet gravende palingen en kan dus beschouwd worden als niet gespecialiseerd.

IV.2 *Heteroconger hassi* and *H. longissimus* - De osteologie en myologie van de kop en staartvin worden besproken in deze staartgravende vissen. De aanwezigheid van kleine kaakspieren en grote ogen kan vermoedelijk gerelateerd worden aan hun zuigende voedingswijze. Aangezien *H. hassi* en *H. longissimus* graven met de staart eerst, kan vermoed worden dat schedelversterkingen overbodig zijn, wat de aanwezigheid van dunne, niet overlappende beenderen kan verklaren. Dit kan echter ook gerelateerd zijn aan miniaturisatie. De staartvin van deze soorten vertoont verschillende aanpassingen voor hun gravende levenswijze, resulterend in een sterk en puntig uiteinde. Modificaties ter hoogte van de spieren, ten opzichte van teleosten in het algemeen, zijn eveneens aanwezig. Deze zouden de beweeglijkheid van de caudal vinstralen beperken en aldus meer stevigheid bieden waardoor de staarttip tijdens het graven niet of minder zou buigen.

**IV.3** *Pisodonophis boro* - Opmerkelijk aan deze soort is de mogelijkheid om zowel met de kop als met de staart eerst te graven. De morfologie van de kop en de staartvin worden beschreven. Veel aspecten van de kopmorfologie van beide kopgravers (*P. boro* and *M. edwardsi*) zijn gelijkaardig en hoogst waarschijnlijk gerelateerd aan hun gravende levenswijze. Het koplateraal zijlijn systeem in *P. boro* is echter niet gemodificeerd zoals in *M. edwardsi*. De afwezigheid van externe openingen in *M. edwardsi* kunnen gerelateerd worden aan hun permanente ondergrondse levenswijze (terwijl het systeem toch functioneel blijkt door de modificaties), terwijl in *P. boro* de aanwezigheid van dergelijke openingen gerelateerd zou zijn aan het gebruik ervan om de omgeving te scannen. De staartvin van *P. boro* en de heterocongrine palingen zijn gelijkaardig gemodificeerd voor het staartgraven. In *P. boro* zijn beide uiteinden van het lichaam aangepast om de bodem te penetreren. De in- en uitwendige modificaties zijn echter meer uitgebreid en uitgesproken ter hoogte van de staart. Aangezien de kop niet alleen gebruikt wordt om te graven maar ook tussenkomt in andere functies zoals respiratie en voeding, kunnen beperkingen ('constraints') en compromissen ('trade-offs') ter hoogte van de kop terug gevonden worden.

**IV.4.3** *Anguilla anguilla* - De craniale variatie resulterend in twee extreme phenotypes, nl breed-koppige en smal-koppige palingen, worden hier multidisciplinaire bestudeerd. Deze studie toont aan dat beide phenotypes syntopisch voorkomen in het schelde-Lippensbroek en over geheel België. Alle methodes die in deze studie worden aangewend duiden op de aanwezigheid van kop-dimorfisme in grootte (aangetoond a.h.v. biometrie) en vorm (a.h.v. morfometrie). De craniale variatie wordt significant beter beschreven door een bimodale distributie dan door een unimodale. De fenotypische variatie is weerspiegeld in de uitwendige kopvorm (voornamelijk breedte en hoogte van de kop en lengte van de onderkaak) maar ook in de vorm van de schedel (preorbitale lengte, hoogte van de schedel, breedte en lengte van postorbital zone, lengte en inclinatie van het sphenotische uitsteeksel and lengte van de pterotische en epiotische uitsteeksels).

**IV.4.2** *Anguilla anguilla* - In deze studie worden morfologische en quantitative verschillen in craniale spieren van beide fenotypes, breed-koppige en smal-koppige palingen, bestudeerd en beschreven. Bijtkrachten en functionele eigenschappen van het bijtapparaat worden voorspeld aan de hand van een biomechanisch model. De massa van de kaakspieren van de breed-koppige palingen is ongeveer drie keer hoger in vergelijking met dat van smal-koppige palingen van gelijke lengte. Het A3-deel vertoont minder verschillen tussen beide fenotypes wat kan verklaard worden door ruimtelijke beperkingen opgelegd aan dit dieper gelegen spierdeel. De massa van de levator arcus palatini en dilatator operculi is hoger bij de breed-koppige palingen. Het verschil in massa van de

levator operculi en protractor hyoidei is minder uitgesproken tussen de twee fenotypes. De voorspelde grootte van de kracht die kan gegenereerd worden door de kaakspieren in de breed-koppige palingen is ongeveer twee keer de grootte van deze voorspeld voor de smal-koppige palingen en is eveneens weerspiegeld in structurele verschillen in het voedingsapparaat. Deze verschillen zijn vermoedelijk voordelig voor de toegenomen piscivore voeding en rotatievoeding in breed-koppige palingen.

**IV.4.3** *Conger conger* - De craniale osteologie en myologie wordt beschreven in deze niet gravende soort en wordt vervolgens vergeleken met deze van gravende soorten. De schedelmorfologie van twee niet gravende soorten (*A. anguilla* and *C. conger*) verschilt zeer weinig. De vorm van de schedel verschilt wel opmerkelijk tussen niet gravers, kopgravers en staartgravers. De morfologie van de onderkaak, kaakspieren en hiermee geassocieerde structurele modificaties zijn gelijkaardig in de hier bestudeerde palingen met uitzondering van de staartgravers. Deze verschillen zijn waarschijnlijk eerder gerelateerd aan een verschillende voedingswijze (zuigvoeding in staartgravers).

**IV.4.1** *Conger conger* en *Anguilla anguilla* - De osteologische en myologische kenmerken van de staartvin bij twee niet gravende palingen, *A. anguilla* and *C. conger*, worden beschreven. De palingsoorten die niet graven en met de kop eerst graven, hebben minder verstevigde staartvinnen en blijken langere en beweeglijke caudale vinstralen (in horizontaal en vertikaal vlak) te bezitten. Dorso-ventrale bewegingen van de caudale vinstralen zijn minder vanzelfsprekend bij *H. hassi*, *H. longissimus* en *P. boro* waar de caudale vinstralen kort zijn en gefixeerd door een dikke bedekkende weefsellaag. Deze morfologische aanpassingen zijn voordelig daar ze een effectieve penetratie van het sediment bevorderen. Hoewel de staartvinspiers bij Anguilliformes in het algemeen gereduceerd zijn, zijn deze in the staartgravers toch meer uitgesproken. Bovendien is een 'trade-off' tussen flexibiliteit en stevigheid in de staartvin vermoedelijk aanwezig. De spieren van de caudale vin bieden hoogst waarschijnlijk zowel flexibiliteit en bilaterale beweeglijkheid als stevigheid om extreem buigen te vermijden.

**IV.** Dit hoofdstuk toont de morfologische beschrijvingen en discussie van verschillende aspecten van het craniale en postcraniale Bauplan in verlengde vertegenwoordigers van de Ostariophysi.

**V.1** *Channallabes apus* - In deze studie wordt de informatieve waarde van wervelvorm voor systematische doeleinden bestudeerd, met verlengde clariide katvissen als 'case study'. Twee hypotheses kunnen naar voor gebracht worden om de aanwezigheid van de aangetoonde wervel variatie te verklaren: (1) interspecifieke variatie en (2) intraspecifieke variatie. Er kan besloten worden dat wervelmorfologie en -vorm een goed

en bruikbaar middel is in systematische studies. Maar, met betrekking tot *C. apus*, is het momenteel (zie VII.4) niet duidelijk op welk niveau (soort of subsoort) de variatie in wervel vorm verklarend is.

**V.2** *Channallabes apus* - De inter- en intraspecifieke variatie in de benige elementen van de staartvin van verlengde clariide soorten wordt bestudeerd en besproken. De grootste variatie wordt gevonden in hypurale fusies en in haemaal- en neuraalstekels. De geobserveerde morfologische variatie blijkt geografisch onafhankelijk te zijn, in tegelstelling tot wat verkregen werd op basis van andere elementen zoals de vorm van de wervels.

**V.3** *Channallabes apus* en *Clarias gariepinus* - De spieren van de staartvin bij een fusiforme en een verlengde clariide soort worden beschreven. Deze van de verlengde soort, *C. apus* zijn gereduceerd in vergelijking met deze van de fusiforme soort *C. gariepinus* en andere teleosten. Reducties worden geobserveerd in de interraddialia, de afwezigheid van de infra- en supracarinalis posterior spieren en in de oorsprong van de flexor dorsalis en flexor ventralis.

**IV.** Dit hoofdstuk toont de morfologische beschrijvingen en discussie van verschillende aspecten van het craniale en postcraniale Bauplan in verlengde vertegenwoordigers van de Acanthopterygii.

**VI.1.1** Mastacembelidae - Deze studie richt zich op de craniale myologie van Mastacembelidae met *M. marcheii*, *M. brichardi* en *M. mastacembelus* als 'case studies'. De uitbreiding van de kaakspier bij *M. brichardi* doet zich voornamelijk voor ter hoogte van de A1 en A2 delen van de adductor mandibulae. De grootte van de A3 is vermoedelijk gelimiteerd. Gebaseerd op de kaakspiergrootte en hoogte van de cononoid processus kan een hogere bijtkracht vermoed worden, wat weerspiegeld is in dieetverschillen. Sommige aspecten van de schedel, suspensorium en infraorbitale beenderen zijn gereduceerd, evenals de ogen. Deze modificaties zijn mogelijk gerelateerd aan de expansie van de kaakspieren, doch miniaturisatie kan niet uitgesloten worden.

**VI.1.2** Mastacembelidae - De morfologie van de staartvinnen wordt beschreven bij *Mastacembelus mastacembelus*, met gescheiden mediane vinnen, en *M. marcheii* en *M. brichardi* met confluerende mediane vinnen. De resultaten doen vermoeden dat er geen relatie bestaat tussen skeletale reducties en myologische reducties in deze bestudeerde soorten. *M. marcheii* en *M. brichardi* ontbreken uitsluitend de carinalis posterior spieren, vergeleken met *M. mastacembelus*, wat vermoedelijk gerelateerd is aan de confluentie van de onpare vinnen.

VI.2 Trichiuridae - Deze studie biedt een gedetailleerde beschrijving van de craniale spieren bij *Aphanopus carbo* en *Trichiurus lepturus*. Verschillen in insertie van de epaxiale supracarinale spieren worden opgemerkt. Deze verschillen zijn waarschijnlijk gerelateerd aan het verschil in hoogte van de supraoccipitale kam. Verder wordt aan de hand van een biomechanisch model het mondsluitingsmechanisme in deze trichiuriden bestudeerd. Deze studie illustreert dat 'trade-offs' niet alleen m.b.t. verschillende aspecten van voeden zelf (vb. hard bijten en snel sluiten) beschouwd moeten worden maar ook tussen voeden en voortbeweging, als we de functionele morfologie van het kaaksysteem volledig willen begrijpen.

VII In de 'General Discussion' worden alle data van deze studie gecombineerd. De vooropgestelde functionele-morfologische componentenanalyse wordt kritisch besproken. Eerst worden alle vergelijkingsmodellen (soorten groepen), die ontkoppeld zijn voor een bepaalde component, afzonderlijk beschouwd en vervolgens als model aanvaard of verworpen. Uit deze vergelijkende studie blijkt duidelijk dat de beschouwde componenten een zeer nauw verbonden netwerk vormen binnen het craniale systeem, wat de afbakening van effecten tengevolge van een bepaalde component verhindert. In een tweede onderdeel wordt de verkregen informatie geprojecteerd op de verlengde clariide referentie soort, *C. apus*. Er kan besloten worden dat mogelijke modificatie componenten, ongeacht hoeveel of welke worden beschouwd, onderling zeer nauw verbonden zijn en bovendien onrechtstreeks een effect kunnen uitoefenen op verschillende andere structurele elementen. Als derde aspect worden enkele hypotheses met betrekking tot convergente evolutie in verlengde vissen en enkele voorbeelden uitgewerkt. Meerdere morfologische elementen zijn convergent bij soorten die onderhevig zijn aan een groter aandeel gelijkaardige natuurlijke selectiedruk. Verder wordt het resultaat van evolutie ook sterk beïnvloed door 'constraints' en 'trade-offs'. Tenslotte worden nog enkele beschouwingen met betrekking tot het gebruik van wervel morfologie en morfologische studies in het algemeen aangekaart.

**IX**

Literature Cited





## LITERATURE CITED

- ADAMS DC, ROHLF FJ. 2000. Ecological character displacement in *Plethodon*: Biomechanical differences found from a geometric morphometric study. *Proceedings of the National Academy of Science of the United States of America*. 97(8): 4106-4111.
- ADAMS DC, ROHLF FJ, AND SLICE DE. 2004. Geometric morphometrics: ten years of progress following the 'revolution'. *Italian Journal of Zoology*. 71(1):5-16.
- ADRIAENS D, AERTS P, VERRAES W. 2001. Ontogenetic shift in mouth opening mechanisms in a catfish (Clariidae, Siluriformes): a response to increasing functional demands. *Journal of Morphology*. 35: 181-208.
- ADRIAENS D, DEVAERE S, TEUGELS GG, DE KEGEL B, VERRAES W. 2002. Intraspecific variation in limblessness in vertebrates: a unique example of microevolution. *Biological Journal of the Linnean Society*. 75: 367-377.
- ADRIAENS D, VERRAES W, TAVERNE L. 1997. The cranial lateral-line system in *Clarias gariepinus* (Burchell, 1822) (Siluroidei: Clariidae): morphology and development of canal related bones. *European Journal of Morphology*. 35(3): 181-208.
- ADRIAENS D, VERRAES W. 1997. Ontogeny of the cranial musculature in *Clarias gariepinus* (Siluroidei: Clariidae): the adductor mandibulae complex. *Journal of Morphology*. 229: 255-269.
- AFMSC, ATLANTIC STATES MARINE FISHERIES COMMISSION. 2004. Public Information Document for potential changes to the Interstate fishery Management Plan for American eel. American Eel Plan Development Team. Washington: USA.
- AGNÈSE JF, TEUGELS GG. 2005. Insight into the phylogeny of African Clariidae (Teleostei, Siluriformes): Implications for their body shape evolution, biogeography, and taxonomy. *Molecular Phylogenetics and Evolution*. 36 (3): 546-553.
- ALEXANDER RM. 1965. Structure and function in the catfish. *Journal of Zoology (London)*. 148: 88-152
- ANON A. 2000. Environment and biology of deep-water species *Aphanopus carbo* in NE Atlantic: basis for its management (BASBLACK). Final report of the EU study project CT 97/0084. DGXIV European Commission. pp 95.
- AOYAMA J, SHINODA A, SASAI S, MILLER MJ, TSUKAMOTO K. 2005. First observations of the burrows of *Anguilla anguilla*. *Journal of fish biology*. 67:1534-1543.
- AOYAMA J, KOBAYASHI T, TSUKAMOTO K. 1996. Phylogeny of eels suggested by mitochondrial DNA sequences. *Nippon Suisan Gakkaishi*. 62: 370-375.
- ARRATIA G. 1983. The caudal skeleton of ostariophysan fishes (Teleostei): intraspecific variation in Trichomycteridae (Siluriformes). *Journal of Morphology*. 177: 213-229.
- ARRATIA G. 1997. Basal teleosts and teleostean phylogeny. *Palaeo Ichthyologica*. Vol 7. Verlag Friedrich Pfeil, München.
- ARRATIA G. 1999. The monophyly of Teleostei and stem-group teleosts. In: *Mesozoic fishes 2, Systematics and fossil record*. Arratia G, Schultze HP. Verlag Dr. Friedrich Pfeil, München, Germany. pp265-334.

- ARRATIA G. 2003A. The catfish head skeleton - An overview. In: Catfishes. Arratia G, Kapoor AS, Chardon M, Diogo R, eds. Enfield, Science Publishers, Inc.
- ARRATIA G. 2003B. The siluriform postcranial skeleton. In: Catfishes. Arratia G, Kapoor AS, Chardon M, Diogo R, eds. Enfield, Science Publishers, Inc.
- ARNOLD SJ. 1992. Constraints on phenotypic evolution. *The American Naturalist*. 140: 85-107.
- ASANO H. 1962. Studies on the congrid eels of Japan. *Bulletin Misaki Marine Biology Institute Kyoto University*. 1: 1-71.
- ATKINSON RJA, TAYLOR AC. 1991. Burrows and burrowing behavior of fish. *Symposia of the Zoological Society of London*. 63: 133-155.
- ATKINSON RJA, PULLIN RSV. 1996. Observations on the burrows and burrowing behaviour of the red band-fish, *Cepola rubescens* L. *Marine Ecology - Pubblicazioni della stazione Zoologica di Napoli I*. 17 (1-3): 23-40.
- AUBRET F, SHINE R, BONNET X. 2004. Adaptive plasticity in snakes. *Nature*. 431: 261-262.
- BANTSEEV V, MORAN KL, DIXON DG, TREVITHICK JR, SIVAK JG. 2004. Optical properties, mitochondria and sutures of lenses of fishes: a comparative study of nine species. *Canadian Journal of Zoology*. 82: 86-93.
- BAREL CDN. 1983. Towards a constructional morphology of cichlid fishes (Teleostei, Perciformes). *Netherlands Journal of Zoology*. 33(4): 357-424.
- BAREL CDN. 1984. Form-relations in the context of constructional morphology: the eye and suspensorium of lacustrine cichlidae (Pisces, Teleostei). *Netherlands Journal of Zoology*. 34:439-502.
- BASTROP R, STREHLOW B, JSS K, STURMBAUER C. 2000. A new molecular phylogenetic hypothesis for the evolution of freshwater eels. *Molecular Phylogenetics and Evolution*. 14: 250-258.
- BATH H. 1960. Über die Körperhaut des "Röhrenaals "*Xarifania hassi*" (Heterocongrinae). *Cell and Tissue Research*. 51:728-734.
- BEAK INTERNATIONAL INCORPORATED. 2001. The decline of American eel, (*Anguilla rostrata*) in the Lake Ontario/St. Lawrence river ecosystem: a modelling approach to identification of data gaps and research priorities. Report for Lake Ontario Committee. Ontario: Beak International Incorporated.
- BELOUZE A. 2001. Compréhension morphologique et phylogénique des traxons actuels et fossiles rapportés aux Anguilliformes (poissons, téléostéens). PhD-thesis. Université Claude Bernard Lyon I.
- BELOUZE A, GAYET M, ATALLAH C, 2003. The first Anguilliformes: II Paraphyly of the genus *Urenchelys* Woodward, 1900 and phylogenetic relationships. *Geobios*. 36: 351-378.
- BENJAMIN M, SANDHU JS. 1990. The structure and ultrastructure of the rostral cartilage in the spiny eel, *Macroglyptus siamensis* (Teleostei: Mastacembeloidei). *Journal of Anatomy*. 169: 37-47.
- BERTIN L. 1942. Les Anguilles: Variation, Croissance, Euryhalinité, Toxicité, Hermaphrodisme, juvénile et sexualité, Migrations, Métamorphoses. Payot. p218.
- BICUDO JEPW, JOHANSEN K. 1979. Respiratory gas exchange in the airbreathing fish *Synbranchus marmoratus*. *Environmental Biology of Fishes*. 4(1): 55-64.

- BOCK WJ, SHEAR CH R. 1972. A staining method for gross dissection of vertebrate muscles. *Anatomischer Anzeiger*. 130: 222-227.
- BÖHLKE EB. 1989. Fishes of the Western North Atlantic. Part 9, Sears Foundation for Marine Research, New Haven.
- BÖHLKE EB, McCOSKER JE, BÖHLKE JE. 1989. Family Muraenidae. In: Böhlke EB, editor. Fishes of the Western North Atlantic. Part 9, Sears Foundation for Marine Research, New Haven. p104-206.
- BÖHLKE EB. 1989b. Methods and Terminology. In: Böhlke EB, editor. Fishes of the western North Atlantic. New Haven: Conn Search Found Mar Res. pp1-8.
- BÖHLKE J. 1957. On the occurrence of garden eels in the Western Atlantic, with a synopsis of the Heterocongrinae. *Proceedings of the Academy of Natural Science of Philadelphia*. CIX: 59-79.
- BONE Q, MARSHALL NB, BLAXTER JHS. 1995. *Biology of Fishes*. sec edition. Great Britain: Chapman and Hall. pp 323.
- BONE Q. 1971. On the scabbard fish *Aphanopus carbo*. *Journal of the Marine Biological Association UK*. 51: 219-225.
- BOOKSTEIN FL, CHERNOFF B, ELDER R, HUMPHRIES J, SMITH G, STRAUSS R. 1985. Morphometrics in evolutionary biology. The geometry of size and change changes, with examples from fishes. Philadelphia Academic Natural Sciences: Special Publication.
- BOOKSTEIN FL. 1991. *Morphometric Tools for Landmark Data. Geometry and Biology*. Cambridge University Press. pp 435.
- BORCHI CE, GIANNONI SM, ROIG VG. 2002. Eye reduction in subterranean mammals and eye protective behavior in *Ctenomys*. *Journal of Neotropical Mammalogy*. 9: 123-134.
- BOULENGER GA. 1908. A revision of the African silurid fishes of the subfamily Clariinae. *Proceedings of the Zoological Society*. 2: 1062-1069.
- BOULENGER GA. 1911. *Catalogue of the fresh-water fishes of Africa in the British Museum (Natural History)*. Vol2. London: printed by order of the Trustees.
- BOWLER PJ. 2005. Variation from Darwin to the modern synthesis. In: variation, a central concept in biology. Hallgrímsson B, Hall BK, eds. New York: Academic. pp 9-27.
- BOZZANO A, 2003. Vision in the rufus snake eel, *Ophichthus rufus*: adaptive mechanisms for a burrowing life-style. *Marine Biology*. 143:167-174.
- BRAINERD EL, SIMONS RS. 2000. Morphology and function of lateral hypaxial musculature in salamanders. *American Zoologist*. 40(1): 77-86.
- BREWER MJ. 2003. Discretisation for inference on normal mixture models. *Statists and Computing*. 13: 209-219.
- BRITZ R, KOTTELAT M. 2003. Descriptive Osteology of the Family Chaudhuriidae (Teleostei, Synbranchiformes, Mastacembeloidei), with a Discussion of its Relationships. *American Museum Novitates*. 3418: 1-62.
- BURGESS WE. 1989. *An atlas of Freshwater and marine catfish: a preliminary survey on the Siluriformes*. T.F.H. Publications, Berkshire.

- CABUY E, ADRIAENS D, VERRAES W, TEUGELS GG. 1999. Comparative study on the cranial morphology of *Gymnallabes typus* (Siluriformes: Clariidae) and their less anguilliform relatives, *Clariallabes melas* and *Clarias gariepinus*. *Journal of Morphology*. 240: 169-194.
- CALDER WA. 1976. Energetics of small body size and high latitude the Rufous Hummingbird in coastal Alaska. *International journal of Biometeorology*. 20(1): 23-35.
- CALDWELL MW. 2003. "Without a leg to stand on": on the evolution and development of axial elongation and limblessness. *Canadian Journal of Earth Sciences*. 40: 573-588.
- CAROLL AM, WAINWRIGHT PC, HUSKEY SH, COLLAR DC, TURINGHAN RG. 2004. Morphology predicts suction feeding performance in centrarchid fish. *Journal of Experimental Biology*. 207: 3873-3881.
- CASIMIR MJ, FRICKE HW. 1971. Zur Function, Morphologie und Histochemie der Schwanzdrüse bei Röhrenaalen (Pisces, Apodes, Heterocongridae). *Marine Biology*. 9: 339-346.
- CASTLE PHJ, RANDALL JE. 1999. Revision of Indo-Pacific garden eels (Congridae: Heterocongrinae), with descriptions of five new species. *Indo-Pacific Fishes*. 30: 2-53.
- CASTLE PHJ. 1968. A contribution to a revision of the moringuid eels. Special Publication 3. Rhodes University Department of Ichthyology, Grahamstown, South Africa p1-29.
- CASTLE PHJ. 1999. A new species of garden eel from the eastern Pacific with comments on *Heteroconger digueti* (Pellegrin) and related nominal species. *Bulletin of marine science*. 64(3): 407-417.
- CAU A, MANCONI P. 1984. Relationship of feeding, reproductive cycle and bathymetric distribution in *Conger conger*. *Marine Biology*. 81(2): 147-151.
- CHANET B, WAGEMANS F. 1997. Presence of double spines on the second preural centrum of the turbot *Scophthalmus maximus* L., 1758 (Pleuronectiformes: Scophthalmidae). *Belgian Journal of Zoology*. 127: 115-122.
- CHAPMAN LJ, CHAPMAN CA, NORDLIE FG, ET AL. 2002. Physiological refugia: swamps, hypoxia tolerance and maintenance of fish diversity in the Lake Victoria region. *Comparative Biochemistry and Physiology A - Molecular and Integrative Physiology*. 133(3): 421-437.
- CHARDON M, PARMENTIER E, VANDEWALLE P. 2003. Morphology, development and evolution of the Weberian apparatus in catfish. In: *Catfishes*. Arratia G, Kapoor, Chardon M, Diogo R, eds. Science Publishers, Enfield, USA. vol. 1, pp 71-119.
- CHENG CH, KAWASAKI T, HIANG KP, HO CH. 2001. Estimated distribution and movement of hairtail *Trichiurus lepturus* in the Aru Sea, based on the logbook records of trawlers. *Fisheries science*. 67: 3-13.
- CHIOU WD, CHEN CY, WANG CM, CHEN CT. 2006. Food and feeding habits of ribbonfish *Trichiurus lepturus* in coastal waters of South-Western Taiwan. *Fisheries science*. 72: 373-381.
- CHOI HF. 2006. Een vergelijkende biomechanische studie van het zwemmen en graven bij twee aalvormige beenvissen: *Pisodonophis boro* en *Heteroconger hassi* (Anguilliformes). Master-thesis. *Evolutionary Morphology of Vertebrates*, Ghent University.
- CHOI HF, DE SCHEPPER N, HERREL A, AERTS P, ADRIAENS D. SUBMITTED. A comparative kinematical study of the swimming locomotion in two burrowing anguilliform bony fish: *Pisodonophis boro* and *Heteroconger hassi* (Anguilliformes). *Journal of Experimental Biology*.
- COAD BW, MCALLISTER DE. 2007. Dictionary of ichthyology. Internet address: <http://www.briancoad.com/Dictionary/M.htm>.

- COATES M, RUTA M. 2000. Nice snake, shame about the legs. *Tree*. 15(12): 503-507.
- COHN MJ, TICKLE C. 1999. Developmental basis of limblessness and axial patterning in snakes. *Nature*. 399(6735): 474-479.
- COLLAR DC, NEAR TJ, WAINWRIGHT PC. 2005. Comparative analysis of morphological diversity: Does disparity accumulate at the same rate in two lineages of centrarchid fishes? *Evolution* 59(8): 1783-1794.
- COLLETTE BB, CHAO LN. 1975. Systematics and morphology of the bonitos (*Sarda*) and their relatives (Scombridae, Sardini). *Fisheries bulletin*. 78(3): 516-625.
- COSTA WJEM, LE BAIL PY. 1999. *Fluviphylax palikur*: A new poeciliid from the rio Oiapoque basin, northern Brazil (Cyprinodontiformes : Cyprinodontoidei), with comments on miniaturization in *Fluviphylax* and other neotropical freshwater fishes. *Copeia*. (4): 1027-1034.
- COSTA G, CHUBB JC, VELTKAMP CJ. 2000. Cystacanths of *Bolbosoma vasculosum* in the black scabbard fish *Aphanopus carbo*, oceanic horse mackerel *Trachurus* and common dolphin *Delphinus delphis* from Madeira, Portugal. *Journal of Helminthology*. 74: 113-120.
- CUTWA MM, TURINGAN RG. 2000. Intralocality variation in feeding biomechanics and prey use in *Archosargus probatocephalus* (Teleostei, Sparidae), with implications for the ecomorphology of fishes. *Environmental Biology of Fishes*. 59(2): 191-198.
- D'AOUT K, AERTS P. 1999. A kinematic comparison of forward and backward swimming in the eel *Anguilla anguilla*. *Journal of Experimental Biology*. 202 (11): 1511-1521.
- DAGET J. 1964. Le crane des téléostéens, I. Origine et mise en place des tissus squelettogènes chez l'embryon. Mésomésenchyme et ectomésenchyme. *Mémoires du Muséum National d'Histoire Naturelle, Séries A. Zoologique*. 31 : 164-340.
- DANIELS SR, HEIDEMAN NJL, HENDRICKS MGJ, MOKONE ME, CRANDALL KA. 2005. Unraveling evolutionary lineages in the limbless fossorial skink genus *Acontias* (Sauria : Scincidae): are subspecies equivalent systematic units? *Molecular Phylogenetics and Evolution*. 34 (3): 645-654.
- DANNEWITZ J, MAES GE, JOHANSSON L, WICKSTRÖM H, VOLKAERT FAM, JARVI T. 2005. Panmixia in the European eel: a matter of time... *Proceedings of the Royal Society B: biological sciences, London*. 272: 1129-1137.
- DAVID L. 1935. Die Entwicklung der Clariiden und ihre Verbreitung. *Revue De Zoologie Et De Botanique Africaines*. 28: 77-147.
- DE PINNA MCC. 1996. A phylogenetic analysis of the Asian catfish families Sisoridae, Akysidae, and Amblycipitidae, with a hypothesis on the relationships of the neotropical Aspredinidae (Teleostei, Ostariophysi). *Fieldiana: Zoology*. 84: 1-83.
- DE SCHEPPER N, ADRIAENS D, TEUGELS GG, DEVAERE S, VERRAES W. 2004. Intraspecific variation in the postcranial skeleton morphology in African clariids: a case study of extreme phenotypic plasticity. *Zoological Journal of the Linnean Society, London*. 140: 437-446.
- DE SCHEPPER N, ADRIAENS D, DE KEGEL B. 2005. *Moringua edwardsi* (Moringuidae: Anguilliformes): Cranial Specialization for Head-First Burrowing? *Journal of Morphology*. 266: 356-368.
- DE SCHEPPER N, ADRIAENS D, DE KEGEL B. 2007. *Pisodonophis boro* (Ophichthidae: Anguilliformes): Specialization for Head-First and Tail-First Burrowing? *Journal of Morphology*. 268(2): 112-126.

- DE SCHEPPER N, DE KEGEL B, ADRIAENS. IN PRESS A. Morphological Specializations in Heterocongrinae (Anguilliformes: Congridae) Related to Burrowing and Feeding. *Journal of Morphology*. Accepted.
- DE SCHEPPER N, ADRIAENS D, TEUGELS GG, DEVAERE S, VERRAES W. IN PRESS B. Shape variation in the vertebrae of Anguilliform Clariidae (Ostariophysi: Siluriformes): useful tool for taxonomy? *Journal of Afrotropical Zoology*. In press.
- DE SCHEPPER N, LACEUR S, CHRISTIAENS J, VAN LIEFFERINGE C, HERREL A, GOEMANS G, MEIRE P, BELPAIRE C, ADRIAENS D. SUBMITTED A. Variation in cranial morphology of the European eel: broad- and narrow-headedness. *Biological journal of the Linnean Society*. Submitted.
- DE SCHEPPER N, VAN WASSENBERGH S AND ADRIAENS D. SUBMITTED B. Morphology of the jaw system in trichiurids: trade-offs between mouth closing and biting performance. *Biological Journal of the Linnean Society*.
- DEKKER, W, VAN OS B., VAN WILLIGEN J. 1998. Minimal and maximal size of eel. L'Anguille Europeenne. 10<sup>e</sup> Reunion du groupe de travail "Anguille" EIFAC/ICES. Bulletin Francais de Peche et Pecherie, Conseil superieur de la peche, Paris (France).
- DEVAERE S, ADRIAENS D, VERRAES W, TEUGELS GG. 2001. Cranial morphology of the anguilliform clariid *Channallabes apus* (Günther, 1873) (Teleostei: Siluriformes): adaptations related to powerful biting? *Journal of Zoology London*. 255: 235-250.
- DEVAERE S. TEUGELS GG, ADRIAENS D, HUYSENTRUYT F, VERRAES W. 2004. Redescription of *Dolichallabes microphthalmus* (Poll, 1942) (Siluriformes, Clariidae). *Copeia*. 1:108-115.
- DEVAERE S, ADRIAENS D, TEUGELS GG, DE CLERCK NM, POSTNOV AA. 2005A. Skeletal morphology of the holotype of *Gymnallabes nops* Roberts & Stewart, 1976, using micro CT-scanning. *Cybium*. 29(3): 281-293.
- DEVAERE S. 2005B. Taxonomy and evolutionary morphology of Afriacan catfishes (Clariidae), roads to anguilliformity. PHD-thesis. *Evolutionary Morphology of Vertebrates*. Ghent University.
- DEVAERE S, ADRIAENS A, VERRAES W. 2007A. Survey of the anguilliform Clariidae (Teleostei, Siluriformes) of Gabon and Republic of Congo, with description of two new species and key to the African clariid genera. *Belgian journal of Zoology* (in press).
- DEVAERE S, ADRIAENS D, VERRAES W. 2007B. *Channallabes sanghaensis* sp. n., a new anguilliform catfish from the Congo River basin, with some comments on other anguilliform clariids (Teleostei, Siluriformes). *Belgian journal of Zoology* (in press).
- DEVAERE S, JANSEN G, ADRIAENS D, WEEKERS P. 2007C. A phylogeny of the African catfish family (Siluriformes, Clariidae) based on morphological and combined analyses: the road to anguilliformity. *Journal of zoological systematics and evolutionary research* (in press).
- DUELLMAN WE, TRUEB L. 1986. Chapter 13: Musculoskeletal system. In: Duellman WE, Trueb L. *Biology of amphibians*. New York: McGraw-Hill Inc. p289-364.
- EATON TH JR. 1935. Evolution of the upper jaw mechanism in teleost fishes. *Journal of Morphology*. 58: 157-172.
- EASTMAN JT. 1980. The caudal skeleton of catostomid fishes. *The American Midland Naturalist*. 103: 133-148.
- EGE V. 1939. A revision of the genus *Anguilla* Shaw: a systematic, phylogenetic and geographical study. *Dana Report*. 16: 1-256.

- EHMCKE J, CLEMEN G. 2003. The skull structure of six species of Mesoamerican plethodontid salamanders (Amphibia, Urodela). *Annals of Anatomy-Anatomische Anzeiger*. 185(3): 253-261.
- ENDLER JA. 1982. Convergent and divergent effects of natural selection on color patterns in two fish faunas. *Evolution*. 36(1): 178-188.
- FERRY-GRAHAM LA, WAINWRIGHT PC, BELLWOOD DR, 2001A. Prey capture in long-jawed butterflyfishes (Chaetodontidae): the functional basis of novel feeding habits. *Journal of experimental Marine Biology and Ecology* 256: 167-184.
- FERRY-GRAHAM LA, WAINWRIGHT PC, HULSEY CD, BELLWOOD DR. 2001B. Evolution of mechanics of long jaws in Butterflyfishes (Family Chaetodontidae). *Journal of Morphology* 248: 120-143.
- FIGUEIREDO I, BORDALO-MACHADO P, REIS S, SENA-CARVALHO D, BLASDALE T. 2003. Observations on the reproductive cycle of the black scabbardfish (*Aphanopus carbo* Lowe, 1839) in the NE Atlantic. *ICES Journal of Marine Science*. 60(4): 774-779.
- FILLEUL A, LAVOUÉ S. 2001. Basal teleosts and the question of elopomorph monophyly. Morphological and molecular approaches. *Comptes-rendus de l'Académie des Sciences de Paris, Life Science*. 324: 393-399.
- FINK SV, FINK WL. 1981. Interrelationships of the ostariophysan fishes (Teleostei). *Zoological Journal of the Linnean Society*. 72: 297-353.
- FINK SV, FINK WL. 1996. *Interrelationships of ostariophysan fishes (Teleostei)*. Academic Press. London.
- FOREY PL, LITTLEWOOD DTJ, RITCHIE P, MEYER A. 1996. Interrelationships of elopomorph fishes. In: Stiassny MLJ, Parenti LR, Johnson GD. Eds. *Interrelationships of Fishes*. Academic Press, San Diego. pp175-191.
- FRICKE HW. 1969. Okologische und verhaltensbiologische Beobachtungen an den Röhrenallen *Gorgasia sillneri* und *Taenioconger hassi* (Pisces, Heteroncongriidae). *Zeitung für Tierpsychologie*. 27:1076-1099.
- FRIEL JP, LUNDBERG JG. 1996. *Micromyzon akamai*, gen et sp nov, a small and eyeless banjo catfish (Siluriformes: Aspredinidae) from the river channels of the lower Amazon basin. *Copeia*. 3: 641-648.
- FRIEL JP, WAINWRIGHT PC. 1998. Evolution of Motor patterns in Tetraodontiform fishes: does muscle duplication lead to functional diversification? *Brain Behavior and Evolution*. 52:159-170.
- FRIEL JP, WAINWRIGHT PC. 1999. Evolution of complexity in motor patterns and jaw musculature of tetraodontiform fishes. *Journal of Experimental Biology*. 202(7): 867-880
- FUJITA K. 1992. Ontogeny of the caudal skeleton in the clariid catfish *Clarias batrachus*. *Japanese Journal of Ichthyology*. 38(4): 430-432
- GABRIEL ML. 1944. Factors affecting the number and form of vertebrae in *Fundulus heteroclitus*. *The Journal of Experimental Zoology*. 95: 105-147.
- GAGO FJ. 1998. Osteology and phylogeny of the cutlassfishes (Scombridae: Trichiuridae). *Contributions in Science*. 476: 1-79.
- GANS C. 1973. Locomotion and burrowing in limbless vertebrates. *Nature*. 242: 414-415.
- GANS C. 1975. Tetrapod limblessness: evolution and functional corollaries. *American Zoologist*. 15: 455-467.

- GILLIS GB. 1996. Undulatory locomotion in elongate aquatic vertebrates: anguilliform swimming since Sir James Gray. *American Zoologist*. 36: 656-665.
- GILLIS GB. 1997. Anguilliform locomotion in an elongate salamander (*Siren intermedia*): Effects of speed on axial undulatory movements. *Journal of Experimental Biology*. 200 (4): 767-784.
- GILLIS GB. 1998. Environmental effects on undulatory locomotion in the American eel *Anguilla rostrata*: kinematics in water and on land. *Journal of Experimental Biology*. 201: 949-961.
- GOEMANS G, BELPAIRE C. 2004. The eel pollutant monitoring network in Flanders, Belgium. Results of 10 years monitoring. *Organohalogen Compounds*. 66: 1834-1840.
- GORDON SM. 1954. The eel genus *Stilbiscus*. *Copeia*. 1:11-15.
- GOSLINE WA. 1956. The Hawaiian fishes of the family Moringuidae: Another eel problem. *Copeia*. 1: 9-18.
- GOSLINE WA. 1971. Functional morphology and classification of teleostean fishes. Honolulu: University Press of Hawaii. p268.
- GOSLINE WA. 1975. The palatine-maxillary mechanism in catfishes, with comments on the evolution and zoogeography of modern Siluroids. Occasional papers of the Californian Academy of Sciences. 120: 1-31.
- GOSLINE WA. 1980. The evolution of some structural systems with reference to the interrelationships of modern lower teleostean fish groups. *Japanese Journal of Ichthyology*. 21:1-24.
- GOSLINE WA. 1983. The relationships of the mastacembelid and synbranchid fishes. *Japanese journal of Ichthyology*. 29(4): 323-328.
- GOSLINE WA. 1997. Functional morphology of the caudal skeleton in teleostean fishes. *Ichthyological Research*. 44: 137-141.
- GRAHAM JB. 1997. Air-Breathing Fishes: Evolution, Diversity and Adaptation. California. Academic Press. 2: 13-63.
- GRANDE L, EASTMAN JT. 1986. A review of Antarctic ichthyofaunas in the light of new fossil discoveries. *Palaeontology*. 29: 113-137.
- GRASSÉ PP. 1958. *Traité de zoologie, anatomie, systématique, biologie*. In: *Tome XIII, Agnathes et poissons*, secondaires fascicule. Grassé PP, ed. Paris: Masson.
- GREENWOOD PH. 1961. A revision of the genus *Dinopterus* Blgr. (Pisces, Clariidae) with notes on the comparative anatomy of the suprabranchial organs in the Clariidae. *Bulletin of the British Museum of Natural History, Zoology*. 7: 217-241.
- GREENWOOD PH, ROSEN DE, WEITZMAN SH, MYERS GS. 1979. Phylogenetic studies of teleostean fishes, with a provisional classification of living forms. In: *Readings in ichthyology*. Love MS, Cailet GM, eds. Goodyear Publishing Company, Santa Monica, California. p73-94.
- GREENWOOD PH, ROSEN DE, WEITZMAN SH, MYERS GS. 1966. Phylogenetic studies of teleostean fishes, with a provisional classification of living forms. *Bulletin of the American Museum for Natural History*. 131, pp. 339-456.
- HAFFER J. 1982. General aspects of the refuge theory. In: *Biological diversification in the Tropics*. Prance GT, ed. New York, Columbia University Press. 6-24.



- HALLGRIMSSON B, HALL BK. 2005. Variation and variability: Central concepts in biology. In: Variation, a central concept in biology. Hallgrímsson B, Hall BK, eds. New York: Academic Press. pp 1-7.
- HANKEN J, WASSERSUG R. 1981. The visible skeleton. A new double-stain technique reveals the nature of the "hard" tissues. *Functional Photography*. 16: 22-26.
- HANKEN J. 1983. Miniaturization and its effects on cranial morphology in plethodontid salamanders, genus *Thorius* (Amphibia, Plethodontidae): II. The fate of the brain and sense organs and their role in skull morphogenesis and evolution. *Journal of Morphology*. 177: 255-268.
- HANKEN J. 1993. Chapter 4: Adaptation of bone growth to miniaturization of body size. In: Hall BK, ed. Bone: Bone Growth. CRC Press, Inc. Vol 7: 79-104.
- HANKEN J, WAKE D. 1993. Miniaturization of Body Size: Organismal Consequences and Evolutionary Significance. *Annual Review of Ecological Systems*. 24: 501-19.
- HASSAN ES. 1989. Chapter 10: Hydrodynamic imaging of the surroundings by the lateral line of the blind cave fish *Anoptichthys jordani*. In: The mechanosensory lateral line. Coombs S, Görner P, Münz H. New York: Springer-Verlag Inc.
- HELFMAN GS, CLARK JB. 1986. Rotational feeding: overcoming gape-limited foraging in anguillid eels. *Copeia* 3:679-685.
- HELFMAN GS, COLLETTE BB, FACEY DE. 1997. Chapter 8: Functional morphology of locomotion and feeding. In: The diversity of fishes. Helfman GS, Collette BB, Facey DE. London: Blackwell Science, Inc p101-116.
- HELFMAN GS, WINKELMAN DL. 1991. Energy trade-offs and foraging mode choice in American eels. *Ecology* 72:310-318.
- HENDRY AP, GRANT PR, GRANT BR, FORD HA, BREWER MJ, PODOS. J. 2006. Possible human impacts on adaptive radiation: beak size bimodality in Darwin's finches. *Proceedings of the Royal Society B: biological sciences*, London 273: 1887-1894.
- HERREL A, ADRIAENS D, VERRAES W, AERTS P. 2002. Bite performance in clariid fishes with hypertrophied jaw adductors as deduced by bite modelling. *Journal of Morphology*. 253: 196-205.
- HIBBITS TJ, FITZGERALD LA. 2005. Morphological and ecological convergence in two natricine snakes. *Biological journal of the Linnean Society*. 85: 363-371.
- HILDEBRAND CM. 1995. Analysis of Vertebrate Structure. 4<sup>th</sup> edn. New York: John Wiley and Sons Inc.
- HOWE KM. 1979. First records of Oregon of the pelagic fishes *Paralepis atlantica*, *Gonostoma atlanticum*, and *Aphanopus carbo*, with notes on the anatomy of *Aphanopus carbo*. *Fishery Bulletin*. 77(3): 701-703.
- HOLCIK J, JEDLIČKA L. 1994. Geographical variation of some taxonomically important characters in fishes: the case of the bitterling *Rhodeus sericeus*. *Environmental Biology of Fishes*. 41: 147-170.
- HUBERT N, BONILLO C, PAUGY D. 2005. Early divergence among the Alestidae (Teleostei, Ostariophyses, Characiformes): Mitochondrial evidences and congruence with morphological data. *Comptes Rendus Biologies*. 328(5): 477-491.

- HULET WH, ROBINS CR. 1989. The evolutionary significance of the leptocephalus larva. In: Böhlke, EB, ed. Fishes of the Western North Atlantic. Part 9. Vol 2. Sears Foundation for Marine Research, New Haven. pp669-677.
- HUYSENTRUYT F, ADRIAENS D, TEUGELS GG, DEVAERE S, HERREL A, VERRAES W, AERTS P. 2004. Diet composition in relation to morphology in some African anguilliform clariid catfishes. *Belgian Journal of Zoology*. 134(1): 41-46.
- INOUE JG, MIYA M, TSUKAMOTO K, NISHIDA M. 2004. Mitogenomic evidence for the monophyly of elopomorph fishes (Teleostei) and the evolutionary origin of the leptocephalus larva. *Molecular Phylogenetics and Evolution*. 32(1): 274-286.
- INOUE JG, MIYA M. 2001. Phylogeny of the basal teleosts, with special reference to the Elopomorpha. *Japanese Journal of Ichthyology*. 48: 75-91 (in Japanese with English abstract).
- IRSCHICK DJ. 2002. Evolutionary approaches for studying functional morphology: examples from studies of performance capacity. *Integrative and Comparative Biology*. 42: 278-290.
- JARVIK E. 1980. Basic structure and evolution of vertebrates. Vol 1. Jovanovisch HB (ed.). Academic Press, London.
- JOCKUSH EL. 1997. Geographic variation and phenotypic plasticity of number of trunk vertebrae in slender salamanders, *Batrachoseps* (Caudata: Plethodontidae). *Evolution*. 51(6): 1966-1982.
- JANSEN G, DEVAERE S, WEEKERS PHH, ADRIAENS D. 2006. Phylogenetic relationships and divergence time estimate of African anguilliform catfish (Siluriformes: Clariidae) inferred from ribosomal gene and spacer sequences. *Molecular Phylogenetics and Evolution*. 38(1): 65-78.
- JOHNSON GD, PATTERSON C. 1993. Percomorph Phylogeny - A survey of Acanthomorphs and a new proposal. *Bulletin of Marine Science*. 52 (1): 554-626.
- JOHNSON GD. 1986. Scombroid phylogeny: an alternative hypothesis. *Bulletin of Marine Science*. 39(1): 1-41.
- JÜRGENS KD, FONS R, PETERS T. 1996. Heart and respiratory rates and their significance for convective oxygen transport rates in the smallest mammal, the Etruscan shrew *Suncus etruscus*. *Journal of Experimental Biology*. 199 (12): 2579-2584.
- KAATZ I, STEWART DS. 1997. The evolutionary origin and functional divergence of sound production in fish: catfish stridulation mechanisms. *Journal of Morphology*. 232 (3): 272.
- KAMMERER CF, GRANDE L, WESTNEAT MW. 2005. Comparative and developmental functional morphology of the jaws of living and fossil gars (Actinopterygii: Lepisosteidae). *Journal of Morphology*. 267(9): 1017-1031.
- KORFF WL, WAINWRIGHT PC. 2004. Motor pattern control for increasing crushing force in the striped burrfish (*Chilomycterus schoepfi*). *Zoology*. 107: 335-346.
- KOTTELAT M, BRITZ R, HUI TH, WITTE KE. 2006. *Paedocypris*, a new genus of Southeast Asian cyprinid fish with a remarkable sexual dimorphism, comprises the world's smallest vertebrate. *Proceedings of the Royal Society B- Biological Sciences*. 273(1589): 895-899.
- KRAMER DL, McCLURE M. 1982. Aquatic surface respiration, a widespread adaptation to hypoxia in tropical freshwater fishes. *Environmental Biology of Fishes*. 7(1): 47-55.
- KWOK KY, NI IH. 2000. Age and growth of cutlassfishes, *Trichiurus spp.*, from the South China Sea. *Fishery Bulletin*. 98: 748-758.

- LAKSHMI K, SRINIVASA RAO K. 1989. Postcranial skeleton of the marine catfish *Arius tenuispinis* (Osteichthyes: Siluriformes, Ariidae). *Journal of Morphology*. 202: 361-377.
- LAMMENS EH, VISSER JT. 1989. Variability of mouth width in European eel, *Anguilla anguilla*, in relation to varying feeding conditions in three Dutch lakes. *Environmental Biology of Fishes*. 26: 63-75.
- LANDE R. 1978. Evolutionary mechanisms of limb loss in tetrapods. *Evolution*. 32: 73-92.
- LAUDER GV. 2000. Function of the caudal fin during locomotion in fishes: Kinematics, flow visualization, and evolutionary patterns. *American Zoologist*. 40(1): 101-122.
- LAUDER GV, DRUCKER G. 2004. Morphology and experimental hydrodynamics of fish fin control surfaces. *IEEE Journal of Oceanic Engineering*. 29:556-571.
- LÊ HLV, LECOINTRE G, PERASSO R. 1993. A 28S rRNA-based phylogeny of the gnathostomes: first steps in the analysis of conflict and congruence with morphologically based cladograms. *Molecular Phylogenetics and Evolution*. 2: 31-51.
- LECOINTRE G, NELSON G. 1996. Clupeomorpha, sister-group of Ostariophysii. In: Stiassny MLJ, Parenti LR, Johnson GD. eds. 1996. *Interrelationships of Fishes*, Academic Press, San Diego. pp193-207.
- LEE MSY. 1998. Convergent evolution and character correlation in burrowing reptiles: Towards a resolution of squamate relationships. *Biological Journal of the Linnean Society*. 65: 369-453.
- LEVINTON AE, GIBBS RH, HEALE, DAWSON CE. 1985. Standards in herpetology and ichthyology: Part 1. Standard symbolic code for institutional resource collections in herpetology and ichthyology. *Copeia* 3: 802-832.
- LIAO JC. 2002. Swimming in needlefish (Belonidae): anguilliform locomotion with fins. *The Journal of Experimental Biology*. 205: 2875-2884.
- LIEM KF, OSSE JWM. 1975. Biological versatility, evolution, and food resources exploitation in African cichlid fishes. *American Zoologist*. 15: 427-454.
- LIEM KF. 1980. Acquisition of energy by teleosts: adaptive mechanisms and evolutionary patterns. In: *Environmental Physiology of fishes*. Ali MA, ed. New York, Plenum press. 299-334.
- LIN YS, TZENG CS, HWANG JK. 2005. Reassessment of morphological characteristics in freshwater eels (genus *Anguilla*, Anguillidae) shows congruence with molecular phylogeny estimates. *Zoologica Scripta*. 34 (3): 225-234.
- LOSOS JB, WALTON BM, BENNETT AF. 1993. Trade-offs between sprinting and clinging ability in Kenyan chameleons. *Functional Ecology*. 7: 281-286.
- LUNDBERG JG, BASKIN JN. 1969. The caudal skeleton of the catfishes, order Siluriformes. *American Museum Novitates*. 2398: 1-19.
- LYTHGOE J, LYTHGOE G. 1991. *Fishes of the Sea: the North Atlantic and Mediterranean*. The MIT Press.
- MARTINS AS, HAIMOVICI M. 1997. Distribution, abundance and biological interactions of the cutlassfish *Trichiurus lepturus* in the southern Brazil subtropical convergence ecosystem. *Fisheries Research*. 30: 217-227.
- MATTHES H. 1964. *Les poissons du lac Tumba et de la region D'Ikela*. Unpubl. PhD-thesis. Nijmegen, the Netherlands.

- MCCOSKER JE, BÖHLKE EB, BÖHLKE JE. 1989. Family Ophichthidae. In: Böhlke EB, editor. Fishes of the western North Atlantic. Sears Foundation for Marine Research, New Haven. pp254-412.
- MCDOWELL SM. 1973. Order Heteromi (Notacanthiformes). In Böhlke EB, ed. Fishes of the Western North Atlantic. Sears Foundation for Marine Research, New Haven. p1-228.
- MEASEY GJ, HERREL A. 2006. Rotational feeding in caecilians: putting a spin on the evolution of cranial design. *Biological Letters*. 2(4): 485-487.
- MECKLENBURG CW. 2003A. Family Ptilichthyidae Jordan and Gilbert 1883 - Quillfishes. *Calif Acad Sci Annotated Checklists of Fishes* 12:1-3.
- MECKLENBURG CW. 2003B. Family Scytalinidae Jordan and Evermann 1898 - Graveldivers. *Calif Acad Sci Annotated Checklists of Fishes* 11:1-3.
- MENDEZ J, KEYS A. 1960. Density and composition of mammalian muscle. *Metabolism*. 9: 184-188.
- MILLER PJ. 1979. Adaptiveness and implications of small size in teleosts. *Symposia of the Zoological Society of London*. 44: 263-306.
- MONOD T. 1968. Le complexe urophore des poissons téléostéens. *Mémoires de l' Institut Fondamental d'Afrique Noire*. 81: 1-705.
- MONTGOMERY JC. 1989. Chapter 28: Lateral line detection of planktonic prey. In: Coombs S, Görner P, Münz H. eds. *The mechanosensory lateral line*. New York: Springer-Verlag Inc.
- MOOI RD, GILL AC. 2004. Notograptidae, sister to *Acanthoplesiops* Regan (Teleostei: Plesiopidae: Acanthoclininae), with comments on biogeography, diet and morphological convergence with Congrogadinae (Teleostei: Pseudochromidae). *Zoological Journal of the Linnean Society*. 141: 179-205
- MORATO T, SOLA E, GROS MP, MENEZES G. 1999. Diets of forkbeard (*Physis physis*) and conger eel (*Conger conger*) off the Azores during spring of 1996 and 1997. *Life and marine sciences*. 17A: 51-64.
- NAKAMURA I, PARIN NV. 1993. Snake mackerels and cutlassfishes of the world (families Gempylidae and Trichiuridae). *FAO Fisheries Synopsis*. 125(15): 136p
- NARICI M. 1999. Human skeletal muscle architecture studied in vivo by non-invasive imaging techniques: functional significance and applications. *Journal of Electromyography and Kinesiology*. 9: 97-103.
- NAVAS CA, ANTONIAZZI MM, CARVALHO JE, CHAUI-BERLINK JG, JAMES RS, JARED C, KOHLSORF T, SILVA MDP, WILSON RS. 2004. Morphological and physiological specialization for digging in amphisbaenians, an ancient lineage of fossorial vertebrates. *Journal of Experimental Biology*. 207: 2433-2441.
- NELSON JN. 1994. *Fishes of the world*. New York, John Wiley and Sons p378.
- Ng, HH. 2003. *Clarias insolitus*, a new species of clariid catfish (Teleostei: Siluriformes) from southern Borneo. *Zootaxa*. 284: 1-8.
- NORTON SF, BRAINERD EL. 1993. Convergence in the feeding mechanics of ecomorphologically similar species in the Centrarchidae and Cichlidae. *Journal of Experimental Biology*. 176: 11-29.
- NURSALL JR. 1963. The hypurapophysis, an important element of the caudal skeleton. *Copeia*. 2: 458-459.

- OLASO I, RODRIGUEZ-MARIN E. 1995. Alimentación de veinte especies de peces demersales pertenecientes a la división VIIIc del ICES. Otoño 1991. Informes Técnicos, Centro Oceanográfico de Santander, Instituto Español de Oceanografía. 157: 56.
- O'SULLIVAN S, MORIARTY C, DAVENPORT J. 2004. Analysis of the stomach contents of the European conger eel *Conger conger* in Irish waters. Journal of the Marine Biological Association (UK). 84: 823-826.
- PANKHURST NW, LYTTHGOE JN. 1983. Changes in vision and olfaction during sexual maturation in the European eel *Anguilla anguilla* (L.). Journal of Fish Biology. 23: 229-240.
- PARENTI LR. 1993. Relationships of atherinomorph fishes (Teleostei). Bulletin of Marine Science. 52: 170-196.
- PARIN NV, NAKAMURA I. 2002. Trichiuridae. Scabbardfishes (hairtails, frostfishes). In: K.E. Carpenter (ed.) FAO species identification guide for fishery purposes. The living marine resources of the Western Central Atlantic. Vol. 3: Bony fishes part 2 (Opistognathidae to Molidae), sea turtles and marine mammals. p 1825-1835.
- PARRA-OLEA G, WAKE DB. 2001. Extreme morphological and ecological homoplasy in tropical salamanders. Proceedings of the national academy of science (PNAS). 98(14): 7888-7891.
- PASI BM, CARRIER DR. 2003. Functional trade-offs in the limb muscles of dogs selected for running vs. fighting. Journal of Evolutionary Biology. 16(3): 541-541.
- PELLEGRIN J. 1927. La disparition des nageoires paires chez les poissons Africains du groupe des clariinés. Annales Des Sciences Naturelles, (Zoologie) Paris. 10: 209-222
- PEPIN P, KOSLOW JA, PEARRE JRS. 1988. Laboratory study of Foraging by Atlantic Mackerel, *Scomber scombrus*, on natural zooplankton Assemblages. Fish Aquaculture. 45: 879-887.
- POLL, M., 1942. Description d'un genre nouveau de Clariidae originaire de Congo Belge. Revue de Zoologie et de Botanique Africaines. 36: 96-100.
- POLL M. 1943. Description du *Tanganikallabes mortiauxi*, gen. nov., sp. n., de la famille des Clariidae. Revue de Zoologie et de Botanique Africaines. 37(1-2): 126-133.
- POLL M. 1973. Les yeux des poissons aveugles Africains et de *Caecomastacembelus brichardi* Poll en particulier. Annales du Spéléologie. 28: 221-230.
- POLL M. 1977. Les genres nouveaux *Platyallabes* et *Platyclarias* comparés au genre *Gymnallabes* (GTHR. Synopsis nouveau des genres de Clariidae. Bulletin de la Classe des Sciences. 5: 122-149.
- POLL M. 1957. Redescription du *Gymnallabes tihoni* Poll 1944, Clariidae microphthalme du Stanley-Pool (Congo Belge). Revue de Zoologie et de Botanique Africaines. 55: 237-248.
- PORTER HT, MOTTA PJ. 2004. A comparison of strike and prey capture kinematics of three species of piscivorous fishes: Florida gar (*Lepisosteus platyrhincus*), redfin needlefish (*Strongylura notata*), and great barracuda (*Sphyraena barracuda*). Marine Biology. 145(5): 989-1000.
- POUGH HF, ANDREWS RM, CADLE JE, CRUMP ML, SAVITZKY AH, WELLS KD. 1998. Chapter 8: Body support and locomotion. In: Pough HF et al eds. Herpetology. New Jersey: Prentice Hall.
- PROMAN JM, REYNOLDS JD. 2000. Differences in head shape of the European eel, *Anguilla anguilla*. Fisheries Management and Ecology. 7: 349-354.

- RAFFERTY KL, HERRING SW, MARSHALL CD. 2003. Biomechanics of the rostrum and the role of facial sutures. *Journal of Morphology*. 257: 33-44.
- RAMZU M, MEUNIER FJ. 1999. Descripteurs morphologiques de la zonation de la colonne vertébrale chez la truite arc-en-ciel *Oncorhynchus mykiss* (Wlbaum, 1792) (Teleostei, Salmoniformes). *Annales des Sciences Naturelles*. 3: 87-97.
- REGAN CT. 1909. On the anatomy and classification of the scombroid fishes. *Annals and Magazine of Natural History*. 8(3): 66-75.
- REGAN CT. 1911. The classification of the teleostean fishes of the order Ostariophysi: 1. Cyprinoidea. *Annals and Magazine of Natural History*. 8(8): 13-32.
- REGAN CT. 1912. The osteology and classification of the teleostean fishes of the order Apodes. *Annals and Magazine of Natural History*. 10: 377-387.
- REISS KZ. 2001. Using Phylogenies to Study Convergence: The Case of the Ant-Eating Mammals. *American Zoologist*. 41(3): 507-525.
- RICHTSMIEIER JT, LELE SR, COLE III TM. 2005. Landmark Morphometrics and the analysis of variation. In: variation, a central concept in biology. Hallgrímsson B, Hall BK, eds. New York: Academic. pp 49-70.
- RIEPEL OC. 1996. Miniaturization in tetrapods: consequences for skull morphology. In: Miller PJ, editor. *Miniature vertebrates*. Oxford: Clarendon Press pp15-45.
- RINGUET S, MUTO F, RAYMAKERS C. 2002. Eels: their harvest and trade in Europe and Asia. *Traffic Bulletin* 19: 2-27.
- ROCKWELL H, EVANS FG, PHEASANT HC. 1938. The comparative morphology of the vertebrate spinal column. Its form as related to function. *Journal of Morphology*. 63: 87-117.
- ROBERTS TR. 1973. Interrelationships of ostariophysans. In: *Interrelationships of Fishes*. Greenwood PH, Miles RS, Patterson C. eds. Academic Press. 53(suppl.1): 373-395.
- ROBERTS T, STEWART DJ. 1976. An ecological and systematical survey of fishes in the rapids of the lower Zaire or Congo river. *Bulletin of the Museum of Comparative Zoology*. 147: 239-317.
- ROBINS CR. 1989. The phylogentic relationships of the Anguilliform fishes. In: Böhlke EB, editor. *Fishes of the western North Atlantic*. New Haven: Conn Search Found Mar Res p9-23.
- ROFF DA, MOSTOWY S, FAIRBAIRN DJ. 2002. The evolution of trade-offs: testing predictions on response to selection and environmental variation. *Evolution, International Journal of Organic Evolution*. 56(1): 84-95.
- ROHLF FJ, SLICE DE. 1990. Extensions of the procrustes method for the optimal superimposition of landmarks. *Systematic Zoology*. 39: 40-59.
- ROHLF FJ. 1990. Morphometrics. *Annual Review of Ecology and Systematics*. 21: 299-316.
- ROHLF FJ. 1993. Relative warp analysis and an example of its application to mosquito wings. In: *Contributions to Morphometrics*. Marcus LF, Bello E, García-Valdecasas A, eds. Madrid: CSIC. pp131-159.
- ROHLF FJ. 1996. Morphometric space, shape components and the effects of linear transformations. In *Advances in Morphometrics*. Marcus LF, Corti M, Loy A, Naylor GJP, Slice DE, eds. New York, Plenum Press. pp117-129.
- ROHLF FJ. 1998. *TpsSmall: Thin Plate Spline Small Variation Analysis*. New York: State University of New York at Stony Brook.

- ROHLF FJ. 2000. TpsRegr: Thin Plate Spline Shape Regression. Stony Brook, New York: State University of New York at Stony Brook.
- ROHLF FJ. 2001A. TpsDig: Thin Plate Spline Digitise. Stony Brook, New York: State University of New York at Stony Brook.
- ROHLF FJ. 2001B. TpsRelw: Thin Plate Spline Relative Warp Analysis. Stony Brook, New York: State University of New York at Stony Brook.
- ROJO AL. 1991. Dictionary of evolutionary fish osteology. CRC Press Inc.
- ROSEN DE, GREENWOOD PH. 1976. A fourth neotropical synbranchid eel and the phylogeny and systematics of synbranchiform fishes. Bulletin of American Museum of Natural History. 1-69.
- ROSENBLATT RH. 1967. The osteology of the congrid eel *Gorgasia punctata* and the relationships of the Heterocongrinae. Pacific Science. XXI: 91-97.
- SABAJ MH, PAGE LM, LUNDBERG JG, FERRARIS CJ JR, ARMBRUSTER JW, FRIEL JP, MORRIS PJ. 2006. All catfish Species Inventory Website. Internet address: <http://clade.acnatsci.org/allcatWsh>.
- SAHINOZ E, DOGU Z, ARAL F. 2006. Development of embryos in *Mastacembelus mastacembelus* (Bank & Solender, 1794) (Mesopotamian spiny eel) (Mastacembelidae). Aquacultural Research. 37(16): 1611-1616.
- SANTOS FB, CASTRO RMC. 2003. Activity, habitat utilization, feeding behaviour, and diet of the samd moray *Gymnothorax ocellatus* (Anguilliformes, Muraenidae) in the South Western Atlantic. Biota Neotropica 3(1): 1-7.
- SCHAEFER SA, LAUDER GV. 1996. Testing historical hypotheses of morphological change: biomechanical decoupling in loricarioid catfishes. Evolution. 50(4): 1661-1675.
- SCHONDUBE JE, DEL RIO CM. 2003. The flowerpiercers' hook: an experimental test of an evolutionary trade-off. Proceedings of the Royal Society B- Biological Sciences. 270(1511): 195-198.
- SCHULTZE HP, ARRATIA G. 1988. Reevaluation of the caudal skeleton of certain actinopterygian fishes: II. *Hiodon*, *Elops* and *Albula*. Journal of Morphology. 195: 257-303.
- SCHULZE T, KAHL U, RADKE RJ, BENNDORF J. 2004. Consumption, abundance and habitat use of *Anguilla anguilla* in a mesotrophic reservoir. Journal of fish Biology. 65(6): 1543-1562.
- SCHWEID R. 2004. Consider the eel, a natural and gastronomic history. Da Capo Press. University of North Carolina press.
- Schwenk K, Wagner GP. 2003. Constraints. In: Keywords and concepts in evolutionary developmental biology. Hall, BK, Olson M, eds. Harvard University Press, London. 52-61.
- SHINE R. 1986. Evolutionary advantages of limblessness: evidence from the pygopodid lizards. Copeia. 2:525-529.
- SIBBING FA, NAGELKERKE L. 2001. Resource partitioning by Lake Tana barbs predicted from fish morphometrics and prey characteristics. Reviews in Fish Biology and Fisheries. 10: 393-437.
- SKULASON S, SMITH TB. 1995. Resource polymorphisms in vertebrates. Trends in Ecology and Evolution. 10:366-370.

- SMITH DG, CASTLE PHJ. 1972. The eel genus *Neoconger* Girard: systematics, osteology, and life history. *Bulletin of Marine Sciences*. 22: 196-249.
- SMITH DG. 1989A. Family Anguillidae. In: Böhlke EB, ed. *Fishes of the Western North Atlantic*. Sears Foundation for Marine Research, New Haven. p25-47.
- SMITH DG. 1989B. Family Congridae. In: Böhlke EB, ed. *Fishes of the western North Atlantic*. Sears Foundation for Marine Research, New Haven. p460-567.
- SMITH DG. 1989c. Family Heterenchelyidae. In: Böhlke EB, ed. *Fishes of the western North Atlantic*. Sears Foundation for Marine Research, New Haven. p48-54.
- SMITH DG. 1989D. Family Moringuidae. In: Böhlke EB, ed. *Fishes of the western North Atlantic*. Sears Foundation for Marine Research, New Haven. p55-71.
- SMITH DG. 1990. Congridae. In: Check-list of the fishes of the eastern tropical Atlantic (CLOFETA). Quéro JC, Hureau JC, Karrer C Post A, Saldanha L, eds. JNICT Lisbon, SEI Paris, UNESCO Paris. Vol 1. p156-167.
- SOARES-PORTO LM, WALSH SJ, NICO LG, NETTO JM. 1999. A new species of *Gelanoglanis* from the Orinoco and Amazon river basins, with comments on miniaturization within the genus (Siluriformes: Auchenipteridae: Centromochlinae). *Ichthyological Exploration of Freshwaters*. 10(1): 63-72.
- SOKAL RR, ROHLF FJ. 1995. *Biometry: The principals and practice of statistics in biological research*. Third edition. Freeman and Company. New York.
- STARKIE A. 2003. Management issues relating to the European eel, *Anguilla anguilla*. *Fisheries Management and Ecology*. 10: 361-364.
- STEARNS SC. 1989. The evolutionary significance of phenotypic plasticity. *Bioscience*. 39: 436-445.
- STEARNS SC. 1992. *The evolution of life histories*. New York: Oxford University Press.
- STIASSNY MLJ. 1986. The limits and relationships of the acanthomorph teleosts. *Journal of Zoology (London)*. 1(41): 1-460.
- STUDHOLME AL, PACKER DB, BERRIEN PL, JOHNSON DL, ZETLIN CA, MORSE WW. 1999. Atlantic Mackerel, *Scomber scombrus*, life history and habitat characteristics. NOAA Technical Memorandum NMFS-NE. 141: 1-35.
- SUBRAMANIAN A. 1984. Burrowing behaviour and ecology of the crab-eating Indian snake eel *Pisoodonophis boro*. *Environmental Biology of Fishes*. 10: 195-202.
- SUDA Y. 1996. Osteology and musculature attachments of the Japanese jack mackerel, *Trachurus japonicus*. *Bulletin of Marine Science*. 58(2): 438-493.
- SUN Z, LEE E, HERRING SW. 2004. Cranial sutures and bones: growth and fusion in relation to mastication strain. *Anatomical Records. Part A*. 276A: 150-161.
- SWAN SC, GORDON JDM, SHIMMIELD T. 2003. Preliminary investigations on the uses of otolith microchemistry for stock discrimination of the deep-water Black Scabbardfish (*Aphanopus carbo*) I the North East Atlantic. *Journal of the Northwest Atlantic Fishery Science*. 31: 221-231.
- TAVERNE L. 1986. L'évolution de l'antorbitaire et son incidence sur la phylogénie des Téléostéens primitives. *Biologisch Jaarboek Dodonea*. 54: 142-160.



- TAVERNE L. 1999. Ostéologie et positoin systématique d'*Arratiaelops vectensis* gen. nov., téléostéen élopiforme du Waldien (Crétacé inférieur) d'Angleterre et de Belgique. Bulletin de l'Institut Royal des Sciences Naturelles de Belgique. 69: 77-93.
- TESCH FW. 2003. The eel. 5<sup>th</sup> edn. Blackwell Publishing Company.
- TEUGELS GG. 1986. A systematic revision of the African species of the genus *Clarias* (Pisces, Clariidae). Annales de Musée Royal de l'Afrique Centrale, Science Zoologiques. 247: 1-199.
- TEUGELS GG. 1996. Taxonomy, phylogeny and biogeography of catfishes (Ostariophysi, Siluroidei): an overview. Aquatic Living Resources. 9: 9-34
- Teugels GG, Adriaens D. 2003. Taxonomy and phylogeny of Clariidae - An overview. In: Catfishes. Arratia G., Kapoor BG, Chardon M, Diogo R, eds. Science Publishers, Inc., Enfield (USA), Chapter 16, Vol. 1: 465-487.
- THUROW F. 1958. Untersuchungen über die spitz und breitzköpfigen Varianten des Flussaales. Archives für Fischerei Wissenschaft. 9: 79-97.
- TILAK R, KANJI SK. 1969. Studies on the osteology of *Pisoodonophis boro* (Hamilton). Gegenbaurs Morphologisches Jahrbuch. 113: 501-523.
- TÖRLITZ H. 1922. Anatomische und entwicklungsgeschichtliche Beiträge zur Artfrage unseres Flussaales. Zeitschrift für Fischerei 21: 1-48.
- TRAUTNER J. 2006. Rapid identification of European (*Anguilla anguilla*) and North American eel (*Anguilla rostrata*) by polymerase chain reaction. Information für Fischereiforschung. 53: 49-51.
- TRAVERS RA. 1984A. A review of the Mastacembeloidei, a suborder of synbranchiform teleost fishes Part I: Anatomical descriptions. Bulletin of the British Museum of Natural History, Zoological series. 46 (1): 1-133.
- TRAVERS RA. 1984B. A review of the Mastacembeloidei, a suborder of synbranchiform teleost fishes Part II: Phylogenetic analysis. Bulletin of the British Museum of Natural History, Zoological series. 47 (2): 83-150.
- TREWAVAS E. 1932. A contribution to the classification of the fishes of the order Apodes, based on the osteology of some rare eels. Proceedings of the Zoological Society, London. 43: 639-659.
- TRUEMAN ER, ANSELL AD. 1969. The mechanism of burrowing into soft substrata by marine animals. Oceanogr Mar Biol Ann Rev. 7: 315-366.
- TSENG MC, TZENG WN, LEE SC. 2003. Historical decline in the Japanese Eel *Anguilla japonica* in Northern Taiwan inferred from temporal genetic variations. Zoological Studies. 42: 556-563.
- TSUKAMOTO K, AOYAMA J. 1998. Evolution of freshwater eels of the genus *Anguilla*: a probable scenario. Environmental Biology of Fishes. 52: 139-148.
- TUCKER DW. 1956. Studies on the trichiuroid fishes - 3 A preliminary revision of the family Trichiuridae. Bulletin of the British Museum of Natural History, Zoology. 4(3): 73-131.
- TURINGAN RG, WAINWRIGHT PC, HENSLEY DA. 1995. Interpopulation variation in prey use and feeding biomechanics in Caribbean Triggerfishes. Oecologia. 102(3): 296-304.

- TURINGAN RG, WAINWRIGHT PC. 1993. Morphological and functional bases of durophagy in the Queen Triggerfish, *Balistes vetula* (Pisces, Tetraodontiformes). *Journal of Morphology*. 215: 101-118.
- TYLER JC, SMITH CL. 1992. Systematic significance of the burrow form of seven species of garden eels (Congridae: Heterocongrinae). *American Museum Novitates*. 3037: 1-13.
- VAN GINNEKEN GJT. 2006A. Simulated migration of European eel (*Anguilla anguilla*, Linnaeus 1758). PHD thesis. The Netherlands: Wageningen University.
- VAN GINNEKEN V. 2006B. Baanbrekend onderzoek in voorplanting aal. *Visionair. Verstand van vissen*. 1: 36-39 (In Dutch).
- VAN GINNEKEN V, ANTONISSEN E, MÜLLER UK BOOMS R., EDING E, VERRETH J, VAN DEN THILLART G. 2005. Eel migration to the Sargasso: remarkably high swimming efficiency and low energy costs. *The journal of Experimental biology*. 208: 1329-1335.
- VANHOODYONCK B, VAN DAMME R. 2001. Evolutionary trade-offs in locomotor capacities in lacertid lizards: are splendid sprinters clumsy climbers? *Journal of Experimental Biology*. 14(1): 46-54.
- VAN LEEUWEN JL, MULLER M. 1983. The recording and interpretation of pressures in prey-sucking fish. *Netherlands Journal of Zoology*. 33: 425-475.
- VAN VALEN L. 2005. The statistics of variation. In: variation, a central concept in biology. Hallgrímsson B, Hall BK, eds. New York, Academic. pp29-48.
- VAN WASSENBERGH S, AERTS P, ADRIAENS D, HERREL A. 2005. A dynamical model of mouth closing movements in clariid catfishes: the role of enlarged jaw adductors. *Journal of Theoretical Biology*. 234:49-65.
- VAN WASSENBERGH S, HERREL A, ADRIAENS D, AERTS P. 2004. Effects of jaw adductor hypertrophy on buccal expansions during feeding of airbreathing catfishes (Teleostei, Clariidae). *Zoomorphology*. 123:81-93.
- VAN WASSENBERGH S, HERREL A, ADRIAENS D, HUYSENTRUYT F, DEVAERE S, AERTS P. 2006. A catfish that can strike its prey on land. *Nature*. 448: 881.
- VETTER B. 1878. Untersuchungen zur vergleichenden Anatomie der Kiemen-und Kiefermuskulatur der Fische. *Zeitschrift für Naturwissenschaften*. 12: 431-550.
- VIGLIOLA L, GALZIN R, HARMELIN-VIVIEN ML, MAZEAS F, SALVAT B. 1996. Les Hétérocongrinae (Téléostei: Congidae) de la pente externe de Moorea (Ile de la société, Polynésie Française): distribution et biologie. *Cybiurn*. 20: 379-393.
- VREVEN EJ. 2001. A systematic revision of the African spiny-eels (Mastacembelidae; Synbranchiformes). PhD-thesis. Katholieke Universiteit Leuven.
- VREVEN EJ. 2005. Mastacembelidae (Teleostei; Synbranchiformes) subfamily division and African generic division: an evaluation. *Journal of Natural History*. 39(4): 351-370.
- WEBB PW. 1984. Body form, locomotion and foraging in aquatic vertebrates. *American Zoologist*. 24(1): 170-120.
- WAINWRIGHT PC, RICHARD BA. 1995. Predicting patterns of prey use from morphology of fishes. *Environmental Biology of Fishes*. 44(1-3): 97-113.
- WAKE MH. 1986. The morphology of *Idiocranium-Russeli* (Amphibia, Gymnophiona), with comments on miniaturization through heterochrony. *Journal of Morphology*. 189(1): 1-16

- WALKER, J. A. 1997. Ecological morphology of lacustrine threespine stickleback *Gasterosteus aculeatus* L. (Gasterosteidae) body shape. *Biological Journal of the Linnean Society*. 61: 3-50.
- WANG CH, KUO C.H, MOK HK, AND LEE SC. 2003. Molecular phylogeny of elopomorph fishes inferred from mitochondrial 12S ribosomal RNA sequences. *Zoological Sciences*. 32: 231-241
- WARD AB, BRAINERD EL. 2007. Evolution of axial patterning in elongate fishes. *Biological journal of the Linnean Society*. 90(1): 97-116.
- WATERS JM, McDOWALL RA. 2005. Pylogenetics of the australasian mudfish: evolution of an eel-like body plan. *Molecular phylogenetics and Evolution*. 37(2): 417-425.
- WEITZMAN SJ, VARI RP. 1988. Miniaturization in South-American freshwater fishes - An overview and discussion. *Proceedings of the Biological Society of Washington*. 101(2): 444-465.
- WESTNEAT MW. 1994. Transmission of force and velocity in the feeding mechanisms of labrid fishes (Teleostei, Perciformes). *Zoomorphology*. 114: 103-118.
- WESTNEAT MW. 2003. A biomechanical model for analysis of muscle force, power output and lower jaw motion in fishes. *Journal of Theoretical Biology*. 223: 269-281.
- WESTNEAT MW. 2004. Evolution of levers and linkages in the feeding mechanisms of fishes. *Integrative and Comparative Biology*. 44: 378-389.
- WG EEL. 2006. FAO European Inland Fisheries Advisory Commission: International Council for the exploration of the Sea. Report of the 2006 session on the joint EIFAC/ICES working group on eels. ICES CM 2006/ACFM: 16. p352.
- WIENS JJ, CHIPPINDALE PT, HILLIS DM. 2003. When are phylogenetic analyses misled by convergence? A case study in Texas cave salamanders. *Systematic Biology*. 52(4): 501-514.
- WIENS JJ, SLINGLUFF JL. 2001. How lizards turn into snakes: a phylogenetic analysis of body-form evolution in anguid lizards. *Evolution*. 55: 2303-2318.
- WINTERBOTTOM R. 1974. A descriptive synonymy of the striated muscles of the Teleostei. *Proceedings of the Academy of Natural Sciences of Philadelphia*. 125(12): 225-317.
- WIRTH T, BERNATCHEZ L. 2003. Decline of North Atlantic eels: a fatal synergy? *Proceedings of the Royal Society B: biological sciences, London*. 270: 681-688.
- WITHERS PC. 1981. Physiological correlates of limblessness and fossoriality in Scincid lizards. *Copeia*. 1: 197-204.
- WOJCIECHOWSKI J. 1972. Observations on the biology of cutlassfish *Trichiurus lepturus* L. (Trichiuridae) of Mauritania shelf. *Acta Ichthyologica et Piscatoria*. 11(2): 67-75.
- YABE M, UYENO T. 1996. Anatomical description of *Normanichthys crockeri* (Scorpaeniformes, Incertae sedis: Family Normanichthyidae). *Bulletin of Marine Science*. 58 (2): 494-510.



**X**

Publication List



## PUBLICATION LIST DE SCHEPPER NATALIE

- DE SCHEPPER N, ADRIAENS D, TEUGELS GG, DEVAERE S, VERRAES W. 2004.** Intraspecific variation in the postcranial skeleton morphology in African clariids: a case study of extreme phenotypic plasticity. *Zoological Journal of the Linnean Society*, London. 140: 437-446.
- DE SCHEPPER N, ADRIAENS D, DE KEGEL B. 2005.** *Moringua edwardsi* (Moringuidae: Anguilliformes): Cranial Specialization for Head-First Burrowing? *Journal of Morphology*. 266: 356-368.
- DE SCHEPPER N, ADRIAENS D, DE KEGEL B. 2005.** Cranial morphological specializations related to burrowing: A case study of head-and tail-first-burrowing *Pisodonophis boro*. *Integrative and Comparative Biology*. 45 (6): 985-985.
- DE SCHEPPER N, ADRIAENS D, DE KEGEL B. 2007.** *Pisodonophis boro* (Ophichthidae: Anguilliformes): Specialization for Head-First and Tail-First Burrowing? *Journal of Morphology*. 268(2): 112-126.
- DE SCHEPPER N, DE KEGEL B, ADRIAENS. IN PRESS A.** Morphological Specializations in Heterocongrinae (Anguilliformes: Congridae) Related to Burrowing and Feeding. *Journal of Morphology*. Accepted.
- DE SCHEPPER N, ADRIAENS D, TEUGELS GG, DEVAERE S, VERRAES W. IN PRESS B.** Shape variation in the vertebrae of Anguilliform Clariidae (Ostariophysi: Siluriformes): useful tool for taxonomy? *Journal of Afrotropical Zoology*. Accepted.
- DE SCHEPPER N, LACEUR S, CHRISTIAENS J, VAN LIEFFERINGE C, HERREL A, GOEMANS G, MEIRE P, BELPAIRE C, ADRIAENS D. SUBMITTED A.** Variation in cranial morphology of the European eel: broad- and narrow-headedness. *Biological journal of the Linnean Society*. Submitted.
- DE SCHEPPER N, VAN WASSENBERGH S AND ADRIAENS D. SUBMITTED B.** Morphology of the jaw system in trichiurids: trade-offs between mouth closing and biting performance. *Biological Journal of the Linnean Society*.
- CHOI HF, DE SCHEPPER N, HERREL A, AERTS P, ADRIAENS D. SUBMITTED.** A comparative kinematical study of the swimming locomotion in two burrowing anguilliform bony fish: *Pisodonophis boro* and *Heteroconger hassi* (Anguilliformes). *Journal of Experimental Biology*.





# Evolutionary morphology of body elongation in teleosts: aspects of convergent evolution

## II - Figures, Tables and Addendum

Thesis submitted to obtain the degree of  
Doctor in Sciences (Biology)

Proefschrift voorgedragen tot het bekomen  
van de graad van Doctor in de Wetenschappen (Biologie)

Academiejaar 2006-2007

Rector: Prof. Dr. Paul Van Cauwenberge

Decaan: Prof. Dr. Herwig Dejonghe

Promotor: Prof. Dr. Dominique Adriaens

De Schepper Natalie



Universiteit Gent  
Faculteit Wetenschappen  
Vakgroep Biologie

Evolutionary  
Morphology of  
Vertebrates





**A**

Figures

Fig. I- 1

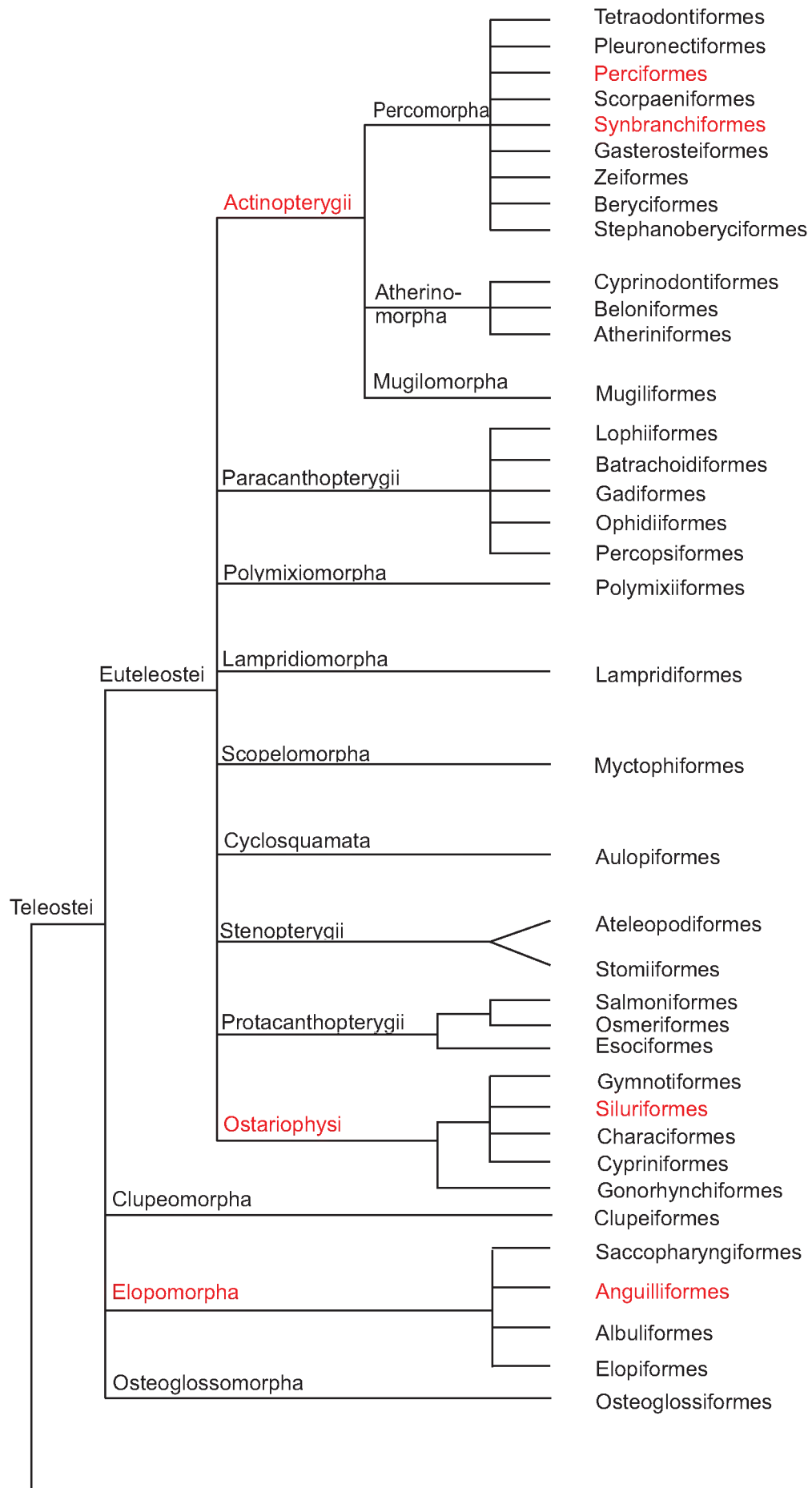


Fig. I- 1: Hierarchy of higher taxa of fishes, modified after Nelson (1994). Taxa examined in this study and in which body elongation has evolved are indicated in red.

Fig. 1- 2

A, Clariidae

B, *Channallabes apus*

C, *Clarias gariepinus*

a, *Heterobranchus longifilis*

b, *Dinopterus cunningtoni*

c, *Clarias poensis*

d, *clariallabes melas*

e, *Clariallabes variabilis*

f, *Gymnallabes typus*

g, *Channallabes apus*

o-fr, os frontale

o-io-II, III, IV, os infraorbitale I, II, III

o-lac, os lacrimale

o-leth, os lateroethmoideum

o-meth, os mesethmoideum

o-par-soc, os parieto-supraoccipitale

o-pt, os pteroticum

o-sph, os sphenoticum

o-spop, os suprapraeoperculare

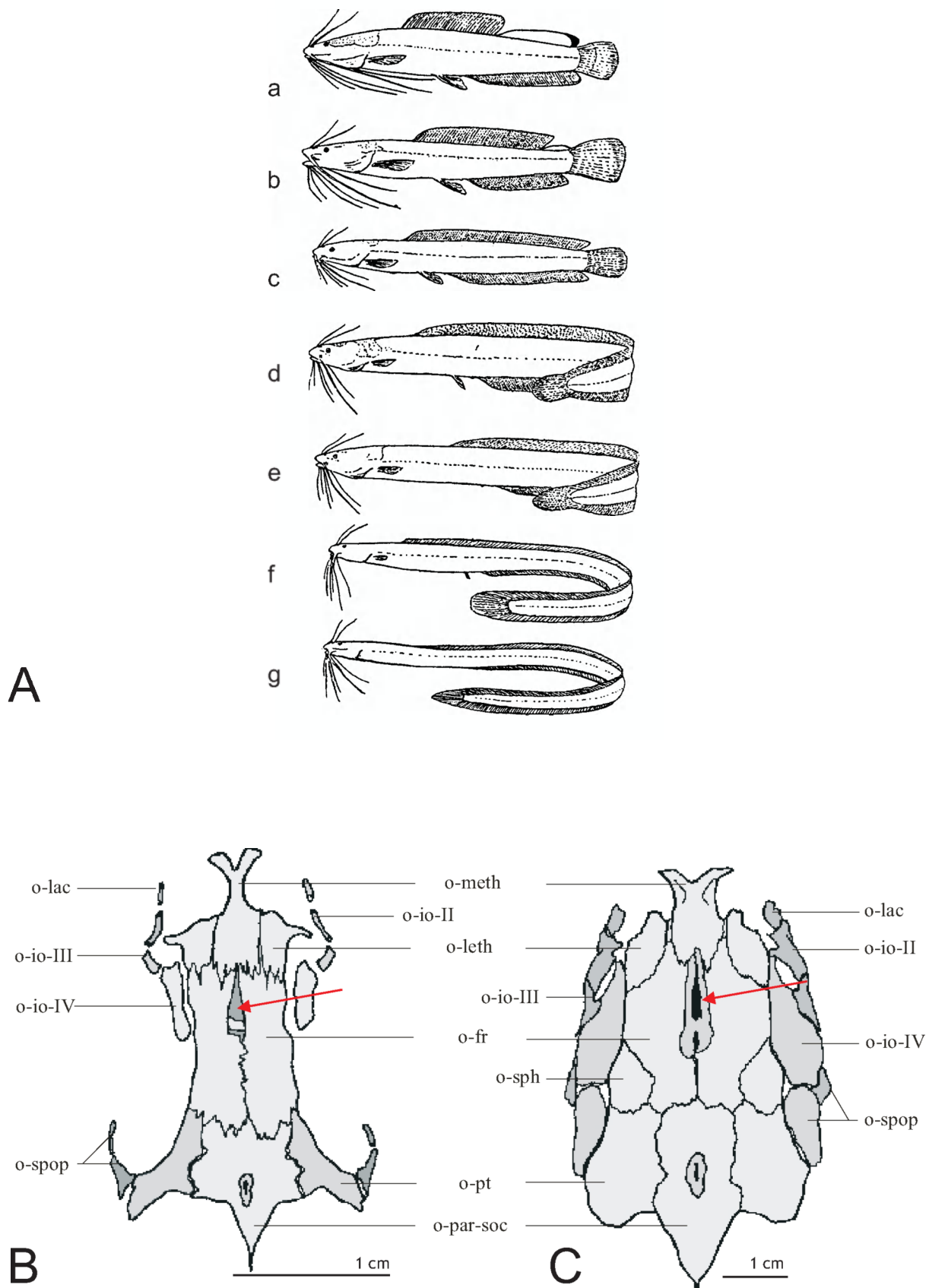


Fig. I- 2 **A**: Habitus of representatives of the family Clariidae, forming an apparent orthogenetic series from fusiform to anguilliform species (after Pellegrin, 1927). In the mean time, it has been proven that body elongation has evolved at least four times independently, originating from a *Clarias*-like ancestor. **B**: Dorsal view of the skull of *Channallabes apus* (after Devaere, 2005b). **C**: Dorsal view of the skull of *Clarias gariepinus* (after Devaere et al., 2007c). Arrows indicate the dorsal fontanel-like space between the frontal bones.

Fig. 1- 3

A, *Channallabes apus*

B - C, left side *Clarias gariepinus*, right side *Channallabas apus*



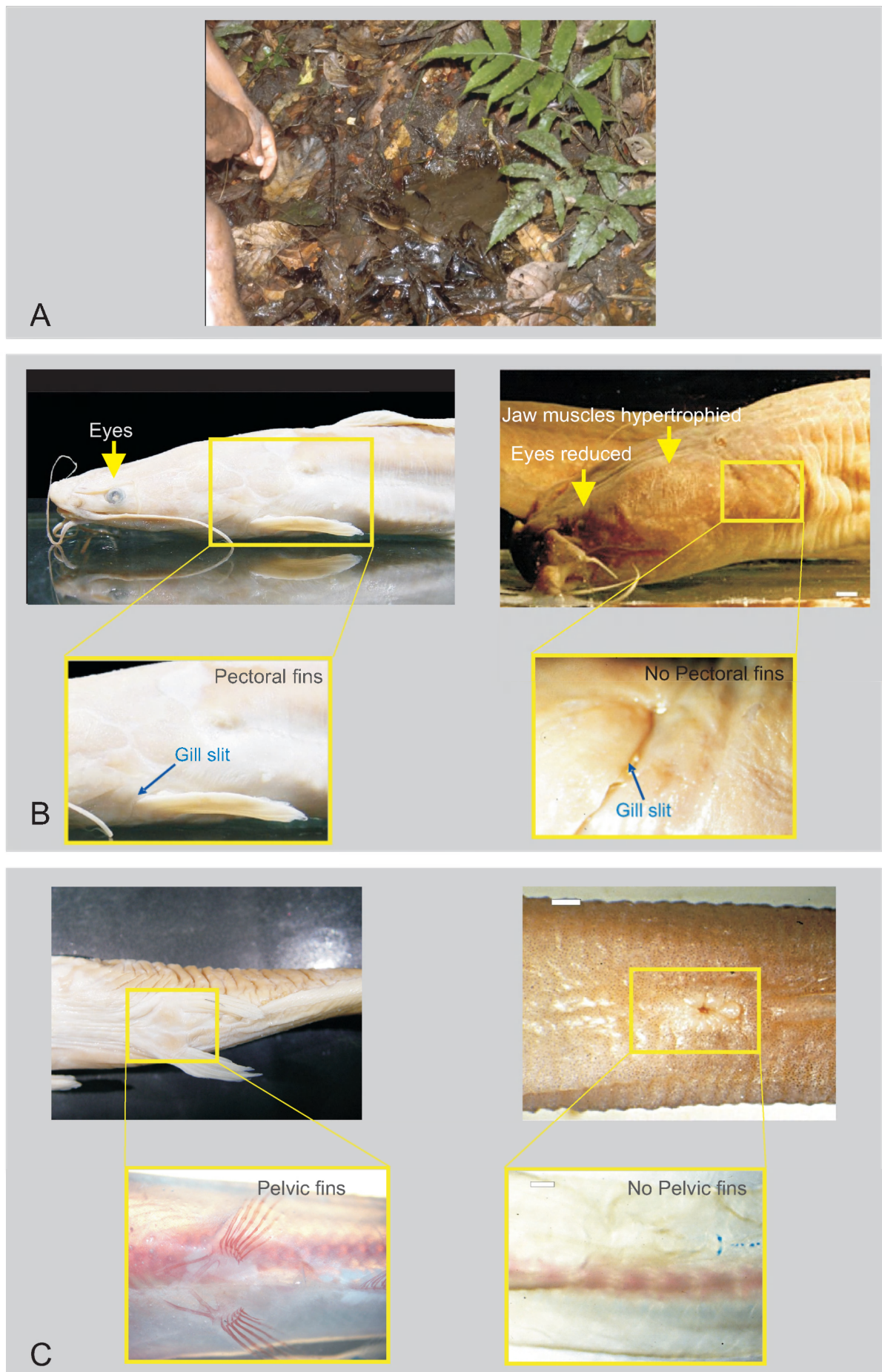


Fig. I- 3 A: Habitat of *Channallabas apus*, burrowed in the mud in swampy areas of Gabon (picture from Adriaens D). **B** and **C**: Pictures on the left side represent *Clarias gariepinus* (after Adriaens et al., 2002), whereas those on the right side represent *Channallabas apus* (with courtesy of Devaere S). Differences in development of the eyes, jaw muscles, pectoral and pelvic fins are indicated.

Fig. 1- 4

A, *Clarias gariepinus*

B, *Clariallabes longicauda*

C, *Gymnallabes typus*

D, *Channallabes apus*

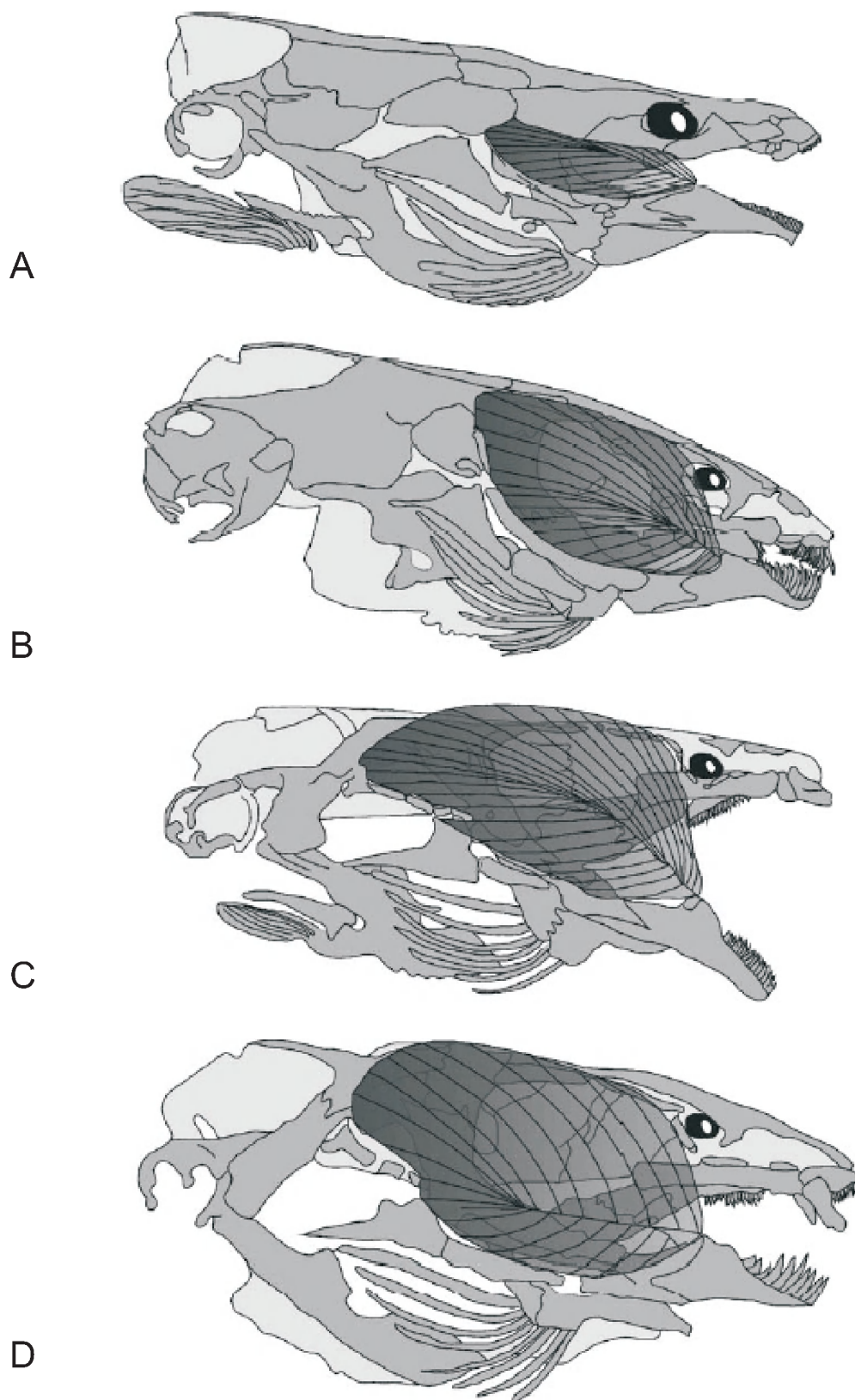


Fig. I- 4: The osteocranium and jaw muscles (transparent dark grey) in lateral view of four clariid species with increasing size of jaw muscles. (A) *Clarias gariepinus*, (B) *Clariallabes longicauda*, (C) *Gymnallabes typus*, (D) *Channallabes apus*. In *Clarias gariepinus*, part of the jaw muscles is covered by bones. (modified after Van Wassenbergh et al., 2005).

Fig. 1- 5

A, Anguilliformes

B, *Pisodonophis boro*

C, *Moringua edwardsi*

D, *Conger conger*

E, *Heteroconger hassi*

F, *Anguilla anguilla*

G, *Heteroconger longissimus*

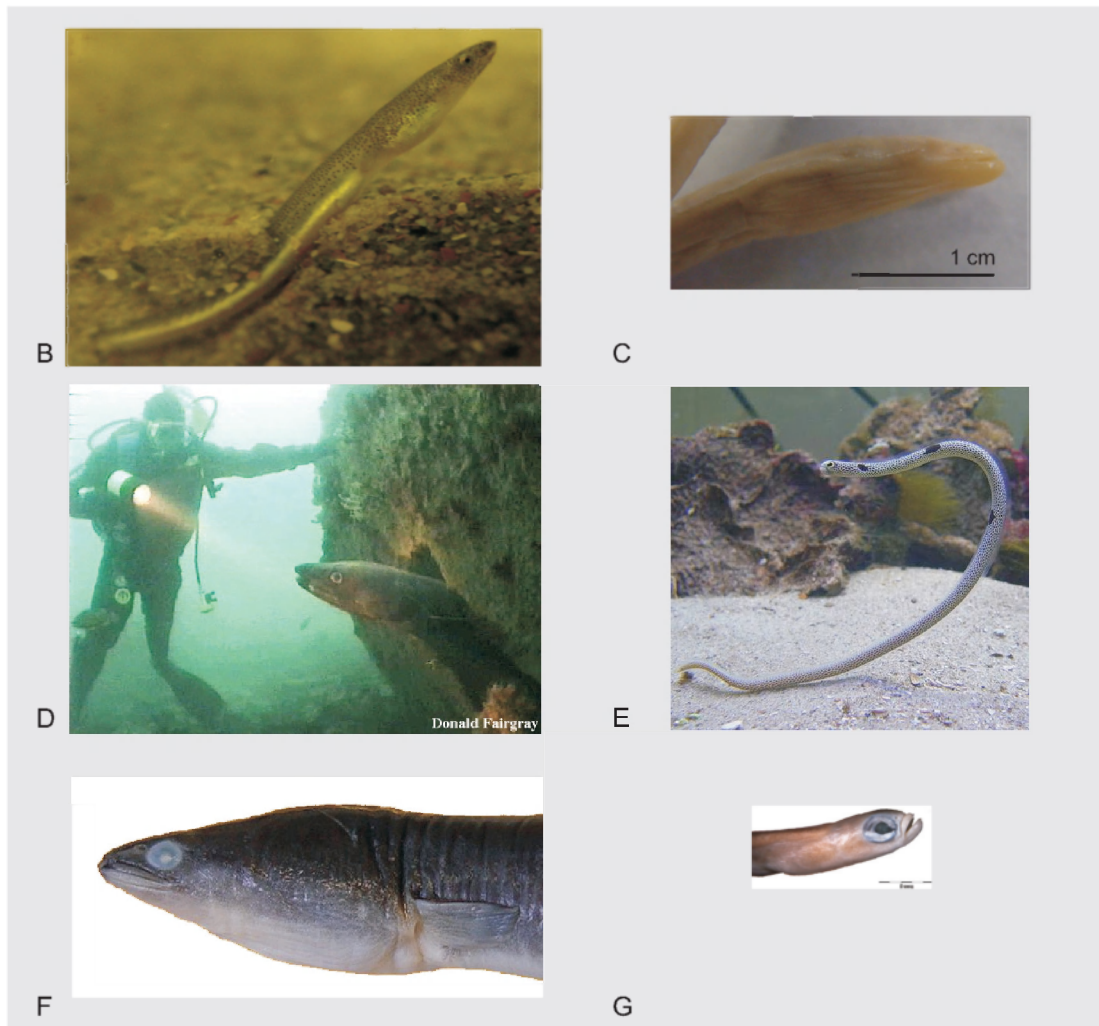
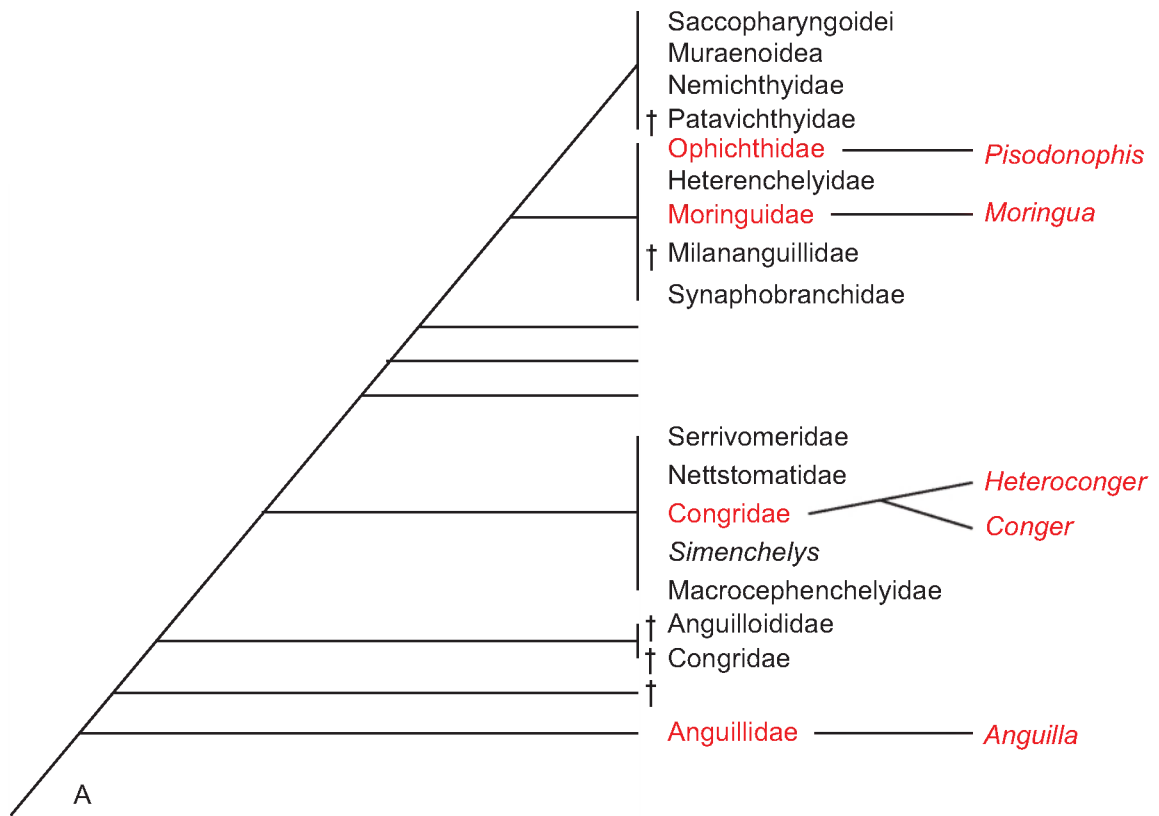


Fig. I- 5: (A) Hypothesis of the relationships of the anguilliform families. Phylogenetic tree of Anguilliformes based on 30 extant species and 21 fossil taxa. (modified after Belouze, 2001, fig. 184). Species (and their respective family) examined in this study are highlighted. Habitus of (B) *Pisodonophis boro*, (C) *Moringua edwardsi*, (D) *Conger conger* (from <http://web.ukonline.co.uk/aquarium/pages/conger.html>), (E) *Heteroconger hassi*, (F) *Anguilla anguilla*, (G) *Heteroconger longissimus*.

Fig. 1- 6

A, *Platyclarias machadoi*

B, *Platyallabes tihoni*

C, *Channallabes*

D, *Dolichallabes microphthalmus*

E, *Gymnallabes typus*

F, *Clarias gariepinus*

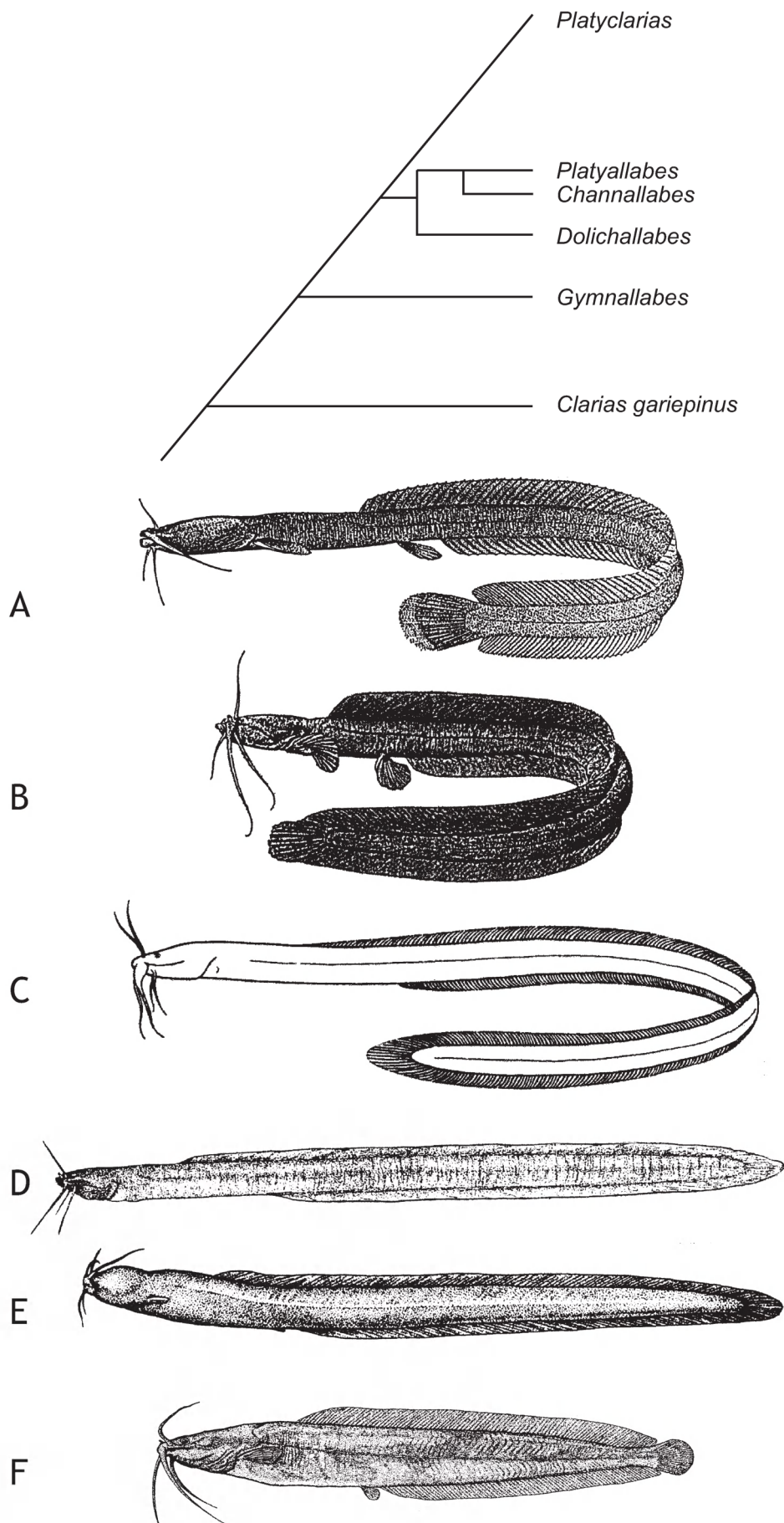


Fig. I- 6: Hypothesis of the relationships of the clariid species. Phylogenetic tree of the Clariidae (modified after Devaere, 2005B, plate V.2-7). Only the species, examined in this dissertation are presented and illustrated (after Devaere, 2005).

Fig. 1- 7

A, Trichiuridae

B, *Aphanopus carbo*

C, *Trichiurus lepturus*



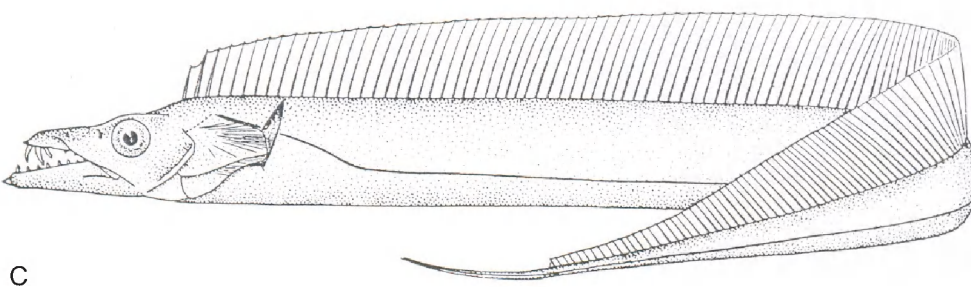
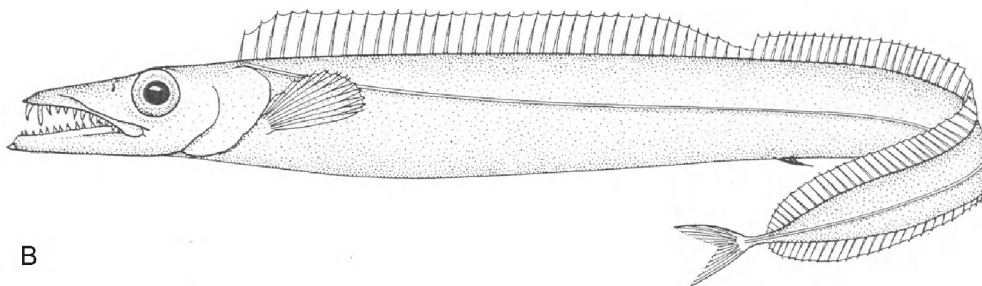
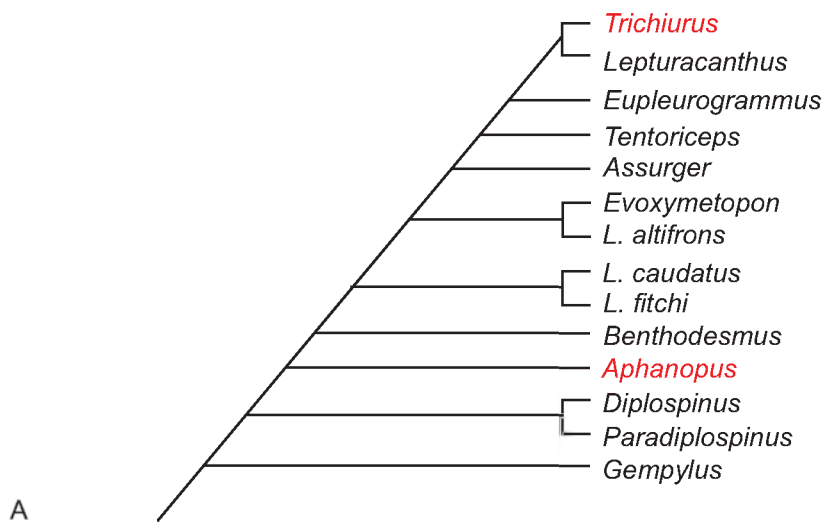


Fig. I- 7 A: Hypothesis of the relationships of the trichiurid species (modified after Gago, 1998, Fig. 6). Trichiurid species used in this study are highlighted. Habitus of (B) *Aphanopus carbo* and (C) *Trichiurus lepturus* (after Parin and Nakamura, 2002).


Fig. 1- 8


A, Mastacembelidae


B, *Mastacembelus mastacembelus*

C, *M. marcheii*

D, *M. brichardi*

 *Mastacembelus mastacembelus*

 *M. marcheii*

 *M. brichardi*

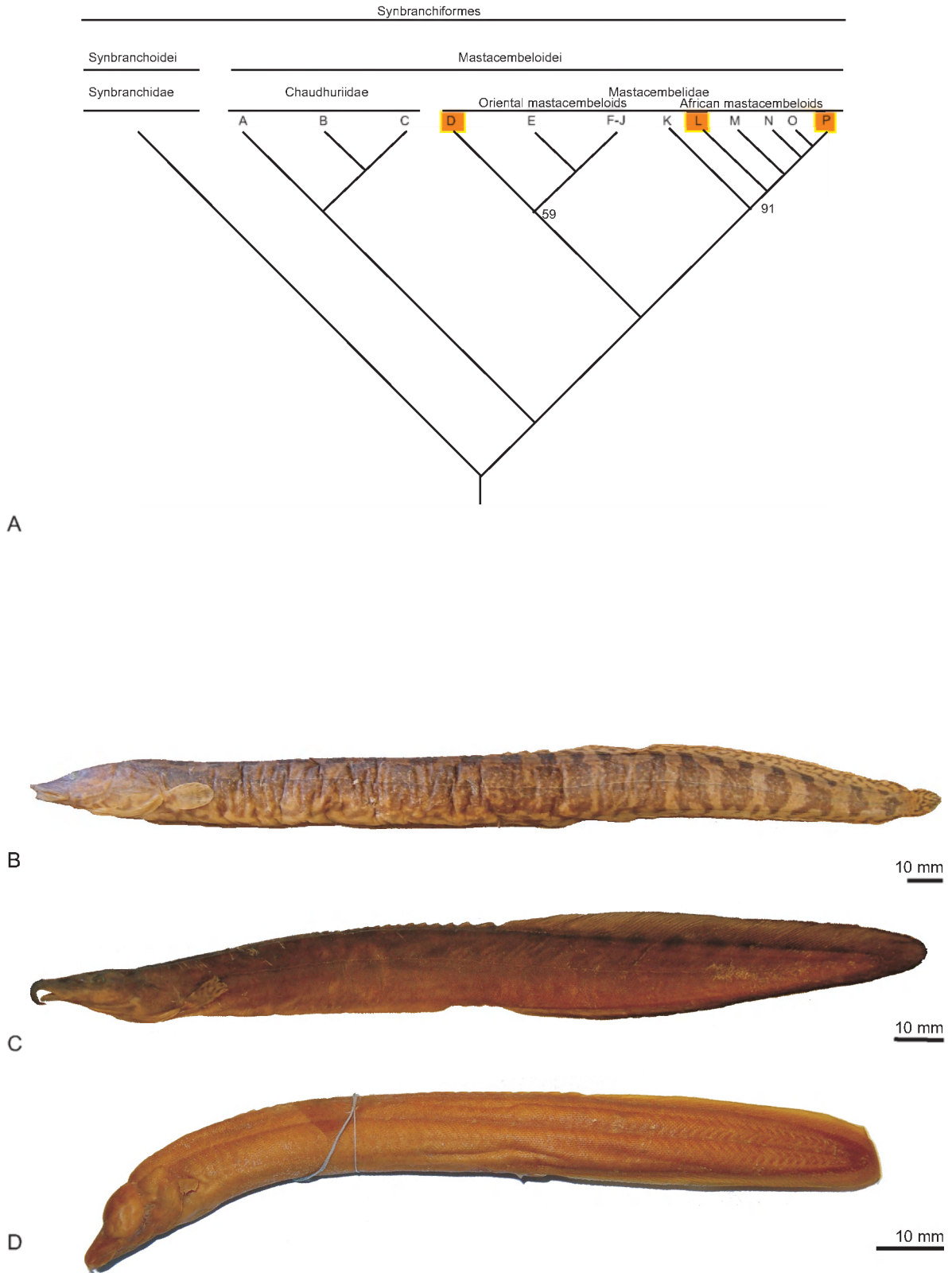


Fig. I- 8 A: Hypothesis of the relationships of the Mastacembelidae (modified after Travers, 1984B). The mastacembelids examined in this study are indicated in orange: (D) *Mastacembelus mastacembelus*, (L) *M. Marcheii*, (P) *M. brichardi*. Habitus of (B) *Mastacembelus mastacembelus*, (C) *M. marcheii* and (D) *M. Brichardi*.

Fig. III.1- 1



Fig. III.1- 1: Picture of sampling site: Scheldt- Lippensbroek. The Lippensbroek is a controlled inundation area connected to the Scheldt.

Fig. III.1- 2

- 1: Northern population (Oyem-region)
- 2: Eastern population (Makokou-region)
- 3: Southern population
  - 3a: Franceville-region,
  - 3b: Congo-basin.

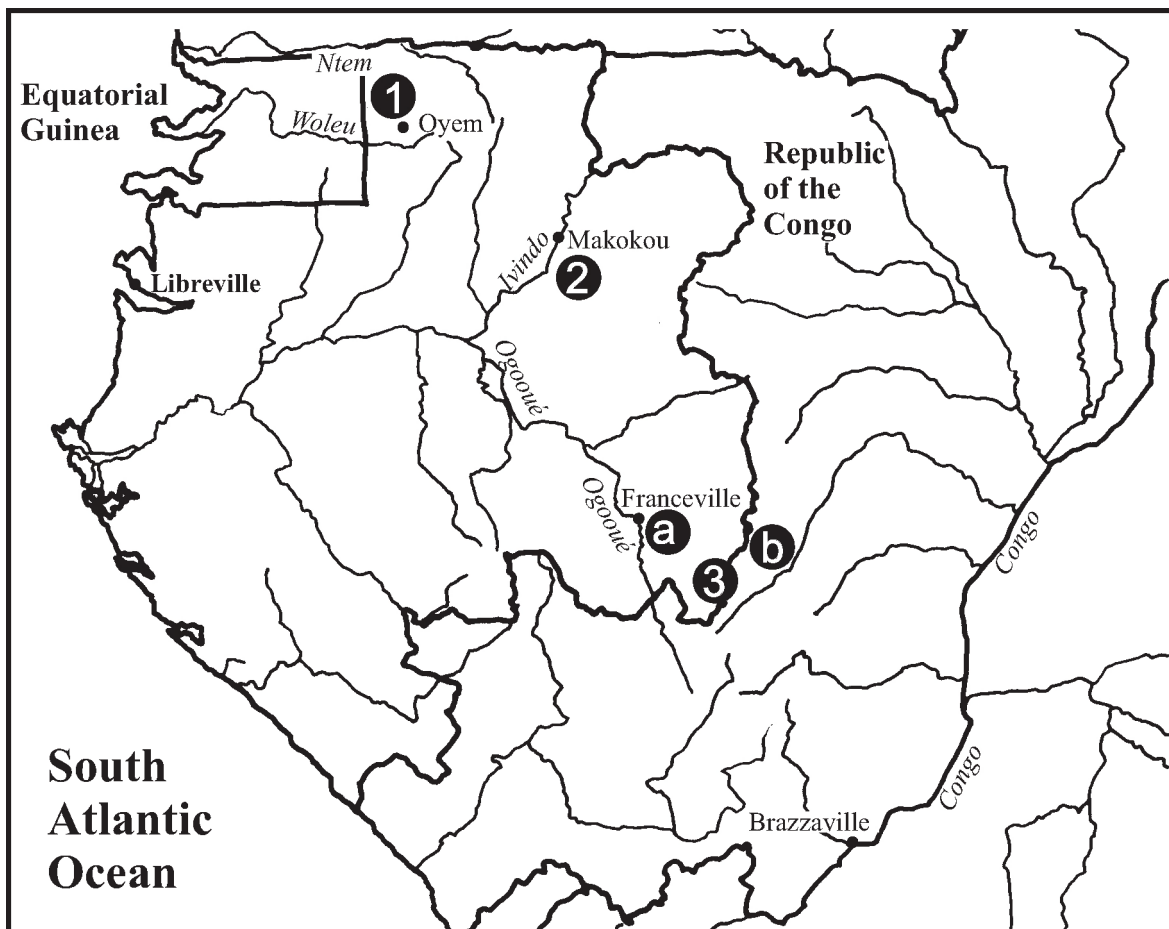


Fig. III.1- 2: Illustration of the geographic location of the sampling locations in Gabon. 1: Northern population (Oyem-region), 2: Eastern population (Makokou-region), 3: Southern population, 3a: Franceville-region, 3b: Congo-basin.

Fig. III.2- 1

*Anguilla anguilla*

A, the neurocranium in lateral view

- 1 LL1: posterior margin of tooth row on ventral surface of premaxillo-ethmovomerine complex;
- 2 LL2: anterior tip of the premaxillo-ethmovomerine complex;
- 3 LL3: anterior tip of the pterotic;
- 4 LL4: rostral tip of sphenotic process;
- 5 LL5: dorso-caudal process of epiotic;
- 6 LL6: dorso-caudal process of pterotic;
- 7 LL7: ventro-caudal tip of basioccipital;
- 8 LL8: posterior tip of orbit;
- 9 LL9: dorso-caudal tip of orbit;
- 10 LL10: anterior tip of orbit.

B, the neurocranium in dorsal view

- 1 LD1: rostral tip of the premaxillo-ethmovomerine complex;
- 2 +24 LD2-24: lateral tips of rhombuslike anterior extension of premaxillo-ethmovomerine complex;
- 3 +23 LD3-23: caudal points of the rhombus-like extension;
- 4 +22 LD4-22: rostral tips of the frontal arches;
- 5 +21 LD5-21: rostral tips of the pterotics;
- 6 +20 LD6-20: sutures between pterotic and sphenotic in front of sphenotic processes;
- 7 +19 LD7-19: inclination points of the concave side of the sphenotic processes
- 8 +18 LD8-18: rostral tips of sphenotic processes;
- 9 +17 LD9-17: lateral points of the convex side of the sphenotic processes;
- 10 +16 LD10-16: sutures between pterotic and sphenotic behind sphenotic processes;
- 11 +15 LD11-15: caudal tips of pterotic processes;
- 12 +14 LD12-14: caudal tips of epiotic processes;
- 13 LD13: caudal tip of supraoccipital.



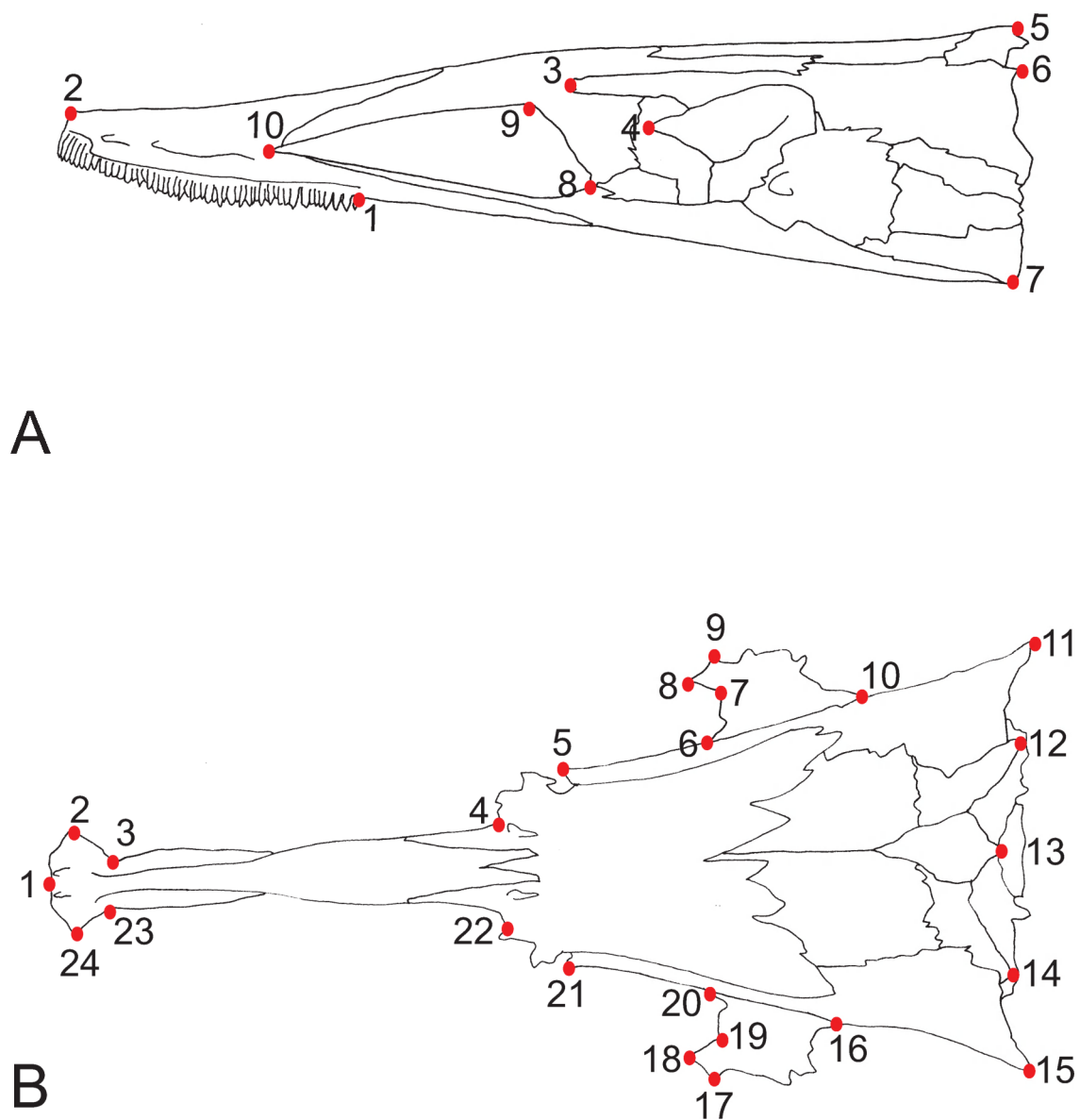


Fig. III.2- 1: Head of *Anguilla anguilla*. Landmarks defined to describe the shape of (A) the neurocranium in lateral view and (B) in dorsal view.

Fig. III.2- 2

*Anguilla anguilla.*

1	L Sn-E L	length from the tip of the snout to the rostral border of the eye in lateral view
2	L Sn-E D	length from the tip of the snout to the rostral border of the eye in dorsal view
3	L Sn-E c	length from the snout to the caudal border of the eye
4	L E-nos r	length from rostral nostril to the rostral border of the eye
5	L Sn-Pe	length from the tip of the snout to the pectoral girdle
6	H H [E r]	height of the head at the level of the rostral border of the eye
7	H H [E c]	height of the head at the level of the caudal border of the eye
8	H H [nos r]	height of the head at the level of the rostral nostril
9	H Pe	height of the body at the level of the pectoral girdle
10	W H [E r]	width of the head at the level of the rostral border of the eye
11	W H [E c]	width of the head at the level of the caudal border of the eye
12	W H [nos r]	width of the head at the level of the rostral nostril
13	W Pe	width of the body at the level of the pectoral girdle
14	D	length of the lower jaw, from the tip of the lower jaw to the angle of the mouth
15	H E	height of the eye
16	L E	length of the eye
17	IOD r	interorbital distance at the level of the rostral border of the eye
18	IOD c	interorbital distance at the level of the caudal border of the eye
19	IOD m	interorbital distance at the centre of the eye

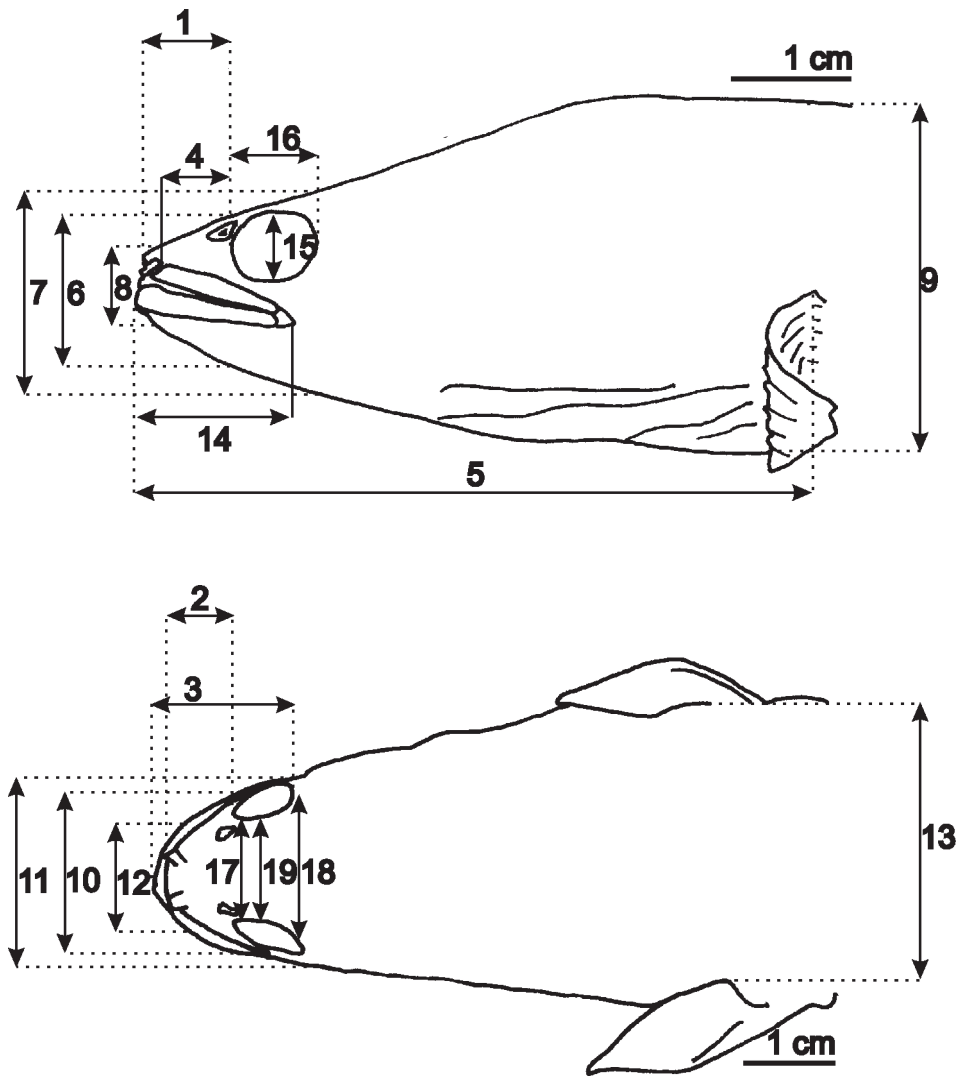


Fig. III.2- 2: Illustration of the cranial measurements on the head of *Anguilla anguilla*.

Fig. III.2- 3

*Aphanopus carbo*

$L_m$  = input-lever

$\beta$  = angle between the lower jaw length axis and the input-lever,

$\sigma$  = angle between the input-lever and the line of action of the jaw muscle,

$\theta$  = average angle of pennation.

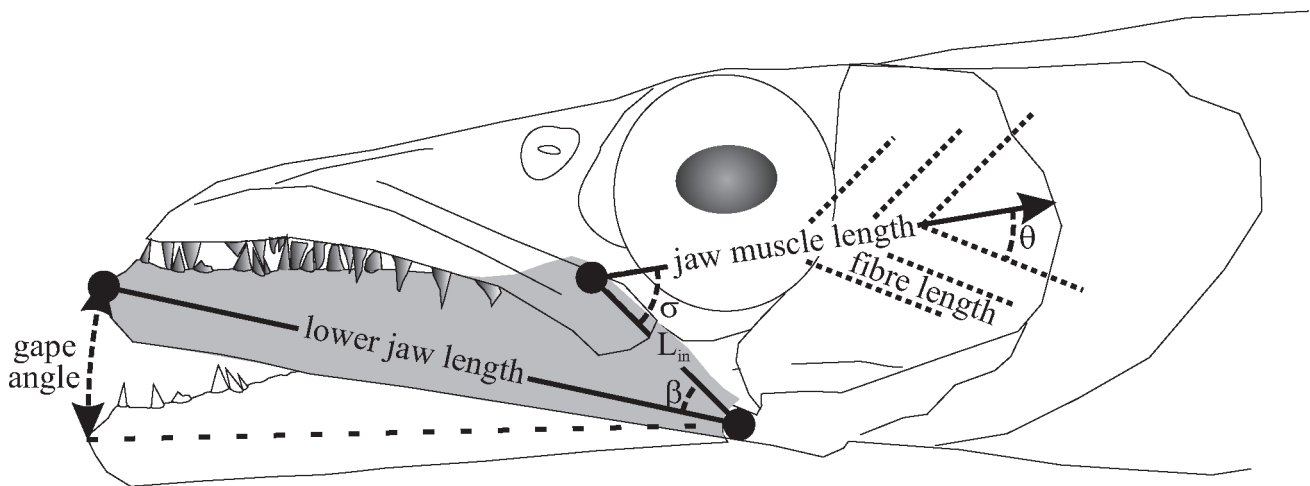


Fig. III.2- 3: Schematic representation (for *Aphanopus carbo*) of the variables of the lower jaw lever system used for model calculations of bite force and mouth closing movements.  $\sigma$  = angle between the lower jaw length axis and the input-lever ( $L_{in}$ ),  $\theta$  = angle between the input-lever ( $L_{in}$ ) and the line of action of the jaw muscle,  $\beta$  = average angle of pennation.

Fig. IV.1- 1

*Moringua edwardsi*

AdNas, adnasal  
B lat Syst, body lateral line system  
c AdNas, adnasal canal  
c Et, ethmoid canal  
c IO, infraorbital canal  
c Md, mandibular canal  
c Ot, otic canal  
c POp, preopercular canal  
c SO, supraorbital canal  
Cav, cavity  
cm F, frontal commissure  
cm ST, supratemporal commissure  
L Nas W, lateral wing of Nasal  
Nas, nasal  
P int, internal pores  
PO, preopercle  
PostO, postorbital

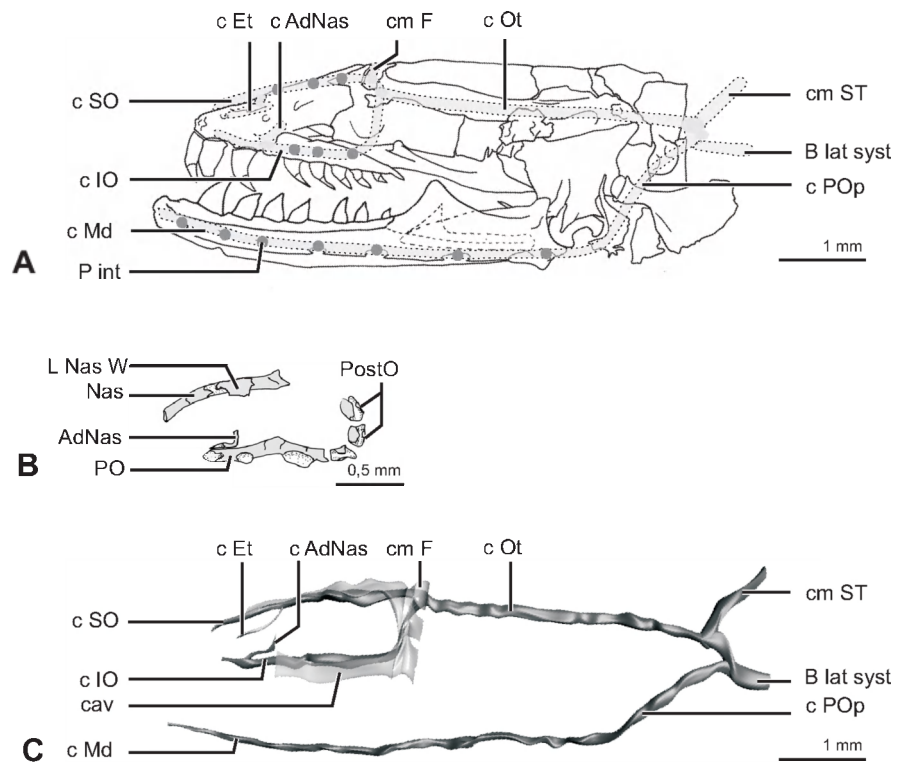


Fig. IV.1- 1: The cranial lateral line system of *Moringua edwardsi*. **A**: Lateral view of the composing canals. Dark dots illustrate internal sensory pores. The orbital pores are in contact with the dermal cavities. **B**: Lateral view of circumorbital bones of the cranial lateral line system. **C**: 3-D reconstruction of the cranial lateral line system, with position of the dermal cavities.

Fig. IV.1- 2

*Moringua edwardsi*

A2v, subdivision of the adductor mandibulae  
A2m, subdivision of the adductor mandibulae  
AdNas, adnasal  
AH, adductor hyomandibulae  
Ang, angular complex  
AO, adductor operculi  
apo, aponeurosis  
BH, basihyal  
BOc, basioccipital  
c IO, infraorbital canal  
c Md, mandibular canal  
c Ot, otic canal  
c POp, preopercular canal  
c SO, supraorbital canal  
Cav, cavity  
CH A, anterior ceratohyal  
CH P, posterior ceratohyal  
cm F, frontal commissure  
ct, connective tissue  
Epax, epaxials  
Epi, epiotic  
ExOc, exoccipital  
ExOc, exoccipital  
F, frontal  
FA, frontal arch  
HHAd, hyohyoidei adductores  
Hyp, hypaxials  
IOp, interopercle  
L Ang-IOp, angulo-interopercular ligament  
L BH-CH, basihyo-ceratohyal ligament  
L Prim, primordial ligament  
L UH-CH, urohyo-ceratohyal ligament  
LO, levator operculi  
M, Meckel's cartilage  
Mx, maxillary  
Par, parietal  
PH, protractor hyoidei  
P-Hm, pars hyomandibularis  
PH $\alpha$ ,  $\alpha$  subdivision of protractor hyoidei  
PH $\beta$ ,  $\beta$  subdivision of protractor hyoidei  
PO, preopercle  
PostO, postorbital  
Pr cor, coronoid process  
Pr D Op, dorsal opercular process  
Pr PSph, parasphenoidal process  
Pro, prootic  
PSph, parasphenoid  
Pt, pterotic  
SOC ri, supraoccipital ridge  
SOc, supraoccipital  
T A2 v, tendon of A2 v  
T LO, tendon of the levator operculi  
UH, urohyal



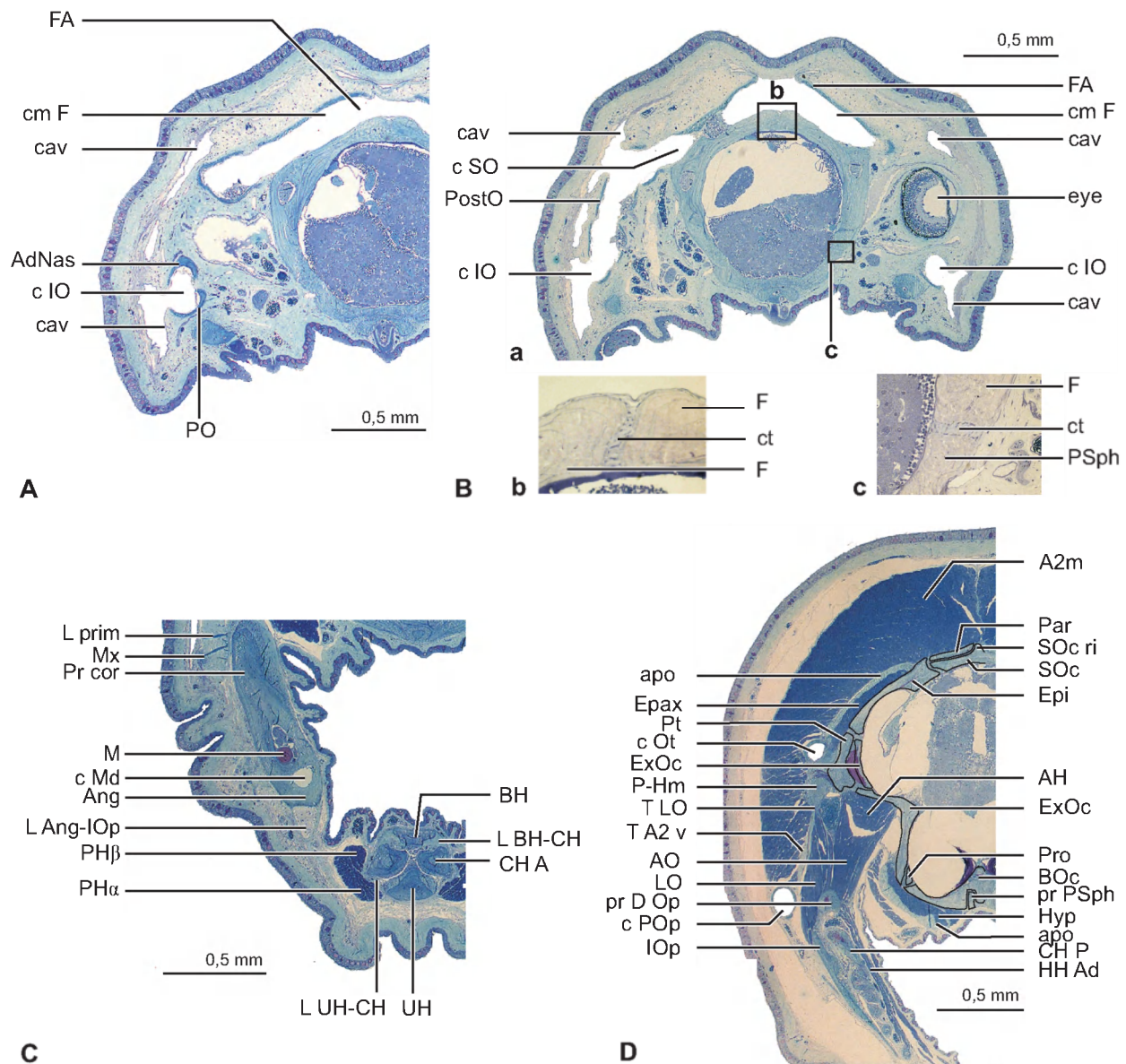


Fig. IV.1- 2: **A**: Cross section of the head of *Moringua edwardsi* at the level of the frontal commissure. **Ba**: Cross section at the level of the fusion between the supra- and infraorbital canal. Inserts show scarf joints and connective tissue between frontals (**Bb**) and between frontals and parasphenoid (**Bc**). **C**: Cross section at the level of the hyoid apparatus. **D**: Cross section at the level of the occipital region. Lines surrounding the bones are manually drawn to improve the visualization of the borderlines.

Fig. IV.1- 3

*Moringua edwardsi*

af Mx- Etv A, anterior maxillo-premaxillo-ethmovomerine articular facet  
af Mx- Etv P, posterior maxillo-premaxillo-ethmovomerine articular facet  
af Susp A, anterior suspensorial articular facet  
af Susp P, posterior suspensorial articular facet  
BOc, basioccipital  
Epi, epiotic  
ExOc, exoccipitals  
F, frontal  
FA, frontal arch  
Hm, hyomandibula  
IOp, interopercle  
Mx, maxillary  
Op, opercle  
Orb, orbital  
Par, parietal  
PMx-Etv, premaxillo-ethmovomerine complex  
POp, preopercle  
PP, pterygoid  
Pr PSph, parasphenoidal process  
Pro, prootic  
PSph, parasphenoid  
Pt, pterotic  
PtSph, pterosphenoid  
Q, quadrate  
SOc, supraoccipital  
Sph, sphenotic

Fig. IV.1- 4

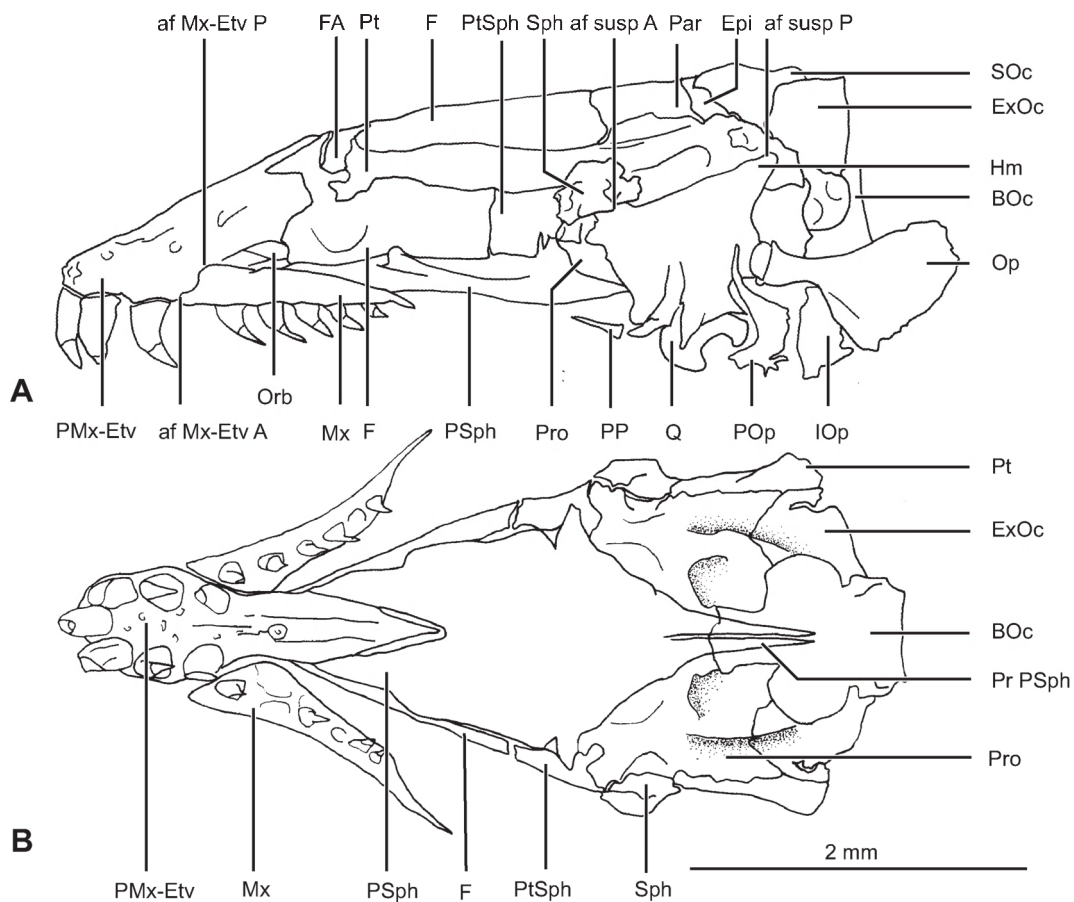


Fig. IV.1- 3: Illustration of the position of the cranial bones of *Moringua edwardsi* in (A) lateral view and (B) ventral view.



Fig. IV.1- 4: Schematic illustration of joint types between skull bones in *Moringua edwardsi*. A: Scarf joint - The cranial bones are connected by connective tissue and form scarf joints, with tapering edges. B: Extended scarf joint - The cranial bones of skull roof (frontals, parietals, supraoccipital, epiotics and exoccipitals) show a high amount of overlap, formed by the extension of the scarf joints. The frontals are interconnected by scarf joints and connected to the parietals by extended scarf joints. C: Butt joint - These have straight sutures and nearly square edges.

Fig. IV.1- 5

*Moringua edwardsi*

ac Md, mandibular articulation condyle  
ac Op, opercular articulation condyle  
af Op, opercular articulation facet  
af Susp A, anterior suspensorial articulatory facet  
af Susp P, posterior suspensorial articulatory facet  
Hm, hyomandibula  
IOP, interopercle  
L Ang-IOP, angulo-interopercular ligament  
L Ang-POp, angulo-preopercular ligament  
L Hm-CH, hyomandibulo-ceratohyal ligament  
L IOP-CH, interoperculo-ceratohyal ligament  
L Op-IOP, operculo-interopercular ligament  
L Pop-Op, preoperculo-opercular ligament  
L PP, pterygoid ligament  
Op, opercle  
POp, preopercle  
PP, pterygoid  
Q, quadrate  
SOp, subopercle

Fig. IV.1- 6

*Moringua edwardsi*

ac Md, mandibular articulation condyle  
Ang, angular complex  
BH, basihyal  
CH A, anterior ceratohyal  
CH P, posterior ceratohyal  
D, dentary  
L Ang-IOP, angulo-interopercular ligament  
L Ang-POp, angulo-preopercular ligament  
L Hm-CH, hyomandibulo-ceratohyal ligament  
L IOP-CH, interoperculo-ceratohyal ligament  
PH $\alpha$ ,  $\alpha$  subdivision of protractor hyoidei  
PH $\beta$ ,  $\beta$  subdivision of protractor hyoidei  
Pr cor, coronoid process  
R Br, branchiostegal ray  
SH, sternohyoideus  
T PH A, anterior tendon of protractor hyoidei  
T PH P, posterior tendon of protractor hyoidei  
T PH $\beta$  P, posterior tendon of  $\beta$  subdivision of protractor hyoidei  
T SH, tendon of sternohyoideus  
UH, urohyal

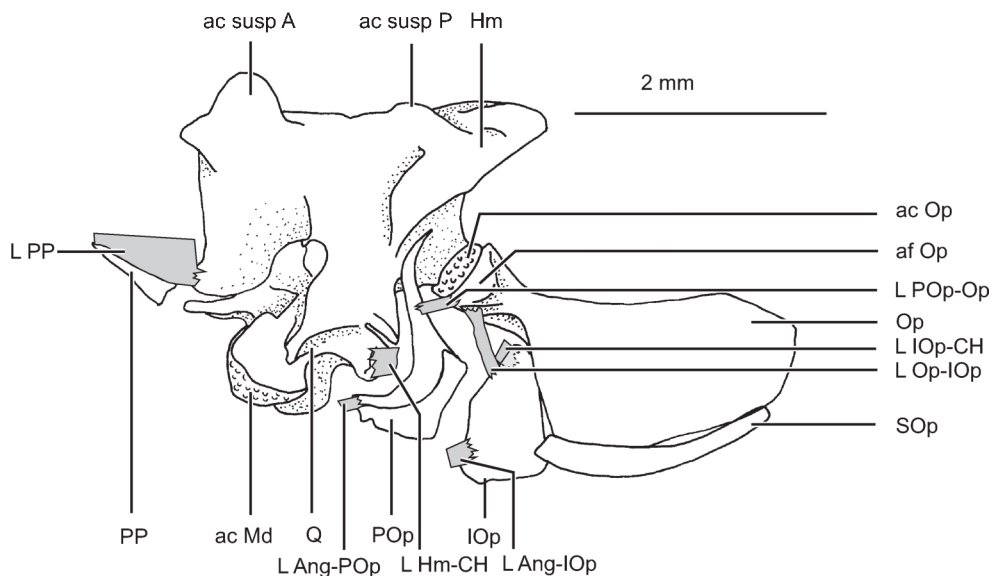


Fig. IV.1- 5: Lateral view of the suspensorium of *Moringua edwardsi*.

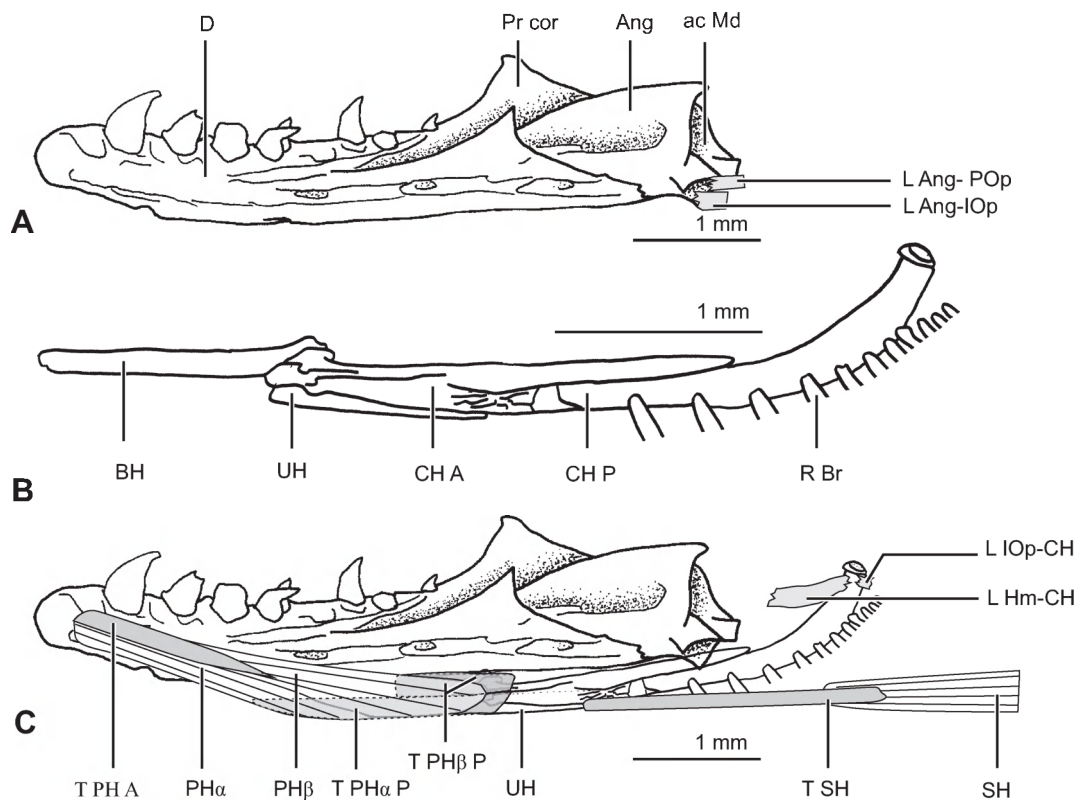


Fig. IV.1- 6: A: Medial view of the lower jaw of *Moringua edwardsi*. B: Lateral view of the hyoid apparatus. C: Left lower jaw and left muscle bundle of the protractor hyoidei is removed. Dotted lines indicate part of the tendons being covered by the right muscle bundle.

Fig. IV.1- 7

*Moringua edwardsi*

A1, A2d, A2m, A2v, A3, A<sub>0</sub> subdivisions of the adductor mandibulae complex

AAP, adductor arcus palatini

AH, adductor hyomandibulae

AO, adductor operculi

DO, dilatator operculi

Epax, epaxials

L Prim, primordial ligament

LAP, levator arcus palatini

LO, levator operculi

T A2m, tendon of subdivisions A2m

T DO, tendon of dilatator operculi

T LAP, tendon of levator arcus palatini

T LO, tendon of levator operculi

Fig. IV.1- 8

*Moringua edwardsi*

F2, generated forces by the adductor mandibulae subdivision A2

F3, generated forces by the adductor mandibulae subdivision A3

Fh 2, Fh 3, horizontal component of force

Fv 2, Fv 3, vertical component of force

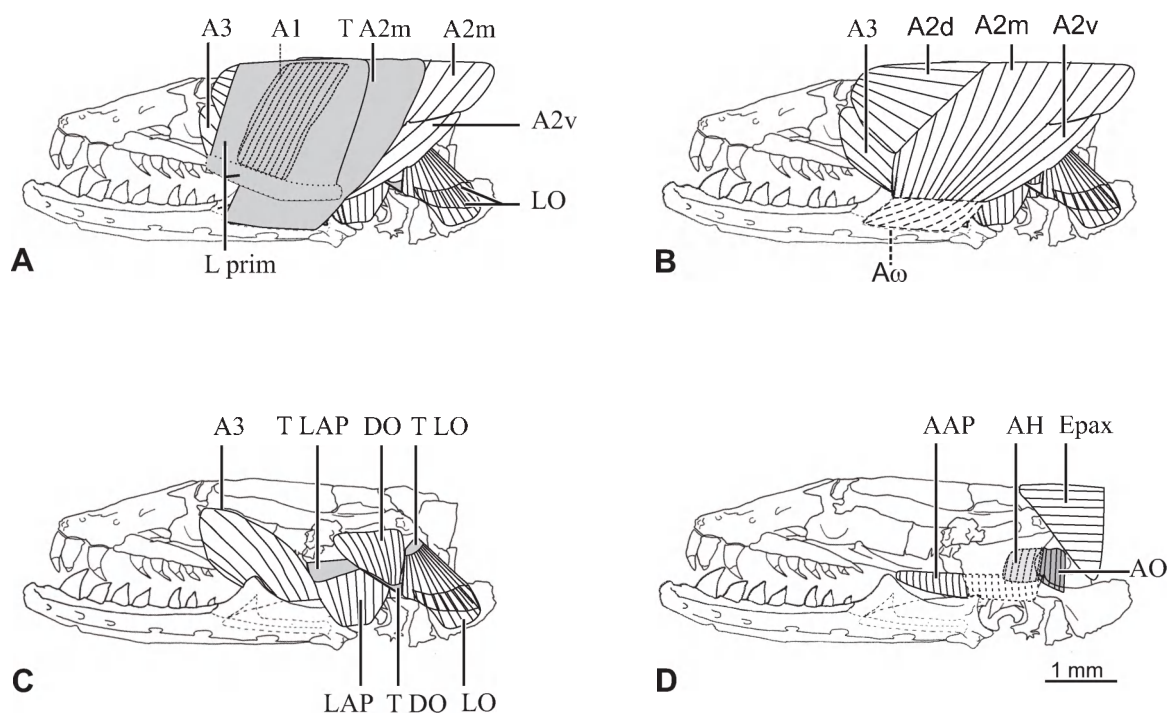


Fig. IV.1- 7: Lateral view of the cranial muscles *Moringua edwardsi*. Dotted lines indicate parts of structures being covered by other elements. **A:** Skin is removed. **B:** Primordial ligament and A1 are removed, exposing the adductor mandibulae complex with dorsal (A2d), medial (A2m), ventral (A2v) and mandibular (A $\omega$ ) part. **C:** The adductor mandibulae complex is removed, except for the A3. **D:** Opercular muscles are removed.

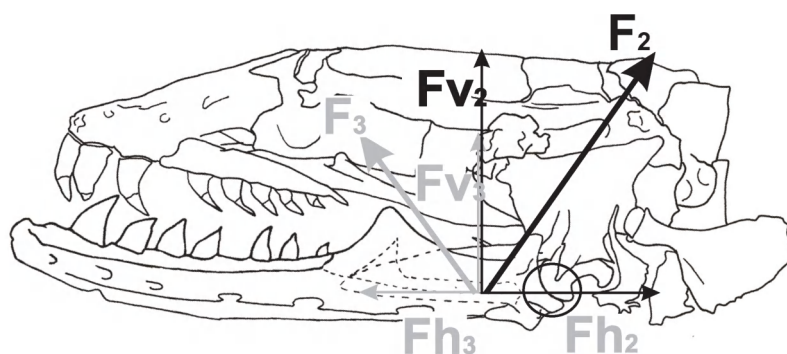


Fig. IV.1- 8: Schematic illustration of the generated forces by the adductor mandibulae A2 ( $F_2$ ) and A3 ( $F_3$ ) with respectively their horizontal ( $F_{h2}$  and  $F_{h3}$ ) and vertical components ( $F_{v2}$  and  $F_{v3}$ ). The horizontal components run in the opposite direction, reducing the pressure in the joint between the lower jaw and the quadrate (encircled).

Fig. IV.1- 9

*Moringua edwardsi*

Cfr, caudal fin rays

FD, flexor dorsalis

FV, flexor ventralis

H pl D, dorsal hypural plate

H1, H2, hypural 1 and 2

HL, hypochordal longitudinalis

Hph, hypurapophysis

Ir, interradials

PU1, first preural centrum

Px, proximalis

UN, uroneural

Us, urostyle



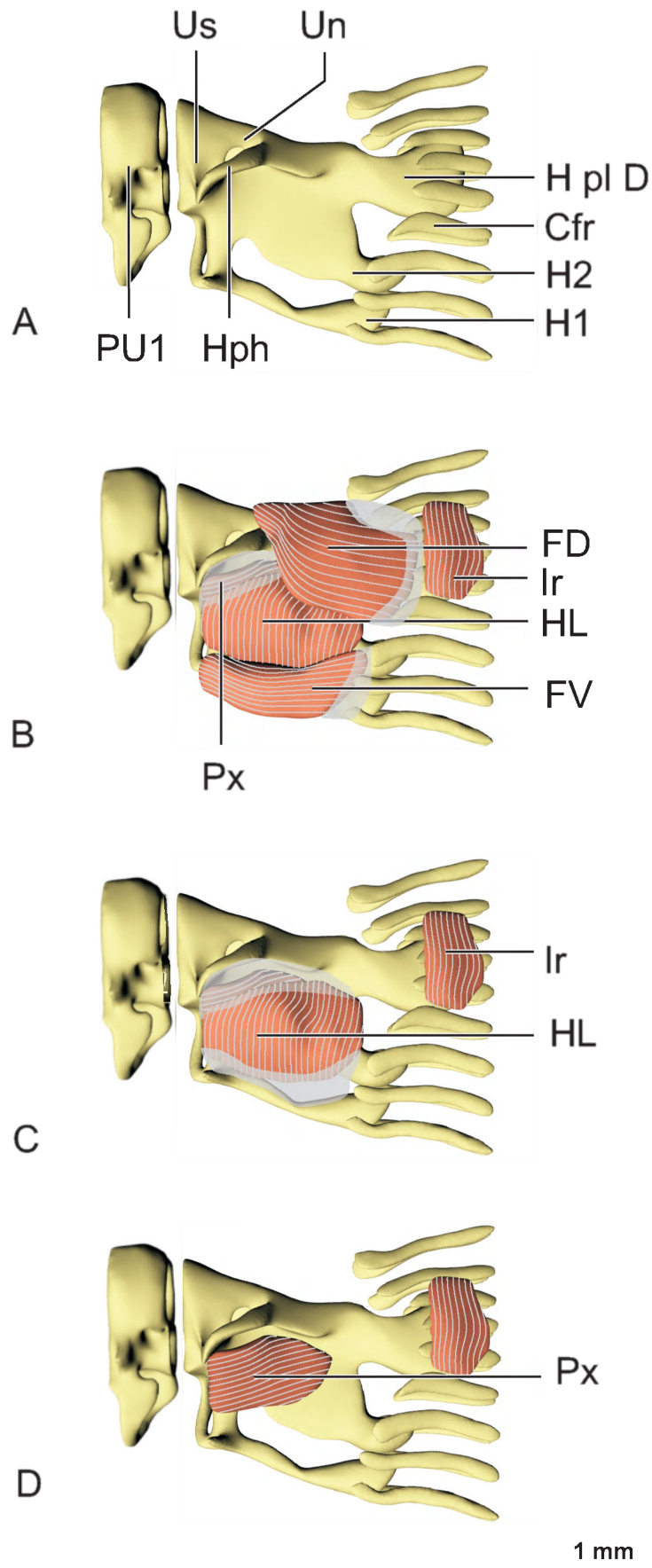


Fig. IV.1- 9: 3-D reconstruction of the tail of *Moringua edwardsi*. Tendons are shown in transparent grey. A: The caudal skeleton in lateral view. B: The epaxials and hypaxials are removed. C: The flexor dorsalis and ventralis are removed. D: The hypochordal longitudinalis is removed.

Fig. IV.1- 10

*Heteroconger hassi*

ac Mx- Etv A, anterior maxillo-premaxillo-ethmovomerine articular condyle  
ac Mx- Etv P, posterior maxillo-premaxillo-ethmovomerine articular condyle  
af Susp A, anterior suspensorial articular facet  
af Susp P, posterior suspensorial articular facet  
af V-PP, vomero-ptyergoidal articular facet  
BOc, basioccipital  
BSph, basisphenoid  
c SO, supraorbital canal  
D, dentary  
Epi, epiotic  
ExOc, exoccipitals  
F, frontal  
IOp, interopercle  
Mx, maxillary  
Nas, nasal  
Op, opercle  
P Mx, pedicel of maxillary  
Par, parietal  
PMx-Etv, premaxillo-ethmovomerine complex  
POp, preopercle  
Pr BSph, Basisphenoidal process  
Pro, prootic  
Pr Sph, sphenotic process  
PSph, parasphenoid  
Pt, pterotic  
PtSph, pterosphenoid  
R Br, branchiostegal ray  
SOc, supraoccipital  
Sph, sphenotic  
Susp, suspensorium.

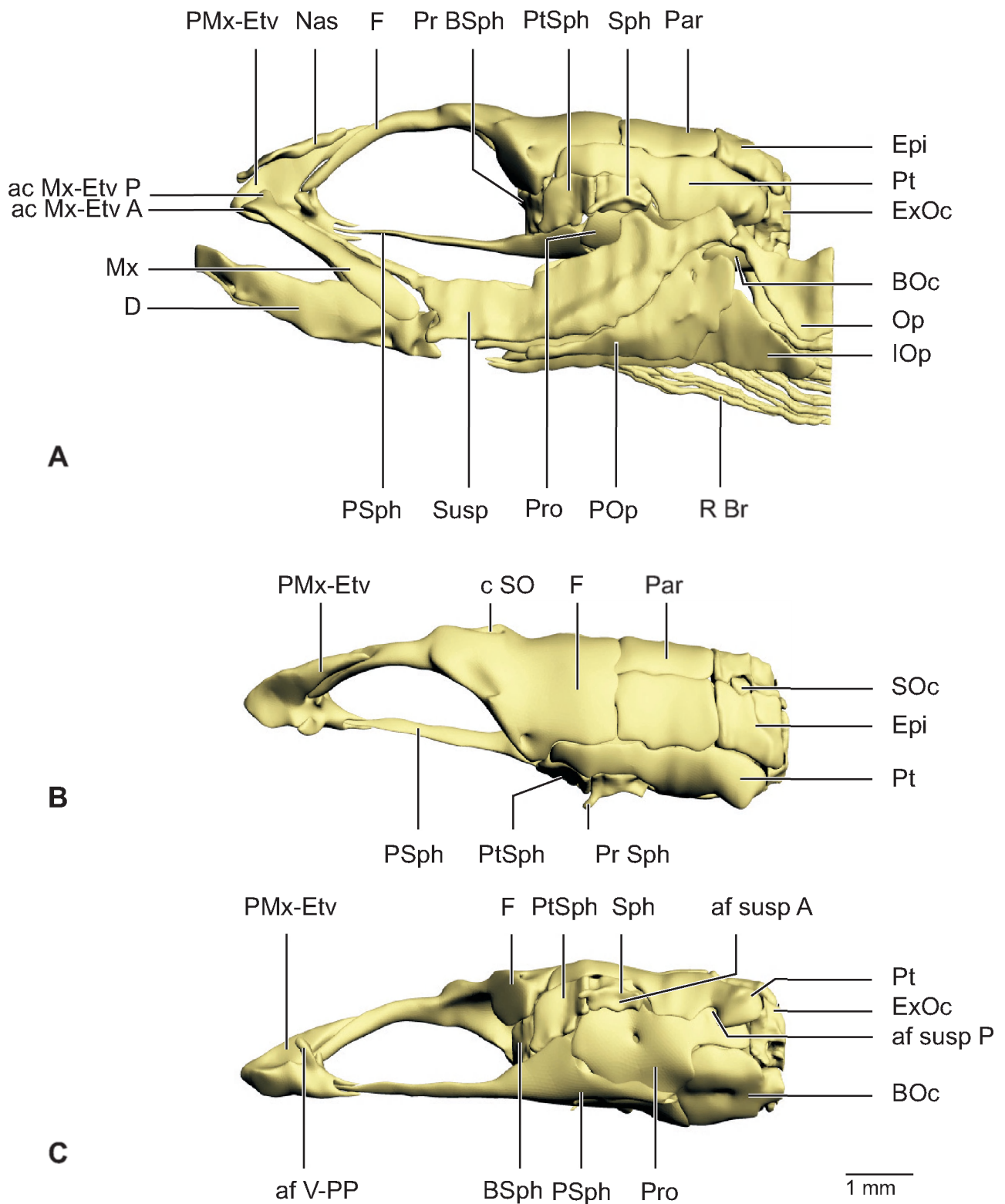


Fig. IV.1- 10: A: 3-D reconstruction of the skull of *Heteroconger hassi* in lateral view. B: 3-D reconstruction of the neurocranium, with the splanchnocranium removed, in dorso-lateral view and (C) ventro-lateral view. The suspensorium (quadrate, hyomandibula and pterygoid), lower jaw (angular and dentary complex) and hyoid arch (anterior and posterior ceratohyal) are considered in this reconstruction as one unit.

Fig. IV.1- 11

*Heteroconger hassi*

ac Md, mandibular articular condyle of the quadrate  
Ac Op, opercular articular condyle of the hyomandibula  
ac susp A, anterior suspensorial condyle of the hyomandibula  
ac susp P, posterior suspensorial condyle of the hyomandibula  
af CH, articular facet of the anterior ceratohyal  
af D Op, rostro-dorsal articular facet of the opercle  
af Md, mandibular articular facet  
Ang, angular complex  
c Et, ethmoid canal  
c IO, infraorbital canal  
c MD, mandibular canal  
c Ot, otic canal  
c POp, preopercular canal  
c SO, supraorbital canal  
CH A, anterior ceratohyal  
CH P, posterior ceratohyal  
cm ST, supratemporal commissure  
M, Meckel's cartilage  
D, dentary  
Hm, hyomandibula  
IOp, interopercle  
Op, opercle  
PO, preorbital  
POp, preopercle  
PostO, postorbital  
PP, pterygoid  
Pr Ang, angular process  
Pr cor, coronoid process  
Pr D Op, rostro-dorsal process of the opercle  
Q, quadrate  
R Br, branchiostegal ray  
SOp, subopercle  
SubO, suborbital

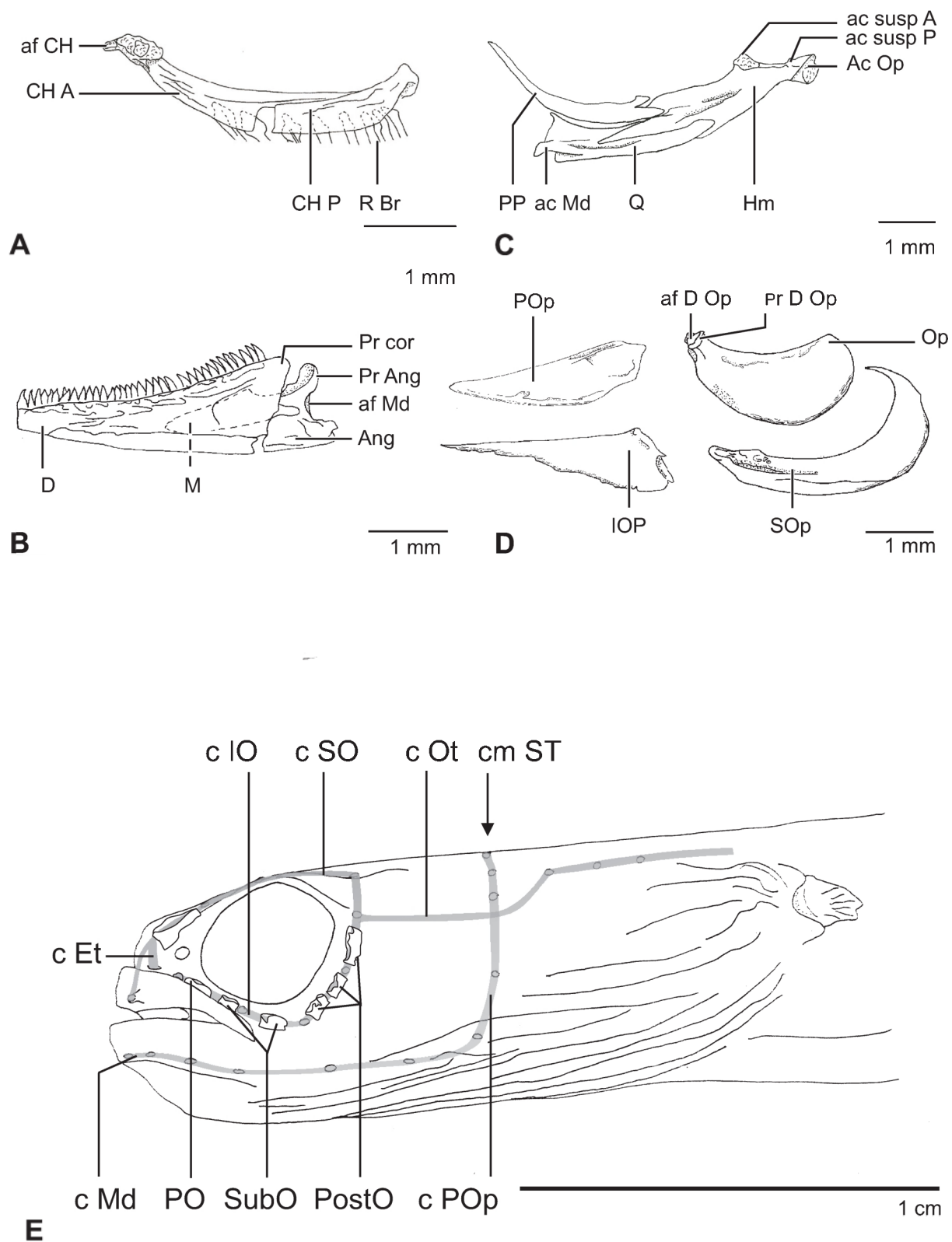


Fig. IV.1- 11. *Heteroconger hassi*. **A**: The anterior and posterior ceratohyals in medial view. **B**: The lower jaw in lateral view. **C**: The quadrate, hyomandibula and pterygoid in lateral view. **D**: The opercular apparatus in lateral view. **E**: Illustration of the composing canals, commissure, pores and circumorbital elements of the cephalic lateral line system.

Fig. IV.1- 12

*Heteroconger hassi*

A2, subdivision of adductor mandibulae complex  
AAP, adductor arcus palatini  
AO, adductor operculi  
D, dentary complex  
DO, dilatator operculi  
Epax, epaxials  
Epi, epiotic  
F, frontal  
HH Ad, hyohyoidei adductores  
HH Inf, hyohyoideus inferior  
Int, intermandibularis  
IOp, interopercle  
LAP, levator arcus palatini  
LO, levator operculi  
Op, opercle  
Par, parietal  
PH, protractor hyoidei  
POp, preopercle  
Pro, prootic  
PSph, parasphenoid  
Pt, pterotic  
PtSph, pterosphenoid  
SCar A, supracarinalis anterior  
Sph, sphenotic  
Susp, suspensorium  
T A2, T A3, tendon of A2, A3  
T DO, tendon of dilatator operculi  
T LAP, tendon of levator arcus palatini  
T LO, tendon of levator operculi  
T PH P, posterior tendon of protractor hyoidei.

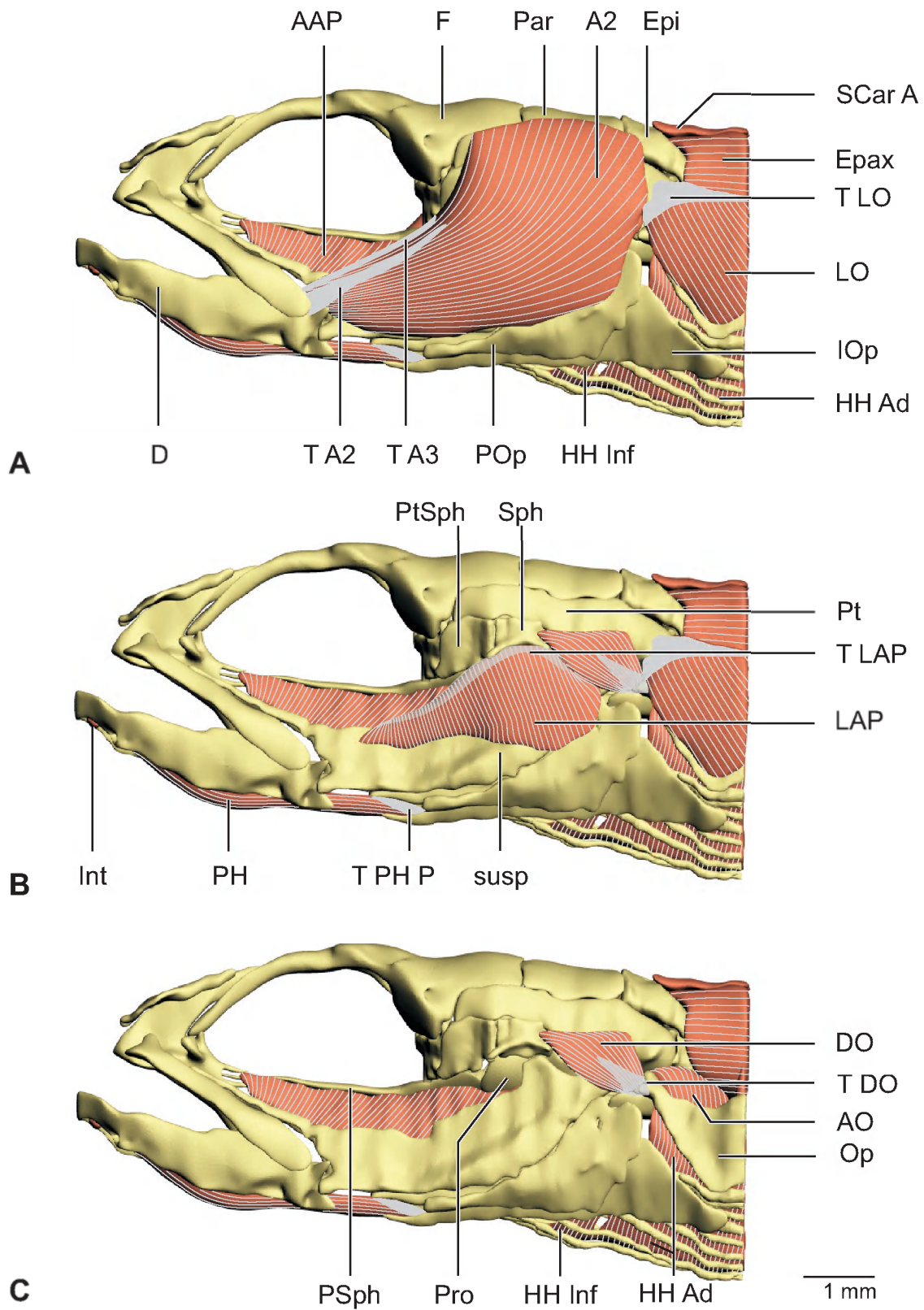


Fig. IV.1- 12: 3-D reconstruction of the cranial muscles of *Heteroconger hassi*. A: The skin is removed. B: The adductor mandibulae complex is removed. C: The levator arcus palatini and levator operculi are removed.

Fig. IV.1- 13

*Heteroconger hassi*

A2, A3, A $\omega$ , subdivisions A2, A3, A $\omega$  of the adductor mandibulae complex

Mx maxillary

Q, quadrate

T A2, A3, A $\omega$ , tendon of subdivisions A2, A3, A $\omega$



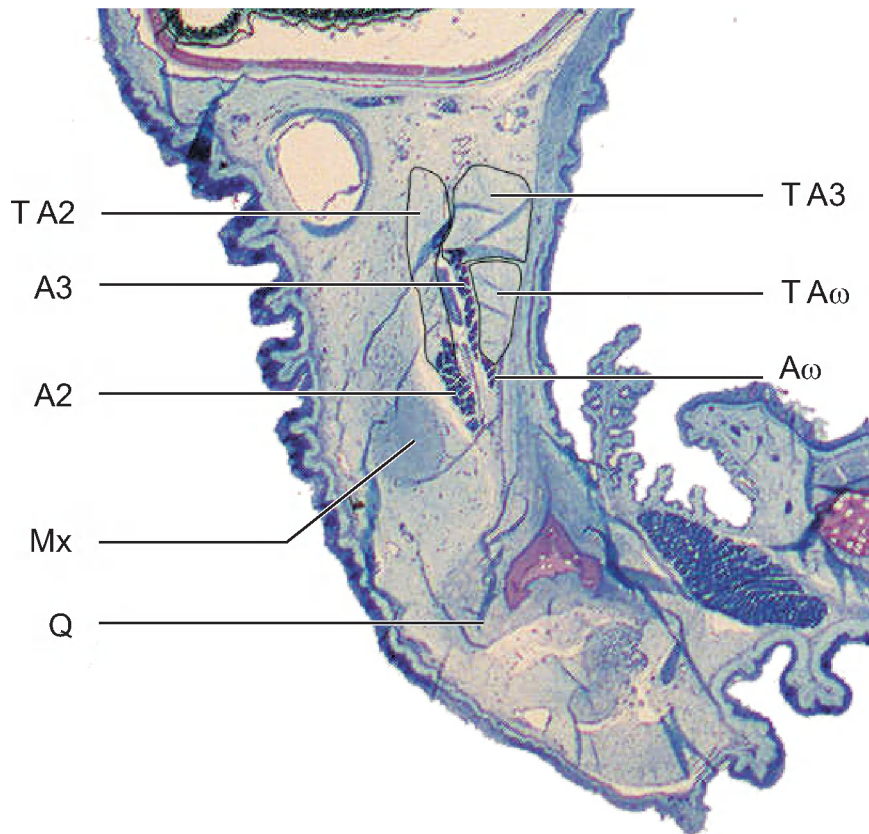


Fig. IV.1- 13: Cross-section at the level of the anterior part of the adductor mandibulae complex of *Heteroconger hassi*, just behind the quadrato-mandibular articulation. The tendons of each adductor mandibulae subdivision are illustrated.

Fig. IV.1- 14

*Heteroconger hassi*

A2, A3, subdivisions A2, A3 of the adductor mandibulae complex  
AAP, adductor arcus palatini  
AH, adductor hyomandibulae  
AO, adductor operculi  
apo, aponeurosis  
BH, basihyal  
CH A, anterior ceratohyal  
CH P, posterior ceratohyal  
D, dentary complex  
DO, dilatator operculi  
HH Ad, hyohyoidei adductores  
HH Inf, hyohyoideus inferior  
Int, intermandibularis  
IOp, interopercle  
LAP, levator arcus palatini  
LO, levator operculi  
Op, opercle  
PH, protractor hyoidei  
POp, preopercle  
SH, sternohyoideus  
SOp, subopercle  
Susp, suspensorium  
T A2, A3, A $\omega$ , tendon of subdivisions A2, A3, A $\omega$   
T PH A, anterior tendon of protractor hyoidei  
T PH P, posterior tendon of protractor hyoidei  
T SH, tendon of sternohyoideus  
UH, urohyal

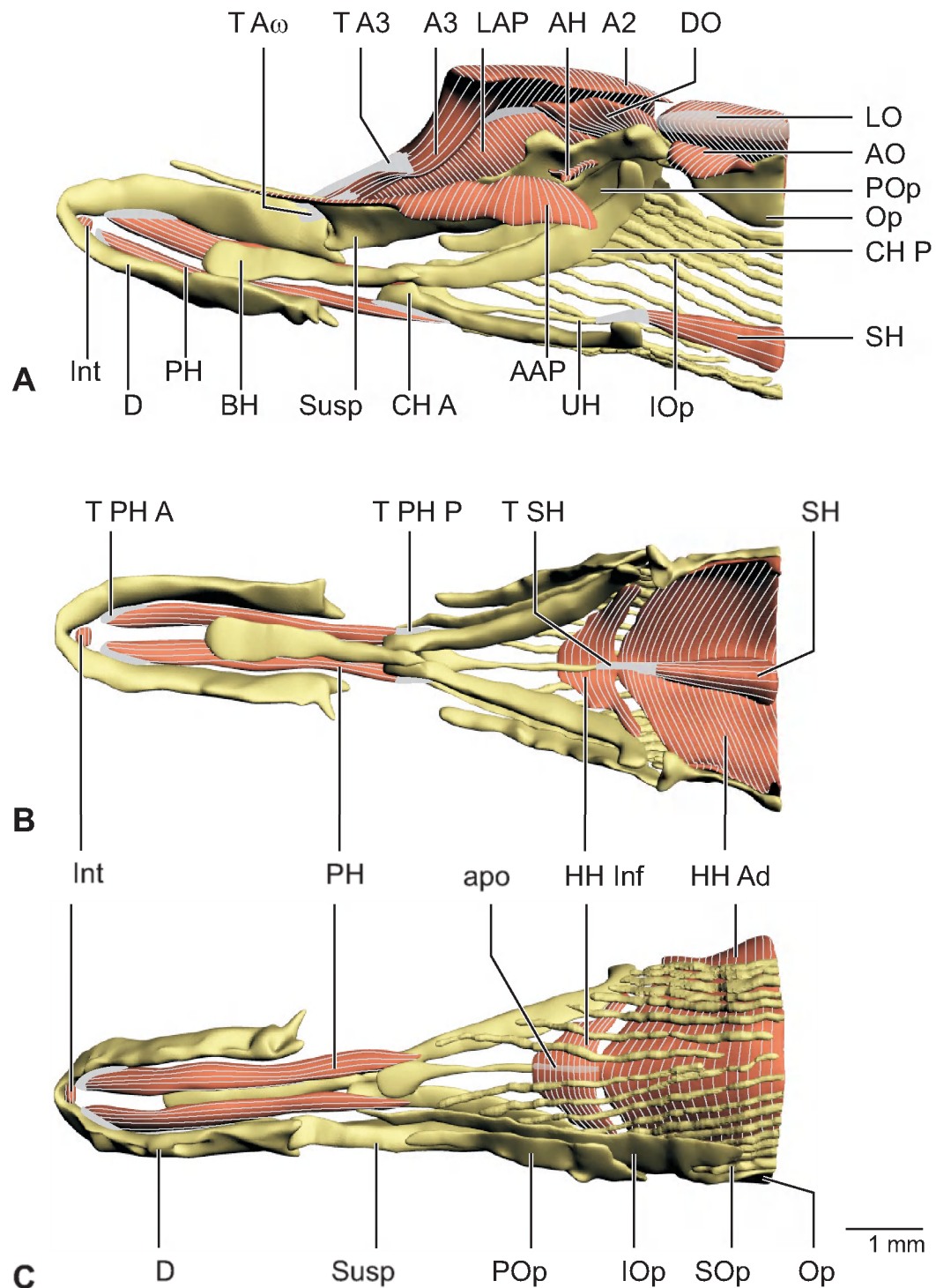


Fig. IV.1- 14: 3-D reconstruction of the splanchnocranium and associated muscles of *Heteroconger hassi*. A: The neurocranium and the suspensorium and opercular apparatus of the left side are removed to allow medial view of the muscles. Illustration of the protractor hyoideus, hyohyoideus inferioris and hyohyoidei adductores (B) in dorsal view (suspensoria of both sides are removed, while the opercular apparatus of both sides are illustrated) and (C) in ventral view (the suspensorium and opercular apparatus of the right side are removed).

Fig. IV.1- 15

*Heteroconger longissimus*

af Mx- Etv A, anterior maxillo-premaxillo-ethmovomerine articular facet  
af Mx- Etv P, posterior maxillo-premaxillo-ethmovomerine articular facet  
af Susp A, anterior suspensorial articular facet  
af Susp P, posterior suspensorial articular facet  
af V-PP, vomero-ptyergoidal articular facet  
BOc, basioccipital  
BSph, basisphenoid  
Epi, epiotic  
ExOc, exoccipitals  
F, frontal  
IOp, interopercle  
Op, opercle  
Orb, orbital  
Par, parietal  
PMx-Etv, premaxillo-ethmovomerine complex  
POp, preopercle  
Pr BSph, Basisphenoidal process  
Pr F, frontal process  
Pro, prootic  
PSph, parasphenoid  
Pt, pterotic  
PtSph, pterosphenoïd  
SOc, supraoccipital  
Sph, sphenotic

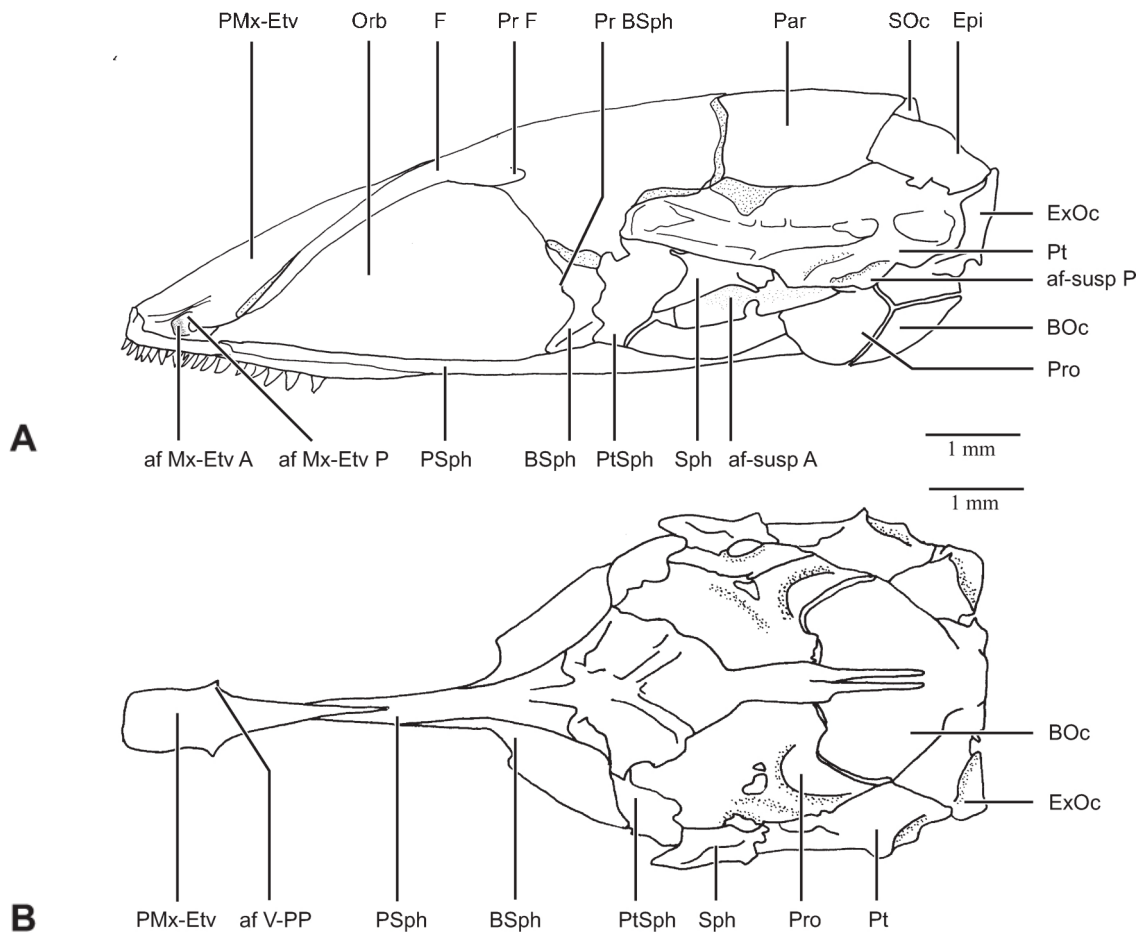
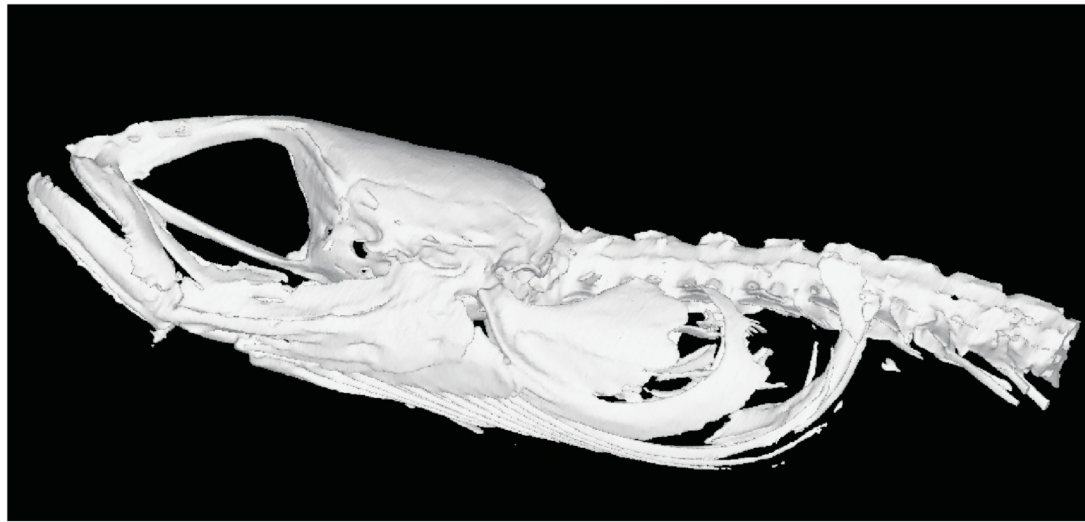


Fig. IV.1- 15: Illustration of the neurocranium of *Heteroconger longissimus* (A) in lateral view and (B) in ventral view.

Fig. IV.1- 16

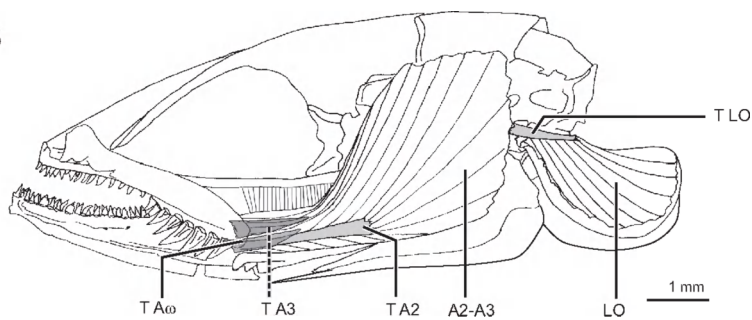
*Heteroconger longissimus*

A2, A3, A $\omega$ , subdivisions A2, A3, A $\omega$  of the adductor mandibulae complex  
AAP, adductor arcus palatini  
AH, adductor hyomandibulae  
AO, adductor operculi  
apo, aponeurosis  
Cl, cleithrum  
D, dentary complex  
DO, dilatator operculi  
HH Ad, hyohyoidei adductores  
HH Inf, hyohyoideus inferior  
IOp, interopercle  
LAP, levator arcus palatini  
LO, levator operculi  
Op, opercle  
PH, protractor hyoidei  
POp, preopercle  
Q, quadrate  
R Br, branchiostegal ray  
SH, sternohyoideus  
SOp, subopercle  
T A2, A3, A $\omega$ , tendon of subdivisions A2, A3, A $\omega$   
T DO, tendon of dilatator operculi  
T LAP, tendon of levator arcus palatini  
T LO, tendon of levator operculi  
T PH A, anterior tendon of protractor hyoidei  
T SH, tendon of sternohyoideus  
UH, urohyal

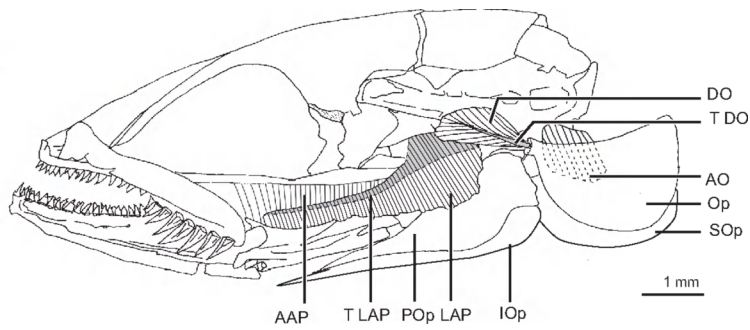


A

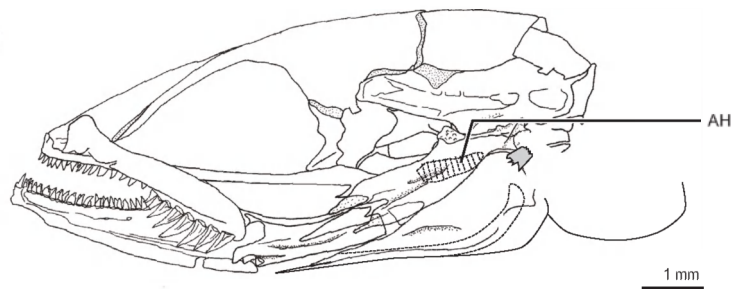
B



C



D



E

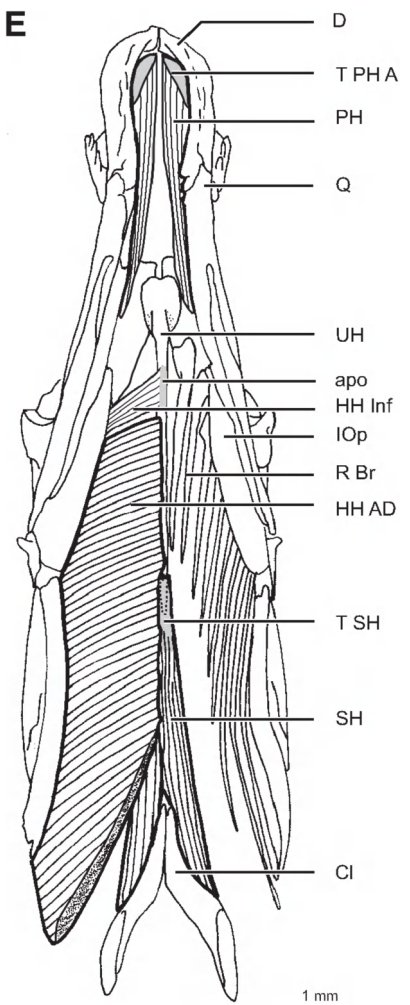


Fig. IV.1- 16: A: cranium of *Heteroconger longissimus* in lateral view (Ct-scanning). B: Cranial muscles of *Heteroconger longissimus*. C: The adductor mandibulae complex and the levator operculi are removed. D: The levator arcus palatini, dilator operculi, adductor operculi and adductor arcus palatini are removed. E: The protractor hyoideus, hyochoideus inferioris and hyochoidei adductores in ventral view. The branchiostegal rays are removed on the right side.

Fig. IV.1- 17

*Heteroconger hassi*

Afr, anal fin ray  
Cfr, caudal fin rays  
Dfr, dorsal caudal fin ray  
Epax, epaxials  
FD, flexor dorsalis  
FV, flexor ventralis  
H f, hypural fenestra  
H pl D, dorsal hypural plate  
H pl V, ventral hypural plate  
HL, hypochordal longitudinalis  
Hph, hypurapophysis  
Hyp, hypaxials  
NA PU1, neural arch of first preural centrum  
ParH, parhypural  
PU1, first preural centrum  
Ptg, pterygiophore  
Px, proximalis  
T Epax, tendon of epaxials  
T FD, tendon of the flexor dorsalis  
T FV, tendon of the flexor ventralis  
T HL, tendon of the hypochordal longitudinalis  
T Hyp, tendon of hypaxials  
UN, uroneural  
Us, urostyle



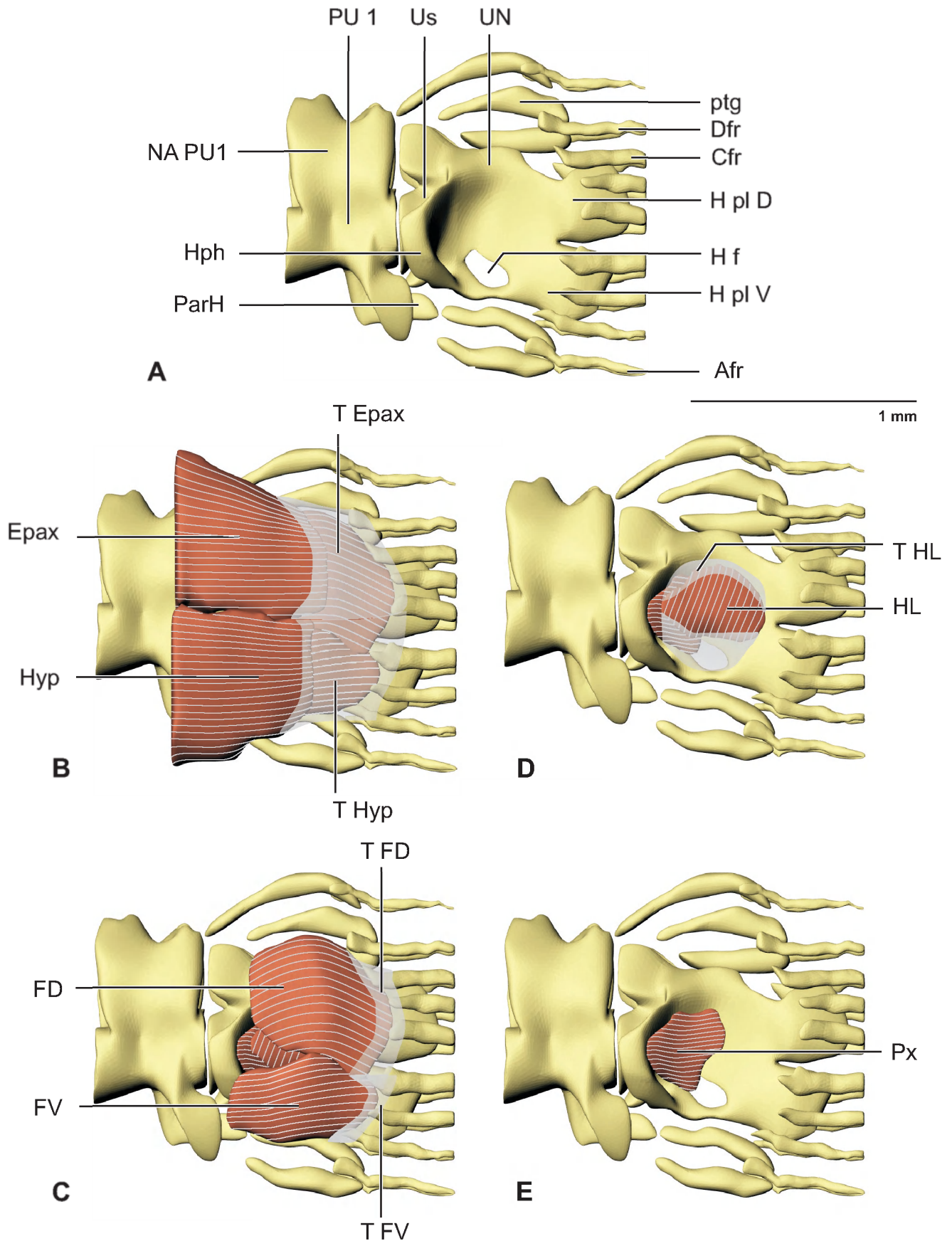


Fig. IV.1- 17: 3-D reconstruction of the tail of *Heteroconger hassi*. Tendons are shown in transparent grey. A: The caudal skeleton in lateral view. B: The intrinsic caudal musculature. C: The epaxials and hypaxials are removed. D: The flexor dorsalis and ventralis are removed. E: The hypochochordal longitudinalis is removed.

Fig. IV.1- 18

*Heteroconger longissimus*

Afr, anal fin ray  
Cfr, caudal fin rays  
D fr, dorsal caudal fin ray  
Epax, epaxials  
FD, flexor dorsalis  
FV, flexor ventralis  
H f, hypural fenestra  
H pl D, dorsal hypural plate  
H pl V, ventral hypural plate  
HL, hypochordal longitudinalis  
Hph, hypurapophysis  
Hyp, hypaxials  
NA PU1, neural arch of first preural centrum  
ParH, parhypural  
PU1, first preural centrum  
Px, proximalis  
T Epax, tendon of epaxials  
T FD, tendon of the flexor dorsalis  
T FV, tendon of the flexor ventralis  
T HL, tendon of the hypochordal longitudinalis  
T Hyp, tendon of hypaxials  
UN, uroneural  
Us, urostyle

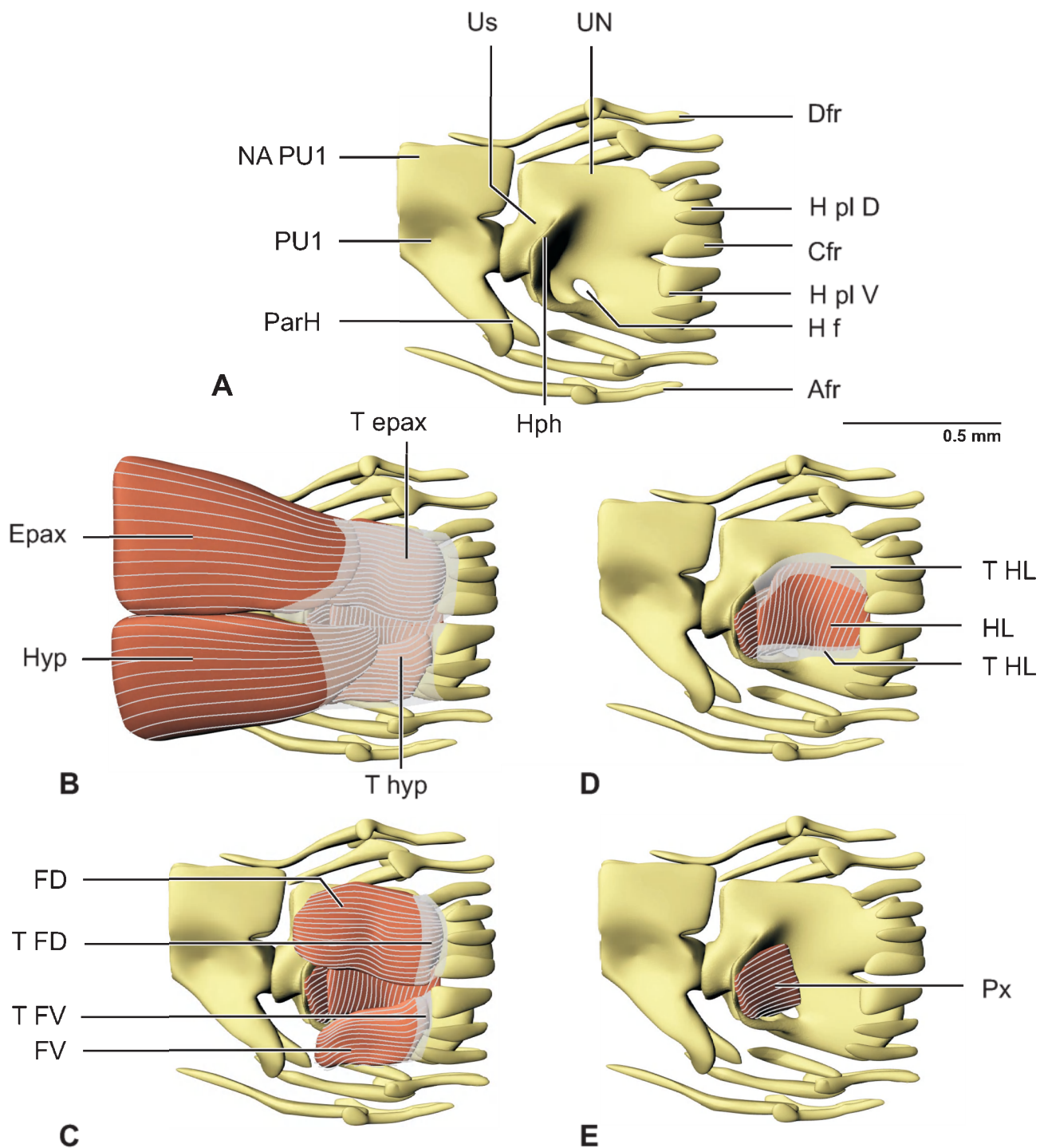


Fig. IV.1- 18: 3-D reconstruction of the tail of *Heteroconger longissimus*. Tendons are shown in transparent grey. A: The caudal skeleton in lateral view. B: The intrinsic caudal musculature. C: The epaxials and hypaxials are removed. D: The flexor dorsalis and ventralis are removed. E: The hypochordal longitudinalis is removed.

Fig. IV.1- 19: Cross-section at the level of the sphenotic wing in (A) *Heteroconger hassi*, (B) *Heteroconger longissimus* and (C) *Moringua edwardsi*. Differences in hypertrophy of the adductor mandibulae complex (A2) are clearly visible.

A2 subdivision of adductor mandibulae complex

AAP, adductor arcus palatini

AH, adductor hyomandibulae

C Ot, otic canal

CH, ceratohyal

F, frontal

Hm, hyomandibula

IOP, interopercle

LAP, levator arcus palatini

POp, preopercle

Pr Sph, sphenotic process

PSph, parasphenoid

Pt, pterotic

T LAP, tendon of levator arcus palatini

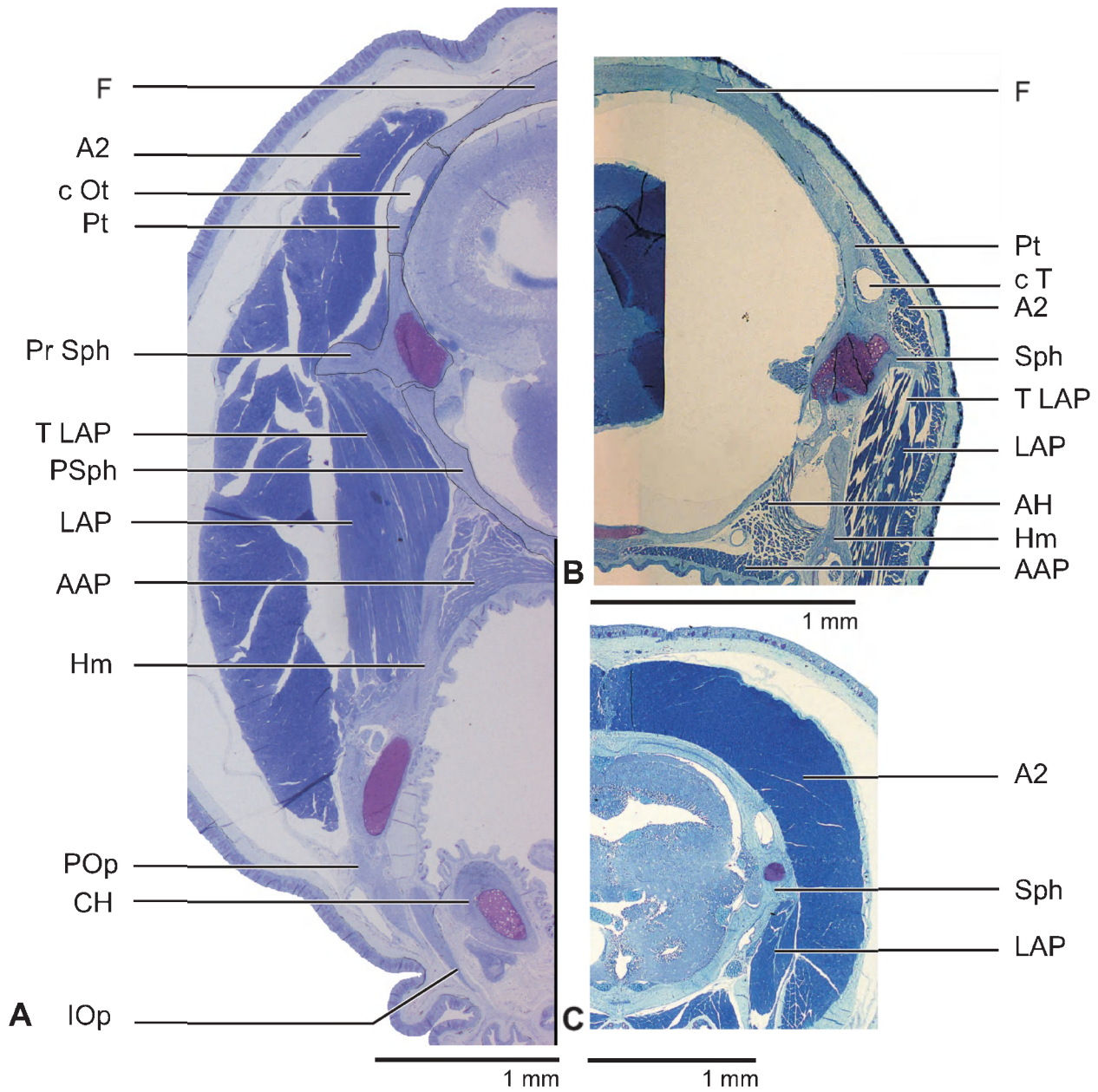


Fig. IV.1- 19: Cross-section at the level of the sphenotic wing in (A) *Heteroconger hassi*, (B) *Heteroconger longissimus* and (C) *Moringua edwardsi*. Differences in hypertrophy of the adductor mandibulae complex (A2) are clearly visible. Some cranial bones are outlined.

Fig. IV.1- 20

*Pisodonophis boro*

Ac Md, mandibular articular condyle of the hyomandibula  
Ac Op, opercular articular condyle of the hyomandibula  
Ac Susp A, anterior suspensorial condyle of the hyomandibula  
Ac susp P, posterior suspensorial condyle of the hyomandibula  
Ang, angular complex  
BH, basihyal  
BOc, basioccipital  
BSph, basisphenoid  
CH, ceratohyal  
D, dentary complex  
Epi, epiotic  
ExOc, exoccipital  
F, frontal  
IOp, interopercle  
Mx, maxilla  
Op, opercle  
P F, frontal commissural pore  
Par, parietal  
PMx-Etv, Premaxillo-ethmovomerine complex  
POp, preopercle  
PP, pterygoid  
Pr D Op, dorsal process of the opercle  
Pro, prootic PSph, parasphenoid  
Pt, pterotic  
PtSph, pterosphenoid  
SOc ri, supraoccipital ridge  
SOp, subopercle  
Sph, sphenotic  
Susp, suspensorium  
UH, urohyal.

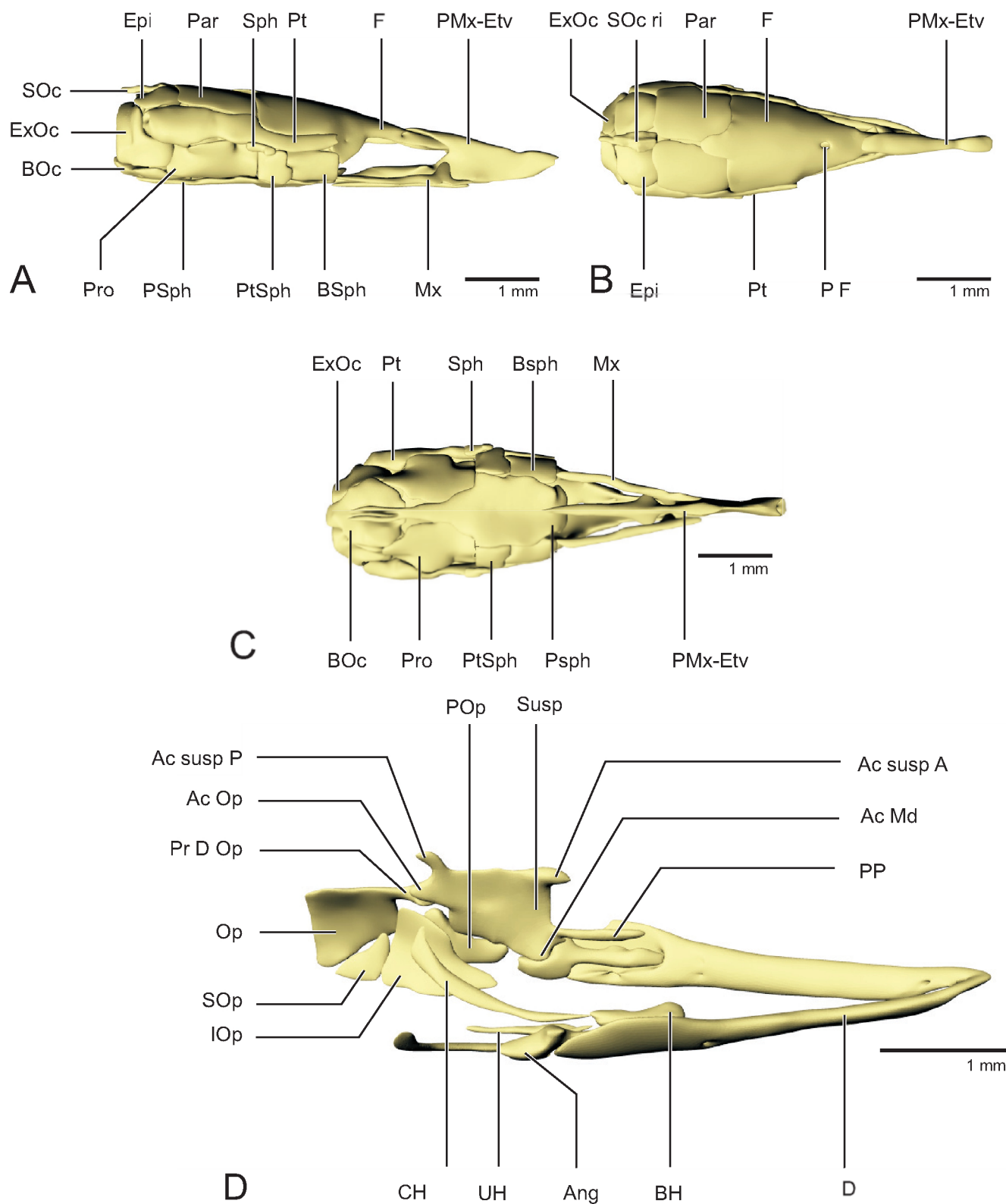


Fig. IV.1- 20: 3D reconstruction of the neurocranium of *Pisodonophis boro* in (A) lateral view, (B) dorsal view and (C) ventral view. D: Illustration of the lower jaw, suspensorium, hyoid and opercular apparatus of *P. boro*. The image is slightly turned to the right, exposing the medial surfaces. Because the quadrate, hyomandibula and pterygoid are strongly interconnected, they are considered in this reconstruction as one unit.

Fig. IV.1- 21

*Pisodonophis*

A1, A2, A2m, A3, A $\omega$ , subdivisions of the adductor mandibulae complex  
apo, aponeurosis  
ct, connective tissue  
Epax, epaxial  
Epi, epiotic  
F, frontal  
L prim, primordial ligament  
Par, parietal  
Pr cor, processus coronoideus  
Pro, prootic  
PSph, parasphenoid  
Pt, pterotic  
PtSph, pterosphenoid  
SOc ri, supraoccipital ridge  
Soc, supraoccipital  
T A1, T A2, tendon of subdivisions.



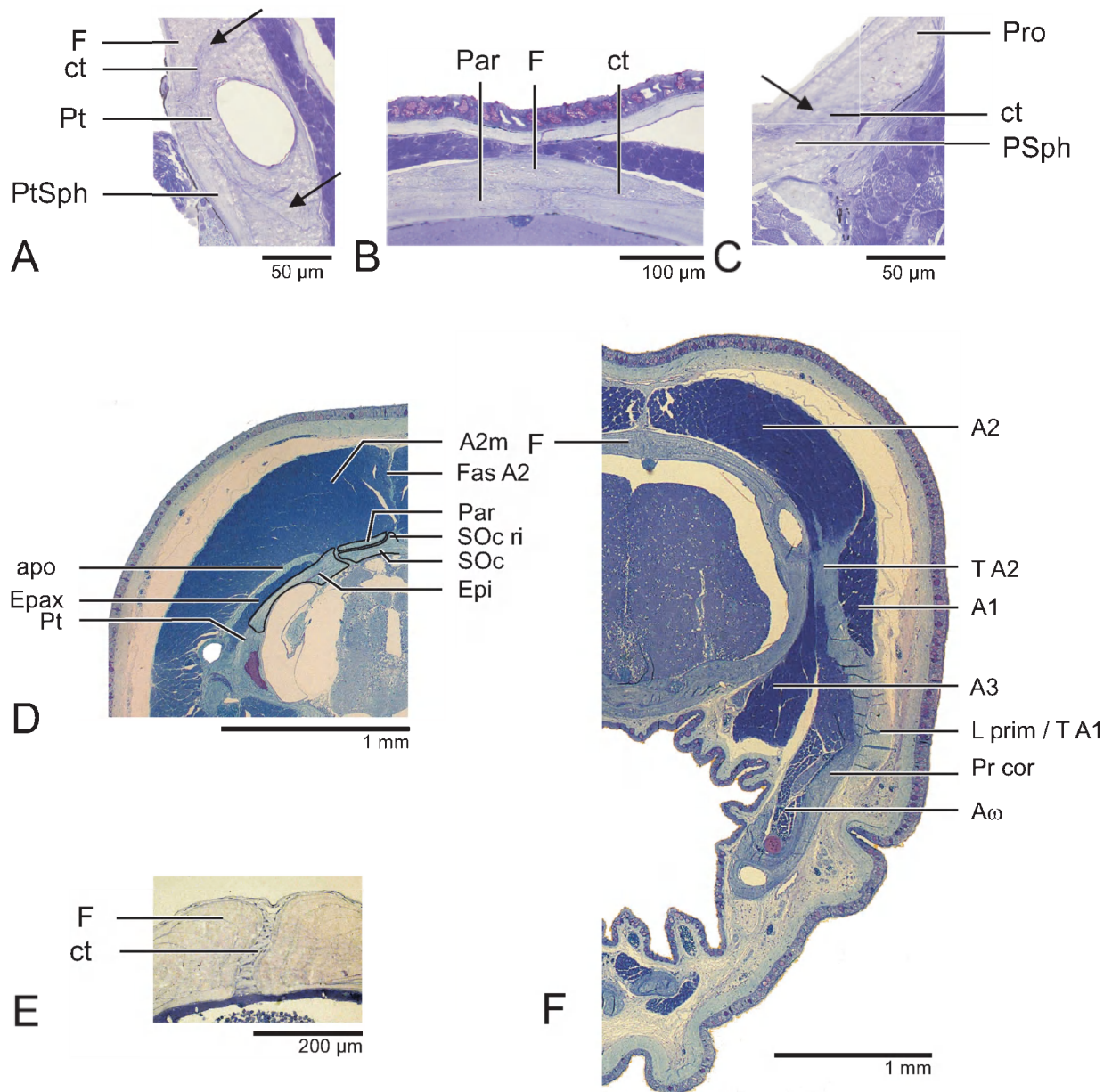


Fig. IV.1- 21: Cross sections of the cranium of *Pisodonophis boro* (A, B, C) and *Moringua edwardsi* (D, E, F). The cranium is fortified by the presence of heavily ossified bones which are strongly interconnected. The arrows indicate oblique edges of the joints. A: Scarf joints between frontal, pterotic and pterosphenoid in *P. boro*. B: Area of overlap between frontal and parietals formed by the extension of the oblique edges of the joints in *P. boro*. C: Scarf joints between parasphenoid and prootic in *P. boro*. D: Aponeurosis between adductor mandibulae complex and epaxials in *M. edwardsi*. E: Scarf joints between frontals in *M. edwardsi*. F: Cross section of the head of *M. edwardsi* at the level of the insertion of the adductor mandibulae complex.

Fig. IV.1- 22

*Pisodonophis boro*

c Et, ethmoid canal  
c IO, infraorbital canal  
c Md, mandibular canal  
c POp, preopercular canal  
c SO, supraorbital canal  
c Ot, otic canal  
cm F, frontal commissure  
cm ST, supratemporal commissure  
Nas, nasal  
PO, preorbital  
PostO, postorbital  
SubO, suborbital.

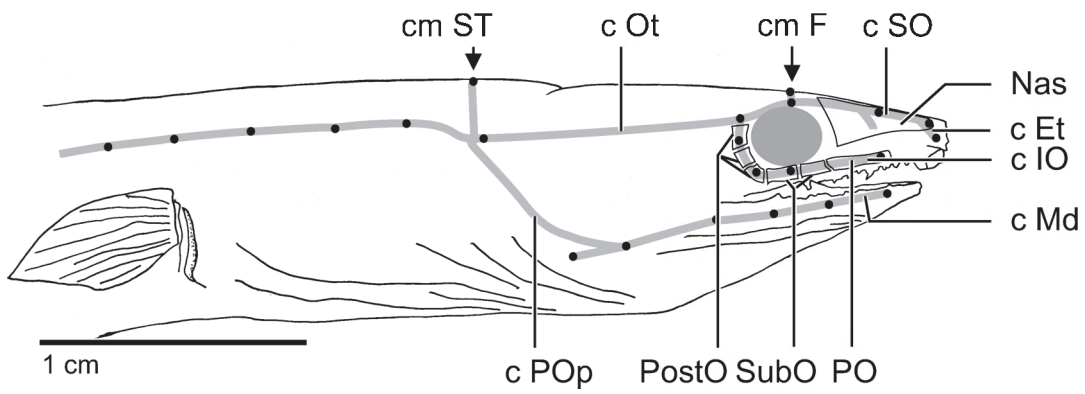


Fig. IV.1- 22: The cephalic lateral line system of *Pisodonophis boro*. Black dots indicate external pores.

Fig. IV.1- 23

*Pisodonophis boro*

A1, A2, A3, Aw, subdivisions of adductor mandibulae complex

DO, dilatator operculi

L prim, primordial ligament

LAP, levator arcus palatini

LO, levator operculi

PH, protractor hyoidei

T A1, T A2, tendons of subdivisions

T DO, tendon of dilatator operculi

T LAP, tendon of levator arcus palatini

T LO, tendon of levator operculi

T PH A, anterior tendon of protractor hyoidei

T PH P, posterior tendon of protractor hyoidei.

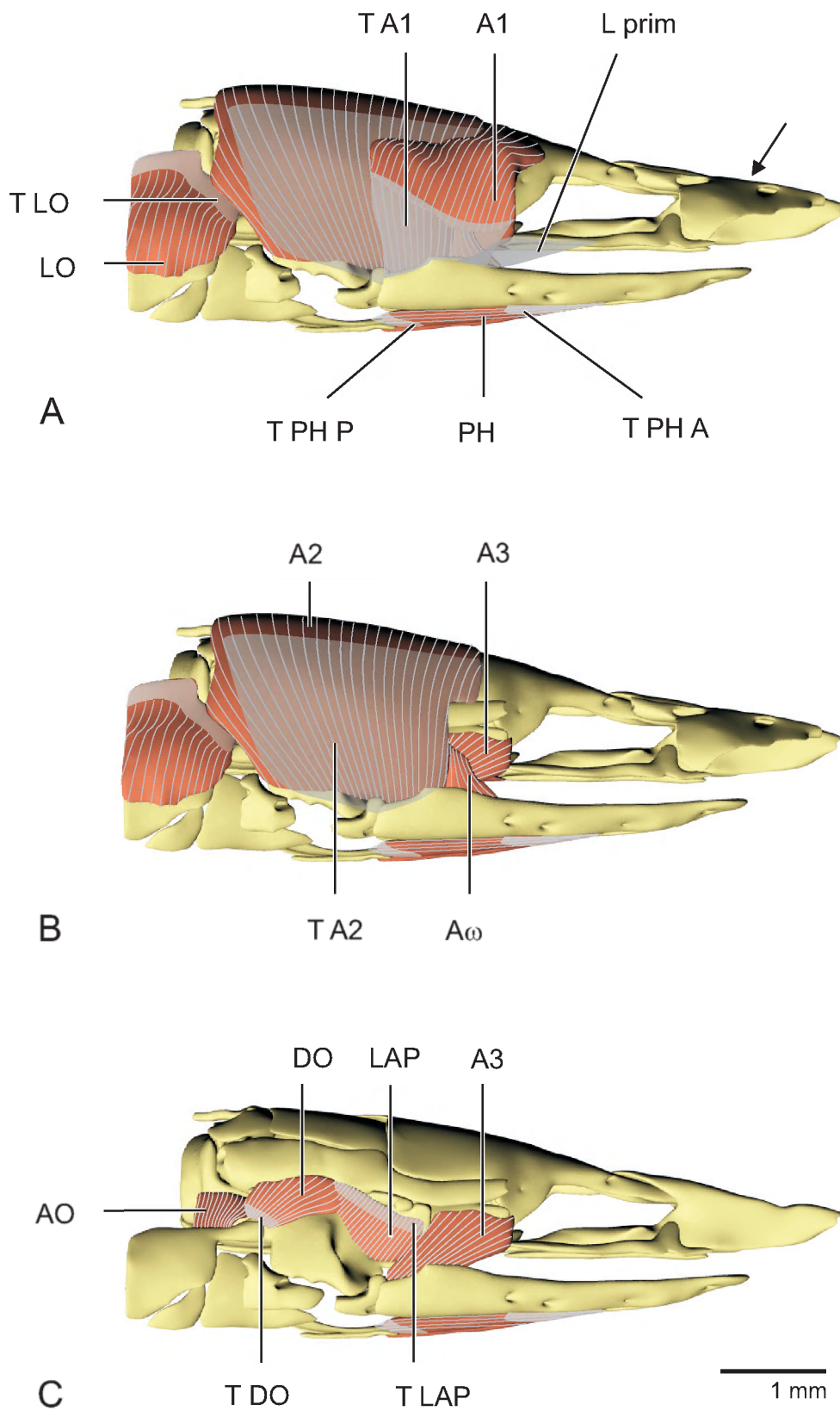


Fig. IV.1- 23: 3D reconstruction of the cranial muscles of *Pisodonophis boro*. The nasal is indicated by an arrow. **A** : The skin is removed **B**: the A1 of the adductor mandibulae complex is removed **C**: A2 and A $\omega$  of the adductor mandibulae complex and LO are removed. .

Fig. IV.1- 24

*Pisodonophis boro*

A3, A $\omega$ , subdivisions of adductor mandibulae complex A $\omega$

AAP, adductor arcus palatini

AH, adductor hyomandibulae

AO, adductor operculi

PH, protractor hyoidei

T A3, tendons of subdivisions

T PH A, anterior tendon of protractor hyoidei

T PH P, posterior tendon of protractor hyoidei

T SH, tendon of sternohyoideus.

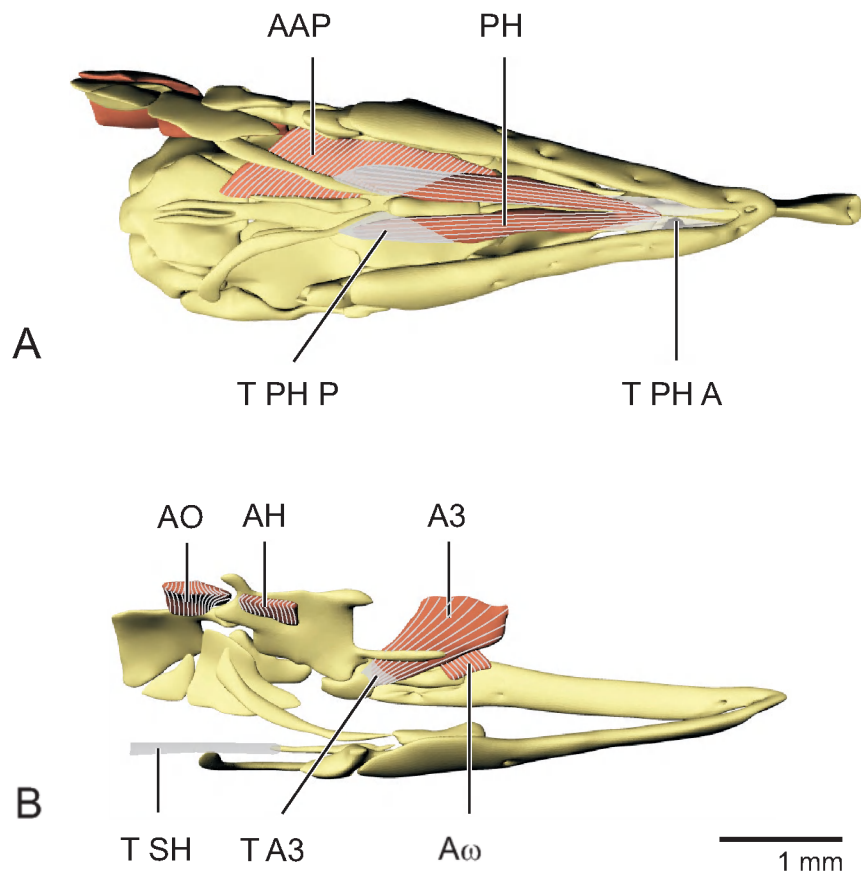


Fig. IV.1- 24: 3D reconstruction of the cranial muscles of *Pisodonophis boro*. **A**: cranial muscles in ventral view, adductor mandibulae complex is removed **B**: neurocranium is removed to show the small muscles situated between the neurocranium and suspensorium (adductor hyomandibulae) or between the neurocranium and the opercle (adductor operculi). This image is slightly laterally inclined. Branchiostegal rays and hyohyoideus are not shown.

Fig. IV.1- 25

*Pisodonophis boro*

A1, A2, A3, A $\omega$ , subdivisions of the adductor mandibulae complex  
AAP, adductor arcus palatini  
Ang, angular complex  
AO, adductor opeculi  
apo, aponeurosis  
BOC, basioccipital  
DO, dilatator operculi  
Epax, epaxials  
Epi, epiotic  
ExOc, exoccipitals  
HH, hyohyoideus  
Hyp, hypaxials  
IOp, interopercle  
L prim, primordial ligament  
LO, levator operculi  
Op, opercle  
P ST, supratemporal pore  
POp, preopercle  
PP, pterygoid  
Pr cor, processus coronoideus  
Pt, pterotics  
R Br, branchiostegal rays  
SOc, supraoccipital  
SOp, subopercle  
T A1, A2, tendons of subdivisions  
T SH, tendon of the sternohyoideus.



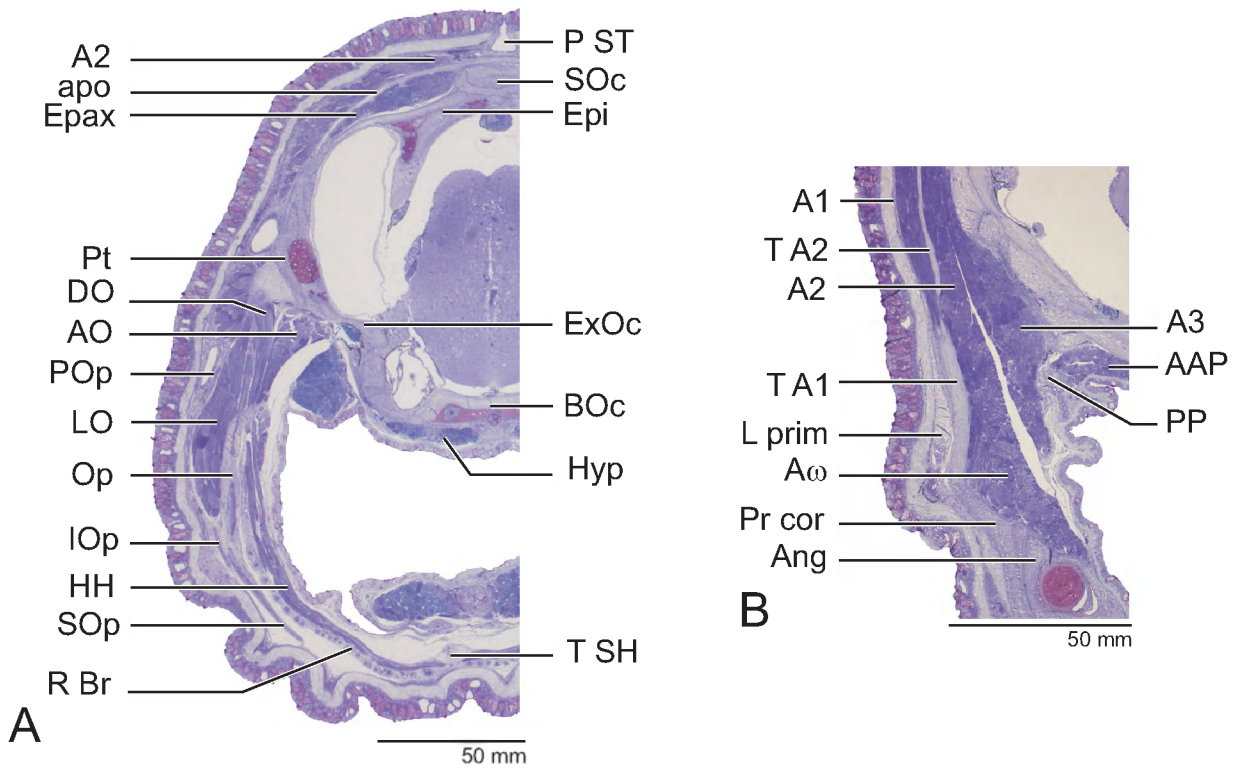


Fig. IV.1- 25: A: Cross section of the head of *Pisodonophis boro* at the level of the supraoccipital. B: cross section at the level of the insertion of the A1 and A2 onto the lower jaw.

Fig. IV.1- 26

*Pisodonophis boro*

HA PU2, hemal arch of second preural centrum  
Hph, hypurapophysis  
Hpl D, dorsal hypural plate  
Hpl V, ventral hypural plate  
NA PU1, neural arch of first preural centrum  
NA PU2, neural arch of second preural centrum  
ParH, parhypural  
PU1, first preural centrum  
PU2, second preural centrum  
UN, uroneural  
Us, urostyle.

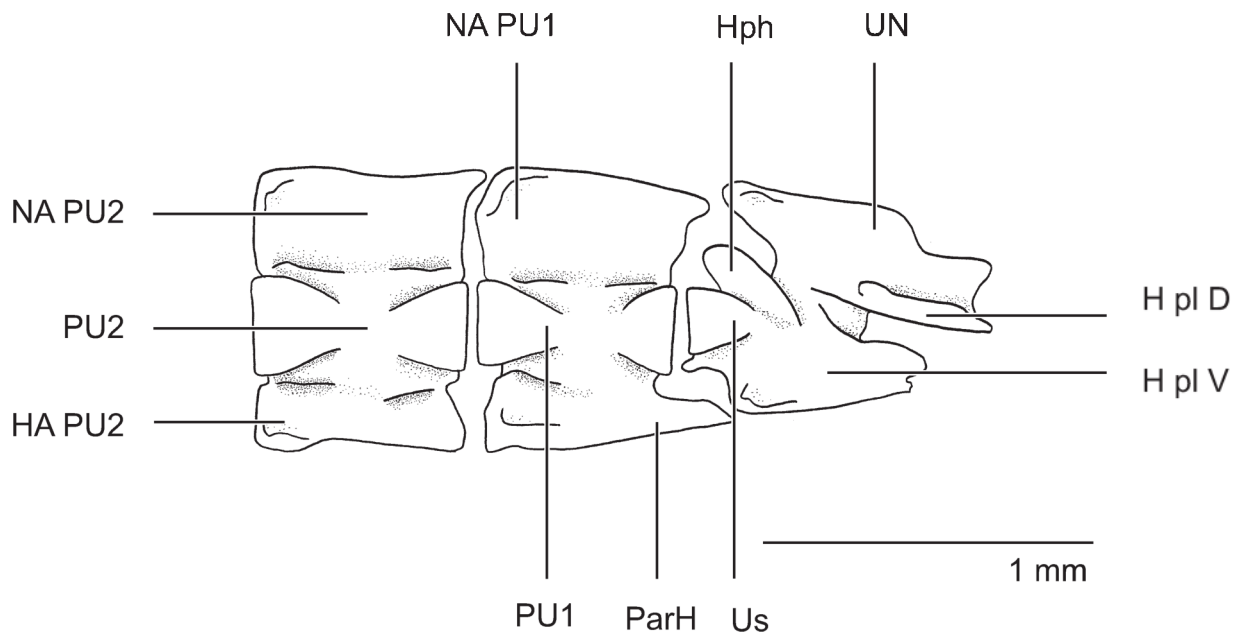


Fig. IV.1- 26: Illustration of the osteological characteristics of the caudal skeleton of *Pisodonophis boro* in lateral view.

Fig. IV.1- 27

*Pisodonophis boro*

Cfr, caudal fin rays  
FD, flexor dorsalis  
FV, flexor ventralis  
HL, hypochordal longitudinalis  
Hph, hypurapophysis  
H pl D, dorsal hypural plate  
H pl V, ventral hypural plate  
NA PU1, neural arch of first preural centrum  
ParH, parhypural  
PU1, first preural centrum  
Px, proximalis  
T FD, tendon of the flexor dorsalis  
T FV, tendon of the flexor ventralis  
T HL, tendon of the hypochordal longitudinalis  
UN, uroneural  
Us, urostyle

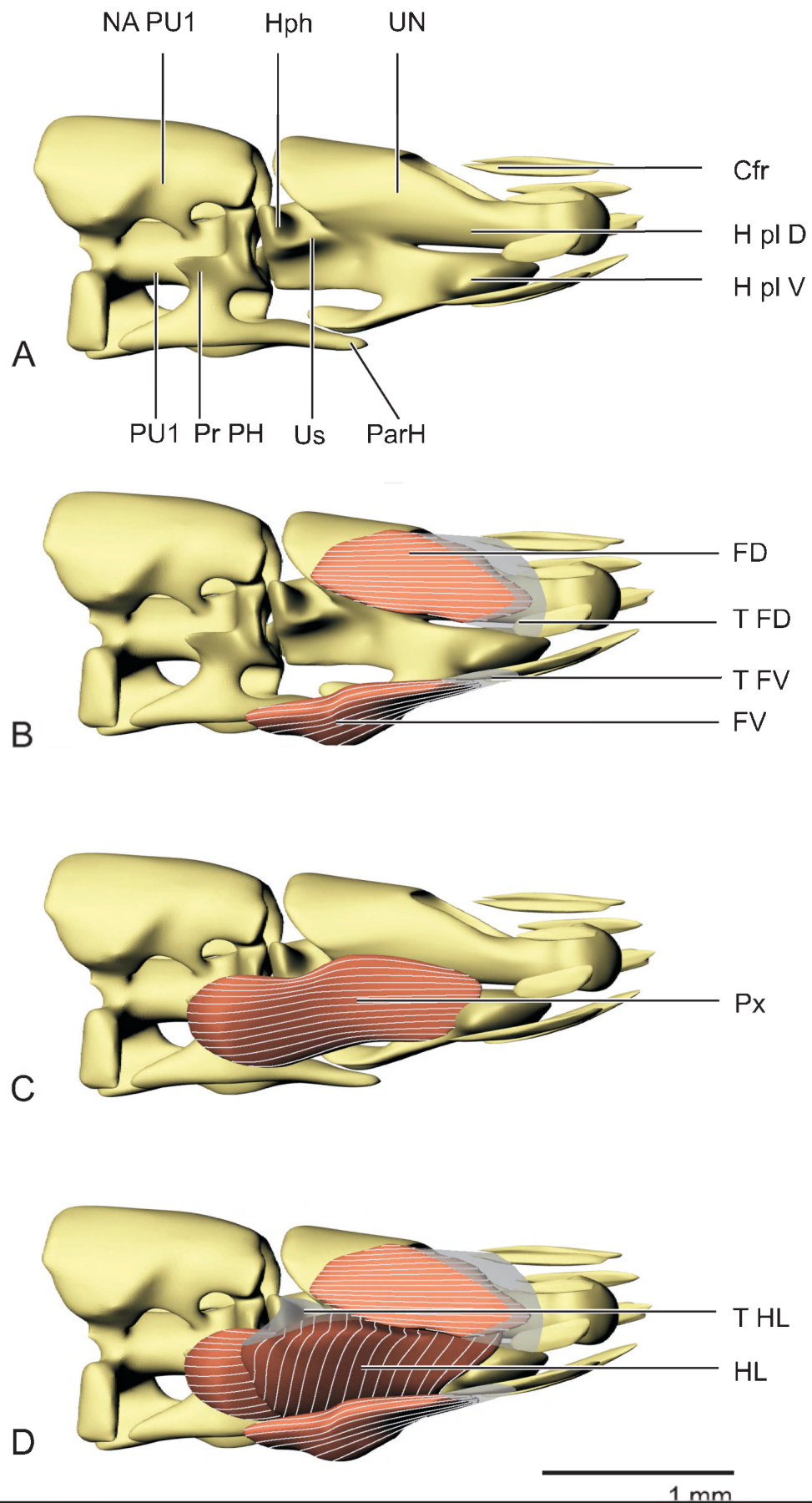


Fig. IV.1- 27: 3D reconstruction of the tail of *Pisodonophis boro*. Tendons are shown in transparent grey. **A:** The caudal skeleton in lateral view. **B-C-E:** The intrinsic caudal musculature.

Fig. IV.1- 28

A, C, *Pisodonophis boro*

B, *Moringua edwardsi*

D, *Heteroconger longissimus*

c IO, infraorbital canal

c SO, supraorbital canal

Nas, nasal

olf, olfactory chamber

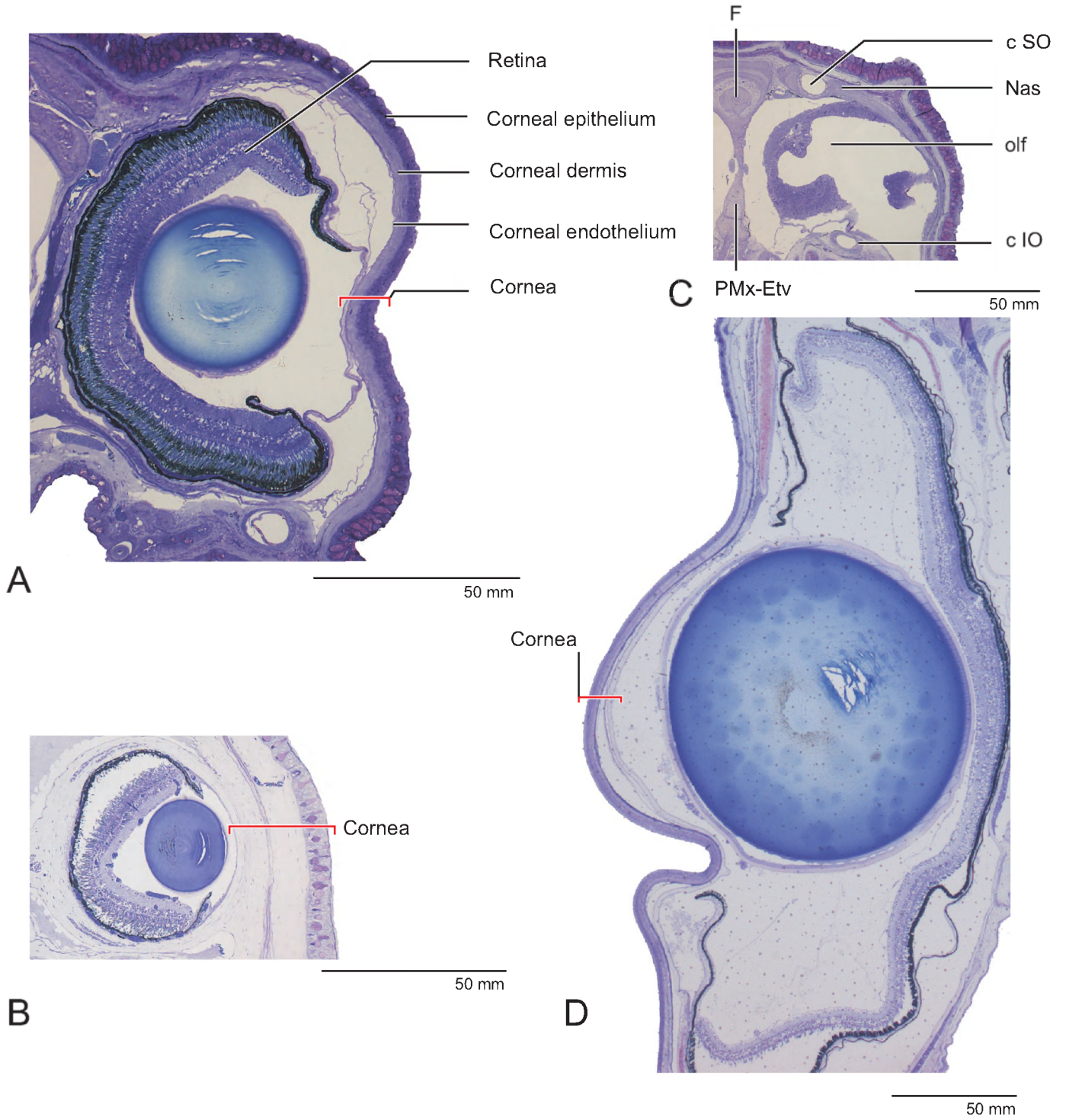


Fig. IV.1- 28: Cross section at the level of the eye in (A) *Pisodonophis boro*, (B) *Moringua edwardsi* and (D) *Heteroconger longissimus*. C: the olfactory organ, covered by the winglike nasal in *P. boro*.

Fig. IV.2.1- 1

*Anguilla anguilla*

bh, basihyal  
bo, basioccipital  
bs, basisphenoid  
ch1, anterior ceratohyal  
ch2, posterior ceratohyal  
de, dentary  
eo, exoccipital  
ep, epiotics  
fm, foramen magnum  
fr, frontal  
hm, hyomandibula  
if, orbita  
io, interopercle  
ma, maxillary  
na, nasal  
op, opercle  
pa, parietal  
po, preopercle  
pp, pterygoid  
ps, parasphenoid  
pt, pterotic  
pts, pterosphenoid  
pv, premaxillo-ethmovomerine complex  
qu, quadrate  
SO, suborbital  
sp, sphenotic  
su, subopercle  
uh, urohyal



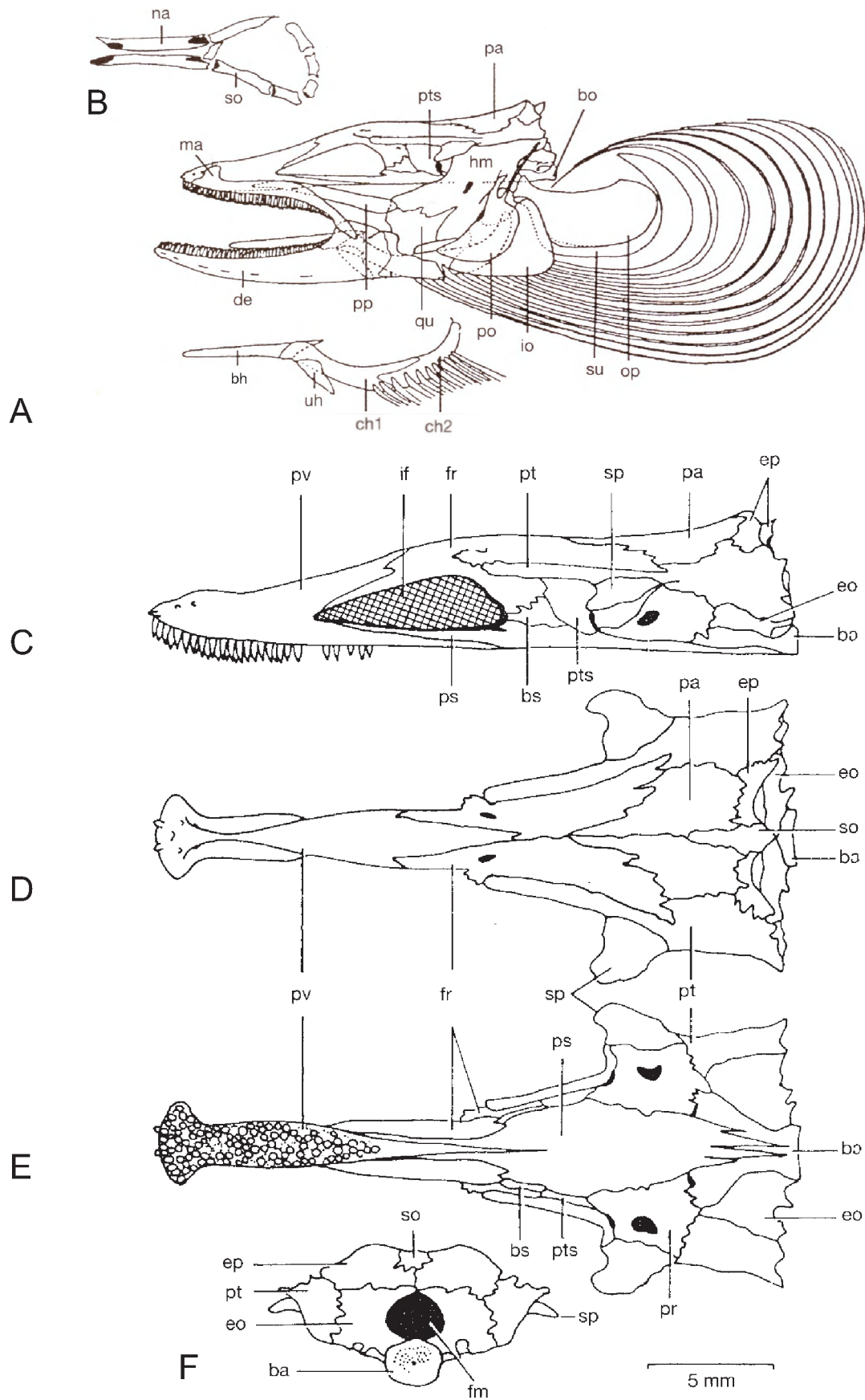


Fig. IV.2.1- 1: Illustration of the cranial osteology of *Anguilla anguilla* (modified after Tesch, 2003). A: The skull in lateral view. B: Detail of the circumorbital series. The neurocranium of *Anguilla anguilla* in lateral view (C); dorsal view (D); ventral view (E) and in caudal view (F).

Fig. IV.2.1- 2

*Anguilla anguilla*

H H [E r], head height at the level of the rostral border of the eye

W H [E c], width of the head at the level of the caudal border of the eye

IOD c, interorbital distance at the level caudal border of the eye

TL, total length

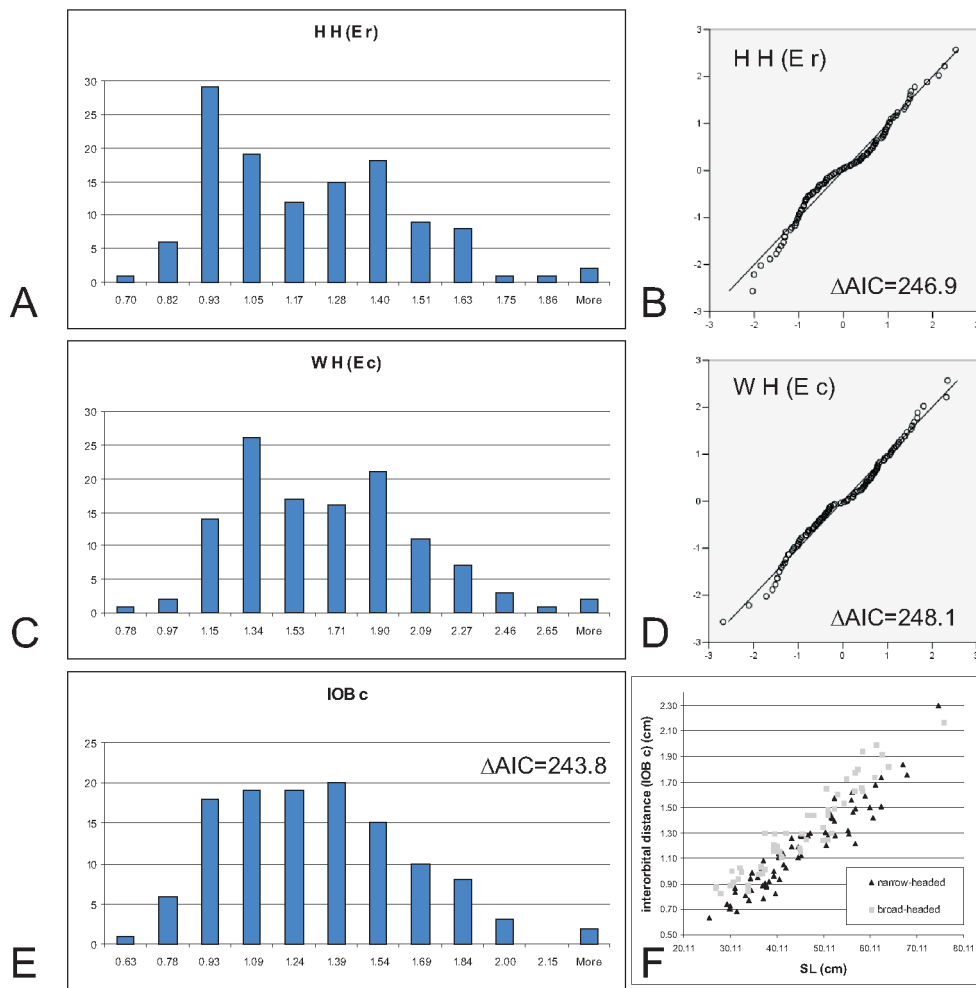


Fig. IV.2.1- 2: Frequency histograms and normality plots of (a, b) head height at the level of the rostral border of the eye (H H [E r]); (c, d) width of the head at the level of the caudal border of the eye (W H [E c]); (e) Frequency histogram of interorbital distance at the level caudal border of the eye (IOD c). Bimodality can not clearly be deduced visually, but is supported by Brewers' bimodality test and clearly visible in its plot versus Total Length (f). (F) Absolute value of IOD c plotted versus Total Length.

Fig. IV.2.1- 3

*Anguilla anguilla*

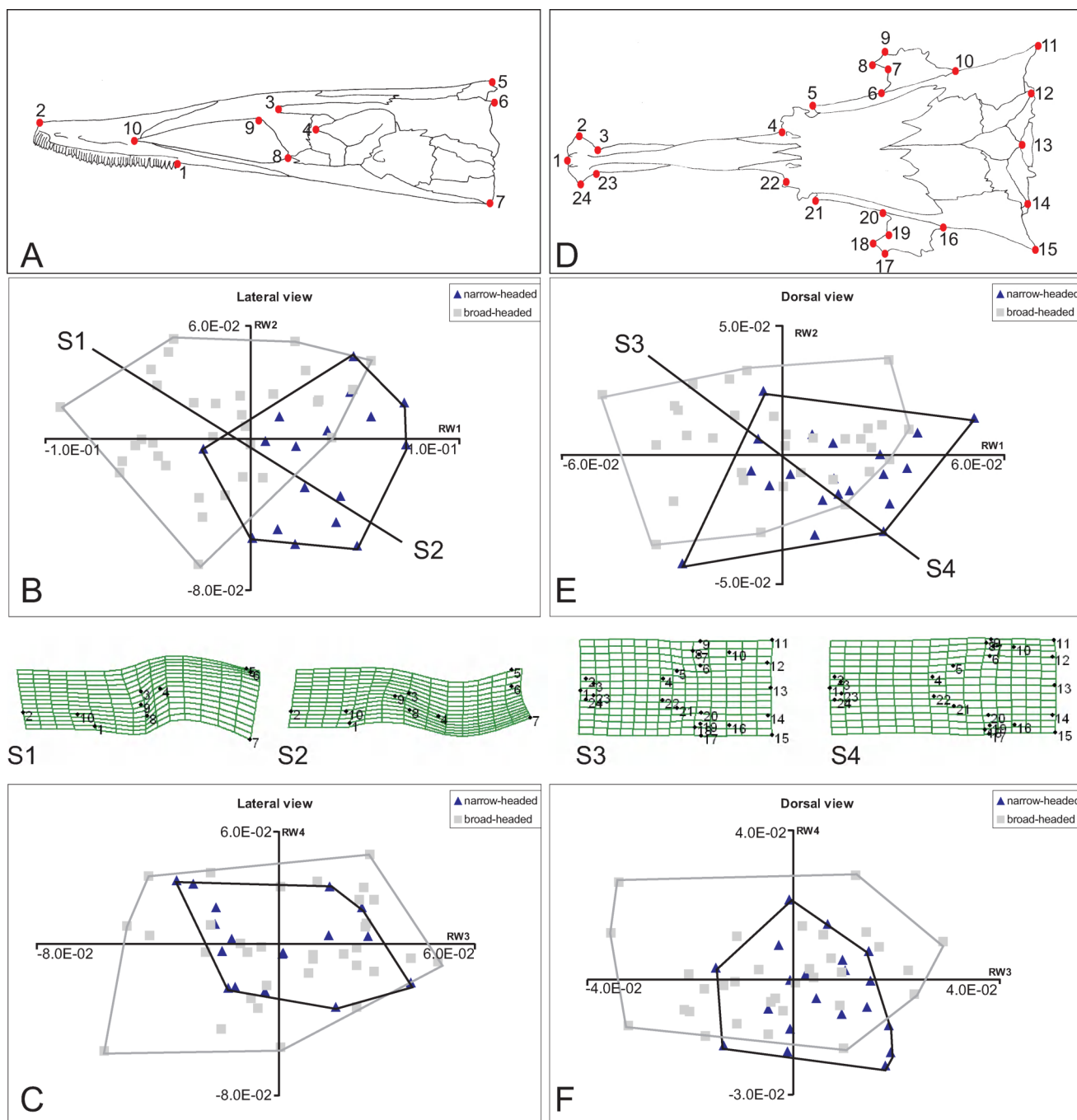


Fig. IV.2.1- 3: Results of morphometric analysis of the skull shape in lateral view (A-C) and dorsal view (D-F). (A, D) Illustration of the landmarks indicating the position defined on the skull. Landmarks used in analyses are taken on pictures (no drawings). (B, E) plot of first relative warp (RW1) versus second relative warp (RW2) and (C, F) plot of third relative warp (RW3) versus fourth relative warp (RW4). The landmark configurations of the extreme broad-headed specimens (S1) and (S3) are visualized and the main shape differences with extreme narrow-headed specimens are visualized using vectors.

Fig. IV.2.2- 1

*Anguilla anguilla*

1e Br R, first branchiostegal ray, broadened and extremely curved in *Anguilla anguilla*

A1, A2, A3, subdivisions of the adductor mandibulae complex

AAP, adductor arcus palatini

AO, adductor operculi

D, dentary

DO, dilatator operculi

Epax, epaxials

HH ad, hyohyoideus adductores

Hyp, hypaxials

IOP, interopercle

LAP, levator arcus palatini

LO, levator operculi

Mx, maxillary

Op, opercle

PH, protractor hyoidei

POp, preopercle

T A1-A2, tendon of subdivision A1 and A2

T PH P, posterior tendon of protractor hyoidei

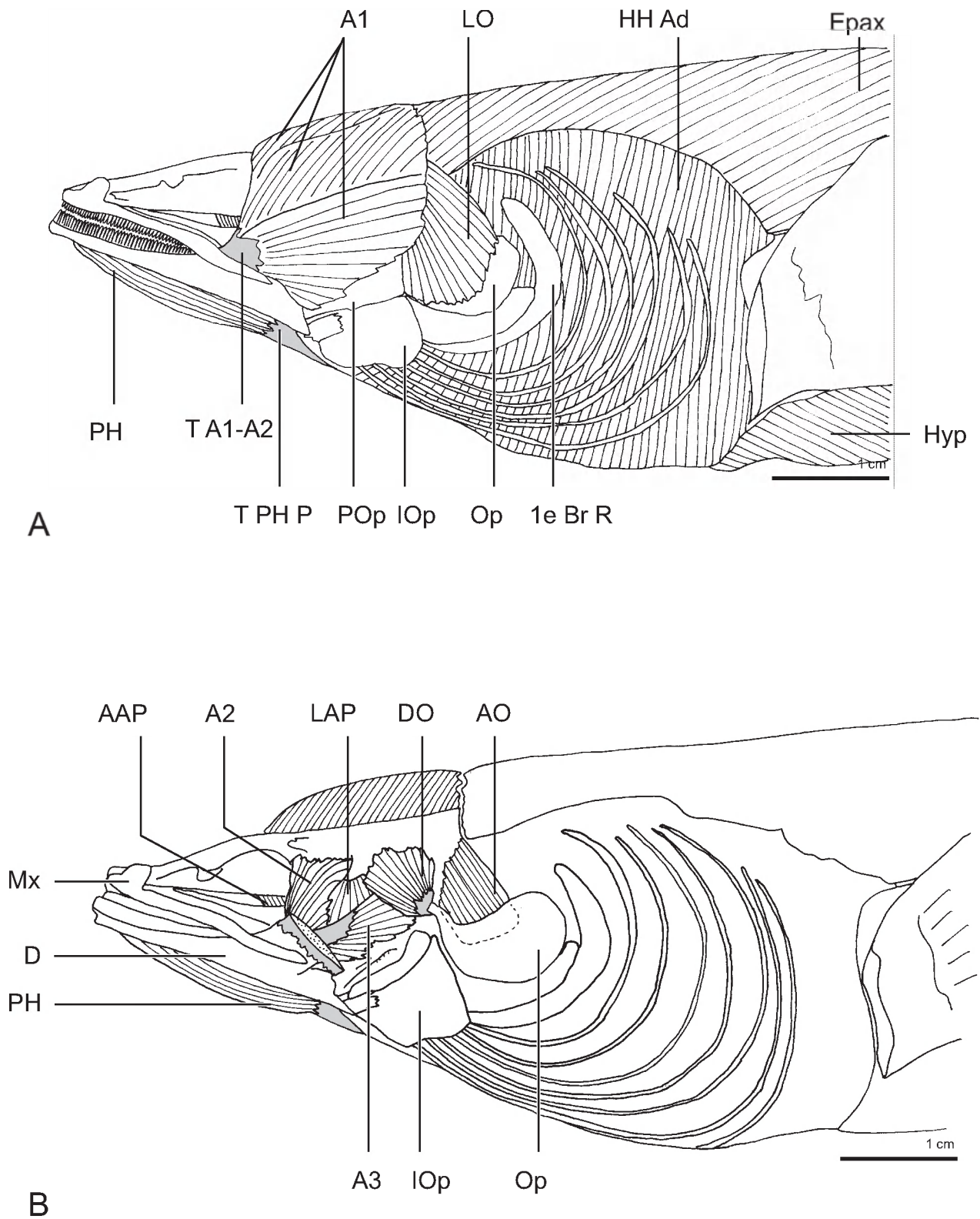


Fig. IV.2.2- 1: **A**: Lateral view of the head musculature of a narrow-headed specimen of *Anguilla anguilla*. Skin is removed **B**: Lateral view of head musculature, A1 and A2 subdivision of the cheek musculature and levator operculi are removed.

Fig. IV.2.2- 2

*Anguilla anguilla.*

LO, levator operculi

A1, subdivision of the adductor mandibulae complex

PH, protractor hyoidei

T PH A, anterior tendon of protractor hyoidei

D, dentary

IOP, interopercle

Op, opercle

HH ad, hyohyoideus adductores

SH, sternohyoideus

T SH, tendon of sternohyoideus



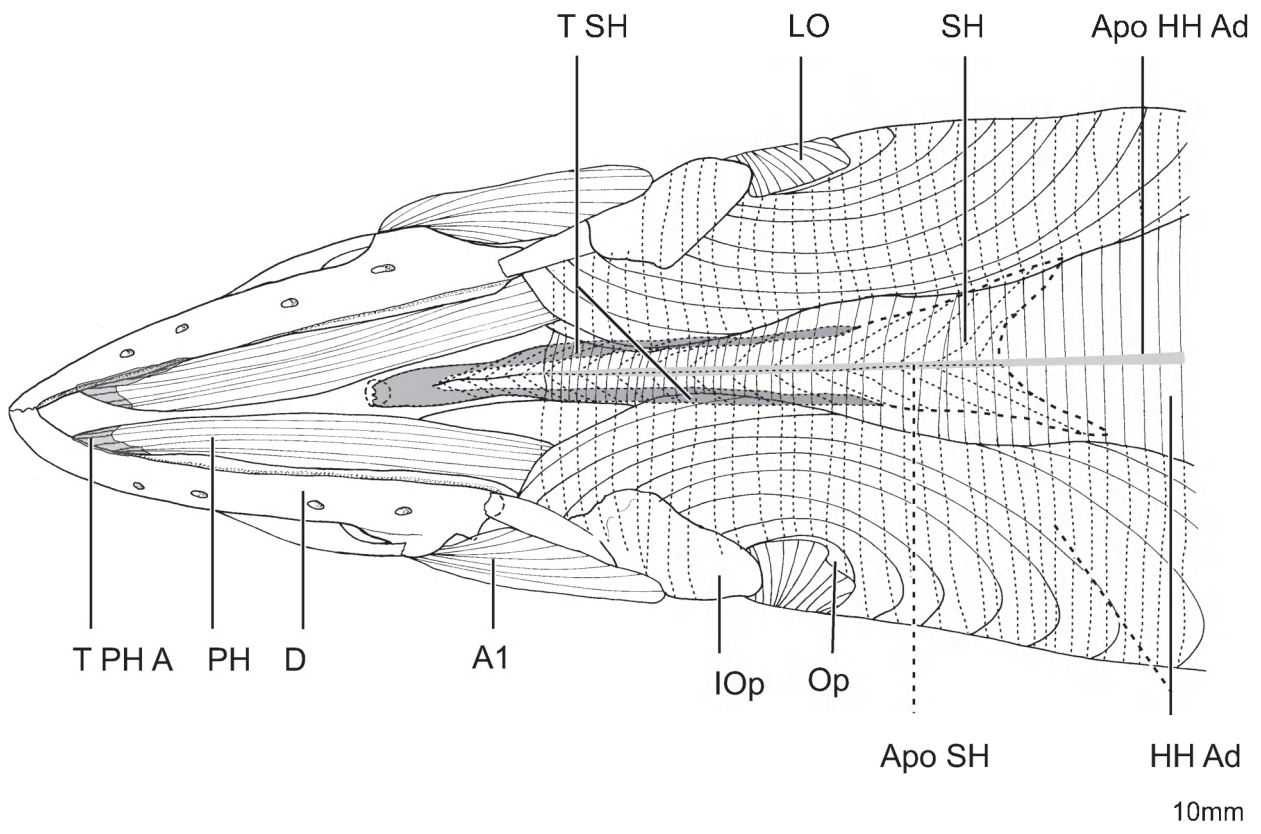


Fig. IV.2.2- 2: Ventral view of head musculature of a narrow-headed specimen of *Anguilla anguilla*.

Fig. IV.2.2- 3

*Anguilla anguilla*

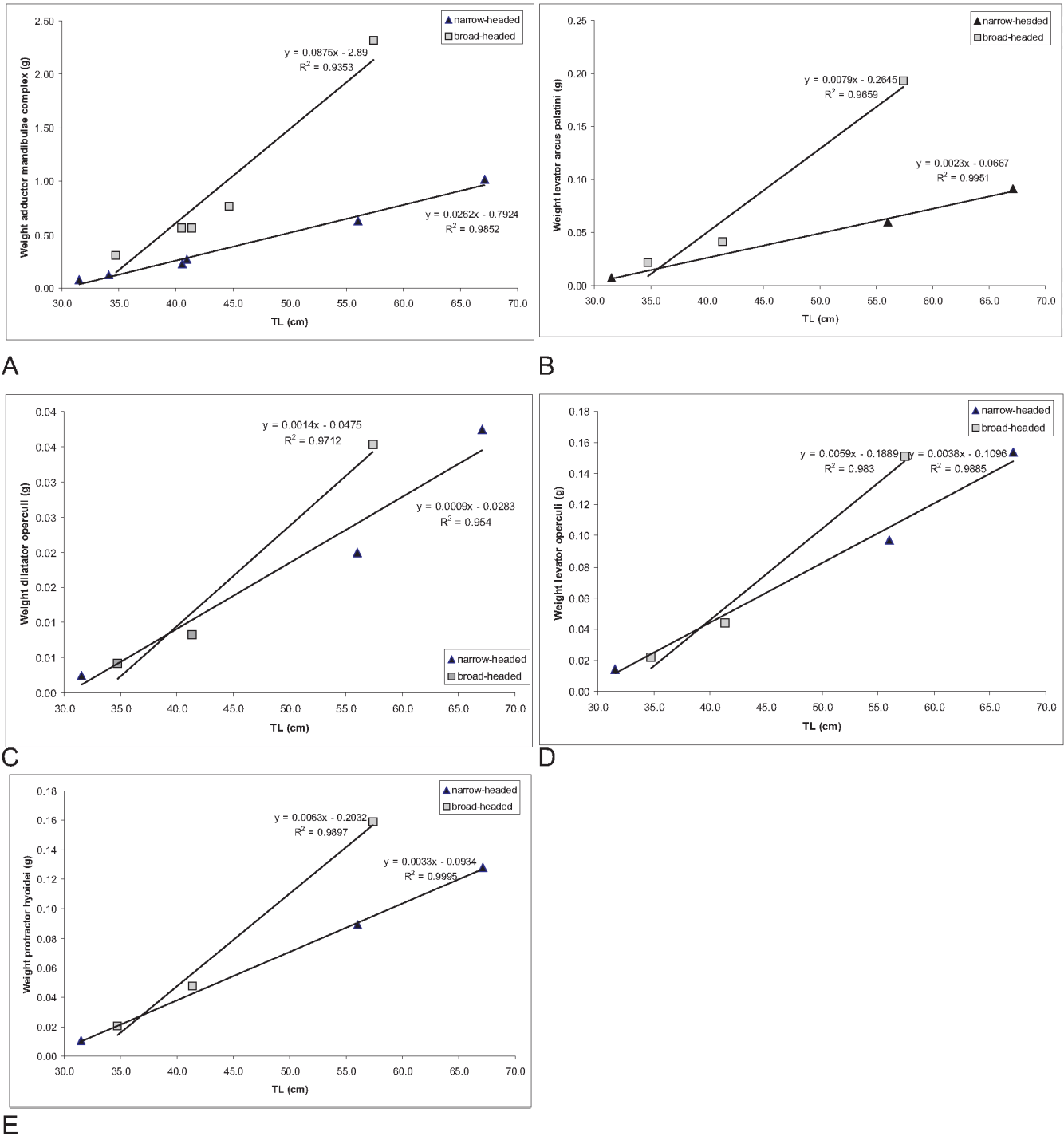


Fig. IV.2.2- 3: Scatterplot of the weight (g) of the (A) Adductor mandibulae complex, (B) the levator arcus palatini, (C) dilatator operculi, (D) levator operculi and (E) protractor hyoidei of broad-headed and narrow-headed eels with respect to total length (cm).

Fig. IV.2.2- 4

*Anguilla anguilla*

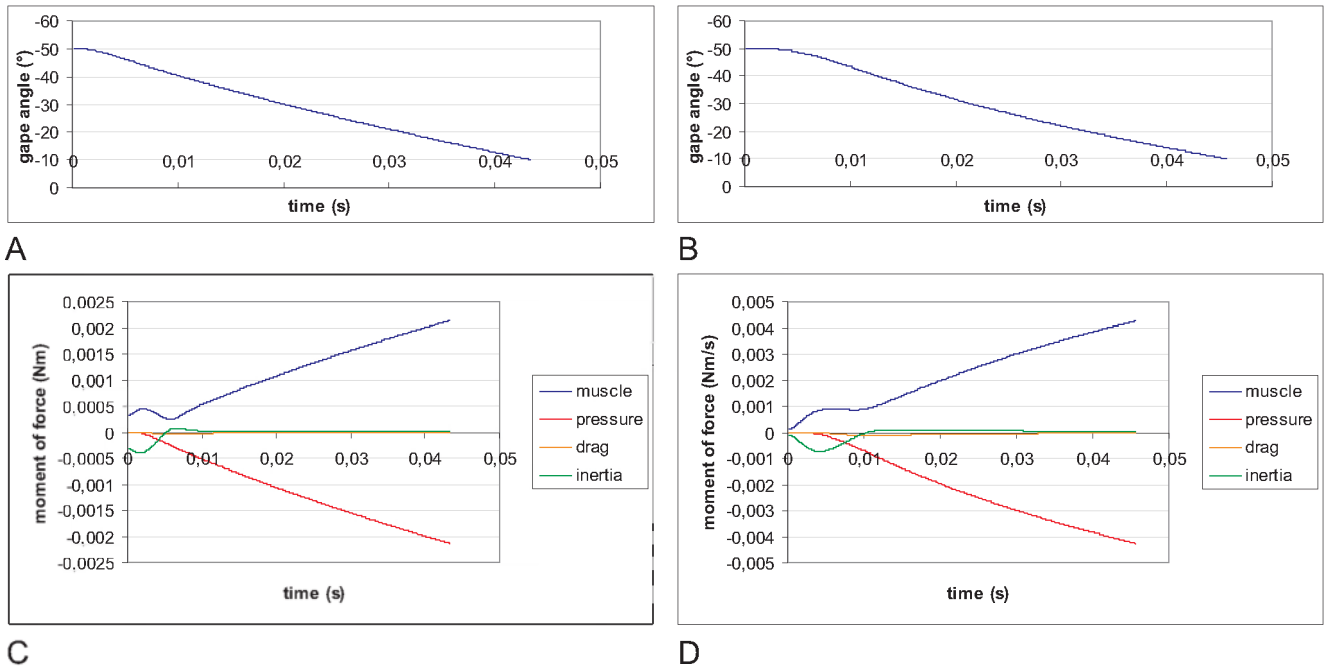


Fig. IV.2.2- 4: Model output (Van Wassenbergh et al., 2005) of the forces involved during jaw closure. The total musculature force needed to overcome drag, buccal pressures and inertia of the lower jaw are represented (A) for broad-headed eels and (B) narrow-headed eels.

Fig. IV.2.3- 1

*Conger conger*

Br R, branchiostegal rays

D, dentary

Hm, hyomandibula

IOP, Interopercle

Mx, maxillary

Nc, neurocranium

Op, opercle

POp, preopercle

PP, pterygoid

Q, quadrate

SOp, subopercle

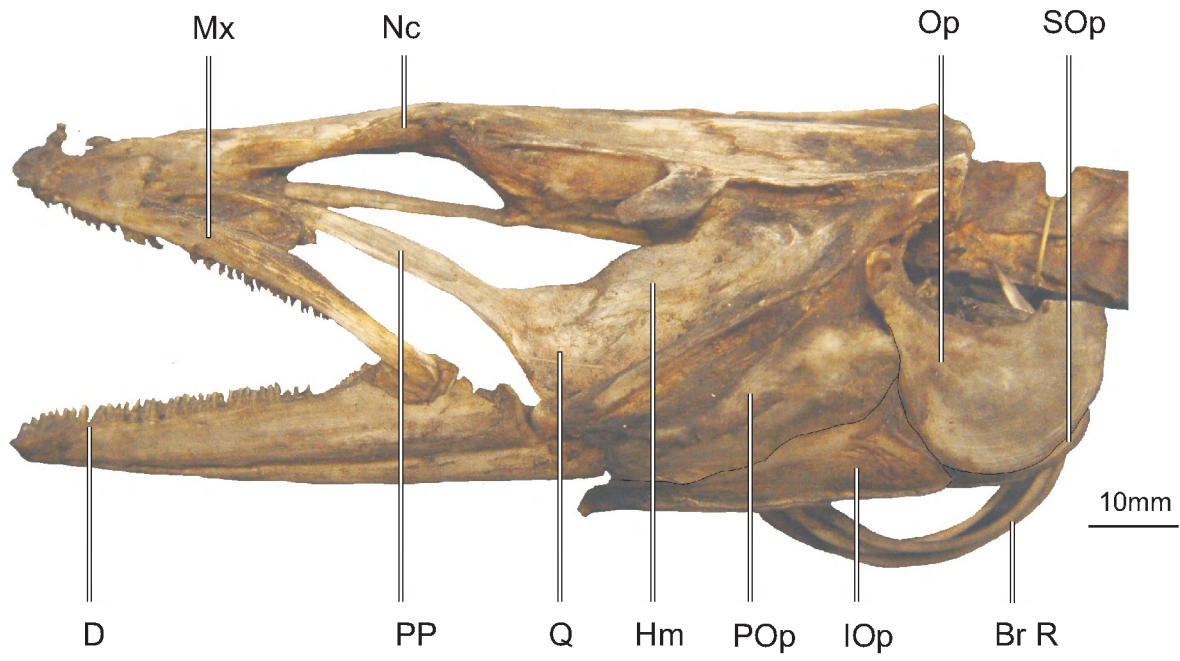


Fig. IV.2.3- 1: Lateral view of the skull of *C. Conger*.

Fig. IV.2.3- 2

*Conger conger*

af Mx- Etv A, anterior maxillo-premaxillo-ethmovomerine articular facet  
af Mx- Etv P, posterior maxillo-premaxillo-ethmovomerine articular facet  
af Susp A, anterior suspensorial articular facet  
af Susp P, posterior suspensorial articular facet  
af V-PP, vomero-ptyergoidal articular facet  
BOc, basioccipital  
BSph, basisphenoid  
Epi, epiotic  
ExOc, exoccipitals  
F, frontal  
Fo Di, fossa dilatator  
Fo ST, fossa subtemporalis  
Par, parietal  
PMx-Etv, Premaxillo-ethmovomerine complex  
Pr BSph, basisphenoidal process  
Pr ExOc, exoccipital process  
Pr F, frontal process  
Pro, prootic  
Pro, prootic  
PSph, parasphenoid  
Pt, pterotic  
PtSph, pterosphenoid  
SOc, supraoccipital  
Sph, sphenotic



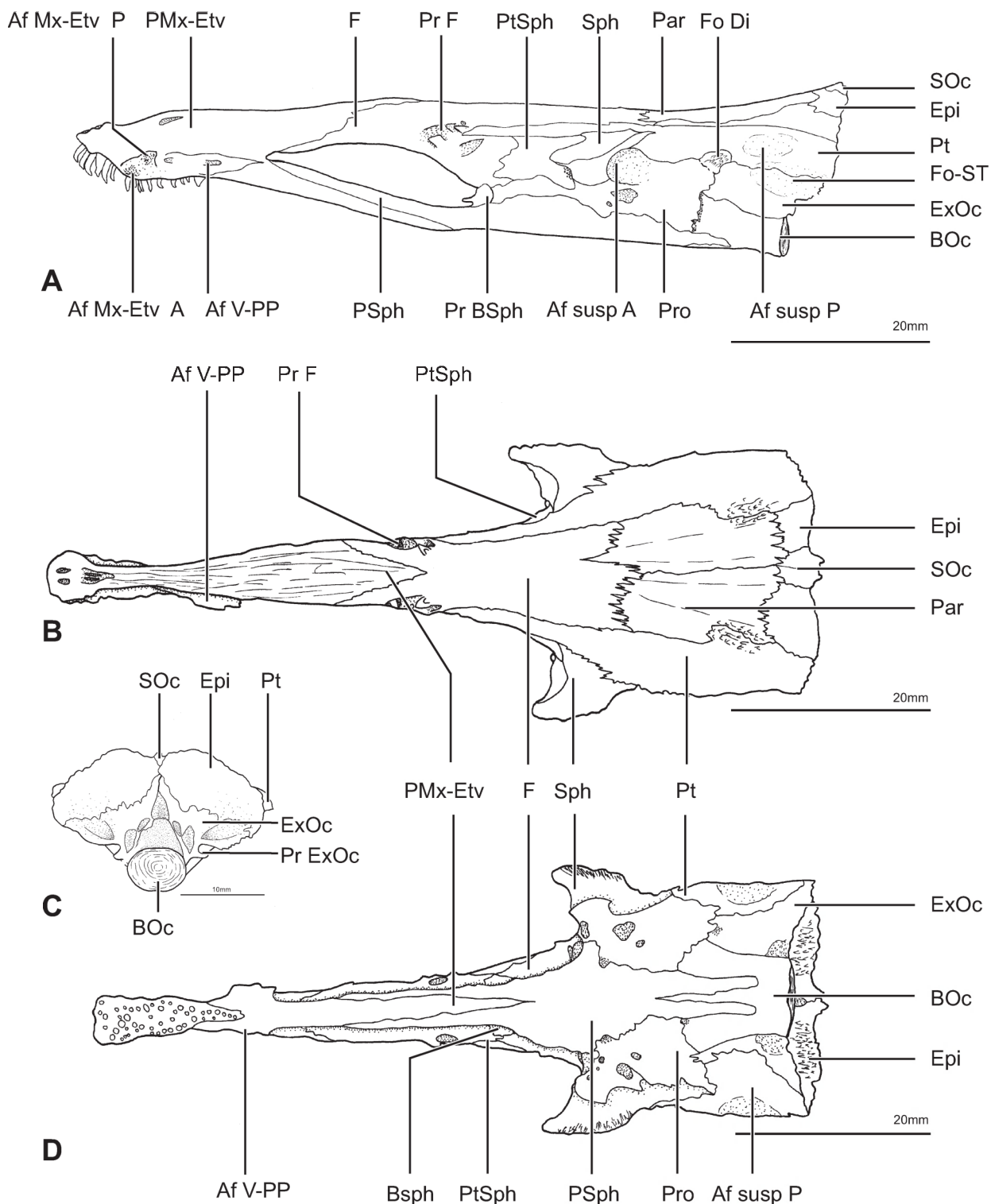


Fig. IV.2.3- 2: Illustration of the position of the cranial bones of *C. conger* in (A) lateral view, (B) dorsal view, (C) caudal view and (D) ventral view.

Fig. IV.2.3- 3

*Conger conger*

ac Md, mandibular articular condyle of the quadrate  
ac susp A, anterior suspensorial condyle of the hyomandibula  
ac susp P, posterior suspensorial condyle of the hyomandibula  
ac V-PP, vomero-ptyergoidal articular condyle  
Af Op, opercular articular facet for the hyomandibula  
c POp, preopercular canal  
Hm, hyomandibula  
IOp, interopercle  
Longit ridge, suspensorial longitudinal ridge  
Op, opercle  
POp, preopercle  
PP, pterygoid  
Pr D Op, rostro-dorsal process of the opercle  
Pr IOp, interopercular process  
Q, quadrate  
SOp, subopercle

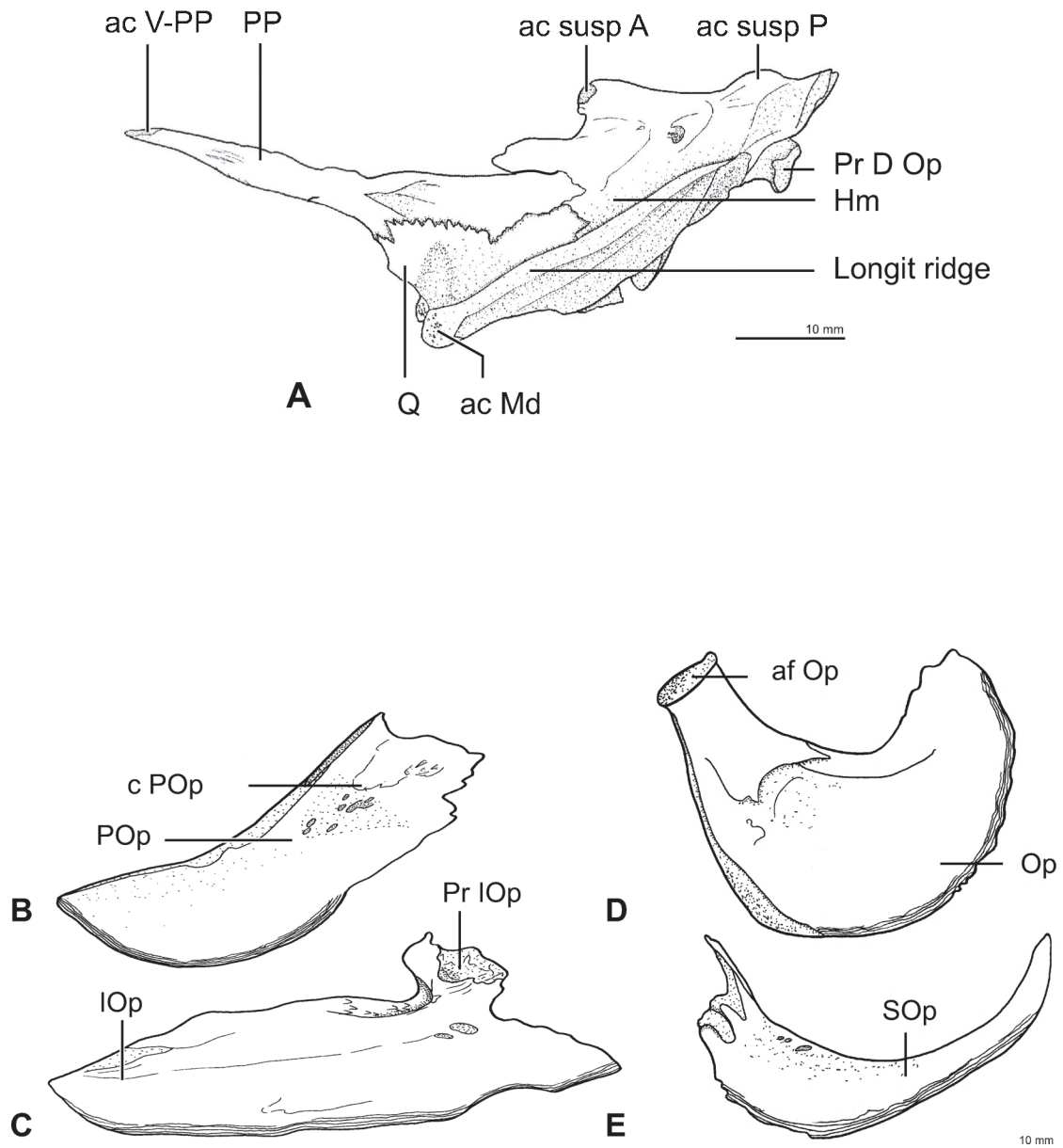


Fig. IV.2.3- 3: Lateral view of (A) the suspensorium; (B) the preopercle; (C) the interopercle; (D) the opercle; (E) the subopercle.

Fig. IV.2.3- 4

*Conger conger*

Af Md, mandibular articular facet

Ang, angular complex

C Md, mandibular canal

D, dentary

M, Meckels' cartilage

Pr cor, coronoid process

Pr RA, retroarticular process

Sym, symphysis

T inn, inner row of teeth

T out, outer row of teeth

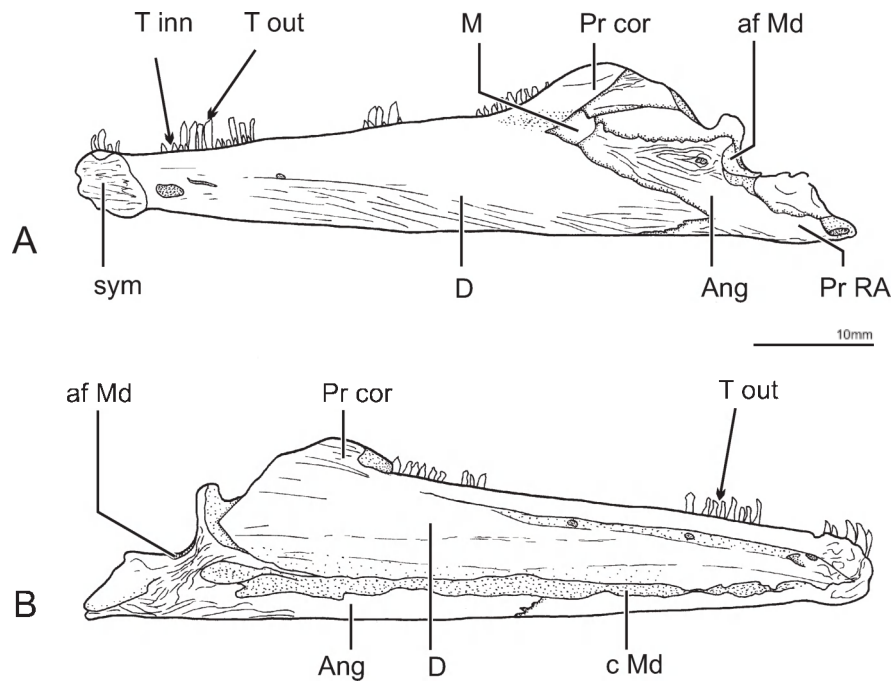


Fig. IV.2.3- 4: Lateral (A) and medial (B) view of the dentary of *C. Conger*.

Fig. IV.2.3- 5

*Conger conger*

ac CH P, articular condyle of the posterior ceratohyal  
af CH A, articular facet of the anterior ceratohyal  
af Mx- Etv A, anterior maxillo-premaxillo-ethmovomerine articular facet  
af Mx- Etv P, posterior maxillo-premaxillo-ethmovomerine articular facet  
Af UH-BH, urohyal-basihyal articular facet  
Af UH-CH, urohyal-ceratohyal articular facet  
BH, basihyal  
Br R, branchiostegal ray  
CH A, anterior ceratohyal  
CH P, posterior ceratohyal  
Pr UH, urohyal process  
UH, urohyal

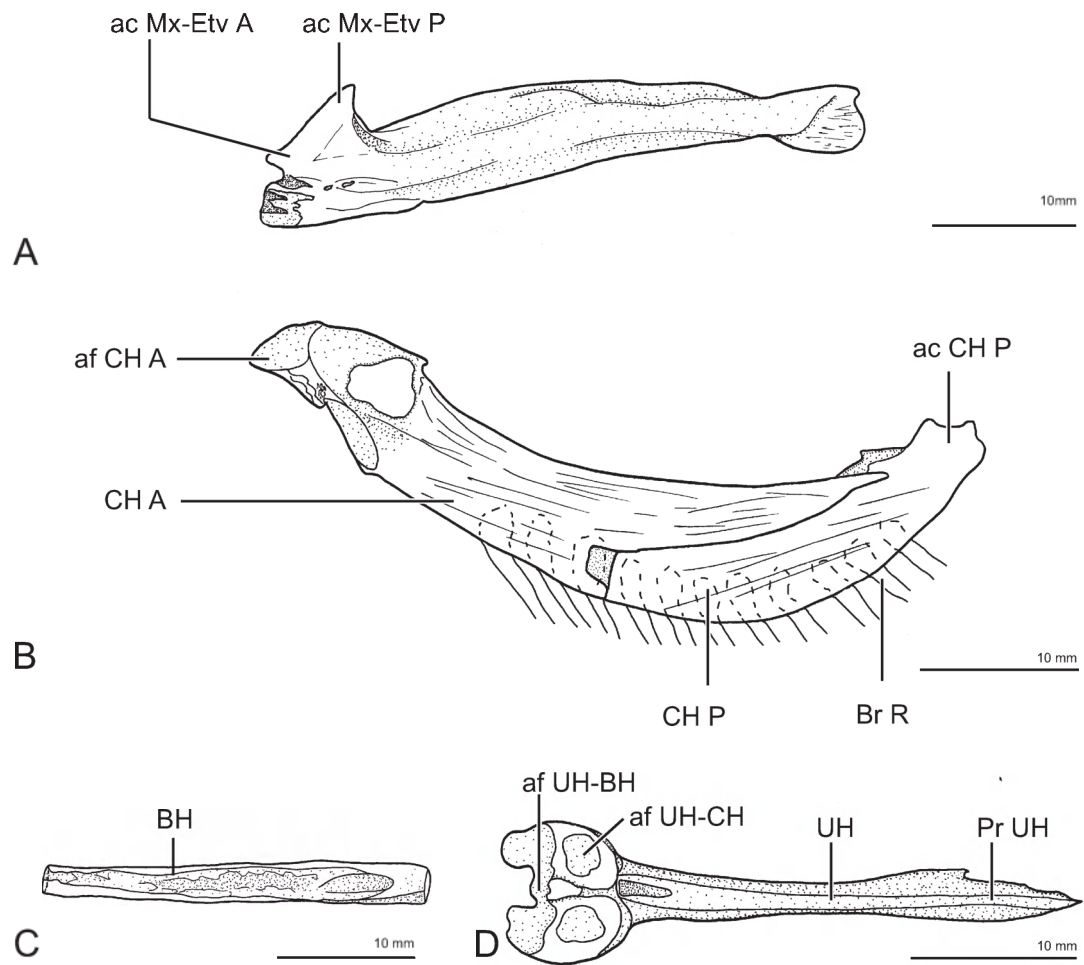


Fig. IV.2.3- 5 **A:** the maxillary in lateral view; **B:** the ceratohyal with branchiostegal rays in lateral view; **C:** the basihyal in lateral view; **D:** the urohyal in dorsal view.

Fig. IV.2.3- 6

*Conger conger*

A1, A2, A3, subdivisions the adductor mandibulae complex  
apo, aponeurosis

HH Ad, hyohyoidei adductores

LO, levator operculi

PH, protractor hyoidei

T A1, A2, A3, tendon of subdivisions A1, A2, A3

T LO, tendon of levator operculi

Epax, epaxials

L Ang-POp, angulo-poreopercular ligament

L Mx-D, maxillo-dental ligament

L Prim, primordial ligament

ms H, horizontal myoseptum



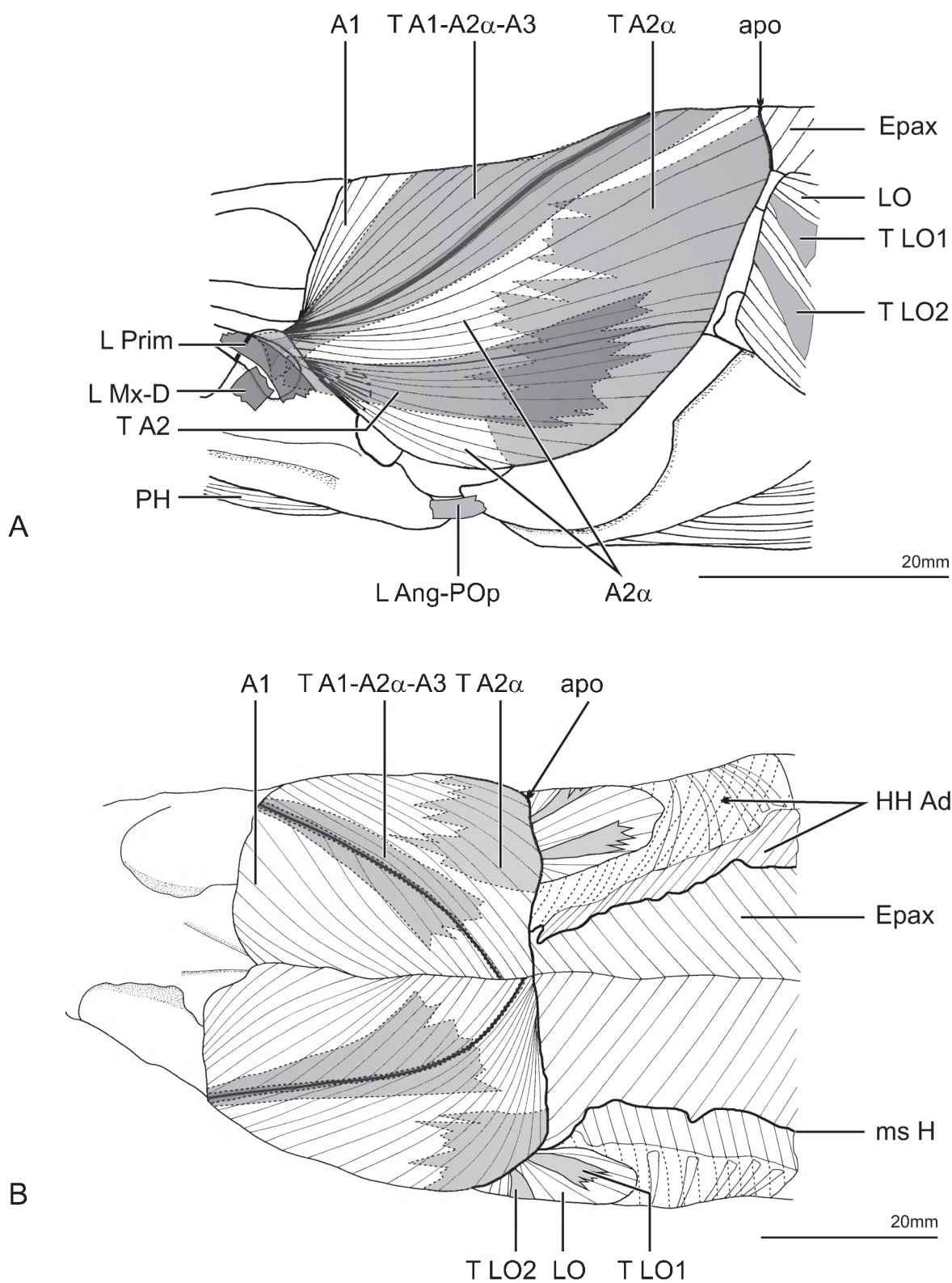


Fig. IV.2.3- 6 A: Lateral view of the cranial muscles of *C. conger*. Dotted lines indicate parts of structures being covered by other elements. Skin is removed. B: Dorsal view of the expanded adductor mandibulae complex. The epaxials are connected to the former by an aponeurosis. The epaxials are laterally partially removed to show the hyohyoideus muscles.

Fig. IV.2.3- 7

*Conger conger*

A1, A2, A3, A $\omega$ , subdivisions the adductor mandibulae complex  
DO, dilatator operculi  
Epax, epaxials  
HH Ad, hyohyoidei adductores  
Hyp, hypaxials  
L Ang-CH, angulo-ceratohyal ligament  
L Ang-IOP, angulo-interopercular ligament  
L Ang-POp, angulo-poreopercular ligament  
L Mx-D, maxillo-dental ligament  
L POp-Op, preoperculo-opercular ligament  
L PP-Mx, pterygoidal-maxillar ligament  
L Prim, primordial ligament  
LAP, levator arcus palatini  
LO, levator operculi  
ms H, horizontal myoseptum  
PH, protractor hyoidei  
T A1, A2, A3, A $\omega$ , tendon of subdivisions A2, A3, A $\omega$   
T DO, tendon of dilatator operculi  
T LO, tendon of levator operculi

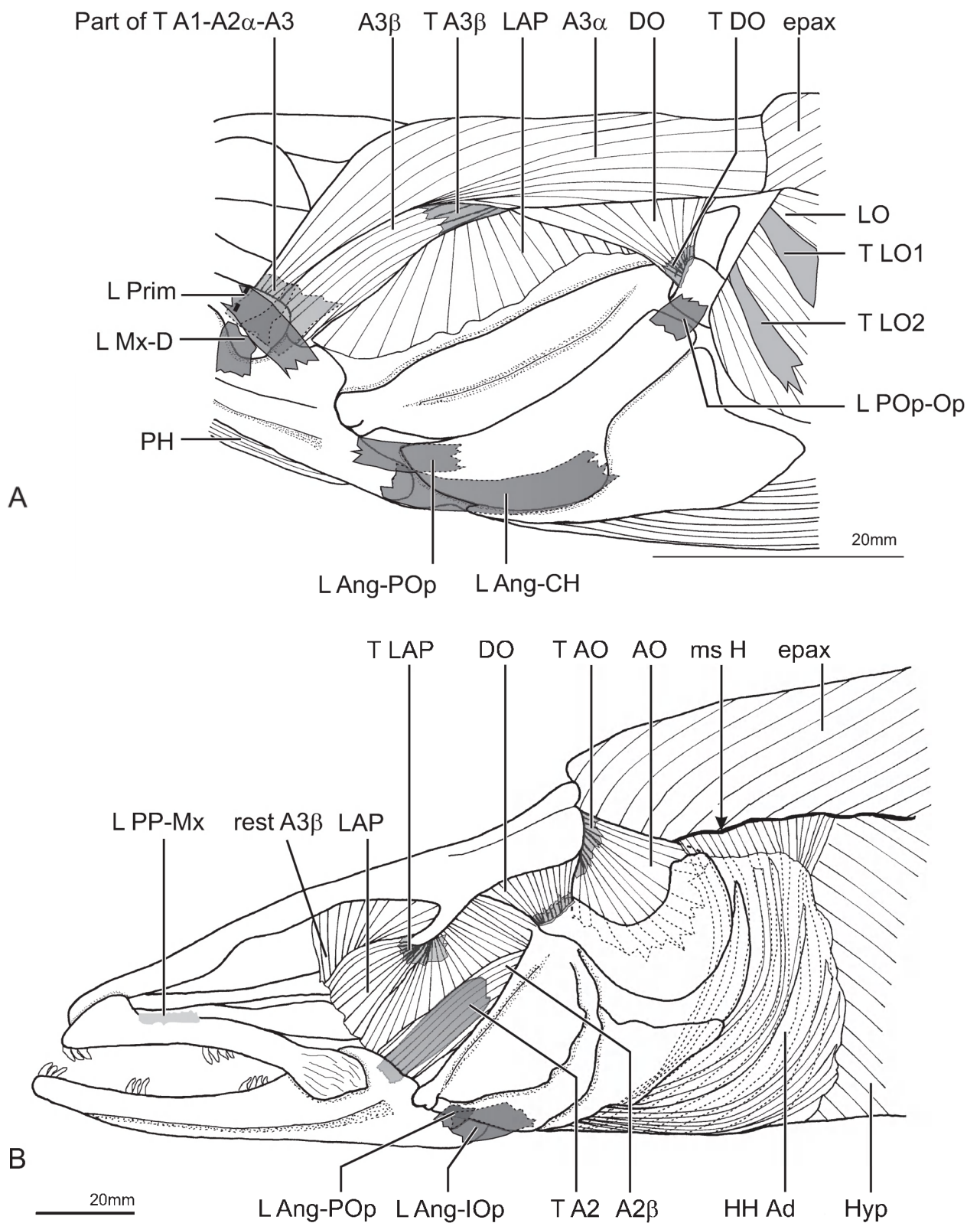
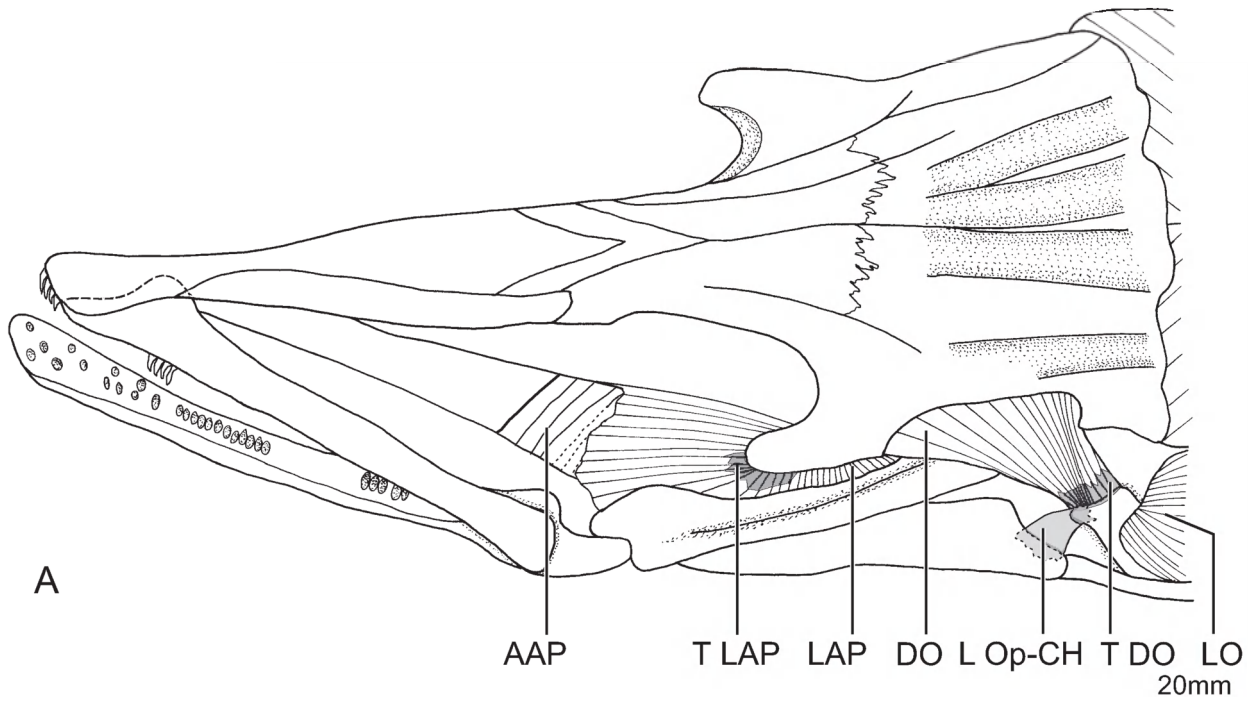


Fig. IV.2.3- 7: Lateral view of the cranial muscles of *C. conger*. **A:** The A1 and A2 are removed, exposing the A3 $\alpha$  and A3 $\beta$ . **B:** The A3 $\alpha$  and A3 $\beta$  are removed.

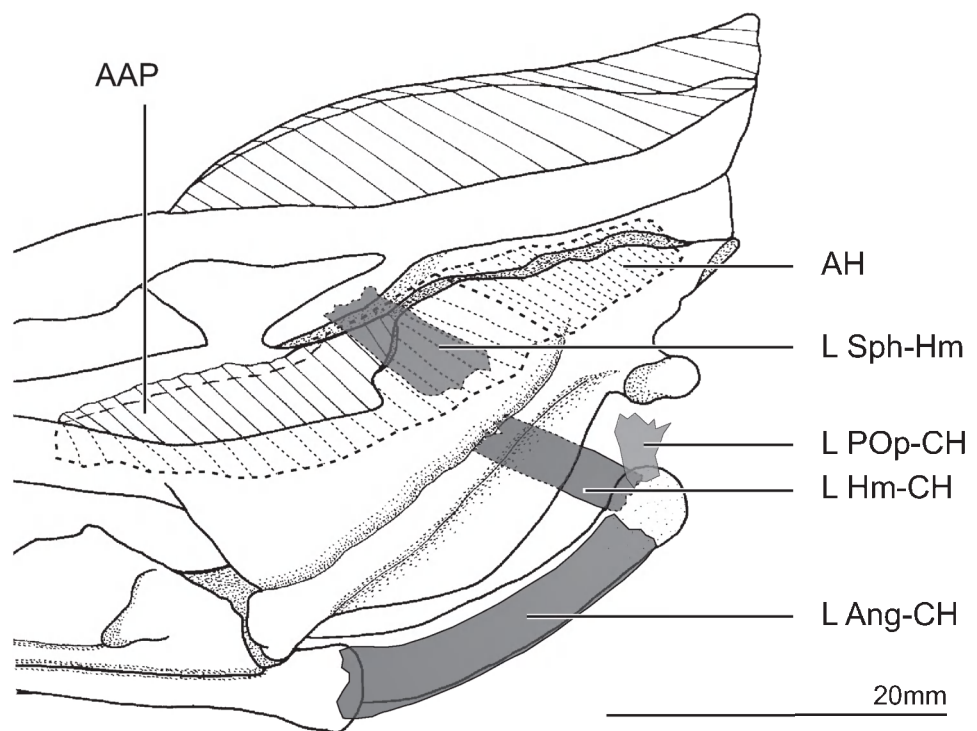
Fig. IV.2.3- 8

*Conger conger*

AAP, adductor arcus palatini  
AH, adductor hyomandibulae  
L Ang-CH, angulo-ceratohyal ligament  
L Hm-CH, hyomandibulo-ceratohyal ligament  
L Op-CH, operculo-ceratohyal ligament  
L POp-CH, preoperculo-ceratohyal ligament  
L Sph-Hm, sphenotic-hyomandibular ligament  
LAP, levator arcus palatini  
LO, levator operculi  
T DO, tendon of dilatator operculi  
T LAP, tendon of levator arcus palatini  
T LO, tendon of levator operculi  
HH Ad, hyohyoidei adductores



A



B

Fig. IV.2.3- 8 A: Dorso-lateral view of the cranial muscles of *C. conger*. The adductor mandibulae complex and LO are removed. B: Lateral view of the cranial muscles with indication of the position of the muscles underneath the suspensorium.

Fig. IV.2.3- 9

*Conger conger*

A2, subdivision the adductor mandibulae complex

AH, adductor hyomandibulae

AO, adductor operculi

apo HH Ad, aponeurosis of the hyohyoidei adductores

apo, aponeurosis

Epax, epaxials

HH Ad, hyohyoidei adductores

L Ang-IOp, angulo-interopercular ligament

L IOp-CH, interoperculo-ceratohyal ligament

L POp-CH, preoperculo-ceratohyal ligament

ms H, horizontal myoseptum

PH, protractor hyoidei

SH, sternohyoideus

T AO, tendon of adductor operculi

T PH, tendon of protractor hyoidei

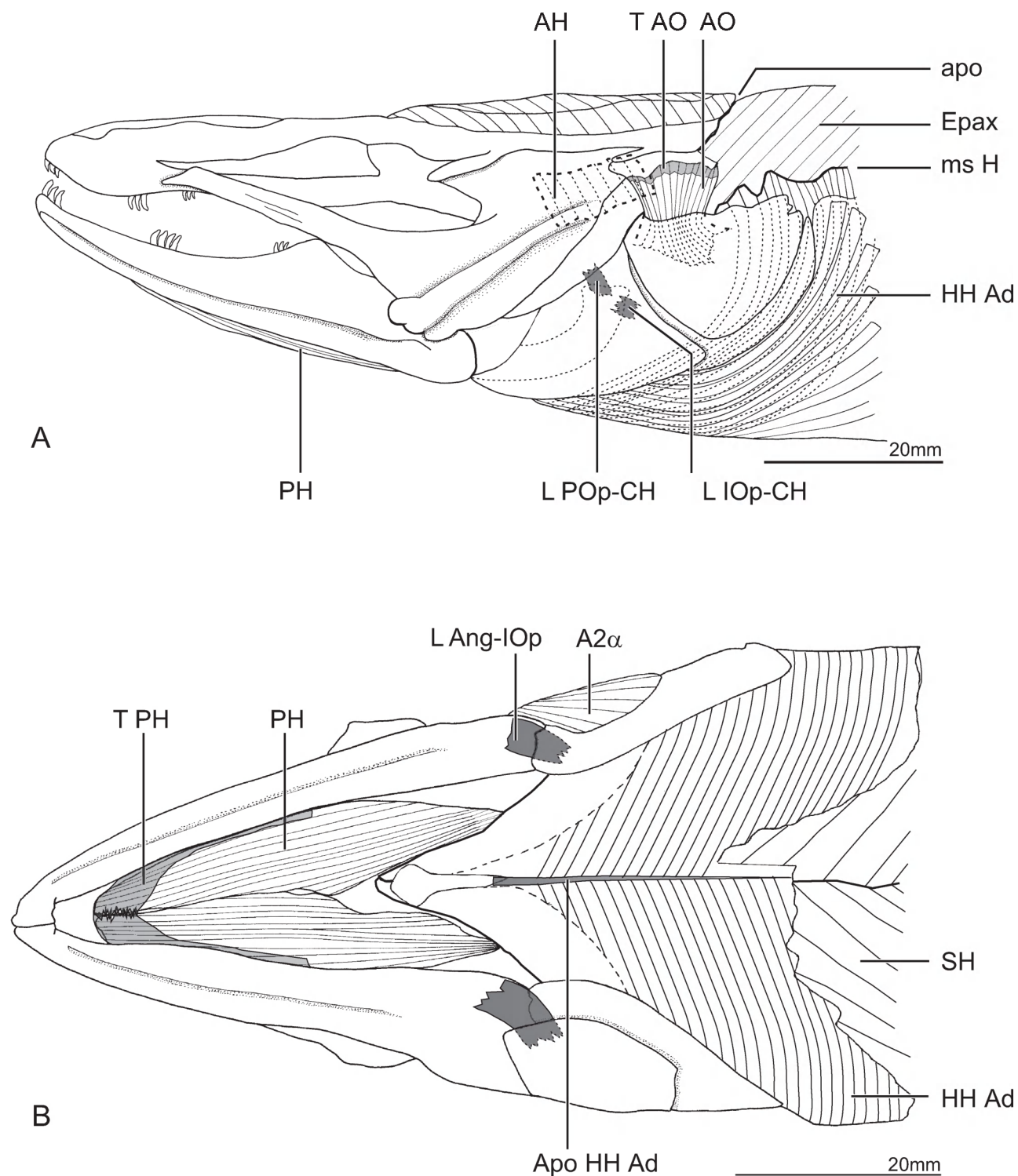


Fig. IV.2.3- 9 **A:** Lateral view of the cranial muscles of *C. conger*. Adductor mandibulae complex, AAP, LAP, LO and DO are removed. **B:** Ventral view of the cranial muscles of *C. Conger*. Branchiostegal rays are removed to visualize the hyohyoidei adductores.

Fig. IV.2.3- 10:

A, *Anguilla anguilla*

B, *Conger conger*

C, *Moringua edwardsi*

D, *Pisodonophis boro*

E, *Heteroconger longissimus*



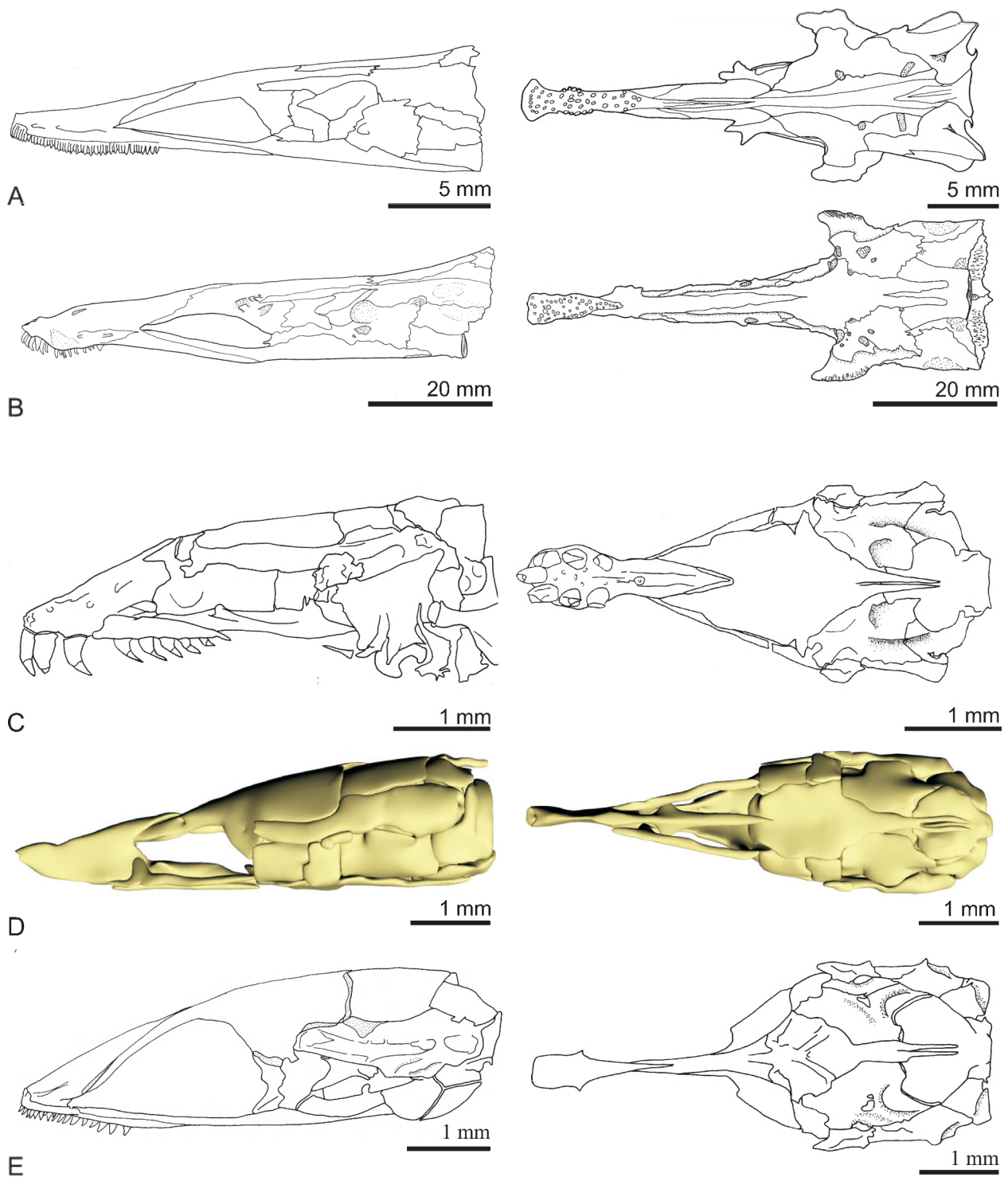


Fig. IV.2.3- 10: Illustration of the neurocrania in lateral view (left column) and ventral view (right column) of 5 Anguilliform species: A: *Anguilla anguilla*, B: *Conger conger*, C: *Moringua edwardsi*, D: *Pisodonophis boro*, E: *Heteroconger longissimus*. Neurocrania are scaled to equal size. Differences in orbit size (and consequent eye size), snout length, skull height and width become more apparent.

Fig. IV.2.3- 11

A, Relative length of the ethmoid region  
B, Relative length of the orbits

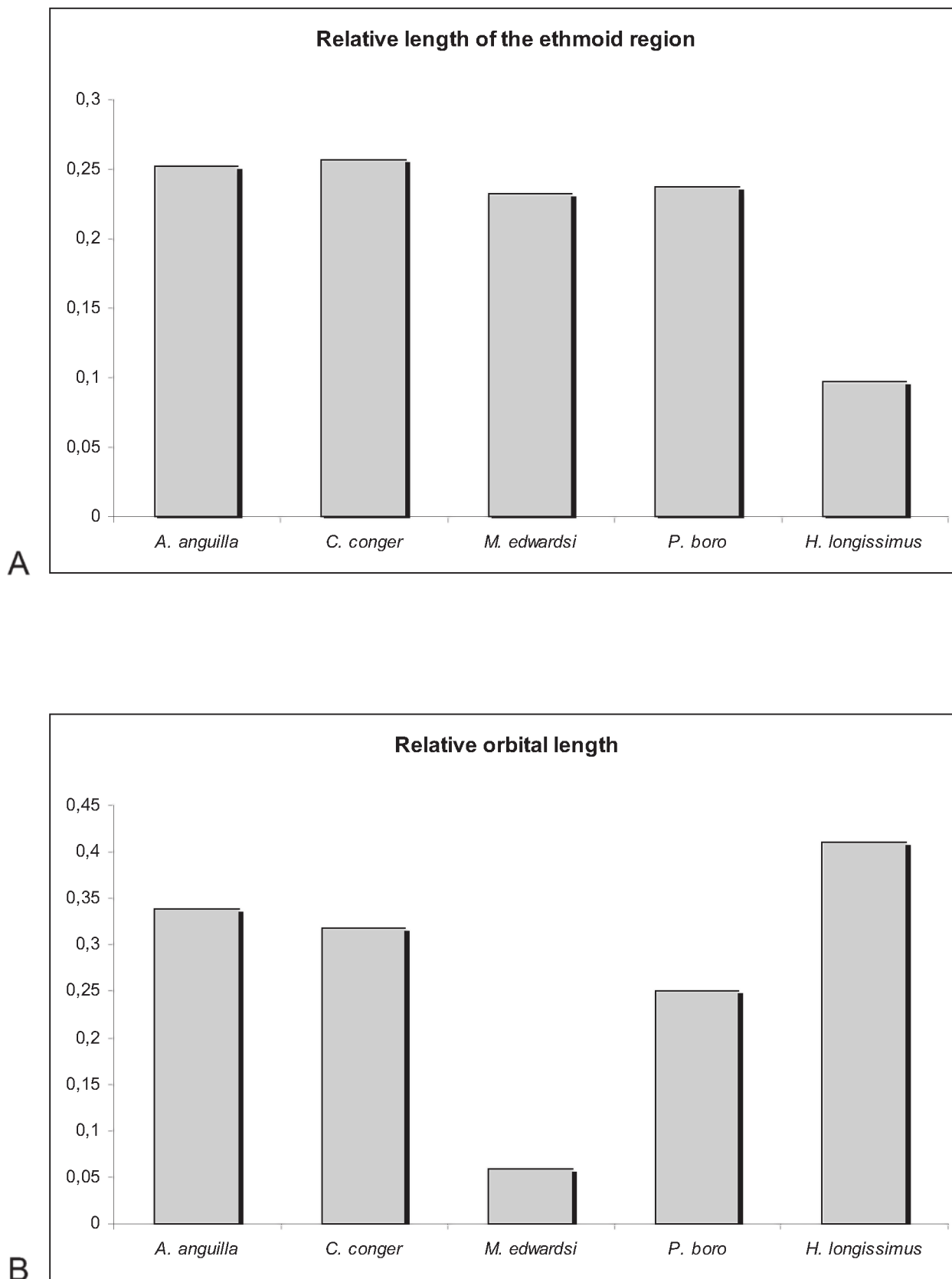


Fig. IV.2.3- 11. The mean of cranial lengths defined for *Anguilla anguilla*, *Conger conger*, *Moringua edwardsi*, *Pisodonophis boro*, *Heteroconger longissimus*. A: Relative length of the ethmoid region. Ethmoid region is measured from the tip of the premaxillo-ethmovomerine complex to the anterior corner of the orbit and expressed with respect to postorbital length. B: Relative length of the orbits. Length is measured from the anterior corner to the posterior corner of the orbit and expressed with respect to postorbital length.

Fig. IV.2.3- 12

A, *Pisodonophis boro*

B, *Heteroconger longissimus*

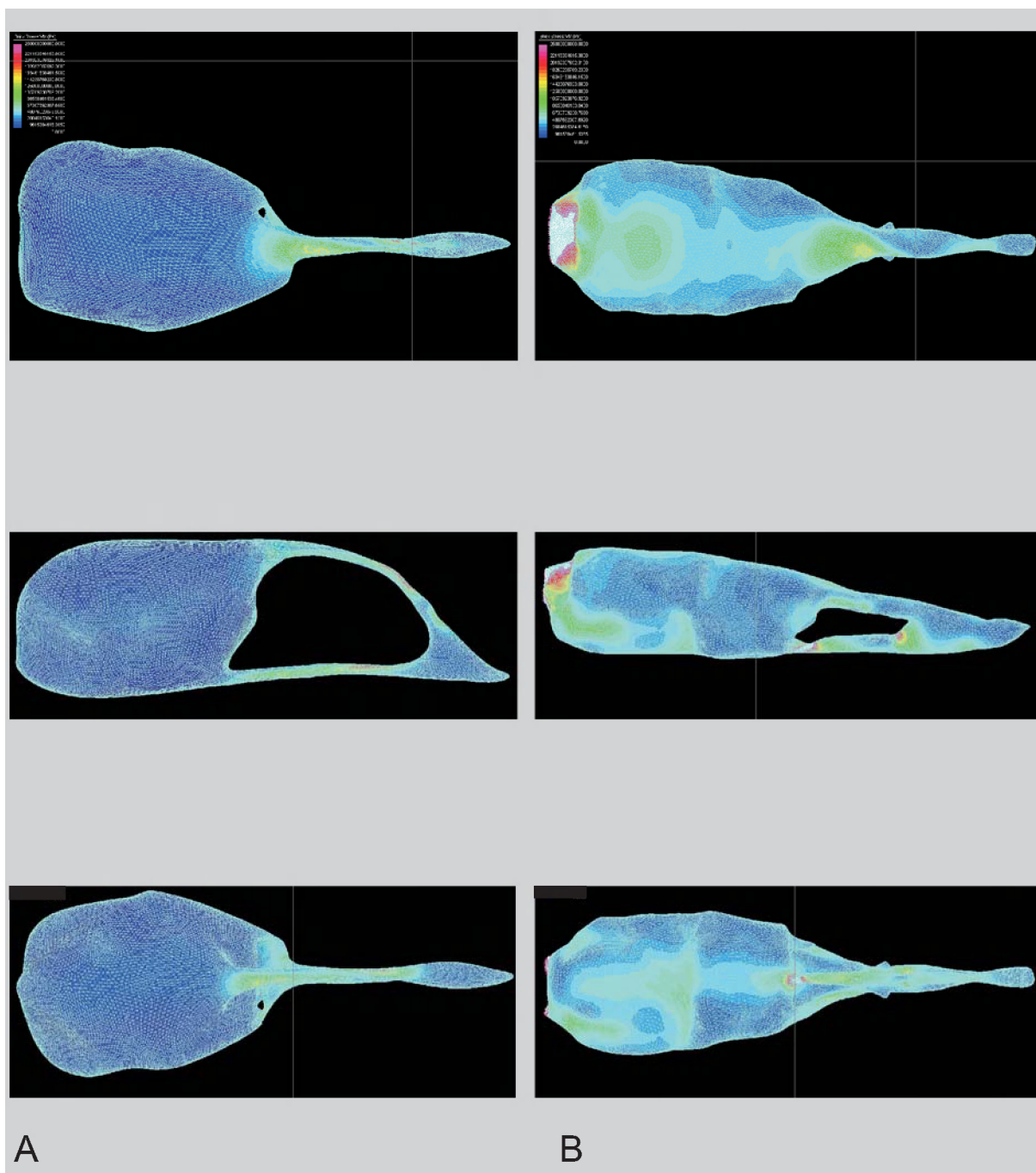


Fig. IV.4.3- 12: Illustration of stress-distribution as a result of frontal and antero-lateral loads in the neurocrania of (A) *Pisodonophis boro* and (B) *Heteroconger longissimus*. White regions indicate higher stress levels than could be shown by the colour legend.

Fig. IV.2.4- 1

A, *Anguilla anguilla*

B, *Conger conger*

C, *Pisodonophis boro*

D, *Moringua edwardsi*

E, *Heteroconger hassi*

F, *Heteroconger longissimus*

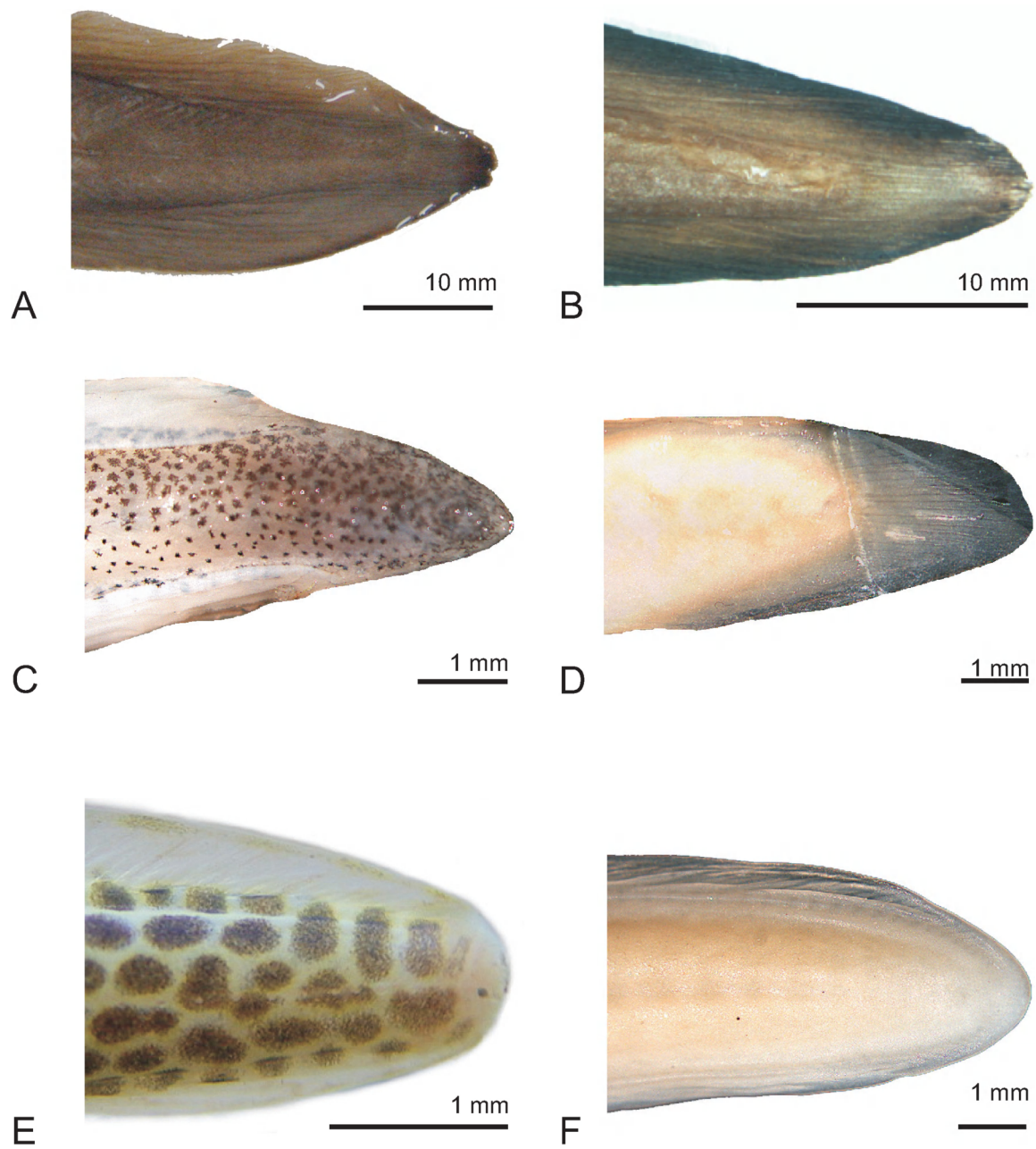


Fig. IV.2.4- 1: The external morphology of the caudal fin of (A) *Anguilla anguilla*, (B) *Conger conger*, (C) *Pisodonophis boro*, (D) *Moringua edwardsi*, (E) *Heteroconger hassi*, (F) *Heteroconger longissimus*.

Fig. IV.2.4- 2

A, *Anguilla anguilla*

B, *Conger conger*

C, *Pisodonophis boro*

D, *Moringua edwardsi*

E, *Heteroconger hassi*

F, *Heteroconger longissimus*



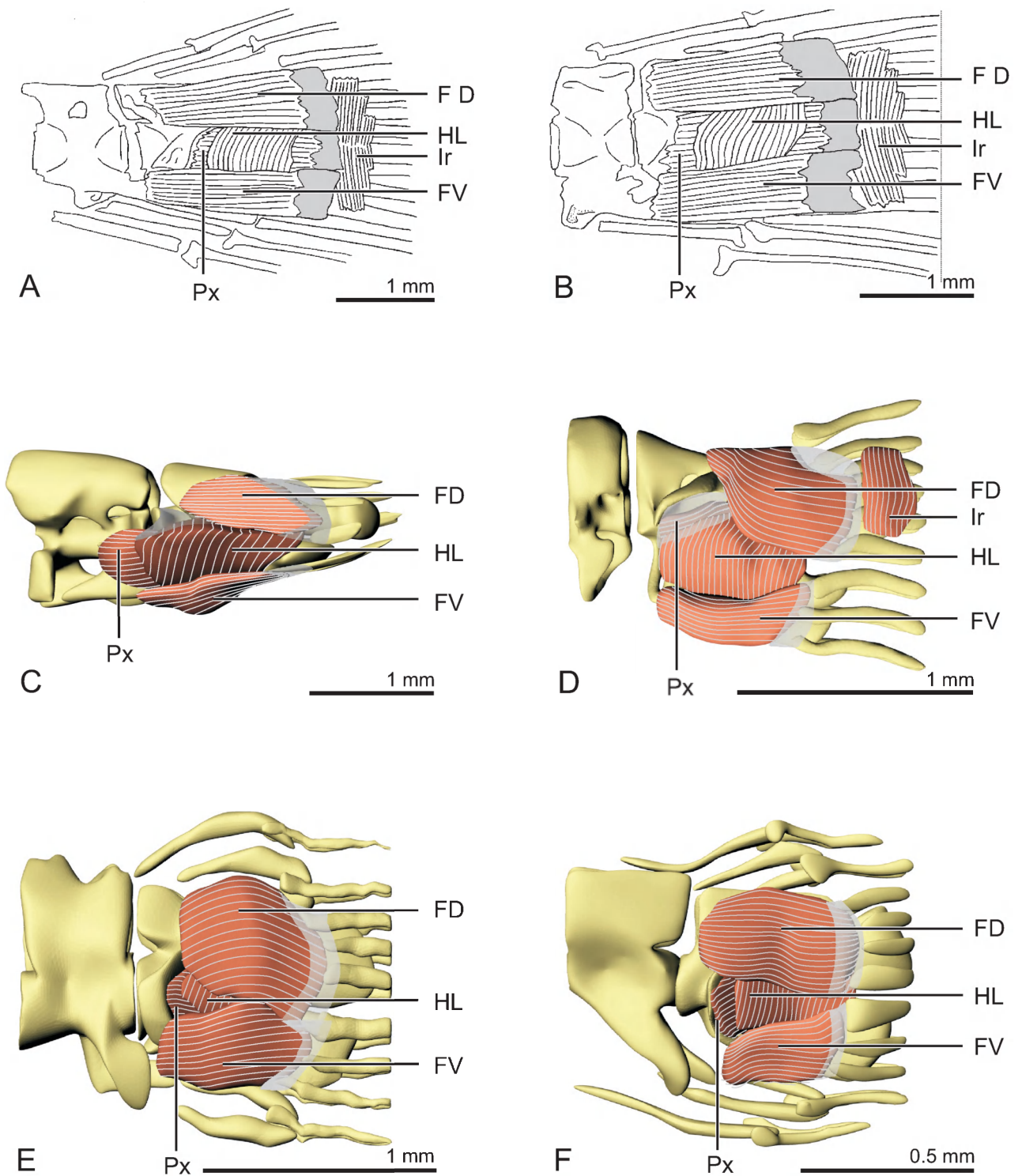


Fig. IV.2.4- 2: The musculature of the caudal fin of (A) *Anguilla anguilla*, (B) *Conger conger*, (C) *Pisodonophis boro*, (D) *Moringua edwardsi*, (E) *Heteroconger hassi*, (F) *Heteroconger longissimus*.

Fig. IV.2.4- 3

A, *Anguilla anguilla*

B, *Conger conger*

C, *Pisodonophis boro*

D, *Moringua edwardsi*

E, *Heteroconger hassi*

F, *Heteroconger longissimus*

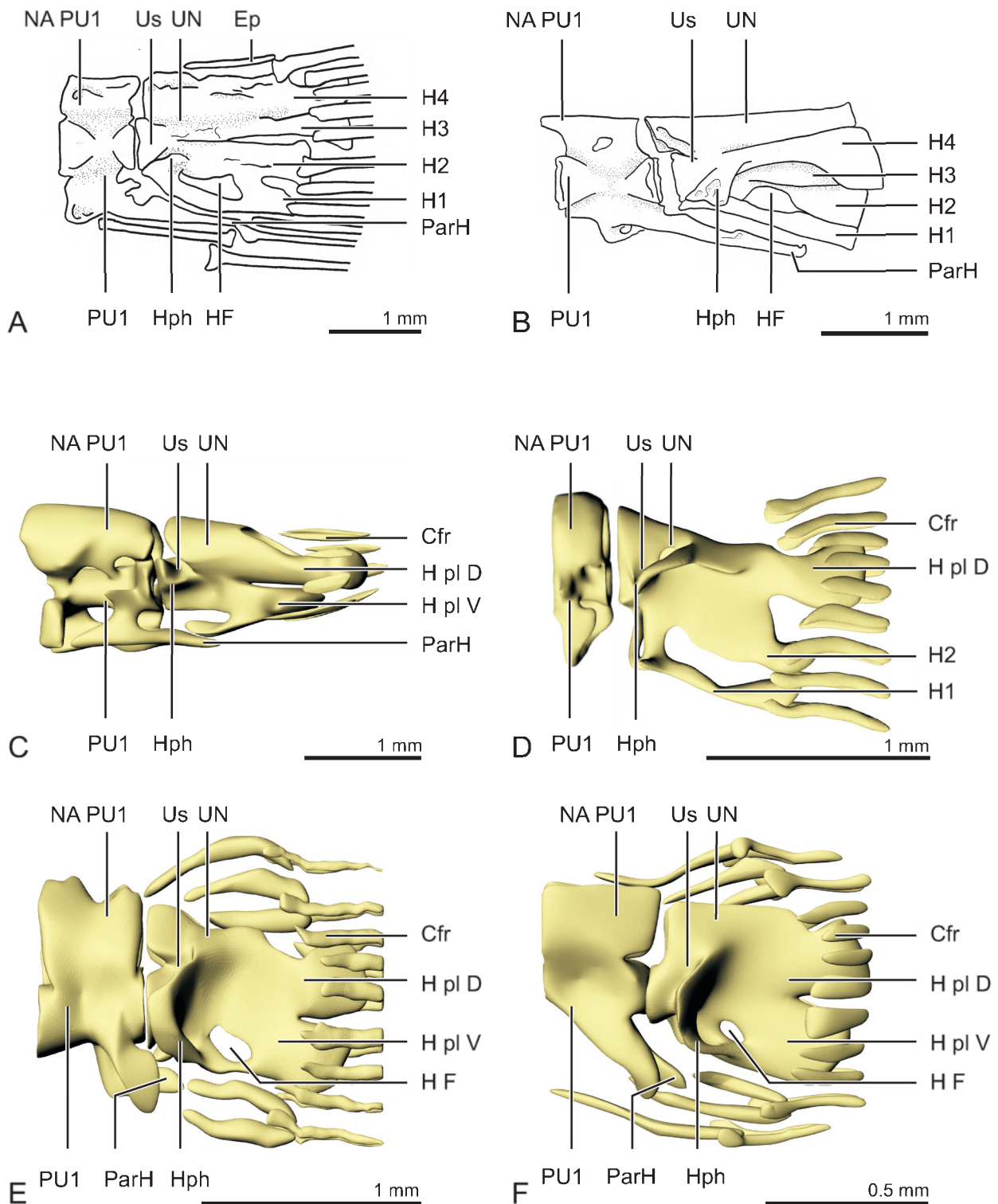


Fig. IV.2.4- 3: The osteology of the tail of (A) *Anguilla anguilla*, (B) *Conger conger*, (C) *Pisodonophis boro*, (D) *Moringua edwardsi*, (E) *Heteroconger hassi*, (F) *Heteroconger longissimus*.

Fig. V.1- 1

*Clarias gariepinus*

H, hypural

PH, parhypural

EP, epural

CC, compound centrum

U, urostyl

PU, preural centrum

HPU, hemal spine of the preural centrum

NPU, neural spine of the preural centrum

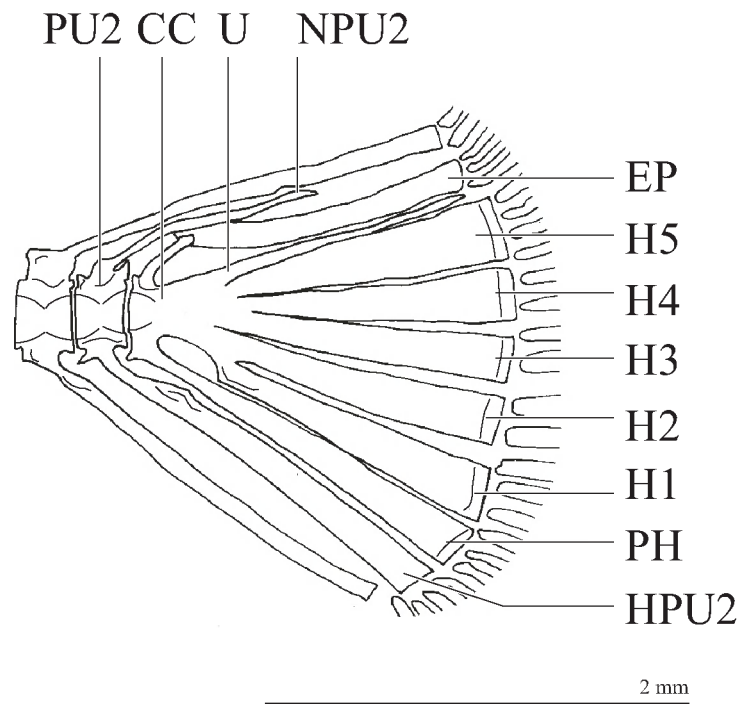


Fig. V.1- 1: The caudal skeleton of *Clarias gariepinus* shows no hypural fusions

Fig. V.1- 2

A, *Platyclarias machadoi*

B, *Platyclarias machadoi*

C, *Platyallabes tihoni*

D, *Gymnallabes typus*

E, *Gymnallabes typus*

F, *Dolichallabes microphthalmus*

H, hypural

PH, parhypural

EP, epural

CC, compound centrum

U, urostyl

PU, preural centrum

HPU, hemal spine of the preural centrum

NPU, neural spine of the preural centrum

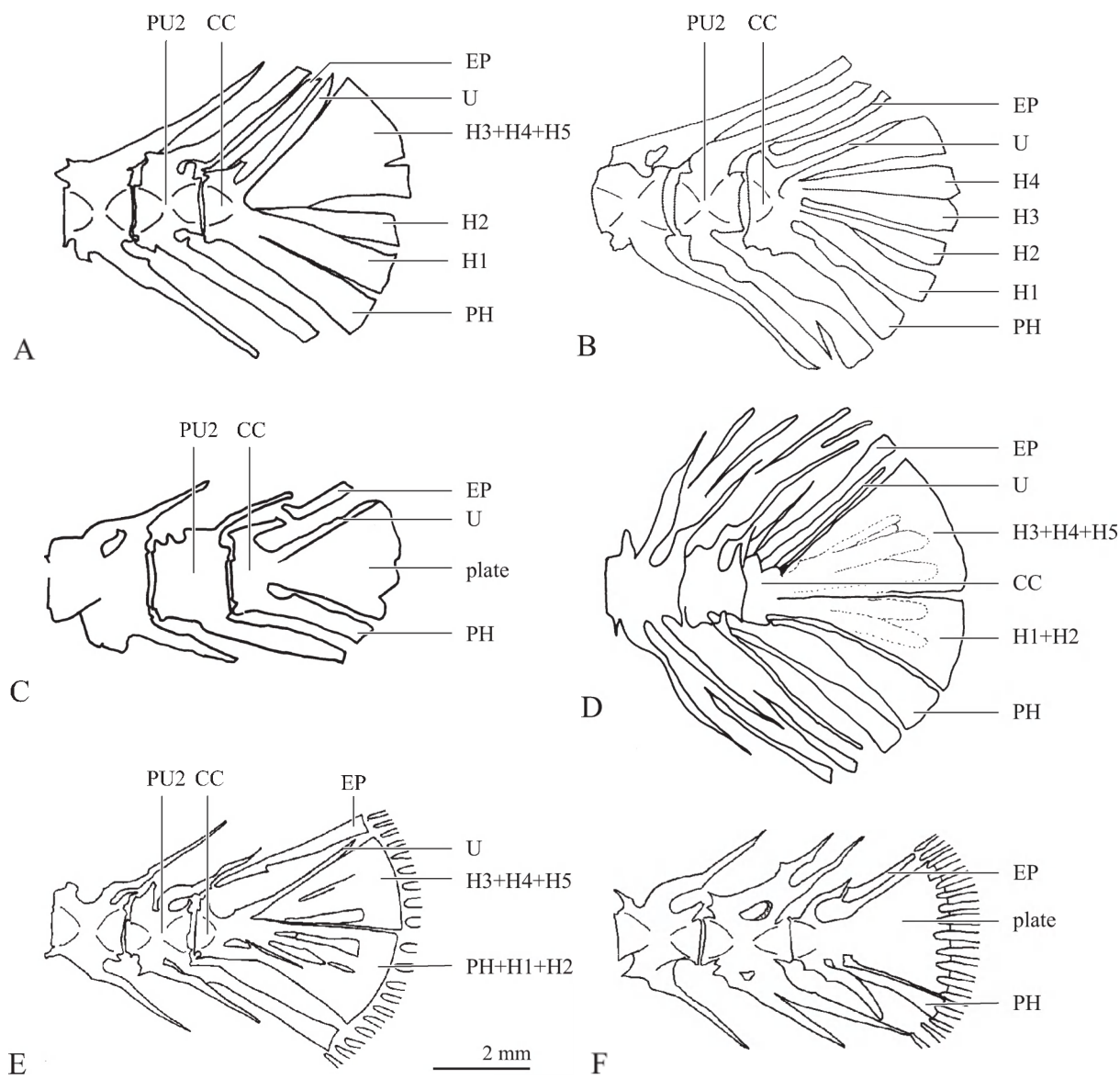


Fig. V.1- 2: The caudal skeleton of A: *Platyclarias machadoi*, B: *Platyclarias machadoi* (modified after Poll, 1977), C: *Platyallabes tihoni* (modified after Poll, 1977), D: *Gymnallabes typus* (modified after Poll, 1977), E: *Gymnallabes typus*, F: *Dolichallabes microphthalmus*

Fig. V.1- 3

*Channallabes apus*

H, hypural

PH, parhypural

EP, epural

CC, compound centrum

U, urostyl

PU, preural centrum

HPU, hemal spine of the preural centrum

NPU, neural spine of the preural centrum



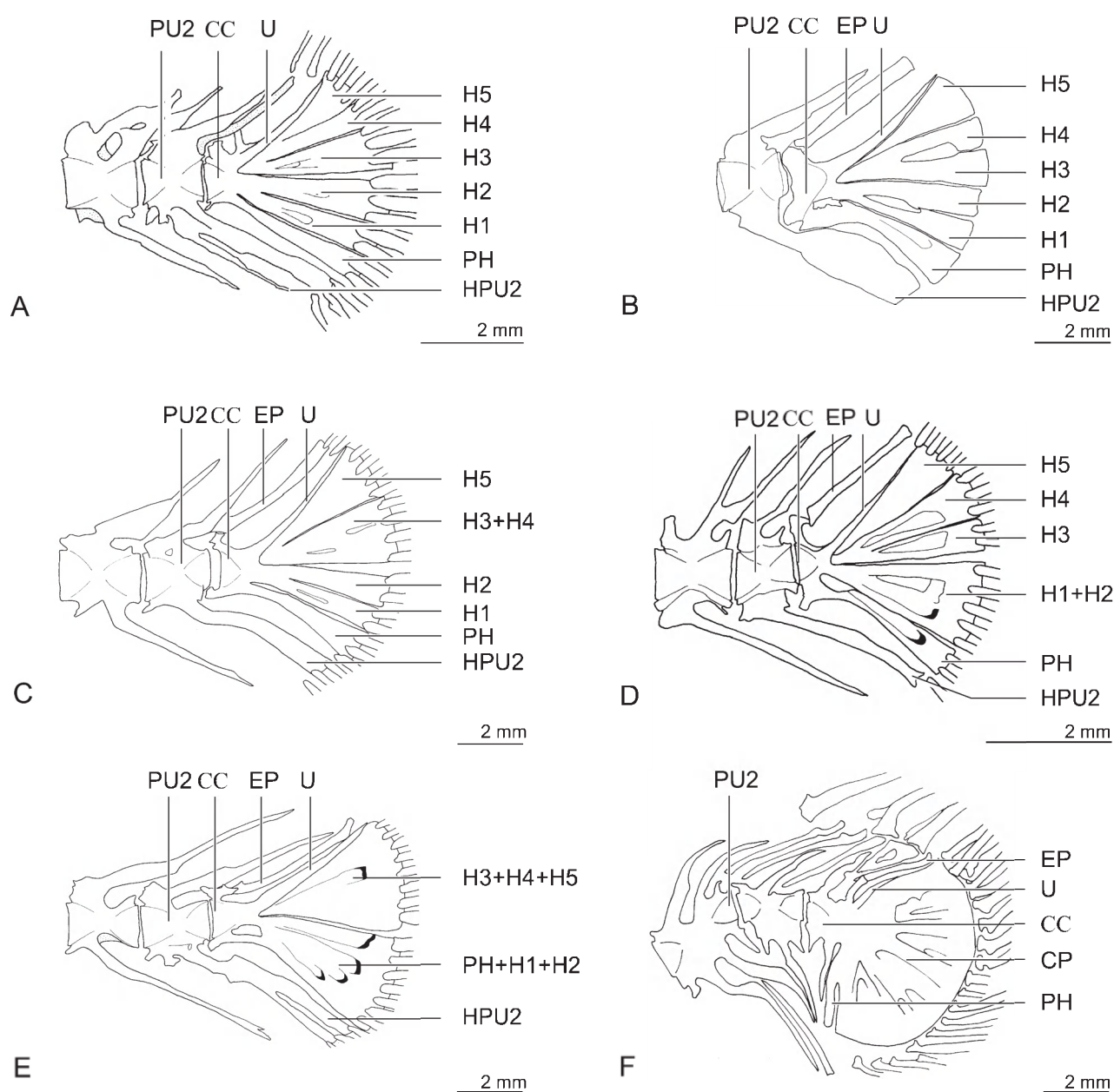


Fig. V.1- 3: Morphological variation in the caudal skeleton of *Channallabes apus*: **A:** The unfused configuration: 5 separate H and a separate PH, no EP is present; the left as well as the right neural arch of PU2 each bear a neural spine; **B:** partial fusions of H1 and H2 and H3 and H4, the EP is supported by the right half of the neural arch of CC; **C:** H3 and H4 are fused; the EP is fused with the neural spine of PU2; **D:** H1 and H2 are fused; the neural spine of PU3 is branched; **E:** PH and H1 and H2 are fused, forming a ventral plate; H3, H4 and H5 are fused forming a dorsal plate; **F:** the PH and H1-H5 are fused forming one caudal plate.

Fig. V.1- 4

*Channallabes apus*

H, hypural

PH, parhypural

EP, epural

CC, compound centrum

U, urostyl

PU, preural centrum

HPU, hemal spine of the preural centrum

NPU, neural spine of the preural centrum

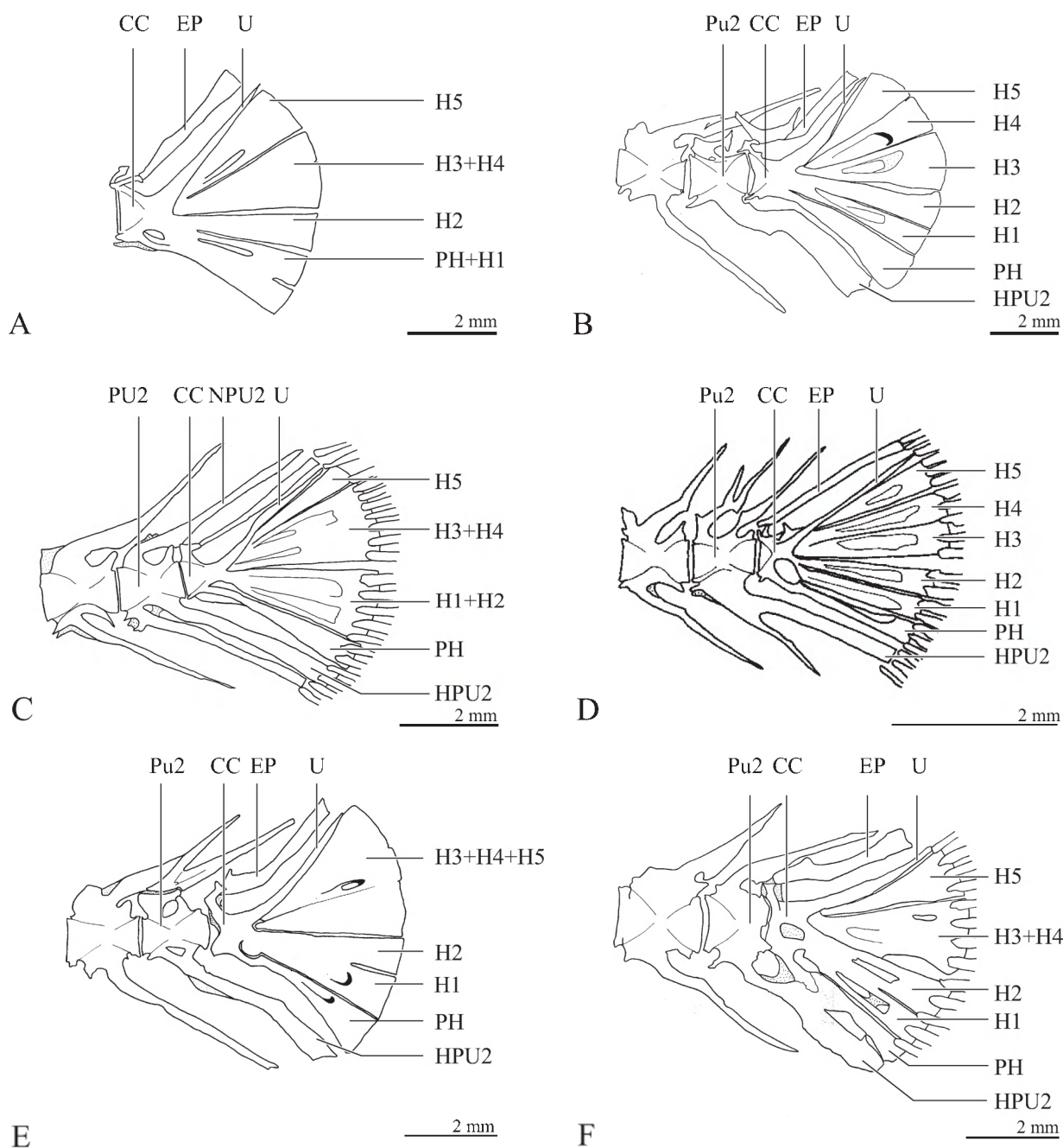


Fig. V.1- 4: Morphological variation in the caudal skeleton of *Channallabes apus*: A: The unfused configuration: H1-H5 are separated and a separate PH, no EP is present; the left as well as the right neural arch of PU2 each bear a neural spine; B: partial fusions of H1 and H2 and H3 and H4, the EP is supported by the right half of the neural arch of the CC; C: H3 and H4 are fused; the EP is fused with the neural spine of the PU2; D: H1 and H2 are fused; the neural spine of the PU3 is branched; E: the PH and H1 and H2 are fused, forming a ventral plate; H3, H4 and H5 are fused forming a dorsal plate; F: the PH and H1-H5 are fused forming one caudal plate.

Fig. V.1- 5

*Heteropneustes fossilis*

PH, parhypural

EP, epural

CC, compound centrum

Fig. V.1- 6

SL, standard length

ABD, abdominal body depth

Dm, *Dolichallabes microphthalmus*

Pt, *Platyallabes tihoni*

Ca, *Channallabes apus*

Pm, *Platyclarias machadoi*

Gt, *Gymnallabes typus*

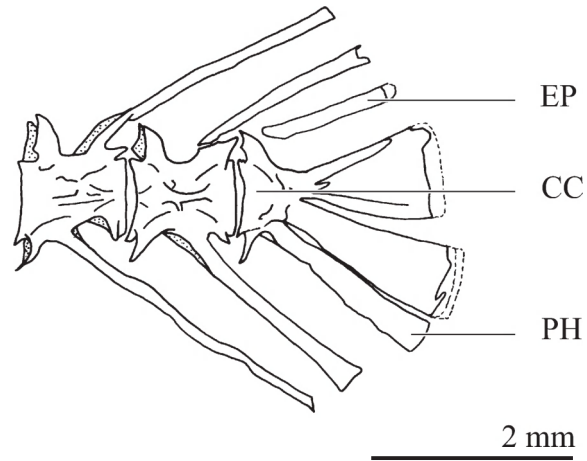


Fig. V.1- 5: The caudal skeleton of *Heteropneustes fossilis*.

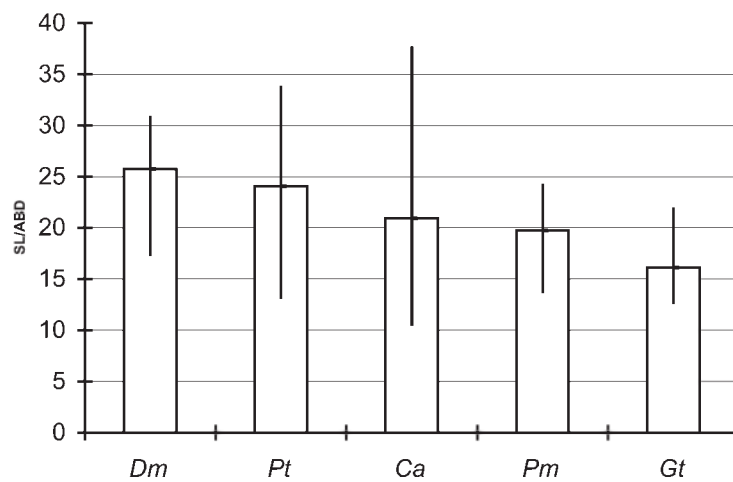


Fig. V.1- 6: A graphic representation of the degree of anguilliformity (SL/ABD). The average, maximum and minimum of the ratio is shown for each species.

Fig. V.1- 7

- A, *Anguilla rostrata*
- B, *Moringua edwardsi*
- C, *Assurger anzac*
- D, *Neconger vermiformis*
- E, *Hypoptychus dybowski*
- F, *Tripterion atriceps*
- G, *Pythonichthys sp.*

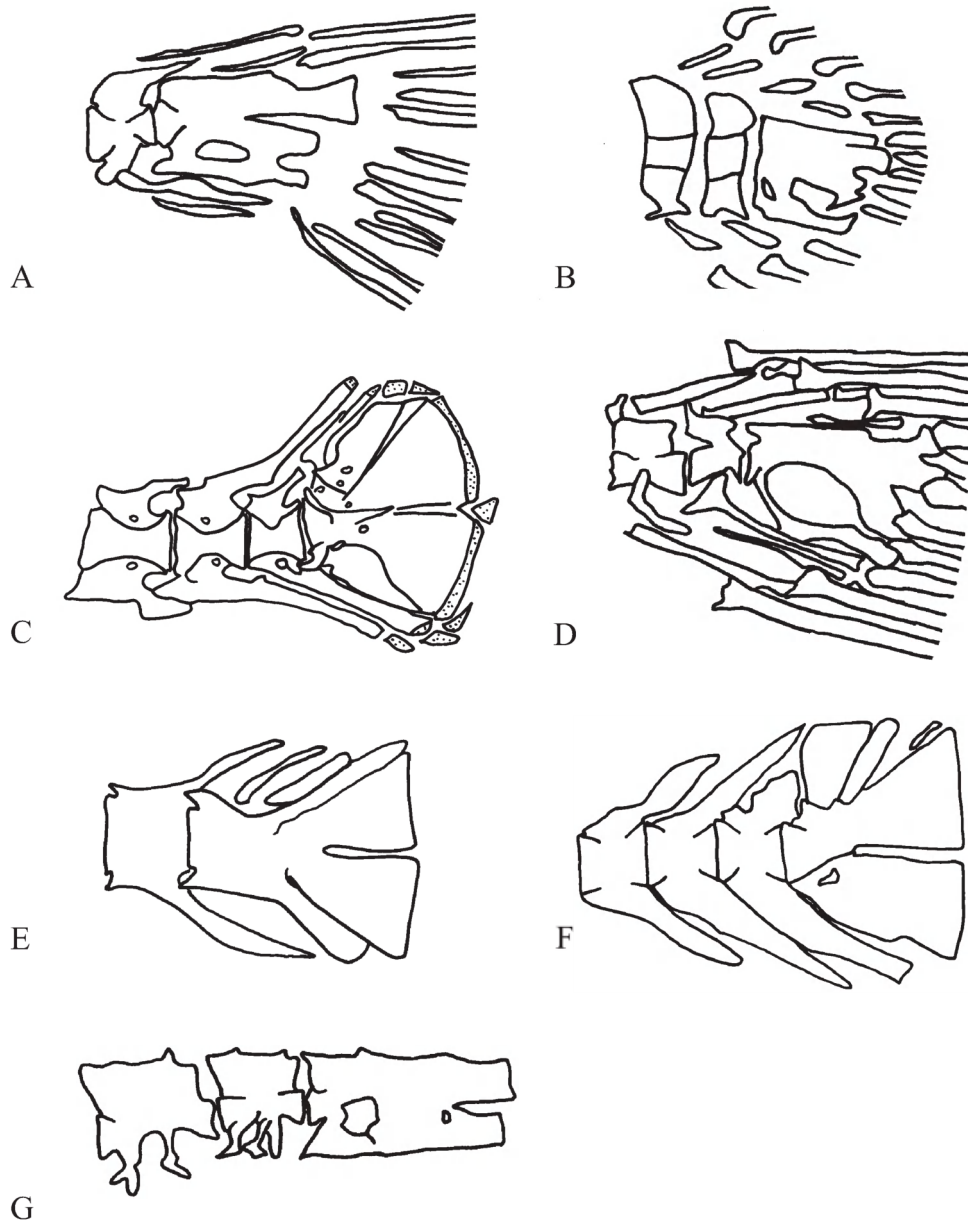


Fig. V.1- 7: Lateral view of the caudal skeleton of A: *Anguilla rostrata* (Anguillidae) (modified after Smith & Castle, 1972); B: *Moringua edwardsi* (Moringuidae) (modified after Smith & Castle, 1972); C: *Assurger anzac* (Trichiuridae) (modified after Gago, 1998); D: *Neoconger vermiformis* (Moringuidae) (modified after Smith & Castle, 1972); E: *Hypoptychus dybowskii* (Hypoptychidae) (modified after Gosline, 1963); F: *Tripterion atriceps* (Tripterygiidae) (modified after Gosline, 1963); G: *Pythonichthys* sp. (Heterenchelyidae) (modified after Smith & Castle, 1972).

Fig. V.2- 1

A, *Clarias gariepinus*

B, *Clarias gariepinus*

C, *Channallabes apus*

EPAX, epaxials

FD, flexor dorsalis

FDS, Flexor dorsalis superior

FV, flexor ventralis

FVI, flexor ventralis inferior

HL, hypochordal longitudinalis

HYP, hypaxials

ICAR P, infracarinalis posterior

PU, preural centrum

SCAR P, supracarinalis posterior



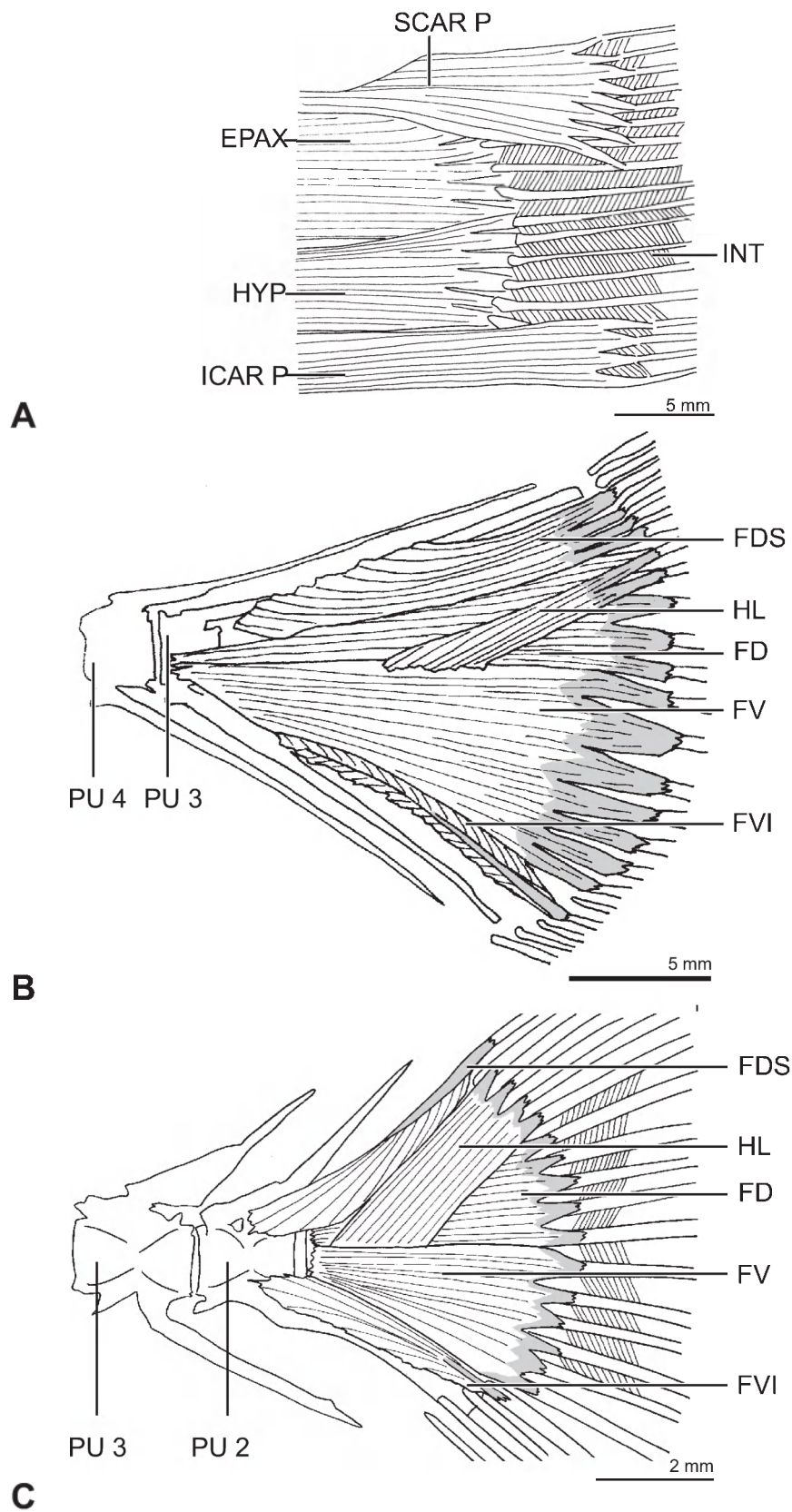


Fig. V.2- 1: The musculature of the caudal fin. **A:** The skin of the tail of *Clarias gariepinus* is removed. **B:** The supracarinal muscles, epaxials and hypaxials of the tail of *Clarias gariepinus* are removed. **C:** The epaxial and hypaxial muscles of *Channallabes apus* are removed. Supracarinalis muscles are absent.

Fig. VI.1.1- 1

A, *Mastacembelus sinensis*

B, *Pillaia*

C, *Chaudhuria*

D, unresolved polytomy, assemblage of 6 species

*Mastacembelus armatus*, *M. erythrotaenia*, ***M. mastacembelus***, *M. oatesii*, *M. unicolor*, *M. aiboguttatus*

E, unresolved polytomy, assemblage of 6 species

*M. guentheri*, *M. keithi*, *M. perakensis*, *M. circumcinctus*, *M. caudicellatus*, *M. maculates*

F-J, nested series of synapomorphic characters,

F, *M. zebrinus*

G, *M. pancalus*

H, *M. aculeatus*

I, *M. aral*

J, *M. siamensis*

K, unresolved polytomy, assemblage of 16 species

*M. albomaculatus*, *M. cunningtoni*, *M. ellipsifer*, *M. flavidus*, *M. frenatus*, *M. micropectus*, *M. moorii*,  
*M. ophidium*, *M. plagiostomus*, *M. platysoma*, *M. tanganicae*, *M. zebratus*, *M. congicus*, *M. shiranus*,  
*M. stappersii*, *M. vanderwaali*

L, unresolved polytomy, assemblage of 15 species

*M. batesii*, *M. brevicauda*, *M. flavomarginatus*, *M. goro*, *M. greshoffi*, *M. liberiensis*, *M. loennbergii*,  
*M. longicauda*, ***M. marchii***, *M. marmoratus*, *M. niger*, *M. nigromarginatus*, *M. reticulatus*, *M. sclateri*, *M. ubangensis*

M, *M. paucispinus*

N, the undescribed species

O, *M. brachyrhinus*

P, ***M. brichardi*** ; Q, *M. latens* ; R, *M. crassus* ; S, *M. aviceps*

59, (numbers according to those used by Travers, 1984b) synapomorphic character state for Mastacembelinae (Oriental); 4 separate, autogenous hypurals

91, Hypural plates, generally 2, tendency for parhypural fusion to ventral edge of lower plate, 8-10 principal fin rays and confluent caudal fin

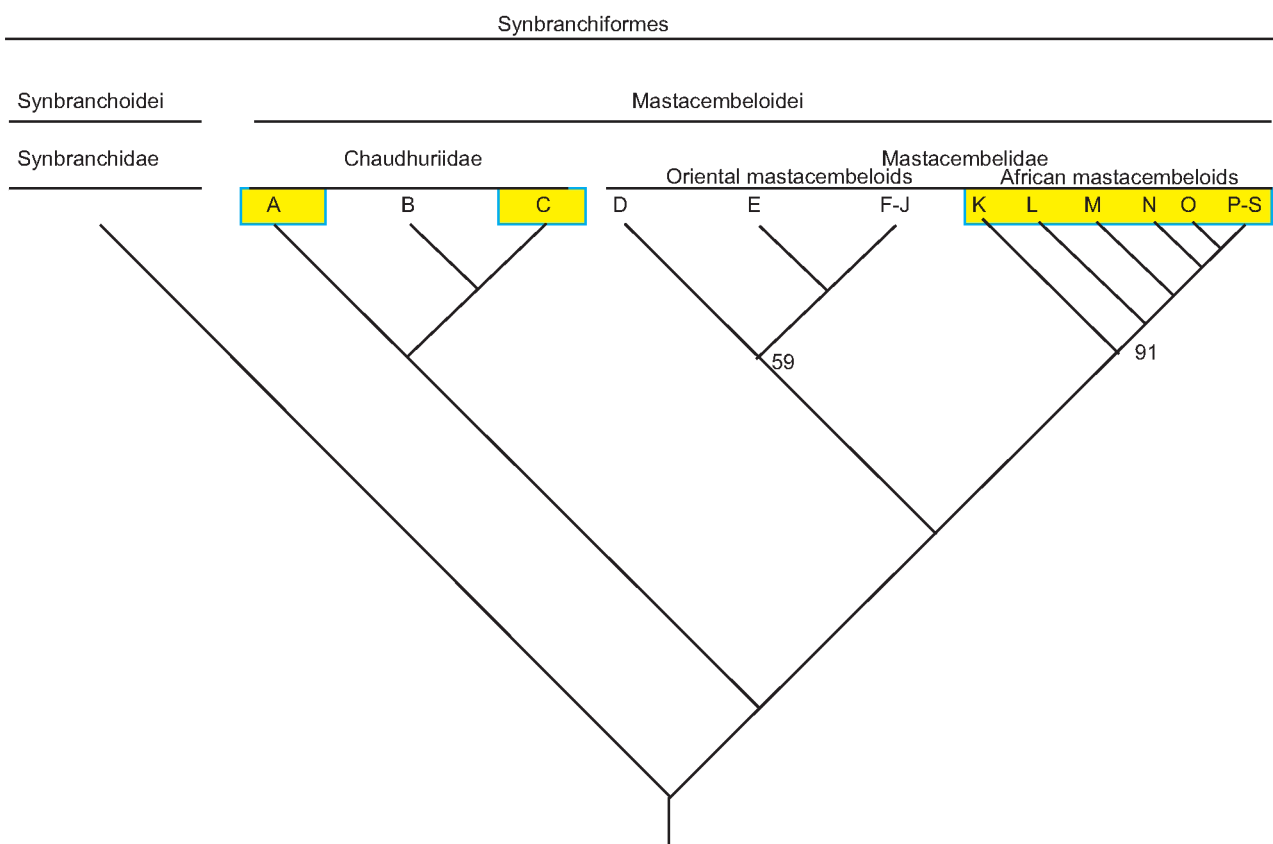


Fig. VI.1.1- 1: Phylogeny of the Mastacembeloidei after Travers 1984b. Lineages convergent in body elongation, fused hypurals and lower number of caudal fin rays are indicated in orange.

Fig. VI.1.1- 2

*Mastacembelus marcheii*

A1, A2, A3, Aw, subdivisions of the adductor mandibulae complex  
AAP, adductor arcus palatini  
AH, adductor hyomandibulae  
AO, adductor operculi  
Br R, branchiostegal rays  
D, dentary  
DO, dilatator operculi  
EcPt, ectopterygoid  
EnPt, endopterygoid  
HH Ab, hyohyoideus abductor  
HH Ad, hyohyoidei adductores  
Hm, hyomandibula  
INT, intermandibularis  
IntO, intraoperculi  
IOp, interopercle  
IOrb1, first infraorbital  
LAP, levator arcus palatini  
LO, levator operculi  
MtPt, metapterygoid  
Mx, maxillary  
Nas, nasal  
Nc, neurocranium  
Op, opercle  
PAL, palatinum  
PH, protractor hyoidei  
POp, preopercle  
Pr BSph, basisphenoidal process  
Q, quadrate  
SOp, subopercle  
Sym, symplecticum  
T A1, A2, A3 tendon of subdivisions of the adductor mandibulae complex

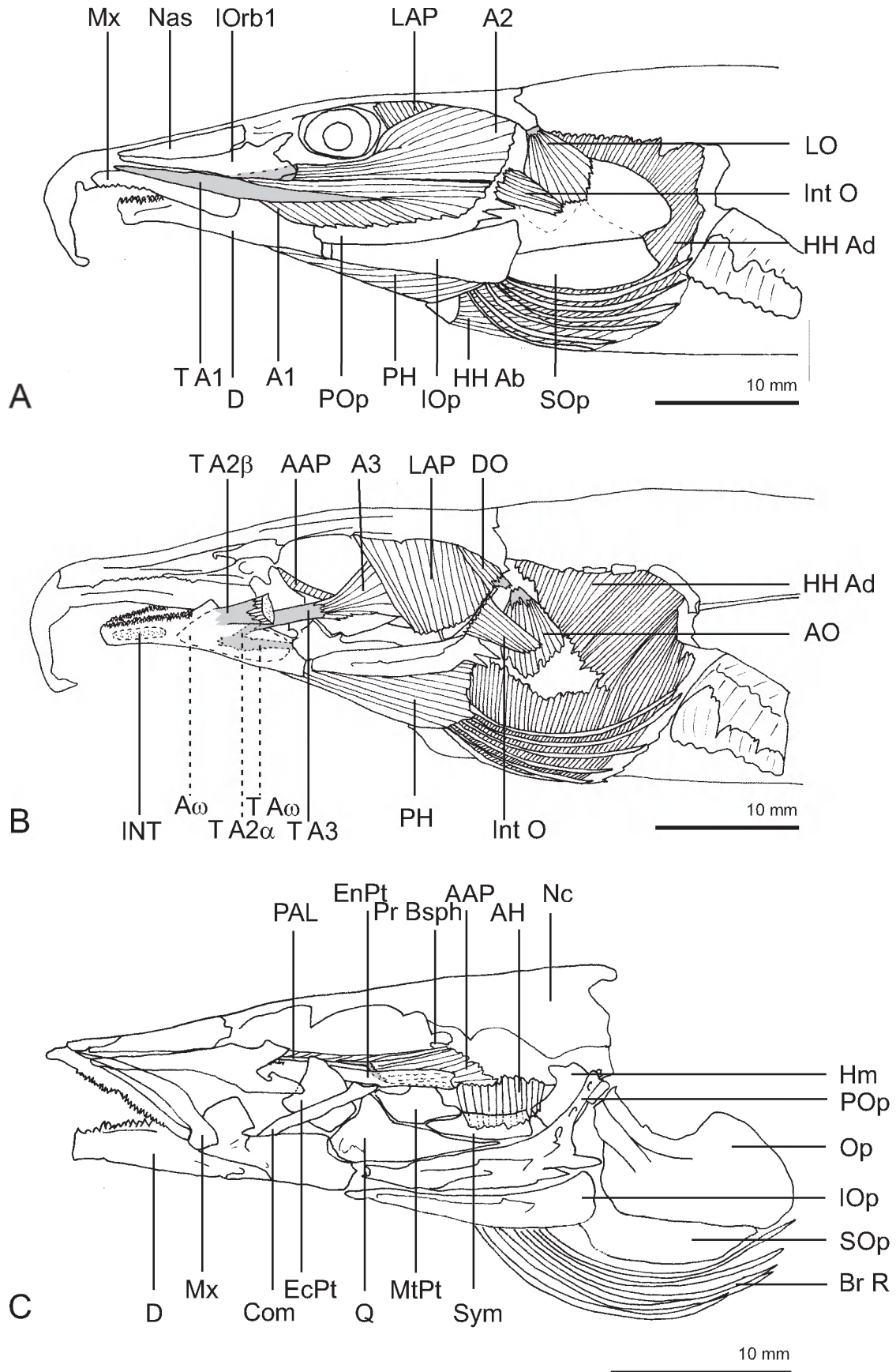


Fig. VI.1.1- 2: Cranial musculature of *Mastacembelus marcheii*. A: Skin is removed. B: Subdivision A1 and A2, opercle, levator operculi are removed. C: Most cranial muscles are removed, except the adductor arcus palatini and adductor hyomandibulae..

Fig. VI.1.1- 3

*Mastacembelus marcheii*

A1, subdivision of the adductor mandibulae complex

CH, ceratohyal

HH Ab, hyohyoideus abductor

HH Ad, hyohyoidei adductores

IOp, interopercle

PH, protractor hyoidei

SH, sternohyoideus

SOp, subopercle

T PH A, anterior tendon of protractor hyoidei

T SH, tendon of sternohyoideus

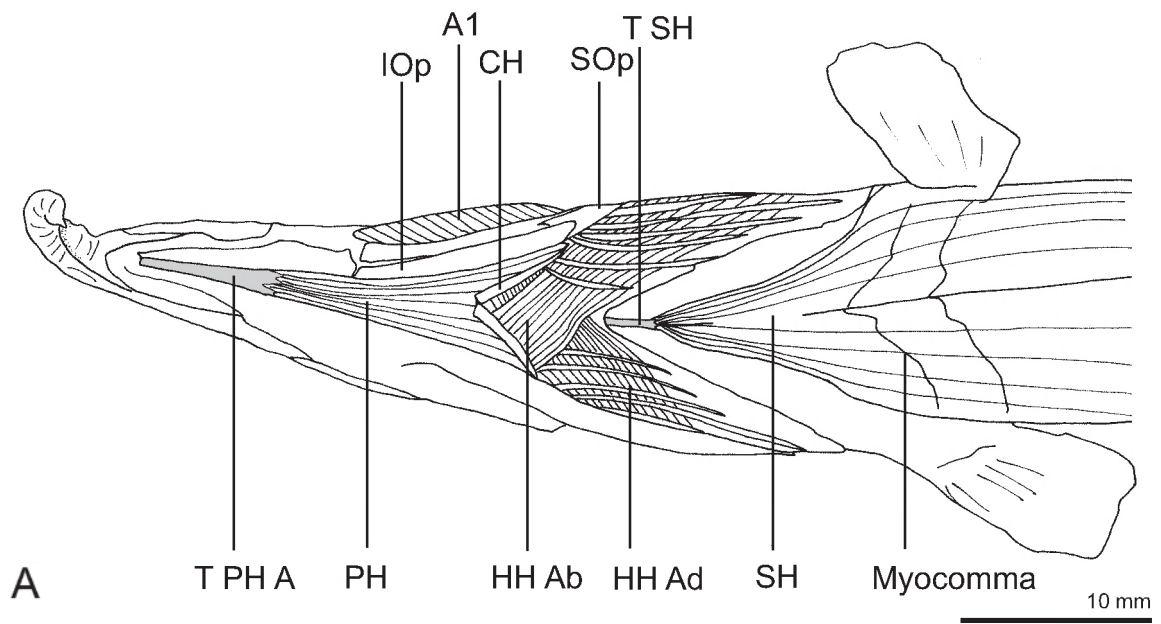


Fig. VI.1.1- 3: Cranial musculature in ventral view of *Mastacembelus marcheii*.

Fig. VI.1.1- 4

*Mastacembelus brichardi*

A1, A2, A3, Aw, subdivisions of the adductor mandibulae complex

D, dentary

HH Ab, hyohyoideus abductor

HH Ad, hyohyoidei adductores

IntO, intraoperculi

IOP, interopercle

IOrb1, first infraorbital

LAP, levator arcus palatini

LO, levator operculi

Mx, maxillary

Nas, nasal

PH, protractor hyoidei

POp, preopercle

SOP, subopercle

T A1, A2, A3 tendon of subdivisions of the adductor mandibulae complex



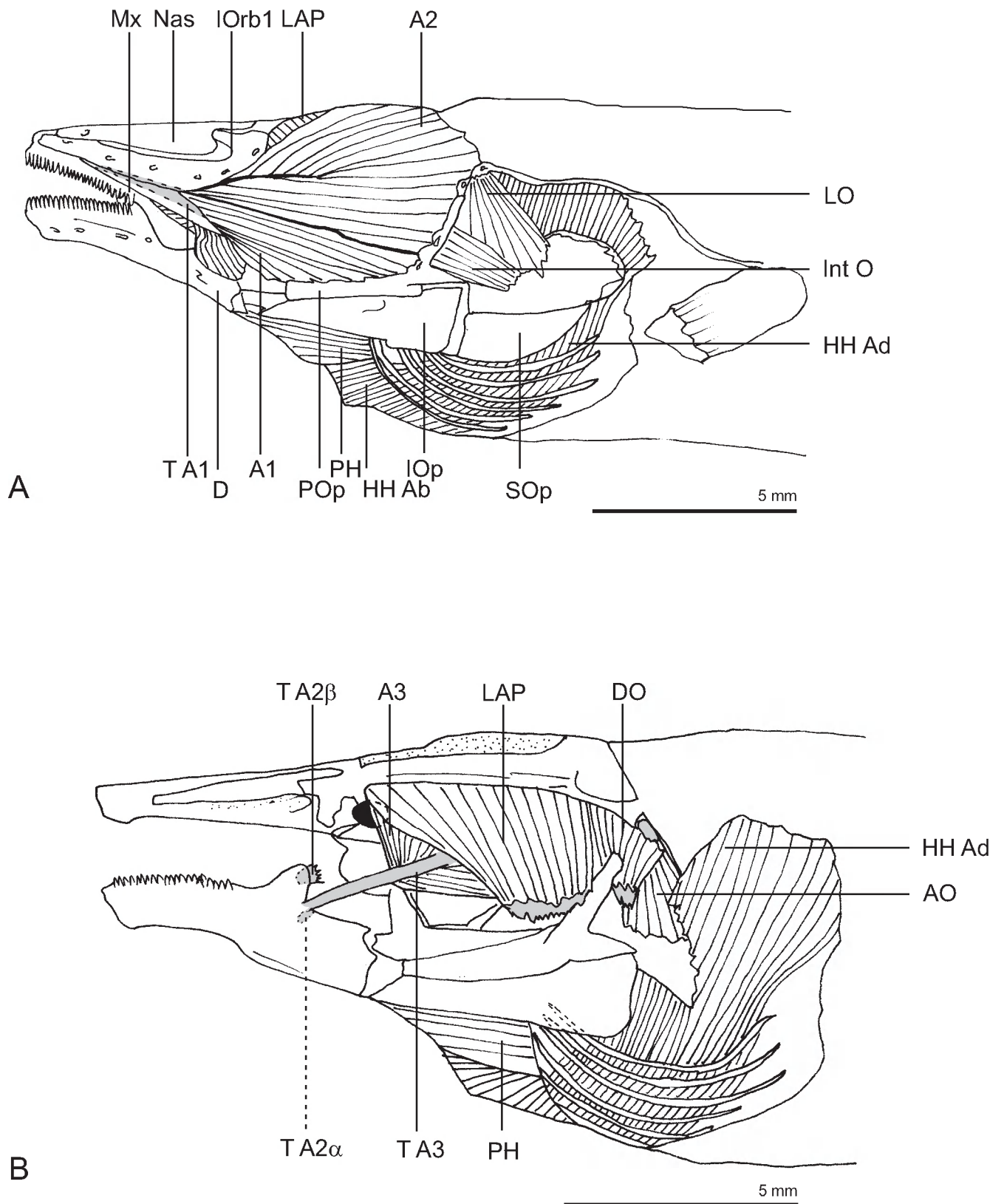


Fig. VI.1.1- 4: Cranial musculature of *Mastacembelus brichardi*. A: Skin is removed. B: Subdivision A1 and A2, opercle, levator operculi are removed.

Fig. VI.1.1- 5

A, *Mastacembelus mastacembelus*

B, *Mastacembelus marchei*

C, *Mastacembelus brichardi*

LO, levator operculi

A1, A2, subdivisions of the adductor mandibulae complex

IntO, interopercularis

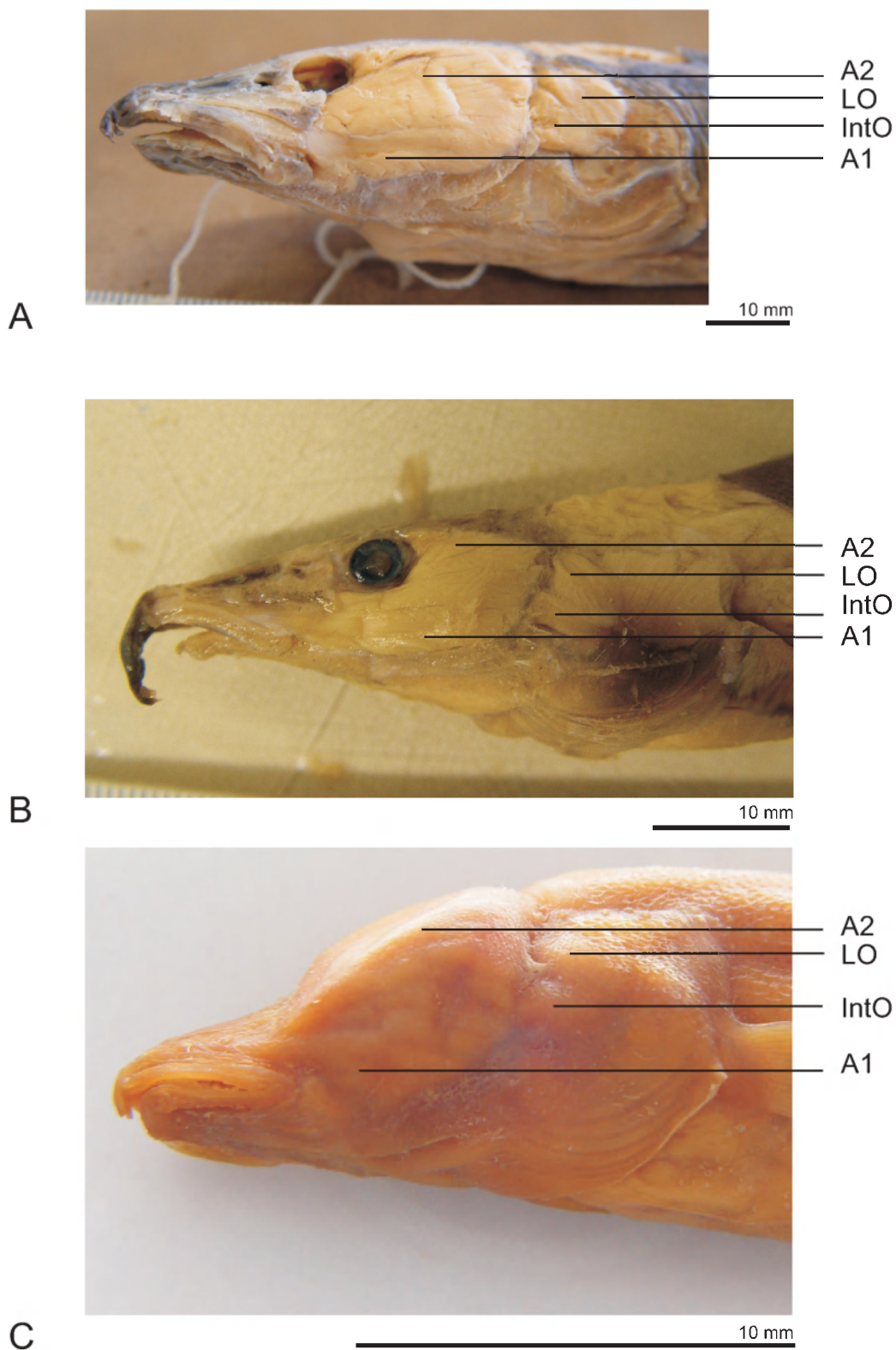


Fig. VI.1.1- 5: Photo illustration of the cranial musculature. The skin removed in A and B. **A:** *Mastacembelus mastacembelus* with moderate to large jaw muscles. **B:** *Mastacembelus marcheji*, with small jaw muscles. **C:** *Mastacembelus brichardi*, with extremely enlarged jaw muscles.

Fig. VI.1.2- 1

A, *Mastacembelus mastacembelus*

B, *Mastacembelus marcheii*

C, *Mastacembelus brichard*

D fin, dorsal fin

A fin, anal fin

C fin, caudal fin

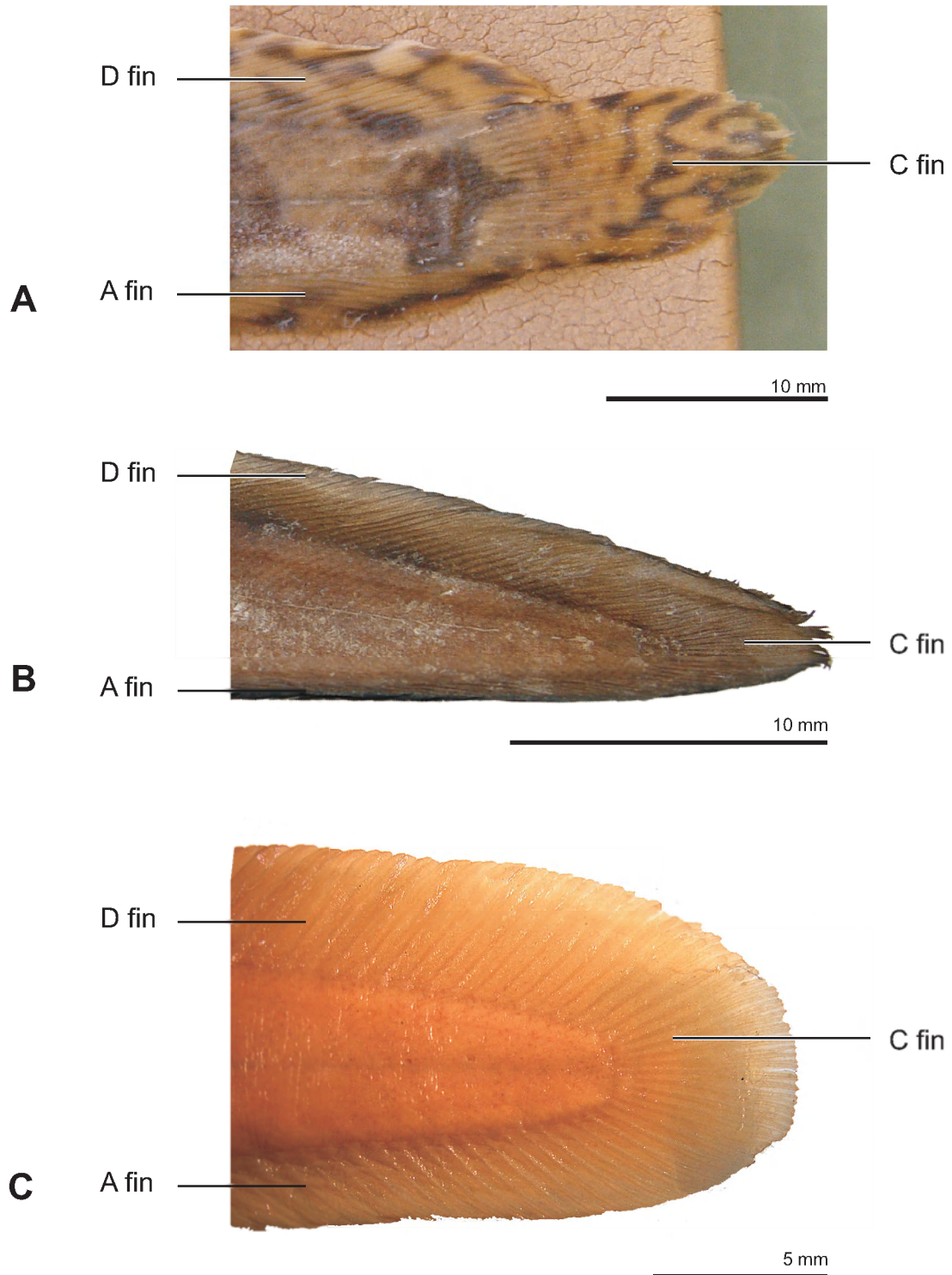


Fig. VI.1.2- 1: Photo illustration of the external morphology of the tail. A: *Mastacembelus mastacembelus*, B: *Mastacembelus marcheii*, C: *Mastacembelus brichardi*.

Fig. VI.1.2- 2

*Mastacembelus mastacembelus*

HL, hypochordal longitudinalis  
Epax, epaxials  
Hyp, hypaxials  
SCar P, supracarinalis posterior  
ICar P, infracarinalis posterior  
INT, interradians  
FV, flexor ventralis  
FD, flexor dorsalis  
FVI, flexor ventralis inferior  
FVE, flexor ventralis externus  
FDS, flexor dorsalis superior  
PU3, third preural vertebra

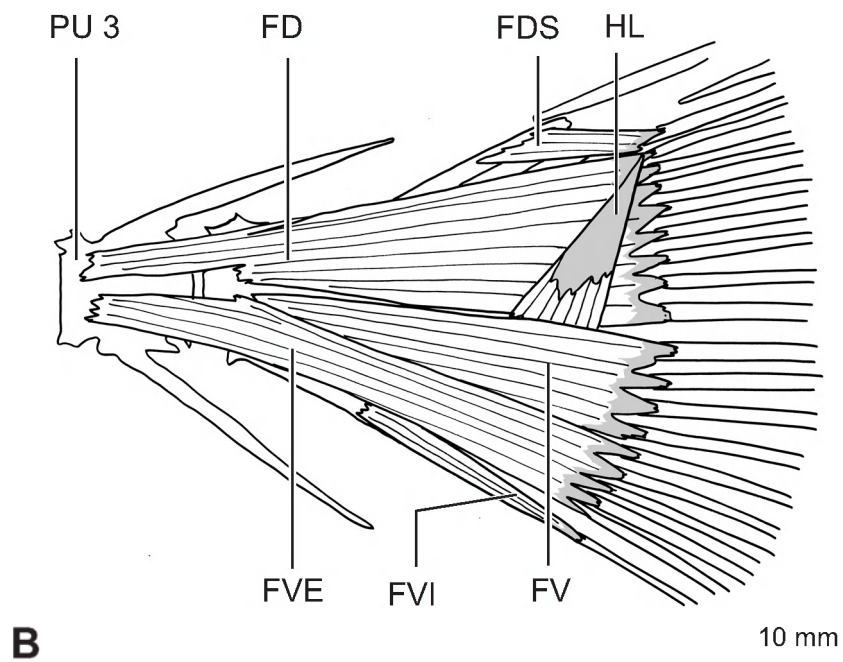
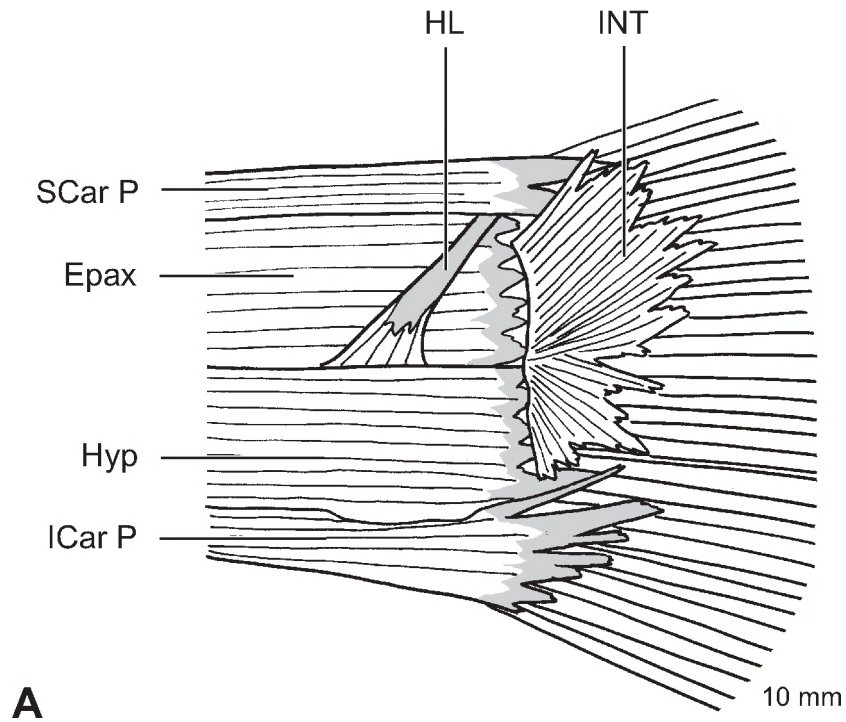


Fig. VI.1.2- 2: The caudal fin musculature of the Oriental species *Mastacembelus mastacembelus*. A: skin is removed. B: body musculature, carinalis muscles and interradians are removed, exposing the caudal fin musculature.

Fig. VI.1.2- 3

**A**, *Mastacembelus marcheii*  
**B**, *Mastacembelus brichardi*

INT, interradials

FV, flexor ventralis

FD, flexor dorsalis

FVI, flexor ventralis inferior

FVE, flexor ventralis externus

FDS, flexor dorsalis superior

PU3, third preural vertebra

HL, hypochordal longitudinalis



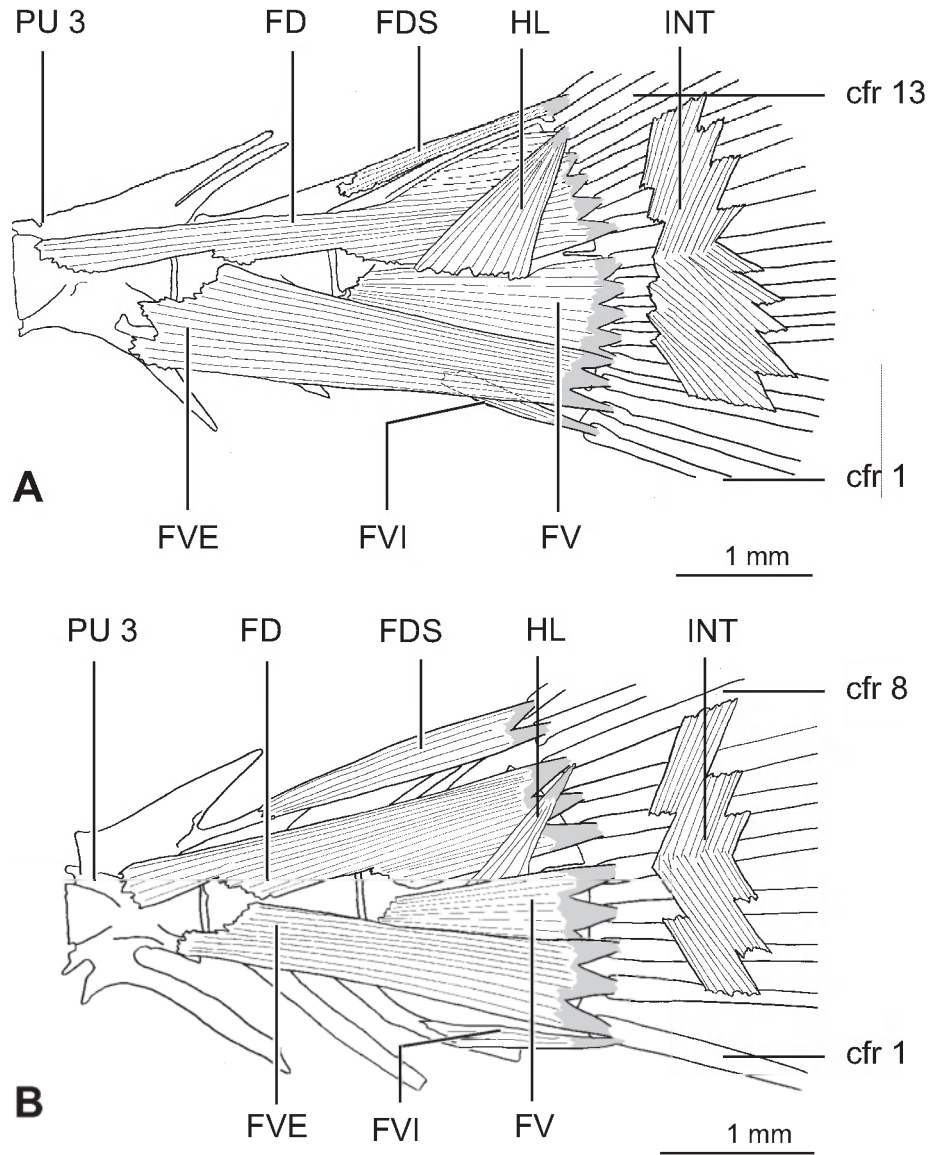


Fig. VI.1.2- 3: The caudal fin musculature of the African species. Skin and body musculature are removed.  
**A:** *Mastacembelus marchei*. **B:** *Mastacembelus brichardi*.

Fig. VI.2- 1

*Aphanopus carbo*

$L_{in}$  = input-lever

$\beta$  = angle between the lower jaw length axis and the input-lever,

$\sigma$  = angle between the input-lever and the line of action of the jaw muscle,

$\theta$  = average angle of pennation.

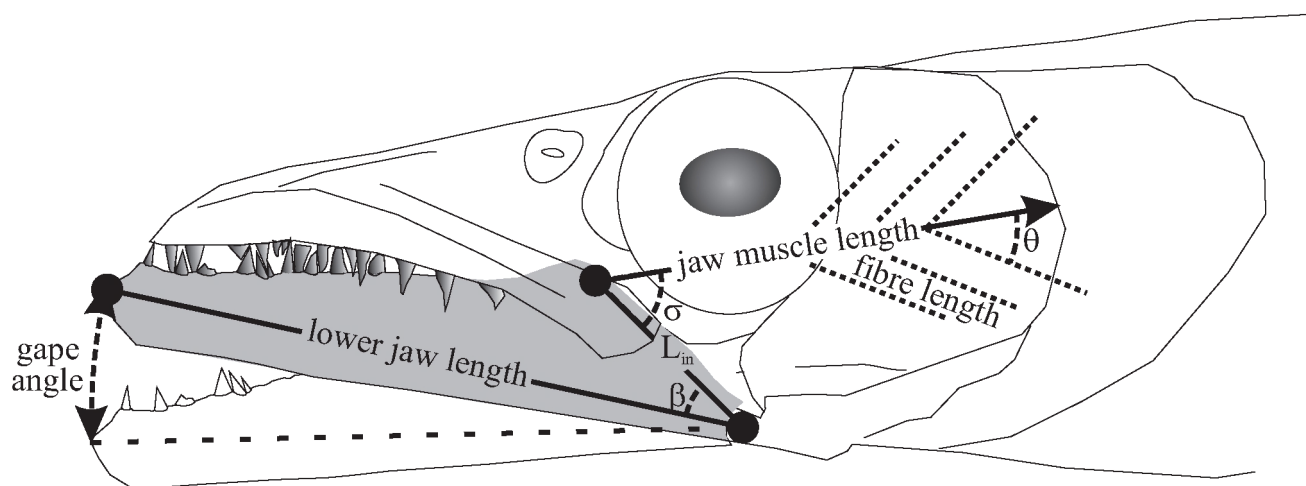


Fig. VI.2- 1 Schematic representation of the variables of the lower jaw lever system used for model calculations of bite force and mouth closing movements.  $\theta$  = angle between the lower jaw length axis and the input-lever ( $L_{in}$ ),  $\theta$  = angle between the input-lever ( $L_{in}$ ) and the line of action of the jaw muscle,  $\theta$  = average angle of pennation.

Fig. VI.2- 2

A, *Aphanopus carbo*  
B, *Trichiurus lepturus*

A1, A2, subdivisions of the adductor mandibulae complex

Epax, epaxials

L Prim, primordial ligament

Pr C Op, caudal opercular process

Pr D Op, dorsal opercular process

Scar A, supracarinalis anterior

T Mx, tendon of subdivision of adductor mandibulae inserting on the maxillary

T sh, tendinous sheet

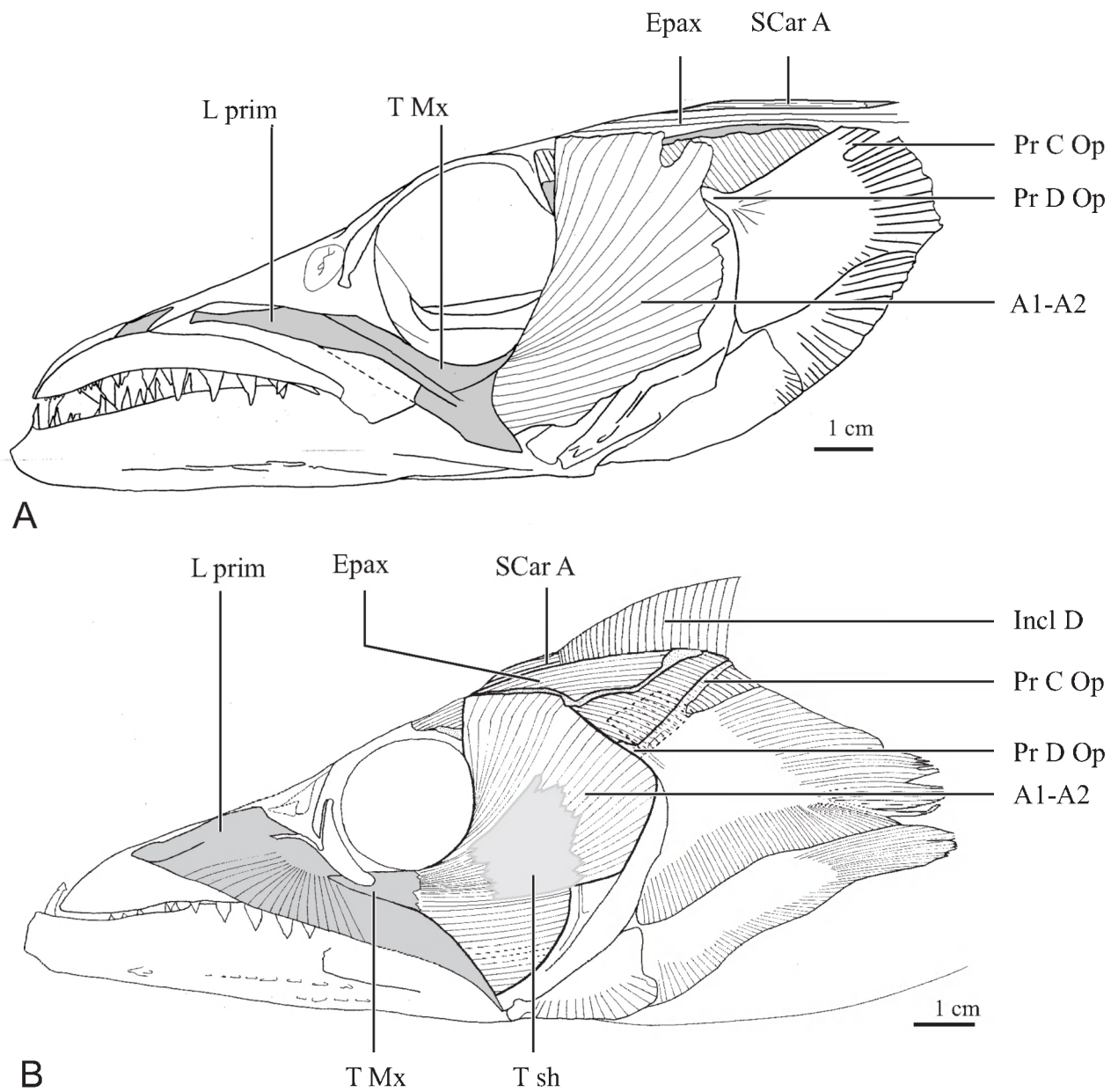


Fig. VI.2- 2: Lateral view of the cranial muscles of A: *Aphanopus carbo* and B: *Trichiurus lepturus*. Skin is removed. Dotted lines indicate parts of structures being covered by other elements. Tendons are illustrated in grey.

Fig. VI.2- 3

**A**, *Aphanopus carbo*  
**B**, *Trichiurus lepturus*

A3, subdivision of the adductor mandibulae complex

AAP, adductor arcus palatini

AO, adductor operculi

DO D, dorsal part of the dilatator operculi

DO V, ventral part of the dilatator operculi

LAP, levator arcus palatini

LO, levator operculi

r Hm, hyomandibular ridge

T DO, tendon of the dilatator operculi

T LAP, tendon of levator arcus palatine

T LO, tendon of levator operculi

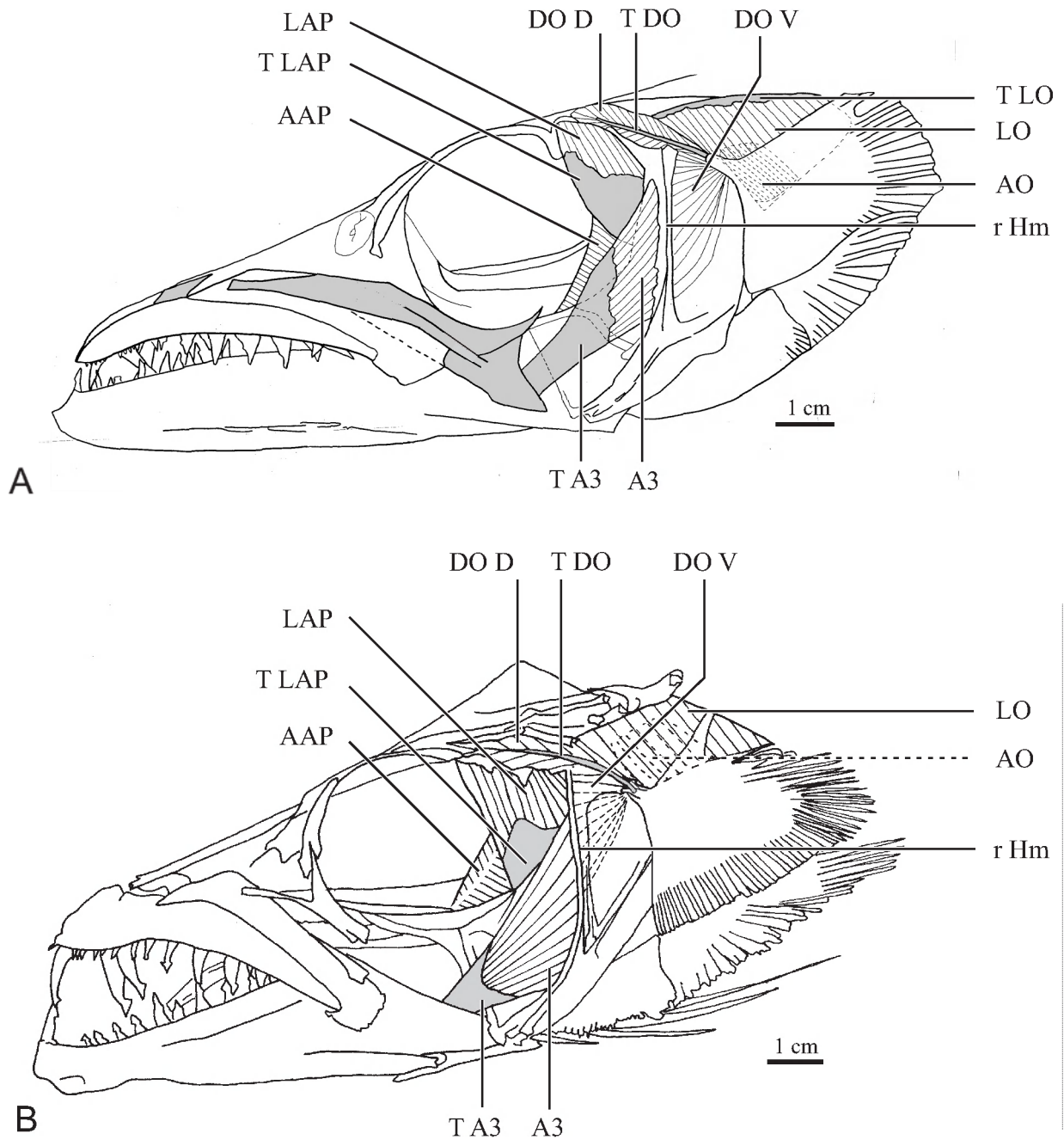


Fig. VI.2- 3: Lateral view of the cranial muscles of A: *Aphanopus carbo* and B: *Trichiurus lepturus*. A1-A2 of the adductor mandibulae complex is removed. Dotted lines indicate parts of structures being covered by other elements. Tendons are illustrated in grey.

Fig. VI.2- 4

**A**, *Aphanopus carbo*  
**B**, *Trichiurus lepturus*

A1, A2, A3, A $\infty$  subdivisions of the adductor mandibulae complex  
Int, intermandibularis

T A1, A2, A3, A $\infty$ , subdivisions of the adductor mandibulae complex

T A $\infty$ -IOp, tendon between A $\infty$  and interopercle

T A $\infty$ -Q, tendon between A $\infty$  and quadrate

T Mx, tendon of subdivision of adductor mandibulae inserting on the maxillary



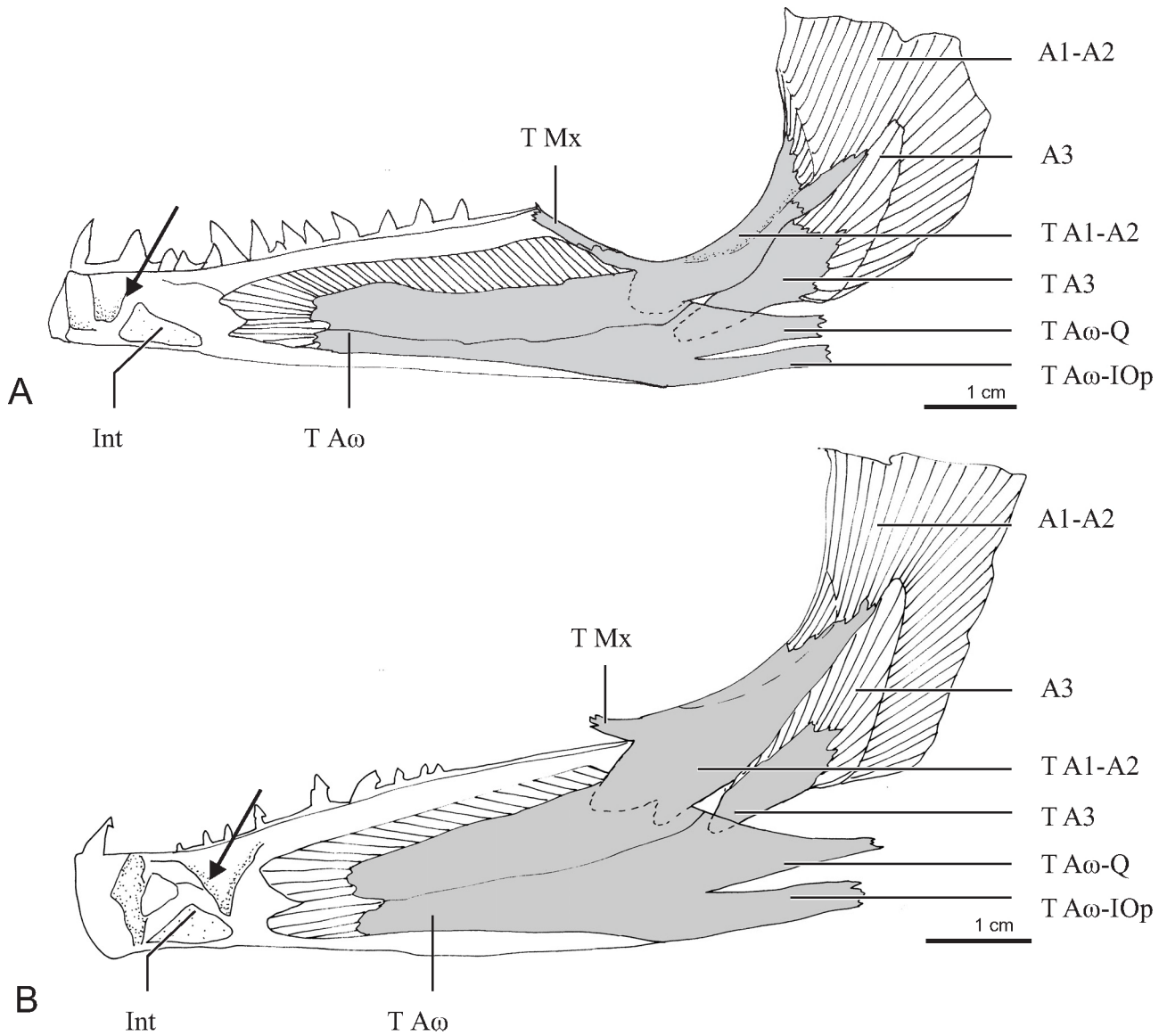


Fig. VI.2- 4: Medial view of lower jaw and adductor mandibulae complex of A: *Aphanopus carbo* and B: *Trichiurus lepturus*. Arrows indicate space in lower jaw in which fangs of upper jaw fit.

Fig. VI.2- 5

A, *Aphanopus carbo*  
B, *Trichiurus lepturus*

BH, basihyal  
CH A, anterior ceratohyal  
CH P, posterior ceratohyal  
D HH, dorsal hypohyal  
HH Ab, hyohyoideus abductor  
HH Ad, hyohyoidei adductores  
Int, intermandibularis  
PH $\alpha$ , PH $\beta$ , subdivisions of the protractor hyoidei  
R Br, branchiostegal rays  
T PH A, anterior tendon of protractor hyoidei  
T PH $\alpha$  P, posterior tendon of  $\alpha$  subdivision protractor hyoidei  
T PH $\beta$  P, posterior tendon of  $\beta$  subdivision protractor hyoidei

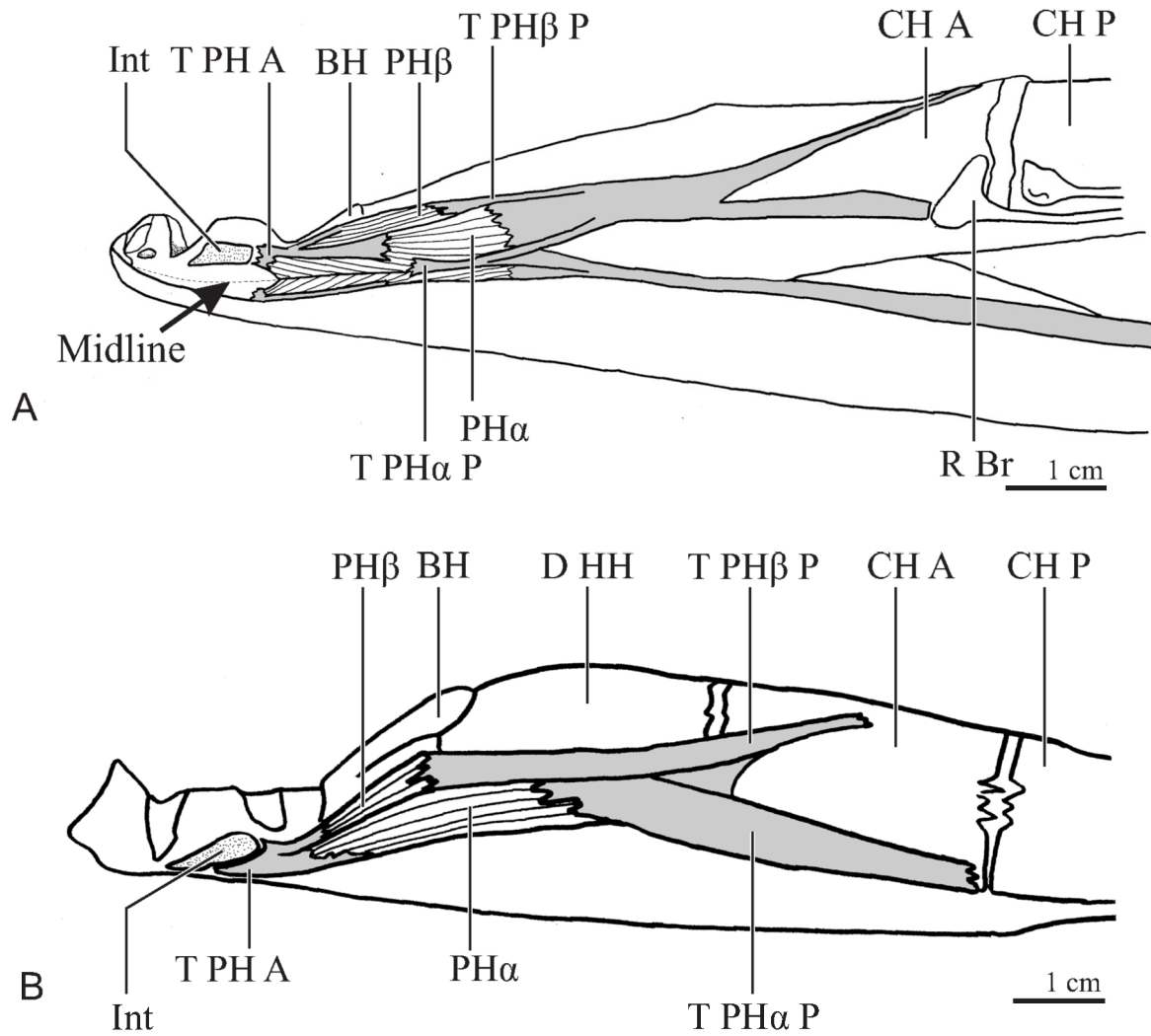


Fig. VI.2- 5: Lateral view of ventral muscles, antero-medial surface of lower jaw and medial surface of ceratohyals are visible, right lower jaw and right half of the hyoid arch are removed. A: *Aphanopus carbo*. Lower jaw is slightly turned over to the right, visualizing the ventral surface partially. Ventral midline is indicated by arrow. B: *Trichiurus lepturus*.

Fig. VI.2- 6

**A**, *Aphanopus carbo*  
**B**, *Trichiurus lepturus*

BH, basihyal  
CH A, anterior ceratohyal  
CH P, posterior ceratohyal  
D HH, dorsal hypohyal  
HH Ab, hyohyoideus abductor  
HH Ad, hyohyoidei adductores  
L BH-HH, basiho-hypohyal ligament  
L UH-HH, uroho-hypohyal ligament  
R Br, branchiostegal rays  
T HH Ab A, anterior tendon of hyohyoideus abductor  
T HH Ab P, posterior tendon of hyohyoideus abductor  
UH, urohyal  
V HH, ventral hyohyal

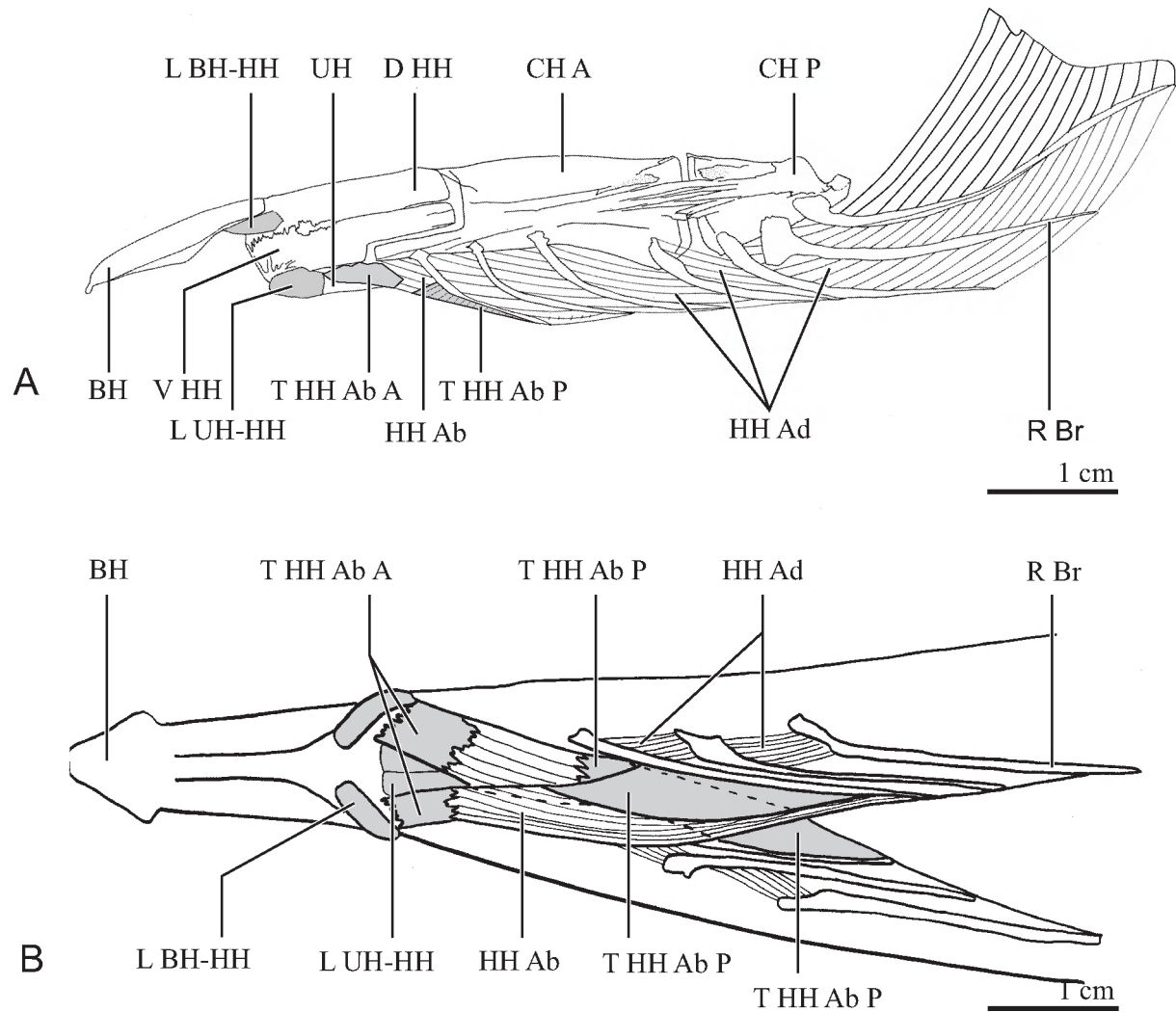


Fig. VI.2- 6: Hyohyoideus muscle complex. A: Lateral view of hyohyoideus muscles in *Aphanopus carbo*; B: Ventral view of hyohyoideus muscles in *Trichiurus lepturus*. Only the anterior bundles of the hyohyoidei adductores are drawn, the posterior fibres also interconnect the successive branchiostegal rays and finally run to the medial side of the opercle as is the case in A. *Carbo*.

Fig. VI.2- 7

A, *Aphanopus carbo*  
B, *Trichiurus lepturus*

BH, basihyal  
Cl, cleithrum  
Fa, fascia  
GL, gill lamellae  
Hyp, hypaxials  
PhC E, pharyngoclavicularis externus  
PhC I, pharyngoclavicularis Internus  
SH, sternohyoideus  
T SB, sternobranchial tendon  
T SH, tendon of sternohyoideus  
UH, urohyal

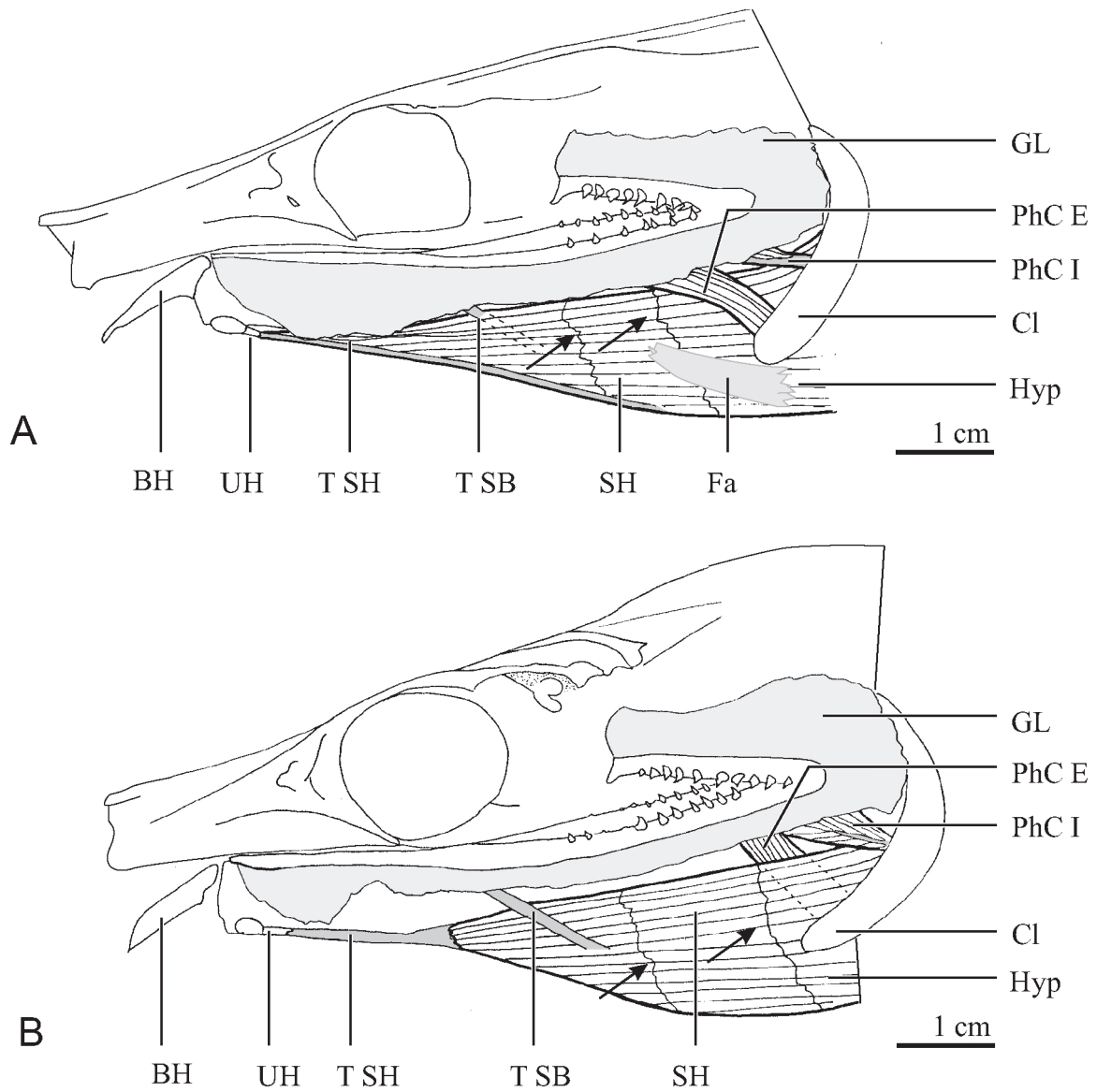


Fig. VI.2- 7: Lateral view of the sternohyoideus. Lower jaws, upper jaws and cranial muscles are removed, gill lamellae (pale grey) are partially cut and tendons are indicated in dark grey. Arrows show myocommata. A: *Aphanopus carbo*; B: *Trichiurus lepturus*.

Fig. VI.2- 8

*Aphanopus carbo*  
*Trichiurus lepturus*

Fig. VI.2- 9

*Aphanopus carbo*  
*Trichiurus lepturus*



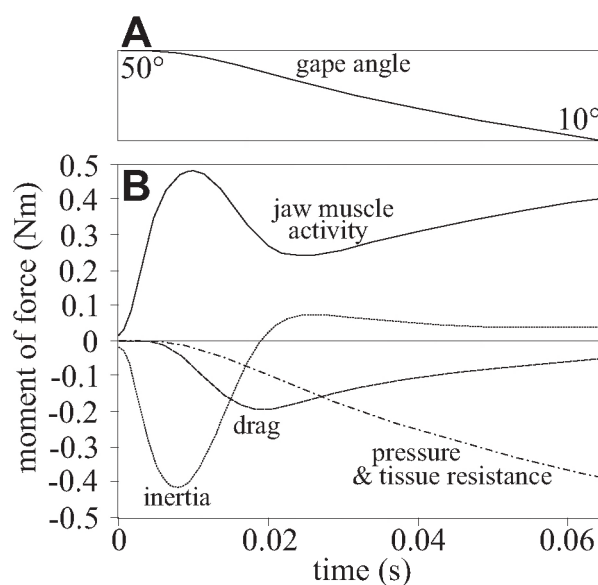


Fig. VI.2- 8 Model output of the moments of force (B) involved during a simulation of a mouth closure in *A. carbo* (cranial length of 160.6 mm) from a gape angle of 50° to 10° (A). Positive moments contribute to mouth closure, while negative moments work against mouth closure. The final lower jaw angle of 10° represents the moment of impact on a prey item. See text for further explanation.

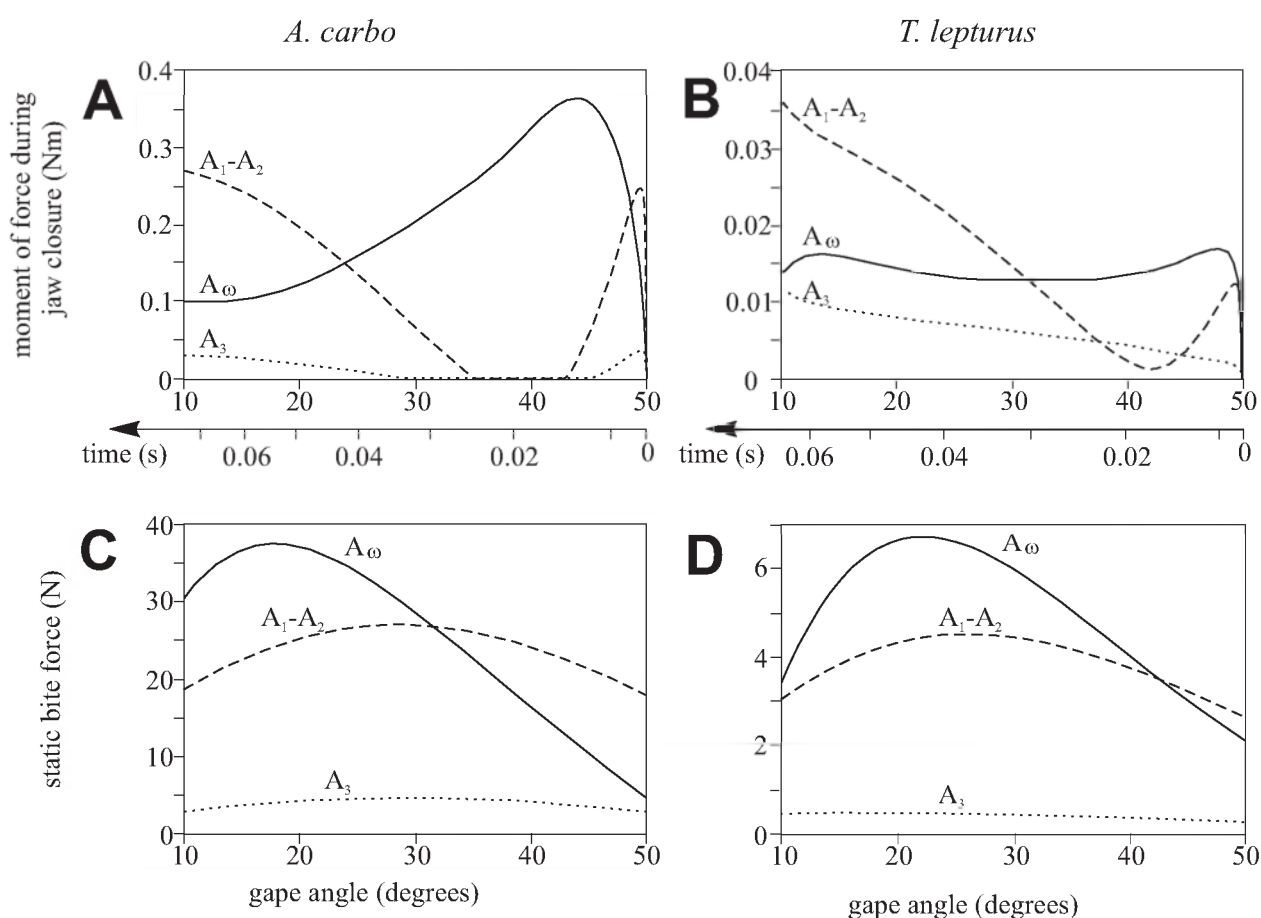


Fig. VI.2- 9 Model output of moment of force (A, B) during a lower jaw adduction from a gape angle of 50° to 10°, and maximal static bite force at the tip of (and perpendicular to) the lower jaw in function of gape angle (C, D) produced by each of the subdivisions of the adductor mandibulae complex ( $A_\omega$ ,  $A_1-A_2$ ,  $A_3$ ). Note that the higher moments and forces generated by *A. carbo* (left) with respect to *T. lepturus* (right) are partly due to its larger size (cranial lengths of 160.6 mm vs. 100.3 for *T. lepturus*), and partly because of the relatively larger cross-sectional area of the jaw muscles (Table VI.2- 2). Further information is given in the text.

Fig. VI.2- 10

*Aphanopus carbo*  
*Trichiurus lepturus*

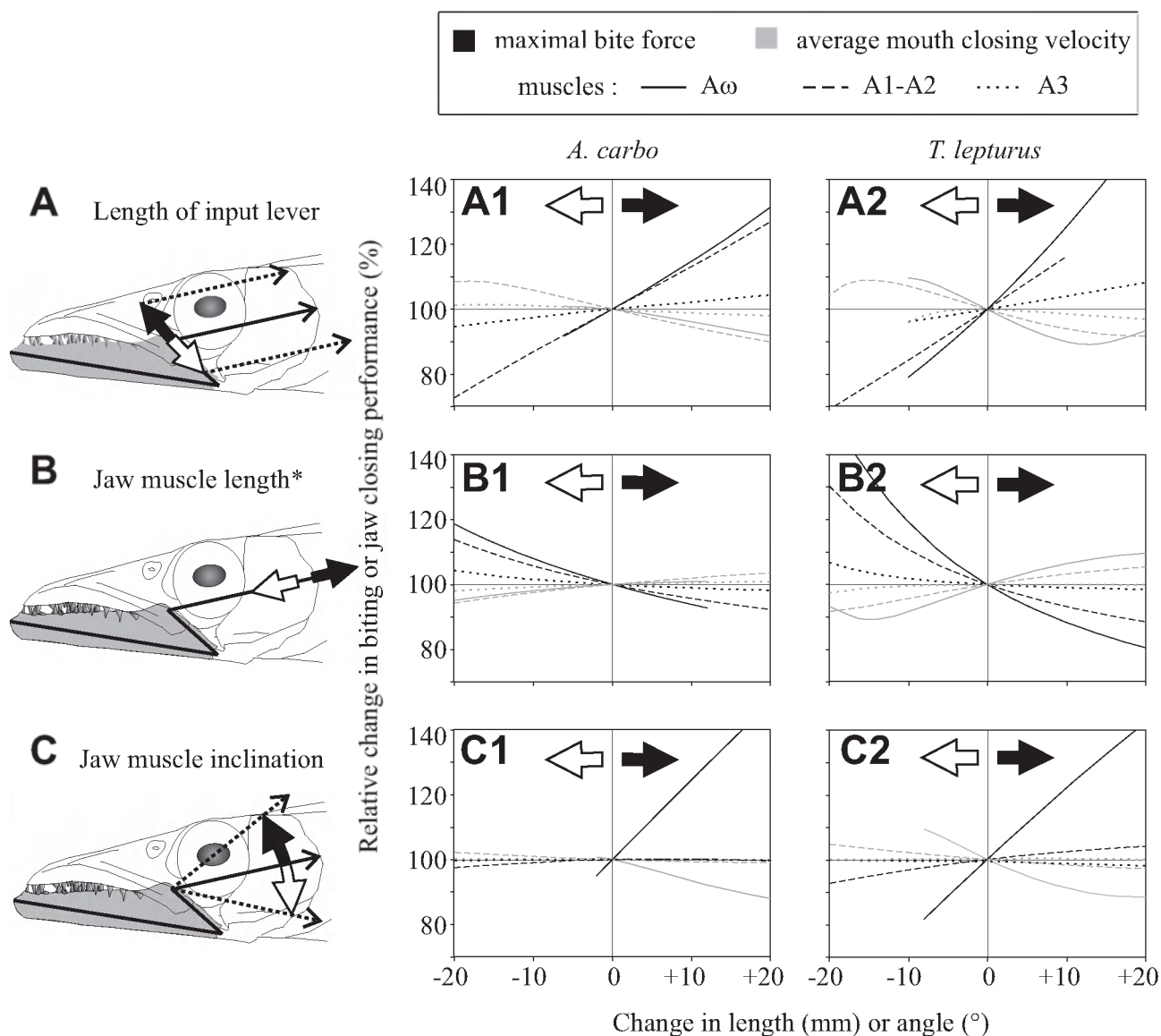


Fig. VI.2- 10 Effects of specific morphological changes to the jaw system (schematically illustrated in A, B, C; left column) on biting and mouth closing ( $50^{\circ}$  to  $10^{\circ}$  gape) performance as calculated by the model for *A. carbo* (cranial length of 160.6 mm) and *T. lepturus* (cranial length of 100.3 mm). The measured configuration of the jaw system of each species corresponds to the central point in the graphs where all curves intersect (0 mm or  $0^{\circ}$ ; 100%). Each morphological change was implemented for each muscle separately (see top for legend), while the model simulations were run with simultaneous activation of all muscles. In this way, the relative importance of modifications to each muscle is also displayed on the graphs. Note that, with few exceptions (see text for further information), increasing biting and mouth closing performance require morphological changes in the opposite direction. This demonstrates the functional trade-off between both functions, and illustrates that the jaw system of both trichiurid species is a compromise between forceful biting and quickly snapping of the jaws. As expected from the relative contribution of each of the adductor mandibulae subdivisions to jaw-closing power (Fig. VI.2- 9A, B) and bite force (Fig. VI.2- 9C, D), changes to the  $A_{\omega}$  generally have the largest impact on jaw closing and biting performance, while changes to the  $A_3$  have the smallest effects on the overall performances. The \* denotes that muscle volume was kept constant by adjusting the physiological cross-sectional area.

Fig. VII.3- 1

*Channallabes apus*

ant, antorbital;  
apal, autopalatine;  
fr, frontal;  
io-II, infraorbital II;  
io-III, infraorbital III;  
io-IV, infraorbital IV;  
lac, lacrimal;  
leth, lateral ethmoid;  
meth, mesethmoid;  
mnd, mandibula;  
mx, maxilla;  
ns, nasal;  
op, opercle;  
par-soc, parietosupraoccipital;  
prmx, premaxilla;  
pt, pterotic;  
pt-scl, posttemporo-supracleithrum;  
pvm, prevomer;  
sph, sphenotic;  
spop, suprapreopercular.

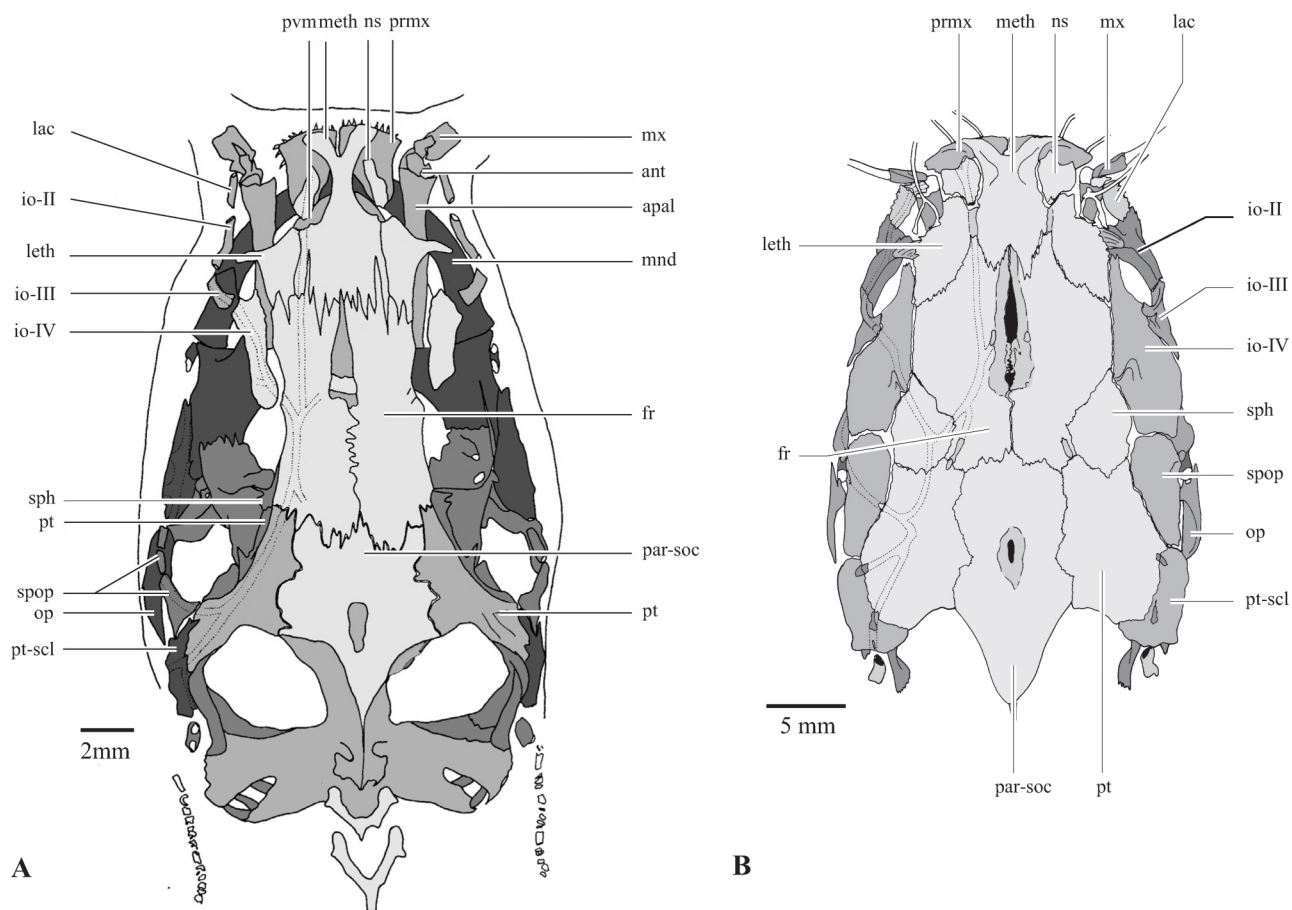


Fig. VII.3- 1: Dorsal view of the skull of **(A)** *Channallabes apus* (258 mm TL) (KMMA 175247±270); **(B)** *Clarias gariepinus* (127 mm SL).

Fig. VII.3- 2

*Channallabes apus*

ang-c, angulosplenio-articuloretroarticular complex;  
ant, antorbital;  
apal, autopalatine;  
boc, basioccipital;  
ch-a, anterior ceratohyal;  
ch-p, posterior ceratohyal;  
cl, cleithrum;  
cor, coracoid;  
den-c, dentosplenio-mentomeckelium complex;  
enp, entopterygoid;  
eoc, exoccipital;  
fr, frontal;  
hh-d, dorsal hypohyal;  
hh-v, ventral hypohyal;  
hm, hyomandibula;  
iop, interopercle;  
io-II, infraorbital II;  
io-III, infraorbital III;  
io-IV, infraorbital IV;  
lac, lacrimal;  
leth, lateral ethmoid;  
l-an-ch, ligamentum angulo-ceratohyale;  
l-an-iop, ligamentum angulo-interoperculare;  
meth, mesethmoid;  
mp, metapterygoid;  
mx, maxilla;  
ns, nasal;  
op, opercle;  
osph, orbitosphenoid;  
para, parasphenoid;  
par-soc, parieto-supraoccipital;  
pop, preopercle;  
pp-v4, parapophysis of vertebra 4;  
pp-v5, parapophysis of vertebra 5;  
prmx, premaxilla;  
prot, prootic;  
psph, pterosphenoid;  
pt, pterotic,  
pt-scl, posttemporo-supracleithrum;  
pvm, prevomer;  
puh, parurohyal;  
q, quadrate;  
r-br-VIII, branchiostegal ray VIII;  
sph, sphenotic;  
spl, splenial;  
spop, suprapreopercle;  
susp, suspensorium;  
v6, vertebra 6

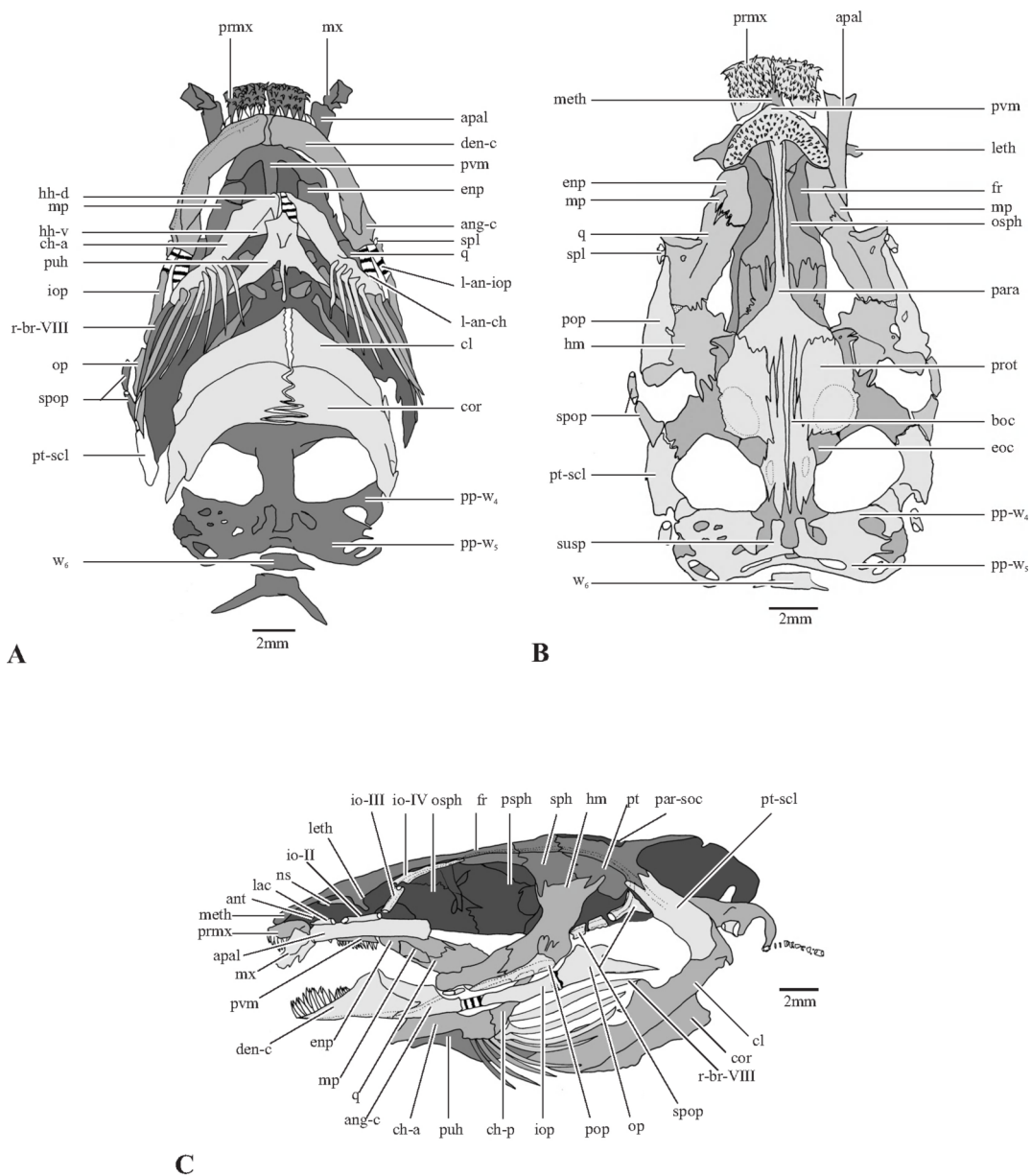


Fig. VII.3- 2: Skull of *Channallabes apus* (258 mm SL) (KMMA 175247±270). **(A)** ventral view of the skull; **(B)** ventral view of the neurocranium; **(C)** lateral view of the skull.

Fig. VII.3- 3

*Channallabes apus*

ang-c, angulosplenio-articuloretroarticular complex;  
apal, autopalatine;  
cl, cleithrum;  
den-c, dentosplenio-mentomeckelium complex;  
fr, frontal;  
hm, hyomandibula;  
iop, interopercle;  
io-II, infraorbital II;  
io-III, infraorbital III;  
io-IV, infraorbital IV;  
leth, lateral ethmoid;  
l-an-iop, ligamentum angulo-interoperculare,  
l-op-iop, ligamentum operculo-interopercle;  
meth, mesethmoid;  
mm-hh-ad, musculus hyohyoidei adductores;  
mnd-b-ex, external mandibular  
barbel; mx, maxilla;  
m-A2A3', musculus adductor mandibulae A2A3';  
m-A3'', musculus adductor mandibulae A3''';  
m-ad-ap, musculus adductor arcus palatini;  
m-ad-op, musculus adductor operculi;  
m-dil-op, musculus dilatator operculi;  
m-ex-t, musculus extensor tentaculi;  
m-l-ap, musculus levator arcus palatini;  
m-l-op, musculus levator operculi; m-pc-h-v, musculus protractor hyoidei pars ventralis;  
m-re-t, musculus retractor tentaculi;  
ns, nasal;  
n-b, nasal barbel;  
op, opercle;  
par-soc, parietosupraoccipital;  
psph, pterosphenoid;  
pop, preopercle;  
pt, pterotic;  
pt-scl, posttemporo-supracleithrum;  
q, quadrate;  
r-br-VIII, branchiostegal ray VIII;  
sph, sphenotic;  
spl, splenial;  
spop, suprapreopercle;  
tr-hm-VII, truncus hyomandibularis nervus facialis.



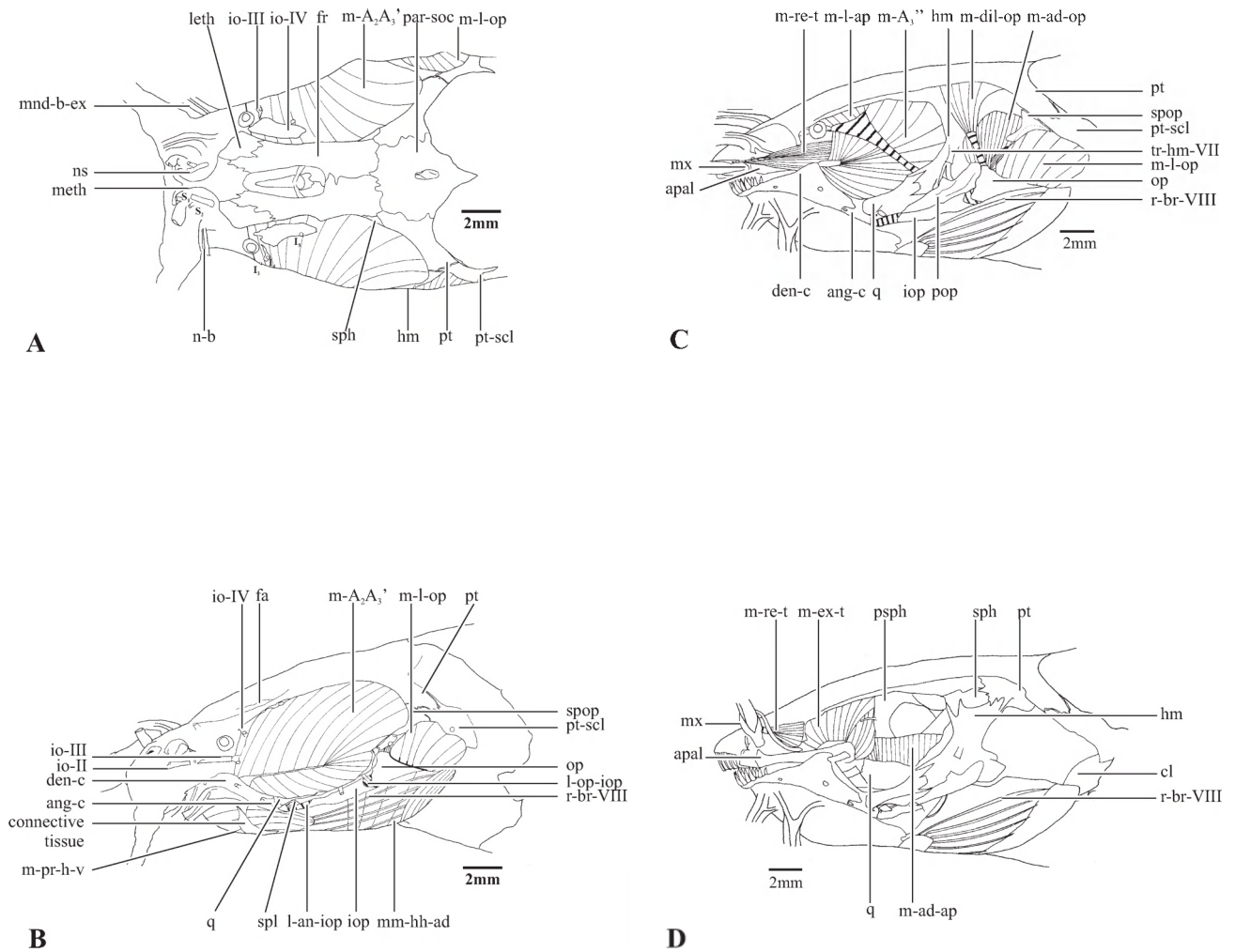


Fig. VII.3- 3: The head musculature of *Channallabes apus* (236 mm SL) (KMMA 175247±270). (A) dorsal view, skin and barbels are removed; (B) lateral view, skin and barbels are removed; (C) lateral view, external jaw muscle is removed; (D) lateral view, internal jaw muscle and the opercular muscles are removed.

Fig. VII.3- 4

*Channallabes apus*

ang-c, angulosplenio-articuloretroarticular complex;  
apal, autopalatine;  
cl, cleithrum;  
den-c, dentosplenio-mentomeckelium complex;  
fr, frontal;  
hm, hyomandibula;  
iop, interopercle;  
io-II, infraorbital II;  
io-III, infraorbital III;  
io-IV, infraorbital IV;  
leth, lateral ethmoid;  
l-an-iop, ligamentum angulo-interoperculare,  
l-op-iop, ligamentum operculo-interopercle;  
meth, mesethmoid;  
mm-hh-ad, musculus hyohyoidei adductores;  
mnd-b-ex, external mandibular  
barbel; mx, maxilla;  
m-A2A3', musculus adductor mandibulae A2A3';  
m-A3'', musculus adductor mandibulae A3''';  
m-ad-ap, musculus adductor arcus palatini;  
m-ad-op, musculus adductor operculi;  
m-dil-op, musculus dilatator operculi;  
m-ex-t, musculus extensor tentaculi;  
m-l-ap, musculus levator arcus palatini;  
m-l-op, musculus levator operculi; m-pc-h-v, musculus protractor hyoidei pars ventralis;  
m-re-t, musculus retractor tentaculi;  
ns, nasal;  
n-b, nasal barbel;  
op, opercle;  
par-soc, parietosupraoccipital;  
psph, pterosphenoid;  
pop, preopercle;  
pt, pterotic;  
pt-scl, posttemporo-supracleithrum;  
q, quadrate;  
r-br-VIII, branchiostegal ray VIII;  
sph, sphenotic;  
spl, splenial;  
spop, suprapreopercle;  
tr-hm-VII, truncus hyomandibularis nervus facialis.

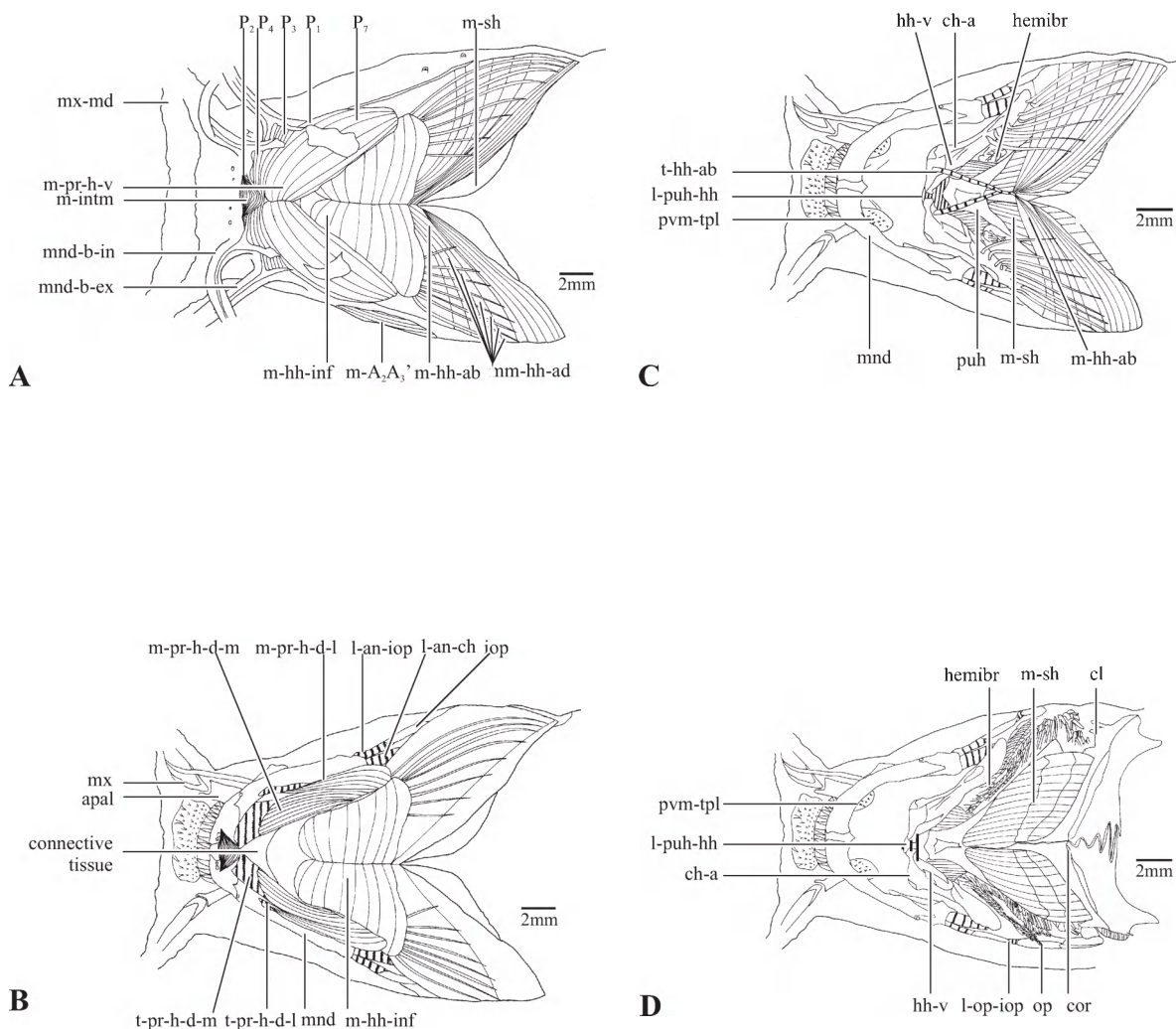


Fig. VII.3- 4: Ventral view of the head musculature of *Channallabes apus* (236 mm SL) (KMMA 175247±270). (A) skin and barbels are removed; (b) ventral part of the hyoid protractor is removed; (c) hyoid protractor, intermandibular and hyohyoideus inferior are removed; (d) hyohyoideus abductor and the hyohyoidei adductores are removed.



**B**

Tables



<b>Scheldt-Estuary</b>	<b>D AIC</b>	<b>Factor loadings PCA</b>		
		<b>1</b>	<b>2</b>	<b>3</b>
L Sn-E L	228.0	-0.116	0.1137	-0.143
L Sn-E D	243.2	-0.1269	0.1582	-0.1318
D	239.3	-0.217	0.2361	-0.3749
H H (E r)	242.6	-0.1344	-0.0258	-0.2181
H H (E c)	250.2	-0.184	-0.1478	-0.2294
H E	218.4	-0.0602	-0.1108	0.0448
L E	233.2	-0.0666	-0.0475	0.0281
H H (nos r)	210.1	-0.0638	0.0215	-0.1695
L E-nos r	234.3	-0.0854	0.0773	-0.0969
W H (E r)	238.8	-0.1788	0.1246	-0.3517
W H (E c)	247.9	-0.2095	-0.0312	-0.3059
IOB r	243.3	-0.1363	-0.1068	-0.1312
IOB c	243.9	-0.1748	-0.1539	-0.1157
IOB m	231.8	-0.1291	-0.0883	-0.18
L Sn-E c	273.8	-0.1891	0.0568	-0.0776
W pe	243.2	-0.3209	-0.4962	0.0388
H Pe	248.1	-0.3792	-0.5264	0.1774
L Sn-Pe	260.3	-0.6475	0.4853	0.5387
W H (nos r)	203.9	-0.0932	0.2036	-0.2666
		94.76%	1.75%	0.92%
<b>INBO</b>	<b>D AIC</b>			
H H (E c)	724.7			
IOB m	557.4			
L Sn-Pe	1056.4			
W pe	859.8			

Table IV.2.1- 1:  $\Delta$ AIC (comparing the fit of a single normal distribution to that of a mixture of two normal distributions) is given for each measurement taken on specimens collected in the Scheldt-Lippensbroek and for the specimens collected in water systems across Belgium (INBO).





		TL (cm)	BW(g)	Add Mand g	% BW	LAP g	% BW	DO g	% BW	LO g	% BW	PH g	% BW
<b>narrow-</b>	<b>230506 LB2P10</b>	31,5	44,7	0,08	1,72	0,01	0,17	0,01	0,06	0,01	0,31	0,01	0,24
<b>headed</b>	<b>220806 LB4P1</b>	56,0	331,5	0,63	1,89	0,06	0,18	0,02	0,06	0,10	0,29	0,09	0,27
	<b>220806 S1P3</b>	67,1	519,5	1,02	1,96	0,09	0,18	0,04	0,07	0,15	0,30	0,13	0,25
	<b>220806 LB2P2</b>	34,1	58,0	0,12	2,14								
	<b>220806 S1P14</b>	40,6	107,1	0,23	2,11								
	<b>220806 LB2P4</b>	41,0	135,8	0,27	1,97								
<b><i>mean</i></b>					1,97		0,18		0,06		0,30		0,25
<b>broad-</b>	<b>220806 S1P10</b>	34,7	58,0	0,31	5,29	0,02	0,38	0,00	0,07	0,02	0,38	0,02	0,35
<b>headed</b>	<b>220806 S1P18</b>	41,4	105,1	0,56	5,37	0,04	0,40	0,01	0,08	0,04	0,42	0,05	0,46
	<b>220806 S1P6</b>	57,4	420,1	2,31	5,51	0,19	0,46	0,04	0,08	0,15	0,36	0,16	0,38
	<b>220806 S1 P10</b>	34,7	58,0	0,31	5,34								
	<b>220806 LB2 P8</b>	40,5	100,7	0,56	5,59								
	<b>220806 S1 P15</b>	44,7	137,4	0,77	5,58								
<b><i>mean</i></b>					5,45		0,41		0,08		0,39		0,40

Table IV.2.2- 1: data weight cranial muscles expressed as pro mille of body weight.



Number of specimens and %		Pattern of hypural fusion
17	(45%)	PH; H1; H2; H3; H4; H5
1	(3%)	(PH+H1+H2); (H3+H4+H5)
4	(11%)	PH; (H1+H2); H3; H4; H5
3	(8%)	PH; (H1+H2); (H3+H4); H5
3	(8%)	PH; (H1+H2); (H3+H4+H5)
7	(19%)	PH; H1; H2; (H3+H4); H5
1	(3%)	(PH+H1); H2; (H3+H4); H5
1	(3%)	(PH+H1+H2+H3+H4+H5)

Table V.1- 1: Summary of the observed patterns of hypural fusion in *Channallabes apus* (Abbreviations: H: hypural; PH: parhypural).



Species	code	TL (mm)	ParH	H	cfr
<b>Oriental</b>					
<i>Mastacembelus mastacembelus</i>	IR-068	404	1	3	18
	IR-012	292	1	4	20
	IR-110	448	1	4	19
	IR-003	224	1	4	20
<b>African</b>					
<i>Mastacembelus marcheii</i>	MM1	210	1	2	12
	MM2	280	1	2	13
	MM3	323	1	2	12
<i>Mastacembelus brichardi</i>	MB1	158	1	2	8
	MB2	114	1	2	8
	MB3	121	1	2	8

Table VI.1.2- 1: Osteological traits of the caudal skeleton. TL, total length; ParH, parhypural (1 if not fused); H, total amount of hypurals, cfr, total amount of caudal fin rays.



Species	lower jaw length (mm)	lower jaw width (mm)	Muscle	$L_{in}$ (mm)	$\beta$	Muscle length (mm)	$\sigma$	$PCSA$ (cm <sup>2</sup> )	$\theta$	avg. fibre length (mm)
<i>T. lepturus</i>	76.9	8.5	A <sub>00</sub>	34.4	10	54.5	20	2.51	6	6.6
<i>CL=100.3 mm</i>			A <sub>1-A2</sub>	24.0	26	45.9	52	0.99	32	17.5
			A <sub>3</sub>	10.1	22	32.3	45	0.27	25	14.0
<i>A. carbo</i>										
<i>CL=160.6 mm</i>	136.9	16.4	A <sub>00</sub>	53.6	10	106.2	20	16.84	12	13.4
	(85.5)	(10.2)		(33.5)		(66.3)		(6.57)		(8.37)
			A <sub>1-A2</sub>	27.3	38	72.0	68	7.79	30	27.3
				(17.0)		(45.0)		(3.04)		(17.0)
			A <sub>3</sub>	23.8	36	44.0	75	1.50	28	20.2
				(14.9)		(27.5)		(0.59)		(12.6)

Table VI.2- 1: Biometric data of the closing system of the lower jaw.  $CL$  = cranial length,  $L_{in}$  = inlever length,  $\theta$  = angle between the longitudinal axis of the lower jaw and  $L_{in}$ ,  $\theta$  = inclination of the line of action of the muscle with respect to  $L_{in}$ ,  $PCSA$  = physiological cross-sectional area (both sides included),  $\theta$  = average angle of pennation. For *A. carbo*, also values scaled isometrically with respect to the  $CL$  of *T. lepturus* are shown underneath the measured values. All variables were measured in specimens with closed mouths (gape angle = 0°; see also Fig. VI.2- 1).





---

code	SL min	SL max	SL mean	HL min	HL max	HL mean	n
<i>M edwardsi</i>	172	219	197	13.4	17.3	15.4	3
<i>H longissimus</i>	225	268	245	12.8	15.3	14.0	5
<i>H hassi</i>	218	286	249	14.3	20.0	16.6	5
<i>P boro</i>	85	309	185	7.7	27.0	16.8	8
<i>C conger</i>	523	1644	1207	78.4	246.6	181.1	4
<i>A anguilla</i>	256	760	454	31.6	88.5	54.3	121
<i>M brichardi</i>	114	158	131	19.2	25.0	21.1	3
<i>M marchei</i>	210	323	271	33.5	48.4	41.5	3
<i>M mastacembelus</i>	224	448	342	37.4	71.9	56.2	4

---

Table VII- 1: Minimum, maximum and mean values of Standard length (SL) and Head length (HL) of the examined species. Values expressed in mm.





# Addendum



A: Sample 250406

Part 1

Code	TL	We	L Sn-E L	L Sn-E D	L Sn-E c	L E-nos r	L Sn-Pe	H H (Er)
250406 LB1 P1	340	69	0.82	0.87	1.20	0.59	4.23	0.91
250406 LB1 P2	295	36	0.66	0.69	0.89	0.47	3.41	0.83
250406 LB1 P3	406	143	0.86	0.92	1.44	0.57	5.13	1.07
250406 LB2 P1	584	400	1.21	1.22	1.88	0.92	6.67	1.58
250406 LB2 P2	312	43	0.81	0.86	1.08	0.54	4.11	0.96
250406 LB2 P3	370	98	0.70	0.78	1.22	0.56	4.18	1.06
250406 LB2 P4	625	450	1.30	1.37	1.90	0.94	6.81	1.61
250406 LB2 P5	385	75	0.91	1.01	1.39	0.65	5.03	0.92
250406 LB2 P6	420	172	0.94	1.00	1.53	0.74	5.79	1.24
250406 LB2 P7	326	54	0.76	0.83	1.16	0.53	4.12	0.91
250406 LB3 P1	380	81	0.75	0.82	1.18	0.59	4.60	0.93
250406 LB3 P2	508	282	1.37	1.46	1.82	0.96	6.87	1.57
250406 LB3 P3	335	70	0.72	0.79	1.08	0.61	4.16	0.89
250406 LB3 P4	464	192	0.92	1.03	1.60	0.71	5.61	1.39
250406 S1 P1	680	390	1.39	1.47	2.15	1.00	7.78	1.47
250406 S1 P10	301	50	0.73	0.78	1.01	0.55	3.60	0.94
250406 S1 P11	372	75	0.77	0.82	1.14	0.52	4.41	0.98
250406 S1 P12	412	131	0.92	1.05	1.49	0.66	5.54	1.20
250406 S1 P13	299	34	0.73	0.78	1.08	0.54	3.98	0.77
250406 S1 P14	302	39	0.60	0.63	0.90	0.41	3.70	0.87
250406 S1 P2	500	241	1.22	1.34	1.82	0.83	6.49	1.40
250406 S1 P3	505	292	0.99	1.04	1.58	0.80	5.81	1.26
250406 S1 P4	480	203	1.08	1.16	1.73	0.81	5.91	1.37
250406 S1 P5	450	165	0.92	0.97	1.49	0.62	5.15	1.23
250406 S1 P6	420	115	0.86	0.90	1.26	0.59	4.70	1.16
250406 S1 P7	362	76	0.77	0.85	1.19	0.59	4.41	1.12
250406 S1 P8	570	372	1.23	1.26	1.79	0.83	6.04	1.38
250406 S1 P9	380	70	0.76	0.79	1.13	0.58	4.12	0.92



A: Sample 250406

Part 2

Code	H H (Ec)	H H (nos r)	H Pe	W H (Er)	W H (Ec)	W H (nos r)	W Pe
250406 LB1 P1	1.12	0.56	1.67	1.13	1.24	0.83	1.83
250406 LB1 P2	0.89	0.46	1.61	0.87	0.98	0.67	1.44
250406 LB1 P3	1.41	0.70	2.48	1.22	1.52	0.87	2.24
250406 LB2 P1	1.87	0.82	3.40	1.80	2.08	1.17	3.37
250406 LB2 P2	1.03	0.56	1.71	0.98	1.09	0.73	1.56
250406 LB2 P3	1.38	0.57	2.18	1.14	1.33	0.83	1.97
250406 LB2 P4	1.92	0.87	3.68	1.75	2.10	1.10	3.32
250406 LB2 P5	1.11	0.50	2.14	1.19	1.31	0.75	1.85
250406 LB2 P6	1.60	0.71	2.85	1.58	1.80	1.05	2.55
250406 LB2 P7	1.06	0.53	1.94	1.07	1.29	0.78	1.56
250406 LB3 P1	1.15	0.55	1.95	0.97	1.16	0.63	1.73
250406 LB3 P2	1.87	0.88	3.37	1.95	2.14	1.28	3.01
250406 LB3 P3	1.06	0.47	1.92	0.94	1.08	0.74	1.75
250406 LB3 P4	1.63	0.54	2.74	1.38	1.70	0.92	2.49
250406 S1 P1	1.80	0.93	3.93	1.97	2.29	1.37	3.51
250406 S1 P10	1.03	0.52	1.73	0.92	1.02	0.61	1.58
250406 S1 P11	1.15	0.57	1.91	0.93	1.11	0.71	1.71
250406 S1 P12	1.50	0.68	2.37	1.54	1.67	1.40	2.12
250406 S1 P13	0.89	0.47	1.51	0.88	0.94	0.69	1.38
250406 S1 P14	0.98	0.44	1.62	0.76	0.94	0.56	1.34
250406 S1 P2	1.69	0.69	2.84	1.74	1.92	1.18	2.57
250406 S1 P3	1.57	0.67	2.87	1.39	1.63	0.88	2.56
250406 S1 P4	1.67	0.75	3.02	1.52	1.91	0.99	2.76
250406 S1 P5	1.50	0.70	2.58	1.34	1.61	0.86	2.43
250406 S1 P6	1.30	0.67	2.26	1.10	1.33	0.78	1.97
250406 S1 P7	1.28	0.66	2.13	1.20	1.40	0.70	1.95
250406 S1 P8	1.81	0.57	3.06	1.46	1.76	0.86	2.86
250406 S1 P9	1.11	0.54	1.93	1.05	1.27	0.72	1.74





A: Sample 250406

Part 3

Code	D	H E	L E	IODr	IODc	IODm
250406 LB1 P1	1.31	0.42	0.47	0.70	0.84	0.54
250406 LB1 P2	1.06	0.29	0.30	0.64	0.74	0.58
250406 LB1 P3	1.56	0.54	0.65	0.80	1.15	0.75
250406 LB2 P1	2.13	0.58	0.65	1.23	1.65	1.25
250406 LB2 P2	1.23	0.33	0.34	0.64	0.84	0.65
250406 LB2 P3	1.38	0.46	0.51	0.76	0.98	0.69
250406 LB2 P4	2.30	0.59	0.64	1.38	1.74	1.19
250406 LB2 P5	1.62	0.44	0.52	0.79	0.92	0.65
250406 LB2 P6	1.79	0.54	0.54	1.03	1.30	0.96
250406 LB2 P7	1.23	0.40	0.44	0.76	1.00	0.73
250406 LB3 P1	1.27	0.43	0.48	0.70	0.89	0.64
250406 LB3 P2	2.37	0.61	0.71	1.31	1.65	1.25
250406 LB3 P3	1.23	0.36	0.42	0.65	0.81	0.70
250406 LB3 P4	1.62	0.55	0.70	0.94	1.25	0.73
250406 S1 P1	2.30	0.74	0.87	1.37	1.76	1.18
250406 S1 P10	1.16	0.35	0.40	0.63	0.71	0.56
250406 S1 P11	1.22	0.40	0.43	0.66	0.79	0.56
250406 S1 P12	1.75	0.41	0.57	0.90	1.11	0.88
250406 S1 P13	1.17	0.32	0.35	0.59	0.71	0.53
250406 S1 P14	1.02	0.34	0.40	0.54	0.73	0.58
250406 S1 P2	2.15	0.50	0.59	0.94	1.24	0.84
250406 S1 P3	1.56	0.55	0.62	0.97	1.31	0.94
250406 S1 P4	1.73	0.58	0.66	1.08	1.44	0.92
250406 S1 P5	1.60	0.46	0.59	0.90	1.18	0.83
250406 S1 P6	1.33	0.48	0.50	0.86	1.03	0.74
250406 S1 P7	1.30	0.43	0.45	0.79	0.98	0.73
250406 S1 P8	1.86	0.55	0.65	1.07	1.22	0.80
250406 S1 P9	1.22	0.40	0.44	0.75	0.88	0.65



B: Sample 230506

Part 1

Code	TL	We	L Sn-E L	L Sn-E D	L Sn-E c	L E-nos r	L Sn-Pe	H H (Er)
230506 LB1 P1	519	228	0.97	1.07	1.56	0.68	6.51	1.32
230506 LB2 P1	556	349	0.99	1.02	1.47	0.68	6.40	1.32
230506 LB2 P10	315	45	0.69	0.70	0.97	0.54	3.62	0.80
230506 LB2 P2	525	262	1.09	1.12	1.72	0.81	6.45	1.52
230506 LB2 P3	527	279	0.87	1.01	1.51	0.62	5.85	1.32
230506 LB2 P4	510	223	1.08	1.13	1.66	0.70	6.15	1.30
230506 LB2 P5	473	226	1.02	1.06	1.50	0.77	5.56	1.22
230506 LB2 P6	509	188	1.16	1.21	1.65	0.82	6.22	1.36
230506 LB2 P7	402	122	0.91	0.96	1.38	0.60	5.22	1.02
230506 LB2 P8	367	83	0.69	0.77	1.18	0.57	4.36	0.90
230506 LB2 P9	344	55	0.73	0.78	1.19	0.59	4.28	0.83
230506 LB3 P1	510	247	1.02	1.12	1.61	0.79	6.36	1.30
230506 LB3 P10	322	59	0.79	0.82	1.31	0.60	4.64	0.99
230506 LB3 P11	376	83	0.69	0.77	1.20	0.55	3.96	0.98
230506 LB3 P12	272	32	0.76	0.77	1.11	0.65	4.47	0.88
230506 LB3 P13	281	35	0.70	0.67	1.06	0.53	3.79	0.85
230506 LB3 P2	510	270	1.08	1.21	1.74	0.79	6.17	1.40
230506 LB3 P3	455	168	0.98	1.01	1.40	0.77	5.80	1.14
230506 LB3 P4	403	129	0.93	0.93	1.27	0.67	5.39	1.16
230506 LB3 P5	451	186	0.83	0.84	1.26	0.68	5.21	1.28
230506 LB3 P6	376	96	0.83	0.87	1.32	0.64	5.19	1.02
230506 LB3 P7	368	89	0.79	0.86	1.24	0.61	4.37	0.91
230506 LB3 P8	305	44	0.83	0.86	1.23	0.63	4.54	1.04
230506 LB3 P9	398	120	0.73	0.70	1.00	0.53	4.20	0.81
230506 LB4 P1	501	193	0.98	1.04	1.53	0.74	5.91	1.24
230506 LB4 P2	525	320	0.93	1.06	1.63	0.67	6.07	1.26
230506 LB4 P3	370	73	0.78	0.81	1.14	0.59	4.64	0.88
230506 LB4 P4	309	54	0.71	0.72	1.11	0.56	3.83	0.92
230506 LB4 P5	405	108	0.82	0.88	1.27	0.62	4.67	1.10
230506 LB4 P6	395	102	0.79	0.88	1.23	0.60	4.82	0.90
230506 LB4 P7	376	92	0.77	0.85	1.28	0.60	4.62	0.96
230506 LB4 P8	302	42	0.79	0.68	0.97	0.54	3.82	0.83
230506 SF1 P1	760	816	1.43	1.55	2.35	1.12	8.85	1.98
230506 SF1 P2	545	305	1.17	1.23	1.54	0.79	6.25	1.47
230506 SF1 P3	624	400	1.03	1.16	1.78	0.86	7.32	1.38
230506 SF2 P1	410	126	0.86	0.88	1.33	0.66	5.13	1.11
230506 SF2 P2	550	352	1.13	1.25	1.77	0.88	6.73	1.53
230506 SF2 P3	553	282	1.09	1.13	1.65	0.87	6.30	1.30



B: Sample 230506

Part 2

Code	H H (Ec)	H H (nos r)	H Pe	W H (Er)	W H (Ec)	W H (nos r)	W Pe
230506 LB1 P1	1.49	0.71	2.98	1.59	1.82	1.12	2.72
230506 LB2 P1	1.62	0.71	3.26	1.40	1.69	0.95	2.96
230506 LB2 P10	1.01	0.45	1.58	0.94	1.07	0.61	1.46
230506 LB2 P2	1.76	0.69	3.11	1.68	1.89	1.08	2.65
230506 LB2 P3	1.73	0.70	3.01	1.48	1.82	0.86	2.64
230506 LB2 P4	1.49	0.67	3.01	1.61	1.82	0.98	2.53
230506 LB2 P5	1.47	0.64	2.84	1.42	1.65	0.92	2.66
230506 LB2 P6	1.55	0.69	2.76	1.60	1.74	1.10	2.38
230506 LB2 P7	1.32	0.56	2.40	1.46	1.61	0.89	2.15
230506 LB2 P8	1.17	0.51	2.01	1.05	1.30	0.77	1.74
230506 LB2 P9	1.01	0.47	1.81	1.01	1.14	0.73	1.53
230506 LB3 P1	1.46	0.66	2.98	1.50	1.78	0.91	2.43
230506 LB3 P10	1.26	0.56	2.32	1.01	1.21	0.71	1.91
230506 LB3 P11	1.14	0.51	2.10	1.10	1.31	0.77	1.73
230506 LB3 P12	1.18	0.52	2.05	1.06	1.19	0.74	1.82
230506 LB3 P13	1.06	0.47	1.70	1.02	1.10	0.71	1.40
230506 LB3 P2	1.63	0.73	3.08	1.57	1.86	1.13	2.71
230506 LB3 P3	1.42	0.65	2.98	1.33	1.49	0.91	2.50
230506 LB3 P4	1.37	0.58	2.60	1.21	1.48	0.84	2.31
230506 LB3 P5	1.66	0.66	2.58	1.48	1.66	0.72	2.22
230506 LB3 P6	1.35	0.59	2.56	1.21	1.50	0.62	2.35
230506 LB3 P7	1.15	0.50	2.10	0.95	1.28	0.74	1.81
230506 LB3 P8	1.23	0.60	2.26	1.12	1.34	0.79	1.96
230506 LB3 P9	1.00	0.43	1.68	0.98	1.05	0.73	1.56
230506 LB4 P1	1.57	0.69	2.82	1.57	1.80	1.11	2.51
230506 LB4 P2	1.65	0.72	3.20	1.31	1.77	0.97	3.04
230506 LB4 P3	1.05	0.45	1.87	1.03	1.20	0.71	1.74
230506 LB4 P4	1.16	0.50	1.91	1.07	1.22	0.71	1.66
230506 LB4 P5	1.37	0.57	2.20	1.15	1.35	0.76	2.01
230506 LB4 P6	1.09	0.51	2.79	1.13	1.28	0.73	1.89
230506 LB4 P7	1.15	0.61	2.21	1.18	1.33	0.81	2.11
230506 LB4 P8	1.03	0.44	2.65	1.02	1.17	0.66	2.55
230506 SF1 P1	2.53	1.05	4.48	2.39	2.84	1.05	3.98
230506 SF1 P2	1.77	0.76	3.19	1.83	1.95	1.15	2.95
230506 SF1 P3	1.74	0.68	3.47	1.56	1.87	0.95	2.86
230506 SF2 P1	1.46	0.59	2.42	1.29	1.53	0.87	2.20
230506 SF2 P2	2.07	0.78	3.36	1.86	2.30	1.08	3.03
230506 SF2 P3	1.68	0.69	3.13	1.53	1.76	1.10	2.84



B: Sample 230506

Part 3

Code	D	H E	L E	IODr	IODc	IODm
230506 LB1 P1	2.02	0.48	0.62	1.06	1.30	1.00
230506 LB2 P1	1.63	0.59	0.65	1.03	1.29	0.91
230506 LB2 P10	1.17	0.39	0.39	0.53	0.69	0.52
230506 LB2 P2	1.92	0.53	0.60	1.11	1.49	1.04
230506 LB2 P3	1.39	0.59	0.70	0.93	1.28	0.85
230506 LB2 P4	1.86	0.59	0.62	1.14	1.44	1.00
230506 LB2 P5	1.72	0.52	0.61	0.94	1.30	0.88
230506 LB2 P6	1.82	0.50	0.57	1.04	1.25	0.82
230506 LB2 P7	1.58	0.50	0.52	0.95	1.20	0.82
230506 LB2 P8	1.20	0.43	0.51	0.72	1.03	0.65
230506 LB2 P9	1.15	0.42	0.48	0.74	0.95	0.60
230506 LB3 P1	1.68	0.56	0.62	1.04	1.28	0.86
230506 LB3 P10	1.35	0.48	0.55	0.83	1.03	0.64
230506 LB3 P11	1.24	0.45	0.47	0.75	0.91	0.60
230506 LB3 P12	1.13	0.44	0.48	0.73	0.88	0.60
230506 LB3 P13	1.13	0.34	0.41	0.68	0.82	0.62
230506 LB3 P2	1.79	0.55	0.60	1.13	1.48	1.12
230506 LB3 P3	1.57	0.52	0.56	0.96	1.28	0.84
230506 LB3 P4	1.44	0.46	0.52	0.81	1.15	0.72
230506 LB3 P5	1.55	0.46	0.49	0.86	1.16	0.81
230506 LB3 P6	1.41	0.54	0.52	0.93	1.30	0.94
230506 LB3 P7	1.33	0.38	0.56	0.76	1.02	0.67
230506 LB3 P8	1.35	0.41	0.47	0.79	1.00	0.71
230506 LB3 P9	1.18	0.36	0.40	0.68	0.83	0.61
230506 LB4 P1	1.83	0.52	0.57	0.99	1.35	1.00
230506 LB4 P2	1.77	0.77	0.70	1.09	1.57	1.01
230506 LB4 P3	1.22	0.44	0.50	0.71	0.89	0.66
230506 LB4 P4	1.07	0.36	0.43	0.68	0.91	0.63
230506 LB4 P5	1.42	0.47	0.51	0.90	1.11	0.72
230506 LB4 P6	1.28	0.48	0.55	0.84	1.00	0.70
230506 LB4 P7	1.30	0.49	0.54	0.77	1.02	0.67
230506 LB4 P8	1.08	0.34	0.35	0.75	0.89	0.62
230506 SF1 P1	2.74	0.97	0.98	1.87	2.17	1.26
230506 SF1 P2	1.91	0.56	0.59	1.13	1.54	1.09
230506 SF1 P3	1.80	0.67	0.74	1.18	1.51	1.02
230506 SF2 P1	1.52	0.50	0.58	0.88	1.12	0.68
230506 SF2 P2	2.11	0.70	0.84	1.37	1.73	1.32
230506 SF2 P3	1.72	0.49	0.55	1.10	1.32	1.06





C: Sample 220806

Part 1

Code	TL	We	L Sn-E L	L Sn-E D	L Sn-E c	L E-nos r	L Sn-Pe	H H (Er)
220806 LB2 P1	748	635	1.71	1.76	2.65	1.25	8.62	1.87
220806 LB2 P2	341	58	0.73	0.78	1.04	0.46	4.02	0.91
220806 LB2 P3	446	135	0.83	0.96	1.38	0.62	5.41	0.98
220806 LB2 P4	410	136	0.65	0.69	1.25	0.55	4.34	0.92
220806 LB2 P5	372	107	0.76	0.77	1.26	0.57	4.02	0.89
220806 LB2 P6	415	124	0.78	0.84	1.34	0.67	4.94	1.05
220806 LB2 P7	348	67	0.82	0.90	1.29	0.62	4.73	0.83
220806 LB2 P8	405	101	0.95	1.03	1.43	0.71	4.94	0.97
220806 LB4 P1	560	332	1.20	1.30	1.84	0.86	6.50	1.26
220806 LB4 P2	415	111	0.77	0.82	1.28	0.55	4.83	0.91
220806 S1 P1	600	410	1.02	1.11	1.79	0.73	6.40	1.39
220806 S1 P10	347	58	0.74	0.76	1.10	0.51	4.07	0.82
220806 S1 P10B	640	532	1.30	1.40	2.09	1.03	7.36	1.57
220806 S1 P11	318	49	0.72	0.72	1.10	0.52	4.05	0.88
220806 S1 P12	339	58	0.73	0.77	1.12	0.56	3.97	0.88
220806 S1 P13	256	27	0.61	0.63	0.92	0.39	3.16	0.70
220806 S1 P14	406	107	0.71	0.79	1.27	0.55	4.70	0.93
220806 S1 P15	447	137	0.95	0.98	1.47	0.65	5.18	1.00
220806 S1 P16	627	481	1.69	1.72	2.51	1.18	7.88	1.55
220806 S1 P17	612	473	1.10	1.27	1.90	0.85	6.89	1.37
220806 S1 P18	414	105	0.80	0.83	1.31	0.55	4.65	1.02
220806 S1 P19	508	209	0.94	1.00	1.54	0.68	5.57	0.98
220806 S1 P2	515	216	1.18	1.21	1.67	0.83	5.85	1.18
220806 S1 P20	270	29	0.62	0.72	0.94	0.53	3.35	0.73
220806 S1 P21	611	458	1.45	1.47	2.17	1.00	7.61	1.46
220806 S1 P3	671	520	1.60	1.69	2.52	1.28	7.93	1.82
220806 S1 P4	524	222	1.05	1.10	1.60	0.77	5.64	1.03
220806 S1 P5	510	208	1.04	1.17	1.65	0.77	5.87	1.32
220806 S1 P6	574	420	1.04	1.00	1.65	0.75	6.30	1.44
220806 S1 P7	454	130	0.81	0.87	1.40	0.62	5.08	1.01
220806 S1 P8	395	105	0.79	0.85	1.30	0.57	4.56	0.86
220806 S1 P9	312	48	0.65	0.73	1.11	0.47	3.76	0.71



C: Sample 220806

Part 2

Code	HH (Ec)	HH (nos r)	H Pe	WH (Er)	WH (Ec)	WH (nos r)	W Pe
220806 LB2 P1	2.64	1.06	5.02	2.08	2.58	1.45	3.81
220806 LB2 P2	1.06	0.43	1.84	0.89	1.02	0.55	1.75
220806 LB2 P3	1.32	0.53	2.57	1.19	1.39	0.73	2.24
220806 LB2 P4	1.30	0.46	2.47	0.95	1.19	0.58	2.22
220806 LB2 P5	1.25	0.45	2.26	1.11	1.27	0.63	1.99
220806 LB2 P6	1.28	0.48	2.36	1.17	1.39	0.82	2.10
220806 LB2 P7	1.11	0.41	1.97	1.00	1.19	0.67	1.77
220806 LB2 P8	1.21	0.45	2.25	1.14	1.39	0.78	1.91
220806 LB4 P1	1.75	0.68	3.36	1.55	1.79	0.94	2.89
220806 LB4 P2	1.20	0.51	2.21	1.09	1.28	0.73	2.05
220806 S1 P1	1.79	0.64	3.93	1.49	1.93	0.90	3.30
220806 S1 P10	1.02	0.37	1.71	0.90	1.09	0.59	1.55
220806 S1 P10B	2.01	0.68	3.84	1.93	2.27	1.15	3.55
220806 S1 P11	1.11	0.46	1.95	1.01	1.18	0.68	1.67
220806 S1 P12	1.15	0.43	1.82	0.90	1.22	0.61	1.82
220806 S1 P13	0.86	0.35	1.41	0.65	0.78	0.42	1.22
220806 S1 P14	1.12	0.46	2.27	0.91	1.12	0.60	1.88
220806 S1 P15	1.26	0.54	2.37	1.20	1.38	0.75	2.23
220806 S1 P16	2.10	0.74	4.20	2.00	2.45	1.23	3.44
220806 S1 P17	1.87	0.67	3.51	1.59	1.99	0.90	3.13
220806 S1 P18	1.20	0.53	2.38	1.17	1.42	0.71	2.07
220806 S1 P19	1.42	0.50	2.73	1.18	1.41	0.66	2.27
220806 S1 P2	1.60	0.60	3.05	1.59	1.71	0.97	2.72
220806 S1 P20	0.90	0.36	1.58	0.89	1.09	0.61	1.35
220806 S1 P21	2.10	0.66	3.84	1.89	2.22	1.11	3.54
220806 S1 P3	2.25	0.95	4.47	2.01	2.23	1.20	3.61
220806 S1 P4	1.52	0.51	2.86	1.39	1.60	0.87	2.67
220806 S1 P5	1.72	0.62	3.35	1.53	1.81	0.87	2.62
220806 S1 P6	1.89	0.60	3.69	1.72	2.11	0.76	3.11
220806 S1 P7	1.26	0.49	2.31	1.24	1.44	0.74	2.10
220806 S1 P8	1.18	0.42	2.20	1.11	1.30	0.70	2.12
220806 S1 P9	0.92	0.37	1.68	0.84	1.04	0.59	1.46



C: Sample 220806

Part 3

Code	D	H E	L E	IODr	IODc	IODm
220806 LB2 P1	3.03	0.85	0.98	1.81	2.30	1.65
220806 LB2 P2	1.19	0.37	0.40	0.68	0.77	0.59
220806 LB2 P3	1.47	0.50	0.52	0.95	1.19	0.86
220806 LB2 P4	1.15	0.55	0.57	0.92	1.11	0.79
220806 LB2 P5	1.05	0.53	0.53	0.87	1.09	0.68
220806 LB2 P6	1.38	0.50	0.47	0.95	1.05	0.73
220806 LB2 P7	1.28	0.43	0.46	0.80	0.99	0.64
220806 LB2 P8	1.15	0.47	0.54	0.91	1.14	0.70
220806 LB4 P1	2.10	0.70	0.74	1.20	1.56	1.12
220806 LB4 P2	1.39	0.47	0.50	0.82	1.05	0.61
220806 S1 P1	1.79	0.66	0.68	1.18	1.50	1.13
220806 S1 P10	1.18	0.37	0.40	0.69	0.85	0.58
220806 S1 P10B	2.27	0.74	0.77	1.36	1.82	1.30
220806 S1 P11	1.18	0.44	0.48	0.75	0.94	0.54
220806 S1 P12	1.09	0.36	0.42	0.81	0.89	0.63
220806 S1 P13	1.07	0.26	0.32	0.55	0.63	0.41
220806 S1 P14	1.15	0.46	0.55	0.74	0.94	0.60
220806 S1 P15	1.42	0.52	0.56	0.86	1.11	0.70
220806 S1 P16	2.68	0.69	0.85	1.54	1.92	1.44
220806 S1 P17	1.96	0.67	0.72	1.40	1.68	1.15
220806 S1 P18	1.26	0.51	0.53	0.80	1.14	0.64
220806 S1 P19	1.57	0.53	0.59	0.90	1.20	0.83
220806 S1 P2	1.79	0.52	0.58	1.17	1.45	1.07
220806 S1 P20	1.12	0.35	0.42	0.69	0.87	0.55
220806 S1 P21	2.31	0.75	0.80	1.35	1.74	1.28
220806 S1 P3	2.77	0.75	0.75	1.48	1.84	1.38
220806 S1 P4	1.82	0.63	0.65	0.96	1.39	0.94
220806 S1 P5	1.75	0.60	0.68	1.12	1.25	1.15
220806 S1 P6	1.95	0.70	0.75	1.45	1.80	1.31
220806 S1 P7	1.36	0.47	0.58	0.89	1.12	0.72
220806 S1 P8	1.35	0.46	0.54	0.80	0.96	0.67
220806 S1 P9	1.22	0.51	0.51	0.71	0.87	0.57



D: Sample 181006

Part 1

Code	TL	We	L Sn-E L	L Sn-E D	L Sn-E c	L E-nos r	L Sn-Pe	H H (Er)
181006 LB2 P1	614	498	1.31	1.54	2.24	1.01	8.02	1.71
181006 LB2 P2	518	301	1.08	1.06	1.65	0.75	5.61	1.37
181006 LB2 P3	433	145	0.90	0.99	1.44	0.69	5.41	1.04
181006 LB2 P4	432	121	1.01	1.09	1.62	0.72	5.58	1.02
181006 LB2 P5	451	139	0.92	0.98	1.44	0.72	4.88	1.12
181006 LB3 P1	395	95	0.82	0.88	1.37	0.61	4.64	0.89
181006 S1 P1	565	363	1.09	1.19	1.76	0.77	6.65	1.31
181006 S1 P10	568	304	1.33	1.44	1.93	1.01	7.07	1.42
181006 S1 P12	361	79	0.75	0.79	1.29	0.58	4.29	0.79
181006 S1 P13	563	300	0.89	1.23	1.81	0.70	6.07	1.19
181006 S1 P14	569	399	1.24	1.30	2.08	0.84	6.52	1.41
181006 S1 P2	521	281	1.05	1.11	1.88	0.77	6.03	1.21
181006 S1 P3	531	230	1.37	1.45	2.04	1.03	6.95	1.28
181006 S1 P4	590	421	1.24	1.37	2.04	0.91	6.68	1.41
181006 S1 P5	569	420	1.06	1.15	1.82	0.78	6.58	1.22
181006 S1 P6	585	467	1.05	1.23	1.98	0.88	7.05	1.55
181006 S1 P7	468	180	0.92	1.01	1.51	0.67	5.44	1.06
181006 S1 P8	394	99	0.81	0.83	1.54	0.63	4.48	0.89
181006 S1 P9	396	132	0.83	0.87	1.48	0.59	4.73	0.95
181006 S2 P1	456	158	1.19	1.28	1.83	0.90	6.24	1.27
181006 S2 P2	607	401	1.22	1.29	1.83	0.92	6.72	1.41
181006 S2 P3	585	364	1.11	1.24	1.94	0.79	7.13	1.30
181006 S2 P4	467	166	1.15	1.21	1.70	0.89	6.02	1.09





D: Sample 181006

Part 2

Code	H H (Ec)	H H (nos r)	H Pe	W H (Er)	W H (Ec)	W H (nos r)	W Pe
181006 LB2 P1	2.21	1.01	3.86	2.37	2.65	1.53	3.65
181006 LB2 P2	1.79	0.58	3.19	1.47	1.74	0.80	3.10
181006 LB2 P3	1.30	0.57	2.51	1.34	1.46	0.70	2.25
181006 LB2 P4	1.28	0.57	2.31	1.38	1.48	0.90	2.16
181006 LB2 P5	1.53	0.62	2.42	1.38	1.53	0.70	2.17
181006 LB3 P1	1.11	0.43	2.14	1.17	1.38	0.79	1.83
181006 S1 P1	1.69	0.59	3.43	1.44	1.76	1.01	2.90
181006 S1 P10	1.79	0.71	3.36	1.86	2.06	1.12	2.82
181006 S1 P12	1.10	0.40	2.08	0.95	1.24	0.60	1.86
181006 S1 P13	1.88	0.60	2.97	1.45	1.87	0.92	2.95
181006 S1 P14	1.78	0.70	3.77	1.59	2.00	0.88	3.16
181006 S1 P2	1.53	0.67	3.15	1.65	1.78	1.03	2.64
181006 S1 P3	1.59	0.56	3.15	1.79	1.98	0.98	2.74
181006 S1 P4	1.78	0.72	3.68	1.72	1.90	1.01	2.85
181006 S1 P5	1.61	0.60	3.12	1.53	1.68	0.82	2.76
181006 S1 P6	2.00	0.74	3.57	1.71	2.18	1.01	3.14
181006 S1 P7	1.38	0.50	2.65	1.38	1.58	0.80	2.24
181006 S1 P8	1.17	0.45	2.10	1.05	1.40	0.54	2.04
181006 S1 P9	1.41	0.55	2.58	1.23	1.60	0.81	2.37
181006 S2 P1	1.73	0.62	2.74	1.65	1.80	1.04	2.46
181006 S2 P2	1.68	0.73	3.51	1.77	1.95	0.94	3.02
181006 S2 P3	1.88	0.62	3.45	1.66	2.07	1.13	3.12
181006 S2 P4	1.45	0.54	2.87	1.49	1.63	0.91	2.48



D: Sample 181006

Part 3

Code	D	H E	L E	IODr	IODc	IODm
181006 LB2 P1	2.75	0.75	0.92	1.63	1.99	1.52
181006 LB2 P2	1.65	0.62	0.54	1.18	1.42	0.95
181006 LB2 P3	1.62	0.45	0.51	0.93	1.26	0.85
181006 LB2 P4	1.70	0.54	0.60	0.95	1.19	0.81
181006 LB2 P5	1.47	0.51	0.55	0.99	1.28	0.79
181006 LB3 P1	1.46	0.47	0.51	0.87	1.16	0.72
181006 S1 P1	2.06	0.61	0.66	1.03	1.46	1.01
181006 S1 P10	2.28	0.57	0.64	1.30	1.63	1.20
181006 S1 P12	1.37	0.43	0.50	0.70	0.95	0.57
181006 S1 P13	1.62	0.78	0.81	1.21	1.62	1.12
181006 S1 P14	1.85	0.79	0.87	1.40	1.77	1.28
181006 S1 P2	1.80	0.66	0.70	1.20	1.41	1.05
181006 S1 P3	2.12	0.70	0.75	1.34	1.60	1.12
181006 S1 P4	2.19	0.63	0.80	1.15	1.59	1.15
181006 S1 P5	1.99	0.67	0.76	1.15	1.49	0.98
181006 S1 P6	1.88	0.76	0.79	1.54	1.94	1.40
181006 S1 P7	1.64	0.51	0.55	1.07	1.28	0.84
181006 S1 P8	1.27	0.72	0.77	0.93	1.20	0.81
181006 S1 P9	1.47	0.75	0.68	1.05	1.29	0.79
181006 S2 P1	1.98	0.51	0.65	1.13	1.29	1.06
181006 S2 P2	1.98	0.62	0.63	1.23	1.42	1.18
181006 S2 P3	1.82	0.60	0.78	1.20	1.63	1.04
181006 S2 P4	1.84	0.56	0.60	1.06	1.44	0.97



code	site	TL	We	L Sn-Pe	IOB m	H H (Ec)	W Pe
030318 GN4 P5	GN4	332	62.7	38.8	1.05	5.52	11.44
030318 GN4 P6	GN4	287	34.2	35.25	1.31	4.68	11.61
030318 GN4 P4	GN4	286	33.5	37.38	1.15	4.62	9.3
030318 GN4 P2	GN4	395	100.8	43.83	1.59	7.37	12
030318 GN4 P1	GN4	349	70.6	41.75	1.59	5.72	12.23
030318 GN4 P3	GN4	490	202.8	64.45	2.69	12.71	20.86
030319 GN2A P2	GN2	350	80.4	37.82	1.27	6.71	13.74
030319 GN2A P3	GN2	354	57.7	45.5	1.79	5.71	13.89
030319 GN2A P1	GN2	362	83.3	52.39	2.28	9.25	13.79
030319 GN2A P4	GN2	320	56.8	40.07	1.23	6.83	12.55
030319 GN2A P5	GN2	342	73.3	43.1	1.99	6.4	14.5
030319 GN2A P9	GN2	443	148.6	65.11	3	12.55	17.18
030319 GN2A P8	GN2	309	52.5	36.35	1.29	5.46	13.53
030319 GN2A P6	GN2	328	57.7	39.73	1.57	6.74	11.06
030319 GN2A P7	GN2	315	55.7	36.35	1.81	7.14	10.72
030319 GN2A P10	GN2	326	43.1	39.26	1.4	7.38	10.3
030616 GB1 P1	GB1	590	411	71.64	4.17	15.03	28.03
030325 BRK P6	BRK	413	126	51.21	2.24	8.58	15.67
030325 BRK P3	BRK	563	333.4	66.39	2.69	11.46	26.95
030325 BRK P8	BRK	299	40.5	33.72	1.58	5.5	10.47
030325 BRK P1	BRK	541	272.3	68.76	4.4	14.34	24.95
030325 BRK P2	BRK	567	293.1	43.56	2.66	12.54	21.48
030325 BRK P5	BRK	494	186.3	61.13	2.79	10.04	20.96
030325 BRK P4	BRK	557	300.8	67.53	4.03	12.59	20.2
030325 BRK P7	BRK	500	240.3	58.67	3.74	12.5	21.55
030409 DEM 3A P1	DEM3	595	466.7	73.79	4.52	16.2	24.84
030409 DEM 3A P2	DEM3	252	35.4	27.54	1.28	4.34	9.49
030319 GN2 P5	GN2	342	73.3	46.2	1.58	7.73	14.64
030319 GN2 P1	GN2	362	83.3	45.97	2.16	7.88	13.54
030319 GN2 P4	GN2	320	56.8	35.61	1.74	6.54	11.84
030319 GN2 P3	GN2	354	57.7	39.4	1.74	7.28	14.89
030319 GN2 P2	GN2	350	80.4	36.17	1.8	6.13	10.9
030325 HGK P2	HGK	390	99.8	47.76	1.88	7.24	15.36
030325 HGK P3	HGK	371	87.3	40.16	1.98	7.42	12.89
030325 HGK P5	HGK	393	110.4	54.24	2.92	8.61	16.49
030325 HGK P1	HGK	432	133.4	53.63	3.05	10.28	16.82
030325 HGK P4	HGK	334	94.8	45.45	2.32	8.16	12.55
030507 DIJ6 P1	DIJ6	488	243.8	57.06	4.78	10.22	18.05
030508 DIJ8 P1	DIJ8	472	203.9	58.41	2.59	9.06	18.65
030506 DIJ1 P1	DIJ1	524	311.7	56.77	3.85	12.39	18.57
030507 DIJ4 P1	DIJ4	475	233.6	57.08	4.23	9.66	19.73
030508 DIJ6A P1	DIJ6	398	121.8	45.79	2	8.45	14.47
030508 DIJ6A P3	DIJ6	292	35.3	36.6	1.69	5.16	11.72
030508 DIJ6A P2	DIJ6	473	141.2	55.41	4.18	10.67	17.37
030604 NEK P9	NEK	443	159.3	66.25	4.32	12.7	17.87
030604 NEK P10	NEK	412	136.4	51.79	2.6	10.39	17.83
030604 NEK P5	NEK	356	99.4	43.87	1.67	7.19	13.24
030604 NEK P8	NEK	417	132.2	52.05	2.42	9.34	14.8
030604 NEK P7	NEK	364	83.3	45.97	1.5	7.12	12.32
011105 BPG P3	BGP	396	126.6	48.19	2.53	7.2	16.14
011105 BPG P2	BGP	450	126.4	59.09	4.85	10.44	18.91
011105 BPG P1	BGP	425	122.3	53.27	5.76	9.32	16.95
011105 BPG P9	BGP	411	105.6	49.94	4.27	10.52	19.09
011105 BPG P6	BGP	406	109.4	48.71	3.24	9	12.68
010928 RM1 P1	RM	377	86.7	45.42	2.5	9.85	13.17

Add III.2- 2: The absolute values of cranial measurements of *Anguilla anguilla* specimens from the INBO- eel pollutant monitoring network.



code	site	TL	We	L Sn-Pe	IOB m	H H (Ec)	W Pe
010928 RM1 P2	RM	425	127.3	59.41	4.85	11.4	17.99
010516 WLL P1	WLL	383	89.8	48.22	4.62	8.57	15.27
010516 WLL P5	WLL	507	292.8	60.49	4.89	14.73	21.81
010516 WLL P2	WLL	384	92.6	40.65	4.54	7.6	10.41
010516 WLL P3	WLL	433	145.2	56.74	4.23	11.35	15.82
010919 NP1A P1	NP1A	318	47.1	34.99	2.78	7.31	9.68
010919 NP1A P2	NP1A	305	53.7	39.78	2.69	7.83	13.15
010919 NP1A P7	NP1A	387	114.3	45.54	3.28	10.02	19.66
010919 NP1A P8	NP1A	354	80.7	42.43	2.86	8.57	18.03
010919 NP1A P3	NP1A	343	61.1	42.37	2.78	7.13	16.38
010514 IK2 P4	IK2	350	76	40.21	2.56	7.86	13.45
010514 IK2 P1	IK2	340	68.2	41.7	2.86	8	13.98
010514 IK2 P3	IK2	368	71.1	41.57	2.21	7.49	14.53
010514 IK2 P2	IK2	381	80.3	46.57	3.49	9.05	20.02
010514 IK2 P10	IK2	342	70	43.01	2.58	8.11	17.95
011001 SK P1	SK	500	200.3	61.27	7.67	15.21	25.03
011001 SK P2	SK	790	882.4	88.12	14	22.48	33.98
011018 OSZ P7	OSZ	338	66.3	41.63	2.73	8.49	14.51
011018 OSZ P5	OSZ	380	74.8	45.26	3.94	9.65	17.81
011018 OSZ P1	OSZ	414	122.9	48.83	4.16	10.84	17.02
011018 OSZ P3	OSZ	348	63.7	47.82	3.27	9.12	16.87
011018 OSZ P4	OSZ	439	138.3	52.02	4.45	11.16	19.28
010606 WIK P1	WIK	566	384.9	68.25	4.44	14.77	34.49
010606 WIK P2	WIK	604	503.2	74.23	4.45	12.98	38.36
011023 KLD1A P7	KLD1A	406	94.7	50.31	4.07	10.52	19.73
011023 KLD1A P11	KLD1A	369	85.9	46.08	2.47	9.2	17.58
011023 KLD1A P4	KLD1A	396	100.3	40.36	3.26	8.75	15.64
011023 KLD1A P1	KLD1A	428	144.1	47.29	2.99	9.64	21.05
011023 KLD1A P9	KLD1A	398	101.2	43.91	3.76	8.54	17.59
010810 COM P11	COM	439	130.9	58.54	4.35	11.03	24.94
010810 COM P10	COM	407	83.1	51.46	2.96	9.71	16.79
010810 COM P12	COM	322	48.1	39.26	1.52	7.39	14.41
010810 COM P19	COM	343	64.6	49.51	3.71	8.05	19.49
010810 COM P15	COM	384	101.9	51.54	4.04	11.56	22.22
010810 COM P13	COM	342	72.7	42.39	1.87	7.61	17.18
010810 COM P14	COM	330	63.8	37.88	1.49	7.16	16.2
010810 COM P18	COM	357	65.2	46.08	2.35	8.76	15.08
010810 COM P1	COM	586	383.9	76.61	7.94	16.38	35.29
010810 COM P7	COM	559	333.3	78.74	7.18	17.18	34.92
010810 COM P5	COM	485	197.8	65.42	5.54	11.22	28.11
010810 COM P21	COM	533	185.2	71.97	6.9	16.29	32.75
020909 IK1B P8	IK1B	340	60.6	41.84	2.26	7.13	14.34
020909 IK1B P7	IK1B	342	80.9	40.61	2.31	7.17	16.9
020909 IK 1B P10	IK1B	355	78.1	41.62	2.25	6.75	15.74
020909 IK 1B P9	IK1B	360	78.2	43.69	2.27	6.86	15.86
020909 IK1B P6	IK1B	438	136.5	57.66	3.31	11.49	23.68
020909 IK1BP5	IK1B	358	97.1	41.74	1.66	7.47	18.27
020909 IK1B P2	IK1B	366	78.2	38.05	2.62	8.43	15.49
020909 IK1B P1	IK1B	432	144.7	56.41	3.94	12.09	23.02
020909 IK1B P3	IK1B	365	86.3	40.81	1.94	6.57	19.05
020909 IK1B P4	IK1B	386	96.5	49.33	2.07	8.48	19.18
020909 IK2A P8	IK2A	398	115.8	42.44	1.94	7.99	17
020909 IK2A P4	IK2A	411	130.2	41.81	3.39	7.48	18.6
020909 IK2A P10	IK2A	393	82.6	42.07	3.26	7.86	17.15
020909 IK2A P5	IK2A	358	110.3	40.54	1.81	6.6	20.45

Add III.2- 2: The absolute values of cranial measurements of *Anguilla anguilla* specimens from the INBO- eel pollutant monitoring network.





code	site	TL	We	L Sn-Pe	IOB m	H H (Ec)	W Pe
020909 IK2A P9	IK2A	366	107	40.35	1.78	6.47	18.01
020909 IK2A P1	IK2A	371	122.8	45.21	1.88	7.99	18.23
020909 IK2A P3	IK2A	363	91.1	42.91	2.33	7.74	18.53
020909 IK2A P6	IK2A	393	126.4	42.63	2.01	7.93	22.41
020909 IK2A P2	IK2A	357	109.7	40.53	2.22	7.39	18.48
020909 IK2A P7	IK2A	354	83.4	41.55	2.01	7.03	18
021008 KBH1C P10	KBH1C	475	177.9	56.53	4.18	9.5	21.14
021008 KBH1C P9	KBH1C	509	209.4	65.2	3.8	11.57	24.47
021008 KBH1C P8	KBH1C	444	154.5	56.58	3.86	9.18	17.47
021008 KBH1C P4	KBH1C	555	311.8	77.55	5.77	13.91	30.39
021008 KBH1C P1	KBH1C	381	92.7	50.23	2.78	7.71	19.18
021008 KBH1C P7	KBH1C	373	82.5	42.09	2.02	6.27	17.79
021008 KBH1C P6	KBH1C	494	200.8	69.39	5.28	11.85	21.35
021008 KBH1C P2	KBH1C	470	209.7	43.97	2.37	7.73	21.34
021008 KBH1C P3	KBH1C	386	102.8	45.49	2.14	7.11	17.74
021008 KBH1C P5	KBH1C	610	425.1	75.22	6.65	16.21	31.92
021104 HV2 P10	HV2	325	48.8	41.62	2.31	5.42	11.74
021104 HV2 P1	HV2	352	72.8	38.42	1.53	6.74	16.98
021104 HV2 P3	HV2	348	65.3	41.12	2.23	6.72	14.56
021104 HV2 P4	HV2	365	61.5	48.47	2.61	7.55	16.35
021104 HV2 P5	HV2	324	44.4	38.15	1.71	5.05	13.23
021104 HV2 P9	HV2	336	55.5	41.46	1.82	7.3	14.02
021104 HV2 P8	HV2	335	60.4	39.18	1.39	5.03	13.69
021104 HV2 P7	HV2	335	65.7	43.61	2.87	6.48	14.12
021104 HV2 P6	HV2	320	53.3	37.38	1.67	5.04	13.65
021104 HV2 P2	HV2	348	68.8	43.15	1.73	5.79	13.27
020909 IK1A P6	IK1A	430	156.4	48.62	2.52	8.65	17.72
020909 IK1A P8	IK1A	357	77.6	50.38	2.38	8.07	16.93
020909 IK1A P9	IK1A	418	161.4	48.66	2.04	6.69	17
020909 IK1A P7	IK1A	419	155.4	45.88	1.76	6.32	17.62
020909 IK1A P3	IK1A	365	77.9	46.66	2.41	7.46	16.46
020909 IK1A P10	IK1A	348	62.1	38.35	1.41	5.14	16.44
020909 IK1A P5	IK1A	383	101.5	43.76	1.87	6.53	14.51
020909 IK1A P2	IK1A	354	95.8	42.37	2.21	7	14.71
020909 IK1A P1	IK1A	352	73.5	51.17	2.15	7.92	15.37
020909 IK1A P4	IK1A	408	112.6	58.75	2.55	8.46	18.62
021017 WBV8 P5	WBV8	322	57.6	40.08	1.47	4.35	9.95
021017 WBV8 P10	WBV8	369	72.5	42.5	1.79	5.88	11.46
021017 WBV8 P8	WBV8	330	42.1	37.93	1.59	5.51	11.48
021017 WBV8 P2	WBV8	368	94.9	40.55	1.77	6.65	12.31
021017 WBV8 P9	WBV8	343	83.5	40.21	1.41	6.15	12.28
021017 WBV8 P1	WBV8	396	99.6	48.59	1.52	6.9	14.41
021017 WBV8 P4	WBV8	416	131.5	48.3	1.96	7.66	17.66
021017 WBV8 P3	WBV8	352	82.9	44.87	2.4	6.02	12.54
021017 WBV8 P6	WBV8	368	88.5	40.87	1.69	6.04	12.81
030915 KDS2 P1	KDS2	411	119.7	55.26	3.52	8.77	18.43
030915 KDS2 P2	KDS2	760	770.5	102.81	13.2	24.24	36.94
030915 KDS4 P1	KDS4	570	383.4	81.41	7.82	17.45	30.16
030915 KDS4 P6	KDS4	382	92.2	48.74	1.91	8.24	15.91
030915 KDS4 P5	KDS4	459	143.3	62.37	5.87	11.59	23.24
030915 KDS4 P4	KDS4	266	25.4	35.63	1.62	4.88	10.47
030915 KDS4 P3	KDS4	458	173.7	48.1	2.31	8.53	19.91
030319 GN3 P1	GN3	337	56.7	39.78	1.86	5.81	14.72
030319 GN3 P2	GN3	340	59.1	39.57	2.46	5.95	14.51
030915 KDS3 P9	KDS3	484	191.9	61.17	5.16	11.66	21.84

Add III.2- 2: The absolute values of cranial measurements of *Anguilla anguilla* specimens from the INBO- eel pollutant monitoring network.



code	site	TL	We	L Sn-Pe	IOB m	H H (Ec)	W Pe
030915 KDS3 P2	KDS3	525	184	73.06	5.51	13.87	20.38
030915 KDS3 P1	KDS3	489	175.4	65.51	4.25	11.74	20.81
030915 KDS3 P6	KDS3	493	197.9	66.15	4.65	13.83	21.57
030915 KDS3 P7	KDS3	559	299.4	74.98	5.08	13.67	22.01
030915 KDS3 P5	KDS3	531	197.1	70.74	4.2	12.73	20.15
030915 KDS3 P8	KDS3	561	333.2	71.3	5.37	14.54	29.87
030915 KDS3 P4	KDS3	493	309.8	64.56	3.62	11.97	21.56
030915 KDS P3	KDS3	561	335.3	67.94	4.48	13.71	23.57
030304 MOT P1	MOT	567	341.8	66.18	5.08	14.51	21.88
030304 MOT P2	MOT	555	282.1	75.6	5.35	15.67	23.77
030514 LEV P4	LEV	250	33.3	29.26	1.15	3.63	10.77
030514 LEV P3	LEV	233	21.1	26.19	0.92	3.52	8.13
030514 LEV P5	LEV	229	19.9	26.64	1.09	3.68	8.88
030514 LEV P2	LEV	589	527.1	80.11	8.1	25.33	30.94
030514 LEV P1	LEV	675	759.1	84.29	7.13	21.03	30.71
030515 PDV P1	PDV	370	81.5	41.35	1.42	6.07	13.63
030515 PDV P3	PDV	306	62.3	37.44	1.28	5.11	12.55
030515 PDV P4	PDV	369	104.5	42.35	1.4	5.45	11.82
030515 PDV P5	PDV	307	54.6	37.52	1.36	5.42	12.25
030515 PDV P6	PDV	310	65.4	39.23	1.39	5.13	12.25
030515 PDV P2	PDV	325	62.9	39.01	1.47	5.09	11.45
030515 PDV P8	PDV	285	47.6	34.01	1.25	4.48	10.74
030515 PDV P7	PDV	324	74.8	38.21	1.51	5.52	12.8
030320 NKE P6	NKE	373	80.3	51.77	2.67	7.45	12.67
030320 NKE P7	NKE	370	74.7	46.26	1.93	7.09	12.55
030320 NKE P3	NKE	391	94.6	41.49	2.74	7.81	12.15
030320 NKE P10	NKE	347	67.1	37.63	1.61	6.49	11.61
030320 NKE P1	NKE	452	142	53.74	1.98	7.31	11.98
030320 NKE P2	NKE	406	110.8	51.32	1.79	7.2	13.49
030320 NKE P8	NKE	356	71.3	40.07	1.8	6.55	12.45
030320 NKE P9	NKE	347	64	37.79	1.84	5.71	12.59
030320 NKE P5	NKE	383	94.8	45.74	1.98	6.95	12.86
030320 NKE P4	NKE	386	115.5	43.54	2.04	7.36	15.94
030325 OPK P5	OPK	336	69.7	40.28	1.48	4.67	11.85
030325 OPK P4	OPK	357	70	46.41	1.61	5.01	12.34
030325 OPK P3	OPK	383	96.7	44.89	1.43	6.77	12.27
030325 OPK P1	OPK	458	138.8	54.51	1.71	7.22	14.21
030325 OPK P2	OPK	492	236.6	61.69	2.25	9.88	17.67
030604 NEK P1	NEK	390	98.8	46.45	2.48	7.39	13.96
030604 NEK P2	NEK	367	89.6	46.75	1.86	7.85	16.22
030604 NEK P6	NEK	380	93.2	51.94	2.17	8.27	13.6
030604 NEK P4	NEK	384	98.9	45.17	1.67	7.02	11.83
030604 NEK P3	NEK	369	85.5	50.45	1.94	7.44	11.61
030327 RLK P2	RLK	350	87.5	42.71	1.8	7.07	11.92
030327 RLK P4	RLK	308	51.1	36.96	1.55	5.32	10.42
030327 RLK P3	RLK	344	66.2	41.57	1.86	6.25	11.91
030327 RLK P1	RLK	313	59	40.37	1.86	6.16	11.26
030604 BBV P5	BBV	348	87.1	43.65	1.36	6.91	15.42
030604 BBV P7	BBV	372	92.9	41.19	1.86	7.37	11.7
030604 BBV P4	BBV	381	98.8	47.4	2.24	7.47	14.58
030604 BBV P8	BBV	370	114.5	45.85	1.53	7.7	15.45
030604 BBV P6	BBV	383	113.3	47.28	2.15	7.61	15.52
030604 BBV P3	BBV	355	86.8	43.25	1.38	7.34	13.33
030604 BBV P1	BBV	392	96.3	48.49	1.82	8.4	14
030604 BBV P2	BBV	384	117.7	45.82	1.79	8.11	14.45

Add III.2- 2: The absolute values of cranial measurements of *Anguilla anguilla* specimens from the INBO- eel pollutant monitoring network.



code	site	TL	We	L Sn-Pe	IOB m	H H (Ec)	W Pe
030604 BBV P9	BBV	350	85.6	44.98	1.93	7.8	12.27
030604 BBV P10	BBV	384	104.7	45.43	1.57	7.44	14.99
030409 DEM4 P1	DEM4	448	173.7	50.91	2.41	9.48	18.63
030320 KN2 P6	KN2	328	57.7	57.54	2.41	8.99	18.63
030320 KN2 P5	KN2	342	73.3	46.67	2.17	6.78	12.89
030320 KN2 P7	KN2	315	55.7	42.36	1.53	7.45	15.72
030320 KN2 P3	KN2	354	57.7	54.3	2.75	10.97	19.81
030320 KN2 P1	KN2	362	83.3	47.04	2.36	8.86	15.95
030320 KN2 P9	KN2	443	148.6	48.76	2.21	9.04	17.24
030320 KN2 P2	KN2	350	80.4	53.66	3.48	10.47	19.35
030320 KN2 P4	KN2	320	56.8	47.15	1.65	6.92	14.59
030320 KN2 P8	KN2	309	52.5	56.31	2.51	9.58	20.96
030320 KN2 P10	KN2	326	43.1	44.96	1.81	6.92	13.78
030607 DA P2	DA	374	111.2	43.81	1.59	7.29	17.63
030607 DA P3	DA	482	215.4	62.02	2.44	10.44	20.32
030607 DA P4	DA	377	117.8	47.14	1.91	8.02	18.61
030607 DA P1	DA	440	136.9	54.31	1.62	7.96	17.41
0306 KAL P1	KAL	930	1962.4	106.62	16.99	27.26	57.11
0306 KAL P2	KAL	955	1766	120.46	13.51	29.12	53.16
0306 KAL P3	KAL	985	2019	104.58	14.76	29.91	53.66
0306 KAL P4	KAL	770	948.8	100.88	10.05	21.39	45.14
0306 KAL P5	KAL	703	657	88.76	7.21	19.17	34.44
0306 KAL P6	KAL	1023	2284	111.56	13.13	26.77	63.38
0306 KAL P7	KAL	726	682.4	87.17	7.52	19.67	39.22
030915 KDS4A P1	KDS4A	407	129.6	54.91	2.37	10.44	18.56
030915 KDS4A P2	KDS4A	315	43	37.32	1.99	7.23	12.24
030915 KDS4A P3	KDS4A	388	101.9	50.35	1.67	7.44	15.04
030915 KDS4A P4	KDS4A	383	92	52.95	2.74	8.58	18.69
030915 KDS4A P5	KDS4A	447	124.8	62.55	2.84	8.44	17.65
030915 KDS4A P6	KDS4A	438	151.7	51.99	2.54	8.24	17.99
030915 KDS4A P7	KDS4A	456	160.5	55.43	2.86	7.94	19.39
030915 KDS4A P8	KDS4A	428	125.5	53.43	2.41	9.16	18.77
030915 KDS4A P9	KDS4A	434	140.4	52.44	2.03	8.81	19.12
030915 KDS4A P10	KDS4A	362	80.8	42.5	1.47	5.51	12.51
030915 KDS8 P2	KDS8	398	110.7	56.79	2.69	8.95	16.62
030915 KDS8 P4	KDS8	390	101.1	46.08	1.57	8.56	15.25
030915 KDS8 P3	KDS8	437	141.9	57.01	2.26	8.8	17.55
030915 KDS8 P5	KDS8	400	113.9	47.72	1.96	7.78	16.96
030915 KDS8 P1	KDS8	675	522.3	88.42	7.06	24.07	45.21
030917 KDS7 P10	KDS7	399	76.9	56.52	2.54	9.79	16.75
030917 KDS7 P3	KDS7	602	301	59.84	3.89	14.47	26.19
030917 KDS7 P8	KDS7	553	310.5	70.26	7.04	15.8	30.26
030917 KDS7 P2	KDS7	406	81.2	53.62	2.06	9.46	15.68
030917 KDS7 P9	KDS7	507	217.9	65.89	4.46	15.13	26.92
030917 KDS7 P7	KDS7	385	76.2	47.23	4.22	7.64	15.17
030917 KDS7 P1	KDS7	460	164.4	56.11	3.46	11.13	15.88
030917 KDS7 P6	KDS7	407	113	55.93	2.98	9.32	16.15
030917 KDS7 P4	KDS7	523	171	67.7	3.37	12.34	18.8
030917 KDS7 P5	KDS7	564	306.6	69.11	5.15	12.12	19.94
030915 KDS7B P4	KDS7B	313	44.6	45.25	1.86	7.53	13.69
030915 KDS7B P5	KDS7B	365	82.1	53.68	3.32	10.87	16
030915 KDS7B P6	KDS7B	510	212	68.15	6.68	16.23	26.44
030915 KDS7B P3	KDS7B	319	46	41.77	1.64	6.64	9.81
030915 KDS7B P1	KDS7B	331	52.7	45.49	2.13	8.34	13.54
030915 KDS7B P2	KDS7B	465	150.4	69.91	4.52	13.36	17.55

Add III.2- 2: The absolute values of cranial measurements of *Anguilla anguilla* specimens from the INBO- eel pollutant monitoring network.



code	site	TL	We	L Sn-Pe	IOB m	H H (Ec)	W Pe
030915 KDS7B P7	KDS7B	510	156.9	65.22	2.46	11.13	21.19
030917 KDS6 P2	KDS6	442	209.3	59.72	3.62	13.36	17.78
030917 KDS6 P8	KDS6	384	91.5	53.06	2.38	8.6	15.05
030917 KDS6 P9	KDS6	482	213.5	71.52	4.44	17.44	22.28
030917 KDS6 P10	KDS6	340	53.3	48.33	2.99	9.12	15.33
030917 KDS6 P7	KDS6	402	134	50.51	3.53	11.04	17.47
030917 KDS6 P6	KDS6	380	99.9	49.06	3.49	8.06	16.32
030917 KDS6 P3	KDS6	401	64	52.94	2.89	8.3	14.34
030917 KDS6 P1	KDS6	358	71.4	45.86	1.74	6.12	12.93
030917 KDS6 P5	KDS6	463	199.3	59.35	5.48	12.54	25.34
030917 KDS6 P4	KDS6	390	124.2	49.69	2.91	8.28	18.89
030902 DEM2 P3	DEM2	351	62.5	45.26	3.7	6.96	16.66
030902 DEM2 P2	DEM2	553	341.1	67.52	7.42	13.86	28.67
030902 DEM2 P1	DEM2	613	520.3	76.52	8.12	20.15	34.29
030915 KDS5 P1	KDS5	425	108.5	54.51	4.27	12.72	19.54
030915 KDS5 P2	KDS5	356	81	44.07	3.06	9.06	17.57
030915 KDS5 P3	KDS5	603	372.3	83.67	7.59	18.54	29.25
030915 KDS5 P4	KDS5	578	374.2	90.82	7.56	18.52	37.47
030915 KDS5 P5	KDS5	513	232.2	72.81	4.99	16.98	26.15
030915 KDS5 P6	KDS5	537	279.1	73.83	6.81	18.73	29.48
030915 KDS5 P7	KDS5	424	128.8	53.66	4.23	10.06	19.62
030915 KDS5 P8	KDS5	378	102.7	47.16	2.52	8.2	18.15
030915 KDS7A P1	KDS7A	323	48.8	40.7	1.72	7.55	14.71
030915 KDS7A P2	KDS7A	422	123	55.54	5.18	17.26	22.79
030915 KDS7A P3	KDS7A	470	192.8	78.62	6.28	17.76	30.3
030915 KDS7A P4	KDS7A	437	157.6	68.28	5.44	14.36	20.07
030915 KDS7A P5	KDS7A	538	266.1	79.01	7.69	22.25	33.98
030623 LE6 P1	LE6	476	191.1	58.19	3.52	14.43	19.37
030623 LE6 P2	LE6	380	84.9	47.42	2.01	9.78	15.08
030623 LE6 P3	LE6	510	249.3	66.76	3.99	16.07	27.38
030623 LE6 P4	LE6	364	89.2	48.83	2.25	8.87	16.65
030623 LE6 P5	LE6	367	86.2	49.9	2.07	9.88	17.52
030623 LE6 P6	LE6	337	64.2	41.6	2.53	9.71	15.3
030623 LE6 P7	LE6	365	90.8	47.95	2.28	9.66	17.68
030623 LE6 P8	LE6	365	73.7	45.22	2.4	7.51	17.04
030623 LE1 P1	LE1	344	63	42.19	2.62	7.29	15.92
030623 LE1 P2	LE1	593	407	76.08	4.56	18.26	26.04
030623 LE1 P3	LE1	319	39.1	40.7	2.21	6.43	13.48
030623 LE1 P4	LE1	285	32.3	35.71	1.76	5.79	11.5
030623 LE1 P5	LE1	602	281.1	69.32	4.95	15.58	28.17
030902 DEM6 P1	DEM6	541	248.9	67.29	4.33	17.04	25.59
030902 DEM6 P2	DEM6	561	334.7	64.83	5.76	15.36	24.43
030623 L P1	L	702	683	93.04	8.28	27.64	30.71
030623 L P2	L	518	250	70.38	4.51	15.01	23.91
030623 L P3	L	352	75.9	44.92	2.92	9.38	16.14
030623 L P4	L	640	659.8	84.7	6.71	22.54	33.96
030623 L P5	L	502	207.4	66.06	5.24	15	23.27
030623 L P6	L	326	55.7	39.88	2.93	7.74	18.12
030623 L P7	L	393	96.1	44.69	2.65	8.74	14.37
030623 L P8	L	563	344.5	67.86	4.38	15.96	27.93
030623 L P9	L	411	120.5	54.71	3.08	10.63	19.54
030623 L P10	L	395	111.9	47.1	2.41	8.38	15.86
030925 KN2C P1	KN2C	494	216.1	53.7	4.52	14.51	19.15
030925 KN2C P2	KN2C	478	224.3	53.74	4.22	15.31	22.73
030925 KN2C P3	KN2C	425	107.9	48.98	2.92	9.97	18.98

Add III.2- 2: The absolute values of cranial measurements of *Anguilla anguilla* specimens from the INBO- eel pollutant monitoring network.





code	site	TL	We	L Sn-Pe	IOB m	H H (Ec)	W Pe
030925 KN2C P4	KN2C	399	101.9	50.01	4.71	10.09	20.77
030925 KN2C P5	KN2C	387	86.6	43.12	3.29	9.63	19.32
030925 KN2C P6	KN2C	380	91.2	50.31	3.52	10.24	17.33
030925 KN2C P7	KN2C	385	68.3	46.61	3.74	10.22	15.37
030925 KN2C P8	KN2C	379	70.5	40.36	2.89	8.6	13.62
030925 KN2C P9	KN2C	371	75.8	42.23	3.22	8.57	17.89
030925 KN2C P10	KN2C	342	57.9	42.35	3.18	7.87	16.14
030917 KDS6A P1	KDS6A	392	94.6	53.89	4.19	8.64	17.56
030917 KDS6A P2	KDS6A	365	68.9	48.5	3.67	8.79	18.49
030917 KDS6A P3	KDS6A	410	90.8	49.06	2.64	9.33	18.79
030917 KDS6A P4	KDS6A	437	128.1	57.09	4.76	12.17	22.6
030917 KDS6A P5	KDS6A	396	109.8	52.98	3.35	11.76	20.56
030917 KDS6A P6	KDS6A	398	101.6	53.85	3.67	10.66	21.27
030917 KDS6A P7	KDS6A	427	123.3	53.49	3.39	9.14	18.33
030917 KDS6A P8	KDS6A	390	94.6	46	3.42	11.73	18.87
030917 KDS6A P9	KDS6A	353	64.3	45.73	2.83	8.62	15.81
030917 KDS6A P10	KDS6A	432	137.6	57.62	4.17	13.01	21.96
030904 DEM P1	DEMI	520	271.8	66.08	4.2	14.75	25.81
030904 DEM P2	DEMI	637	477.5	73.76	7.01	20.59	33.72
020523 KLD4 P1	KLD4	385	86.8	46.47	3.93	9.85	17.81
020523 KLD4 P2	KLD4	407	97.7	45.44	3.3	8.78	15.03
020523 KLD4 P3	KLD4	421	104.8	48.56	3.28	12.34	14.84
020523 KLD4 P4	KLD4	381	81.2	44.03	3.29	9.35	16.65
020523 KLD4 P5	KLD4	376	83.2	48.37	3.15	10.03	15.59
020523 KLD4 P6	KLD4	480	194.5	53.07	3.74	11.06	19.79
020523 KLD4 P7	KLD4	427	119.9	53.31	3.77	11.46	17.59
020523 KLD4 P8	KLD4	501	217.9	61.2	4.39	13.68	19.54
020523 KLD4 P9	KLD4	495	225.3	49.08	3.47	13.52	21.19
020523 KLD4 P10	KLD4	444	145.1	50.97	4.99	14.86	22.83
020515 MA2 P1	MA2	575	278	64.76	4.68	13.93	22.08
020515 MA2 P2	MA2	402	76.5	44.96	3.4	9.55	14.98
020515 MA2 P3	MA2	523	259.2	65.45	5.28	14.64	24.22
020515 MA2 P4	MA2	508	212.3	58.63	5.66	16.81	23.39
020515 MA2 P5	MA2	398	95.3	46.79	3.3	9.72	21.77
020515 MA2 P6	MA2	397	113.4	47.68	4	10.94	20.75
020515 MA2 P7	MA2	633	505.5	78.58	6.83	19.04	31.89
020515 MA2 P8	MA2	456	153.5	50.03	4.55	13.55	17.91
020515 MA2 P9	MA2	364	83.7	43.16	3.15	8.34	16.78
020515 MA2 P10	MA2	356	67.6	40.76	4.53	9.32	13.04
020626 KLD4 P1	KLD4	407	120	43.82	3.82	11.94	20.01
020626 KLD4 P2	KLD4	494	197	59.92	5.74	18.81	24.88
020626 KLD4 P3	KLD4	503	188.5	64.67	5.97	10.42	21.21
020626 KLD4 P4	KLD4	509	234	77.6	5.96	19.18	24.55
020626 KLD4 P5	KLD4	517	265.6	62.55	4.58	14.04	20.72
020626 KLD4 P6	KLD4	537	318.6	66.28	5.85	16.84	24.22
020626 KLD4 P7	KLD4	583	352.1	67.38	6.22	19.2	26.37
020626 KLD4 P8	KLD4	573	328.7	79.88	8.85	23.47	29.23
020626 KLD4 P9	KLD4	600	397.9	82.77	8.8	23.45	29.08
020626 KLD4 P10	KLD4	620	387	74.52	5.85	20.23	27.45
020515 MA2A P1	MA2A	597	455.6	84.59	7.37	23.59	33.2
020515 MA2A P2	MA2A	569	293	72.1	7.76	17.65	30.57
020515 MA2A P3	MA2A	387	105.3	48.65	5.54	12.15	14.8
020515 MA2A P4	MA2A	507	220.1	60.2	5.63	16.3	25.08
020515 MA2A P5	MA2A	574	409.7	66.27	4.8	20.54	31.44
020515 MA2A P6	MA2A	517	265	66.36	6.99	15.8	28.13

Add III.2- 2: The absolute values of cranial measurements of *Anguilla anguilla* specimens from the INBO- eel pollutant monitoring network.



code	site	TL	We	L Sn-Pe	IOB m	H H (Ec)	W Pe
020514 MA3B P1	MA3B	503	210.2	50.77	3.71	17.68	21.36
020514 MA3B P2	MA3B	486	207.3	56.09	4.22	12.73	21.32
020514 MA3B P3	MA3B	523	232.4	50.82	6.07	14.59	25.13
020514 MA3B P4	MA3B	530	262.4	61.34	5.16	14.1	25.17
020514 MA3B P5	MA3B	536	272.8	62.66	5.2	15.38	23.04
020619 KLD4 P1	KLD4	433	150.3	53.71	4.91	13.83	19.11
020619 KLD4 P2	KLD4	565	268.5	75.98	6.16	18.64	24.42
020619 KLD4 P3	KLD4	416	108.4	52.53	5.89	12.86	19.36
020619 KLD4 P4	KLD4	480	177.5	63.78	6.1	15.24	23.8
020619 KLD4 P5	KLD4	462	151.3	55.77	3.6	11.88	15.81
020619 KLD4 P6	KLD4	575	295.8	69.29	6.26	15.47	24.15
020619 KLD4 P7	KLD4	404	98.3	51.74	4.08	12.52	15.9
020619 KLD4 P8	KLD4	389	75.6	49.71	3.7	9.39	14.52
020619 KLD4 P9	KLD4	443	120.6	57.13	4.82	10.92	16.95
020318 LLS P1	LLS	387	79.9	52.6	2.88	10.9	15.1
020318 LLS P2	LLS	354	68.4	43.8	2.7	9.72	14.76
020318 LLS P3	LLS	427	78.9	47.81	3.33	10.51	14.19
020318 LLS P4	LLS	380	68.9	43.09	2.98	9.54	18.97
020318 LLS P5	LLS	390	80	46.73	3.32	9.51	13.75
020318 LLS P6	LLS	435	137.3	54.01	4.4	12.63	21.69
020523 GS2 P1	GS2	356	112.6	45.45	3.87	9.92	17.71
020523 GS2 P2	GS2	383	112.2	45.47	3.42	10.07	17.52
020523 GS2 P3	GS2	334	64	38.58	2.63	7.24	12.49
020523 GS2 P4	GS2	376	135.1	44.39	3.41	11.43	16.71
020523 GS2 P5	GS2	316	50.3	38.75	3.29	7.08	15.14
020523 GS2 P6	GS2	323	62.9	38.02	2.06	10.3	13.49
020523 GS2 P7	GS2	325	81.5	38.48	2.84	7.04	14.36
020523 GS2 P8	GS2	340	76.5	40.55	3.08	8.91	16.11
020514 MA3A P1	MA3A	450	176.9	55.17	5.58	13.36	24.68
020514 MA3A P2	MA3A	474	202.6	53.87	5.14	14.48	21.45
020514 MA3A P3	MA3A	436	141.7	51.12	3.39	12.75	19.55
020514 MA3A P4	MA3A	472	200.6	58.25	5.12	12.39	23.65
020514 MA3A P5	MA3A	454	181.4	50.04	5.36	14.02	17.25
020514 MA3A P6	MA3A	459	199.3	56.71	3.79	12.46	20.56
020514 MA3A P7	MA3A	486	223	53.71	4.76	15.67	23.16
020514 MA3A P8	MA3A	494	245.3	58.63	4.62	16.31	20.02
020514 MA3A P9	MA3A	576	262.9	65.29	7.57	20.34	36.38
020514 MA3A P10	MA3A	530	268.4	61.5	5.03	17.65	30.29
020327 DE3A P1	DE3A	466	197.4	56.29	4.3	15.04	19.84
020327 DE3A P2	DE3A	416	133	47.33	4.76	10.82	17.36
020327 DE3A P3	DE3A	382	121.6	52.38	4.52	11.24	18.21
020513 MA3C P1	MA3C	405	104.6	41.44	4.1	8.92	19.98
020513 MA3C P2	MA3C	563	315.6	69.91	6.1	18.47	29.03
020513 MA3C P4	MA3C	528	372	57.53	4.6	13.23	25.84
020513 MA3C P5	MA3C	444	163	57.57	4.88	14.41	24.75
020513 MA3C P6	MA3C	540	293.4	48.9	5.37	15.77	25.98
020513 MA3C P7	MA3C	468	174.7	58.01	4.28	15.15	20.15
020513 MA3C P8	MA3C	528	302	56.22	4.56	14.32	26.19
020513 MA3C P9	MA3C	566	397.6	74.77	6.39	18.86	35.44
020614 BEV1 P2	BEV1	310	52.4	37.17	2.53	8.49	12.67
020614 BEV2 P1	BEV2	506	369.8	76.19	6.3	19.86	25.74
020404 WMX P1	WMX	453	157.2	60.98	4.29	13.96	25.46
020404 WMX P2	WMX	524	284.2	74.09	5.63	18.84	31.76
020404 WMX P3	WMX	585	381.8	65.88	5.71	14.79	27.01
020404 WMX P4	WMX	503	286.6	64.07	4.44	15.49	30.27

Add III.2- 2: The absolute values of cranial measurements of *Anguilla anguilla* specimens from the INBO- eel pollutant monitoring network.



code	site	TL	We	L Sn-Pe	IOB m	H H (Ec)	W Pe
020404 WMX P5	WMX	503	262	59.69	5.42	15.05	26.27
020404 WMX P6	WMX	371	96.3	46.1	2.72	10.74	20.27
020404 WMX P7	WMX	334	66.4	41	3.22	8.99	18.69
020328 DE3B P2	DE3B	576	431.7	67.93	5.2	17.87	32.87
020604 SCH3C P4	SCH3C	436	167.6	49.89	3.05	11.97	22.2
020604 SCH3C P5	SCH3C	500	237.9	55.1	4.21	13.96	17.67
020604 SCH3C P6	SCH3C	428	156.4	57.18	4.45	13.35	17.4
020604 SCH3C P7	SCH3C	413	136.2	44.58	5.02	12.94	20.98
020604 SCH3C P8	SCH3C	359	94.7	42.79	3.49	11.72	17.39
020604 SCH3C P9	SCH3C	375	89.2	46.9	3.78	11.69	15.08
020604 SCH3C P10	SCH3C	400	125.9	47.38	2.76	11.28	16.68
020617 KLD1A P1	KLD1A	546	231.8	64.9	3.87	14.63	22.28
020617 KLD1A P2	KLD1A	460	161.2	53.08	4.53	11.52	20.86
020617 KLD1A P3	KLD1A	468	137.4	54.89	5.29	15.12	20.25
020617 KLD1A P4	KLD1A	576	323.5	63.87	7.07	16.11	21.03
020515 MA1 P1	MA1	692	562.7	79.65	7.46	20.33	34.39
020515 MA1 P2	MA1	406	113	51.47	3.86	12.88	20.53
020515 MA1 P3	MA1	433	128.8	48.98	4.19	11.91	20.44
020515 MA1 P4	MA1	402	111.5	53.51	3.91	12.23	19.95
020515 MA1 P5	MA1	626	436.2	76.96	6.17	21.26	33.95
020515 MA1 P6	MA1	556	280	72.4	6.08	17.81	29.77
020515 MA1 P7	MA1	450	157.2	59.16	5.83	12.56	22.27
020311 JEK P1	JEK	664	567.9	73	6.85	22.82	30.56
020311 JEK P3	JEK	590	381	69.25	5.29	17.04	28.59
020327 DE3 P1	DE3	553	397.4	66.11	6.04	19.85	28.91
020404 KN1 P1	KN1	372	69.8	53.72	4.34	12.98	18.14
020404 KN1 P2	KN1	331	57.3	43.96	4	10.68	18.37
020404 KN1 P3	KN1	366	55	43.01	3.57	8.46	15.28
020404 KN1 P4	KN1	472	150.3	67.08	7.02	15.26	26.48
020404 KN1 P5	KN1	385	92.8	48.17	4.18	12.54	21.5
020404 KN1 P6	KN1	300	33.8	34.36	3.04	8.5	16.47
020404 KN1 P7	KN1	295	40.6	36.06	2.7	7.82	13.67
020404 KN1 P8	KN1	301	40.1	31.91	3.59	8.39	15.82
020404 KN1 P9	KN1	304	33.7	37.29	1.97	9.02	13.94
020328 DE4A P1	DE4A	407	114.5	47.01	4.84	14.78	19.95
020328 DE4A P2	DE4A	389	101.5	52.67	4.61	15.35	21.88
020328 DE4A P3	DE4A	419	122	46.34	4.71	13.5	20.06
020328 DE4A P4	DE4A	476	206.6	58.04	4.08	17.48	25.29
020328 DE4A P5	DE4A	472	222	57.83	6.37	17.93	23.28
020328 DE4A P6	DE4A	372	96.2	51.44	4.74	13.14	21.68
020328 DE4A P7	DE4A	480	193.9	61.67	5.66	17.44	22.27
020328 DE4A P8	DE4A	352	73.8	51.73	4.51	10.28	18.61
020513 MA3E P1	MA3E	487	211.5	58.45	3.96	12.45	26.27
020513 MA3E P2	MA3E	480	213.3	57.95	5.21	14.87	25.41
020513 MA3E P3	MA3E	441	180	52.08	3.77	12.21	20.47
020513 MA3E P4	MA3E	411	108.7	48.48	4.31	11.71	19.22
020513 MA3E P5	MA3E	454	150.5	55.14	4.21	11.62	20.14
020513 MA3E P6	MA3E	436	146.5	52.47	4.1	12.82	19.1
020513 MA3E P7	MA3E	422	124.4	54.37	4.5	13.3	20.22
020513 MA3E P8	MA3E	476	185.6	55.45	5.21	13.46	23.22
020513 MA3E P9	MA3E	434	153.7	51.68	3.56	13.05	18.12
020513 MA3E P10	MA3E	416	119.8	50.57	4.89	11.2	19.1
020606 SCH4A P1	SCH4A	372	116.3	50.75	3.73	12.11	18
020606 SCH4A P2	SCH4A	431	185.5	49.09	4.37	13.03	20.12
020606 SCH4A P3	SCH4A	419	139.2	53.87	3.54	11.91	17.4

Add III.2- 2: The absolute values of cranial measurements of *Anguilla anguilla* specimens from the INBO- eel pollutant monitoring network.



code	site	TL	We	L Sn-Pe	IOB m	H H (Ec)	W Pe
020606 SCH4A P4	SCH4A	377	110.6	46.68	4.08	9.65	16.03
020606 SCH4A P5	SCH4A	445	203.5	54.88	4.64	13.8	18.98
020606 SCH4A P6	SCH4A	417	149.9	48.91	4.23	11.1	20.24
020606 SCH4A P7	SCH4A	482	216.5	58.93	5.27	14.75	20.24
020606 SCH4A P8	SCH4A	472	223	63.59	5.25	13.91	22.91
020606 SCH4A P9	SCH4A	475	248.2	55.05	4.38	13.86	23.19
020606 SCH4A P10	SCH4A	428	185.1	47.01	4.63	10.56	19.58
020514 MA2B P1	MA2B	584	369.2	81.6	8.33	21.85	32.21
020514 MA2B P2	MA2B	456	181.1	51.58	4.48	12.75	20.19
020514 MA2B P3	MA2B	500	278.2	55.39	5.09	13.71	25.98
020514 MA2B P4	MA2B	447	133.6	59.91	4.75	12.89	22.11
020514 MA2B P5	MA2B	459	215	54.13	5.8	15.39	21.27
020514 MA2B P6	MA2B	465	184.9	62.56	5.04	16.42	23.74
020514 MA2B P7	MA2B	383	118.7	60.76	5.75	19.17	27.71
020514 MA2B P8	MA2B	522	323.3	44.05	4.66	11.63	18.71
020514 MA2B P9	MA2B	640	550.9	94.88	10.85	19.54	39.39
020514 MA2B P10	MA2B	618	475.8	82.6	8.37	20.91	40.86
020916 OMD P1	OMD	400	109.5	51.78	4.9	11.75	22.87
020916 OMD P3	OMD	351	91.2	39.69	4.03	10.28	18.58
020916 OMD P4	OMD	360	92.7	42.67	3.14	8.64	21.42
020916 OMD P5	OMD	405	94.2	57.09	4.49	15.08	20.13
020916 OMD P6	OMD	420	133.4	55.56	4.23	11.97	21.67
020916 OMD P7	OMD	420	109.6	48.91	4.86	10.98	23.56
020916 OMD P8	OMD	365	88	44.71	4.33	10.63	22.19
020916 OMD P9	OMD	355	79.9	43.88	4	8.91	18.42
020916 OMD P10	OMD	360	74.3	53.03	4.83	10.85	20.65
021023 OSK P1	OSK	432	128.1	53.79	4.07	13.22	21.58
021023 OSK P2	OSK	456	151.3	71.73	6.32	14.93	23.57
021023 OSK P3	OSK	325	64.8	42.01	2.97	8.91	15.03
021023 OSK P4	OSK	337	63.4	39.85	3.51	10.97	15.6
021023 OSK P5	OSK	297	37.1	40.34	2.95	8.1	12.42
021023 OSK P6	OSK	345	68.2	46.55	3.68	9.51	14
021023 OSK P7	OSK	423	148.1	63.47	5.17	18.28	26.88
021023 OSK P8	OSK	330	51.6	43.51	3.68	12.69	11.81
021023 OSK P9	OSK	319	55.1	42.61	3.84	10.49	12.32
020604 SCH3A P2	SCH3A	524	346.4	59.88	5.4	14.66	25.6
020604 SCH3A P3	SCH3A	580	431.8	67.7	6.91	19.98	27.06
020604 SCH3A P4	SCH3A	417	136.8	48.72	4.5	13.39	16.54
020604 SCH3A P5	SCH3A	350	83.3	45.24	4.28	11.69	15.35
020613 KLD2A P1	KLD2A	534	255.8	63.39	5.64	15.48	20.56
020613 KLD2A P2	KLD2A	564	296.9	68.48	6	19.13	25.03
020613 KLD2A P3	KLD2A	546	270	54.54	4.48	11.99	25.21
020613 KLD2A P4	KLD2A	650	508.1	71.09	6.2	16.26	26.93
020613 KLD2A P5	KLD2A	572	346.4	64.54	5.99	15	24.97
020613 KLD2A P6	KLD2A	537	263	64.32	5.64	13.49	22.73
020613 KLD2A P7	KLD2A	506	116.5	58.94	5.59	14.36	20.54
020604 SCH4B P1	SCH4B	407	132.3	55.27	4.67	13.33	20.11
020604 SCH4B P2	SCH4B	419	132.3	48.23	4.62	11.61	17.83
020513 MA3D P4	MA3D	423	146.8	48.07	4.44	11.71	18.49
020513 MA3D P5	MA3D	466	197.7	60.51	4.56	12.4	19.62
020513 MA3D P2	MA3D	547	277.5	61.42	4.16	12.12	23.95
020513 MA3D P3	MA3D	462	151.1	52.09	4.23	9.93	16.78
020513 MA3D P6	MA3D	544	292.7	71.65	8.64	18.73	30.54
020513 MA3D P7	MA3D	475	198.8	62.84	5.68	18.08	25.31
020513 MA3D P8	MA3D	477	187.1	66.2	5.98	16.14	23.16

Add III.2- 2: The absolute values of cranial measurements of *Anguilla anguilla* specimens from the INBO- eel pollutant monitoring network.





code	site	TL	We	L Sn-Pe	IOB m	H H (Ec)	W Pe
020513 MA3D P9	MA3D	455	149.4	54.99	3.35	11.71	19.59
020513 MA3D P10	MA3D	524	292.6	57.69	3.87	15.41	24.33
020328 DE3C P2	DE3C	465	210.8	62.86	5.65	14.78	22.52
020328 DE3C P3	DE3C	503	287.3	68.53	7.39	18.26	32.37
020328 DE3C P4	DE3C	529	341.8	80.78	7.38	18.56	29.94
020328 DE3C P5	DE3C	400	120	51.76	5.17	14.75	18.13
020328 DE3C P6	DE3C	368	70.9	51.24	4.01	10.3	16.54
020328 DE3C P7	DE3C	435	197.5	57.12	4.7	15.34	21.83
020328 DE3C P8	DE3C	476	208	63.7	6.5	17.6	24.89
020328 DE3C P9	DE3C	366	114	49.64	5.95	12.61	17.82
020328 DE3C P10	DE3C	457	171.3	62.65	6.4	16.16	31.43
020514 MA3 P1	MA3	558	341.4	75.34	8.3	20.39	29.38
020514 MA3 P2	MA3	454	173.3	80.32	7.39	16.55	24.72
020514 MA3 P3	MA3	578	347.5	61.41	5.49	12.06	23.24
020514 MA3 P4	MA3	573	435.4	68.66	6.88	14.35	30.57
020403 MNB P1	MNB	459	165.4	67.33	5.03	14.18	26.08
020403 MNB P2	MNB	370	100.5	42.83	4.17	10.44	19.58
020403 MNB P3	MNB	323	67.3	36.93	3.03	8.3	14.93
020403 MNB P4	MNB	345	80.6	37.07	2.85	8.5	17.78
020403 MNB P5	MNB	518	223	58.91	4.88	16.01	21.14
020403 MNB P6	MNB	508	289.5	59.02	6.1	19.03	25.08
020902 OMS P1	OMS	432	140.5	61.82	6	15.28	27.22
020902 OMS P2	OMS	432	125.7	57.3	5.14	13.47	22.81
020902 OMS P3	OMS	382	74.7	46.65	4.15	10.84	16.57
020902 OMS P4	OMS	399	87	48.44	4.14	12.49	16.75
020902 OMS P5	OMS	414	129.5	56.3	4.57	11.4	21.1
020902 OMS P6	OMS	369	70.5	45.75	4.01	8.12	18.83
020902 OMS P7	OMS	373	91	50.97	4.15	12.26	18.93
020902 OMS P8	OMS	419	115.6	55.34	4.05	14.21	19.43
020902 OMS P9	OMS	440	148.2	65.18	5.52	14.65	23.58
020902 OMS P10	OMS	426	112.6	58.95	5.92	13.34	26.19
021009 KBH2 P1	KBH2	414	109.5	54.14	4.5	13.42	20.94
021009 KBH2 P2	KBH2	349	66.8	44.35	3.61	10.22	18.39
020207 KLD4 P1	KLD4	593	273.7	71.17	8.26	17.77	25.94
020604 SCH3C P1	SCH3C	441	175.1	58.67	5.02	13.36	23.24
020604 SCH3C P2	SCH3C	463	210.3	58.44	7.43	13.21	24.93
020604 SCH3C P3	SCH3C	345	68.4	36.85	2.96	8.72	15.9
020506 PV1 P1	PV1	342	101.7	46.35	3.14	10.19	18.06
020604SCH3B P1	SCH3B	536	298.3	69.94	8.64	15.94	28.29
020506 PV2 P1	PV2	317	69.5	40.61	3.69	9.16	18.78
020506 PV2 P2	PV2	347	80.4	40.96	3.36	8.33	14.92
021010 KBH3 P1	KBH3	348	77.8	43.18	3.83	9.53	17.07
021010 KBH3 P2	KBH3	344	70.1	43.15	3.62	9.94	15.57
021010 KBH3 P3	KBH3	344	71.5	43.59	4.33	10.16	18.25
021010 KBH3 P4	KBH3	295	38.2	33.19	4.18	8.14	13.48
020508 MVX P1	MVX	336	79.8	39.57	3.68	8.92	17.98
020508 MVX P2	MVX	323	78.5	41.42	3.45	9.99	18.67
020523 GS1 P1	GS1	356	86.5	45	5.28	10.91	16.52
020523 GS1 P2	GS1	478	217.4	54.24	5.03	11.61	23.98
021007 KBH1 P1	KBH1	402	114.7	48.48	4.1	11.67	15.18
021007 KBH1 P2	KBH1	419	120.7	45.69	4.4	12.23	18.43
021007 KBH1 P3	KBH1	357	81.6	43.68	3.65	11.27	17.5
020403 VNX P1	VNX	388	91.1	59.42	4.01	11.77	18.46
020403 VNX P2	VNX	325	56.4	40.87	2.98	9.95	14.94
020402 BGX P1	BGX	346	63.6	40.07	3.42	10.34	15.82

Add III.2- 2: The absolute values of cranial measurements of *Anguilla anguilla* specimens from the INBO- eel pollutant monitoring network.



code	site	TL	We	L Sn-Pe	IOB m	H H (Ec)	W Pe
020402 BGX P2	BGX	321	43.2	38.3	3.45	8.69	14.66
020321 ZLO P1	ZLO	380	88.6	48.84	5.57	13.22	17.58
020424 AA P1	AA	532	328.2	59.33	6.71	15.12	32.74
020528 ED1 P1	ED1	436	161	57.56	5.04	14.84	22.77
020604 SCH3A P1	SCH3A	554	415.3	80.73	8.45	19.15	32.3
020508 ZGL P1	ZGL	307	54.3	43.22	3.75	11.46	15.93
020508 ZGL P2	ZGL	470	166.1	65.24	7.64	16.84	25.38
020314 ZB P1	ZB	480	292.5	63.3	6.25	16.08	25.67
020402 ASA P1	ASA	424	124.9	56.52	5.29	16.95	20.13
020507 KBR P1	KBR	335	83.6	44.84	3.46	9.99	21.32
020507 KBR P2	KBR	323	70.1	42.41	3.61	8.28	14.34
020507 KBR P3	KBR	317	61.6	42.68	3.29	7.03	16.03
020529 HBN P1	HBN	343	69.8	47.92	4.54	10.2	18.55
020528 DBU P1	DBU	472	195.2	58.31	6.68	16.23	25.96
020523 KLB P1	KLB	366	105.7	37.69	4.4	10.64	17.53
020523 KLB P2	KLB	384	122.6	43.22	4.04	14.27	18.17
020523 KLB P3	KLB	341	77.1	39.69	3.95	13.93	16.71
020523 KLB P4	KLB	367	111.5	43.77	4.93	10.94	19.67
020523 KLB P5	KLB	339	83.9	39.01	3.67	9.33	16.77
020528 ED2 P1	ED2	477	239.2	55.73	6.33	17.5	22.01
020528 ED2 P2	ED2	347	84.1	44.59	4.05	11.96	17.33
020528 ED2 P3	ED2	314	56.3	40.03	4.07	9.14	17.02
020528 ED2 P4	ED2	297	60	36.18	2.28	9.41	12.12
010420 HEL P1	HEL	380	120	44.46	1.96	7.93	17.24
010420 HEL P10	HEL	348	83.9	39.77	1.41	6.57	10.12
010420 HEL P2	HEL	362	102.4	43.14	1.65	6.86	14.52
010420 HEL P3	HEL	374	97.7	40.22	1.34	7.81	12.45
010420 HEL P4	HEL	353	92.4	42.2	1.76	7.27	14.83
010511 ZBR P1	ZBR	870	1340.2	87.88	7.44	18.88	42.42
010511 ZBR P2	ZBR	885	1276.1	93.29	10.31	22.69	39.38
010511 ZBR P3	ZBR	1015	1836.7	104.05	12.43	23.78	42.37
010517 ZWL P1	ZWL	426	118.8	51.39	2.58	8.95	18.75
010517 ZWL P2	ZWL	394	122	52.62	4.02	10.15	16.79
010517 ZWL P3	ZWL	423	113	53.43	2.26	10.5	18.27
010517 ZWL P4	ZWL	545	343.1	67.3	5	13.77	24.78
010517 ZWL P5	ZWL	600	454.3	68.38	5.71	17.86	28.56
010607 IB1 P1	IB1	381	88	41.74	2.36	7.31	13.9
010607 IB1 P2	IB1	414	122.2	42.01	2.98	9.27	13.97
010607 IB1 P3	IB1	370	89.7	41.05	2.17	8.63	14.46
010607 IB1 P4	IB1	378	90.9	40.85	1.83	6.51	11.85
010607 IB1 P5	IB1	346	77.1	40.73	2.2	8.25	13.28
010810 COM P16	COM	419	114.8	54.11	1.97	10.35	21.64
010810 COM P17	COM	432	122.2	57.18	3.63	11.19	22.69
010810 COM P2	COM	426	157.7	58.28	3.21	10.38	23.82
010810 COM P20	COM	503	204.3	65.11	3.86	12.1	26.71
010810 COM P3	COM	448	178.1	57.19	3.56	9.05	22.12
010810 COM P4	COM	357	76	37.77	1.42	5.93	12.03
010810 COM P6	COM	453	217.8	61.87	3.56	10.64	22.28
010810 COM P8	COM	408	120.4	59.16	2.74	10.62	20.4
010810 COM P9	COM	375	86.7	51.36	2.89	9.32	20.22
010920 NP2 P1	NP2	448	171	54.63	4.23	12.14	26.74
010920 NP2 P2	NP2	419	142.2	48.36	2.14	8.53	16.66
010920 NP2 P5	NP2	417	106.5	48.05	2.34	8.5	14.99
010920 NP2 P6	NP2	443	149.8	51.69	2.1	8.58	15.99
010920 NP2 P9	NP2	398	119.8	49.99	2.81	8.44	17.2

Add III.2- 2: The absolute values of cranial measurements of *Anguilla anguilla* specimens from the INBO- eel pollutant monitoring network.



code	site	TL	We	L Sn-Pe	IOB m	H H (Ec)	W Pe
010928 RM1 P1	RM	377	86.7	44.35	1.79	8.2	13.98
010928 RM1 P2	RM	425	127.3	57.12	4.63	12.23	18.13
011023 KLD2 P1	KLD2	402	110	46.52	2.18	8.99	16.9
011023 KLD2 P5	KLD2	381	77.7	41.53	1.76	7.33	11.99
011023 KLD2 P6	KLD2	453	175.6	49.37	2.09	9.32	20.47
011023 KLD2 P8	KLD2	392	108.6	42.56	1.56	6.73	14.43
011023 KLD2 P9	KLD2	431	115	45.12	2.33	8.3	15.22
011105 BPG P1	BGP	425	122.3	48.65	2.79	9.43	16.65
011105 BPG P2	BGP	450	126.4	61.69	5.75	12.6	17.99
011105 BPG P6	BGP	406	109.4	46.51	2.59	8.8	14.42
011105 BPG P9	BGP	411	105.6	49.89	3.27	10.54	18.18
011105BPG P3	BGP	396	126.6	47	2.28	10.18	16.98
020605 GBO P1	GBO	306	68	38.91	1.98	6.02	14.22
020605 GBO P2	GBO	457	202	55.23	2.84	9.49	20.45
020605 GBO P3	GBO	346	89.1	42.85	1.92	8.58	15.3
020605 GBO P4	GBO	400	140.9	55.05	3.2	9.51	18.06
020924 KZ P1	KZ	383	97	39.26	1.48	6.78	13.27
020924 KZ P10	KZ	351	78.3	38.3	1.38	6.62	12.45
020924 KZ P2	KZ	386	88.7	43.23	1.33	7.45	13.33
020924 KZ P3	KZ	436	144.9	47.8	2.33	8.26	15.8
020924 KZ P4	KZ	380	103.6	41.34	2.07	7.98	14.7
020924 KZ P5	KZ	421	110.7	56.6	2.92	9.03	21.32
020924 KZ P6	KZ	398	99.9	46.7	2.29	8.01	16.93
020924 KZ P7	KZ	389	105.7	40.59	1.96	7.25	15.5
020924 KZ P8	KZ	382	95.6	40.96	1.55	6.47	13.86
020924 KZ P9	KZ	430	145.2	49.43	2.09	7.95	15.99
021007 KBH1A P1	KBH1A	332	99	47.48	2.17	8.53	16.71
021007 KBH1A P2	KBH1A	371	70.4	42.31	1.74	6.56	13.9
021007 KBH2A P1	KBH2A	412	121	47.84	4.08	10.19	16.2
021007 KBH4 P1	KBH4	485	197.5	56.11	2.98	10.02	16.94
021007 KBH4 P2	KBH4	413	120.8	46.9	2.49	9.37	16.71
021007 KBH4 P3	KBH4	459	150.7	60.74	4.68	10.86	19.9
021007 KBH5 P1	KBH5	454	152.9	54.55	2.99	10.64	16.05
021007 KBH5 P10	KBH5	349	77.2	43.46	2.77	7.91	11.8
021007 KBH5 P2	KBH5	443	123.1	52.51	2.26	8.32	20.32
021007 KBH5 P3	KBH5	372	92.1	46.02	1.91	8.67	17.88
021007 KBH5 P4	KBH5	443	137.1	58.5	3.14	9.63	17.98
021007 KBH5 P5	KBH5	370	87.8	46.75	2.35	9.1	14.18
021007 KBH5 P6	KBH5	443	136.3	52.85	3.02	8.8	14.58
021007 KBH5 P7	KBH5	361	71.8	46.57	2.24	8.15	14.64
021007 KBH5 P8	KBH5	443	137.2	54.9	2.96	10.88	18.82
021007 KBH5 P9	KBH5	361	89.9	42.2	1.84	8.8	15.01
021009 KBH1D P10	KBH1D	373	84.4	40.95	1.23	7.85	16.72
021009 KBH1D P2	KBH1D	471	160.7	53.58	4.01	10.35	17.5
021009 KBH1D P3	KBH1D	472	200.7	56.02	2.96	9.71	20.39
021009 KBH1D P4	KBH1D	452	159.3	57.33	3.83	10.48	19.24
021009 KBH1D P5	KBH1D	448	163.2	49.11	3.31	8.99	20.76
021009 KBH1D P6	KBH1D	431	149.9	51.68	2.48	10.44	17.41
021009 KBH1D P7	KBH1D	453	172.2	57.16	3.2	10.94	21.28
021009 KBH1D P8	KBH1D	377	96.4	42.8	2.06	10.08	13.63
021009 KBH1D P9	KBH1D	490	201.4	61.94	2.92	10.45	19.84
021009 KBH1DP1	KBH1D	440	172	56.7	3.89	11.38	18.51
021014 WBV6 P11	WBV6	423	119.2	48.91	2.29	9.12	15.34
021014 WBV6 P12	WBV6	423	130.5	50.74	1.76	7.89	20.01
021014 WBV6 P13	WBV6	398	89.5	49.06	1.79	8.91	17.59

Add III.2- 2: The absolute values of cranial measurements of *Anguilla anguilla* specimens from the INBO- eel pollutant monitoring network.



---

code	site	TL	We	L Sn-Pe	IOB m	H H (Ec)	W Pe
021014 WBV6 P14	WBV6	400	116.3	48.99	2.3	7.18	17.79
021014 WBV6 P15	WBV6	362	96.5	44.13	1.73	6.12	13.34
021017 WBV8 P7	WBV8	365	95.3	42.84	2.23	7.54	14.44
021104 HVX P1	HVX	550	395.2	68.6	4.28	14.66	28.74
021104 HVX P2	HVX	354	74.4	43.71	1.99	9.25	15.34
021104 HVX P3	HVX	573	371.4	71.28	4.3	15.48	26.18
021104 HVX P4	HVX	349	68.9	39.99	1.47	7.66	12.01
021104 HVX P5	HVX	312	48.8	36.99	1.43	7.68	9.21
021104 HVX P6	HVX	297	51.1	36.1	1.35	6	11.86
021104 HVX P7	HVX	337	57.7	41.81	2.13	9.55	13.92

---







